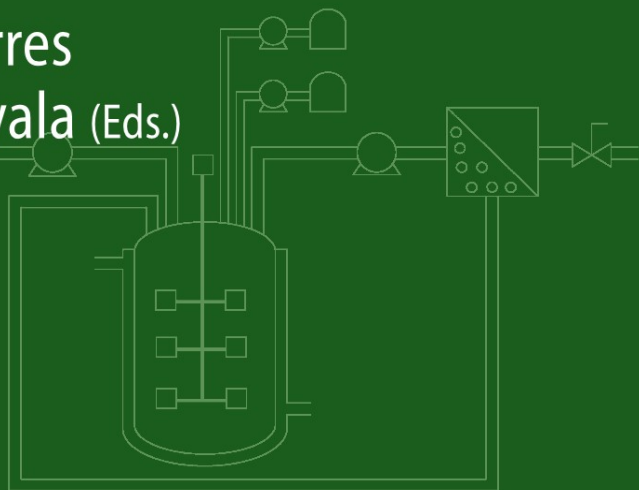


E. Torres
M. Ayala (Eds.)



Biocatalysis Based on Heme Peroxidases

Peroxidases as Potential
Industrial Biocatalysts

 Springer

Biocatalysis Based on Heme Peroxidases

Eduardo Torres • Marcela Ayala
Editors

Biocatalysis Based on Heme Peroxidases

Peroxidases as Potential
Industrial Biocatalysts

 Springer

Editors

Dr. Eduardo Torres
Benemérita Universidad
Autónoma de Puebla
Centro de Química
Ciudad Universitaria
72570 Puebla
México
eduardo.torres@icbuap.buap.mx

Dr. Marcela Ayala
Universidad Nacional Autónoma
de México
Instituto de Biotecnología
Av. Universidad, Col. Chamilpa 2001
62210 Cuernavaca, Morelos
México
maa@ibt.unam.mx

ISBN 978-3-642-12626-0 e-ISBN 978-3-642-12627-7
DOI 10.1007/978-3-642-12627-7
Springer Heidelberg Dordrecht London New York

Library of Congress Control Number: 2010932759

© Springer-Verlag Berlin Heidelberg 2010

This work is subject to copyright. All rights are reserved, whether the whole or part of the material is concerned, specifically the rights of translation, reprinting, reuse of illustrations, recitation, broadcasting, reproduction on microfilm or in any other way, and storage in data banks. Duplication of this publication or parts thereof is permitted only under the provisions of the German Copyright Law of September 9, 1965, in its current version, and permission for use must always be obtained from Springer. Violations are liable to prosecution under the German Copyright Law.

The use of general descriptive names, registered names, trademarks, etc. in this publication does not imply, even in the absence of a specific statement, that such names are exempt from the relevant protective laws and regulations and therefore free for general use.

Cover design: WMXDesign GmbH, Heidelberg, Germany

Printed on acid-free paper

Springer is part of Springer Science+Business Media (www.springer.com)

Preface

The last systematic description of heme peroxidases was published in 1999 by Brian Dunford, from the University of Alberta in Canada. The book *Heme peroxidases* covers discussion on three-dimensional structure, reaction mechanism, kinetics, and spectral properties of representative enzymes from bacterial, plant, fungal, and animal origin. Since 1999, vast information on basic but also applied aspects of heme peroxidases has been generated. We believe fusion of these two aspects will benefit research of those dedicated to development of biocatalytic process. The aim of this book is to present recent advances on basic aspects such as evolution, structure–function relation, and catalytic mechanism, as well as applied aspects, such as bioreactor and protein engineering, in order to provide the tools for rational design of enhanced biocatalysts and biocatalytic processes. The book does not include an exhaustive listing of references but rather a selected collection to enrich discussion and to allow envisioning future directions for research.

This book is organized in three parts. In Part I, current knowledge of structure and mechanism of peroxidases is covered. From the molecular phylogeny, going through the influence of structural factors over oxidative ability to the molecular mechanism of catalysis, the authors intend to provide an understanding of peroxidases at the molecular level. The understanding of the fundamental behavior of peroxidases will allow further adequation, design, and/or optimization of peroxidase-based catalysis to a particular process. In Part II, research on potential applications of peroxidases in several fields is presented and discussed. New processes for the fine chemicals industry, creation of new materials with novel properties, and biotransformation of compounds found in polluted water and soil are the topics included in this part. Finally, Part III presents the challenges that must be overcome in order to develop commercially feasible peroxidase-based industrial processes. As discussed in Chap. I, lowering the cost of the biocatalyst is essential; thus, low cost production and increased stability is discussed in this part. A compendium of useful information on peroxidases is to be found at the end of

the book, containing from biochemical properties such as molecular weight and isoelectric point to spectroscopic properties and kinetic data.

We would like to thank all the recognized experts that participated as authors in this book. We are also indebted to Prof. Michael A. Pickard, emeritus professor from the University of Alberta, who dedicated all his professional life to the study of peroxidases, and who made significant contributions in the areas of microbial metabolism and fungal enzymes, particularly with chloroperoxidase from *Caldariomyces fumago*, for helpful discussion and editorial assistance.

Puebla/Cuernavaca, 2010

Marcela Ayala
Eduardo Torres

Contents

1 Introduction	1
Marcela Ayala and Eduardo Torres	
Part I Molecular and Structural Aspects of Peroxidases	
2 Molecular Phylogeny of Heme Peroxidases	7
Marcel Zámocký and Christian Obinger	
3 Structural and Functional Features of Peroxidases with a Potential as Industrial Biocatalysts	37
Francisco J. Ruiz-Dueñas and Angel T. Martínez	
4 Redox Potential of Peroxidases	61
Marcela Ayala	
5 Catalytic Mechanisms of Heme Peroxidases	79
Paul R. Ortiz de Montellano	
Part II Prospective Usage of Peroxidases in Industry	
6 Potential Applications of Peroxidases in the Fine Chemical Industries	111
Luigi Casella, Enrico Monzani, and Stefania Nicolis	
7 Grafting of Functional Molecules: Insights into Peroxidase-Derived Materials	155
Gibson S. Nyanhongo, Endry Nugroho Prasetyo, Tukayi Kudanga, and Georg Guebitz	

8 Applications and Prospective of Peroxidase Biocatalysis in the Environmental Field	179
Cristina Torres-Duarte and Rafael Vazquez-Duhalt	
Part III Challenges in the Application of Peroxidases	
9 Enzyme Technology of Peroxidases: Immobilization, Chemical and Genetic Modification	209
Adriana Longoria, Raunel Tinoco, and Eduardo Torres	
10 Reactor Engineering	245
Juan M. Lema, Carmen López, Gemma Eibes, Roberto Taboada-Puig, M. Teresa Moreira, and Gumersindo Feijoo	
11 Deactivation of Hemeperoxidases by Hydrogen Peroxide: Focus on Compound III	291
Brenda Valderrama	
12 Heterologous Expression of Peroxidases	315
Sandra de Weert and B. Christien Lokman	
13 A Compendium of Bio-Physical-Chemical Properties of Peroxidases	335
Humberto Garcia-Arellano	
Index	353

Contributors

Marcela Ayala Instituto de Biotecnología, UNAM. Av. Universidad 2001, Chamilpa, 62210 Cuernavaca, Morelos, México, maa@ibt.unam.mx

Luigi Casella Dipartimento di Chimica Generale, Università di Pavia, Via Taramelli 12, 27100 Pavia, Italy, bioinorg@unipv.it

Sandra de Weert Institute of Biology Leiden, Leiden University, Sylviusweg 72, 2333BE Leiden, The Netherlands, s.de.weert@biology.leidenuniv.nl

Gemma Eibes Department of Chemical Engineering, School of Engineering, University of Santiago de Compostela, Santiago de Compostela E-15782, Spain

Gumersindo Feijoo Department of Chemical Engineering, School of Engineering, University of Santiago de Compostela, Santiago de Compostela E-15782, Spain

Humberto Garcia-Arellano Departamento de Ingeniería Química y Bioquímica, Instituto Tecnológico de Veracruz, Calz. M.A. De Quevedo 2779, C.P. 91860 Veracruz, Mexico, hgarcia.arellano@itver.edu.mx

Georg Guebitz Institute of Environmental Biotechnology, Graz University of Technology, Petersgasse 12/1, A-8010 Graz, Austria

Tukayi Kudanga Institute of Environmental Biotechnology, Graz University of Technology, Petersgasse 12/1, A-8010 Graz, Austria

Juan M. Lema Department of Chemical Engineering, School of Engineering, University of Santiago de Compostela, Santiago de Compostela E-15782, Spain, juan.lema@usc.es

B. Christien Lokman HAN BioCentre, Laan van Scheut 2, 6525 EM Nijmegen, The Netherlands, christien.lokman@han.nl

Carmen López Department of Chemical Engineering, School of Engineering, University of Santiago de Compostela, Santiago de Compostela E-15782, Spain

Adriana Longoria Instituto de Biotecnología, UNAM. Av. Universidad 2001. Col. Chamilpa, Cuernavaca 62210, Morelos, México, yanni@ibf.unam.mx

Angel T. Martínez Centro de Investigaciones Biológicas, CSIC, Ramiro de Maeztu 9, E-28040 Madrid, Spain

Enrico Monzani Dipartimento di Chimica, Generale Università di Pavia, Via Taramelli 12, 27100 Pavia, Italy, enrico.monzani@unipv.it

M. Teresa Moreira Department of Chemical Engineering, School of Engineering, University of Santiago de Compostela, Santiago de Compostela E-15782, Spain

Stefania Nicolis Dipartimento di Chimica Generale, Università di Pavia, Via Taramelli 12, 27100 Pavia, Italy, stefania.nicolis@unipv.it

Gibson S. Nyanhongo Institute of Environmental Biotechnology, Graz University of Technology, Petersgasse 12/1, A-8010 Graz, Austria

Christian Obinger Metalloprotein Research Group, Division of Biochemistry, Department of Chemistry, University of Natural Resources and Applied Life Sciences, Muthgasse 18, A-1190 Vienna, Austria

Paul R. Ortiz de Montellano Department of Pharmaceutical Chemistry, University of California, San Francisco, CA 94158-2517, USA

Endry Nugroho Prasetyo Institute of Environmental Biotechnology, Graz University of Technology, Petersgasse 12/1, A-8010 Graz, Austria

Francisco J. Ruiz-Dueñas Centro de Investigaciones Biológicas, CSIC, Ramiro de Maeztu 9, E-28040 Madrid, Spain

Raunel Tinoco Instituto de Biotecnología, UNAM. Av. Universidad 2001. Col. Chamilpa, Cuernavaca 62210, Morelos, México, raunel@ibt.unam.mx

Roberto Taboada-Puig Department of Chemical Engineering, School of Engineering, University of Santiago de Compostela, Santiago de Compostela E-15782, Spain

Cristina Torres-Duarte Instituto de Biotecnología, UNAM, Av. Universidad 2001. Col. Chamilpa, 62210 Cuernavaca, Morelos, México

Eduardo Torres Benemérita Universidad Autónoma de Puebla. Centro de Química. Ciudad Universitaria, 72570 Puebla, México, eduardo.torres@icbuap.buap.mx

Brenda Valderrama Departamento de Medicina Molecular y Bioprocesos, Instituto de Biotecnología, Universidad Nacional Autónoma de México, Morelos, Mexico, brenda@ibt.unam.mx

Rafael Vazquez-Duhalt Instituto de Biotecnología, UNAM, Av. Universidad 2001. Col. Chamilpa, 62210 Cuernavaca, Morelos, México, vazquduh@ibt.unam.mx

Marcel Zámocký Institute of Molecular Biology, Slovak Academy of Sciences, Dúbravská cesta 21, SK-84551 Bratislava, Slovakia, marcel.zamocky@boku.ac.at

Chapter 1

Introduction

Marcela Ayala and Eduardo Torres

World population is expected to increase from 6.5 billion in 2005 to 8.3 billion by 2030. Simultaneously, the average per capita income could rise from USD 5,900 in 2005 to USD 8,600, a 46% increase. A larger population with increased acquisitive power, along with the challenge of developing environmentally sustainable processes will be the driving force for the emergence of bioeconomy. According to the Organization for Economic Cooperation and Development (OECD), biotechnology-derived products could represent 2.7% of the GDP of OCDE countries by 2030, with the largest contribution arising from applications in industry and primary production (agriculture, forestry, and fishing), followed by health applications. According to the forecast, the bioeconomy growth will be particularly important in developing countries [1]. Sustainable development requires the preservation of (a) vital environmental factors, such as biodiversity, clean water, clean air, and clean soil; (b) renewable sources; and (c) technological capabilities to develop alternative processes, based on renewable sources. Biotechnology is able to support sustainable development by improving the efficiency of processes to lower the environmental impact. It is also able to manage polluted water and soil, to maintain the availability of vital nonrenewable resources.

In the 1990s, the US Environmental Protection Agency (EPA) introduced the term “green chemistry” to describe “chemical technologies that reduce or eliminate the use or generation of hazardous substances in the design, manufacture and use of chemical products”. The accomplishment of green chemistry should consider the environmental impact of a product from a cradle-to-grave perspective, including all aspects of the entire life cycle, from raw material to product use and disposal. A guide to achieve sustainability, the 12 principles of green engineering proposed by Anastas and Warner, comprehends the integration of several elements, such as renewable raw material, efficient catalysts, low environmental impact solvents, high atom efficiency, minimum waste generation, and water and energy consumption [2]. Life cycle assessments (LCAs) are valuable tools to measure the sustainability of a process. In the case of biotechnologies, LCAs of bioprocesses or bio-derived products are not as abundant as for conventional chemical processes; however, from the different stages involved in a bioprocess, several opportunities for improvement

may be detected [3], as shown in Fig. 1.1. One of them is biocatalyst performance, as also pointed out by the OECD when analyzing the impact of biotechnologies on sustainable industry [4]. On this subject, the new generation of biocatalysts for the twenty-first century should meet a certain performance level to compete with existing or alternative technologies; the characteristics of these improved biocatalysts are summarized in Table 1.1.

As an example, it has been estimated that for the industrial production of fine chemicals, biotransformations should accomplish a minimum space–time yield of $0.1 \text{ g l}^{-1} \text{ h}^{-1}$ and a minimum final product concentration of 1 g l^{-1} , while for pharmaceuticals, the minimum requirements are $0.001 \text{ g l}^{-1} \text{ h}^{-1}$ and 0.1 g l^{-1} for volumetric productivity and product concentration, respectively [6]. Analysis of enzymes with recognized industrial potential, such as cytochrome P450, showed that some of the parameters are already within industrially relevant ranges [7]. The improvements achieved with these biocatalysts through protein, cell, and process engineering are based on the understanding of their molecular arrangement and catalytic mechanisms.

This book gathers and analyzes information of both basic and applied aspects of heme peroxidases. Peroxidases are oxidoreductases that catalyze the oxidation of a wide range of molecules, using peroxide as electron acceptor. Although they have been proposed for applications in several fields (see for example [8, 9]) there are few industrial processes that utilize peroxidases. The commercial applications of these enzymes are reduced to diagnosis and research [10]. Unfortunately, the

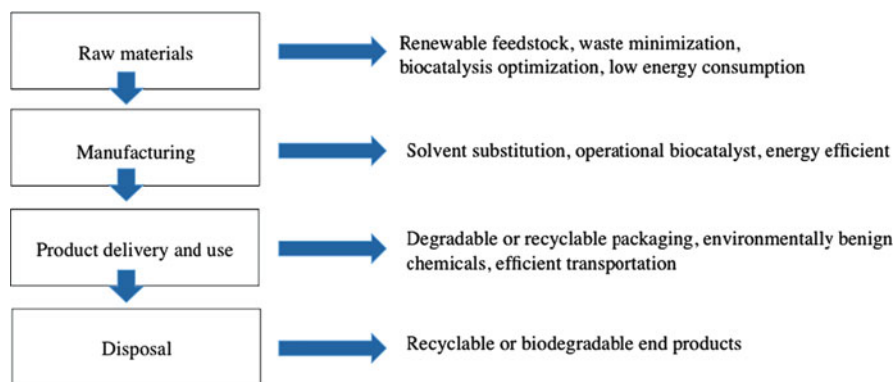


Fig. 1.1 Green industrial biotechnology applied from cradle-to-grave. Adapted from [3]

Table 1.1 Performance metrics of improved biocatalysts [5]

Characteristic	Goal
Temperature stability	Up to 120–130°C
Activity in water or organic solvent	100 to 10,000-fold over current levels
Productivity	10 to 100-fold increase
Turnover rate	Comparable to current chemicals catalysts
Lifetime durability	Months to years

economic feasibility of peroxidase-based processes has not been always assessed. Figure 1.2 shows the publication of scientific articles found in the Science Citation Index Expanded database with the word “peroxidase” on the title, for the last 100 years. For the last 30 years, the number of publications is steady and around 400 per year. It is significant to notice that more than 25% correspond to the area of basic biochemistry and molecular biology. Thus, one may consider that current understanding is mature enough to allow the design of peroxidase-based applications. However, less than a third of the publications could be considered applied or engineering-related research.

In order to successfully develop peroxidase-based biocatalysis, it is imperative to take into account not only operational criteria but also economic factors. Although the performance of peroxidases in terms of total turnover is already included in some of the research proposing peroxidase-based applications, the economic factor is usually overlooked. One of the few examples that consider both technical and economic aspects is the analysis of the enantioselective production of styrene epoxide, a high value product catalyzed by chloroperoxidase from *Caldariomyces fumago*. The analysis assumed that heterologous expression could reduce the enzyme cost from USD 5 million/kg (actual cost of the purified enzyme from vendors such as Chirazym) to USD 50,000/kg. Even under this assumption, the biocatalyst represents 95% of production costs. This analysis highlighted the imperative need to develop efficient, low cost expression systems for peroxidases. It also allowed concluding that both activity and stability of the peroxidase had to

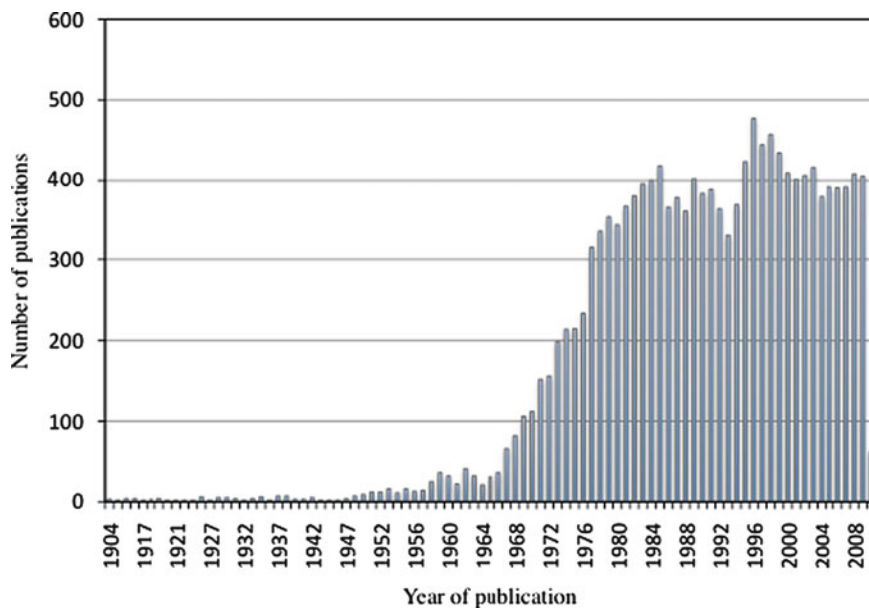


Fig. 1.2 Scientific articles related to peroxidases, as found on the Science Citation Index Expanded [11]

improve at least 10-fold for the process to compete with conventional chemical technologies [12]. At this point, it should be noted that even when enzyme cost is high (from USD 100 to 100,000/kg), the important consideration is cost contribution to the final product [13]; thus, at the moment, peroxidases have an opportunity to produce high value products that consume a low amount of biocatalyst.

Stability, activity, and specificity of an enzyme are thus the fundamental parameters that control the development of an industrial application. In the case of peroxidases, a great amount of information is available regarding structural and mechanistic factors that govern the catalytic performance, as well as the stability of these enzymes. It is also encouraging that enzyme engineering is able to increase the stability of the enzymes in non natural environments, such as the presence of organic solvents and high temperatures, by means of genetic engineering or chemical modification. Bioengineering is a crucial step in determining the feasibility of a process by focusing on productivity. The virtuous cycle would then involve optimizing a biocatalyst by taking into consideration its performance on a given reactor. In conclusion, understanding of all aspects of peroxidase catalysis allows the consideration of the design of better enzymes through a combination of molecular tools such as genetic engineering and chemical modification. The basic aspects of peroxidase catalysis as well as the challenges and tools to overcome them are discussed in the next sections.

References

1. OECD (2009) The bioeconomy to 2030: designing a policy agenda. OECD report. OECD, Washington, DC. ISBN ISBN-978-92-64-03853-0
2. Anastas PT, Zimmerman JB (2003) Through the 12 principles of green engineering. *Environ Sci Technol* 37:95A–101A
3. Hatti-Kaul R, Tornvall U, Gustafsson L et al (2007) Industrial biotechnology of bio-based chemicals: a cradle-to-grave perspective. *Trends Biotechnol* 25:119–124
4. OECD (2001) The application of biotechnology to industrial sustainability, OECD report. OECD, Washington DC
5. Department of Energy (1999) New biocatalysts: essential tools for a sustainable 21st century chemical industry. Department of energy, Washington DC. <http://www.stormingmedia.us/12/1256/A125634.html>. Accessed February 2010
6. Straathof AJJ, Panke S, Schmid A (2002) The production of fine chemical by biotransformations. *Curr Opin Biotechnol* 13:548–556
7. Julsing M, Cornelissen S, Buhler B et al (2008) Heme-iron oxygenases: powerful industrial biocatalysts? *Curr Opin Chem Biol* 12:177–186
8. Alvarado B, Torres E (2009) Recent patents in the use of peroxidases. *Rec Pat Biotechnol* 3:88–102
9. Vazquez-Duhalt R, Quintero Ramirez R (2004) Petroleum biotechnology: development and perspectives. Elsevier Science, Amsterdam
10. Aehle W (2004) Enzymes in industry. Wiley, New York
11. Isi Web of Knowledge <http://isiwebofknowledge.com/>. Accessed February 2010
12. Borole AP, Davison BH (2007) Techno-economic analysis of biocatalytic processes for production of alkene poxides. *Appl Biochem Biotechnol* 136–140:437–449
13. Rozzell JD (1999) *Bioorg Med Chem* 7:2253

Part I
Molecular and Structural Aspects
of Peroxidases

Chapter 2

Molecular Phylogeny of Heme Peroxidases

Marcel Zámocký and Christian Obinger

Contents

2.1	Systematic Classification of Peroxidases	8
2.2	The Peroxidase–Cyclooxygenase Superfamily	9
2.2.1	Bacterial Members: Peroxicins, Peroxidockerins, Primordial Peroxidases	10
2.2.2	Bacterial, Fungal, and Animal Cyclooxygenases	12
2.2.3	Ecdysozoan and Echinozoan Peroxinectins	12
2.2.4	Ecdysozoan and Deuterostomian Peroxidases	12
2.2.5	Chordata Peroxidases	16
2.3	The Peroxidase–Catalase Superfamily	17
2.3.1	Class I: Peroxidases	19
2.3.2	Class II: Manganese, Lignin Peroxidases, and Versatile Peroxidases	23
2.3.3	Class III: Plant Secretory Peroxidases	23
2.4	Di-Heme Peroxidase Family	26
2.5	Dyp-Type Heme Peroxidase Family	26
2.6	Haloperoxidase Family	30
2.7	Conclusions	32
	References	32

Abstract All currently available gene sequences of heme peroxidases can be phylogenetically divided in two superfamilies and three families. In this chapter, the phylogenetics and genomic distribution of each group are presented. Within the peroxidase–cyclooxygenase superfamily, the main evolutionary direction developed peroxidatic heme proteins involved in the innate immune defense system and in biosynthesis of (iodinated) hormones. The peroxidase–catalase superfamily is widely spread mainly among bacteria, fungi, and plants, and particularly in Class I led to the evolution of bifunctional catalase–peroxidases. Its numerous fungal representatives of Class II are involved in carbon recycling via lignin degradation, whereas Class III secretory peroxidases from algae and plants are included in various forms of secondary metabolism. The family of di-heme peroxidases are predominantly bacteria-inducible enzymes; however, a few corresponding genes were also detected in archaeal genomes. Four subfamilies of dyp-type peroxidases capable of degradation of various xenobiotics are abundant mainly among bacteria

and fungi. Heme-haloperoxidase genes are widely spread among sac and club fungi, but corresponding genes were recently found also among oomycetes. All described families herein represent heme peroxidases of broad diversity in structure and function. Our accumulating knowledge about the evolution of various enzymatic functions and physiological roles can be exploited in future directed evolution approaches for engineering peroxidase genes *de novo* for various demands.

2.1 Systematic Classification of Peroxidases

It is already well established that peroxidases are ubiquitous and abundant enzymes in all forms of life. Even in strictly anaerobic bacteria [1, 2], hydroperoxidases play an essential function mainly in signaling and maintaining oxygen tolerance. Primal blue-green algae (i.e., cyanobacterial predecessors) that appeared about 3.2 billion years ago must have been among the first organisms that elaborated mechanisms for the detoxification of partially reduced, reactive oxygen species as a consequence of their oxygen-evolving photosystem [3]. A significant increase in the level of atmospheric oxygen at the beginning of Proterozoic (i.e., between 2.45 and 2.32 billion years ago) [4] necessarily led to further sophisticated evolution of both prokaryotic and eukaryotic antioxidative stress responses, with peroxidases and catalases being among the most prominent enzymatic factors [5]. The genome sequencing projects of last two decades have shed light on the presence of numerous gene orthologs and paralog variants of heme peroxidase gene families in almost all known genomes. The full-length coding sequences (both DNA and amino acids) are the base for any comprehensive higher-level phylogenetic reconstruction, and with increasing number and reliability of sequence data, our evolutionary views are improving. We have attempted to collect all available peroxidase sequences in the PeroxiBase [6] <http://peroxidase.isb-sib.ch>. Out of 6,861 known peroxidase sequences collected in PeroxiBase (January 2010), more than 73% of them code for heme-containing peroxidases. In the majority of cases, heme *b* is the prosthetic group, and its evolutionary highly conserved amino acid surroundings influences its reactivity. All currently known heme-containing peroxidases can be divided in two main superfamilies and three families. Contrary to some recently published opinions [7], the in-depth phylogenetic analysis clearly reveals that almost all of these heme peroxidase coding genes have very ancient prokaryotic origins probably dating back to the rise of atmospheric oxygen. All (super)families described below represent their own peculiar mode of evolution in maintaining and regulating the heme reactivity. The classical division into plant and animal heme peroxidases nowadays appears to be obsolescent and not appropriate. There are numerous examples of interkingdom distribution for members of most herein described gene families. It is therefore more suitable to name the appropriate groupings according to peculiar reaction specificity in each observed (super)family. As a special case of hydroperoxidases, heme-containing catalases represent a very abundant gene family [8, 9], but they will not be analyzed in this contribution as they dominantly exhibit catalatic

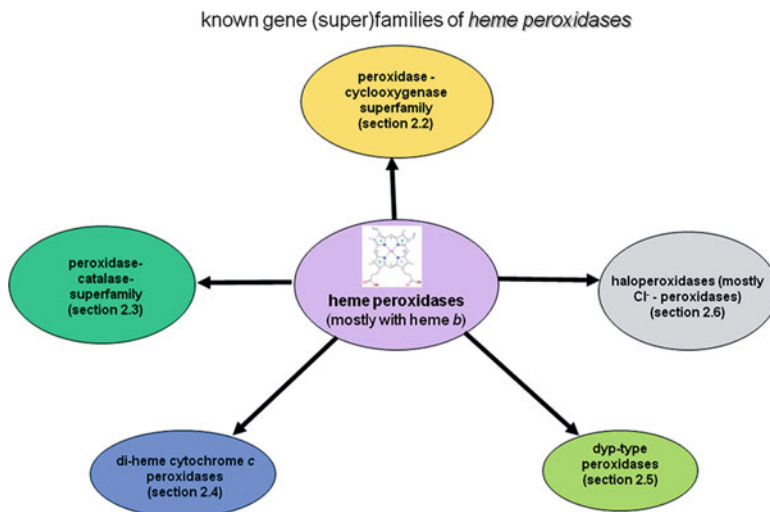


Fig. 2.1 Overview of all heme peroxidase (super)families

activity and their peroxidatic reaction mode is only of marginal importance. Here, first, we present an overview of the two ubiquitous heme peroxidase superfamilies, followed by the description of the phylogeny of three less abundant but physiologically and biotechnologically important heme peroxidase families. In Fig. 2.1, a brief overview of all types of heme peroxidases addressed in this chapter is presented.

2.2 The Peroxidase–Cyclooxygenase Superfamily

The peroxidase–cyclooxygenase superfamily, named after its most typical activity profiles [10], represents one of the two main evolutionary streams of heme peroxidase development in the living world. Currently, there are 371 sequences of peroxidases belonging to this superfamily that are collected in PeroxiBase (January 2010), but many further sequences are expected to be added from recent sequencing projects. In the corresponding Pfam database at <http://www.ebi.ac.uk/interpro/>, there are already over 820 entries for PF03098 or IPR002007, describing this superfamily. The PROSITE profile “peroxidase_3” counts up to 807 protein sequences matching these criteria. The importance of the peroxidase–cyclooxygenase superfamily is underlined by the fact that its numerous representatives are involved in the innate immune system, e.g., [11]. This is true not for the mammalian peroxidases alone, which have undergone the most complicated evolutionary step. Even several peroxidases from the bacterial predecessor clades [12] are supposed to be involved in unspecific defense mechanisms. The overall phylogeny is outlined in Fig. 2.2. Seven main clades representing distinct subfamilies are well segregated in the reconstructed unrooted phylogenetic tree (with 160 full sequences involved

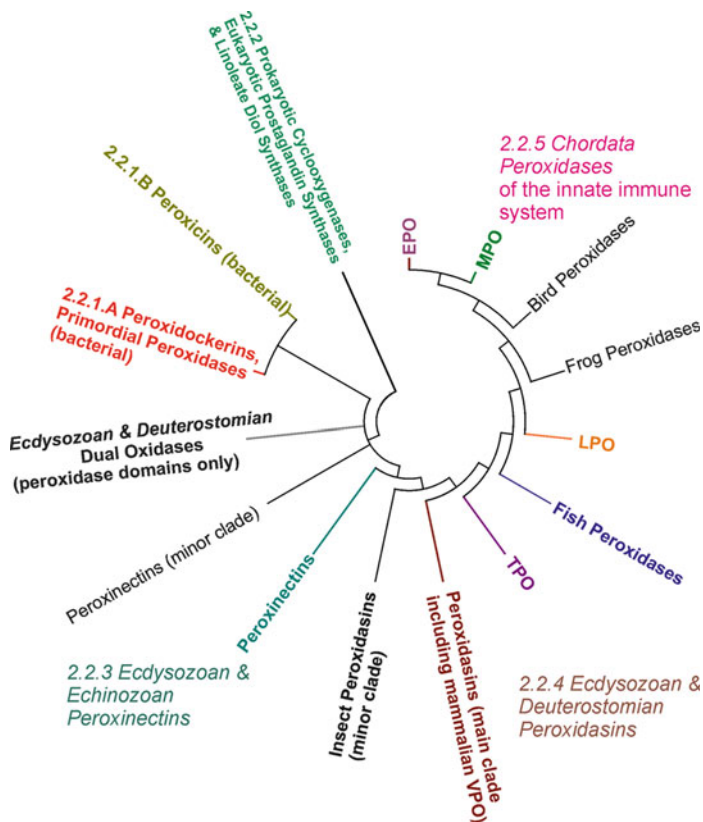


Fig. 2.2 Phylogenetic relationships within the peroxidase–cyclooxygenase superfamily. This *circle tree* was obtained in MEGA package [13] after compressing all resolved branches from 160 full sequences of this superfamily to main clades. Seven subfamilies [10] are clearly discernible

in the analysis). From the occurrence of multiple paralogs of otherwise conserved peroxidase genes in addition to the rare occurrence of pseudogenes, it was concluded that this superfamily obeys the rules of birth-and-death model of multigene family evolution [10, 14]. Details for each of the seven subfamilies with the exception of dual oxidases will be presented in the following subchapters. In dual oxidases, the peroxidase domain has lost its functional residues, and its physiological role remains elusive [15].

2.2.1 Bacterial Members: Peroxicins, Peroxidockerins, Primordial Peroxidases

Bacterial members represent the most ancient forms of the peroxidase–cyclooxygenase superfamily that probably remained without significant changes during the

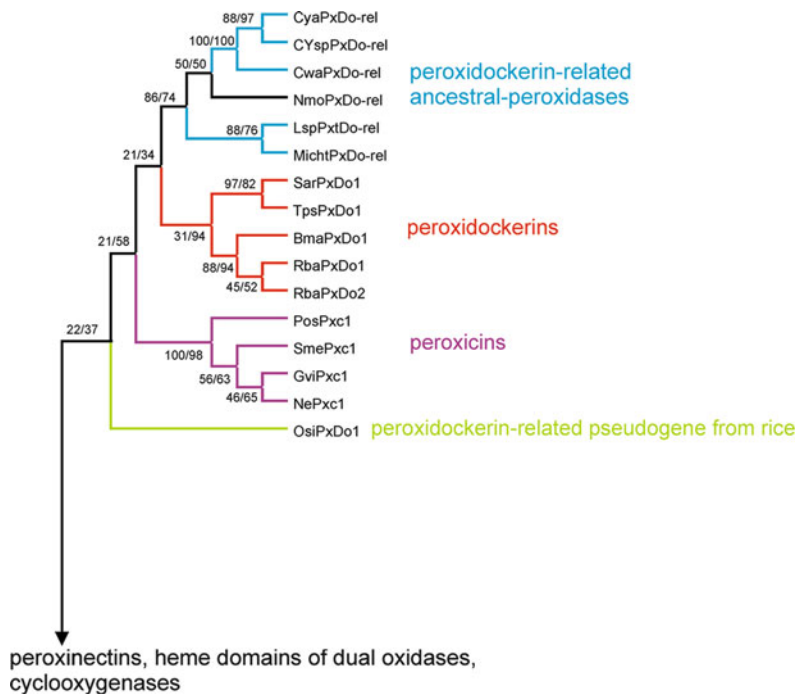


Fig. 2.3 Phylogeny of bacterial representatives of the peroxidase–cyclooxygenase superfamily. The reconstructed tree obtained from the NJ-method of the MEGA package [13] with JTT matrix and 1,000 bootstrap replications is presented. A similar tree was obtained also with ProML-method of the PHYLIP package [16] with 100 bootstraps. *Numbers* in the nodes indicate bootstrap values for NJ and ProML method, respectively. *Abbreviations* of protein names correspond to PeroxiBase

long evolution of this superfamily [3]. There are currently 30 complete sequences entered in PeroxiBase. Open reading frames of primordial peroxidases, containing only the peroxidase domain, can be found mainly in cyanobacteria and also to some extent in proteobacteria. Peroxidockerins represent more complicated gene structures with an additional N-terminal dockerin domain containing dockerin type I repeats with predicted transmembrane helices [10]. Peroxicins are multidomain peroxidases that possess a short N-terminal peroxidase motif besides the normal-length peroxidase domain as well as C-terminal hemolysin-like calcium-binding repeats [12]. These very long C-terminal domains might be involved in defense mechanism against competitor bacteria. Figure 2.3 outlines the reconstructed phylogeny of peroxicins, peroxidockerins, and ancestral peroxidases related to them. The single-domain cyanobacterial genes might represent a molecular fossil of the ancestral peroxidase gene of this superfamily [3].

2.2.2 Bacterial, Fungal, and Animal Cyclooxygenases

Cyclooxygenases diverged rather early from the remaining peroxidase genes of the peroxidase–cyclooxygenase superfamily [10]. This is underlined by the fact that corresponding genes can be found in various organisms ranging from bacteria and fungi to mammals. There are currently 74 sequences entered in PeroxiBase. The eukaryotic genes exhibit a peculiar structure consisting of a N-terminal signal peptide followed by an epidermal growth factor domain, a membrane-binding domain, and the conserved globular peroxidase domain. Two main clades of this subfamily are discernible (Fig. 2.4). In the first subfamily, an evolutionary connection between bacterial cyclooxygenases towards human prostaglandin synthases can be followed. Also the fungal linoleate diol synthases participating in linoleic acid metabolism are located in this clade as a separate branch. In the second main clade, further cyclooxygenase paralogs and alpha dioxygenases are located. Corresponding genes are abundant mainly among fungal and plant genomes, but there are also predecessors among bacterial genes. The clade of typical plant alpha-dioxygenase genes within this subfamily clearly demonstrates that it is not appropriate to name such superfamily as “animal peroxidase” superfamily, although the nomenclature is still present in some databases.

2.2.3 Ecdysozoan and Echinozoan Peroxinectins

The very abundant subfamily of peroxinectins is mainly spread among Ecdysozoa and Echinozoa, i.e., among various arthropods and nematodes. Up to 40 sequences can be found in PeroxiBase. Originally, peroxinectin from crayfish was described as a cell adhesion protein with a peroxidase domain and an integrin-binding motif [17]. Two main clades are visible within the phylogenetic distribution of this subfamily (Fig. 2.5). In the first clade, nematode and squid peroxinectins are dominating, whereas in the second main clade, various gene duplicates of insect and crustacean peroxinectins are located. The fact that until now no vertebrate peroxinectin gene was found can be understood as an impasse of natural evolution of this subfamily within the whole superfamily [10]. Restricted gene variant distribution further supports the proposed evolutionary scheme based on the birth and death model of gene family evolution [14].

2.2.4 Ecdysozoan and Deuterostomian Peroxidasins

Peroxidasins (in humans also designated vascular peroxidases [18]) represent peculiar multidomain peroxidases. In PeroxiBase, 37 sequences are described. During later steps of evolution, the peroxidase domain was fused with immunoglobulin

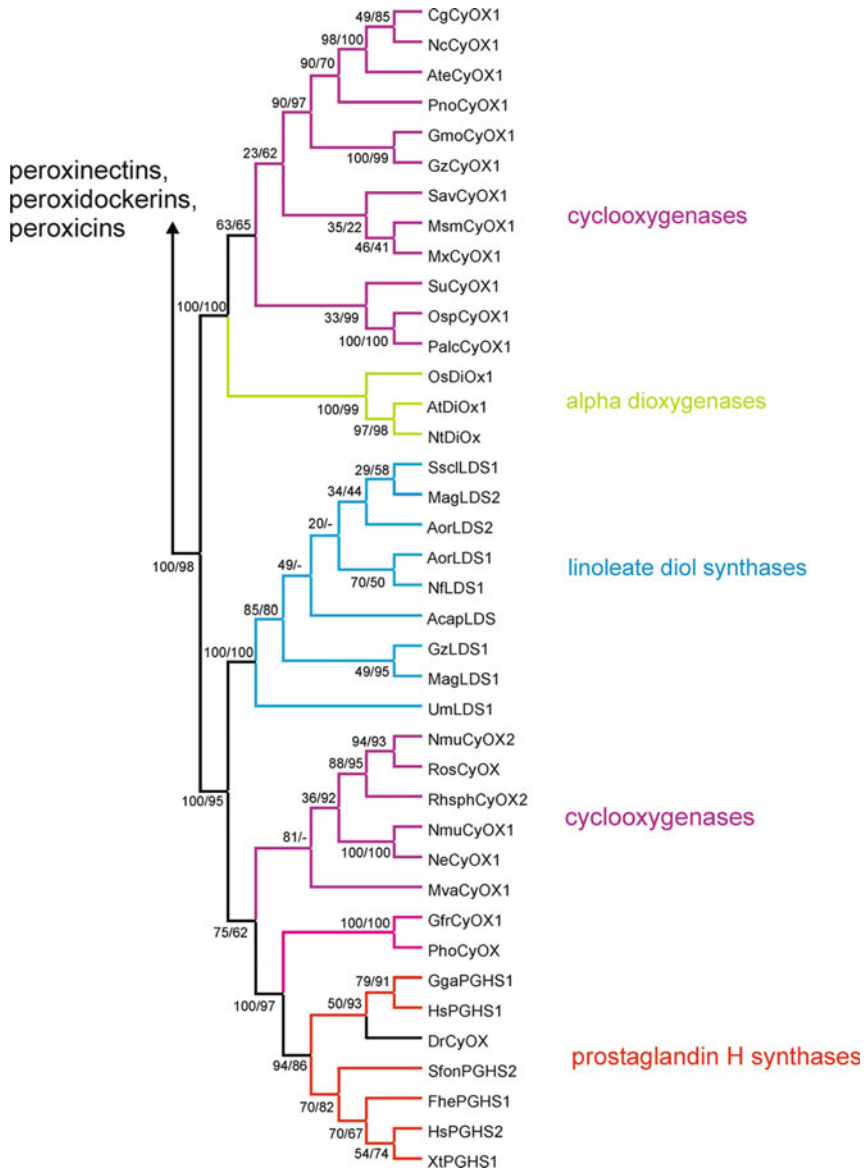


Fig. 2.4 Phylogeny of cyclooxygenases. The reconstructed tree obtained from the NJ-method [13] with JTT matrix and 1,000 bootstrap replications is presented. A similar tree was obtained using the ProML-method [16] and 100 bootstraps. *Numbers* in the nodes indicate bootstrap values obtained for NJ and ProML method, respectively. *Abbreviations* of protein names correspond to PeroxiBase

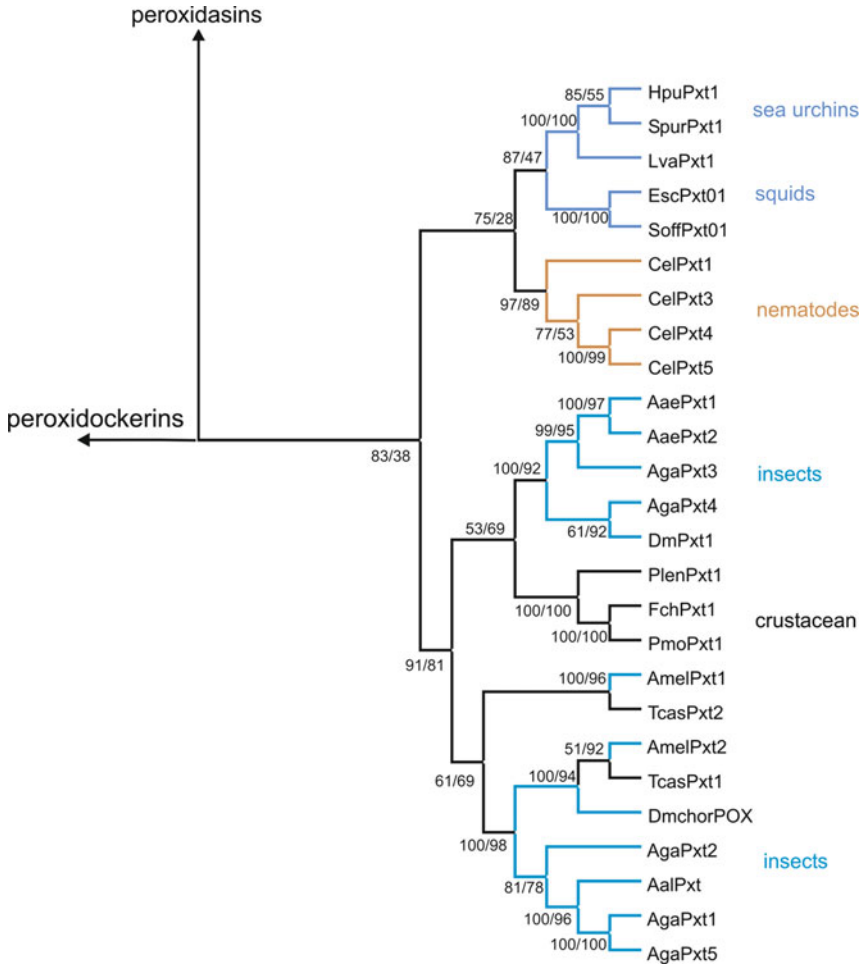


Fig. 2.5 Phylogeny of peroxinectins. The reconstructed tree obtained from the NJ-method [13] with JTT matrix and 1,000 bootstrap replications is presented. A nearly identical tree was obtained also with the ProML method [16] with 100 bootstraps. *Numbers* in the nodes indicate bootstrap values for NJ and ProML method, respectively. *Abbreviations* of protein names correspond to PeroxiBase

domains, suggesting an essential role of this subfamily in the innate immune system. Peroxidases are found both in invertebrates (even in nematodes) and vertebrates including mammals. The first peroxidase was described in *Drosophila* as a multi-domain protein combining the peroxidase domain with extracellular matrix motifs [19]. In humans, these proteins were detected to be most abundant in heart and vascular wall [18]. In PeroxiBase, 37 sequences are deposited (January 2010). A typical peroxidase gene encodes an N-terminal signal peptide followed by leucine-rich repeats (LRR), immunoglobulin domains, the peroxidase domain, and

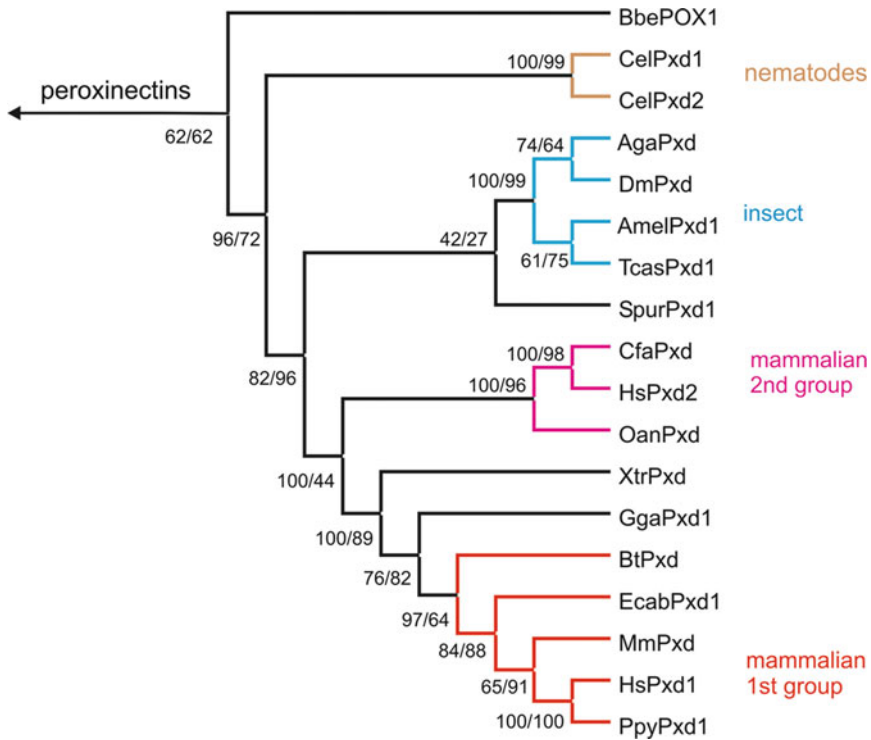


Fig. 2.6 Phylogeny of peroxidases. The reconstructed tree obtained from the NJ-method of the MEGA package [13] is presented. A nearly identical tree was obtained also from ProML method of the PHYLIP package [16]. Numbers in the nodes indicate bootstrap values for NJ and ML methods, respectively. Abbreviations of protein names correspond to PeroxiBase

finally a von Willebrand factor C type (VWC) domain [18]. The LRR regions frequently mediate protein–protein and protein–lipid interactions [20]. The repeated immunoglobulin domains are of the C-2-type. They are closely related to extracellular domains in Class I and Class II major histocompatibility complexes and are supposed to be involved in vascular cell adhesion molecule by binding to integrins [18]. The proposed physiological role of the VWC domain involved in specific protein–protein interactions is mainly in embryonic development and tissue specification [21], but for peroxidases, this function has not yet been proven experimentally. In the presented part of the evolutionary tree (Fig. 2.6), all analyzed peroxidase subfamily members form a single clade with a frequent occurrence of gene duplicates within ecdysozoan and deuterostomian genomes. In mammals, there are apparently one or several peroxidase paralogs (cf. with Sect. 2.2.5) participating in the innate immunity. The phylogenetic position of *Branchiostoma belcheri* (invertebrate) peroxidase is very interesting. It is located at the root of this subfamily and is also the closest homolog to thyroid peroxidases.

2.2.5 Chordata Peroxidases

The sequences coding for well-known and intensively investigated mammalian representatives, myeloperoxidase (MPO), eosinophil peroxidase (EPO), lactoperoxidase (LPO), and thyroid peroxidase (TPO), were phylogenetically analyzed in detail recently [10, 22]. The reconstructed unrooted tree that focused on all available chordata sequences is presented in Fig. 2.7. In the statistically highly supported output, the division in two gene duplicated twin-clades of EPO and MPO with a closely related clade of LPO and more distantly related clade of TPO was observed and also the sites of positive Darwinian selection were elucidated [22]. The phylogenetic distribution of these four monophyletic clades is in accordance with the proposed physiological function: whereas MPO, EPO, and LPO members play key roles in antimicrobial and innate immune responses of mammals [23, 24], TPO is essential in thyroid hormone biosynthesis [25]. The amino acid positions of positive selection detected separately for each clade within the highly evolved peroxidase domain have physiological implications that most likely contributed to the functional diversity within this subfamily. Variants in most of the observed positions are associated with such diverse diseases such as asthma, Alzheimer's disease, and inflammatory vascular disease. It has to be noted that even in the more

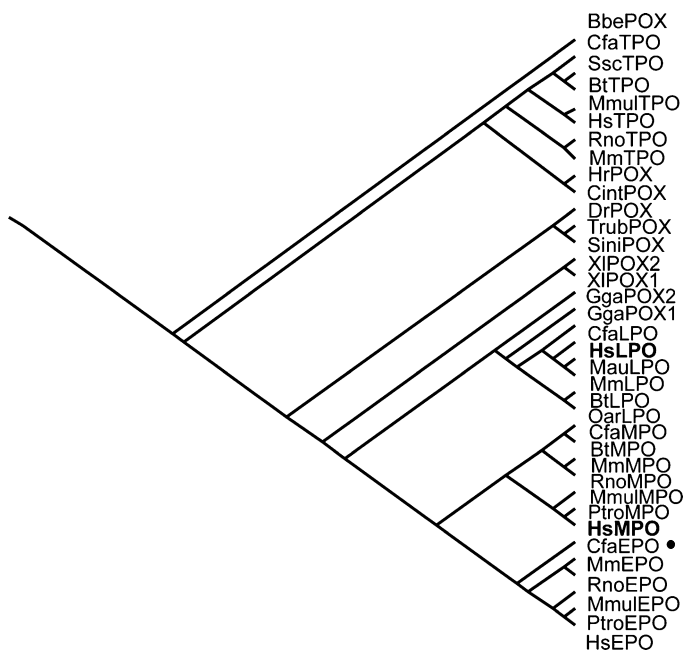


Fig. 2.7 Detail of the reconstructed phylogenetic tree showing the subfamily of vertebrate peroxidases including the mammalian enzymes myeloperoxidase (MPO), eosinophil peroxidase (EPO), lactoperoxidase (LPO), and thyroid peroxidase (TPO). Reproduced from [10] with the permission of John Wiley and Sons (License Nr. 2326000554179)

complex evolutionary tree of this superfamily [10], nonmammalian members are distributed between the well-resolved clades of mammalian peroxidases (cf. Figs. 2.2 and 2.7). For example, between the clades of MPO–EPO and LPO, there are minor clades of bird and amphibian peroxidases of so far unknown physiological role. Very interestingly, XIPOX1 (a frog peroxidase) has been reported to possess a ribonuclease activity [26], thus being involved in the destabilization of albumin mRNA. Furthermore, between the LPO and TPO clades, a minor clade of fish peroxidases is located (cf. Fig. 2.2) also with so far unknown physiological role. In some databases, corresponding (yet putative) proteins are classified as myeloperoxidases (e.g., the Zebrafish sequence), but the sequence analysis reveals that they diverge from mammalian myeloperoxidases in critical amino acid residues [10]. All presented members of this subfamily demonstrate a high level of gene variability and speciation up to modern day mammals. However, future research that mostly focus on the nonmammalian members of this subfamily is of essential importance not only for basic science but also for biotechnological applications.

2.3 The Peroxidase–Catalase Superfamily

This is the currently best known and most intensively studied superfamily of heme peroxidases. Its representatives being among the oldest peroxidases known, e.g., horseradish peroxidase, have been systematically studied since 1930s [27]. In 1940s, yeast cytochrome *c* peroxidase was discovered, but the corresponding sequence was available only in 1982 [28]. In 1980s, the advent of intensively studied fungal lignin and manganese peroxidases occurred with plenty of newly available sequences. In parallel, catalase–peroxidase and ascorbate peroxidases-focused research also brought numerous new representatives. Currently, up to 4,020 protein sequences match the criteria for this superfamily in IPR002016 (PF00141). The first systematic classification of accumulated sequences and structures was performed by Welinder and divided all members of this superfamily in three distinct classes [29]. Class I was identified as containing mainly yeast cytochrome *c* peroxidase, ascorbate peroxidases, and bacterial catalase–peroxidases. Class II is dominated by fungal lignin and manganese peroxidases. Class III is represented by secretory plant peroxidases related to horseradish peroxidase. The whole superfamily was thus first named according to the origin of included members as the superfamily of plant, fungal, and bacterial heme peroxidases. It was shown recently that few representatives occur also in the genomes of *Hydra viridis* [30] and related species belonging to the phylum of *Cnidaria* that is phylogenetically located at the root of animal kingdom [31]. Therefore, it would be more appropriate to name this superfamily as peroxidase–catalase superfamily, i.e., according to main enzymatic activities performed by its members. Such name is similar to the nomenclature used for other families and superfamilies (cf. Sect. 2.2 or Sects. 2.4–2.6) In Peroxi-Base, more than 4,100 sequences of its members can be found (January 2010).

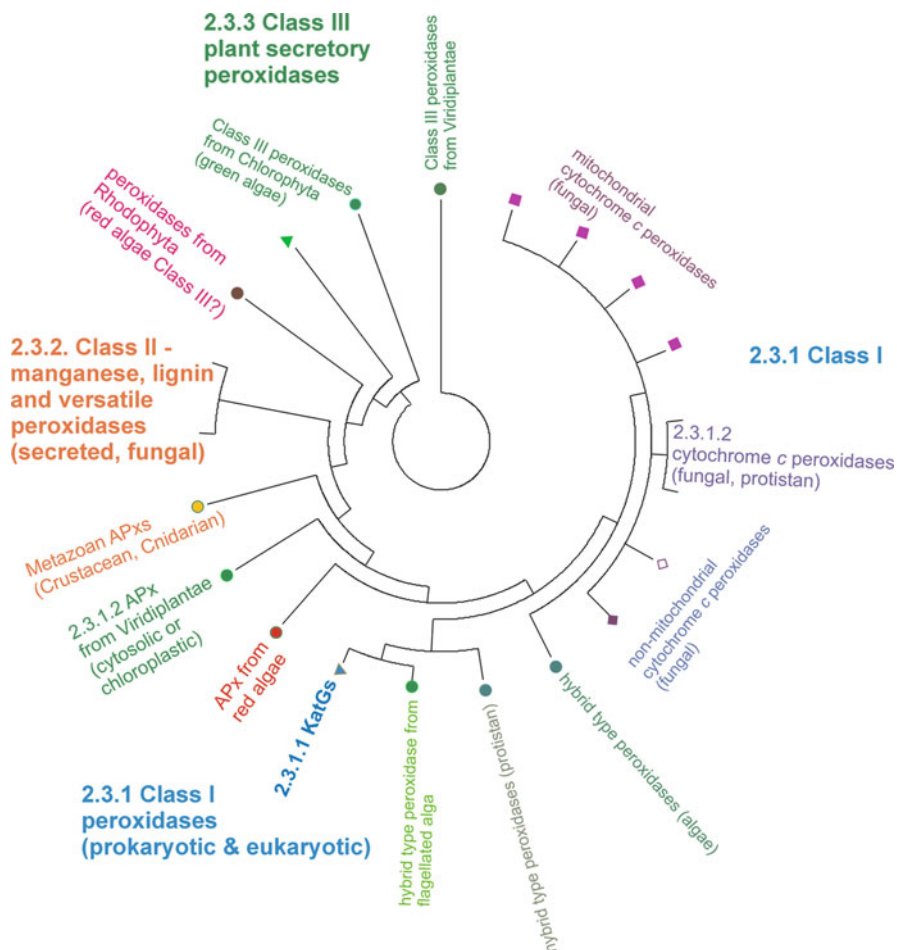


Fig. 2.8 Phylogenetic relationships among heme peroxidases belonging to classes I, II, and III of the peroxidase–catalase superfamily. This circle tree was obtained in MEGA package [13] after compressing all resolved branches from 123 full sequences of this superfamily to main clades. All three classes originally defined in [29] are clearly discernible

The molecular phylogeny was already investigated from various aspects. In general, it was proposed that both Class II and Class III evolved from a common ancestor [32] and (Fig. 2.8). As there is no prokaryotic sequence in the neighborhood of the corresponding phylogenetic node [32], it is very probable that Class II and Class III diverged in already formed ancestral eukaryotic genome. Such a predecessor gene may have diverged after an earlier, very distant gene duplication from ancestral bacterial Class I representative [33]. Details of this event still need to be resolved. Nevertheless, Class II secretory fungal peroxidases and Class III secretory plant peroxidases evolved in parallel after their early division for a long time period, leading to two highly evolved groups of genes within this superfamily.

2.3.1 Class I: Peroxidases

2.3.1.1 Catalase–Peroxidases (KatGs)

It is reasonable to suppose that bifunctionality was at the root of the peroxidase–catalase superfamily since it has been argued that catalytic promiscuity frequently occurred in the evolution of protein superfamilies [34]. Catalase–peroxidases are physiologically active primarily as catalases and their peroxidase functionality *in vivo* is still under discussion [3]. Currently, 366 peroxidases deposited in PeroxiBase match the criteria for designation as catalase–peroxidase. They are phylogenetically distributed among archae (8), eubacteria (305, including also facultative anaerobes), fungi (42), and protists (11). KatG genes reveal a peculiar gene structure [35, 36]. In all sequenced *katG* genes, a tandem gene duplication with different function for each of the duplicated domains is obvious. This gene structure is unique not only within the peroxidase–catalase superfamily but also among all known heme peroxidase families. In the first attempt to reconstruct the evolution of this family within the whole Class I, the tandem gene duplication of *katG* was taken into account [37]. However, the N- and C-terminal domains revealed slight differences in their phylogenetic distribution possibly due to differences in mutational rates. It was proposed that the tandem duplication occurred after the earlier segregation between KatG and cytochrome *c* peroxidase and ascorbate peroxidase branches. Further phylogenetic analysis with 152 full sequences reported recently [38] gave a more detailed insight, although the distribution among the microorganisms is influenced by the fact that *katG* genes are not an essential equipment of the genome and their role can be eventually adopted also with alternative loci (e.g., *katE* encoding typical catalase or genes encoding non heme peroxidases). The most interesting aspect of this family evolution is the occurrence of several lateral gene transfers (LGT). The distribution of known *katG* sequences with most apparent LGT from bacteroidetes towards sac fungi in an unrooted tree is evident from Fig. 2.9. Two basal paralog clades were segregated at the beginning of *katG* gene evolution. In most bacteria, the presence of these two paralogs is rare, but the minor clade 2 contains besides proteobacterial also mostly (but not all) archaean representatives. The main clade 1 contains *katG* genes from almost all bacterial phyla. Mainly among proteobacteria, numerous closely related orthologs are present. Cyanobacterial catalase–peroxidases are located at the root of this clade and also the fungal branch has its origin in later steps of this main clade evolution. The phylogenetic distribution clearly suggests that fungal catalase–peroxidases were segregated from bacteroidetes ancestor via a LGT towards ancient fungi [39]. Further support for this rare LGT event came from differences in G+C content (gene vs. whole genome) and from rare occurrence of introns within fungal *katG* genes. The future research within KatGs with potential biotechnological applications will be probably focused mainly on the elucidation of structure and function of eukaryotic catalase–peroxidases. Besides detection of KatG as a virulence factor in human fungal pathogens such as *Penicillium marneffe*

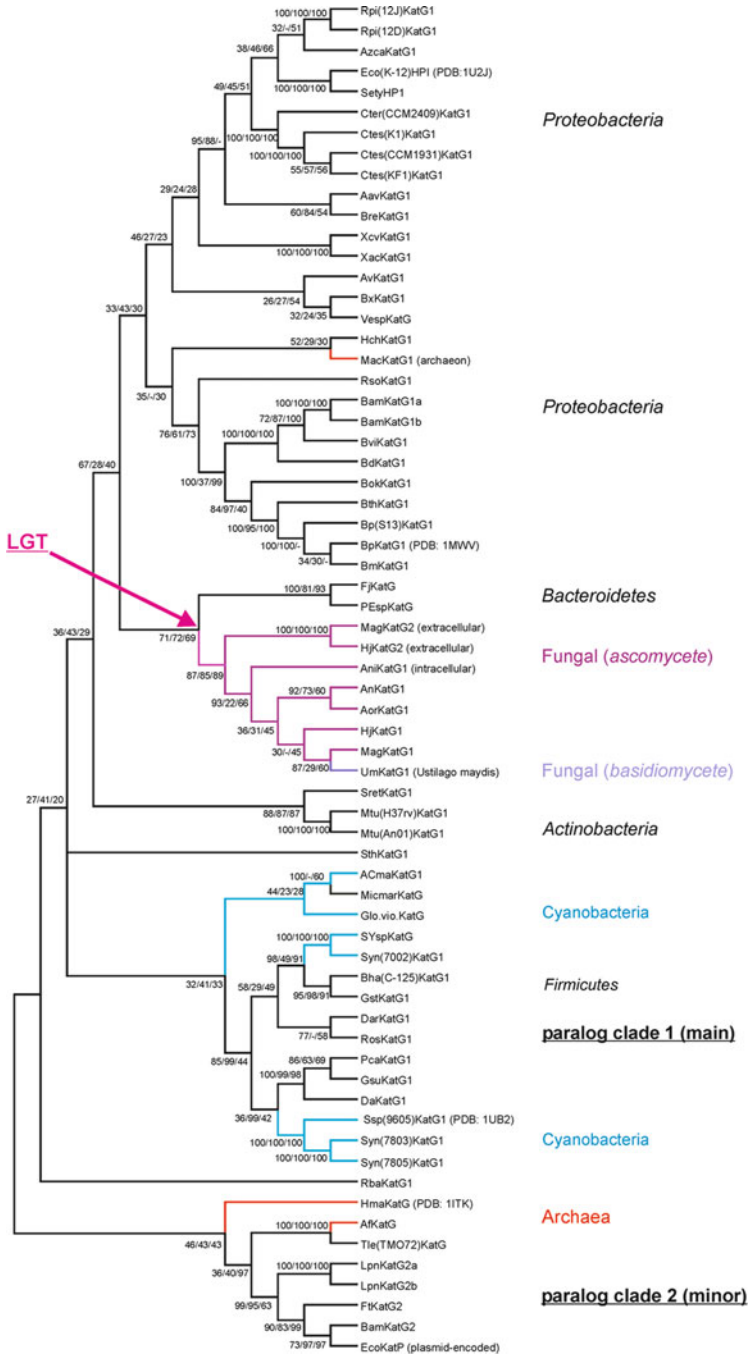


Fig. 2.9 Phylogeny of selected 66 KatGs for the demonstration of the presence of two paralog clades separated very early as well as a lateral gene transfer (LGT) from bacteria to fungi within this gene family. The reconstructed tree obtained with the NJ-method [13] is presented. Nearly

[40], mainly the elucidation of potential role of catalase–peroxidases in phytopathogenic fungi might have a significance for the preservation of culture crops, particularly against attacks of *Gibberella* sp. [41] and *Magnaporthe grisea* [42], two important phytopathogens.

2.3.1.2 Ascorbate Peroxidases, Cytochrome *c* Peroxidases, and Their Putative Hybrid Types

Ascorbate peroxidases (APx) and cytochrome *c* peroxidases (CcP, i.e., single heme cytochrome *c* peroxidase) segregated very early from *katG* genes [33, 37], but the details of this event and the process of gene speciation towards different substrate specificities remain unclear. There are still missing important intermediate sequences and corresponding proteins from, e.g., primitive fungi and protists that could clarify this problem. In PeroxiBase, already 409 ascorbate peroxidases are included (January 2010), but approximately one third of them are only partial sequences that are thus not suitable for higher-level phylogenetic analysis. These partial sequences originate from EST-database and shall indicate their expression profiles in various growth and developmental phases. Soon after its development, the clade of APxs segregated from that of CcPs. All known ascorbate peroxidases are divided into three types according to their cellular location [33]. Chloroplastic APxs diverged in the earlier phase, whereas cytosolic and peroxisomal variants evolved together and were separated only in the later stage of evolution. Of particular interest is the sequence analysis of ascorbate peroxidases in chloroplastic protists, which acquired chloroplasts by endosymbiosis [43].

Detailed phylogeny of fungal cytochrome *c* peroxidases with the inclusion of novel, previously not analyzed sequences mainly from recently finished sequencing projects was recently presented [44]. In Fig. 2.10, an update with 88 full-length sequences (out of 108 known) including also nonfungal protist sequences is depicted. There are three distinct subfamilies that differ in subcellular location. In subfamily I, no signal sequence was detected, suggesting that these are cytosolic CcPs. Subfamily II is the largest one with signal sequence targeting them to mitochondria. The well-known *S. cerevisiae* CcP belongs in this branch. Enzymes from subfamily III, probably the most ancient one, can even possess targeting signals not solely for mitochondria. According to recent data mining (M. Zámocký, unpublished work), there exists a minor but important group of hybrid type APx–CcP sequences in fungal and protistan genomes (Fig. 2.8). In PeroxiBase, 36 sequences of this type are entered (January 2010). These completely unknown peroxidases might represent the missing proteins for the complex phylogenetic reconstruction of this family. Investigation of hybrid type APx–CcP can give novel

←

Fig. 2.9 (*Continued*) identical trees were obtained using the ProML- [16] and the MP-methods [13]. Numbers in the nodes indicate bootstrap values for NJ/MP/ML methods, respectively. Arrow indicates the occurrence of LGT from *Bacteroidetes* towards sac fungi. Abbreviations of protein names correspond to PeroxiBase

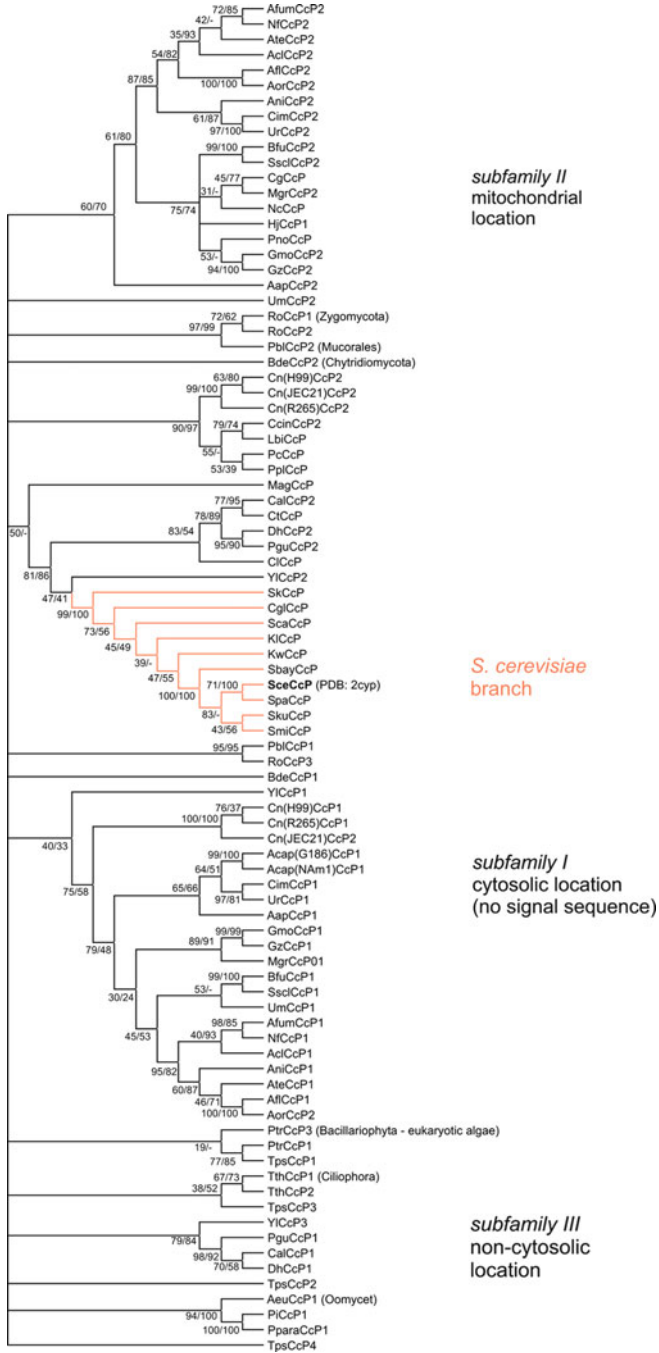


Fig. 2.10 Phylogeny of 88 full sequences coding for fungal and protistan cytochrome *c* peroxidases (CcP). The reconstructed tree obtained from the NJ-method of the MEGA package [13] is presented. A nearly identical tree was obtained with the ProML method of the PHYLIP

aspects to our understanding of substrate specificity of Class I heme peroxidases with yet hardly predictable biotechnological impact.

2.3.2 *Class II: Manganese, Lignin Peroxidases, and Versatile Peroxidases*

Phylogenetic relationships of Class II peroxidases have been already reconstructed in a comprehensive way [32]. Extracellular Class II heme peroxidases are currently known only in the kingdom of fungi (see PeroxiBase for details) and are essentially involved, through various mechanisms, in lignin degradation [45]. There are three main evolutionary groups (i.e., subfamilies) secreted by white rot basidiomycetes: manganese peroxidases (MnP), lignin peroxidases (LiP), and versatile peroxidases (VP). These subfamilies apparently present a gene speciation within one fungal paralog clade. This paralog clade was overwhelmed by frequent gene duplications giving rise to multiple gene variants (e.g., up to eight in *P. chrysosporium*) of both lignin and manganese peroxidases [46]. The same is true also for versatile peroxidases, but the duplication frequency appears to be lower than for LiP [47]. Phylogenetic analysis of 90 Class II peroxidase sequences revealed that this class is a monophyletic group [32] (Fig. 2.11). It was suggested, with good statistical support, that LiPs, VPs, and the classical MnPs from Agaricomycetes are derived from ancient peroxidases with a manganese-dependent activity. Besides LiPs, MnPs, and VPs, there are evolutionary very interesting types of Class II peroxidases that do not fall in either of these distinct lignin degrading groupings. These so called “basal peroxidases” [32] include also sequences from *Coprinopsis cinerea* and *Antrodia cinnamomea* – both fungi that do not produce the white rot of wood. Such “basal peroxidases,” surprisingly closely related with ascomycetous Class II-peroxidase representatives, may have retained some properties of the ancestral Class II forms and are thus best candidates for applications like protein engineering via directed evolution. It will be intriguing to compare the parallel evolutionary history of lignin-forming plants with those of lignin degrading fungi including also their immediate predecessors to get valuable hints about plant and fungi interactions and the role of Class II heme peroxidases in this process.

2.3.3 *Class III: Plant Secretory Peroxidases*

Heme peroxidases of Class III are, in principle, plant-secreted glycoproteins involved in cell elongation, cell wall construction, and differentiation, as well as



package [16]. Numbers in the nodes indicate bootstrap values for NJ and ML methods, respectively. Abbreviations of protein names correspond to PeroxiBase

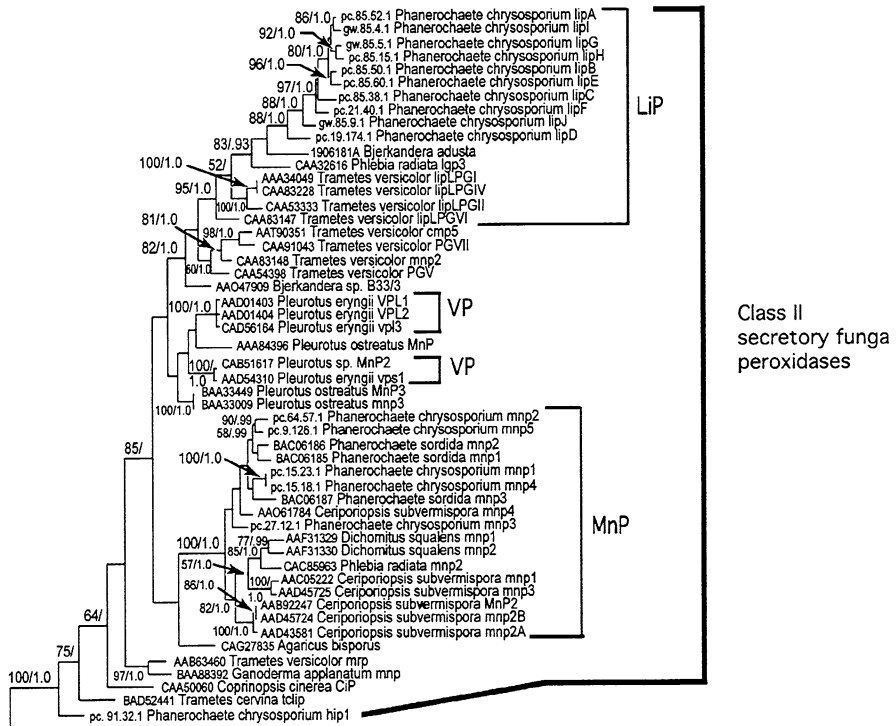


Fig. 2.11 Phylogeny of Class II of the peroxidase–catalase superfamily. Sequences coding for secretory fungal peroxidases: lignin peroxidase (LiP), manganese peroxidase (MnP), and versatile peroxidase (VP) were used for this reconstruction. One of nine equally parsimonious trees is presented. Bootstrap values are indicated before slash, and Bayesian posterior probability values are indicated after the slash. With kind permission from Springer Science & Business Media: Morgenstern et al. [32], Fig. 2

in the defense against various plant pathogens. They are encoded by a surprisingly large number of paralogous genes, but in most genomes of Angiosperm plants, the peroxidase genes of this superfamily (i.e., Class III but also Class I) have additionally undergone numerous gene duplications [48] in a relative recent evolutionary phase. For example, in *Arabidopsis thaliana*, which has served for long time as “model plant,” up to 73 distinct Class III peroxidase genes were detected [49], for *Medicago truncatula* up to 101 Class III genes, for *Oryza sativa* even up to 138 various Class III sequences were entered, and in *Zea mays*, this number reaches a maximum of 151 in the complete genome. The total number of Class III genes entered in PeroxiBase exceeds already 3,000 (January 2010) thus representing over 73% of all entered superfamily members. Monocotyledon peroxidases differ slightly in their sequence fingerprints from Eudicotyledons counterparts [50], but the majority of the *prx* genes is highly conserved throughout the whole Class III. The observed overall sequence similarities lead to the classification of all available

2.4 Di-Heme Peroxidase Family

This average-sized peroxidase family (IPR004852 or PF03150) is present predominantly among various bacteria, but a few archaeal members have also been found recently. So far no eukaryotic representatives were found. It is probable that corresponding genes evolved very early but, compared with other lineages, did not reach their universal coverage. This family is unique in containing two heme groups in one protein moiety thus allowing studies of intramolecular electron transfers [53]. Di-heme cytochrome *c* peroxidases (DiHCcP) reduce hydrogen peroxide to water using cytochrome *c* or cupredoxin. All investigated representatives of this family contain heme *c* prosthetic groups (unlike fungal CcPs) that are covalently linked to the polypeptide chain. DiHCcPs comprise two distinct domains: the electron transferring (E) heme domain and the peroxidatic (P) heme domain with a calcium-binding site at the domain interface [54]. This gene family also includes eubacterial methylamine utilization proteins (MauG), whose significant similarity to DiHCcP was detected earlier [55]. In the case of *Paracoccus denitrificans*, the purified heme protein reveals only marginal peroxidase activity. It appears that MauGs are, in principle, heme-oxygenases that play an important role in the synthesis of a tryptophan tryptophylquinone cofactor for the methylamine dehydrogenase [56]. Thus, it is reasonable to conclude that a massive gene conversion must have occurred during the evolution in this particular clade. Selected DiHCcP representatives were studied from various physiological aspects and were shown to be inducible in low oxygen conditions under the control of FNR protein [57]. PeroxiBase currently covers 110 bacterial DiHCcP sequences, whereas in PFAM over 900 mostly putative sequences are registered. The detailed phylogeny from PeroxiBase entries was reconstructed and is presented in Fig. 2.13. From this output, it is obvious that di-heme cytochrome *c* peroxidases are dominantly spread among all classes of proteobacteria, and in most of them, various orthologs exist. Only a minor clade within *Chlorobia* genomes exists and the two archaean representatives probably originated via lateral gene transfer from proteobacterial genomes. The phylogenetic position of the sole cyanobacterial DiHCcP gene is not highly supported, but it has apparently a common evolutionary history with the *Spirochaetes* representatives. The origin of this peroxidase family appears to be among ancient proteobacteria.

2.5 Dyp-Type Heme Peroxidase Family

Originally named “dye-decolorizing peroxidases,” this protein family is spread among bacteria and fungi with so far ~800 deposited sequences [7]. No archaeal representative could be unequivocally detected so far, although, recently, protein sequences from archaea were reported to belong to the same PFAM family [58] classified as IPR006314 or PF04261. It remains unclear whether the corresponding putative proteins possess all peroxidase domain features. Only one putative eukaryotic gene of nonfungal origin was found in the genome of a slime mold.

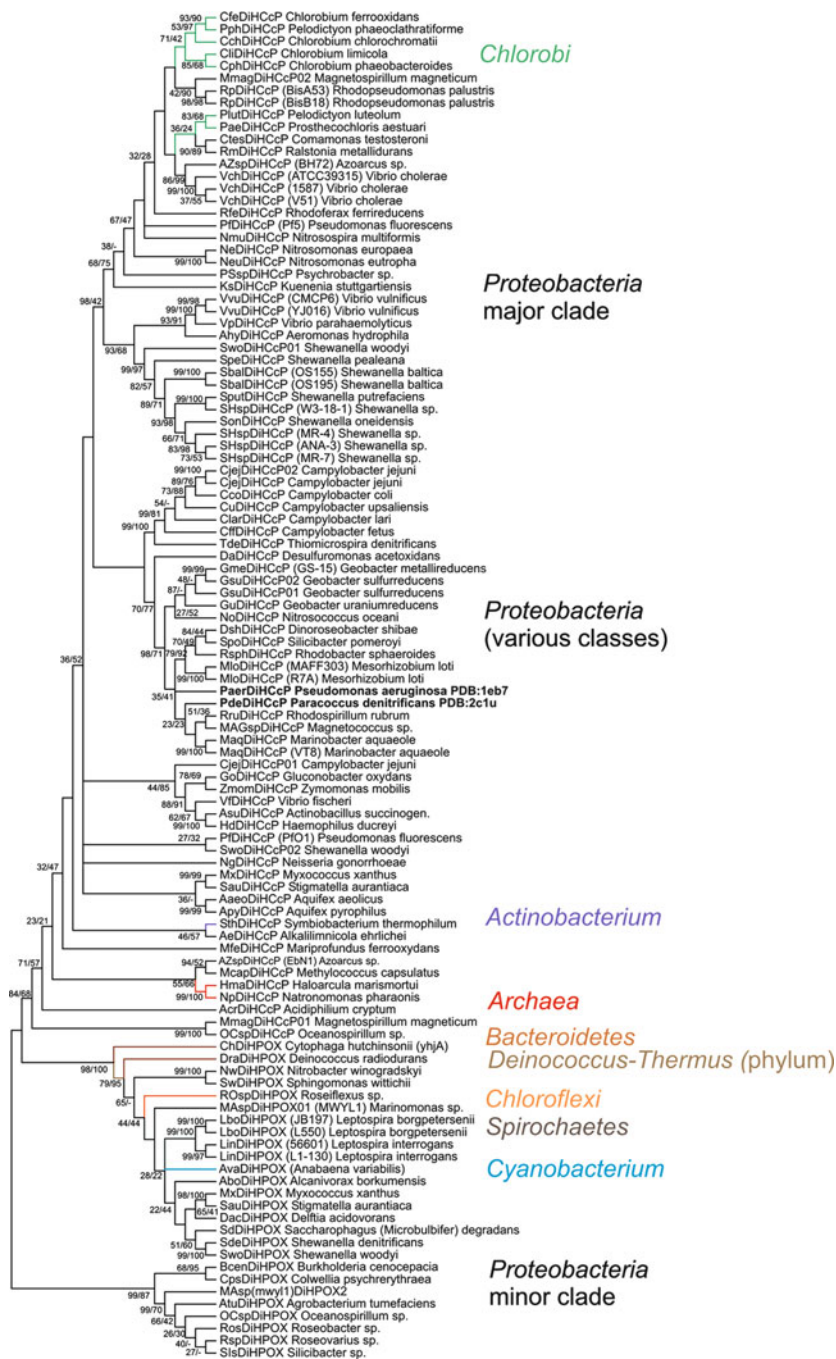


Fig. 2.13 Phylogeny of bacterial di-heme peroxidases. The reconstructed tree obtained from the NJ method of the MEGA package [13] is presented. A very similar tree was obtained also from

Thus apparently, the distribution of the dyp-type peroxidase family is not as universal as demonstrated for the two heme peroxidase superfamilies presented above. In biotechnology, mainly the basidiomycete Dyp-members became popular for their ability to degrade various synthetic disperse dyes, but their physiological role and mainly their physiological electron donors remain obscure and were not addressed by the authors investigating them. It was apparent after their first purifications, without sequence analysis, that they differ significantly in their substrate specificity from known Class II peroxidases that are frequently present in the same club fungi (Sect. 2.3.2) [59] and may interfere in screening of crude samples. In PeroxiBase, 106 sequences of DyP peroxidase family are already registered and annotated (January 2010) but several further can follow from newly sequenced genomes. Possibly in this case, heme peroxidase has evolved to its highest versatility: besides peroxidase activity with, e.g., anthraquinone derivatives serving as electron donors, dyp-type enzymes seem to have also hydrolase and oxygenase activities [7]. This resembles the evolution of di-heme peroxidase towards MauG protein, (Sect. 2.4) but for dyp-type peroxidases, this phenomenon needs more comprehensive analysis. Nevertheless, it is a striking aspect to consider also in future directed evolution experiments whether a heme peroxidase has the internal capacity to evolve towards an oxygenase. A dendrogram of few members of this family was already presented [60] where peroxidases from other families were linked together with Dyp family. This approach is rather problematic as there were only a very limited number of dyp-type sequences included, and the sequence similarity of dyp-type peroxidases to peroxidases from other families described above is too low for a higher-level phylogenetic analysis. All annotated and complete dyp peroxidase sequences from PeroxiBase were collected for the calculation of the unrooted phylogenetic tree presented in Fig. 2.14. Four distinct subfamilies can be clearly defined. According to clade distribution, it can be expected with a high probability that in the first step of their evolution subfamilies A and B diverged from C and D counterparts, and in the later steps subfamilies A and B as well as C and D segregated from each other and their genes have undergone speciations in four directions within the respective subfamilies. There are already 26 solely bacterial subfamily A members. Mainly *E. coli* and *Shigella* sp. genes are very abundant orthologs in this subfamily clade, addressing their potential role in pathogenicity. It has been proposed that YcdB protein from *E. coli* belonging to subfamily A can function as periplasmic peroxidase [61]. Twenty four bacterial and one protozoan member are building subfamily B. Two bacterial representatives of this clade are already known on the structural level [58] thus supporting this phylogenetic overview. The unique eukaryotic variant of this subfamily is at the moment a putative protein that needs to be further characterized. Twenty two solely bacterial C-subfamily members are distributed among proteobacteria, cyanobacteria, and actinobacteria. Corresponding proteins need to be investigated for their



ProML method of the PHYLIP package [16]. Numbers in the nodes indicate bootstrap values for NJ and ML methods, respectively. Abbreviations of protein names correspond to PeroxiBase

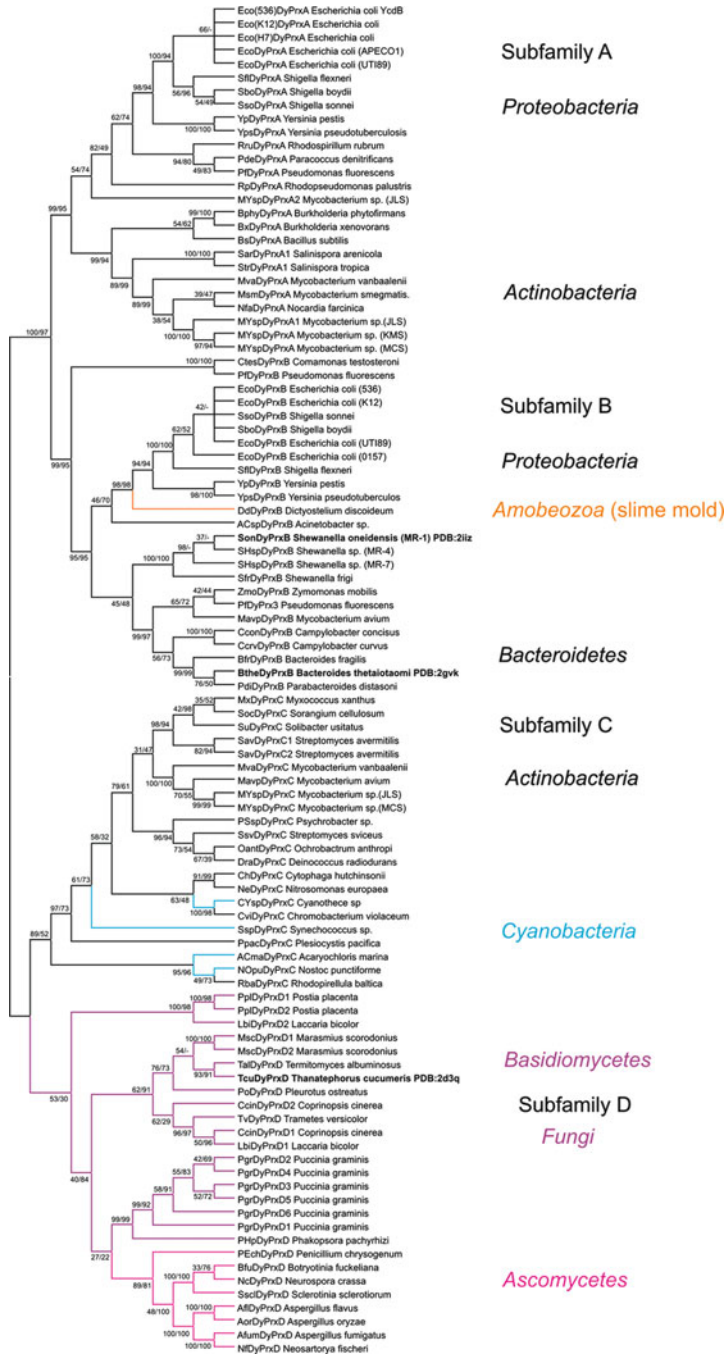


Fig. 2.14 Reconstructed phylogeny of four types of dyp peroxidases. The unrooted tree obtained from the NJ method of the MEGA package [13] is presented. A very similar tree was obtained

substrate specificity as there are only putative sequences within this subfamily. Currently, 27 solely fungal members form subfamily D. *Pleurotus ostreatus* [62], and *Thanatephorus cucumeris* [60] peroxidases are typical basidiomycete examples of this subfamily, the latter also with known 3D structure. Apparently, there are also several ascomycete representatives in this subfamily (Fig. 2.14). Their physiological function and substrate specificity with potential biotechnological applications remain completely unknown at the moment.

2.6 Haloperoxidase Family

Haloperoxidases are abundant mainly among fungi, but a few very similar genes were recently detected also among oomycetes (water molds) that, although in several aspects are similar, do not belong to the monophyletic kingdom of fungi. As a newly defined class within stramenopiles, they are more closely related to plants than animals, and it will be very interesting to screen for haloperoxidase genes in genomes of other stramenopiles. Generally, we have to distinguish between haloperoxidases with prosthetic heme group and nonheme haloperoxidases that are phylogenetically unrelated with this family and can form two different gene families. Heme-thiolate haloperoxidases contain protoporphyrin IX as prosthetic group [63] and can catalyze the oxidative transformation of halides and halophenols. In most databases, they are still described as “chloroperoxidases,” e.g., in IPR000028 or PF01328 counting only around 140 distinct protein sequences (January 2010). The most intensively investigated member is chloroperoxidase from the ascomycete *Caldariomyces fumago* (CCPO) [64]. The evolution of this small peroxidase family resulted, in analogy with other peroxidase families (e.g., Sects. 2.4 and 2.5), in considerable multifunctionality as it possesses besides dehaloperoxidase also remarkable catalase [65] and peroxygenase activities [66]. According to recent opinions on enzyme evolution [34], this haloperoxidase multifunctionality can be understood as another example of ancient peroxidase promiscuity. Moreover, it was mentioned that CCPO (but very probably also other phylogenetic neighbors) is significantly more robust and functions in harsher conditions when compared with all other heme peroxidases [64]. No prokaryotic heme haloperoxidases are annotated so far, suggesting conversion from other gene type, not necessarily a highly specified peroxidase. The reconstructed tree of 63 haloperoxidase members is presented in Fig. 2.15 and demonstrates that heme haloperoxidases form a monophyletic group with frequent gene duplication events. There is a segregation of haloperoxidase representatives between ascomycete (sac) fungi and basidiomycete (club) fungi with gene speciation within particular genomes. However, in some clades, the genes are mixed between these



using ProML of the PHYLIP package [16]. Numbers in the nodes indicate bootstrap values for NJ and ML methods, respectively. Abbreviations of protein names correspond to PeroxiBase

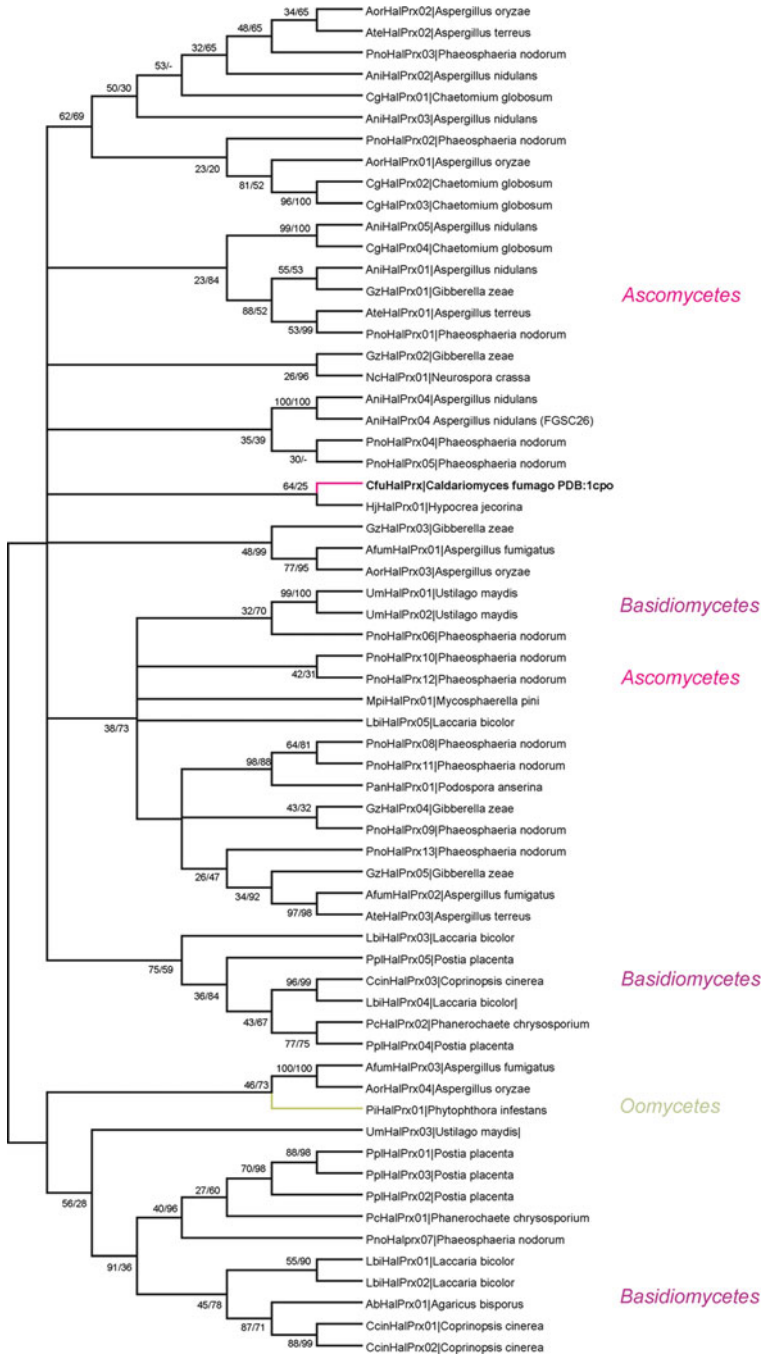


Fig. 2.15 Phylogeny of heme-containing haloperoxidases. The reconstructed tree from the ME-method of the MEGA package [13] is presented. A very similar tree was obtained with the ProML method of the PHYLIP package [16]. *Numbers* in the nodes indicate bootstrap values for ME and ML, respectively. *Abbreviations* of protein names correspond to PeroxiBase

phyla but this phenomenon can be observed also in other peroxidase families (e.g., Sect. 2.3.1.1). The oomycete (non fungal) representative appears to have diverged from related ascomycete genes; however, a more comprehensive analysis with more closely related representatives is needed. Among ascomycetes, basidiomycetes and oomycetes putative heme haloperoxidase genes are abundant mainly in genomes of phytopathogens. The best example is the presence of 13 haloperoxidase genes in the genome of ascomycete *Phaeosphaeria nodorum*, a major pathogen of wheat causing lead diseases and glume blotch. Such unusual, frequent occurrence of gene duplicates of several gene family paralogs within one genome opens interesting questions about their physiological role and possible involvement in host/pathogen interaction.

2.7 Conclusions

The phylogenetic analysis of structural and functional diversity of heme peroxidases can help in the search for new candidates for various biotechnological applications covering all important areas from red through green to white biotechnologies. The phylogenetic output can be also a good starting point for the planning of directed molecular evolution experiments to continue and simulate the natural evolution of peroxidases in the laboratory. This methodology can even lead to *de novo* peroxidase design (inspired by natural evolution) with desired structure and tailored reaction specificity.

References

1. Talwalkar A, Kailasapathy K (2004) The role of oxygen in the viability of probiotic bacteria with reference to *L. acidophilus* and *Bifidobacterium* spp. *Curr Issues Intest Microbiol* 5:1–8
2. Gracieux MV, Tamanai-Shacoori Z, Perez-Chaparro J et al (2008) Expression patterns of genes induced by oxidative stress in *Porphyromonas gingivalis*. *Oral Microbiol Immunol* 23:308–314
3. Bernroither M, Zámocký M, Furtmüller PG et al (2009) Occurrence, phylogeny, structure, and function of catalases and peroxidases in cyanobacteria. *J Exp Bot* 60:423–440
4. Bekker A, Holland HD, Wang PL et al (2004) Dating the rise of atmospheric oxygen. *Nature* 427:117–120
5. Regelsberger G, Jakopitsch C, Plasser L et al (2002) Occurrence and biochemistry of hydroperoxidases in oxygenic phototrophic prokaryotes (cyanobacteria). *Plant Physiol Biochem* 40:479–490
6. Passardi F, Theiler G, Zámocký M et al (2007) PeroxiBase: the peroxidase database. *Phytochemistry* 68:1605–1611
7. Sugano Y (2009) Dyp-type peroxidases comprise a novel heme peroxidase family. *Cell Mol Life Sci* 66:1387–1403
8. Klotz M, Loewen PC (2003) The molecular evolution of catalatic hydroperoxidases: evidence for multiple lateral transfer of genes between prokaryota and from bacteria into eukaryota. *Mol Biol Evol* 20:1098–1112

9. Zámocký M, Furtmüller PG, Obinger C (2008) Evolution of catalases from bacteria to humans. *Antioxid Redox Signal* 10:1527–1547
10. Zámocký M, Jakopitsch C, Furtmüller PG et al (2008) The peroxidase-cyclooxygenase superfamily: reconstructed evolution of critical enzymes of the innate immune system. *Proteins* 72:589–605
11. Söderhall K (1999) Invertebrate immunity. *Dev Comp Immunol* 23:263–266
12. Dick GJ, Podell S, Johnson HA et al (2008) Genomic insights into Mn(II) oxidation by the marine alphaproteobacterium *Aurantimonas* sp. strain SI85-9A1. *Appl Environ Microbiol* 74:2646–2658
13. Tamura K, Dudley J, Nei M et al (2007) MEGA4: Molecular Evolutionary Genetics Analysis (MEGA) Software Version 4.0. *Mol Biol Evol* 24:1596–1599
14. Nei M, Rooney AP (2005) Concerted and birth-and-death evolution of multigene families. *Annu Rev Genet* 39:121–152
15. Felsenstein J (1996) Inferring phylogenies from protein sequences by parsimony, distance, and likelihood methods. *Methods Enzymol* 266:418–427
16. Ris-Stalpers C (2006) Physiology and pathophysiology of the DUOXes. *Antioxid Redox Signal* 8:1563–1572
17. Johansson MW, Lind MI, Holmblad T et al (1995) Peroxinectin, a novel cell adhesion protein from crayfish blood. *Biochem Biophys Res Commun* 216:1079–1087
18. Cheng G, Salerno JC, Cao Z et al (2008) Identification and characterization of VPO1, a new animal heme-containing peroxidase. *Free Radic Biol Med* 45:1682–1694
19. Nelson RE, Fessler RI, Takagi Y et al (1994) Peroxidasin: a novel enzyme-matrix protein of *Drosophila* development. *EMBO J* 13:3438–3447
20. Karaulanov EE, Bottcher RT, Niehrs C (2006) A role for fibronectine-leucine-rich transmembrane cell-surface proteins in homotypic cell adhesion. *EMBO Rep* 7:283–290
21. Zhang J-L, Huang Y, Qiu L-Y et al (2007) von Willebrand factor type C domain-containing proteins regulate bone morphogenetic protein signaling through different recognition mechanisms. *J Biol Chem* 282:20002–20014
22. Loughran NB, O'Connor B, O'Fágáin C et al (2008) The phylogeny of the mammalian heme peroxidases and the evolution of their diverse functions. *BMC Evol Biol* 8:101
23. Klebanoff SJ (1999) Myeloperoxidase. *Proc Assoc Am Phys* 111:383–389
24. Wang J, Slungaard A (2006) Role of eosinophil peroxidase in host defense and disease pathology. *Arch Biochem Biophys* 445:256–260
25. Ruf J, Carayon P (2006) Structural and functional aspects of thyroid peroxidase. *Arch Biochem Biophys* 445:269–277
26. Chernokalskaya E, Dubell AN, Cunningham KS et al (1998) A polysomal ribonuclease involved in the destabilization of albumin mRNA is a novel member of the peroxidase gene family. *RNA* 4:1537–1548
27. Keilin D, Mann T (1937) On the haematin compound of peroxidase. *Proc R Soc Lond* 122B:119–133
28. Kaput J, Goltz S, Blobel G (1982) Nucleotide sequence of the yeast nuclear gene for cytochrome *c* peroxidase precursor. *J Biol Chem* 257:15054–15058
29. Welinder KG (1992) Superfamily of plant, fungal, and bacterial peroxidases. *Curr Opin Struct Biol* 2:388–393
30. Habetha M, Bosch TC (2005) Symbiotic *Hydra* express a plant-like peroxidase gene during oogenesis. *J Exp Biol* 208:2157–2165
31. Myers P, Espinosa R, Parr CS et al (2008) The Animal Diversity Web. <http://animaldiversity.org>
32. Morgenstern I, Klopman S, Hibbett DS (2008) Molecular evolution and diversity of lignin degrading heme peroxidases in the Agaricomycetes. *J Mol Evol* 66:243–257
33. Passardi F, Bakalovic N, Teixeira FK et al (2007) Prokaryotic origins of the non-animal peroxidase superfamily and organelle-mediated transmission to eukaryotes. *Genomics* 89:567–579
34. Khersonsky O, Roodveldt C, Tawfik DS (2006) Enzyme promiscuity: evolutionary and mechanistic aspects. *Curr Opin Chem Biol* 10:498–508

35. Welinder KG (1991) Bacterial catalase-peroxidases are gene duplicated members of the plant peroxidase superfamily. *Biochim Biophys Acta* 1080:215–220
36. Zámocký M, Regelsberger G, Jakopitsch C et al (2001) The molecular peculiarities of catalase-peroxidases. *FEBS Lett* 492:177–182
37. Zámocký M (2004) Phylogenetic relationships in Class I of the superfamily of bacterial, fungal, and plant peroxidases. *Eur J Biochem* 271:3297–3309
38. Passardi F, Zámocký M, Favet J et al (2007) Phylogenetic distribution of catalase-peroxidases: are there patches of order in chaos? *Gene* 397:101–113
39. Zámocký M, Furtmüller PG, Obinger C (2009) Two distinct groups of fungal catalase/ peroxidases. *Biochem Soc Trans* 37:772–777
40. Xi L, Xu X, Liu W et al (2007) Differentially expressed proteins of pathogenic *Penicillium marneffei* in yeast and mycelial phases. *J Med Microbiol* 56:298–304
41. Champeil A, Doré T, Fourbet JF (2004) *Fusarium* head blight: epidemiological origin of the effects of cultural practices on head blight attacks and the production of mycotoxins by *Fusarium* in wheat grains. *Plant Sci* 166:1389–1415
42. Nishizawa Y, Nishio Z, Nakazono K et al (1999) Enhanced resistance to blast (*Magnaporthe grisea*) in transgenic Japonica rice by constitutive expression of rice chitinase. *Theor Appl Genet* 99:383–390
43. Gray MW (1999) Evolution of organellar genomes. *Curr Opin Genet Dev* 9:678–687
44. Zámocký M, Dunand C (2006) Divergent evolutionary lines of fungal cytochrome c peroxidases belonging to the superfamily of bacterial, fungal and plant heme peroxidases. *FEBS Lett* 580:6655–6664
45. Kirk TK, Farrell RL (1987) Enzymatic “combustion”: the microbial degradation of lignin. *Annu Rev Microbiol* 41:465–505
46. Hildén K, Martinéz AT, Hatakka A et al (2005) The two manganese peroxidases Pr-MnP2 and Pr-MnP3 of *Phlebia radiata*, a lignin-degrading basidiomycete, are phylogenetically and structurally divergent. *Fungal Genet Biol* 42:403–419
47. Ruiz-Duenas FJ, Morales M, Garcia E et al (2009) Substrate oxidation sites in versatile peroxidase and other basidiomycete peroxidases. *J Exp Bot* 60:441–452
48. Duroux L, Welinder KG (2003) The peroxidase gene family in plants: a phylogenetic overview. *J Mol Evol* 57:397–407
49. Welinder KG, Justensen AF, Kjaersgard IV et al (2002) Structural diversity and transcription of Class III peroxidases from *Arabidopsis thaliana*. *Eur J Biochem* 269:6063–6081
50. Passardi F, Longet D, Penel C et al (2004) The Class III peroxidase multigenic family in rice and its evolution in land plants. *Phytochemistry* 65:1879–1893
51. Veitch NC (2004) Horseradish peroxidase: a modern view of a classic enzyme. *Phytochemistry* 65:249–259
52. Oliva M, Theiler G, Zámocký M et al (2009) PeroxiBase: a powerful tool to collect and analyse peroxidase sequences from Viridiplantae. *J Exp Bot* 60:453–459
53. Brittain T (2008) Intra-molecular electron transfer in proteins. *Protein Pept Lett* 15:556–561
54. Echalié A, Goodhew CF, Pettigrew GW et al (2006) Activation and catalysis of the di-heme cytochrome c peroxidase from *Paracoccus pantotrophus*. *Structure* 14:107–117
55. Gak ER, Tsygankov YD, Chistoserdov AY (1997) Organization of methylamine utilization genes (mau) in *Methylobacillus flagellatum* KT and analysis of mau mutants. *Microbiology* 143:1827–1835
56. Wang Y, Graichen ME, Liu A et al (2003) MauG, a novel di-heme protein required for tryptophan tryptophylquinone biogenesis. *Biochemistry* 42:7318–7325
57. van Spanning RJ, de Boer AP, Reijnders WN et al (1997) FnrP and NNR of *Paracoccus denitrificans* are both members of the FNR family of transcriptional activators but have distinct roles in respiratory adaptation in response to oxygen limitation. *Mol Microbiol* 23:893–907
58. Zubieta C, Joseph R, Krishna SS et al (2007) Identification and structural characterization of heme binding in a novel dye decolorizing peroxidase, TyrA. *Proteins* 69:234–243

59. Kim SJ, Shoda M (1999) Purification and characterization of a novel peroxidase from *Geotrichum candidum* Dec1 involved in decolorization of dyes. *Appl Environ Microbiol* 65:1029–1035
60. Sugano Y, Muramatsu R, Ichiyangi A et al (2007) DyP, a unique dye-decolorizing peroxidase, represents a novel heme peroxidase family. *J Biol Chem* 282:36652–36658
61. Cartron ML, Mitchell SA, Woodhall MR et al (2007) Preliminary X-ray diffraction analysis of YcdB from *Escherichia coli*: a novel haem-containing and Tat-secreted periplasmic protein with a potential role in iron transport. *Acta Crystallogr Sect F Struct Biol Cryst Commun* 63:37–41
62. Faraco V, Piscitelli A, Sannia G et al (2007) Identification of a new member of the dye-decolorizing peroxidase family from *Pleurotus ostreatus*. *World J Microbiol Biotechnol* 23:889–893
63. Hofrichter M, Ulrich R (2006) Heme-thiolate haloperoxidases: versatile biocatalysts with biotechnological and environmental significance. *Appl Microbiol Biotechnol* 71:276–288
64. Osborne RL, Raner GM, Hager LP et al (2006) *C. fumago* chloroperoxidase is also a dehaloperoxidase: oxidative dehalogenation of halophenols. *J Am Chem Soc* 128:1036–1037
65. Manoj KM, Hager LP (2001) Utilization of peroxide and its relevance in oxygen insertion reactions catalyzed by chloroperoxidase. *Biochim Biophys Acta* 1547:408–417
66. Anh DH, Ullrich R, Benndorf D et al (2007) The coprophilous mushroom *Coprinus radians* secretes a haloperoxidase that catalyzes aromatic peroxygenation. *Appl Environ Microbiol* 73:5477–5485

Chapter 3

Structural and Functional Features of Peroxidases with a Potential as Industrial Biocatalysts

Francisco J. Ruiz-Dueñas and Angel T. Martínez

Contents

3.1	General Structural Characteristics of Heme Peroxidases	38
3.1.1	Superfamily of Plant, Fungal, and Bacterial Peroxidases	38
3.1.2	Superfamily of Mammalian and Other Animal Peroxidases	39
3.1.3	Other Heme Peroxidase (super)Families	42
3.2	Basidiomycete Peroxidases	43
3.2.1	White-Rot Fungal Peroxidases: Biotechnological Interest	43
3.2.2	Evolutionary Relationships of Basidiomycete Peroxidases	44
3.3	Ligninolytic Peroxidases	46
3.3.1	Heme Environment	47
3.3.2	Manganese Oxidation Site	47
3.3.3	LRET Substrate Oxidation at an Exposed Tryptophan	49
3.3.4	Influence of the Catalytic Tryptophan Environment	50
3.4	Heme-Thiolate Peroxidases	51
3.4.1	Heme Environment	52
3.4.2	Substrate Oxidation Sites	53
3.5	Dye-Decolorizing Peroxidases	53
3.6	Conclusions	54
	References	55

Abstract This chapter begins with a description of the main structural features of heme peroxidases representative of the two large superfamilies of plant–fungal–bacterial and animal peroxidases, and the four additional (super)families described to date. Then, we focus on several fungal peroxidases of high biotechnological potential as industrial biocatalysts. These include (1) ligninolytic peroxidases from white-rot basidiomycetes being able to oxidize high redox-potential substrates at an exposed protein radical; (2) heme-thiolate peroxidases that are structural hybrids of typical peroxidases and cytochrome P450 enzymes and, after their discovery in sooty molds, are being described in basidiomycetes with even more interesting catalytic properties, such as selective aromatic oxygenation; and (3) the so-called dye-decolorizing peroxidases that are still to be thoroughly investigated but have been identified in different basidiomycete genomes. The structural–functional

description of these peroxidases includes an analysis of the heme environment and a description of their substrate oxidation sites, with the purpose of understanding their interesting catalytic properties and biotechnological potential.

3.1 General Structural Characteristics of Heme Peroxidases

Since 1984, when the first crystal structure of a heme peroxidase – namely yeast (*Saccharomyces cerevisiae*) cytochrome *c* peroxidase (CCP; PDB entry 2CYP) – was published [1], an increasing number of molecular structures of heme peroxidases have been solved. Currently, there are about 344 structure hits available in the protein data bank (PDB; <http://www.pdb.org>) corresponding not only to polypeptide chains plus cofactors structures, but also to other protein–ligand complexes (up to 129 different ligands including substrates), from over 5,000 heme peroxidase sequences included in PeroxiBase¹ (<http://peroxibase.toulouse.inra.fr>) [2] (nonheme peroxidases also represent a large group of enzymes, with more than 1,800 entries in PeroxiBase).

Over the next few years, it is probable that the number of structures will increase significantly due to the interest of different research groups in heme peroxidase structure–function relationships. Much of this knowledge is being and will be used by different research entities, both academic and commercial, to develop biotechnological, environmental, medical, and other applications based on these enzymes.

Heme peroxidases can be classified into two large superfamilies, and four additional small nonrelated families/superfamilies, the members of each sharing general structural features, described in this first section. Main structural details related to the catalytic properties of some of the most outstanding heme peroxidases with a potential as industrial biocatalysts will be described in the next sections of this chapter.

3.1.1 Superfamily of Plant, Fungal, and Bacterial Peroxidases

The superfamily of plant, fungal, and bacterial heme peroxidases (also called non animal peroxidase superfamily, see Chap. 2) categorizes its components into three classes based on sequence alignment and biological origin, such as initially proposed by K.G. Welinder using the only crystal structure available at that moment (yeast CCP) as a model [3, 4]. Class III is the largest one, with over 3,000 plant peroxidase entries in PeroxiBase, followed by Classes I and II, with over 900 entries

¹Concerning PeroxiBase, note that (1) the database although under permanent updating is not exhaustive; (2) hypothetical peroxidase genes from genomes, and partial sequences, are included; and (3) the information cited here corresponds to January 2010.

corresponding to peroxidases of prokaryotic origin and near 170 fungal peroxidase entries in PeroxiBase, respectively. This superfamily includes monomeric heme peroxidases, in some cases with a very low amino acid sequence identity, sharing the same helical fold independently of the presence (in plant and fungal peroxidases) or absence (in bacterial peroxidases) of disulfide bridges and structural calcium ions. This is illustrated in Fig. 3.1 that shows ribbon diagrams of the molecular structures of selected heme peroxidases, with prokaryotic CCP, basidiomycete lignin peroxidase (LiP), and plant horseradish peroxidase (HRP) as representatives for the three classes of this superfamily. The similar helical topology of the superfamily members is evident in these diagrams, especially in the cases of CCP and LiP, but also in HRP (Fig. 3.1a–c).

The components of this superfamily present an iron–protoporphyrin IX noncovalently bound to the protein, which is located at an internal cavity connected to the solvent by one or two access channels. A main heme access channel is present in all peroxidases, allowing the H_2O_2 to reach the heme iron to activate the enzyme, as well as the entrance of small reducing substrates in classical plant and fungal peroxidases, such as HRP and the soil basidiomycete *Coprinopsis cinerea* (synonym *Coprinus cinereus*) peroxidase (CIP) [5, 6]. A second small channel, also acting as a catalytic site, extends directly to the heme propionates in some members of the superfamily, including prokaryotic ascorbate peroxidase [7] and fungal manganese peroxidase (MnP) [8] and versatile peroxidase (VP) [9] (Fig. 3.2) (the latter discussed in Sect. 3.3.2). As also shown in Fig. 3.1a–c, the heme pocket residues are conserved in LiP and HRP, while the aromatic residues are two tryptophans in CCP, one of them forming a catalytic tryptophanyl radical in CCP (see Sect. 3.3.1 for further description of the LiP heme pocket). Small additional differences affecting single amino acid residues in this and other areas of the protein are responsible for the unique catalytic properties of some enzymes included in this superfamily, as in the case of the different ligninolytic peroxidases [10] described below.

3.1.2 Superfamily of Mammalian and Other Animal Peroxidases

The other large heme peroxidase superfamily includes animal peroxidases [11]. In PeroxiBase, the superfamily of animal peroxidases (including cyclooxygenases and peroxinectins) has over 360 entries, although only around 50 of them correspond to typical mammalian peroxidases. These are predominant α -helical monomeric and dimeric glycosylated enzymes. Each monomer is made up of one (lactoperoxidase, LPO) or two (myeloperoxidase, MPO; eosinophil peroxidase, EPO; and thyroid peroxidase, TPO) polypeptide chains. In the last case, these result from proteolytic processing of a primary translation product yielding a small and a large subunit. The overall structures of the only two mammalian peroxidases determined by X-ray crystallography to date, that is, monomeric LPO and homodimeric MPO [12–14], are very similar as shown in the diagrams included in Fig. 3.1d, e. In the same way,

homology modeling suggests that almost all the regions corresponding to helices in these two crystal structures are well conserved in other mammalian peroxidases [15], such as EPO and TPO.

Diagrams in Fig. 3.1d, e also illustrate the presence of a derivative of iron-protoporphyrin IX covalently bound to the protein by two ester linkages, with participation of two acidic residues (glutamate and aspartate) in all members of this superfamily, and an additional sulfonium linkage involving a methionine residue (Met243) in MPO. This is probably the most important structural feature in these enzymes affecting, among others, heme protection from their highly reactive products [16, 17] and enzymatic catalysis at different levels (including substrate binding and oxidation) [15]. The proximal heme ligand is a histidine residue conserved in all members of this superfamily together with an asparagine, which forms a hydrogen bond with the N_{δ} of the proximal histidine. On the heme

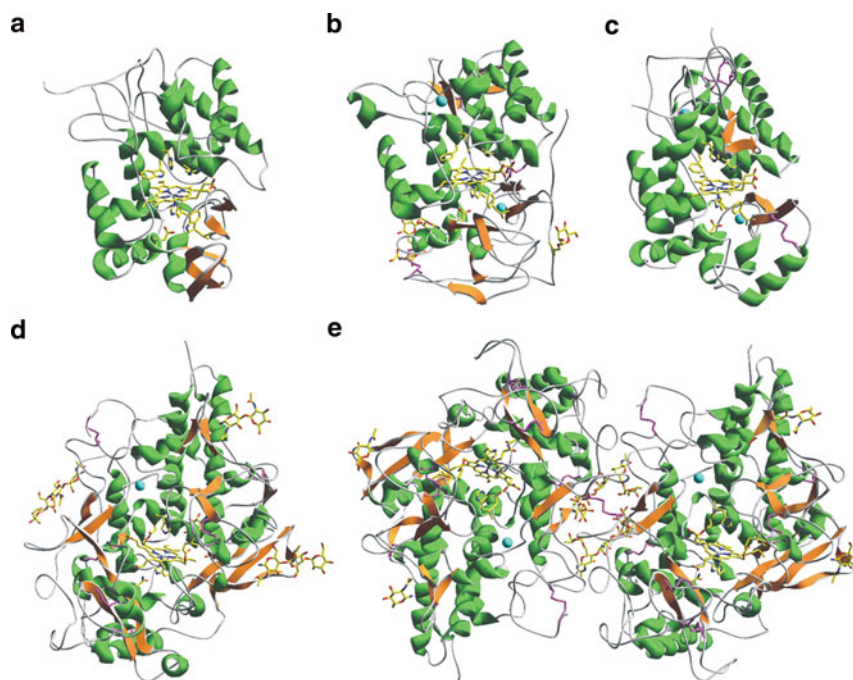


Fig. 3.1 Ribbon diagrams of the molecular structures of representatives for the main heme peroxidase families/superfamilies (a) Yeast CCP; (b) *P. chrysosporium* LiP; (c) HRP; (d) Buffalo LPO; (e) Human MPO; (f) Yeast catalase (tetramer unit); (g) *G. sulfurreducens* di-heme CCP (dimer unit); (h) *L. fumigo* CPO; and (i) *Geotrichum* DyP (based on PDB entries 1CCP, 1LLP, 7ATJ, 2GJM, 1CXP, 1A4E, 3HQ6, 1CPO, and 2D3Q, respectively). Secondary structure (green helices and orange β -strands) is shown together with heme cofactors, some carbohydrate residues (as colored bars) disulfide bridges (pink bars) and some structural ions (blue van der Waals spheres)

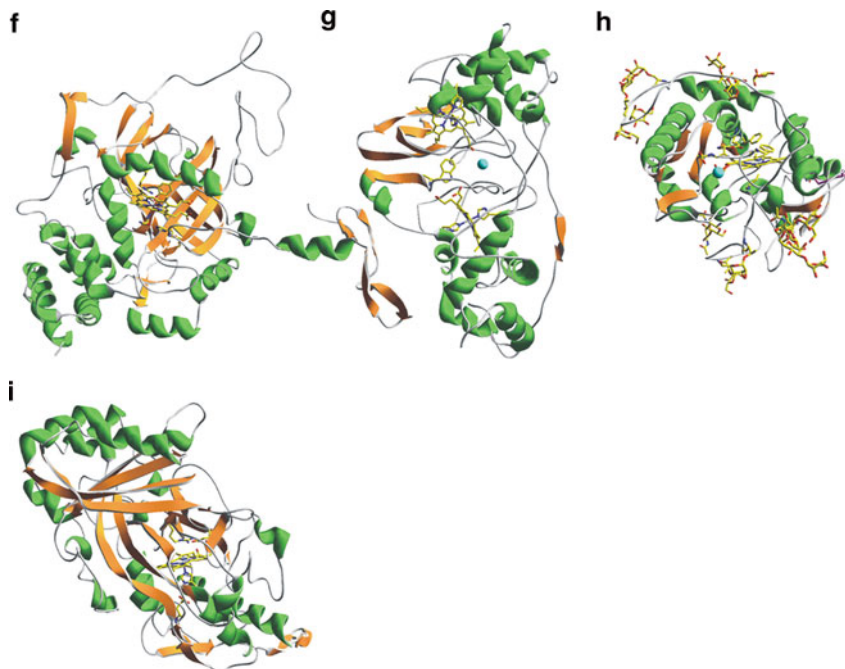
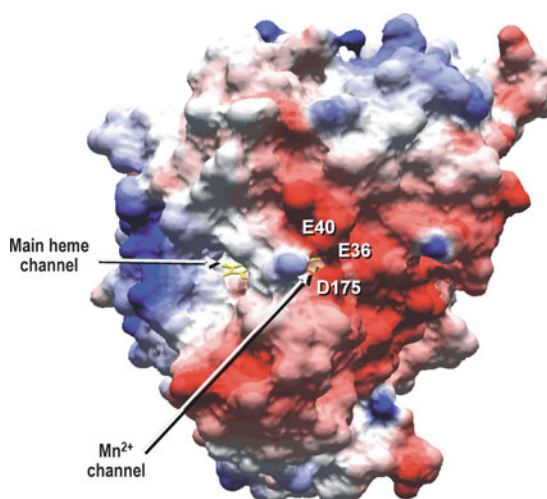


Fig. 3.1 (continued)

Fig. 3.2 Solvent access surface (colors represent electrostatic potentials) showing the main channel providing access to the heme cofactor (in yellow bars) occupying a central cavity (heme pocket); and the second narrow channel present in some peroxidases, such as manganese-oxidizing peroxidases, accessing to the heme propionates (based on the crystal structure of *P. eryngii* VP, PDB 2BOQ)



distal side three additional residues, namely histidine, arginine, and glutamine, are conserved. Moreover, a calcium-binding site is also found, and its coordination suggests that it plays an important structural role both in correctly orienting the

distal histidine in LPO and MPO, and in the interaction between the small and large polypeptide within the monomer of MPO [18]. On the other hand, a disulfide bridge is involved in MPO dimerization, as shown in Fig. 3.1e, and also glycosylation has been suggested to play an important role in dimer formation.

3.1.3 Other Heme Peroxidase (super)Families

Four additional families/superfamilies of heme peroxidases display no sequence homology between each other [2] and exhibit their own structural features. Enzymes with catalase activity are highly polyphyletic including (1) nonheme Mn-containing catalases that are outside the scope of the chapter; (2) prokaryotic catalase–peroxidases that are included in Class I of the first superfamily discussed above; and (3) monofunctional catalases to be discussed here. Moreover, several other heme peroxidases, such as plant peroxidases and chloroperoxidases, also exhibit some catalase activity. The catalase superfamily (over 250 entries in PeroxiBase) includes three phylogenetically separated clades, probably derived from a common ancestor in clade-2 [19]. They are homotetrameric enzymes and differ in the size of subunits, as well as in the heme orientation with respect to the active site histidine. The first complete crystal structure of a catalase was reported from *Penicillium vitale* (a synonym of *Penicillium janthinellum*) [20] only a couple of years after publication of the CCP crystal structure [1], and a preliminary structure had already been reported in *Nature* on 1981 [21]. Moreover, this catalase PDB entry (4CAT) was deposited in 1983, while the first CCP entry (2CYP) was only deposited in 1985. Figure 3.1f shows a diagram of a monomer of the small-unit catalase from yeast (representative of clade-3), which was the second fungal catalase to be solved [22]. This structure lacks the carboxyl-terminal domain present in the *Penicillium* and other large-unit (clade-2) catalases; it also shows the active-site histidine situated above heme ring-III, while the “original” position in catalases seems to be above ring-IV. Conserved residues at the heme environment of catalases are also shown in Fig. 3.1f, including tyrosine acting as fifth iron ligand, and the above-mentioned histidine at the opposite side of the heme (plus arginine and aspartate residues accompanying the two above residues, respectively). Yeast catalase does not bind NADPH tightly (partial occupancy in the crystals) in contrast with other catalases. NADPH seems to play a role in preventing catalase inactivation [23].

Another superfamily is formed by bacterial di-heme CCP (with over 110 entries in PeroxiBase) that are periplasmic enzymes providing protection from oxidative stress. These homodimeric enzymes have a conserved tertiary structure containing two type-*c* hemes covalently attached to two predominantly α -helical domains via a characteristic binding motif. One heme acts as a low redox-potential center where H_2O_2 is reduced, and the other as a high redox-potential center that feeds electrons to the peroxidatic site from soluble electron-shuttle proteins such as cytochrome *c* [24]. In the crystal structure of the *Geobacter sulfurreducens* enzyme shown in Fig. 3.1g, the first heme appears as a bis-histidinyl-coordinated form (and

a methionine occupies one of the axial positions in the second heme). A conserved tryptophan residue and the tightly coordinated Ca^{2+} ion visible between the two heme groups play a key role in facilitating electron transfer between the two redox centers [25, 26].

The two last families/superfamilies are heme-thiolate (halo)peroxidases and dye-decolorizing peroxidases (DyP) (which are considered in more detail in Sects. 3.4 and 3.5, respectively). The heme-thiolate family (with over 60 entries in PeroxiBase) is structurally represented by chloroperoxidase (CPO) from the ascomycete *Leptoxiphium fumago* (synonym: *Caldariomyces fumago*), the only member whose structure has been solved [27]. CPO folds in a unique structure dominated by eight helical segments, and includes one structural cation near the heme propionates, as shown in Fig. 3.1h. It presents a cysteine thiolate as the heme ligand like in cytochrome P450, while the rest of heme peroxidases use a histidine as the axial ligand with the exception of catalases that have a tyrosine ligand, as mentioned above. Finally, DyP has only recently been proposed as a novel heme peroxidase family [28], although a considerable number of entries (over 100) exist in PeroxiBase. The first DyP structure was that from the *Geotrichum*-type anamorph of a basidiomycete identified as *Thanatephorus cucumeris* solved in 2007 [28]. Members of this family range from monomers to hexamers [29] and, as shown in Fig. 3.1i, exhibit a unique structural motif consisting of two sets of antiparallel β -sheets located between two α -helices above the distal area of the noncovalently bound iron–protoporphyrin IX cofactor.

3.2 Basidiomycete Peroxidases

After the above survey on the general molecular structure of the different types of heme peroxidases, a more detailed analysis on the catalytic sites of some heme peroxidases of particular biotechnological interest produced by fungi is presented in Sects. 3.3–3.5. Previously, a description of the biotechnological interest of these enzymes, followed by a structural classification and evolutionary analysis of all the basidiomycete peroxidases, whose sequence is known to date, is presented in the two subsections included below. For a full evolutionary analysis of heme peroxidases, see Chap. 2.

3.2.1 White-Rot Fungal Peroxidases: Biotechnological Interest

Compared with plant and other peroxidases, white-rot fungal peroxidases are characterized by their high redox potential, related to the architecture of the heme environment (see Chap. 4). This is required to perform their role in nature, namely the oxidative biodegradation of the recalcitrant lignin polymer present in the cell wall of all vascular plants [30–32]. By contrast, one of the roles of plant peroxidases

is the oxidation of lignin precursors (monolignols) in the last step of lignin biosynthesis. Monolignols are phenolic and, therefore, no high redox-potential peroxidases are required in plants to generate their phenoxy radicals. Since the resulting polymer is basically nonphenolic (most of the radical condensation reactions involve the *para* position of the aromatic ring), those fungal peroxidases involved in lignin biodegradation were forced to develop high redox potential and other specific degradation mechanisms [33–35] as described in Sect. 3.3.

White-rot fungi, whose name derives from the whitish color of delignified wood, are the only organisms producing high redox-potential ligninolytic peroxidases as confirmed by the recent comparison of the genomes of lignin-degrading (white rot) and cellulose-degrading (brown rot) basidiomycetes [36]. Lignin removal is not only a key step for the recycling of all the carbon fixed by plants in land ecosystems, but also a central issue for the current industrial utilization of wood (e.g., in paper pulp manufacture) as well as for the development of integrated lignocellulose biorefineries for the future production of chemicals, materials, and biofuels [37]. Biotechnology can significantly contribute to this sustainable development, and white-rot fungal peroxidases have biotechnological interest for the modification (or removal) of lignin and other recalcitrant aromatic compounds.

An additional characteristic of white-rot fungal peroxidases is their wide-substrate specificity allowing them to oxidize substrates that shares structural characteristics with lignin units [38]. Among others, these enzymes are able to oxidize phenolic and nonphenolic pollutants [39], pesticides [40], polycyclic aromatic hydrocarbons [41] and industrial dyes [42]. These properties expand the range of applications also to the environmental sector.

3.2.2 Evolutionary Relationships of Basidiomycete Peroxidases

At least 87 basidiomycete heme peroxidases have been described to date, whose evolutionary relationships are shown in Fig. 3.3. It also includes putative peroxidases from the genomes of *Phanerochaete chrysosporium*, *Pleurotus ostreatus*, and *Pycnoporus cinnabarinus*, and two reference ascomycete peroxidases.

The dendrogram shows a large cluster for all the ligninolytic peroxidases (a total of 64) and a few related sequences. Typical MnP (from *P. chrysosporium* and other six basidiomycetes, up to 16 sequences) form group A, which is clearly separated from the rest. Group B is also well-defined and formed by 16 typical LiP sequences (from *P. chrysosporium* and other four basidiomycetes). The typical VP from *Pleurotus* species form two groups (C) that cluster together, but also with group A' including three nontypical MnP from *P. ostreatus*. The only confirmed VP from a different genus (*Bjerkandera* VP) does not cluster with the *Pleurotus* VP, but with group A'' of nontypical MnP that also includes a putative VP. This and other putative VP (also up to a total of 16 VP sequences) were classified as such because of the presence of catalytically relevant residues as discussed below (two other putative VP are included in other groups).

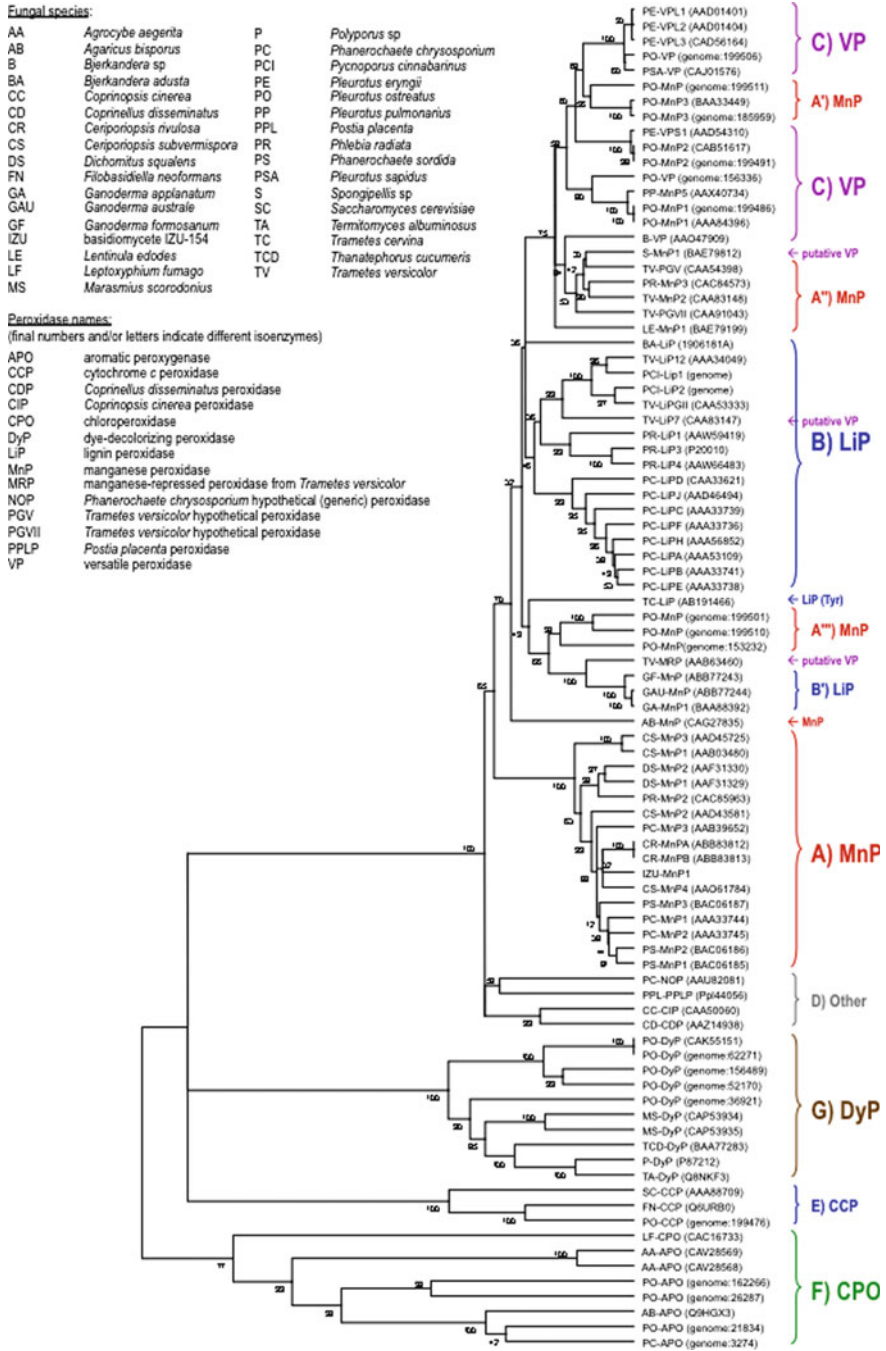


Fig. 3.3 Dendrogram of evolutionary relationships between 87 basidiomycete (and two reference ascomycete) peroxidases, including structural–functional classification based on Ruiz-Dueñas et al. [10] (GeneBank and *P. ostreatus* genome references in parentheses). Amino acid sequence comparisons as Poisson distances and clustering based on UPGMA and “pair-wise deletion” option of MEGA4 [43]

Interestingly, CIP clusters with three other low redox-potential peroxidases from *Coprinellus disseminatus*, and from the genomes of *P. chrysosporium* (NOP) [44] and *Postia placenta* [36] (group **D**), being distantly related to the above large group of ligninolytic peroxidases.

The remaining 21 peroxidases form three groups (evolutionarily very distant from the rest) that include some interesting enzymes, together with basidiomycete CCP (group **E**). The group of CPO-type peroxidases (**F**) is formed by two *Agrocybe aegerita* heme-thiolate peroxidases clustered with a similar peroxidase from *A. bisporus* and four putative CPO-type enzymes – one from the genome of *P. chrysosporium* and the three other from that of *P. ostreatus* – as well as, at a longer distance, with the reference CPO from the ascomycete *L. fumago*. Finally, the last peroxidase group (**G**) corresponds to DyP and includes sequences of the best characterized *Geotrichum* DyP, and several DyP-type enzymes from *Marasmius scorodionius*, *Termitomyces albuminosus*, *P. ostreatus*, and *Polyporus* sp, together with four putative DyP-type sequences from the genome of *P. ostreatus* (Ruiz-Dueñas et al., unpublished results).

In addition to “classical” ligninolytic peroxidases (discussed in Sect. 3.3) the above analysis revealed other basidiomycete peroxidases, including DyP-type and heme-thiolate peroxidases (discussed in Sects. 3.4 and 3.5). The latter present even higher interest than typical CPO because of their ability to catalyze mono-oxygenase reactions on a variety of aromatic compounds [45, 46]. Because of the lack of a published structure, that of related CPO is discussed below as the closest reference. Basidiomycete DyP are still to be thoroughly investigated from both the structural–functional and application points of view, however, its ability to degrade highly recalcitrant dyes that are resistant even to the action of ligninolytic peroxidases [47] also suggest their potential interest as industrial biocatalysts.

3.3 Ligninolytic Peroxidases

Ligninolytic peroxidases, including the LiP, MnP, and VP families [10, 33], form Class II of the superfamily of plant, fungal, and bacterial peroxidases, together with the CIP family from soil basidiomycetes. Structure–function studies of these high redox-potential peroxidases have been performed using a wide array of techniques, including structure analysis by NMR and X-ray diffraction, in combination with stopped-flow spectrophotometry, electron paramagnetic resonance, density functional theory, electron-nuclear double resonance, site-directed mutagenesis, and directed evolution. This multidisciplinary approach has contributed not only to identify the different substrate oxidation sites and structural determinants responsible for other properties of interest [10] but also to improve their catalytic properties and stability to obtain more efficient and robust tailor-made biocatalysts [48–53]. A description of the heme environment and the catalytic sites involved in oxidation of different substrates by ligninolytic peroxidases is provided in the next subsections.

3.3.1 Heme Environment

As in the other members of the superfamily, the heme pocket of ligninolytic peroxidases includes two conserved histidine residues disposed above and below the heme plane (Fig. 3.4a). The second histidine acts as the fifth ligand of the heme iron, occupying a proximal position, while the first one is at a higher distance being, therefore, called distal histidine (by extension, the regions located below and above the heme plane are also called proximal and distal regions).

Four more amino acid residues are conserved at the distal (arginine and phenylalanine) and proximal (aspartate and phenylalanine) sides of the heme pocket in all structurally characterized ligninolytic peroxidases [33], two of them (distal arginine and proximal aspartate) also being conserved in the other members of the superfamily.

The conserved distal histidine and arginine are directly involved in the heterolytic cleavage of H_2O_2 during the two-electron activation of the resting enzyme (containing Fe^{3+}) to form Compound I (containing $\text{Fe}^{4+}=\text{O}$ complex and porphyrin radical) [54]. In the other side of the heme, the N ϵ of the proximal histidine acts as the fifth heme iron ligand, and the strength of this histidine–iron bond modulates the electronegativity of the Fe^{4+} being one of the factors that determine its redox potential in the above-mentioned Compound I, as well as in Compound II (containing $\text{Fe}^{4+}=\text{O}$) formed by one-electron reduction of Compound I by one substrate molecule/ion [55]. For a full discussion on the catalytic mechanism, see Chap. 5.

3.3.2 Manganese Oxidation Site

Basidiomycete MnP and VP oxidize Mn^{2+} to Mn^{3+} in a manganese oxidation site formed by the side-chain carboxylates of three acidic residues (Glu35/36, Glu39/40, and Asp179/175 in MnP/VP from *P. chrysosporium*/*Pleurotus eryngii*) located in front of the most internal heme propionate (with respect to the opening of the main heme channel) and connected to the solvent by a narrow channel [8, 9, 56]. This is illustrated in Figs. 3.2 and 3.5 showing, respectively, the opening of the manganese channel to the solvent, and an axial view of the heme pocket (including the Mn^{2+} ion near the above acidic residues) in the VP crystal structure.

The carboxylates of the above amino acid residues and the heme propionate are responsible for Mn^{2+} binding (two water molecules complete its coordination sphere) and subsequent electron transfer to the peroxide activated heme of MnP and VP. A comparison of the crystal structures in absence and presence of Mn^{2+} (and those of mutated variants unable to bind Mn^{2+}) [8, 9, 60] revealed a variable orientation of the glutamates side chains that suggests a rearrangement during catalysis. This includes (1) an “open-gate” conformation with the glutamate side chains oriented to the solvent (enabling Mn^{2+} access); and (2) a “closed-gate” conformation in which the three acidic side chains fix the Mn^{2+} ion near the propionate carboxylate, where it is finally oxidized.

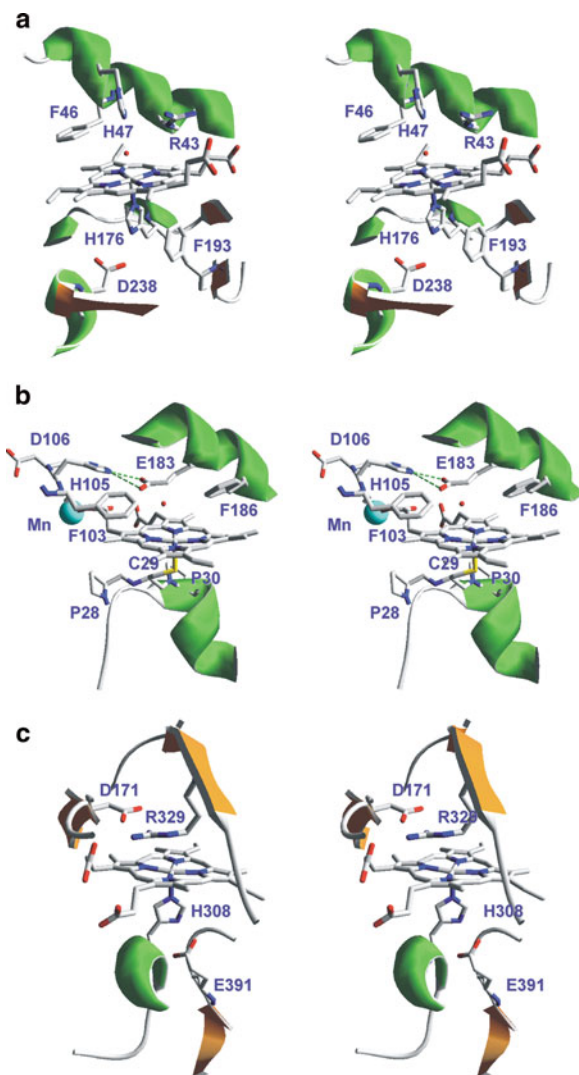


Fig. 3.4 Stereoviews of conserved amino acid residues (and corresponding helices and β -strands) at the proximal (*bottom*) and distal (*top*) sides of the heme pocket in LiP (**a**), CPO (**b**), and DyP (**c**) (some water molecules, as small spheres, and one hydrogen bond are indicated). Based on crystal structures of *P. chrysosporium* LiP (PDB 1LLP), *L. fumigo* CPO (PDB 1CPO) and *Geotrichum* DyP (PDB 2D3Q)

In spite of the high similarity between MnP and VP oxidation sites, crystal structures of wild and recombinant VP, and kinetics of its mutated variants, revealed some significant differences. These result in efficient Mn^{2+} oxidation in the presence of only two of the three residues forming the binding site [9, 61]. Some MnP residues, which are not conserved in VP, could be responsible for these

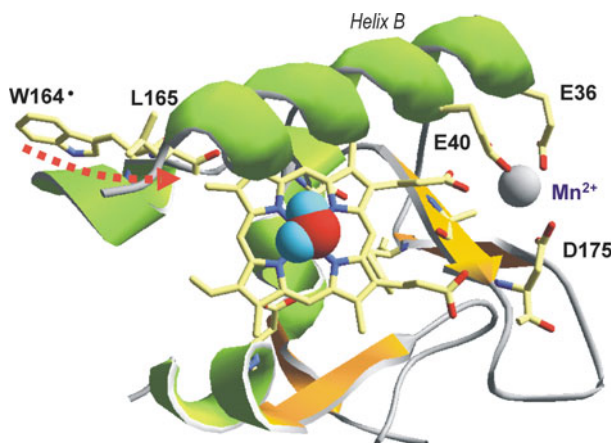


Fig. 3.5 Two substrate oxidation sites in VP: *left*, Oxidation site for high redox-potential substrates (such as VA, RB5, and lignin) by a LRET pathway (*dotted arrow*) from a tryptophan residue forming a catalytic neutral radical (W164 \cdot) to a heme methyl group via a leucine residue [57–59]; *right*, Oxidation site for Mn $^{2+}$, at the internal propionate of heme, involving three acidic amino acid residues [10]. Axial view of the heme region (a water molecule, represented as van der Waals spheres, is seen at the top position on the heme iron)

differences, for example, by contributing to the orientation of the Mn $^{2+}$ ligands in MnP and limiting their mobility. This would be the case of Arg177 forming a salt bridge with Glu35 necessary for the optimal Mn $^{2+}$ ligation geometry in MnP [62] but being absent from VP [9].

3.3.3 LRET Substrate Oxidation at an Exposed Tryptophan

Lignin is the natural substrate of ligninolytic peroxidases. MnP cannot directly oxidize lignin (and nonphenolic lignin model compounds) although it is able to act on its minority phenolic moiety via Mn $^{3+}$ -chelates. In the presence of unsaturated lipids, MnP can also contribute to degradation of nonphenolic lignin by Mn $^{3+}$ initiation of peroxidation reactions that lead to highly reactive lipid radicals [63, 64].

By contrast, the two other ligninolytic peroxidases (LiP and VP) have been demonstrated to directly oxidize nonphenolic lignin model compounds [65–67]. Initially, it was thought that this interaction should be through the main heme access channel (Fig. 3.2), in a similar way to that observed for fungal and plant heme peroxidases oxidizing simple phenolic compounds at this site. In fact, no sooner was the LiP crystal structure solved than the veratryl (3,4-dimethoxybenzyl) alcohol (VA) molecule, a simple nonphenolic aromatic compound, was modeled at the main heme access channel [68]. However, large model compounds (and polymeric lignin) cannot gain access to heme through this channel, whose solvent opening is even smaller than in classical fungal and plant peroxidases [30].

Ligninolytic peroxidases seem to have faced the challenge of overcoming the steric hindrances preventing direct interaction between the heme group and the aromatic lignin polymer by placing an amino acid residue able to form a stable radical at the enzyme surface. This residue is the starting point of a long range electron transfer (LRET) pathway from the enzyme surface, where the substrate is oxidized, to heme (Fig. 3.5, left). The same strategy is followed by other redox proteins, including prokaryotic CCP that oxidizes bulky cytochrome *c* [69].

Although considerable effort has been exerted, ligninolytic peroxidases have not been crystallized as substrate–enzyme complexes, either in the presence of the heterogeneous lignin polymer or with lignin model compounds or other simple aromatic substrates (like VA). Crystallographic and spin-trapping studies provided indirect evidence of a protein radical centered at a tryptophan residue (Trp171) exposed to the solvent in LiP [70, 71]. This protein radical was directly detected for the first time at the equivalent tryptophan residue (Trp164) located at less than 11 Å from heme in VP [57, 58]. Very recently, it has also been detected at Trp171 in a LiP variant, where the tryptophan environment was modified to be similar to that of VP [72].

A few years ago, a different LiP-type peroxidase was reported in the white-rot basidiomycete *Trametes cervina*. This enzyme has an exposed tyrosine residue that seems to be involved in catalysis [73]. Curiously, this catalytic tyrosine occupies the equivalent position to that of an aspartate residue forming the Mn²⁺ oxidation site in MnP and VP. Additional work is necessary to confirm the catalytic role of this amino acid residue.

3.3.4 Influence of the Catalytic Tryptophan Environment

The amino acid residues at the environment of the catalytic tryptophan described above (Fig. 3.6) could be responsible for the differences observed in the oxidation of high redox-potential aromatic substrates by VP and LiP. In this regard, LiP needs redox mediators for oxidation of some compounds that are directly oxidized by VP, such as Reactive Black 5 (RB5) and even polymeric lignin (although model dimers are directly oxidized) [10]. In contrast, VP exhibits a lower efficiency oxidizing VA than LiP.

The lack of LiP activity on RB5 does not seem due to steric hindrances as suggested by Tsukihara et al. [75] but to the existence of a partially negative environment around Trp171 (including Asp264 homologous to VP Arg257, and Asp165 homologous to VP Ser158) compared with the positively charged environment of VP Trp164 (including Lys264 in addition to Arg257) that would favor binding of anionic substrates, such as demonstrated by Ruiz-Dueñas et al. [76].

Conversely, it was demonstrated that three of the five exposed acidic residues around Trp171 in *P. chrysosporium* LiP affected the kinetics of VA oxidation [77] and suggested that a partially acidic environment would stabilize the VA cation radical to act as an enzyme-bond mediator [78]. Interestingly, the RB5-oxidizing activity was

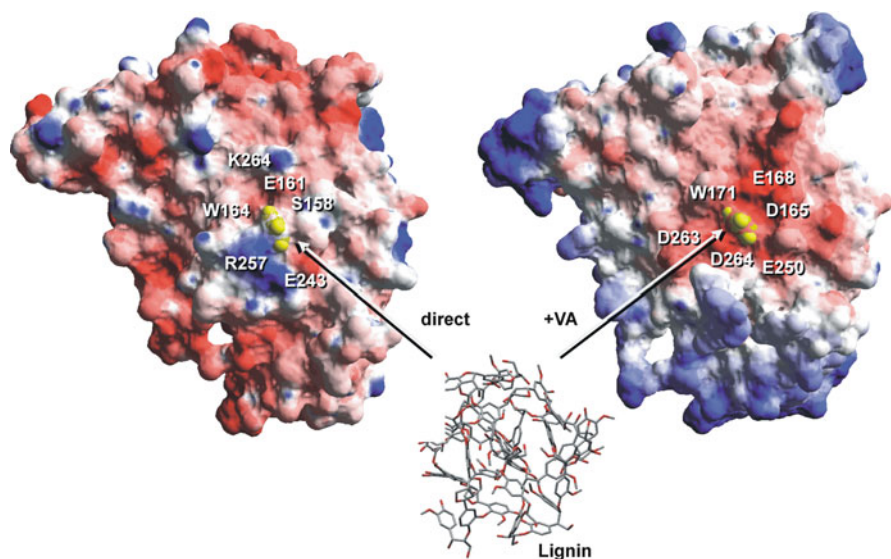


Fig. 3.6 Solvent access surfaces (*colors* represent electrostatic potentials) showing the exposed tryptophan residue (as *yellow* van der Waals spheres) involved in oxidation of lignin and other high redox-potential substrates by VP (**a**) and LiP (**b**). Lignin can be directly oxidized by VP at the tryptophan radical, while LiP requires the simultaneous presence of VA (synthesized by the fungus) acting as an enzyme-bound mediator [74]. Based on VP and LiP crystal structures (PDB 2BOQ and 1LLP, respectively)

restored by adding VA to the R257D VP variant. This suggested stabilization of the VA cation radical by a more acidic Trp164 environment in the mutated VP, similar to that found in LiP. Such behavior is similar to the VA-mediated activity of LiP on RB5 and other substrates, including lignin, and contrasted with their direct oxidation by native VP [79].

Finally, it could also be demonstrated that it is possible to improve VP catalytic properties by modifying the amino acid residues around the catalytic tryptophan. In this sense, simultaneous removal of Arg257 and incorporation of a phenylalanine residue, homologous to LiP Phe267 involved in VA binding [80], resulted in a VP variant with VA transient-state kinetic constants comparable to those of LiP [76].

3.4 Heme-Thiolate Peroxidases

CPO from the sooty mold *L. fumago* is the model enzyme for the heme-thiolate family, and has been described as one of the most versatile of all heme enzymes [81]. Recently, a second type of heme-thiolate peroxidase has been discovered first in *A. aegerita* [82] and latter in cultures and genomes of other basidiomycetes (see Sect. 3.2.2). The new enzyme exhibits a wider biotechnological interest than

CPO due to its ability to transfer oxygen not only to typical CPO substrates but also to different aromatics, such as naphthalene or benzene [45, 46]. Therefore, the name aromatic peroxxygenase has been suggested for the *A. aegerita* heme-thiolate peroxidase [83, 84].

In addition to catalyzing halogenation reactions, heme-thiolate enzyme shares catalytic properties with peroxidases, catalases, and cytochrome P450 monooxygenases, including the ability to perform enantioselective oxygen insertion reactions. These characteristics make them of considerable biotechnological interest in bulk and fine chemistry for selective oxygenations and halogenations, in substitution of more aggressive and less selective chemical processes.

Although CPO was first describe in 1966 [85] it was not until 1995 that its crystal structure was solved [27]. The crystal structure of the novel heme-thiolate aromatic-peroxxygenase from *A. aegerita* has not been yet published, therefore, the CPO molecular structure is described herein as representative for the heme-thiolate peroxidases.

3.4.1 Heme Environment

CPO shares not only catalytic properties but also structural characteristics with both peroxidases and cytochrome P450 enzymes [27]. The heme axial ligand coordinating the catalytic iron corresponds to a thiolate group (Cys29) like in cytochrome P450, although its environment is significantly different (Fig. 3.4b). However, the shared catalytic properties are not exclusively due to this structural determinant, as shown by the fact that the C29H CPO variant retained most of the chlorination, oxygenation, peroxidatic, and catalase activities [86].

On the other hand, a polar environment characterizes the CPO distal side, like in typical heme peroxidases. However, unlike typical peroxidases, which have a second conserved histidine, CPO presents a glutamate residue (Glu183) that seems to play the same role as the catalytic acid–base in peroxide O–O bond cleavage. In fact, Glu183 can be substituted with a histidine residue without completely preventing enzyme activation by H₂O₂ [87].

A histidine residue (His105) is located at the heme distal side in CPO, which is hydrogen bonded to Glu183 and Asp106, conferring to the glutamate side chain high rigidity and the appropriate orientation for catalysis. In the structural arrangement formed by the above residues, only the Glu183 side chain is close enough to the peroxide-binding site to serve a direct catalytic role [27]. In this respect, crystal structures of CPO with different heme coordinating ligands confirmed the rigidity of the active-site architecture with the fixed acid–base catalyst (Glu183) maintaining the hydrogen bond with His105 [88]. Although the above observations explain the mode of Compound I formation in CPO, some results involving chemical modification of histidine residues showed that His105 could be not so critical [89], thus suggesting that some structural flexibility would not affect the CPO half-reaction with H₂O₂.

Additional crystallographic studies of CPO complexes with cyanide and other ligands, allowed to propose a new mechanism of Compound I formation with the incoming H_2O_2 first interacting with Glu138 [90], instead of first binding to heme and then interacting with the catalytic glutamate, as generally considered.

3.4.2 Substrate Oxidation Sites

At least two different catalytic sites have been suggested for the one- and two-electron oxidative reactions catalyzed by CPO [89]. Phenols and large substrates unable to gain access to the heme are presumably oxidized at the enzyme surface by (one-electron) LRET pathways similar to that described in Sect. 3.3.3 for ligninolytic peroxidases, although the catalytic residue exposed to the solvent has not been yet identified.

By contrast, the catalytic site responsible for the halogenation, hydroxylation, and other (two-electron) oxygenation reactions has been better, although not completely, characterized by X-ray crystallography of CPO complexed with several substrates (such as iodide/bromide and cyclopentane-1,3-dione) and other compounds (such as carbon monoxide, thiocyanate, nitrate, acetate, formate and, in a ternary complex, with dimethylsulfoxide and cyanide) [88, 90]. The above substrates bind at the distal side of heme, and the corresponding structures were also useful to establish the mechanism of Compound I formation as discussed above [90].

It has been suggested that the access of typical CPO substrates to the heme pocket is through two (narrow and wide) channels that converge at the heme distal side directly over the $\text{Fe}^{4+}=\text{O}$ center. Kühnel et al. [90] identified three halide-binding sites within the narrow channel suggesting a pathway for the access of halides to the active site. The authors also determined the CPO structure with cyclopentanedione (precursor of the antibiotic caldariomycin synthesized by the fungus *L. fumago*) although the position occupied, sandwiched between the aromatic side chains of Phe186 and Phe103, was considered not to be productive with respect to the chlorination reaction by CPO.

Finally, it is interesting to mention that the above mentioned rigidity at the distal side of heme (involving His105 hydrogen bonds with Glu183 and Asp106) could be related to the observed enantioselectivity of the epoxidation reactions catalyzed by CPO [88].

3.5 Dye-Decolorizing Peroxidases

The first pieces of evidence for the existence of these peroxidases were found in 1995 in a screening for microorganisms decolorizing synthetic dyes [91]. Four years later, the first DyP was purified and characterized from cultures of the *Geotrichum*-type anamorph of a basidiomycete identified as *Thanatephorus cucumeris*, although the

anamorph morphological and other characteristics suggest it could be a different species (most probably *Bjerkandera adusta*). Other DyP-type peroxidases have been reported in different fungi and bacteria [29] but the *Geotrichum* DyP is the best characterized to date.

It has been suggested that DyP-type peroxidases exhibit significant catalytic versatility due to its ability to bleach different dyes (including persistent anthraquinone derivatives), oxidize typical peroxidase substrates such as phenolic compounds [47] and other reactions, such as β -carotene cleavage [92]. Moreover, they exhibit high stability, for example, the *M. scorodnius* peroxidase is exceptionally stable under both high pressure and elevated temperatures [93]. Catalytic properties and stability make this peroxidase family very interesting from a biotechnological point of view, and much work is being carried out to better understand their structure–function relationships. The crystal structure of *Geotrichum* DyP was published 3 years ago by Sugano et al. [28], and two other (bacterial) DyP-type peroxidases have been solved up to now [94]. Only the region surrounding the heme has been exhaustively analyzed, and substrate oxidation sites have not been yet identified.

Three amino acid residues (*Geotrichum* DyP Asp171, His308, and Arg329) are conserved in the heme environment of these peroxidases (Fig. 3.4c). Additionally, an acidic residue (aspartate in *Geotrichum* DyP, Asp391; and glutamate in other DyP-type peroxidases) seems to be also conserved at the heme proximal side. The above histidine residue (His308) acts as the fifth heme iron ligand. However, DyP lacks the distal histidine acting as the acid–base catalyst in Compound I formation. An acidic residue (Asp171) has been proposed to substitute such histidine in DyP, and a unique mechanism, involving Arg329 for charge stabilization, has been suggested for the H_2O_2 reaction in these peroxidases [28].

DyP heme environment has been compared with that of CPO [29]. Although both enzymes differ in the proximal ligand (histidine in DyP and cysteine in CPO), they share the presence of an acidic residue at the distal side (Asp171 in DyP, and Glu183 in CPO) playing the role of an acid–base catalyst. However, some differences exist in the Compound I formation mechanism by both enzymes since Arg329 is thought to assist the reaction in DyP, whereas a histidine residue (His105 mentioned above) has been postulated to be indirectly involved in modulating the acidity/basicity and/or in fixing the position of the carboxyl group of glutamic acid in CPO.

3.6 Conclusions

Heme peroxidases are widespread in prokaryotes, fungi, plants, and animals (over 5,000 entries in the PeroxiBase database) with variable substrate specificities and stabilities, which nowadays can be partially correlated to structural data revealing differences in active-site and global architecture, as well as to the existence of specific oxidation sites and mechanisms (in the near 350 structures deposited in PDB). Some fungal peroxidases have high biotechnological potential as biocatalysts, as suggested by the reactions that they catalyze in nature. Among them, the capacity to

oxidize highly recalcitrant aromatic compounds and dyes is a characteristic of white-rot fungal peroxidases and DyP-type enzymes (in the former case associated to the existence of LRET oxidation mechanisms) while the ability to catalyze site- and stereo-specific hydroxylations and other oxygenation reactions is a characteristic of basidiomycete heme-thiolate peroxidases (related to a specific heme distal-side architecture). Moreover, new heme peroxidases are still to be discovered, as revealed by genome analyses. Structural studies on the most interesting enzymes, including the newest ones, can contribute to the development of peroxidase-based biocatalysts by a combination of rational (e.g., site-directed mutagenesis), nonrational (e.g., directed evolution), and semirational (e.g., combinatorial saturation mutagenesis) approaches. This should result in future new bioproducts and more economic or environmentally friendly peroxidase-based bioprocesses for the production of bulk and fine chemicals, among other industrial and environmental applications.

Acknowledgments The authors thank Martin Hofrichter (University of Zittau, Germany) for useful information on basidiomycete heme-thiolate and DyP-type peroxidases. The financial support of the BIORENEW EU-contract on “White Biotechnology for added value products from renewable plant polymers: Design of tailor-made biocatalyst and new industrial bioprocesses” (NMP2-CT-2006-026456) and the RAPERO Spanish Biotechnology project on “Radical peroxidases” (BIO2008-01533) is acknowledged. F.J.R.-D. thanks the Spanish MICINN for a “Ramón y Cajal” contract.

References

1. Finzel BC, Poulos TL, Kraut J (1984) Crystal structure of yeast cytochrome c peroxidase refined at 1.7 Å resolution. *J Biol Chem* 259:13027–13036
2. Koua D, Cerutti L, Falquet L et al (2009) PeroxiBase: a database with new tools for peroxidase family classification. *Nucleic Acids Res* 37:D261–D266
3. Welinder KG (1992) Superfamily of plant, fungal and bacterial peroxidases. *Curr Opin Struct Biol* 2:388–393
4. Welinder KG, Gajhede M (1993) Structure and evolution of peroxidases. In: Greppin H, Rasmussen SK, Welinder KG et al (eds) *Plant peroxidases: biochemistry and physiology*. University of Copenhagen and University of Geneva, Geneva, pp 35–42
5. Dunford HB (1999) *Heme peroxidases*. Wiley, New York
6. Banci L (1997) Structural properties of peroxidases. *J Biotechnol* 53:253–263
7. Sharp KH, Mewies M, Moody PC et al (2003) Crystal structure of the ascorbate peroxidase-ascorbate complex. *Nat Struct Biol* 10:303–307
8. Sundaramoorthy M, Youngs HL, Gold MH et al (2005) High-resolution crystal structure of manganese peroxidase: substrate and inhibitor complexes. *Biochemistry* 44:6463–6470
9. Ruiz-Dueñas FJ, Morales M, Pérez-Boada M et al (2007) Manganese oxidation site in *Pleurotus eryngii* versatile peroxidase: A site-directed mutagenesis, kinetic and crystallographic study. *Biochemistry* 46:66–77
10. Ruiz-Dueñas FJ, Morales M, García E et al (2009) Substrate oxidation sites in versatile peroxidase and other basidiomycete peroxidases. *J Exp Bot* 60:441–452
11. Kimura S, Ikeda-Saito M (1988) Human myeloperoxidase and thyroid peroxidase, two enzymes with separate and distinct physiological functions, are evolutionarily related members of the same gene family. *Proteins* 3:113–120

12. Zeng J, Fenna RE (1992) X-ray crystal-structure of canine myeloperoxidase at 3 Å resolution. *J Mol Biol* 226:185–207
13. Fiedler TJ, Davey CA, Fenna RE (2000) X-ray crystal structure and characterization of halide-binding sites of human myeloperoxidase at 1.8 angstrom resolution. *J Biol Chem* 275: 11964–11971
14. Singh AK, Singh N, Sharma S et al (2008) Crystal structure of lactoperoxidase at 2.4 angstrom resolution. *J Mol Biol* 376:1060–1075
15. Zederbauer M, Furtmuller PG, Brogioni S et al (2007) Heme to protein linkages in mammalian peroxidases: impact on spectroscopic, redox and catalytic properties. *Nat Prod Rep* 24:571–584
16. Huang LS, Ortiz de Montellano PR (2006) Heme-protein covalent bonds in peroxidases and resistance to heme modification during halide oxidation. *Arch Biochem Biophys* 446:77–83
17. Huang LS, Wojciechowski G, Ortiz de Montellano PR (2006) Role of heme-protein covalent bonds in mammalian peroxidases – Protection of the heme by a single engineered heme-protein link in horseradish peroxidase. *J Biol Chem* 281:18983–18988
18. Furtmüller PG, Zederbauer M, Jantschko W et al (2006) Active site structure and catalytic mechanisms of human peroxidases. *Arch Biochem Biophys* 445:199–213
19. Chelikani P, Fita I, Loewen PC (2004) Diversity of structures and properties among catalases. *Cell Mol Life Sci* 61:192–208
20. Vainshtein BK, Melikadamyán WR, Barynin VV et al (1986) 3-Dimensional structure of catalase from *Penicillium vitale* at 2.0 Å resolution. *J Mol Biol* 188:49–61
21. Vainshtein BK, Melikadamyán WR, Barynin VV et al (1981) 3-Dimensional structure of the enzyme catalase. *Nature* 293:411–412
22. Mate MJ, Zamocky M, Nykyri LM et al (1999) Structure of catalase-A from *Saccharomyces cerevisiae*. *J Mol Biol* 286:135–149
23. Kirkman HN, Galiano S, Gaetani GF (1987) The function of catalase-bound NADPH. *J Biol Chem* 262:660–666
24. Fülöp V, Ridout CJ, Greenwood C et al (1995) Crystal-structure of the di-heme cytochrome-c peroxidase from *Pseudomonas aeruginosa*. *Structure* 3:1225–1233
25. Dias JM, Alves T, Bonifacio C et al (2004) Structural basis for the mechanism of Ca²⁺ activation of the di-heme cytochrome c peroxidase from *Pseudomonas nautica* 617. *Structure* 12:961–973
26. De Smet L, Savvides SN, Van Horen E et al (2006) Structural and mutagenesis studies on the cytochrome c peroxidase from *Rhodobacter capsulatus* provide new insights into structure-function relationships of bacterial di-heme peroxidases. *J Biol Chem* 281:4371–4379
27. Sundaramoorthy M, Turner J, Poulos TL (1995) The crystal structure of chloroperoxidase: A heme peroxidase-cytochrome P450 functional hybrid. *Structure* 3:1367–1377
28. Sugano Y, Muramatsu R, Ichiyanaagi A et al (2007) DyP, a unique dye-decolorizing peroxidase, represents a novel heme peroxidase family. *J Biol Chem* 282:36652–36658
29. Sugano Y (2009) DyP-type peroxidases comprise a novel heme peroxidase family. *Cell Mol Life Sci* 66:1387–1403
30. Ruiz-Dueñas FJ, Martínez AT (2009) Microbial degradation of lignin: How a bulky recalcitrant polymer is efficiently recycled in nature and how we can take advantage of this. *Microb Biotechnol* 2:164–177
31. Kirk TK, Farrell RL (1987) Enzymatic “combustion”: The microbial degradation of lignin. *Annu Rev Microbiol* 41:465–505
32. Kersten P, Cullen D (2007) Extracellular oxidative systems of the lignin-degrading Basidiomycete *Phanerochaete chrysosporium*. *Fungal Genet Biol* 44:77–87
33. Martínez AT (2002) Molecular biology and structure-function of lignin-degrading heme peroxidases. *Enzyme Microb Technol* 30:425–444
34. Martínez AT (2007) High redox potential peroxidases. In: Polaina J, MacCabe AP (eds) *Industrial enzymes: structure, function and applications*. Springer, Berlin, pp 475–486

35. Hammel KE, Cullen D (2008) Role of fungal peroxidases in biological ligninolysis. *Curr Opin Plant Biol* 11:349–355
36. Martínez D, Challacombe J, Morgenstern I et al (2009) Genome, transcriptome, and secretome analysis of wood decay fungus *Postia placenta* supports unique mechanisms of lignocellulose conversion. *Proc Natl Acad Sci USA* 106:1954–1959
37. Martínez AT, Ruiz-Dueñas FJ, Martínez MJ et al (2009) Enzymatic delignification of plant cell wall: from nature to mill. *Curr Opin Biotechnol* 20:348–357
38. Bumpus JA, Tien M, Wright D et al (1985) Oxidation of persistent environmental pollutants by a white rot fungus. *Science* 228:1434–1436
39. Rodríguez E, Nuero O, Guillén F et al (2004) Degradation of phenolic and non-phenolic aromatic pollutants by four *Pleurotus* species: the role of laccase and versatile peroxidase. *Soil Biol Biochem* 36:909–916
40. Dávila-Vázquez G, Tinoco R, Pickard MA et al (2005) Transformation of halogenated pesticides by versatile peroxidase from *Bjerkandera adusta*. *Enzyme Microb Technol* 36:223–231
41. Wang YX, Vázquez-Duhalt R, Pickard MA (2003) Manganese-lignin peroxidase hybrid from *Bjerkandera adusta* oxidizes polycyclic aromatic hydrocarbons more actively in the absence of manganese. *Can J Microbiol* 49:675–682
42. Heinfling A, Martínez MJ, Martínez AT et al (1998) Transformation of industrial dyes by manganese peroxidase from *Bjerkandera adusta* and *Pleurotus eryngii* in a manganese-independent reaction. *Appl Environ Microbiol* 64:2788–2793
43. Tamura K, Dudley J, Nei M et al (2007) MEGA4: Molecular evolutionary genetics analysis (MEGA) software version 4.0. *Mol Biol Evol* 24:1596–1599
44. Larrondo L, Gonzalez A, Perez AT et al (2005) The *nop* gene from *Phanerochaete chrysosporium* encodes a peroxidase with novel structural features. *Biophys Chem* 116:167–173
45. Ullrich R, Hofrichter M (2007) Enzymatic hydroxylation of aromatic compounds. *Cell Mol Life Sci* 64:271–293
46. Ullrich R, Hofrichter M (in press) Novel trends in fungal biooxidation. *The Mycota X: Industrial applications*. Springer, Berlin
47. Kim SJ, Shoda M (1999) Purification and characterization of a novel peroxidase from *Geotrichum candidum* Dec 1 involved in decolorization of dyes. *Appl Environ Microbiol* 65:1029–1035
48. Miyazaki-Imamura C, Oohira K, Kitagawa R et al (2003) Improvement of H₂O₂ stability of manganese peroxidase by combinatorial mutagenesis and high-throughput screening using *in vitro* expression with protein disulfide isomerase. *Protein Eng* 16:423–428
49. Reading NS, Aust SD (2001) Role of disulfide bonds in the stability of recombinant manganese peroxidase. *Biochemistry* 40:8161–8168
50. Miyazaki C, Takahashi H (2001) Engineering of the H₂O₂-binding pocket region of a recombinant manganese peroxidase to be resistant to H₂O₂. *FEBS Lett* 509:111–114
51. Reading NS, Aust SD (2000) Engineering a disulfide bond in recombinant manganese peroxidase results in increased thermostability. *Biotechnol Progr* 16:326–333
52. Ruiz-Dueñas FJ, Morales M, Rencoret J et al (2008) Improved peroxidases (*Peroxidasas mejoradas*). Patent (Spain) P200801292
53. García E, Martínez MJ, Ruiz-Dueñas FJ et al (2009) High redox-potential peroxidases from directed evolution (*Peroxidasas de elevado potencial redox diseñadas por evolución dirigida*). Patent (Spain) application P200930157
54. Hiner ANP, Raven EL, Thorneley RNF et al (2002) Mechanisms of compound I formation in heme peroxidases. *J Inorg Biochem* 91:27–34
55. Banci L, Bertini I, Turano P et al (1991) Proton NMR investigation into the basis for the relatively high redox potential of lignin peroxidase. *Proc Natl Acad Sci USA* 88:6956–6960
56. Gold MH, Youngs HL, Gelpke MD (2000) Manganese peroxidase. *Met Ions Biol Syst* 37:559–586
57. Pérez-Boada M, Ruiz-Dueñas FJ, Pogni R et al (2005) Versatile peroxidase oxidation of high redox potential aromatic compounds: Site-directed mutagenesis, spectroscopic and

- crystallographic investigations of three long-range electron transfer pathways. *J Mol Biol* 354:385–402
58. Pogni R, Baratto MC, Teutloff C et al (2006) A tryptophan neutral radical in the oxidized state of versatile peroxidase from *Pleurotus eryngii*: a combined multi-frequency EPR and DFT study. *J Biol Chem* 281:9517–9526
 59. Ruiz-Dueñas FJ, Pogni R, Morales M et al (2009) Protein radicals in fungal versatile peroxidase: catalytic tryptophan radical in both Compound I and Compound II and studies on W164Y, W164H and W164S variants. *J Biol Chem* 284:7986–7994
 60. Sundaramoorthy M, Kishi K, Gold MH et al (1997) Crystal structures of substrate binding site mutants of manganese peroxidase. *J Biol Chem* 272:17574–17580
 61. Youngs HL, Gelpke MDS, Li DM et al (2001) The role of Glu39 in Mn-II binding and oxidation by manganese peroxidase from *Phanerochaete chrysosporium*. *Biochemistry* 40:2243–2250
 62. Gelpke MDS, Youngs HL, Gold MH (2000) Role of arginine 177 in the Mn^{II} binding site of manganese peroxidase. Studies with R177D, R177E, R177N, and R177Q mutants. *Eur J Biochem* 267:7038–7045
 63. Kapich AN, Korneichik TV, Hatakka A et al (2010) Oxidizability of unsaturated fatty acids and of a non-phenolic lignin structure in the manganese peroxidase-dependent lipid peroxidation system. *Enzyme Microb Technol* 46:136–140
 64. Bao WL, Fukushima Y, Jensen KA et al (1994) Oxidative degradation of non-phenolic lignin during lipid peroxidation by fungal manganese peroxidase. *FEBS Lett* 354:297–300
 65. Mester T, Ambert-Balay K, Ciofi-Baffoni S et al (2001) Oxidation of a tetrameric nonphenolic lignin model compound by lignin peroxidase. *J Biol Chem* 276:22985–22990
 66. Moreira PR, Almeida-Vara E, Malcata FX et al (2007) Lignin transformation by a versatile peroxidase from a novel *Bjerkandera* sp strain. *Int Biodeterior Biodegrad* 59:234–238
 67. Johjima T, Itoh H, Kabuto M et al (1999) Direct interaction of lignin and lignin peroxidase from *Phanerochaete chrysosporium*. *Proc Natl Acad Sci USA* 96:1989–1994
 68. Poulos TL, Edwards SL, Wariishi H et al (1993) Crystallographic refinement of lignin peroxidase at 2 Å. *J Biol Chem* 268:4429–4440
 69. Pelletier H, Kraut J (1992) Crystal structure of a complex between electron transfer partners, cytochrome *c* peroxidase and cytochrome *c*. *Science* 258:1748–1755
 70. Blodig W, Smith AT, Winterhalter K et al (1999) Evidence from spin-trapping for a transient radical on tryptophan residue 171 of lignin peroxidase. *Arch Biochem Biophys* 370:86–92
 71. Choinowski T, Blodig W, Winterhalter K et al (1999) The crystal structure of lignin peroxidase at 1.70 Å resolution reveals a hydroxyl group on the C_β of tryptophan 171: A novel radical site formed during redox cycle. *J Mol Biol* 286:809–827
 72. Smith AT, Doyle WA, Dorlet P et al (2009) Spectroscopic evidence for an engineered, catalytically active Trp radical that creates the unique reactivity of lignin peroxidase. *Proc Natl Acad Sci USA* 106:16084–16089
 73. Miki Y, Tanaka H, Nakamura M et al (2006) Isolation and characterization of a novel lignin peroxidase from the white-rot basidiomycete *Trametes cervina*. *J Fac Agr Kyushu Univ* 51:99–104
 74. Khindaria A, Yamazaki I, Aust SD (1996) Stabilization of the veratryl alcohol cation radical by lignin peroxidase. *Biochemistry* 35:6418–6424
 75. Tsukihara T, Honda Y, Sakai R et al (2008) Mechanism for oxidation of high-molecular-weight substrates by a fungal versatile peroxidase, MnP2. *Appl Environ Microbiol* 74:2873–2881
 76. Ruiz-Dueñas FJ, Morales M, Mate MJ et al (2008) Site-directed mutagenesis of the catalytic tryptophan environment in *Pleurotus eryngii* versatile peroxidase. *Biochemistry* 47:1685–1695
 77. Smith AT, Doyle WA (2006) Engineered peroxidases with veratryl alcohol oxidase activity. Patent (International) WO/2006-114616
 78. Khindaria A, Nie G, Aust SD (1997) Detection and characterization of the lignin peroxidase compound II- veratryl alcohol cation radical complex. *Biochemistry* 36:14181–14185

79. Heinfling A, Ruiz-Dueñas FJ, Martínez MJ et al (1998) A study on reducing substrates of manganese-oxidizing peroxidases from *Pleurotus eryngii* and *Bjerkandera adusta*. FEBS Lett 428:141–146
80. Gelpke MDS, Lee J, Gold MH (2002) Lignin peroxidase oxidation of veratryl alcohol: Effects of the mutants H82A, Q222A, W171A, and F267L. Biochemistry 41:3498–3506
81. Dawson JH, Sono M (1987) Cytochrome P-450 and chloroperoxidase – thiolate-ligated heme enzymes – spectroscopic determination of their active-site structures and mechanistic implications of thiolate ligation. Chem Rev 87:1255–1276
82. Ullrich R, Nuske J, Scheibner K et al (2004) Novel haloperoxidase from the agaric basidiomycete *Agrocybe aegerita* oxidizes aryl alcohols and aldehydes. Appl Environ Microbiol 70:4575–4581
83. Kluge M, Ullrich R, Dolge C et al (2009) Hydroxylation of naphthalene by aromatic peroxygenase from *Agrocybe aegerita* proceeds via oxygen transfer from H₂O₂ and intermediary epoxidation. Appl Microbiol Biotechnol 81:1071–1076
84. Pecyna MJ, Ullrich R, Bittner B et al (2009) Molecular characterization of aromatic peroxygenase from *Agrocybe aegerita*. Appl Microbiol Biotechnol 84:885–897
85. Morris DR, Hager LP (1966) Chloroperoxidase. I. Isolation and properties of crystalline glycoprotein. J Biol Chem 241:1763
86. Yi XW, Mroczko M, Manoj KM et al (1999) Replacement of the proximal heme thiolate ligand in chloroperoxidase with a histidine residue. Proc Natl Acad Sci USA 96:12412–12417
87. Yi XW, Conesa A, Punt PJ et al (2003) Examining the role of glutamic acid 183 in chloroperoxidase catalysis. J Biol Chem 278:13855–13859
88. Sundaramoorthy M, Turner J, Poulos TL (1998) Stereochemistry of the chloroperoxidase active site: crystallographic and molecular-modeling studies. Chem Biol 5:461–473
89. Manoj KM, Hager LP (2008) Chloroperoxidase, a Janus enzyme. Biochemistry 47:2997–3003
90. Kühnel K, Blankenfeldt W, Turner J et al (2006) Crystal structures of chloroperoxidase with its bound substrates and complexed with formate, acetate, and nitrate. J Biol Chem 281:23990–23998
91. Kim SJ, Ishikawa K, Hirai M et al (1995) Characteristics of a newly isolated fungus, *Geotrichum candidum* Dec 1, which decolorizes various dyes. J Ferment Bioeng 79:601–607
92. Scheibner M, Hulsdau B, Zelena K et al (2008) Novel peroxidases of *Marasmius scorodoni* degrade beta-carotene. Appl Microbiol Biotechnol 77:1241–1250
93. Puhse M, Szweda RT, Ma YY et al (2009) *Marasmius scorodoni* extracellular dimeric peroxidase – Exploring its temperature and pressure stability. BBA Proteins Proteomics 1794:1091–1098
94. Zubieta C, Krishna SS, Kapoor M et al (2007) Crystal structures of two novel dye-decolorizing peroxidases reveal a beta-barrel fold with a conserved heme-binding motif. Proteins 69:223–233

Chapter 4

Redox Potential of Peroxidases

Marcela Ayala

Contents

4.1	Introduction	61
4.2	Redox Potential of the Fe(III)/Fe(II) Couple in Heme Proteins	62
4.2.1	Thermodynamics of Ferric Heme Reduction	62
4.2.2	Influence of the Primary Coordination Sphere on Redox Potential	64
4.2.3	Influence of the Protein Matrix on Redox Potential	65
4.3	Redox Potential of Heme Peroxidases	66
4.3.1	Redox Potential of the Catalytic Species	67
4.3.2	Modulation of Redox Potential	68
4.4	Methods to Measure or Estimate Redox Potential of Heme Peroxidases	71
4.5	Conclusions	72
	References	73

Abstract Redox potential of peroxidases greatly influences the range of oxidizable substrates: in principle, peroxidases may only catalyze the oxidation of substrates with lower redox potential. There is substantial information on the factors that modulate the redox potential of heme proteins. Both theoretical and experimental evidence highlight the most significant contributions arising from the interaction of heme iron with the axial ligands, as well as the electrostatic interactions surrounding the heme group. However, for different proteins, the factors contribute to different extents. Understanding the electrochemistry of heme peroxidases is fundamental in order to design enhanced biocatalysts. In this chapter, current knowledge of the forces influencing redox potential of heme peroxidases is reviewed.

4.1 Introduction

Enzymes catalyzing redox reactions in which oxygen serves as the electron acceptor may be divided in two groups: those that catalyze substrate oxidation by electron transfer to the acceptor (oxidases and peroxidases) and those that catalyze substrate

Table 4.1 Reduction reactions using oxygen as electron acceptor catalyzed by heme proteins

Redox reaction	Standard redox potential (E° vs. SHE, V) [1]	Enzymes
$\text{O}_2 + 2\text{H}^+ + 2\text{e}^- \rightleftharpoons \text{H}_2\text{O}_2$	0.070	Oxidases
$\text{O}_2 + 4\text{H}^+ + 4\text{e}^- \rightleftharpoons 2\text{H}_2\text{O}$	1.23	Oxidases
$\text{H}_2\text{O}_2 + 2\text{H}^+ + 2\text{e}^- \rightleftharpoons 2\text{H}_2\text{O}$	1.78	Peroxidases

oxidation by oxygen incorporation into the molecule (monooxygenases and dioxygenases). Theoretically, peroxidases are the most oxidizing enzymes found in nature, according to the redox potential of hydrogen peroxide in Table 4.1.

The ability to both exist in a stable basal state and generate sufficiently oxidizing intermediates in order to specifically transform substrates is the challenge that heme peroxidases face. Redox potential (E°) play a critical role in determining a peroxidase ability to catalyze challenging oxidation reactions. However, it is not the only factor. As in other heme proteins, activity also depends on electrostatic interactions, substrate orientation, and active site topography [2].

How can a simple cofactor, such as heme, give rise to a wide spectrum of protein functionalities? While the Fe(III)/Fe(II) couple has a standard redox potential of 0.77 V, when complexed with a protoporphyrin to form free heme, it may decrease to -0.115 V [3–5]. When heme is introduced into a protein matrix, redox potential shows an impressive variation of around 1 V. The electrochemical data for structurally characterized heme proteins involved in electron transfer and redox catalysis has been compiled at the Heme Protein Database (HPD, <http://heme.chem.columbia.edu/heme>) [6]. The database comprises not only peroxidases but also catalases, oxidases, monooxygenases, and cytochromes. From b-type heme with histidine–tyrosine ligation ($E^\circ = -0.55$ V) to c-type heme with histidine–methionine ligation ($E^\circ = 0.45$ V), the effect of protein matrix shows tremendous versatility in determining the redox state and thus the function of every heme protein. The factors that have been proven to modulate redox potential in heme proteins in general, and peroxidases in particular, will be reviewed in this chapter. In order to design more efficient biocatalysts, assessing the effect of chemical or genetic modifications on redox potential is important to evaluate the design. Thus, the methodology used to determine or estimate redox potential of peroxidases will also be presented.

4.2 Redox Potential of the Fe(III)/Fe(II) Couple in Heme Proteins

4.2.1 Thermodynamics of Ferric Heme Reduction

Early work by Kassner recognized the influence of heme desolvation on the redox potential of heme proteins. This work suggested that the polarity of the heme environment in the protein could be the main modulator of the redox potential

through the preferential stabilization of either the oxidized or reduced forms of iron species [4, 5]. As ferrous heme is neutral and ferric heme has one net positive charge, the latter would be destabilized in a low dielectric media; therefore, the more hydrophobic the heme environment, the more stabilized the ferrous heme and thus the more positive the redox potential would be. Since then, it has been recognized that redox potential modulation is a multifactorial phenomenon, and that the contribution of each factor may vary from protein to protein [7].

The thermodynamic model of the reduction from Fe(III) to Fe(II) in heme proteins, in general, shows that the Gibbs energy change ($\Delta G^{\circ'}$) depends mainly on the bonding interactions at the redox center (ΔG_{cen}) and on the electrostatic interactions between the redox center and the protein and solvent (ΔG_{el}). A third term is related to conformational changes due to redox state (ΔG_{conf}), for example, the tertiary structure conformational change produced upon oxygen binding in hemoglobin and myoglobin; however, this term may be considered negligible for electron transfer in simple proteins.

$$\Delta G^{\circ'} = \Delta G_{\text{cen}} + \Delta G_{\text{el}} + \Delta G_{\text{conf}}.$$

The electrostatic term may be further decomposed in four terms, namely:

- (a) The effect of a low dielectric environment, related to Kassner proposal ($\Delta G_{\text{H}_2\text{O}}$)
- (b) The effect of ions in solution, related to ionic strength (ΔG_{ion})
- (c) The effect of electrostatic interactions between buried heme and buried protein charges (ΔG_{int})
- (d) The effect of electrostatic interactions between buried heme and exposed protein charges (ΔG_{surf})

Due to the difficulty in separating $\Delta G^{\circ'}$ into its different components, an empirical approach is to consider one of the terms constant and assume that the observed differences in $\Delta G^{\circ'}$ are due the other contributing factors. An example of this approach is the selection of a series of heme proteins with the same catalytic site, which are assumed to display the same bonding interactions at the redox center and thus the observed changes are attributed to differences in the electrostatic term [8]. Interesting observations from this simplified model have been made. For example, it has allowed to estimate in a mitochondrial cytochrome *c* the contribution of the desolvation effect described by Kassner, $\Delta G_{\text{H}_2\text{O}}$ [9, 10]; in cases where the heme is buried and thus the electrostatic interactions with buried charges are expected to be high due to the low dielectric environment, it has been estimated ΔG_{int} to be in the range of -6 kJ mol^{-1} for a cytochrome c_{551} , equivalent to a $\Delta E^{\circ'}$ of around 65 mV at 25°C. Finally, the contribution of ΔG_{surf} was found to be 10 kJ mol^{-1} ($E^{\circ'} = -105 \text{ mV}$) compared to a $\Delta G^{\circ'} = -26.4 \text{ kJ mol}^{-1}$ ($E^{\circ'} = 275 \text{ mV}$) for a cytochrome c_{522} , whereas for a cytochrome *c* ΔG_{surf} was -4.6 kJ mol^{-1} ($E^{\circ'} = 48 \text{ mV}$) compared to $\Delta G^{\circ'} = -26.4 \text{ kJ mol}^{-1}$ ($E^{\circ'} = 275 \text{ mV}$).

Another approach is to measure the redox potential at different temperatures and to calculate $\Delta H^{\circ'}$ and $\Delta S^{\circ'}$. However, these thermodynamic terms also depends on both protein intrinsic factors and solvent reorganization effects. In general, the

Table 4.2 Factors influencing the redox potential of heme proteins

	Factor	Effect	References
Primary coordination sphere	Proximal and distal ligand	Influences the stability of different redox states following the hard–soft acid–base principle	[12, 18–23]
	Heme substituents	Electron-withdrawing substituents alter the donor power of the equatorial ligands	[24–27]
Protein matrix	Solvent exposure of heme	A dielectric environment destabilizes ferric heme	[4, 5, 28]
	Electrostatic interactions	Local charges stabilize the ferric heme and decrease the local dielectric	[7, 9, 29–32]

enthalpic contribution is larger than the entropic term [11–16]. The entropic term depends on solvent reorganization and changes in protein structure. Some approximations have been made after a series of assumptions, similar to those described above, such as ignoring the contribution from changes in protein conformation upon reduction. Negative $\Delta S^{\circ'}$ values are observed for metalloproteins in which the metal center is not accessible to the solvent. For peroxidases, however, water molecules are usually present in the active site cavity, thus a positive value for $\Delta S^{\circ'}$ is observed upon heme reduction due to a decreased interaction of water with ferrous heme and therefore a decreased solvent ordering [15]. On the other hand, $\Delta H^{\circ'}$ is mainly determined by the polarity of the heme environment, the donor properties of the heme axial ligand, and the electrostatic interactions between heme and the protein and solvent. It has been observed that a more polar cavity stabilizes ferric heme, therefore resulting in a more positive value for $\Delta H^{\circ'}$ and a decreased value of $E^{\circ'}$. The same effect is observed due to the basic character of the axial ligand, which also favors the oxidized state [16].

The analysis of redox potential modulation in heme proteins has been undertaken through both experimental and theoretical strategies. In particular, the use of simple models such as microperoxidase (MP) and the design of artificial heme proteins or biomimetics has allowed to single out the effect of different factors on redox potential [17, 18]. There are a number of relevant interactions, listed on Table 4.2, related to the thermodynamics terms mentioned above and that have been shown to influence the redox potential of heme proteins and biomimetics. Although they may not entirely explain redox potential modulation, they are the best understood and several examples may be found in the literature.

4.2.2 Influence of the Primary Coordination Sphere on Redox Potential

Regarding the primary coordination sphere of iron, the identity of the axial ligand is critical to determining the chemical reactivity of heme. In general, the interaction between the axial ligand and heme iron follow the hard–soft acid–base principle

(HSAB) [19]. Softer ligands such as methionine sulfur bind with higher affinity to the softer ferrous heme, whereas harder ligands such as histidine imidazole bind preferentially to ferric heme. Thus, soft ligands favor higher redox potentials. Following this line of reasoning, redox potential of bis- and mono-His-ligated MP-8 are -200 and -160 mV, respectively, whereas the value for the His–Met complex is -30 mV [21–23]. Another example using the His–H₂O-ligated MP-11 shows that His–His coordination lowers the redox potential from -134 to -189 mV whereas the His–Met coordination raises the value to -67 mV [12]. Even more important variations were found in cytochrome *c*, with redox potential changing from 300 to 400 mV when varying the identity of the ligand: nitrogen, oxygen, or thiol sulfur [33].

On the other hand, the chemical structure of heme also exerts an important effect on redox potential. The electron withdrawing or donating properties of porphyrin substituents influence in turn the donor power of heme iron equatorial ligands, thus determining the redox potential of that particular heme group [34]. As an example, the electrochemistry of hemochromes, bis-imidazole-ligated hemes, may be compared in order to assess this effect. The redox potential of the bis-imidazole-ligated heme *b* (-235 mV) and Fe(mesoporphyrin IX)(Im)₂ (-285 mV), a model for heme *c*, are significantly lower than the value for hemochrome of heme *a* (-120 mV) [24, 25], which bears a farnesyl group instead of vinyl or thioether moieties. For heme proteins, the effect may be more dramatic, as in the case of blue myoglobin, bearing a Fe(III)(porphycene), with a notably low redox potential of -193 mV, compared to 52 mV for myoglobin [26]. Moreover, the covalent linkage between heme and the protein matrix has been postulated to also exert certain influence on redox potential values. These covalent interactions are present in *c*-type heme proteins (e.g., cytochrome *c*) as thioether linkages, and in animal peroxidases as ester and sulfonium ion bonds, the latter only present in myeloperoxidase (MPO). In the case of MPO, both heme distortion arising from the covalent linkage and the electron withdrawing nature of the positive charge present due to the sulfonium ion are thought to be responsible for decreasing the electron density at the heme group, thus increasing the redox potential of this enzyme [35]. In the case of cytochrome *c*, heme distortion as well as enhancement of the interaction between heme iron and the axial histidine may explain the great range of redox potentials observed for *c*-type heme proteins [36].

4.2.3 Influence of the Protein Matrix on Redox Potential

Beyond the primary coordination sphere, electrostatic interactions serve to modulate the redox potential set by the heme type and axial ligand. Local charges as well as solvent-exposure of heme have been correlated with redox potential in artificial and natural heme proteins. Since 1978, Stellwagen observed an inverse dependence between the redox potential and the exposure of heme to aqueous solvent [28]. On the other hand, the influence of charged residues near the heme group has been analyzed in artificial proteins; for example, the role of negatively charged residues

has been studied in a synthetic heme protein of 124 residues called [H10H24]₂ [37]. The introduction of a glutamic residue at a leucine position in the heme vicinity lowers the redox potential from -156 to -198 mV, presumably by stabilization of ferric heme, whereas the introduction of a glutamine at a glutamic position resulted in a redox potential increase to -104 mV [27]. Regarding biomimetics, the contribution of heme burial has also been measured, showing that the extent to which the heme is buried results in an increase of the redox potential, in line with earlier proposals related to destabilization of the ferric species in a dielectric environment [27, 38–40]. The relative impact of different factors on redox potential may be ranked, in order to provide a rational basis for design of heme proteins: axial coordination (280 mV), metalloporphyrin type (245 mV), heme burial (36–138 mV, up to 500 mV), and local charges (40–135 mV, up to 200 mV) [18].

Theoretical tools have also been employed to understand the electrochemistry of heme proteins. The more successful approaches consider all these factors in order to explain heme electrochemistry. Modern techniques that combine classical continuum electrostatics and molecular mechanics have quantitatively analyzed the modulation of heme redox potential in 42 proteins bearing a, b, and c-type heme and covering an experimental redox potential range from -0.35 to 0.45 V [41]. The strategy considers a low dielectric constant for the protein matrix (4 and 8) as well as the interactions of heme with its ligands, the solvent, and the protein matrix. The model assumes that the effect of the protein on the redox potential may be decomposed in several terms: desolvation energy, interaction with backbone dipoles, and electrostatic interactions with propionates and the rest of the protein. In general, it was observed that heme desolvation raises redox potential, while interaction with propionates is favorable for ferric heme and thus lowers redox potential. Calculations showed a linear correlation that account for 73% of the changes in redox potential. Interestingly, it was shown that there was a poor correlation with redox potential when single terms were considered. For example, heme desolvation accounted for only 20% of the differences observed in redox potential. The conclusion of this theoretical approach and also of this section is that redox potential in heme proteins is not always tuned in the same manner and that different mixtures of forces modulate the redox behavior of each protein.

4.3 Redox Potential of Heme Peroxidases

Redox potential is a catalytically relevant property of heme peroxidases, as in theory, sets the limit for the oxidative ability of the enzyme. An inverse correlation was found between the activity and the redox potential of methoxybenzenes and methoxy-substituted benzyl alcohols for lignin peroxidase (LiP) and horseradish peroxidase (HRP) [42, 43]. These enzymes were able to catalyze the oxidation of methoxybenzenes with redox potential as high as 1.45 V and 1.12 V, respectively [42]. In the case of methoxy-substituted benzyl alcohols, the maximum substrate redox potential was 1.39 V for both enzymes [43]. This type of correlation has allowed ranking enzymes from the more oxidant to the less oxidant. The inverse

correlation between activity and the ionization potential was also observed for the oxidation of polycyclic aromatic compounds. The ionization potential is the energy required to subtract an electron from a molecule. The ionization potential threshold observed for peroxidases are chloroperoxidase (CPO) 8.2 eV [44]; manganese peroxidase 8.1 eV [45, 46]; LiP 7.55 eV [47]; versatile peroxidase 7.42 eV [48]; HRP 7.35 eV [49].

The effect of mutations or chemical modification is mostly measured in terms of changes in peroxidase activity. However, the electron transfer rate depends on the redox potential of the enzyme, so that a more integral characterization should include the electrochemistry of the enzyme. Thus, the modulation of redox potential could also serve for the design of more efficient biocatalysts.

4.3.1 Redox Potential of the Catalytic Species

The importance of combining the ability to exist in a stable basal state and to generate sufficiently oxidizing intermediates for the case of heme peroxidases is explained in terms of the reactivity properties of iron species. In water, free ferrous heme is rapidly oxidized by oxygen to ferric iron, which cannot bind oxygen. However, the protein matrix of oxygen-binding heme proteins such as hemoglobin and myoglobin increases Fe(III)/Fe(II) redox potential relative to free heme, thus stabilizing the reduced state. Moreover, spontaneous oxidation is further reduced *in vivo*, due to the low dielectric environment inside the cell. In comparison, peroxidases display a more negative Fe(III)/Fe(II) redox potential, which allows a stable basal state with a ferric heme, both *in vitro* and *in vivo*. Moreover, the negative redox potential suggests that inside the protein matrix, higher iron oxidation states such as Fe(IV) or Fe(V) would be sufficiently stabilized to be transiently present during the reaction. Additionally, aqueous Fe(III) is able to react with hydrogen peroxide and to generate hydroxyl radicals (Fenton chemistry) [50, 51]; thus, another benefit from a lower redox potential is to prevent the formation of such reactive, unspecific species. Table 4.3 shows the redox potential value of heme peroxidases from the peroxidase–catalase superfamily, according to the classification in Chap. 2, along with other heme proteins with different function for comparison. In this section, the discussion of redox potential will be focused on heme peroxidases belonging to the peroxidase–catalase superfamily, as these enzymes have recognized biotechnological potential.

For peroxidase biocatalysis, the relevant redox couples are Compound I and Compound II, the intermediates present during the catalytic cycle, as described in Chap. 5. However, Fe(III)/Fe(II) redox potential could still be a useful indicator of the oxidizing character of peroxidases. Millis et al. [54] suggested for the first time that the noncatalytic Fe(III)/Fe(II) redox potential could be used to predict the oxidative capacity of a heme peroxidase during turnover. In this work, it was suggested that a more positive Fe(III)/Fe(II) redox potential indicates a higher electron deficiency within the active site, and thus the existence of enzymatic

Table 4.3 Fe(III)/Fe(II) redox potential of various heme proteins

Protein	pH	Redox potential vs. SHE (mV)	Function	References
Cytochrome c	7	247	Mitochondrial electron transfer	[10]
Myoglobin	7	52	Oxygen transport	[26]
Myeloperoxidase	7	5	Innate immune system	[52]
Versatile peroxidase	7.5	5	Ligninolytic activity	[53]
Manganese peroxidase	7	-88 to -93	Ligninolytic activity	[54]
Lignin peroxidase	7	-120 to -140	Ligninolytic activity	[54]
Eosinophil peroxidase	7	-126	Innate immune system	[55]
Chloroperoxidase	6.9	-140	Halogenation of metabolites	[56]
<i>C. cinereus</i> peroxidase	7	-183	Lignification	[15]
Nitrophorin 4	5	-187	NO transport	[57]
Lactoperoxidase	7	-176	Innate immune system	[55]
Cytochrome c peroxidase	6.1	-194	Hydrogen peroxide metabolism	[58]
Horseradish peroxidase	7	-278	Lignification, cell wall formation	[59]
Turnip peroxidase	8	-233 to -160	Lignification, cell wall formation	[60]
Catalase-peroxidase	7	-226	Hydrogen peroxide metabolism	[61]
Human peroxiredoxin	7	-290	Hydrogen peroxide metabolism	[62]
Soybean peroxidase	7	-310	Cell wall formation	[16]

intermediates with higher oxidative capacity. However, no data was shown at that moment.

The two-electron reduction of Compound I to Fe(III) and the one electron reduction of Compound I to Compound II and Compound II to Fe(III) have been estimated by different methods. These methods will be described in the next section, but they differ in the strategy to estimate the redox potential. Two of them rely on spectral determination of equilibrium between redox species [63–65], whereas a third one proposes the use of catalytic measurements [53]. The values obtained with the different methods are shown in Table 4.4. It should be noted these are not standard values. As expected, one of the more oxidant enzymes is the versatile peroxidase, which is able to catalyze the oxidation of Mn(II) to Mn(III) ($E^{\circ'}=1.5$ V). MPO has the highest two-electron redox potential, supporting the fact that only this enzyme is able to catalyze the oxidation of chloride to hypochlorite at neutral pH [72, 73], whereas eosinophil peroxidase performs better at acidic pH [74].

Figure 4.1 shows the correlation between measured redox potentials of Fe(III)/Fe(II) presented in Table 4.3 and estimated redox potentials of Compound II/Fe(III) presented in Table 4.4. In spite of the different methodology, there is a clear tendency for the more oxidant enzymes to present more positive Fe(III)/Fe(II) redox potential values.

4.3.2 Modulation of Redox Potential

The modulation of redox potential in heme peroxidases depends on the factors described in Table 4.2. Iron pentacoordination is conserved among peroxidases, being the most common ligand the N^c from a histidine residue. There are exceptions,

Table 4.4 Estimated redox potentials of heme peroxidases

Enzyme	Redox couple	Redox potential (mV)	References ^a
Horseradish peroxidase	Compound I/Compound II	898; 880	[65, 66]
	Compound II/Fe(III)	900; 870; 890	[53, 63, 66]
Cytochrome c peroxidase	Compound I/Compound II	740	[67]
	Compound II/Fe(III)	1,080	[68]
<i>A. ramosus</i> peroxidase	Compound I/Compound II	915	[69]
	Compound II/Fe(III)	982; 1,180	[53, 69]
Myeloperoxidase	Compound I/Fe(III)	1,160	[70]
	Compound I/Compound II	1,350	[70]
	Compound II/Fe(III)	970	[70]
Lactoperoxidase	Compound I/Fe(III)	1,090	[71]
	Compound I/Compound II	1,140	[71]
	Compound II/Fe(III)	1,040; 980	[53, 71]
Eosinophil peroxidase	Compound I/Fe(III)	1,100	[65]
Versatile peroxidase	Compound II/Fe(III)	1,370	[53]
Soybean peroxidase	Compound II/Fe(III)	950	[53]

^aRespectively, for each redox potential value listed

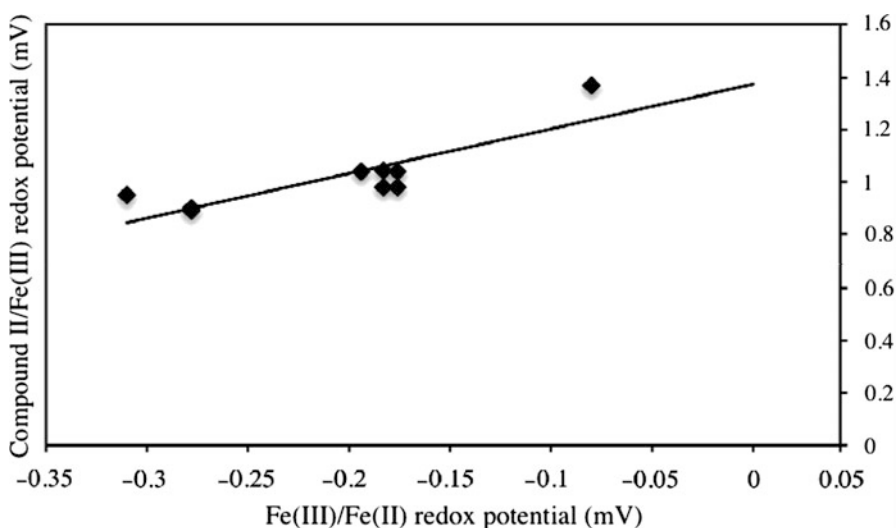


Fig. 4.1 Relation between redox potential of Fe(III)/Fe(II) and Compound II/Fe(III) couples of heme peroxidases. Values were taken from Tables 4.3 and 4.4 for the following proteins: soybean peroxidase, horseradish peroxidase, cytochrome c peroxidase, *C. cinereus* peroxidase, lactoperoxidase, manganese peroxidase

such as the coordination by the cysteine sulfur in CPO from *Caldariomyces fumago* (see Chap. 3). The chemistry of this primary coordination sphere of iron is thus determined by the proximal ligand, with histidine stabilizing higher oxidation states of the heme iron, as described in the previous section. Particularly for heme peroxidases, the combination of a proximal histidine with a polar distal site also enhances the formation of Compound I: both the electron donor effect of histidine (push) and

the hydrogen bonding of the distal histidine and arginine (pull), the “push–pull” concept, facilitate the cleavage of the O–O bond in peroxide [75, 76].

Modulation through diversity in heme chemical structure is small, as most peroxidases contain heme b. However, covalent linkages between the heme and the protein are not present in every peroxidase and might represent a modulating factor. In MPO, the heme is covalently bound to the protein through two ester linkages, as well as through a sulfonium ion linkage. The electron-withdrawing character of the positive charge of the sulfur atom in the sulfonium ion linkage strongly decreases the electron density at the heme iron and thus raises the redox potential of this enzyme (see Table 4.3) [35, 77]. On the other hand, artificial modification of the heme exerts the expected effect when changing the local electron density. Interestingly, this effect is also present when measuring the redox potential of the catalytic species. He et al [78] demonstrated that introduction of diacetyl (electron-withdrawing) groups in the pyrrole ring of HRP increased by 100 mV the redox potential of the Compound I/Compound II couple.

The interactions with residues beyond the primary coordination sphere modulate the heme reactivity to provide high redox potential active sites. Polar amino acids are critical to providing hydrogen bond donors and acceptors that tunes heme chemistry; hydrophobic residues are usually found surrounding the heme group, in particular aromatic residues such as phenylalanine, tryptophan, and histidine that interacts and stabilizes the heme macrocycle through π -stacking and edge-to-face interactions. Moreover, although the general mechanism of peroxidases is similar, there are differences that may further influence the redox potential and thus the oxidative ability of the enzymes. As explained in Chap. 5, in some peroxidases, the temporal electron donor may be an amino acid, instead of the porphyrin ring, thus generating a free radical based on a residue; apparently, the localization of the free radical influences the redox potential of peroxidases.

Beyond the primary coordination sphere, there are recognized factors that modulate the redox potential of heme peroxidases. In particular, the structural factors that tune the chemistry of the proximal histidine are well understood. First, the bond length between heme iron and N^ε from the proximal histidine has been proposed to influence the electron density of heme and thus modulate the redox potential: a longer bond would cause an electron deficiency in the heme, thus increasing the redox potential [79, 80]. The inverse correlation with redox potential may be observed for cytochrome c peroxidase (CcP), LiP, and MPO, with Fe–N^ε lengths of 1.95 ($E^\circ = -0.194$ mV), 2.15 ($E^\circ = -0.120$ mV), and 2.2 Å ($E^\circ = 0.005$ mV), respectively [35, 81]. The relative position of the proximal histidine with respect to heme depends on hydrogen bonding between secondary structure. In LiP, the proximal histidine is displaced around 1 Å from the heme plane, compared to CcP. This displacement arises from a strong hydrogen bond between serine 177 and aspartic 201, which moves the histidine-containing helix away from the heme. The interaction is not present in CcP, as the equivalent 177 position is occupied by an alanine residue [79]. A second factor is related to the basic character of histidine. It has been suggested that strong hydrogen bonding to neighboring residues increases its basicity. The stronger imidazolite character

would stabilize the higher oxidation states, which would lower the redox potential [82, 83]. In this sense, the most important residue is the conserved aspartate in the proximal cavity, which forms a hydrogen bond with the proximal histidine. Substitution with residues that modifies the hydrogen bond network would have an effect on the redox potential of the Fe(III)/Fe(II) couple. In line with this reasoning, substitution with a glutamic residue increased the redox potential of CcP by 70 mV [84], and in *C. cinereus* peroxidase (CiP), the substitution with asparagine lowered the redox potential [85]. However, in MnP, the substitution with a glutamic residue lowered the redox potential [86]. It is thus important to bear in mind the multifactorial character of redox potential modulation and the variable weight that the contribution factors may have, depending on the protein context.

It is also possible to notice a relation between the position of the free radical in Compound I and the redox potential. For example, substitutions of the proximal phenylalanine in HRP with tyrosine or tryptophan residues favors the generation of a Compound I with a residue-based radical, similar to that in CcP [87–89]; in particular, the F221W HRP mutant has an increased redox potential of -178 mV, closer to that of CcP [88]. Experimental evidence and theoretical studies suggest that a lower polarity of the heme proximal environment might favor the retention of the porphyrin-based radical, as determined for HRP, CcP, and ascorbate peroxidase (APX) [89–93]. Fungal peroxidases with higher redox potential and wider biotechnological interest generate a Compound I with a protein-based radical, such as LiP [94, 95] and versatile peroxidase (VP) [96]. These enzymes may be utilized as models to create peroxidases with higher oxidative ability combined with other desirable properties, such as stability and specificity.

4.4 Methods to Measure or Estimate Redox Potential of Heme Peroxidases

In general, the redox potential data for Compound I and Compound II is unavailable. Direct methods such as cyclic voltammetry cannot be used due to the short lifetime of the activated intermediates and irreversibility of the reactions to generate them. The methods that may be found in the literature to estimate redox potential of the catalytic species, Compound I and Compound II, are redox titrations [64, 97, 98], spectroelectrochemistry [99], and catalytic-based estimation [53].

Redox titrations involve determination of equilibrium between the enzyme and a redox agent of known redox potential. The method requires a redox agent with redox potential close to the protein of interest, to ensure reversibility. The protein is exposed to different concentrations of the redox agent, and once equilibrium is attained, the half cell potential is measured with electrodes and the oxidation–reduction state of the proteins is measured by some physical technique, usually UV–Vis spectrophotometry. The concentration of the oxidized and reduced forms is determined at isosbestic points, and thus spectral characterization of redox species (ferric enzyme,

Compound I and Compound II) is required. The standard redox potential is then calculated from the Nernst equation. Errors in redox potentials estimated with this method may be in the order of ± 10 mV. This is the most commonly used method to determine redox potential of peroxidases [63, 66, 68, 69], and the redox agent is frequently K_3IrCl_6 with $E^\circ = 0.93$ V. However, it has been discussed that the species present in the equilibrium might not be equivalent to Compound I and Compound II formed in the presence of peroxide [100]. However, this drawback may be overcome in a recently reported modification of this method [64, 65]. By using stopped-flow spectrophotometry, it has been possible to utilize hydrogen peroxide as the redox agent, with errors of ± 3 mV or less. The redox potentials for mammalian peroxidases in Table 4.4 have been determined following this approach [65, 70, 71].

While the redox titration method is potentiometric, the spectroelectrochemistry method is potentiostatic [99]. In this method, the protein solution is introduced into an optically transparent thin layer electrochemical cell. The potential of the transparent electrode is held constant until the ratio of the oxidized to reduced forms of the protein attains equilibrium, according to the Nernst equation. The oxidation–reduction state of the protein is determined by directly measuring the spectra through the transparent electrode. In this method, as in the redox titration method, the spectral characterization of redox species is required. A series of potentials are sequentially potentiostated so that different oxidized/reduced ratios are obtained. The data is then adjusted to the Nernst equation in order to calculate the standard redox potential of the proteic species. Errors in redox potentials estimated with this method may be in the order of ± 3 mV.

Another option is to estimate the redox potential through catalytic measurements. According to the electron transfer theory developed by Marcus, there is a semilogarithmic correlation between the rate constant and the redox potentials of the enzyme and the substrate [101]. Using a series of phenols with increasingly electron-withdrawing *p*-substituents, the redox potentials for five peroxidases from plant, fungal, and animal origin were estimated [53]. Voltammetric determination of Fe(III)/Fe(II) redox potential is usually accomplished at pH 7, not at the optimal pH for catalysis. The catalytic data utilized in this method is obtained at the optimum pH for each enzyme; thus, it is likely that redox potential estimated in this way may complement the information on the oxidative abilities of peroxidases.

4.5 Conclusions

The complex task of understanding the electrochemistry of heme peroxidases has benefited from combining both experimental and theoretical tools. To date, more than 70% of the factors determining redox potential in heme proteins can be accounted for. More powerful calculations and new experimental techniques will undoubtedly lead to a more detailed comprehension of redox potential modulation; in this way, redox potential could be another criterion when designing new or better

enzymes. The design would then consider the global performance of a biocatalyst: specificity, stability, and oxidative ability.

Acknowledgments Funding from Conacyt 56718 and DGAPA 212510 is acknowledged.

References

1. Atkins P (1997) Physical chemistry. W.H. Freeman, New York
2. Cusanovich MA, Hazzard JT, Meyer TE et al (1989) Electron transfer mechanisms in heme proteins. *J Macromol Sci A* 26:433–443
3. Shack J, Clark WM (1947) Metalloporphyrins: VI. Cycles of changes in systems containing heme. *J Biol Chem* 171:143–187
4. Kassner RJ (1973) Theoretical model for the effects of local nonpolar heme environments on the redox potentials in cytochromes. *J Am Chem Soc* 9:2674–2677
5. Kassner RJ (1972) Effects of nonpolar environments on the redox potentials of heme complexes. *Proc Natl Acad Sci USA* 69:2263–2167
6. Reedy CJ, Elvekrog MM, Gibney BR (2007) Development of a heme protein structure-electrochemical function database. *Nucleic Acids Res* 36:D307–13
7. Moore GR, Pettigrew GW, Rogers NK (1986) Factors influencing redox potentials of electron transfer proteins. *Proc Natl Acad Sci USA* 83:4998–4999
8. Leitch FA, Moore GR, Pettigrew GW (1984) Structural basis for the variation of pH-dependent redox potentials of *Pseudomonas* cytochromes c-551. *Biochemistry* 23:1831–1838
9. Churg AK, Warshel A (1986) Control of the redox potential of cytochrome and microscopic dielectric effects in proteins. *Biochemistry* 25:1675–1681
10. Flatmark T (1967) Multiple molecular forms of bovine heart cytochrome c: V. A comparative study of their physicochemical properties and their reactions in biological systems. *J Biol Chem* 24:2454–2459
11. Battistuzzi G, Borsari M, Rainieri A et al (2002) Redox thermodynamics of the Fe³⁺/Fe²⁺ couple in horseradish peroxidase and its cyanide complex. *J Am Chem Soc* 124:26–27
12. Battistuzzi G, Borsari M, Cowan JA et al (2002) Control of cytochrome c redox potential: axial ligation and protein environment effects. *J Am Chem Soc* 124:5315–5324
13. Battistuzzi G, Borsari M, Cowan JA et al (1999) Redox chemistry and acid–base equilibria of mitochondrial plant cytochromes c. *Biochemistry* 38:5553–5562
14. Battistuzzi G, Borsari M, Sola M (2001) Medium and temperature effects on the redox chemistry of cytochrome c. *Eur J Inorg Chem* 2001:2989–3004
15. Battistuzzi G, Bellei M, De Rienzo F et al (2006) Redox properties of the Fe³⁺/Fe²⁺ couple in *Arthromyces ramosus* class II peroxidase and its cyanide adduct. *J Biol Inorg Chem* 11:586–592
16. Battistuzzi G, Bellei M, Borsari M et al (2005) Axial ligation and polypeptide matrix effects on the reduction potential of heme proteins probed on their cyanide adducts. *J Biol Inorg Chem* 10:643–651
17. Marques HM (2007) Insights into porphyrin chemistry provided by the microperoxidases, the haempeptides derived from cytochrome c. *Dalton Trans* 39:4371–4385
18. Reedy CJ, Gibney BR (2004) Heme protein assemblies. *Chem Rev* 104:617–649
19. Pearson RG (1963) Hard and soft acids and bases. *J Am Chem Soc* 85:3533–3539
20. Tezcan FA, Winkler JR, Gray HB (1988) Effects of ligation and folding on reduction potentials of heme proteins. *J Am Chem Soc* 120:13383–13388
21. Harbury HA, Loach PA (1960) Oxidation-linked proton functions in heme octa- and undecapeptides from mammalian cytochrome c. *J Biol Chem* 235:3640–3645

22. Harbury HA, Cronin JR, Fanger MW et al (1965) Complex formation between methionine and a heme peptide from cytochrome c. *Proc Natl Acad Sci USA* 54:1658–1664
23. Santucci R, Reinhard H, Brunori M (1988) Direct electrochemistry of the undecapeptide from cytochrome c (microperoxidase) at a glassy carbon electrode. *J Am Chem Soc* 110:8536–8537
24. Vanderkooi G, Stotz E (1966) Oxidation-reduction potentials of heme a hemochromes. *J Biol Chem* 241:3316–3323
25. Vanderkooi G, Stotz E (1966) The two forms of the imidazole hemochrome of heme a: a new model for cytochrome a. *J Biol Chem* 241:2260–2267
26. Hayashi T, Dejima H, Matsuo T et al (2002) Blue myoglobin reconstituted with an iron porphycene shows extremely high oxygen affinity. *J Am Chem Soc* 124:11226–11227
27. Shifman JM, Gibney BR, Sharp RE et al (2000) Heme redox potential control in de novo designed four- α -helix bundle proteins. *Biochemistry* 39:14813–14821
28. Stellwagen E (1978) Haem exposure as the determinate of oxidation–reduction potential of haem proteins. *Nature* 275:73–74
29. Gunner MR, Alexov E, Torres E et al (1997) The importance of the protein in controlling the electrochemistry of heme metalloproteins: methods of calculation and analysis. *J Biol Inorg Chem* 2:126–134
30. Warshel A, Papazyan A, Muegge IJ (1997) Microscopic and semimacroscopic redox calculations: what can and cannot be learned from continuum models. *J Biol Inorg Chem* 2:143–152
31. Gunner MR, Alexov E (2000) A pragmatic approach to structure based calculation of coupled proton and electron transfer in proteins. *Biochim Biophys Acta* 1458:63–87
32. Mao JJ, Hauser K, Gunner MR (2003) How cytochromes with different folds control heme redox potentials. *Biochemistry* 42:9829–9840
33. Wallace CJA, Clark-Lewis I (1992) Functional Role of heme ligation in cytochrome c: effects of replacement of methionine 80 with natural and non-natural residues by semi-synthesis. *J Biol Chem* 267:3852–3861
34. Rosales-Hernandez MC, Correa-Basurto J, Flores-Sandoval C et al (2007) Theoretical study of heme derivatives under DFT calculations. *Theochem* 804:81–88
35. Zederbauer M, Furtmuller P, Brogioni S et al (2007) Heme to protein linkages in mammalian peroxidases: impact on spectroscopic, redox and catalytic properties. *Nat Prod Rep* 24:571–584
36. Bowman SE, Bren KL (2008) The chemistry and biochemistry of heme c: functional bases for covalent attachment. *Nat Prod Rep* 25:1118–1130
37. Robertson DE, Farid RS, Moser CC (1994) Design and synthesis of multi-haem proteins. *Nature* 368:425–432
38. Benson DR, Hart BR, Zhu X et al (1995) Design, synthesis and circular dichroism investigation of a peptide-sandwiched mesoheme. *J Am Chem Soc* 117:8501–8510
39. Holm RH, Kennepohl P, Solomon EI (1996) Structural and functional aspects of metal sites in biology. *Chem Rev* 96:2239–2314
40. Gibney BR, Isogai Y, Rabanal F et al (2000) Self-assembly of heme A and heme B in a designed four-helix bundle: implications for a cytochrome c oxidase maquette. *Biochemistry* 39(11041–11049):2
41. Zheng Z, Gunner MR (2009) Analysis of the electrochemistry of hemes with Ems spanning 800 mV. *Proteins* 75:719–734
42. Kersten PJ, Kalyanaraman B, Hammel KE et al (1990) Comparison of lignin peroxidase, horseradish peroxidase and laccase in the oxidation of methoxybenzenes. *Biochem J* 268:475–480
43. Hong F, Jönsson LJ, Lundquist K et al (2006) Oxidation capacity of laccases and peroxidases as reflected in experiments with methoxy-substituted benzyl alcohols. *Appl Biochem Biotechnol* 129–132:303–319

44. Ayala M, Robledo NR, Lopez-Munguia A et al (2000) Substrate specificity and ionization potential in chloroperoxidase-catalyzed oxidation of diesel fuel. *Environ Sci Technol* 34:2804–2809
45. Bogan BW, Lamar RT (1995) One-electron oxidation in the degradation of creosote polycyclic aromatic hydrocarbons by *Phanerochaete chrysosporium*. *Appl Environ Microbiol* 61:2631–2635
46. Bogan BW, Lamar RT, Hammel KE (1996) Fluorene oxidation in vivo by *Phanerochaete chrysosporium* and in vitro during manganese peroxidase-dependent lipid peroxidation. *Appl Environ Microbiol* 62:1788–1792
47. Hammel KE, Kalyanaraman B, Kirk TKJ (1986) Oxidation of polycyclic aromatic hydrocarbons and dibenzo[p]-dioxins by *Phanerochaete chrysosporium* ligninase. *J Biol Chem* 261:16948–16952
48. Wang Y, Vazquez-Duhalt R, Pickard MA (2003) Manganese-lignin peroxidase hybrid from *Bjerkandera adusta* oxidizes polycyclic aromatic hydrocarbons more actively in the absence of manganese. *Can J Microbiol* 49:675–682
49. Cavalieri E, Rogan E (1985) Role of radical cations in aromatic hydrocarbon carcinogenesis. *Environ Health Perspect* 64:69–84
50. Barb WG, Baxendale JH, Hargrave R (1951) Reactions of ferrous and ferric ions with hydrogen peroxide Part 2. The ferric ion reaction. *Trans Faraday Soc* 47:591–616
51. Walling C, Goosen A (1973) Mechanism of the ferric ion catalyzed decomposition of hydrogen peroxide. Effect of organic substrates. *J Am Chem Soc* 95:2987–2991
52. Battistuzzi G, Bellei M, Zederbauer M et al (2006) Thermodynamics of the Fe(III)/Fe(II) couple of human Myeloperoxidase in its high-spin and low-spin forms. *Biochemistry* 45:12750–12755
53. Ayala M, Roman R, Vazquez-Duhalt R (2007) A catalytic approach to estimate the redox potential of heme-peroxidases. *Biochem Biophys Res Commun* 357:804–808
54. Millis CD, Cai D, Stankovich MT et al (1989) Oxidation–reduction potentials and ionization states of extracellular peroxidases from the lignin-degrading fungus *Phanerochaete chrysosporium*. *Biochemistry* 28:8484–8489
55. Battistuzzi G, Bellei M, Vlasits J et al (2010) Redox thermodynamics of lactoperoxidase and eosinophil peroxidase. *Arch Biochem Biophys* 494:72–77
56. Makino R, Chiang R, Hager LP (1976) Oxidation-reduction potential measurements on chloroperoxidase and its complexes. *Biochemistry* 15:4748–4754
57. Taniguchi I, Kai A, Mie Y et al (2004) Spectroelectrochemical study on a function of nitrophorin-4, a heme protein of insecto. Abstract no. 731, 205th meeting of the Electrochemical Society
58. Conroy CW, Tyma P, Daum PH et al (1978) Oxidation-reduction potential measurements of cytochrome c peroxidase and pH dependent spectral transitions in the ferrous enzyme. *Biochim Biophys Acta* 537:62–69
59. Yamada H, Makino R, Yamazaki I (1975) Effects of 2, 4- substituents of deuterio heme upon redox potentials of horseradish peroxidases. *Arch Biochem Biophys* 169:344–353
60. Ricard J, Mazza G, William RJP (1972) Oxidation reduction potentials and ionization states of two turnip peroxidases. *Eur J Biochem* 28:566–578
61. Bellei M, Jakopitsch C, Battistuzzi G et al (2006) Redox thermodynamics of the ferric–ferrous couple of wild-type *Synechocystis* KatG and KatG(Y249F). *Biochemistry* 45:4678–4774
62. Cox AG, Peskin AV, Paton LN et al (2009) Redox potential and peroxide reactivity of human peroxiredoxin. *Biochemistry* 48:6495–6501
63. Hayashi Y, Yamazaki I (1979) The oxidation–reduction potentials of compound I/compound II and compound II/ferric couples of horseradish peroxidases A2 and C. *J Biol Chem* 254:101–106
64. Sorlie M, Seefeldt LC, Parker VD (2000) Use of stopped-flow spectrophotometry to establish midpoint potentials for redox proteins. *Anal Biochem* 287:118–125

65. Arnhold J, Furtmuller PG, Regelsberger G et al (2001) Redox properties of the couple compound I/native enzyme of myeloperoxidase and eosinophil peroxidase. *Eur J Biochem* 268:5142–5148
66. Farhangrazi ZS, Fosset ME, Powers LS et al (1995) Variable temperature spectroelectrochemical study of horseradish peroxidase. *Biochemistry* 34:2866–2871
67. Mondal MS, Fuller HA, Armstrong FA (1996) Direct measurement of the reduction potential of catalytically active cytochrome c peroxidase Compound I: voltammetric detection of a reversible, cooperative two-electron transfer reaction. *J Am Chem Soc* 118:263–264
68. Purcell WL, Erman JE (1976) Cytochrome c peroxidase catalyzed oxidations of substitution inert iron II complexes. *J Am Chem Soc* 98:7033–7037
69. Farhangrazi ZS, Copeland BR, Nakayama T et al (1994) Oxidation-reduction properties of compounds I and II of *Arthromyces ramosus* peroxidase. *Biochemistry* 33:5647–5652
70. Furtmuller PG, Arnhold J, Jantschko W et al (2003) Redox properties of the couples compound I/compound II and compound II/native enzyme of human myeloperoxidase. *Biochem Biophys Res Commun* 301:551–557
71. Furtmuller PG, Arnhold J, Jantschko W et al (2005) Standard reduction potentials of all couples of the peroxidase cycle of lactoperoxidase. *J Inorg Biochem* 99:1220–1229
72. Furtmüller PG, Burner U, Obinger C (1998) Reaction of myeloperoxidase compound I with chloride, bromide, iodide and thiocyanate. *Biochemistry* 37:17923–17930
73. Furtmüller PG, Obinger C, Hsuanyu Y et al (2000) Mechanism of reaction of myeloperoxidase with hydrogen peroxide and chloride ion. *Eur J Biochem* 267:5858–5864
74. Arnhold J, Monzani E, Furtmüller PG et al (2006) Kinetics and thermodynamics of halide and nitrite oxidation by mammalian heme peroxidases. *Eur J Inorg Chem* 19:3801–3811
75. Poulos TL (1988) Heme enzyme crystal structures. *Adv Inorg Biochem* 7:1–36
76. Dawson JH (1988) Probing structure-function relations in heme-containing oxygenases and peroxidases. *Science* 240:433–439
77. Fiedler TJ, Davey CA, Fenna RE (2000) X-ray crystal structure and characterization of halide-binding sites of human myeloperoxidase at 1.8 Å resolution. *J Biol Chem* 275:11964–11971
78. He B, Sinclair R, Copeland BR et al (1996) The structure-function relationship and reduction potentials of high oxidation states of myoglobin and peroxidase. *Biochemistry* 35:2413–2420
79. Banci L (1997) Structural properties of peroxidases. *J Biotechnol* 53:253–263
80. Piontek K, Glumoft T, Winterhalter K (1993) Low pH crystal structure of glycosylated lignin peroxidase from *Phanerochaete chrysosporium* at 2.5 Å resolution. *FEBS Lett* 315:119–124
81. Choinowski T, Błodig W, Winterhalter KH et al (1999) The crystal structure of lignin peroxidase at 1.70 Å resolution reveals a hydroxy group on the C β of tryptophan 171: a novel radical site formed during the redox cycle. *J Mol Biol* 286:809–827
82. Banci L, Bertini I, Turano P et al (1991) Proton NMR investigation into the basis for the relatively high redox potential of lignin peroxidase. *Biochemistry* 88:6956–6960
83. Poulos TL, Kraut J (1981) The stereochemistry of peroxidase catalysis. *J Biol Chem* 255:8199–8205
84. Goodin DB, McRee DE (1993) The Asp-His-Fe triad of cytochrome c peroxidase controls the reduction potential, electronic structure and coupling of the tryptophan free radical to the heme. *Biochemistry* 32:3313–3324
85. Ciaccio C, Rosati A, De Sanctis G et al (2003) Relationships of ligand binding, redox properties, and protonation in *Coprinus cinereus* peroxidase. *J Biol Chem* 278:18730–18737
86. Santucci R, Bongiovanni C, Marini S et al (2000) Redox equilibria of manganese peroxidase from *Phanerochaete chrysosporium*: functional role of residues on the proximal side of the haem pocket. *Biochem J* 349:85–90
87. Miller VP, Goodin DB, Friedman AE et al (1995) Horseradish peroxidase Phe172Tyr mutant. Sequential formation of Compound I with a porphyrin radical cation and a protein radical. *J Biol Chem* 270:181413–181419

88. Morimoto A, Tanaka M, Takahashi S et al (1998) Detection of a tryptophan radical as an intermediate species in the reaction of horseradish peroxidase mutant Phe221Trp and hydrogen peroxide. *J Biol Chem* 273:14753–14760
89. Wirstam M, Blomberg MRA, Siegbahn PEM (1999) Reaction mechanism of compound I formation in heme peroxidases: a density functional theory study. *J Am Chem Soc* 121:10178–10185
90. Bonagura CA, Sundaramoorthy M, Pappa HS et al (1996) An engineered cation site in cytochrome c peroxidase alters the reactivity of the redox active tryptophan. *Biochemistry* 35:6107–6115
91. Jensen GM, Bunte SW, Warshel A et al (1998) Energetics of cation radical formation at the proximal active site tryptophan of cytochrome c peroxidase and ascorbate peroxidase. *J Phys Chem B* 102:8221–8228
92. deVisser SP, Shaik S, Sharma PK et al (2003) Active species of horseradish peroxidase HRP and cytochrome P450: two electronic chameleons. *J Am Chem Soc* 125:15779–15788
93. Barrows TP, Bhaskar B, Poulos TL (2004) Electrostatic control of the tryptophan radical in cytochrome c peroxidase. *Biochemistry* 43:8826–8834
94. Blodig W, Smith AT, WA D et al (2001) Crystal structures of pristine and oxidatively processed lignin peroxidase expressed in *Escherichia coli* and of the W171F variant that eliminates the redox active tryptophan 171. Implications on the reaction mechanism. *J Mol Biol* 305:851–861
95. Miki Y, Tanaka H, Nakamura M et al (2006) Isolation and characterization of a novel lignin peroxidase from the white-rot basidiomycete *Trametes cervina*. *J Fac Agr Kyushu Univ* 5199–5204
96. Perez-Boada M, Ruiz-Duenas FJ, Pogni R et al (2005) Versatile peroxidase oxidation of high redox potential aromatic compounds: site-directed mutagenesis, spectroscopic and crystallographic investigation of three long-range electron transfer pathways. *J Mol Biol* 354:385–402
97. Dutton PL (1978) Redox potentiometry: determination of midpoint potentials of oxidation-reduction components of biological electron-transfer systems. *Methods Enzymol* 54:411–435
98. Wilson GS (1978) Determination of oxidation-reduction potentials. *Methods Enzymol* 54:396–410
99. Heineman WR, Norris BJ, Goelz JF (1975) Measurement of enzyme E° values by optically transparent thin layer electrochemical cells. *Anal Chem* 47:79–84
100. Fergusson RR (1956) On the oxidation of peroxidase by one-electron oxidizing agents. *J Am Chem Soc* 78:741–745
101. Marcus RA, Sutin N (1985) Electron transfers in chemistry and biology. *Biochim Biophys Acta* 811:265–322

Chapter 5

Catalytic Mechanisms of Heme Peroxidases

Paul R. Ortiz de Montellano

Contents

5.1	Introduction	80
5.2	Peroxidase Catalytic Cycle	80
5.2.1	Ferric Peroxidase	82
5.2.2	Compound 0	83
5.2.3	Compound I: Porphyrin Radical	83
5.2.4	Compound I: Protein Radical	84
5.2.5	Compound II	85
5.2.6	Compound III	85
5.3	Self-Processing of Peroxidases	86
5.3.1	Protein Modifications	86
5.3.2	Heme-Protein Crosslinking	88
5.3.3	Heme Modification by Metabolites	89
5.4	Substrate Oxidations	93
5.4.1	Oxidative Properties	93
5.4.2	One-Electron Oxidations	94
5.4.3	Two-Electron Oxidations	98
5.5	Conclusions	101
	References	102

Abstract The hemoprotein peroxidases produce a reactive intermediate, Compound I, whose reactions are controlled by the protein environment. In conventional peroxidases with a histidine iron ligand, access to the Compound I ferryl species is restricted by the protein, favoring the transfer of single electrons from the substrate to an exposed heme edge. If the protein has a suitably placed oxidizable residue such as a tyrosine or tryptophan, it may be preferentially oxidized by the initial Compound I to give an alternative Compound I in which a ferryl species is paired with a protein rather than porphyrin radical cation. In conventional peroxidases, only small substrates have ready access to the ferryl oxygen and undergo a direct two-electron oxidation, although larger substrates can appear to undergo a two-electron oxidation through the stepwise removal of two electrons. In contrast, peroxidases with a thiolate iron ligand have more open distal active sites and are

able to catalyze a range of two-electron oxidations in addition to one-electron peroxidative transformations.

5.1 Introduction

The hemoprotein peroxidases are ubiquitous proteins that catalyze the one-electron oxidation of their substrates employing a peroxide, usually H_2O_2 , as the cosubstrate. Historically, the most studied and best characterized of the peroxidases are horseradish peroxidase (HRP) and cytochrome *c* peroxidase (CcP), although more recently enzymes such as lignin peroxidase (LiP) and ascorbate peroxidase have also been extensively investigated. In parallel with these studies of plant and fungal enzymes, much work has been done on the structure and mechanism of the mammalian peroxidases, particularly myeloperoxidase (MPO) and lactoperoxidase (LPO), for both of which crystal structures are now available. In all of these enzymes, the catalytic center is iron protoporphyrin IX (Fig. 5.1), although in the mammalian proteins this prosthetic group is autocatalytically modified. Despite the differences in the proteins, active sites, and even prosthetic groups, the catalytic mechanisms of all the peroxidases are sufficiently similar that they can be viewed, despite their differences, from a common perspective.

5.2 Peroxidase Catalytic Cycle

The common overall reaction of the peroxidases can be written as in the following equation, where RH is a suitable peroxidase substrate and R' is a free-radical product derived from it:

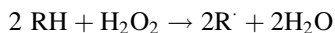
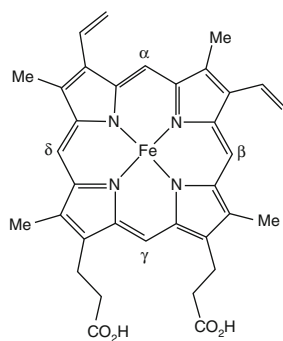


Fig. 5.1 The structure of iron protoporphyrin IX, the prosthetic heme group of the peroxidases except where it is modified by the formation of covalent bonds to the methyl or vinyl groups. The α -, β -, γ -, and δ -*meso*-carbon atoms, defined with respect to the pattern of the ring substituents, are labeled



This net transformation, however, encompasses a more complex mechanism that can be visualized in the generic catalytic cycle shown schematically in Fig. 5.2. Compounds I and II, the critical catalytic intermediates, are readily distinguished from the resting ferric state of the protein by their UV–visible absorption spectra (Table 5.1) [1–4]. Although the exact positions of the maxima show small variations, the spectroscopic properties of HRP are representative of those of all the peroxidases in which the heme iron atom is coordinated to a histidine nitrogen atom. The individual stages of the catalytic cycle are considered below.

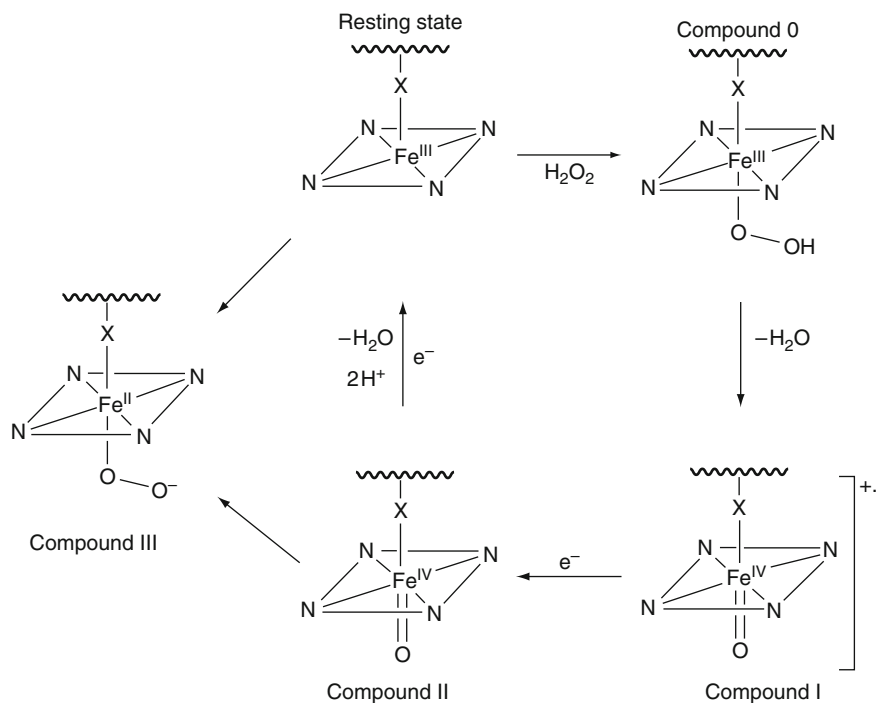


Fig. 5.2 Generic peroxidase catalytic cycle. The *square* of four nitrogens around the iron atom is a representation of the prosthetic heme group of the peroxidase

Table 5.1 Soret absorption maxima for resting state ferric HRP and the Compound I and Compound II catalytic intermediates [1–4]

HRP species	Soret (nm)	Molar absorptivity (mM ⁻¹ cm ⁻¹)	Visible (nm)	Charge transfer (nm)
Ferric	403	102	498, 640	
Compound I	400	54	~525 (sh), 577	622, 651
Compound II	420	105	527, 555	
Compound III	417	108	544, 580	

5.2.1 Ferric Peroxidase

The prosthetic heme in the resting peroxidases is in the ferric state. In HRP and most peroxidases, the iron is five coordinate, high spin [5], with a histidine as the proximal iron ligand and a water molecule in the distal side that is not coordinated to the iron. In HRP, the oxygen of the water molecule is 3.20 Å from the iron [6] and in CcP at a distance of 2.33 Å [7]. In addition to the proximal histidine iron ligand, which in HRP is His170, in CcP His175, and in LiP His176 (Fig. 5.3), most peroxidases have a distal histidine not bound to the heme iron atom that is intimately involved in catalysis. In HRP, this residue is His42, in CcP His52, and in LiP His47. A second important catalytic residue is a distal arginine that through polar interactions facilitates heterolytic cleavage of the peroxide dioxygen bond. In HRP, this residue is Arg38, in CcP Arg48, and in LiP Arg43. Additional residues are thought to promote the formation of Compound I. In HRP, these include Asn70 on the distal side, which by hydrogen bonding to the N–H of His42 enhances its basicity, and Asp247 on the proximal side, which by accepting a hydrogen bond from the proximal histidine increases the negative electron density on the imidazole ring and thereby, through a “push” effect, facilitates O–O bond cleavage. The roles of these residues are supported by mutagenesis studies showing that loss of any of the indicated residues or interactions decreases the catalytic activities of the enzymes, with the distal catalytic histidine being the most important [9–13].

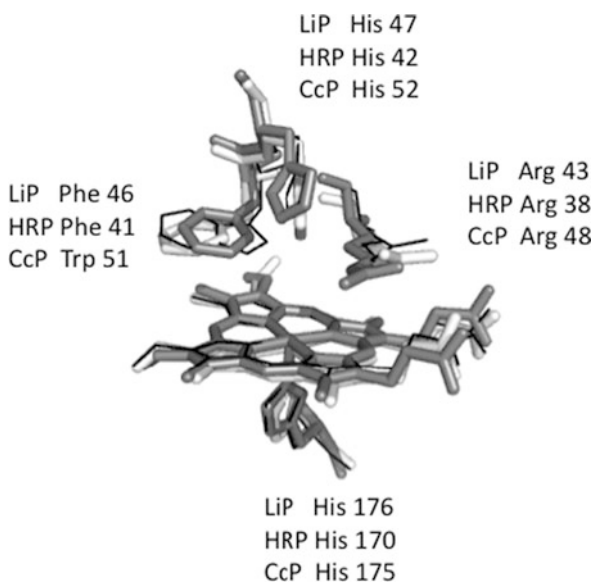


Fig. 5.3 Location of critical catalytic residues relative to the heme group in the active site of LiP (white sticks), HRP (gray sticks), and CcP (black line). The figure is based on [8]

5.2.2 *Compound 0*

The first step of peroxidase catalysis involves binding of the peroxide, usually H_2O_2 , to the heme iron atom to produce a ferric hydroperoxide intermediate $[\text{Fe}(\text{III})\text{--OOH}]$. Kinetic data identify an intermediate prior to Compound I whose formation can be saturated at higher peroxide concentrations. This elusive intermediate, labeled Compound 0, was first observed by Baek and Van Wart in the reaction of HRP with H_2O_2 [14]. They reported that it had absorption maxima at 330 and 410 nm and assigned these spectral properties to the ferric hydroperoxide species $[\text{Fe}(\text{III})\text{--OOH}]$. They subsequently detected transient intermediates with similar spectra in the reactions of HRP with alkyl and acyl peroxides [15]. However, other studies questioned whether the species with a split Soret absorption detected by Baek and Van Wart was actually the ferric hydroperoxide [16–18]. Computational prediction of the spectrum expected for Compound 0 supported the structure proposed by Baek and Van Wart for their intermediate, whereas intermediates observed by others with a conventional, unsplit Soret band may be complexes of ferric HRP with undeprotonated H_2O_2 , that is $[\text{Fe}(\text{III})\text{--HOOH}]$ [19]. Furthermore, computational analysis of the peroxidase catalytic sequence suggests that the formation of Compound 0 is preceded by formation of an intermediate in which the undeprotonated peroxide is coordinated to the heme iron [20]. Indeed, formation of the $[\text{Fe}(\text{III})\text{--HOOH}]$ complex may be required to make the peroxide sufficiently acidic to be deprotonated by the distal histidine residue in the peroxidase active site [21].

5.2.3 *Compound I: Porphyrin Radical*

The conversion of Compound 0 to Compound I requires protonation of the distal oxygen of the ferric hydroperoxide complex so that formation of the ferryl species can be linked to elimination of the distal oxygen as a molecule of water. It is thought that the distal histidine residue in the peroxidase active site is the base that deprotonates the peroxide in the formation of Compound 0. This proton is then delivered by the imidazole to the terminal oxygen of the ferric hydroperoxide complex, catalyzing the O–O bond cleavage that produces Compound I (Fig. 5.4). This general sequence, referred to as the Poulos–Kraut mechanism [22], was first postulated when the structure of CcP became available. The structure of CcP was the first of any peroxidase to be determined. Although more recent work has suggested refinements of this mechanism, its basic features have been confirmed by extensive work.

UV–visible [23], EPR [24, 25], Mössbauer [24], EXAFS [26], and resonance Raman [27] data indicate that Compound I of HRP consists of a ferryl $[\text{Fe}(\text{IV})\text{=O}]$ species combined with a radical cation localized on the porphyrin framework [23, 24], although the porphyrin radical cation is difficult to observe directly by EPR [23, 25].

The crystal structure of Compound I has been determined after its generation by reaction of ferric HRP with peracetic acid [28]. The high reactivity of Compound I

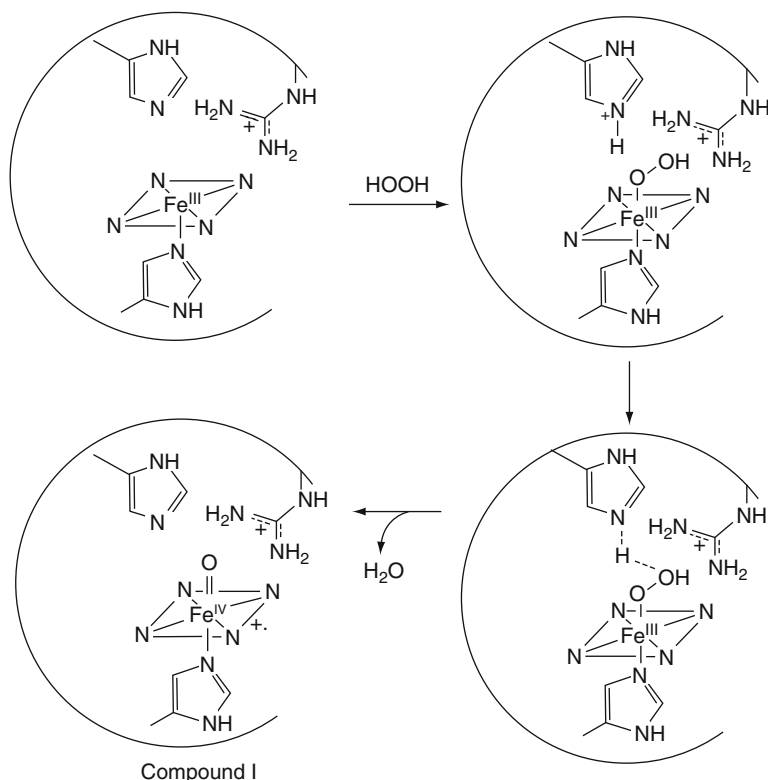


Fig. 5.4 Schematic representation of the Poulos–Kraut peroxidase mechanism in which the conserved distal histidine serves as an acid–base catalyst that transfers a proton from the H_2O_2 to the terminal oxygen after formation of the $[\text{Fe}(\text{III})\text{--OOH}]$ intermediate. The proximal histidine iron ligand and the catalytic histidine and arginine are shown. In HRP, these residues are His170, His 42, and Arg38, respectively

and its sensitivity to reduction by X-rays made it necessary to employ a multiple crystal strategy to obtain the structure. The iron–oxygen bond in the structure is 1.7 Å in length, a value that agrees reasonably well with the 1.64 Å obtained by extended X-ray fine structure (EXAFS) analysis [26]. In general, the iron–oxygen bond length in Compound I is in the range 1.67–1.76 Å [29], consistent with the presence of an unprotonated ferryl oxygen atom. The oxygen of the ferryl group in the HRP crystal structure forms hydrogen bonds with Arg38 and a water molecule that, in turn, is hydrogen bonded to His42 and Arg38 [26].

5.2.4 Compound I: Protein Radical

The Compound I species of many peroxidases, as illustrated for HRP, is characterized by an $[\text{Fe}(\text{IV})\text{=O}]$ ferryl species coupled with a porphyrin radical cation.

However, in some peroxidases, the porphyrin radical cation, if formed at all, is transient and gives way to a Compound I intermediate in which the ferryl species is accompanied by a protein rather than porphyrin radical. The prototypical enzyme of this class is CcP in which Trp191, located adjacent to the proximal iron ligand His175 [30], is oxidized to the radical cation [31]. This intermediate in CcP was historically known as Compound ES to differentiate it from Compound I of enzymes like HRP, although in fact it is an alternative form of Compound I if this intermediate is defined as an enzyme species two oxidation equivalents higher than the resting ferric state. The finding that replacement in HRP of Phe172 by a tyrosine or Phe221 by a tryptophan gives mutant proteins in which the Compound I with a porphyrin radical decays to a Compound I with a protein radical indicates that a key determinant of this shift in the radical location is simply the presence of an appropriately located oxidizable residue [8, 32]. In the CcP Compound I structure, the Fe–O distance is 1.87 Å [7], consistent with the presence of a singly bonded, protonated ferryl oxygen [Fe(IV)–OH], such as that found in Compound II of all the peroxidases.

The different location of the radical in the two types of Compound I structure is relevant, as it causes differences in their spectroscopic properties and results in differential catalytic activities. These differences only apply to Compound I, as the spectroscopic and catalytic properties of Compound II, in which only the ferryl is retained (see below), are similar for all the peroxidases.

In some enzymes, the protein radical appears to participate in substrate oxidation. Evidence exists for the involvement of a surface tryptophan in the oxidation of veratryl alcohol by the ligninase from *Phanerochaete chrysosporium* [33]. Similarly, tryptophan radicals on the surface of the versatile peroxidases from *Pleurotus eryngii* and *Bjerkandera adjusta* [34–36], and a tyrosine in the LiP from *Trametes cervina* [33], are thought to be involved in substrate oxidation.

5.2.5 Compound II

One-electron reduction of Compound I produces Compound II, in which the iron is still present in the [Fe(IV)] state, but the porphyrin radical has been quenched. The crystal structure of HRP Compound II exhibits an iron–oxygen bond length of 1.8 Å [28]. In general, peroxidase Compound II structures have an iron–oxygen bond length of 1.86–1.92 Å, consistent with the presence of a single-bond between these atoms and therefore of a protonated oxygen [Fe(IV)–OH] [29]. The ferryl oxygen in HRP is hydrogen-bonded to Arg38 and to a water molecule that is hydrogen-bonded to His42 and Arg38.

5.2.6 Compound III

Compound III designates a complex in which a molecule of oxygen is bound end-on to the ferrous iron of the peroxidase. It is thus a structure that is close to those of the

oxygen complexes present in oxymyoglobin and oxyhemoglobin. The crystal structure of HRP Compound III shows the oxygen is bound in a bent conformation, with one oxygen atom bound to the iron at a distance of 1.8 Å and a Fe–O–O bond angle of 126° [28]. In HRP, the oxygen atom furthest away from the iron atom is hydrogen-bonded to His42, Arg38, and a water molecule.

Compound III, in which the iron is in the ferrous state, is usually formed when there is a large excess of H₂O₂. It is likely that this intermediate is largely formed by combination of superoxide, generated by the oxidation of H₂O₂, with the ferric enzyme, although superoxide could also be generated by electron transfer from oxidized substrates to molecular oxygen. Compound III is not ordinarily a catalytically active intermediate, although it may play a role in the oxidation of isoniazid by the catalase–peroxidase KatG of *Mycobacterium tuberculosis* [37]. For a more detailed description of Compound III, refer to Chap. 11.

5.3 Self-Processing of Peroxidases

5.3.1 Protein Modifications

In view of the formation of a highly reactive Compound I ferryl species, and the fact that the porphyrin radical cation of this intermediate is reduced in enzymes such as CcP by a protein residue, it is not surprising that permanent covalent modifications are autocatalytically introduced into some protein frameworks. Two examples of autocatalytic protein modification, those of LiP and the catalase–peroxidases, are summarized here to illustrate the maturation of peroxidase protein structures that can have important functional consequences.

LiP catalyzes the degradation of lignin. The enzyme is commonly assayed by its ability to oxidize veratryl alcohol to a diffusible veratryl radical cation that can either oxidize other substrates or is further converted by a second electron removal to the aldehyde (Fig. 5.5). This reaction is thought to mimic the *in vivo* operation of

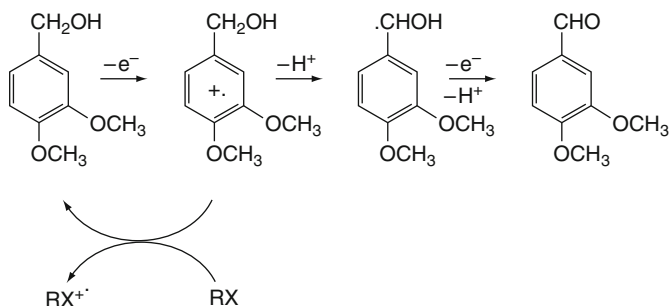


Fig. 5.5 Oxidation of veratryl alcohol to a radical cation that can oxidize other substrates (RX) or can be further oxidized to give veratryl aldehyde

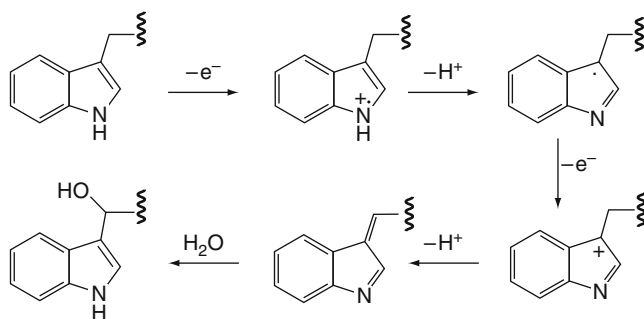


Fig. 5.6 Reaction scheme showing a mechanism for intramolecular, autocatalytic oxidation of Trp71 in LiP to a hydroxylated tryptophan derivative

LiP, where a diffusible radical can facilitate degradation of the relatively impermeable lignin matrix. Interestingly, LiP undergoes a maturation process in which Trp171 is autocatalytically oxidized by insertion of a hydroxyl into the side-chain adjacent to the aromatic ring (Fig. 5.6) [38, 39]. Oxygen is not required for this hydroxylation reaction, suggesting that the hydroxyl group is introduced after formation of a conjugated system via two sequential one-electron oxidations by Michael addition of a water molecule, producing the modified Trp171 residue [38]. The finding that in the presence of veratryl alcohol more catalytic turnovers are required to introduce the modification indicates that the modification is not actually essential for oxidation of this substrate. However, the W171F and W171S mutants are unable to oxidize veratryl alcohol but still oxidize two other small substrates [39, 40]. These results suggest that the Trp171 locus is the binding site for oxidation of veratryl alcohol, but a second site exists for the oxidation of other substrates. It is not clear, however, whether the Trp171 modification is incidental or actually plays a role in the oxidation of veratryl alcohol.

The catalase–peroxidase KatG enzymes are unique in that they have high catalase activity but also a substantial peroxidase activity [41]. One of the unique, highly conserved features of this class of enzymes is the presence of a crosslinked Met–Tyr–Trp tripeptide. Expression of the *M. tuberculosis* KatG in *Escherichia coli* under conditions that prevent catalytic turnover yields an enzyme without the crosslinked peptide, but exposure to low levels of H_2O_2 results in rapid, quantitative introduction of the crosslinks [42]. The tripeptide is clearly the result of an autocatalytic processing event. The crosslinked tripeptide is formed by a series of sequential peroxidative reactions terminated by addition of the Met sulfur to the resulting Michael acceptor (Fig. 5.7). Mutation of the residues involved in tripeptide formation results in a major loss of catalase activity, but conversely a small increase in peroxidase activity [43]. The role of the tripeptide thus appears to be related to the preservation of catalase activity, possibly by helping to reduce the catalase-inactive Compound II to the ferric state [43], but mostly, as the tripeptide radical, by accepting an electron from the Compound III [Fe(II)– O_2] intermediate,

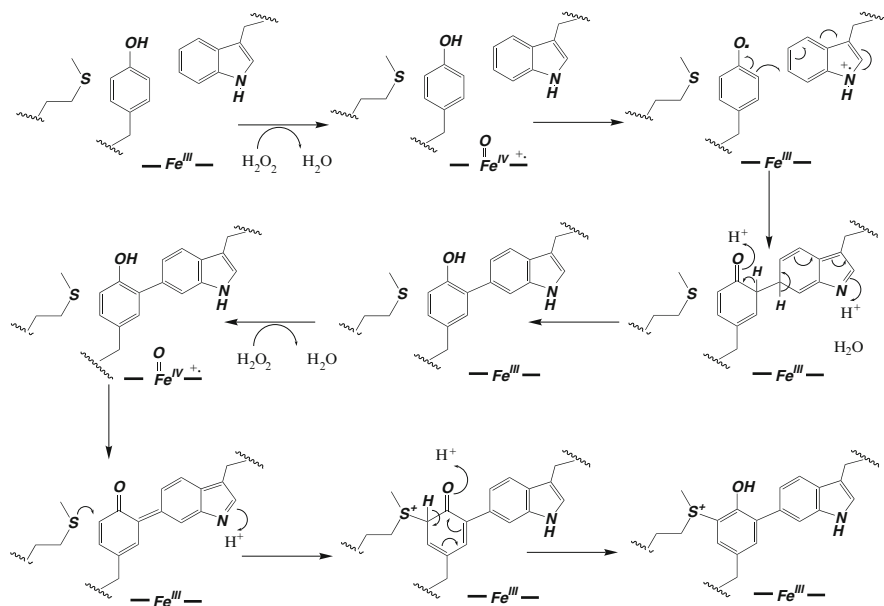


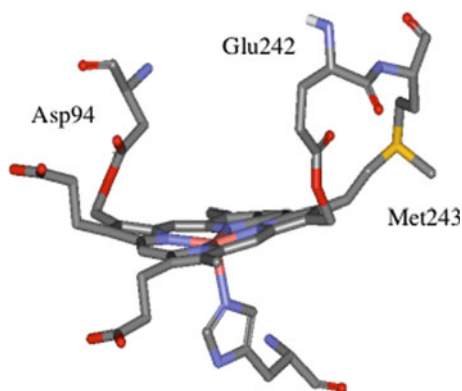
Fig. 5.7 Mechanism proposed for autocatalytic formation of the Met–Tyr–Trp crosslinked tripeptide found in all KatG catalase–peroxidases based on experimental observations with the enzyme from *M. tuberculosis*. The iron between two bars represents the prosthetic heme group

generating a molecule of oxygen and returning the tripeptide radical to the neutral state and the iron to the ferric state [44, 45].

5.3.2 Heme-Protein Crosslinking

Although the mammalian peroxidases catalyze conventional peroxidation reactions, their physiological functions generally involve oxidation of a halide (X⁻) to the halogenating and microbicidal product HOX [46]. This difference in physiological function may help explain why the prosthetic heme group in LPO [47], MPO [48], eosinophil peroxidase [49], and probably thyroid peroxidase is covalently bound to the protein. The crystal structures of LPO and MPO clearly show that covalent ester bonds are formed between the 1- and 5-methyl groups and the carboxyl group of nearby Asp or Glu residues [47, 48]. In MPO, these bonds involve the carboxyl groups of Asp94 and Glu242 (Fig. 5.8). However, a recent study has suggested that the ester bond with Glu242 in the protein isolated from a native source may only be present in a subset of the protein molecules [49]. Unusually, in MPO there is an additional bond between the heme 2-vinyl group and the sulfur of a methionine residue [48]. The two ester bonds to the heme appear

Fig. 5.8 The active site of MPO showing the covalent bonds between the 1- and 5-methyls of the heme and the carboxyl groups of Glu242 and Asp94, respectively. The covalent bond between the 2-vinyl of the heme and the sulfur atom of Met243 is also shown



to be present in eosinophil peroxidase, although they have not been as precisely established [50].

Heterologous studies clearly demonstrate that covalent heme binding is the result of an autocatalytic processing event. Expression of LPO in a baculovirus system yields a protein in which only a fraction of the protein has a covalently bound heme [51]. Incubation of this expressed protein with H_2O_2 , however, results in a high level of covalently bound heme [51, 52]. The mechanism in Fig. 5.9 has been proposed to explain the covalent binding sequence, which in these proteins must occur twice to form the two ester bonds present in the native protein. Interestingly, introduction by site-specific mutagenesis into HRP of a carboxyl group near one of the heme methyl groups yields a protein, the F41E mutant, which on incubation with H_2O_2 quantitatively forms a covalent bond to the heme [53], presumably by the mechanism shown in Fig. 5.9.

The third covalent bond present in MPO is also thought to form by an autocatalytic process, although it has not been clearly demonstrated to do so. However, incubation of an ascorbate peroxidase mutant into which a methionine has been introduced by mutagenesis has been shown to result in covalent attachment of the Met sulfur atom to a heme vinyl group [54]. Although the link is not identical to that in MPO, this finding provides strong circumstantial evidence that the bond in MPO is also formed by an autocatalytic mechanism.

5.3.3 Heme Modification by Metabolites

The free radical products generated by peroxidases are highly reactive species that can, in some instances, covalently modify the heme group of the enzyme (Fig. 5.10). In the case of HRP, the substrates for which this type of reaction has been observed include aryl and alkyl hydrazines [55, 56], the azide anion [57], nitromethane [58], cyclopropanone hydrate [59], and alkyl acids [60]. Free radicals

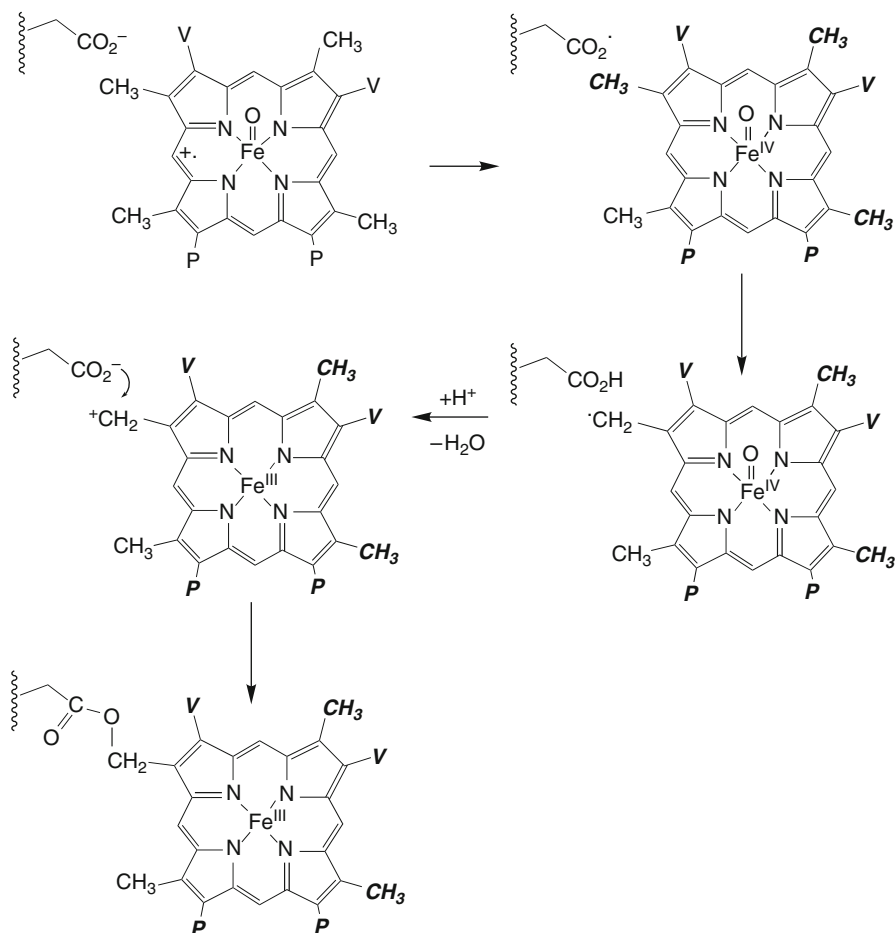


Fig. 5.9 Mechanism proposed for formation of a covalent bond between a heme methyl and a protein carboxyl group. A similar sequence must occur again to form the second heme–protein ester link in the mammalian peroxidases. In the heme structure, V stands for $-\text{CH}=\text{CH}_2$ and P for $-\text{CH}_2\text{CH}_2\text{CO}_2\text{H}$

of relatively high energies readily add at the δ -*meso* carbon of the heme group, as shown in Fig. 5.10, whereas radicals of low reactivity (e.g., nitrite radical) can only add efficiently to the heme vinyl groups (Fig. 5.11) [61]. The C–H bond dissociation energy for the radical of around 90 kcal mol^{-1} appears to define the limit below which addition to the *meso*-position does not occur, although addition to the vinyl groups can, in principle, occur with all the radicals (Table 5.2).

Prosthetic heme modification also occurs in some instances with the two-electron oxidation products formed by peroxidases when they oxidize halide and pseudohalide ions. Thus, the oxidation of bromide by HRP results in the addition of HOBr to one or both of the heme vinyl groups (Fig. 5.11) [62]. Similar reactions are

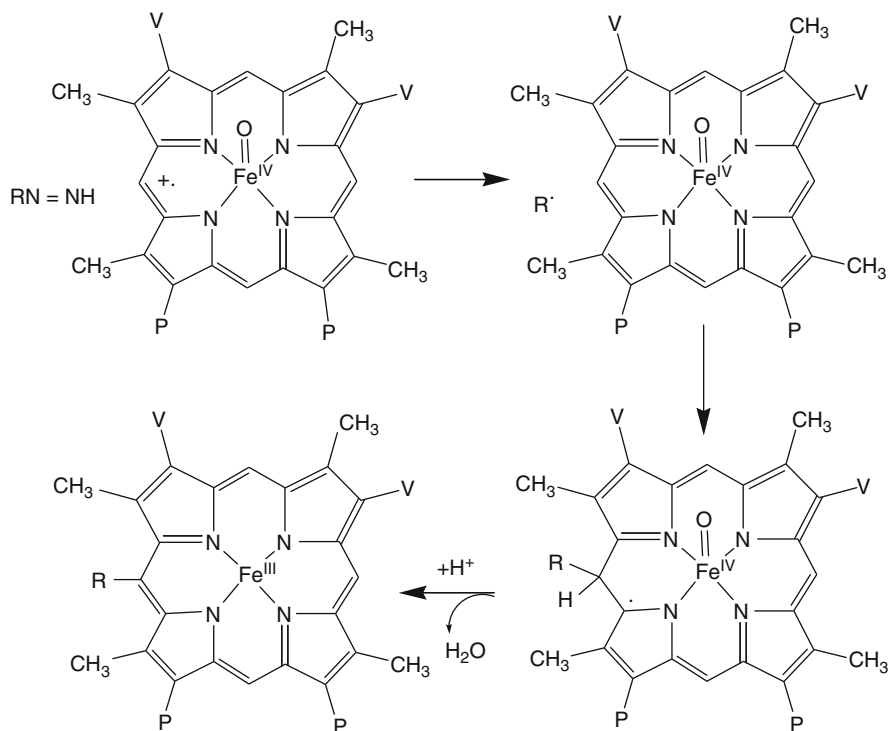


Fig. 5.10 Addition to the δ -meso position of the prosthetic heme of the carbon radical generated when HRP oxidizes a diazene ($\text{RN}=\text{NH}$). The diazene is itself generated by peroxidatic oxidation of the precursor hydrazine (RNHNH_2)

observed with the HOSCN produced by HRP from thiocyanate ion [63]. Even the oxidation of chloride ion, which is mediated very poorly by HRP, results in addition of HOCl to the vinyl groups [62]. The electrophilic metabolites may also react with nucleophilic groups of the protein [64].

Heme modification by the products of peroxidase catalysis has been observed with peroxidases other than HRP, but it does not occur with all peroxidases. Some peroxidases are resistant to these types of reactions. In particular, the mammalian peroxidases are resistant to heme modification by both the free radical and electrophilic metabolites [63]. This resistance is due, at least in part, to the covalent bonds that link the heme to the mature protein. A similar resistance to modification by the HOBr produced by HRP is observed when the reaction is carried out with the F41E mutant in which a covalent bond to the heme has been introduced [65]. However, resistance to radical products can occur even without the presence of covalent links between the heme and the protein. Thus, LiP has a heme that is resistant to modification by phenylhydrazine or azide, although the protein is apparently inactivated by modifications of the protein [66].

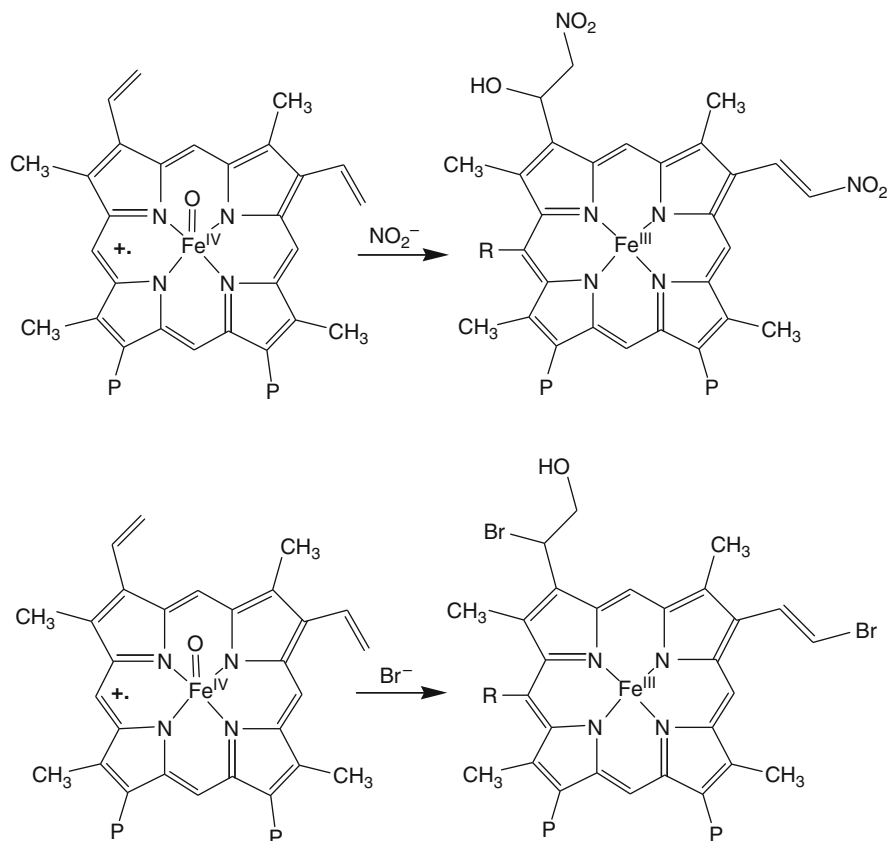


Fig. 5.11 Modification of the vinyl groups of the prosthetic heme of HRP upon catalytic oxidation of nitrite to NO_2^- or Br^- to HOBr. For each reaction, two different modifications of the vinyl groups are shown. These modifications can occur in different combinations. For example in the Br^- reaction, both of the vinyls could be present as bromohydrin [$-\text{CHBrCH}_2\text{OH}$] adducts

Table 5.2 Relationship between the energy of a radical and its ability to add to the *meso*-position of the heme group in HRP [61]

C–H bond	DH ₂₉₈ (kcal mol ⁻¹)	Site of addition to heme of HRP ^a
HCN	126	δ- <i>meso</i>
C ₆ H ₅ –H	113	δ- <i>meso</i>
CH ₃ CO ₂ H	112	δ- <i>meso</i>
CH ₃ –H	105	δ- <i>meso</i> , vinyl
HCl	103	δ- <i>meso</i> , vinyl
CH ₃ CH ₂ –H	101	δ- <i>meso</i>
HNCS	96	δ- <i>meso</i>
HN ₃	92	δ- <i>meso</i>
CH ₃ OO–H	88	vinyl
HBr	88	vinyl
HNO ₂	79	vinyl

^aIn some instances, the F41M mutant of HRP was used to decrease the steric barriers to the active site

5.4 Substrate Oxidations

5.4.1 Oxidative Properties

Peroxidases catalyze the one-electron oxidation of sufficiently oxidizable substrates but generally do not catalyze oxygen transfer reactions in which the ferryl oxygen is transferred to the substrate. This is a key distinction between the peroxidases and monooxygenases despite the fact that both enzymes employ analogous Compound I catalytic species. Computational comparison of Compound I in the peroxidases and cytochrome P450 enzymes suggests that the peroxidase Compound I should actually be competent in oxygen transfer reactions [67]. However, steric constraints imposed on the peroxidase active site play a major role in limiting peroxygenase reactions in favor of simple one-electron oxidations. The crystal structure of HRP shows that the heme group is embedded in a protein crevice with only the δ -*meso*-edge of the heme exposed to the medium (Fig. 5.12) [6]. The heme iron atom is protected, among others, by the catalytic histidine residue (His42) and an adjacent phenylalanine (Phe41). A consequence of this active site topology is that substrates are oxidized by electron transfer to the exposed heme edge without interacting directly with the ferryl oxygen, a reaction trajectory that precludes transfer of the ferryl oxygen to the substrate. This heme edge reactivity was first unmasked by studies showing that the inactivation of HRP and other peroxidases by alkyl and aryl hydrazines resulted from addition of the resulting carbon radicals exclusively to the δ -*meso* carbon atom of the prosthetic heme group (Fig. 5.10)

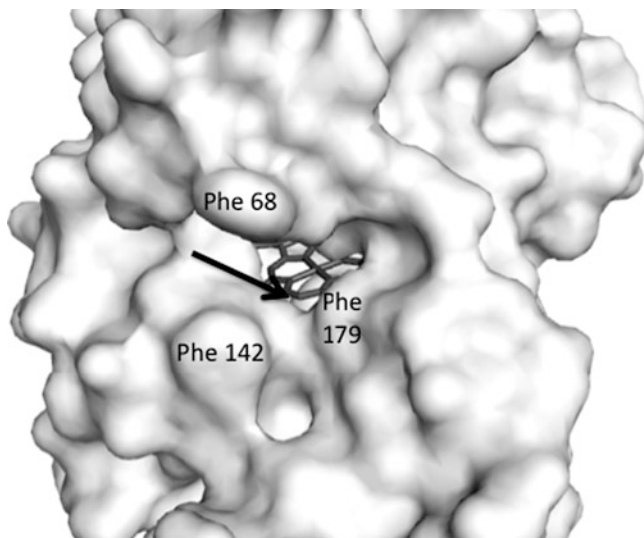


Fig. 5.12 The HRP substrate access channel. The aromatic residues flanking the access channel are *highlighted*. The *arrow*, located in the access channel, points to the δ -*meso*-carbon atom

[55, 56]. The bottom line is that for substrates larger than one or two atoms in size, steric restrictions imposed on the peroxidase active site prevent oxygen transfer reactions and confine substrate–enzyme interactions to the heme edge.

CcP, in contrast to HRP, has two sites for interaction with substrates. Cytochrome *c*, its physiological substrate, binds primarily at a protein surface site facing the carboxyl groups of the heme from which it delivers an electron to the Compound I or II intermediate [68]. The oxidation of guaiacol by CcP, however, is apparently mediated at the δ -*meso* edge of the heme. Autocatalytic inactivation of the enzyme by phenylhydrazine or azide, which results in covalent binding of the phenyl or azide group, respectively, to the δ -*meso* carbon of the heme inhibits oxidation of the small substrates to a much greater extent than it does cytochrome *c* oxidation [69]. Furthermore, reconstitution of the protein with δ -*meso*-substituted hemes suppresses oxidation of guaiacol but has only modest effects on cytochrome *c* oxidation. A channel is present in the CcP crystal structure that leads from the outside of the protein into the active site crevice and terminates near the δ -*meso* edge of the heme [30]. Two sites thus exist for substrate oxidation in CcP, one at the protein surface for the normal protein substrate and a second one for small substrates such as guaiacol within the heme cavity.

As already mentioned, in some enzymes radicals generated on surface tryptophan and tyrosine radicals by electron transfer to the ferryl species are involved in abstraction of electrons from substrates [33–36, 40]. Mutation of Trp171 on the surface of *P. chrysosporium* LiP to a phenylalanine or serine completely suppresses the veratryl alcohol oxidizing activity of the enzyme [40]. A similar depression in the oxidation of veratryl alcohol occurs on mutation of Trp164 in the versatile peroxidase from *P. eryngii* [34, 35].

5.4.2 One-Electron Oxidations

5.4.2.1 Phenols

The classic reaction catalyzed by peroxidases is the one-electron oxidation of phenols. The guaiacol assay for peroxidase activity, an assay that derives from the earliest observation of peroxidase activity [70], involves the one-electron oxidation of guaiacol to a free radical that undergoes subsequent radical–radical combination to give a colored dimeric product (Fig. 5.13) [71]. The ability of substituted phenols to act as substrates and reduce HRP Compound I is controlled by the electronic nature of the substituent [72]. At pH 7.0, the linear Hammett correlation observed between the substituent σ value and the rate of Compound I reduction adheres to the equation $\log k_X/k_H = -6.92\sigma$, where k_X is the rate of the reaction of the substituted phenol and k_H is the rate of the reaction of the unsubstituted phenol. The ability of substituted phenols to reduce Compound II also correlates with the substituent σ -values according to the equation $k_X/k_H = -4.6\sigma$ [73]. As might be expected, correlations have also been shown to exist between the

Fig. 5.13 The oxidation of guaiacol to colored dimeric products underlies the use of guaiacol in a classical peroxidase activity assay. Additional products can be formed

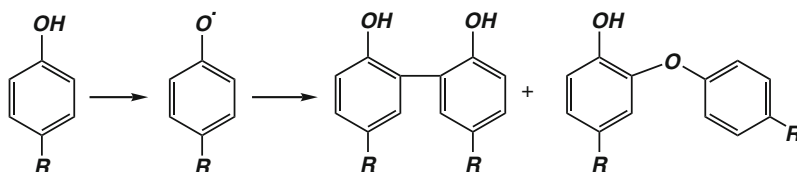
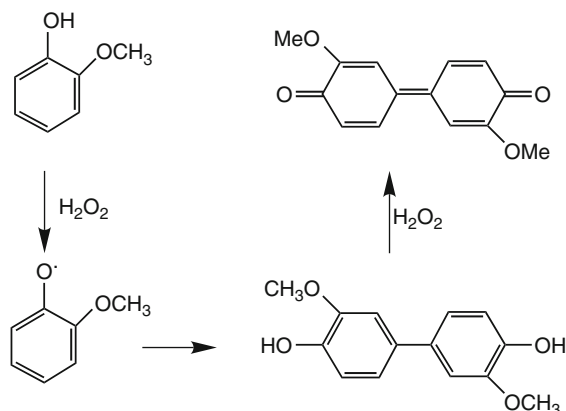


Fig. 5.14 A common peroxidase reaction is the oxidation of phenols to phenolic radicals that condense to give dimeric or oligomeric products. As shown, two orientations are possible for the condensation of the phenolic radicals if the *para*-position is blocked by a group R

calculated redox potentials of the phenols, which are themselves related to the electronic properties of the substituents, and the rates of their oxidation by HRP [74, 75]. These relationships establish that the ability to reduce both Compound I and Compound II increases as the electron donating strength of the substituent increases, with Compound I reduction being more responsive to the electron density in the phenol ring. As the difference in the redox potentials of Compounds I and II at pH 7.0 is small [76], something else must account for the difference in the sensitivity of the rates to the electronic nature of the substituents. One possibility suggested by the evidence that electrons are transferred to the heme edge is that electron transfer is more facile to the heme edge of Compound I, in which the porphyrin is a radical cation, than of Compound II, in which it is an electroneutral porphyrin.

The final products of phenol oxidation are generated by secondary reactions of the radicals produced by the peroxidase. One very common pathway involves dimerization or oligomerization of the radicals, as illustrated in Fig. 5.14 for the oxidation of a *para*-substituted phenol such as tyrosine [R = CH₂CH(NH₂)CO₂H]. The dimerization can occur between two ring carbon atoms or by addition of the oxygen of one phenoxy radical to a ring carbon of the other.

5.4.2.2 Aromatic Amines

Peroxidases also catalyze the one-electron oxidation of aromatic amines to the corresponding radical cations. Studies of the oxidation of substituted anilines by HRP Compounds I and II have established that these reactions are also linearly correlated with the electron donating nature of the substituents [72, 73]. The Hammett equation for the Compound I oxidation of anilines was $k_X/k_H = -7.00\sigma\sigma$, and for the corresponding reaction of Compound II (obtained by a different group) was $k_X/k_H = -5.75\sigma$ [77]. A comparison of the absolute rates of the oxidation of substituted anilines and phenols indicates that the phenols are generally oxidized more rapidly by 1–2 orders of magnitude [72, 77].

The oxidation of aminofluorene by HRP provides a suitable example [78]. The amine group is oxidized to the radical cation that, upon deprotonation, yields the aminofluorenyl radical. This radical can dimerize by nitrogen–nitrogen coupling or by unsymmetrical combination, yielding the products in Fig. 5.15. The nitrogen radical can also be further oxidized to a nitrogen cation that combines with water to give the hydroxylamine derivative. In reality, these products can be further oxidized by HRP, so that higher oxidation products are obtained.

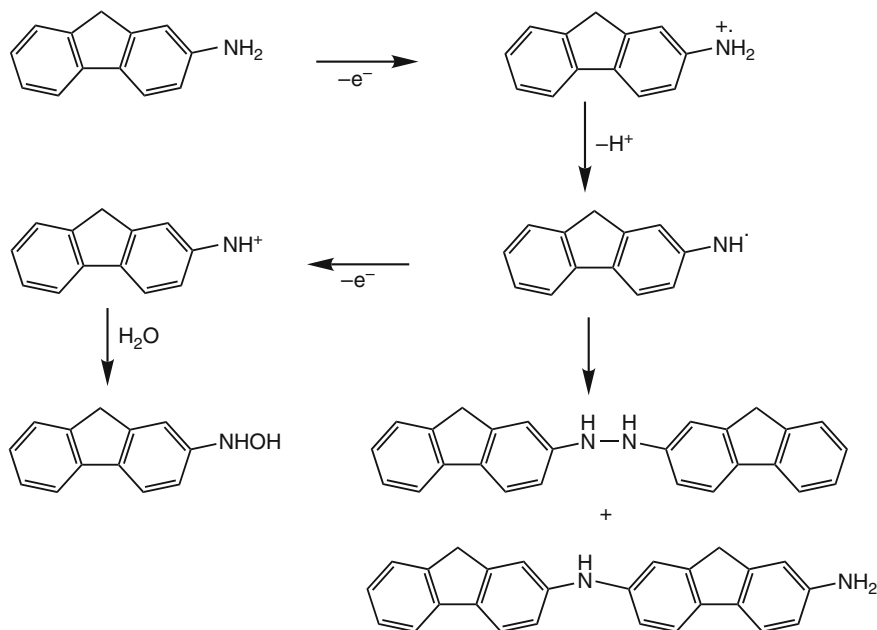


Fig. 5.15 Initial products formed in the oxidation of aminofluorene by HRP. Further oxidative products can occur under the continued catalytic action of the peroxidase

5.4.2.3 Carbon Oxidation

Carbon atoms can be oxidized when they are anionic or bear substantial negative charge due to their incorporation into an appropriate functional group. For example, HRP oxidizes malondialdehyde to a free radical product (Fig. 5.16; [79]). The carbon between the two carbonyl groups in this molecule has a pKa of 4.65 and is therefore present at pH 7 largely in a deprotonated state with the negative charge delocalized over the conjugated system. Phenylbutazone, with a pKa of 4.5 for the carbon between the two carbonyl groups, is also highly ionized in solution and is oxidized by HRP to the corresponding free radical [80].

5.4.2.4 Electron Transfer Relay

Efficient, diffusible peroxidase substrates can play a role in the oxidation of secondary, less efficient, peroxidase substrates. As already mentioned, the veratryl radical produced by LiP can serve to oxidize lignin at sites inaccessible to the enzyme (Fig. 5.5). The same mechanism operates with manganese peroxidases, which oxidize Mn(II) to Mn(III) [81]. The higher valent manganese then diffuses into lignin to mediate the oxidation of relatively inaccessible residues. This mechanism is not limited to lignin degrading enzymes, however. For example, a similar relay has been shown to improve the oxidation of isoniazid by HRP in the presence of chlorpromazine [82]. Chlorpromazine, an efficient substrate for HRP, is converted to a radical cation that, in turn, oxidizes isoniazid (Fig. 5.17). Isoniazid itself is a substrate for HRP, but it is an inefficient substrate and also irreversibly inactivates the enzyme. Using the chlorpromazine radical cation as a mediator results in a rate of isoniazid oxidation several orders of magnitude faster than in its absence. Furthermore, the chlorpromazine electron relay completely protects the peroxidase enzyme from irreversible inactivation.

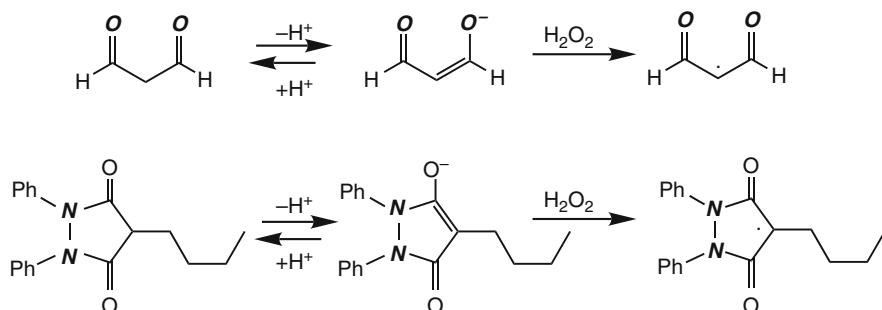


Fig. 5.16 HRP-catalyzed oxidation of malondialdehyde and phenylbutazone, two carbons with an acidic carbon atom

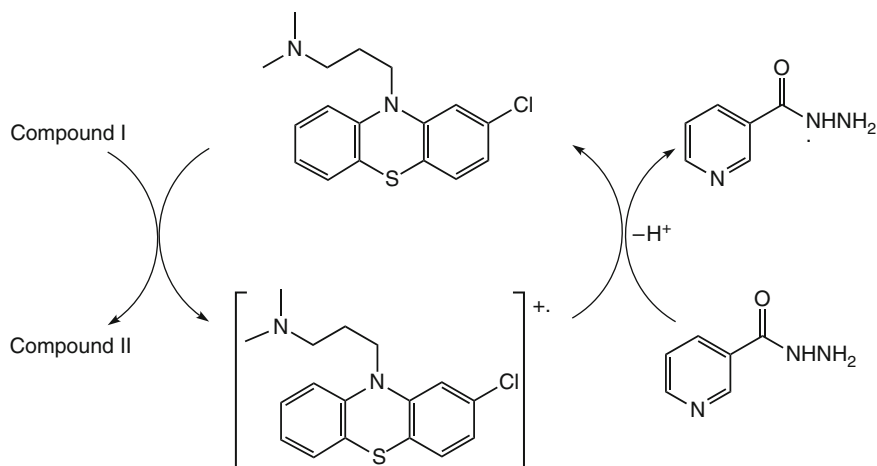


Fig. 5.17 Role of chlorpromazine as an electron relay in the oxidation of isoniazid by HRP. Although isoniazid is directly oxidized by HRP, the reaction is much faster when chlorpromazine, a better substrate, is used as a relay in the oxidation of isoniazid

5.4.3 Two-Electron Oxidations

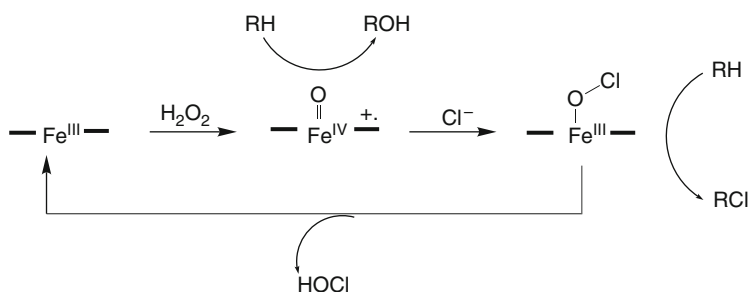
5.4.3.1 Halogenation

Direct, two-electron oxidations are rare for most peroxidase enzymes. The one broad exception is the oxidation of halide and pseudohalide ions, specifically Γ^- , Br^- , Cl^- , and NCS^- . Fluoride ion, in contrast, is not known to be oxidized by these enzymes. The oxidation of Γ^- and NCS^- is common for the peroxidases, whereas that of Br^- is widespread but is usually less effective, and that of Cl^- , among the conventional peroxidases, is only important in the case of MPO [46, 83]. The halogenation activities of the mammalian peroxidases are compared in Table 5.3. As the table shows, chloride ion is oxidized by MPO, particularly at pH 5, but it is a very poor substrate for EPO and LPO. Br^- , Γ^- , and SCN^- are readily oxidized by all three enzymes, but most efficiently by EPO at pH 5 [84–86].

The plant and fungal peroxidases with a histidine iron ligand also do not detectably oxidize chloride ion, although the demonstration that oxidation of chloride ion at acidic pH by HRP and *Arthromyces ramosus* peroxidase results in addition of HOCl to the prosthetic heme vinyl groups illustrates that a low level of activity actually exists [62, 87]. However, Cl^- ions are readily oxidized by the special class of peroxidases exemplified by the haloperoxidases from *Caldariomyces fumago* and *Agroclybe aegerita* [88]. These chloroperoxidases are distinguished by the fact their proximal iron ligand is not a histidine but rather a cytochrome P450-like thiolate ion [89]. Furthermore, the distal catalytic histidine is replaced in chloroperoxidase by a glutamic acid (Glu183), which plays a catalytic role similar to that of the histidine in HRP [90, 91].

Table 5.3 Apparent second order rate constants for the oxidation of halides and thiocyanate at pH 7 and 4.5 by Compound I of MPO, EPO, and LPO

	MPO [84] $\times 10^4$ ($M^{-1} s^{-1}$)		EPO [85] $\times 10^4$ ($M^{-1} s^{-1}$)		LPO [86] $\times 10^4$ ($M^{-1} s^{-1}$)
	pH 7	pH 5	pH 7	pH 5	pH 7
Cl^-	2.5	390	0.31	2.6	—
Br^-	110	3,000	1,900	11,000	4.1
I^-	720	6,300	9,300	>11,000	12,000
SCN^-	960	7,600	10,000	>11,000	20,000

**Fig. 5.18** Schematic representation of the mechanism of haloperoxidases. In the presence of Cl^- , HOCl is formed that (a) diffuses from the active site and oxidizes substrates in the medium, although in some cases, (b) oxidation may occur within the active site. In the absence of Cl^- , thiol-ligated haloperoxidases can (c) catalyze oxygen transfer to their substrates in a cytochrome P450-like reaction

The oxidation of halides by peroxidases results in the formation of the corresponding hypohalides: i.e., HOI, HOBr, HOCl, and HOSCN. Secondary reactions of these products with the halide ions can lead to additional oxidizing species. Thus, HOSCN can produce NCS–SCN by reaction with another NCS⁻ ion [92], and HOCl can be similarly converted to BrCl by bromide ions [93]. The substrate halogenation reactions are the result of reaction with these diffusible metabolites, although it has been argued that substrate halogenation may occur within the active site of the enzyme, either by reaction with the hypohalide before it diffuses out or with a precursor of the hypohalide. Formation of the hypohalide is thought to involve addition of the halide ion (X^-) to the oxygen of Compound I (Fig. 5.18) [84], yielding a transient Fe–OX intermediate that, at least in principle, can itself mediate halogenation reactions before it dissociates from the iron atom to give the hypohalide HOX. Furthermore, it has recently been reported that chlorination by a flavin-dependent halogenase involves not only HOCl but also a chlorinated active site lysine residue that can mediate further substrate halogenation [94]. This is reminiscent of a species called Compound X formed in the reaction of HRP with chlorite, in which a chlorinated protein residue was proposed to be involved in substrate halogenation [95]. Analogous protein-mediated halogenations may occur

with the hemoprotein haloperoxidases, but there is no evidence that this is a significant reaction pathway.

5.4.3.2 Oxygen Transfer

As already indicated, direct oxygen transfer from the peroxidase Compound I intermediate to the substrate does not occur for peroxidases except when the substrate is a small halide or pseudohalide ion. This generalization does not apply, however, to the thiolate-coordinated haloperoxidases. These enzymes not only have a thiolate proximal iron ligand but also a more open distal active site pocket that enables the binding and oxidation of small organic molecules [90, 91]. The oxygen transfer reactions catalyzed by the *Caldariomyces fumago* chloroperoxidase have been extensively investigated and are sufficiently robust to be of biotechnological interest [96]. These reactions include epoxidation of olefins, sulfoxidation of thiol groups, and oxidation of activated (e.g., allylic, propargylic, benzylic) hydrocarbon bonds. In several of these reactions, including the epoxidation of styrene [97], nitrogen oxidation of *p*-chloronitroaniline [98], and hydroxylation of 4-methylanisole [99], it has been specifically demonstrated by ^{18}O -labeling studies that the oxygen incorporated into the substrate derives quantitatively from the peroxide cosubstrate (Fig. 5.19), as required by direct oxygen transfer from Compound I (Fig. 5.18). Analogous reactions are mediated by the thiolate-ligated haloperoxidase from *A. aegerita* [88].

5.4.3.3 Sequential One-Electron Oxidations

Many reactions are known in which oxidation of a substrate by a peroxidase produces a two-electron oxidized product. In general, these reactions can be

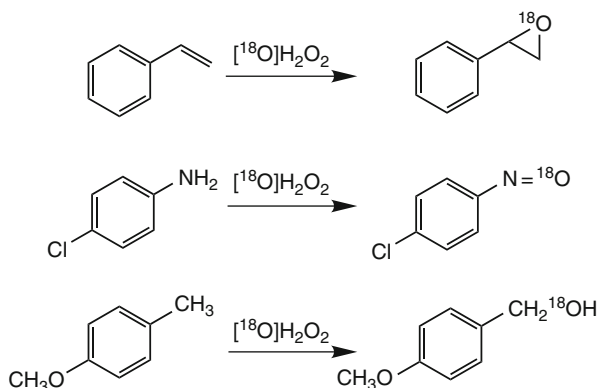


Fig. 5.19 Three oxygen transfer reactions catalyzed by the chloroperoxidase from *Caldariomyces fumago* in which the oxygen transfer was firmly established by ^{18}O isotopic labeling studies

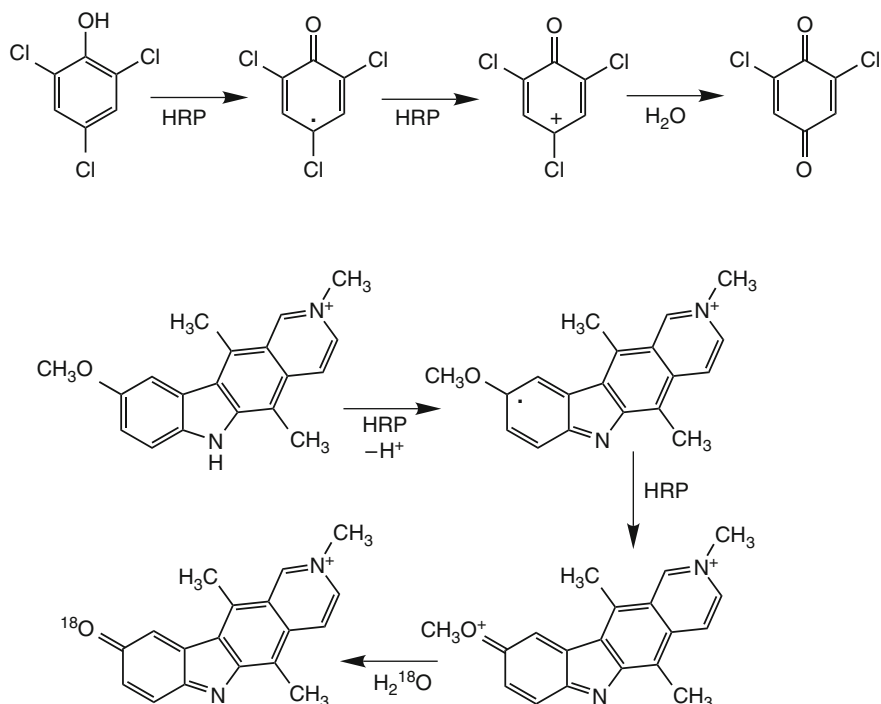


Fig. 5.20 Two examples of reactions in which the final metabolites are obtained by two one-electron oxidations catalyzed by the peroxidase

rationalized by formation of a free radical metabolite followed by a second oxidation of the free radical to the final observed product. The two oxidations can be mediated by sequential electron transfer to Compound I and then Compound II of the same peroxidase or by the action of two different peroxidases. The oxidation of veratryl alcohol to veratryl aldehyde (Fig. 5.5) is a reaction of this type. Two further examples of such reactions are the HRP-catalyzed dechlorination of 2,4,6-trichlorophenol and the oxidation of 9-methoxyellipticine to a quinone–imine (Fig. 5.20) [100, 101]. In the latter reaction, the oxygen of the iminoquinone derives from water, as expected from the indicated mechanism.

5.5 Conclusions

The peroxidases produce a reactive intermediate, Compound I, whose reactions are controlled by the protein environment. In conventional peroxidases with a histidine iron ligand, access to the Compound I ferryl species is restricted by the protein, favoring the transfer of single electrons from the substrate to an exposed heme edge. If the protein has a suitably placed oxidizable residue such as a tyrosine or

tryptophan, it may be preferentially oxidized by the initial Compound I intermediate to an alternative Compound I in which the ferryl species is paired with a protein rather than porphyrin radical cation. In most conventional peroxidases, only small substrates have ready access to the ferryl oxygen and are subject to a two-electron oxidation, although larger substrates can undergo an apparent two-electron oxidation by the stepwise peroxidative removal of two electrons. In contrast, peroxidases with a thiolate iron ligand have more open distal active sites and are able to catalyze a range of two-electron oxidations in addition to one-electron peroxidative transformations.

References

1. Schonbaum GR, Lo S (1972) Interaction of peroxidases with aromatic peracids and alkyl peroxides. *J Biol Chem* 247:3353–3360
2. Dunford HB, Stillman JS (1976) On the function and mechanism of action of peroxidases. *Coord Chem Rev* 19:187–251
3. Makino R, Yamazaki I (1972) Effects of 2, 4-substituents of deuterohemin upon peroxidase functions. I. Preparation and some properties of artificial enzymes. *J Biochem* 72:655–664
4. Dunford HB (1999) Heme peroxidases. Wiley, New York, pp 141–142
5. Smulevich G, Paoli M, Burke JF et al (1994) Characterization of recombinant horseradish peroxidase C and three site-directed mutants, F41V, F41W, and R38K by resonance Raman spectroscopy. *Biochemistry* 33:7398–7407
6. Gajhede M, Schuller DJ, Henriksen A et al (1997) Crystal structure of horseradish peroxidase C at 2.15 Å resolution. *Nat Struct Biol* 4:1032–1038
7. Bonagura CA, Bhaskar B, Shimizu H et al (2003) High-resolution crystal structures and spectroscopy of native and Compound I cytochrome c peroxidase. *Biochemistry* 42:5600–5608
8. Miller VP, Goodin DB, Friedman AE et al (1995) Horseradish peroxidase Phe172->Tyr mutant. Sequential formation of Compound I with a porphyrin radical cation and a protein radical. *J Biol Chem* 270:18413–18419
9. Nagano S, Tanaka M, Ishimori K et al (1996) Catalytic roles of the distal site asparagine-histidine couple in peroxidases. *Biochemistry* 35:14251–14258
10. Newmyer SL, Ortiz de Montellano PR (1995) Horseradish peroxidase His-42 -> Ala, His-42 -> Val, and Phe-41 -> Ala mutants. Histidine catalysis and control of substrate access to the heme iron. *J Biol Chem* 270:19430–19438
11. Rodriguez-Lopez JN, Smith AT, Thorneley RNF (1996) Recombinant horseradish peroxidase isoenzyme C: the effect of distal haem cavity mutations (His42->Leu and Arg38->Leu) on compound I formation and substrate binding. *J Biol Inorg Chem* 1:136–142
12. Erman JE, Vitello LB, Miller MA et al (1993) Histidine 52 is a critical residue for rapid formation of cytochrome c peroxidase compound I. *Biochemistry* 32:9798–9806
13. Vitello LB, Erman JE, Miller MA et al (1993) Effect of arginine-48 replacement on the reaction between cytochrome c peroxidase and hydrogen peroxide. *Biochemistry* 32:9807–9818
14. Baek HK, Van Wart HE (1989) Elementary steps in the formation of horseradish peroxidase Compound I: Direct observation of Compound 0, a new intermediate with a hyperporphyrin spectrum. *Biochemistry* 28:5714–5719
15. Baek HK, Van Wart HE (1992) Elementary steps in the reaction of horseradish peroxidase with several peroxides: Kinetics and thermodynamics of formation of Compound 0 and Compound I. *J Am Chem Soc* 114:718–725

16. Ozaki S, Inada Y, Watanabe Y (1998) Characterization of polyethylene glycolated horseradish peroxidase in organic solvents: Generation and stabilization of a transient catalytic intermediate at low temperatures. *J Am Chem Soc* 120:8020–8025
17. Denisov IG, Makris TM, Sligar SG (2002) Formation and decay of hydroperoxo-ferric heme complex in horseradish peroxidase studied by cryoradiolysis. *J Biol Chem* 277:42706–42710
18. Shintaku M, Matsuura K, Yoshioka S et al (2005) Absence of a detectable intermediate in the Compound I formation of horseradish peroxidase at ambient temperature. *J Biol Chem* 280:40934–40938
19. Harris DL, Loew GH (1996) Identification of putative peroxide intermediates of peroxidases by electronic structure and spectra calculations. *J Am Chem Soc* 118:10588–10594
20. Derat E, Shaik S (2006) The Poulos-Kraut mechanism of Compound I formation in horseradish peroxidase: a QM/MM study. *J Phys Chem B* 110:10526–10533
21. Jones P, Dunford HB (2005) The mechanism of Compound I formation revisited. *J Inorg Biochem* 99:2292–2298
22. Poulos TL, Kraut J (1980) The stereochemistry of peroxidase catalysis. *J Biol Chem* 255:8199–8205
23. Dolphin D, Forman A, Borg DC et al (1971) Compounds I of catalase and horseradish peroxidase: π -cation radicals. *Proc Natl Acad Sci USA* 68:614–618
24. Rutter R, Valentine M, Hendrich MP et al (1983) Chemical nature of the porphyrin π cation radical in horseradish peroxidase Compound I. *Biochemistry* 22:4769–4774
25. Roberts JE, Hoffman BM, Rutter R et al (1981) Electron double resonance of horseradish peroxidase Compound I. Detection of the porphyrin π -cation radical. *J Biol Chem* 256:2118–2121
26. Penner-Hahn JE, Eble KS, McMurry TJ et al (1986) Structural characterization of horseradish peroxidase using EXAFS spectroscopy. Evidence for Fe=O ligation in Compounds I and II. *J Am Chem Soc* 108:7819–7825
27. Palaniappan V, Terner J (1989) Resonance Raman spectroscopy of horseradish peroxidase derivatives and intermediates with excitation in the near ultraviolet. *J Biol Chem* 264:16046–16053
28. Berglund GI, Carlsson GH, Smith AT et al (2002) The catalytic pathway of horseradish peroxidase at high resolution. *Nature* 417:463–468
29. Hersleth H-P, Ryde U, Rydberg P et al (2006) Structures of the high-valent metal-ion haem-oxygen intermediates in peroxidases, oxygenases and catalases. *J Inorg Biochem* 100:460–476
30. Finzel BC, Poulos TL, Kraut J (1984) Crystal structure of yeast cytochrome c peroxidase refined at 1.7 Å resolution. *J Biol Chem* 259:13027–13036
31. Huyett JE, Doan PE, Gurbel R et al (1995) Compound ES of cytochrome c peroxidase contains a Trp π -cation radical: characterization by CW and pulsed Q-band ENDOR spectroscopy. *J Am Chem Soc* 117:9033–9041
32. Morimoto A, Tanaka M, Takahashi S et al (1998) Detection of a tryptophan radical as an intermediate species in the reaction of horseradish peroxidase mutant (Phe-221->Trp) and hydrogen peroxide. *J Biol Chem* 273:14753–14760
33. Miki Y, Morales M, Ruiz-Dueñas FJ et al (2009) *Escherichia coli* expression and *in vitro* activation of a unique ligninolytic peroxidase that has a catalytic tyrosine residue. *Protein Express Purif* 68:208–214
34. Pérez-Boada M, Ruiz-Dueñas FJ, Pogni R et al (2005) Versatile peroxidase oxidation of high redox potential aromatic compounds: site-directed mutagenesis, spectroscopic and crystallographic investigation of three long-range electron transfer pathways. *J Mol Biol* 354:385–402
35. Ruiz-Dueñas FJ, Pogni R, Morales M et al (2009) Protein radicals in fungal versatile peroxidases. Catalytic tryptophan radical in both compound I and compound II and studies on W164Y, W164H, and W164S variants. *J Biol Chem* 284:7986–7994

36. Pogni R, Baratto MC, Giansanti S et al (2005) Tryptophan-based radical in the catalytic mechanism of versatile peroxidase from *Bjerkandera adusta*. *Biochemistry* 44: 44267–44274
37. Ghiladi RA, Medzihradzsky KF, Rusnak FM et al (2005) Correlation between isoniazid resistance and superoxide reactivity in *Mycobacterium tuberculosis* KatG. *J Am Chem Soc* 127:13428–13442
38. Blodig W, Doyle WA, Smith AT et al (1998) Autocatalytic formation of a hydroxy group at C β of Trp171 in lignin peroxidase. *Biochemistry* 37:8832–8838
39. Blodig W, Smith AT, Doyle WA et al (2001) Crystal structures of pristine and oxidatively processed lignin peroxidase expressed in *Escherichia coli* and of the W171F variant that eliminates the redox active tryptophan 171. Implications for the reaction mechanism. *J Mol Biol* 305:851–861
40. Doyle WA, Blodig W, Veitch NC et al (1998) Two substrate interaction sites in lignin peroxidase revealed by site-directed mutagenesis. *Biochemistry* 37:15097–15105
41. Smulevich G, Jakopitsch C, Droghetti E et al (2006) Probing the structure and bifunctionality of catalase-peroxidase (KatG). *J Inorg Biochem* 100:568–585
42. Ghiladi RA, Knudsen GM, Medzihradzsky KF et al (2005) The Met-Tyr-Trp crosslink in *Mycobacterium tuberculosis* catalase-peroxidase (KatG): Autocatalytic formation and effect on enzyme catalysis and spectroscopic properties. *J Biol Chem* 280:22651–22663
43. Ghiladi RA, Medzihradzsky KF, Ortiz de Montellano PR (2005) The role of the Met-Tyr-Trp crosslink in *Mycobacterium tuberculosis* catalase-peroxidase (KatG) as revealed by KatG (M255I). *Biochemistry* 44:15093–15105
44. Suarez J, Ranguelova K, Jarzecki AA et al (2009) An oxyferrous heme/protein-based radical intermediate is catalytically competent in the catalase reaction of *Mycobacterium tuberculosis* catalase-peroxidase (KatG). *J Biol Chem* 284:7017–7029
45. Jakopitsch C, Vlasits J, Wiseman B et al (2007) Redox intermediates in the catalase cycle of catalase-peroxidases from *Synechocystis* PCC 6803, *Burkholderia pseudomallei*, and *Mycobacterium tuberculosis*. *Biochemistry* 46:1183–1193
46. Davies MJ, Hawkins CL, Pattison DI et al (2008) Mammalian heme peroxidases: from molecular mechanisms to health implications. *Antioxidants Redox Signal* 10:1199–1234
47. Singh AK, Singh N, Sharma S et al (2008) Crystal structure of lactoperoxidase at 2.4 Å resolution. *J Mol Biol* 376:1060–1075
48. Fiedler TJ, Davey CA, Fenna RE (2000) X-ray crystal structure and characterization of halide-binding sites of human myeloperoxidase at 1.8 Å resolution. *J Biol Chem* 275:11964–11971
49. Carpena X, Vidossich P, Schroettner K et al (2009) Essential role of proximal histidine-asparagine interaction in mammalian peroxidases. *J Biol Chem* 284:25929–25937
50. Oxvig C, Thomsen A, Overgaard M et al (1999) Biochemical evidence for heme linkage through esters with Asp-93 and Glu-241 in human eosinophil peroxidase. The ester with Asp-93 is only partially formed *in vivo*. *J Biol Chem* 274:16953–16958
51. DePillis GD, Ozaki S, Kuo JM et al (1997) Autocatalytic processing of heme by lactoperoxidase produces the native protein-bound prosthetic group. *J Biol Chem* 272:8857–8860
52. Colas C, Kuo JM, Ortiz de Montellano PR (2002) Asp225 and Glu375 in autocatalytic attachment of the prosthetic heme group of lactoperoxidase. *J Biol Chem* 277:7191–7200
53. Colas C, Ortiz de Montellano PR (2004) Horseradish peroxidase mutants that autocatalytically modify their prosthetic heme group. Insights into mammalian peroxidase heme-protein covalent bonds. *J Biol Chem* 279:24131–24140
54. Metcalfe CL, Ott M, Patel N et al (2004) Autocatalytic formation of green heme: evidence for H₂O₂-dependent formation of a covalent methionine-heme linkage in ascorbate peroxidase. *J Am Chem Soc* 126:16242–16248
55. Ator MA, Ortiz de Montellano PR (1987) Protein control of prosthetic heme reactivity. Reaction of substrates with the heme edge of horseradish peroxidase. *J Biol Chem* 262: 1542–1551

56. Ator MA, David SK, Ortiz de Montellano PR (1987) Structure and catalytic mechanism of horseradish peroxidase. Regiospecific meso alkylation of the prosthetic heme group by alkylhydrazines. *J Biol Chem* 262:14954–14960
57. Ortiz de Montellano PR, David SK, Ator MA et al (1988) Mechanism-based inactivation of horseradish peroxidase by sodium azide. Formation of meso-azidoporphyrin IX. *Biochemistry* 27:5470–5476
58. Porter DJT, Bright HJ (1983) The mechanism of oxidation of nitroalkanes by horseradish peroxidase. *J Biol Chem* 258:9913–9924
59. Wiseman JS, Nichols JS, Kolpak MX (1982) Mechanism of inhibition of horseradish peroxidase by cyclopropanone hydrate. *J Biol Chem* 257:6328–6332
60. Huang L, Colas C, Ortiz de Montellano PR (2004) Oxidation of carboxylic acids by horseradish peroxidase results in prosthetic heme modification and inactivation. *J Am Chem Soc* 126:12865–12873
61. Wojciechowski G, Ortiz de Montellano PR (2007) Radical energies and the regiochemistry of addition to heme groups. Methylperoxy and nitrite radical additions to heme of horseradish peroxidase. *J Am Chem Soc* 129:1663–1672
62. Huang L, Wojciechowski G, Ortiz de Montellano PR (2005) Prosthetic heme modification during halide ion oxidation. Demonstration of chloride oxidation by horseradish peroxidase. *J Am Chem Soc* 127:5345–5353
63. Wojciechowski G, Huang L, Ortiz de Montellano PR (2005) Autocatalytic modification of the prosthetic heme of horseradish but not lactoperoxidase by thiocyanate oxidation products. A role for heme-protein covalent crosslinking. *J Am Chem Soc* 127:15871–15879
64. Davies MJ (2005) The oxidative environment and protein damage. *Biochim Biophys Acta* 1703:93–109
65. Huang L, Wojciechowski G, Ortiz de Montellano PR (2006) Role of heme-protein covalent bonds in mammalian peroxidases. Protection of the heme by a single engineered heme-protein link in horseradish peroxidase. *J Biol Chem* 281:18983–18988
66. DePillis GD, Wariishi H, Gold MH et al (1990) Inactivation of lignin peroxidase by phenylhydrazine and sodium azide. *Arch Biochem Biophys* 280:217–223
67. Kumar D, de Visser SP, Sharma PK et al (2005) The intrinsic axial ligand effect on propene oxidation by horseradish peroxidase versus cytochrome P450 enzymes. *J Biol Inorg Chem* 10:181–189
68. Pelletier H, Kraut J (1992) Crystal structure of a complex between electron transfer partners, cytochrome c peroxidase and cytochrome C. *Science* 258:1748–1755
69. DePillis GD, Sishta BP, Mauk AG et al (1991) Small substrates and cytochrome c are oxidized at different sites of cytochrome c peroxidase. *J Biol Chem* 266:19334–19341
70. Planche LA (1810) Note sur la sophistication de la résine de jalap et sur les moyens de la reconnaître. *Bull Pharm* 2:578–580
71. Booth H, Saunders BC (1956) Studies in peroxidase action. Part X. The oxidation of phenols. *J Chem Soc* :940–948
72. Job D, Dunford HB (1976) Substituent effect on the oxidation of phenols and aromatic amines by horseradish peroxidase Compound I. *Eur J Biochem* 66:607–614
73. Dunford HB, Adeniran AJ (1986) Hammett σ_p correlation for reactions of horseradish peroxidase Compound II with phenols. *Arch Biochem Biophys* 251:536–542
74. Van Haandel MJH, Claassens MMJ, Van der Hout N et al (1999) Differential substrate behaviour of phenol and aniline derivatives during conversion by horseradish peroxidase. *Biochim Biophys Acta* 1435:22–29
75. Gilabert MA, Hiner ANP, García-Ruiz PA et al (2004) Differential substrate behavior of phenol and aniline derivatives during oxidation by horseradish peroxidase: kinetic evidence for a two-step mechanism. *Biochim Biophys Acta* 1699:235–243
76. Hayashi Y, Yamazaki I (1979) The oxidation-reduction potentials of Compound I/Compound II and Compound II/ferric couples of horseradish peroxidases A2 and C. *J Biol Chem* 254:9101–9106

77. Sakurada J, Sekiguchi R, Sato K et al (1990) Kinetic and molecular orbital studies on the rate of oxidation of monosubstituted phenols and anilines by horseradish peroxidase Compound II. *Biochemistry* 29:4093–4098
78. Boyd JA, Eling TE (1984) Evidence for a one-electron mechanism of 2-aminofluorene oxidation by prostaglandin H synthase and horseradish peroxidase. *J Biol Chem* 259:13885–13896
79. Mottley C, Robinson RE, Mason RP (1991) Free radical formation in the oxidation of malondialdehyde and acetylacetone by peroxidase enzymes. *Arch Biochem Biophys* 289:153–160
80. Lakshmi VM, Zenser TV, Mattammal MB et al (1993) Phenylbutazone peroxidatic metabolism and conjugation. *J Pharmacol Exp Ther* 266:81–88
81. Hofrichter M (2002) Review: Lignin conversion by manganese peroxidase (MnP). *Enzyme Microb Technol* 30:454–466
82. Goodwin DC, Grover TA, Aust SD (1997) Roles of efficient substrates in enhancement of peroxidase-catalyzed oxidations. *Biochemistry* 36:139–147
83. Furtmüller PG, Zederbauer M, Jantschko W et al (2006) Active site structure and catalytic mechanisms of human peroxidases. *Arch Biochem Biophys* 445:199–213
84. Furtmüller PG, Burner U, Obinger C (1998) Reaction of myeloperoxidase Compound I with chloride, bromide, iodide, and thiocyanate. *Biochemistry* 37:17923–17930
85. Furtmüller PG, Burner U, Regelsberger G et al (2000) Spectral and kinetic studies on the formation of eosinophil peroxidase compound I and its reactions with halides and thiocyanate. *Biochemistry* 39:15578–15584
86. Furtmüller PG, Jantschko W, Regelsberger G et al (2002) Reaction of lactoperoxidase compound I with halides and thiocyanate. *Biochemistry* 41:11895–11900
87. Huang L, Ortiz de Montellano PR (2007) *Arthromyces ramosus* peroxidase produces two chlorinating species. *Biochem Biophys Res Commun* 355:581–586
88. Hofrichter M, Ullrich R (2006) Heme-thiolate haloperoxidases: versatile biocatalysts with biotechnological and environmental significance. *Appl Microbiol Biotechnol* 71:276–288
89. Dawson JH, Sono M (1987) Cytochrome P-450 and chloroperoxidase: thiolate-ligated heme enzymes. Spectroscopic determination of their active site structures and mechanistic implications of thiolate ligation. *Chem Rev* 87:1255–1276
90. Sundaramoorthy M, Terner J, Poulos TL (1995) The crystal structure of chloroperoxidase: a heme peroxidase-cytochrome P450 functional hybrid. *Structure* 3:1367–1377
91. Sundaramoorthy M, Terner J, Poulos TL (1998) Stereochemistry of the chloroperoxidase active site: crystallographic and molecular-modeling studies. *Chem Biol* 5:461–473
92. Thomas EL (1985) Products of lactoperoxidase-catalyzed oxidation of thiocyanate and halides. In: Pruitt KM, Tenovuo JO (eds) *The lactoperoxidase system. Chemistry and biological significance*. Marcel Dekker, New York, pp 31–53
93. Henderson JP, Byun J, Williams MV et al (2001) Production of brominating intermediates by myeloperoxidase. A transhalogenation pathway for generating mutagenic nucleobases during inflammation. *J Biol Chem* 276:7867–7875
94. Yeh E, Blasiak LC, Koglin A et al (2007) Chlorination by a long-lived intermediate in the mechanism of flavin-dependent halogenases. *Biochemistry* 46:1284–1292
95. Suh YJ, Hager LP (1991) Chemical and transient state kinetic studies on the formation and decomposition of horseradish peroxidase compounds X_I and X_{II}. *J Biol Chem* 266:22102–22109
96. Dembitsky VM (2003) Oxidation, epoxidation, and sulfoxidation reactions catalyzed by haloperoxidases. *Tetrahedron Lett* 59:4701–4720
97. Ortiz de Montellano PR, Choe YS, DePillis G et al (1987) Structure-mechanism relationships in hemoproteins. Oxygenations catalyzed by chloroperoxidase and horseradish peroxidase. *J Biol Chem* 262:11641–11646
98. Doerge DR, Corbett MD (1991) Peroxygenation mechanism for chloroperoxidase-catalyzed N-oxidation of arylamines. *Chem Res Toxicol* 4:556–560

99. Miller VP, Tschirret-Guth RA, Ortiz de Montellano PR (1995) Chloroperoxidase-catalyzed benzylic hydroxylation. *Arch Biochem Biophys* 319:333–340
100. Ferrari RP, Laurenti E, Trotta F (1999) Oxidative dechlorination of 2, 4, 6-trichlorophenol catalyzed by horseradish peroxidase. *J Biol Inorg Chem* 4:232–237
101. Meunier G, Meunier B (1985) Peroxidase-catalyzed *O*-demethylation reactions. Quinone imine formation from 9-methoxyellipticine derivatives. *J Biol Chem* 260:10576–10582

Part II
Prospective Usage of Peroxidases
in Industry

Chapter 6

Potential Applications of Peroxidases in the Fine Chemical Industries

Luigi Casella, Enrico Monzani, and Stefania Nicolis

Contents

6.1	Selective Oxidations Catalyzed by Peroxidases	111
6.1.1	Introduction	111
6.1.2	Reactions Driven by Radical Mechanisms	114
6.1.3	Insertion of Oxygen Atoms into Substrate Molecules	123
6.1.4	Activation of Halogens	129
6.1.5	Activation of Nitrite	130
6.2	Analytical Applications of Peroxidases	132
6.2.1	ELISA	132
6.2.2	Biosensors	133
6.3	Prospective Applications of Peroxidases in the Fine Chemical and Pharmaceutical Industries	135
6.3.1	Native and Modified Peroxidases	135
6.3.2	Proteins with Pseudoperoxidase Activity	136
6.3.3	Heme–Peptide Complexes	139
	References	143

Abstract A description of selected types of reactions catalyzed by heme peroxidases is given. In particular, the discussion is focused mainly on those of potential interest for fine chemical synthesis. The division into subsections has been done from the point of view of the enzyme action, i.e., giving emphasis to the mechanism of the enzymatic reaction, and from that of the substrate, i.e., analyzing the type of transformation promoted by the enzyme. These two approaches have several points in common.

6.1 Selective Oxidations Catalyzed by Peroxidases

6.1.1 Introduction

Chemistry is a very important industrial sector from an economic and social point of view. Chemical industries deal with both large-scale preparations and small-scale productions. The latter include products made by the so called “fine chemical

industries,” which produce chemical compounds with high value. Most of them are drugs or intermediates for drug preparations, but they are used not only in pharmaceutical companies but also for many other applications. Their preparations often require regio- and stereospecific synthesis in order to reduce the number of by-products and generally occur under controlled reaction conditions. The selectivity is commonly achieved by the use of catalysts, which in several cases are constituted by metal complexes. Together with more traditional synthetic methods, an increasing number of processes make use of biocatalysts [1]. In fact, biotransformations can be profitably used in fine chemical industries, in particular when selective and very active catalysts are required. This is because enzymes are chiral molecules with active site characteristics often allowing an easy approach only to molecules with specific shapes. In some cases, the substrates are bound at the active site with a rigid disposition, facilitating its transformation through highly regioselective reactions. The selectivity of enzymatic reaction allows reduction of the quantity and number of by-products, making the process more “environmentally friendly,” a step forward toward green chemistry [2]. In other cases, enzymes have low selectivity in the reaction with substrates; this usually happens when they bear low specificity active sites, allowing free approach of substrates of different types, for instance, carrying different charges, stereocenters, and steric requirements. Here, the negative aspect of the low selectivity is balanced by the possibility of using the biomolecules for transformation of a broad spectrum of substrates, independently of their structure. When the enzyme has oxidative activity, the redox potential of the active species formed in the catalytic cycle is also an important factor determining the type of reactions that can be catalyzed, discriminating between which kind of molecules are potential substrates and which are not (see Chap. 4). An important aspect in using enzymes is that they can perform their reactions in very mild conditions, generally in water but often also in mixed water/organic solvents, and at room temperature. This is important not only from an environmental and economic point of view but also because often the molecules of interest in the fine chemical industry, in particular in drug preparations, have more than one site or functional group, which can undergo modification when the reaction conditions employed are more severe.

Often the positive aspects of using enzymes are counterbalanced by their weak points. With many of them, the use is restricted to water medium since they lose activity or undergo inactivation, denaturation, or even precipitation in the presence of organic solvents. On the other hand, a large number of interesting molecules to be used as substrates show very limited solubility in water, thus requiring an organic cosolvent. This leads to a general problem in the use of biocatalysts for industrial applications, i.e., stability in the (nonphysiological) reaction conditions. Both thermodynamic stability (the capacity to maintain tertiary structure) and kinetic stability (the duration the enzyme remains active) are important here, and a large variety of methods have been devised to increase enzyme stability, including chemical modification, use of additives, lyophilization, immobilization, and protein engineering [3]. With reference to the problem of operation in mixed organic solvents as an example, modification of the exposed residues with polyethylene glycol may be sufficient to enhance the organic solvent compatibility of the protein.

Chemical modification has the drawback that the modified protein often shows a much reduced activity with respect to the native enzyme, and the effect on enzyme selectivity is unpredictable. A further weak point in using biocatalysts is that they are much more expensive with respect to conventional catalysts and, in order to be economically convenient from an industrial point of view, they must show a large number of turnover cycles before degradation. If the enzyme has very high activity and/or it is not excessively precious, its recycle from the product mixture may not be necessary. Otherwise, the protein must also be easily separated from the reaction mixture, without undergoing inactivation.

Heme peroxidases have the potential to be widely used as catalysts in fine chemical preparations. This is because they are enzymes capable of performing a wide variety of oxidation reactions, ranging from radical coupling reactions, to oxygen-atom insertion into substrates, to several types of halogenation processes. Some of them are capable to oxidize, without selectivity, a broad range of electron-rich molecules. The types of catalytic activity exhibited by heme peroxidases are associated with the redox potential of the active species formed in the catalytic cycle, the accessibility of the substrates to their heme active site, and the possibility to generate diffusible halogenating and nitrating species. In spite of their versatility, up to now there are only a few industrial applications of peroxidases, in most cases still at a prospective level, for instance, for bleaching purposes in detergents and in the paper and pulp industry, for degradation of electron-rich aromatic residues in waste waters, for antimicrobial applications, and for the synthesis of phenolic resins. The main limitation has probably to do with the chemistry these enzymes catalyze, which involves as an essential substrate a strong oxidant such as hydrogen peroxide. The scale-up of processes requiring this reagent inevitably leads to a relatively rapid reduction in the performance of peroxidases, which are enzymes of considerable cost. As a matter of fact, industrial applications of enzymes belonging to other classes, and also of many other oxidoreductases that do not use peroxides, are much more extensive [4]. Another problem, with some interesting peroxidases, is their low availability, since large-scale preparation methods are still lacking (see Chap. 12). Unfortunately, these drawbacks are particularly important with chloroperoxidase (CPO), probably the peroxidase with the most interesting reactivity features, from the point of view of organic synthesis, since in many reactions it exhibits interesting stereoselectivity and enantioselectivity properties. CPO is an expensive enzyme, which not only undergoes inactivation in the presence of hydrogen peroxide but also survives only in slightly acidic solution. For these reasons, the current most widespread applications of peroxidases are in the field of immunoassays and as biosensors, in particular for the best known enzyme from horseradish. In these cases, the enzyme is used in very low concentrations and the reaction does not require a selective catalyst but a species capable to generate a radical by oxidation of chromogenic, electron-rich substrates.

As the practical limitations to the use of peroxidases can be overcome, we believe that these enzymes have many potential applications in fine chemistry. This chapter, therefore, aims at summarizing the different reactions promoted by the peroxidases, which could be of interest in fine chemicals preparation. This is because the enzyme

either allows high selectivity in the product or because it performs a difficult reaction in much milder conditions than any other chemical oxidizing agent. Several studies are currently under development for obtaining modified peroxidases with enhanced stability, activity, and selectivity (see Chap. 9). When these goals are achieved, it is expected that the number of technological applications of these versatile enzymes will experience a significant increase.

The following section thus reports a description of selected types of reactions catalyzed by heme peroxidases. In particular, the discussion will focus mainly on those of potential interest for fine chemical synthesis. The division into subsections has been done from the point of view of the enzyme action, i.e., giving emphasis to the mechanism of the enzymatic reaction, and from that of the substrate, i.e., analyzing the type of transformation promoted by the enzyme. These two approaches have several points in common.

6.1.2 Reactions Driven by Radical Mechanisms

Among the various types of reactions catalyzed by peroxidases, those involving a radical mechanism are the most common. The classical peroxidase mechanism involves, after the reaction of the enzyme with hydrogen peroxide, the formation of two active intermediates, namely compound I and compound II [5–7] (for a detailed description see Chap. 5). Compound I is two oxidizing equivalents above the resting enzyme. This active species could be formally described as an iron(V)-oxo species, but in most peroxidases, such as horseradish peroxidase (HRP), it is an iron(IV)-oxo porphyrin radical cation. Also common is the delocalization of the radical on amino acid residues of the peptide chain of the protein, as it occurs, for example, in lactoperoxidase (LPO) and cytochrome *c* peroxidase (CcP) [8–11]. The one-electron reduction of compound I gives rise to compound II. This species is one oxidizing equivalent above the resting enzyme and, in most cases, it is an iron(IV)-oxo species, because it is the radical (either on the porphyrin or on the protein residue/s) that is reduced in compound I. For LPO, it has been reported that in particular conditions in compound II, the oxidizing equivalent could be located on an amino acid residue [8–11].

Both compound I and compound II easily undergo one electron reduction in the presence of suitable reducing agents [12]. The electron transfer between the enzyme and the substrates is facilitated by the presence of the highly delocalized π orbitals of the porphyrin moiety and the presence of protein aromatic residues. In order to be easily oxidized, the substrate must approach the site where the electron transfer takes place. In the case of HRP and many other peroxidases, the electron transfer is very efficient when the substrate also has π orbitals, which can give some overlap with those of the porphyrin, and this occurs when the reducing molecule is localized at the porphyrin edge. The binding of substrates near the porphyrin edge often occurs also with inorganic anions such as iodide, thiocyanide, or nitrite. Usually, the substrate binding site is close to the enzyme surface.

Enzyme selectivity is usually limited because it depends on the interaction between the substrate and hydrophobic and hydrophilic amino acid residues at the active site, but here the degree of substrate immobilization is generally low. After the electron transfer process has occurred, the substrate is transformed into a radical compound that diffuses to the bulk of the solution and evolves according to its chemical properties, generally independently of the enzyme. This implies that the peroxidases rule the yield and the rate of radical formation but, once the latter species has been formed, the product composition and the stereoselectivity of the reaction are essentially dependent on the radical chemical structure and, to some extent, on the solvent and temperature of the reaction.

Another important aspect of peroxidase reactions is the relation between the substrate one-electron redox potential and the redox potential of compound I and compound II, since this restricts the number of possible redox partners (see Chap. 4 for a detailed description). Table 6.1 reports the redox potentials of some selected peroxidases; as it can be seen, the values span an interval ranging from 1.35 V for reduction of myeloperoxidase (MPO) compound I to ≈ 1.0 V for reduction of HRP compound I [13–15]. But the selection of the preferred enzyme for a given radical reaction must consider not only the complementarities in the redox potentials but also the mechanism preferred by the enzyme, since some peroxidases, such as CPO and MPO, and also LPO in some cases, react through a two-electron oxidation mechanism.

There are many molecules that, in the presence of peroxides and peroxidases, can be oxidized by abstraction of one electron; among them, there are electron-rich aromatic molecules, such as phenols, anilines, catechols, and indoles, and also small molecules and anions such as nitrite. In general, the application of this reaction for fine chemical preparations is prevented by the complex pattern of products obtained that is usually a mixture of oligomeric and polymeric compounds.

6.1.2.1 Oxidation of Phenols (oxidative dehydrogenation of phenols)

Most phenols have one electron redox potential, which allows their oxidation by compound I and compound II to phenoxide radicals according to the following reactions:

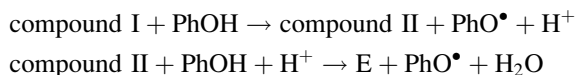


Table 6.1 One-electron reduction potentials of selected peroxidase redox couples

	Enzyme	Compound I/ Compound II	Compound II/ ferric enzyme
1	Myeloperoxidase	1.35 V	0.97 V
2	Lactoperoxidase	1.14 V	1.04 V
3	Horseradish peroxidase	0.97 V	≈ 1 V
4	Chloroperoxidase	≈ 1.3 V	≈ 1.3 V

Entry 1, 2, 3, and 4 are from [13–15], respectively

where the radical in the substrate is localized partly on the oxygen atom and partly on the carbons in *ortho* and *para* positions to the hydroxyl group. This delocalization of the radical on the phenol nucleus accounts for the product composition, since the radical coupling can occur through an *ortho-ortho* process, giving rise to an *o,o'*-biphenyl adduct, or through an *ortho-para* process, forming the so called Pummerer's ketone, a pharmacophoric synthon [16] (Fig. 6.1a).

Notwithstanding the phenol dimers are bulkier compounds with respect to the starting substrate, thus making their access to the peroxidase active site more difficult, they have a lower redox potential and compete with monomeric phenols in the reaction with compound I and compound II. Furthermore, the phenoxy radical can oxidize a phenol dimer to its radical form. This results in the formation of oligomeric and then polymeric compounds at longer reaction times [17]. Thus, if the products of interest are the diphenolic compounds, the reaction must be carried out in mildest conditions and only the products formed in the initial phase have to be collected. But in some cases [18–20], the *o,o'*-biphenyl is the principal product of phenol oxidation, such as with *p*-cresol, tyrosine, etc. All peroxidases can be employed for these reactions, but HRP is usually preferred with respect to other peroxidases due to its higher availability and to its broad specificity. Whole cell

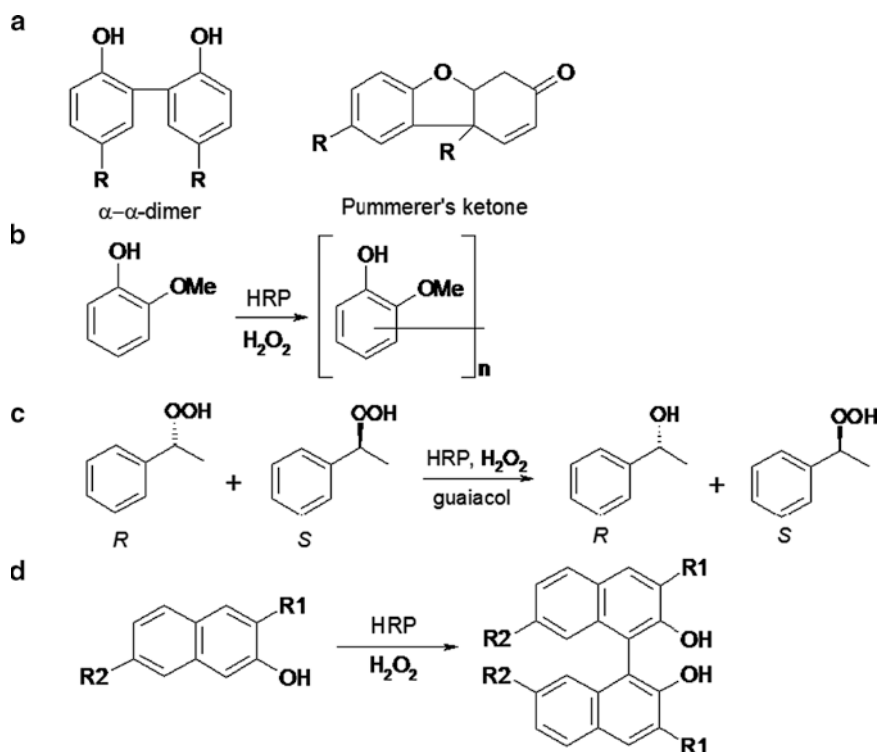


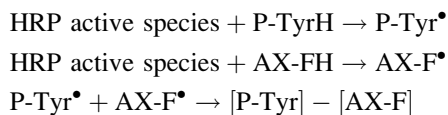
Fig. 6.1 Some examples of peroxidase-catalyzed oxidations of phenols and naphthols; in (d), R1 represents a hydrogen or a bromine atom and R2 a hydrogen, methyl, or carboxymethyl groups

systems have also been employed instead of purified enzymes [21–23]. The peroxidase oxidation of phenols finds application for waste water treatment and for resin preparation [24], but potential applications of this reaction can be envisioned for the synthesis of *o,o'*-biphenyl derivatives as modified natural products with potentiated biological activities [25–29] (Table 6.2).

HRP efficiently catalyzes the polymerization of guaiacol by H₂O₂ (Fig. 6.1b). The reaction occurs easily also with alkyl hydroperoxides. In order to form compound I, these oxidants must reach the iron atom, and may experience an interaction with the amino acids at the distal site of the enzyme. It follows that different alkyl hydroperoxides exhibit different reactivities and, in particular, enantiomers react at different rates. Adam et al [30] took advantage of this property for developing a method for the kinetic resolution of racemic alkyl hydroperoxides. The racemic secondary hydroperoxide was reacted with guaiacol in the presence of HRP. One enantiomer of the oxidant preferentially reacted with the enzyme and was transformed into the corresponding alcohol. The other enantiomer was left behind and accumulated in solution. The enzyme shows high selectivity in this reaction, and often almost enantiopure hydroperoxide can be isolated. In particular, with aryl alkyl-substituted hydroperoxide, it is the (*R*)-isomer of the oxidant that is preferentially transformed into the (*R*)-alcohol, thus leading to the accumulation of the (*S*)-hydroperoxide [30–32] (Fig. 6.1c). Both the formed alcohol and the unreacted hydroperoxide are optically pure, but from a fine chemistry point of view, it is the preparation of the enantiomeric pure oxidant that is the important aspect of this synthesis.

Peroxidases are also active in the oxidation of naphthyl derivatives. In particular, when the substrates are 2-naphthols, the interesting derivatives 1,1'-dinaphthyl-2,2'-diols are formed [23] (Fig. 6.1d). In the presence of suitable substituents blocking the rotation of the naphthyl moieties, chiral binaphthyls can be obtained with enantiomeric enrichment [33, 34].

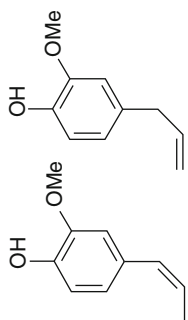
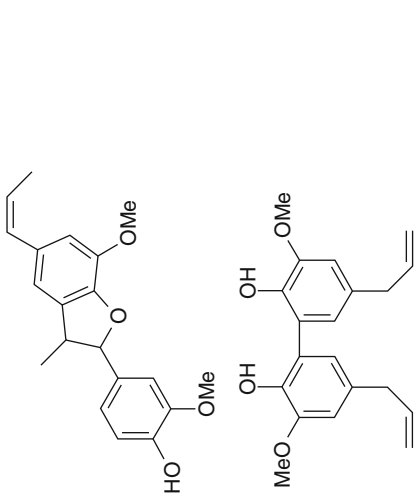
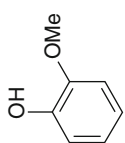
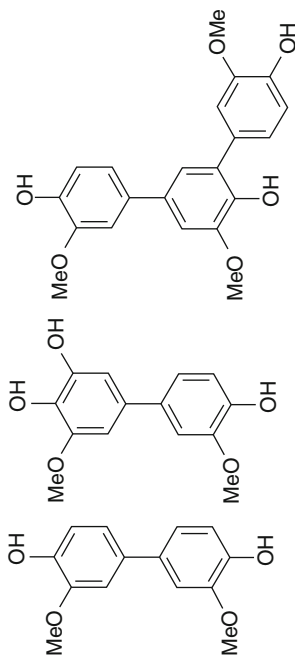
Peroxidases oxidize tyrosines, both as a free amino acid and as a residue in peptides and proteins. When proteins are treated with HRP in the presence of hydrogen peroxide, protein dimers are obtained through the coupling of tyrosyl radicals. HRP can also be used for cross-linking of proteins with polysaccharides [35]. In this case, coupling occurs between a tyrosyl radical in the protein and a radical species on the saccharide:

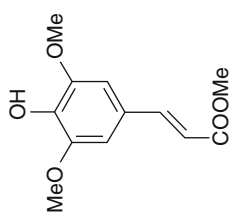


where *P*-TyrH represents a tyrosine residue in a protein and AX-FH an arabinoxylan (AX) containing ester-linked ferulic acid.

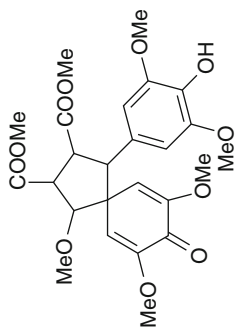
Protein–polysaccharide cross-linking gives rise to protein conjugates with modified properties, such as an enhanced stability to heat, organic solvents, and proteolysis, which could bear biotechnological applications, but could also be used for preparation of gels, foams, and colloids.

Table 6.2 Some products of peroxidase catalyzed phenol oxidation with potential fine chemical applications

	Substrate	Products
1		
2		



3



Entry 1, 2, and 3 are from [25], [26], and [29], respectively

6.1.2.2 Oxidation of Amines

As for the oxidation of phenols, the peroxidase reaction with amines usually gives rise to the formation of polymers. This is the case, for instance, of the oxidation of aniline [36] (Fig. 6.2a).

The peroxidase-catalyzed oxidation of *ortho*-phenylenediamine by hydrogen peroxide can be used for the synthesis of diaminophenazine, the starting material for the preparation of many dyes (Fig. 6.2b).

Again, upon prolonged reaction times, polymerization of the substrate occurs [37]. Often, when the substrates contain nitrogen atoms, the radical mechanism leads to products containing azo groups [38] or iminoxy dimers [39], which can be used as starting materials for the synthesis of complex molecules (Fig. 6.2c). Nonenzymatic reactions afford a complex mixture of radical oxidation products. In addition, in many cases, aryl amines may undergo nitrogen oxidation to the corresponding nitroso compound (see Sect. 6.1.3).

Another type of transformation catalyzed by peroxidases and occurring through a radical mechanism is the demethylation of heteroatoms, such as $-OMe$ and $-NMe$ groups [40–42]. Figure 6.2d shows, as an example, the HRP-catalyzed *O*-demethylation of 9-methoxyellipticine [41]. This reaction occurs through the elimination of methanol in very mild conditions. It should be noted that

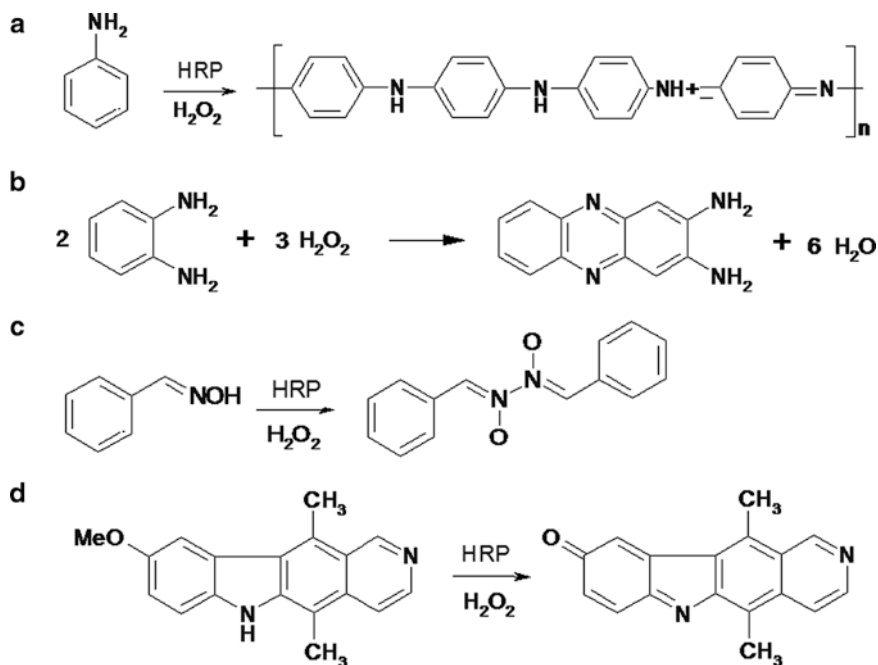


Fig. 6.2 Some examples of peroxidase-catalyzed oxidations of aryl amines, (a) and (b), oxyme, (c) and demethylation of a $-OMe$ group, (d)

demethylation is not an easy reaction to be performed with classical organic chemistry preparative methods.

6.1.2.3 Oxidation of Catechols

By one-electron oxidation, catechols are transformed into semiquinone radicals. These are unstable species and, in solution, undergo dismutation to the corresponding quinone and a molecule of the initial catechol according to the reaction [43] (Fig. 6.3a).

In the presence of bulky groups, such as in 3,5-di-*tert*-butylquinone, the quinone is stable and can be isolated, but in most cases, it easily undergoes other reactions, such as Michael addition by nucleophiles present in solution, including the catechol itself. On the other hand, in some cases, the substrate oxidation can be driven to selected products [44], as in the synthesis of neurotrophic americanol A and isoamericanol by HRP-catalyzed oxidative coupling of caffeic acid [45] (Fig. 6.3b).

With branched catechols carrying nucleophilic groups in the side chains, the ring closure reaction occurs. Typical examples are the peroxidase oxidation of dopa and dopamine, which produce a series of compounds such as dopachrome and dopaminechrome, respectively, which further evolve to compounds related to melanin pigments [46] (Fig. 6.3c).

Synthetic melanic compounds can also be prepared by peroxidase oxidation of dihydroxyindoles. Similarly to phenol oxidation, the reaction proceeds through radical coupling, and the product distribution agrees with the radical delocalization in the semiquinone [47] (Fig. 6.3d).

Catechol oxidation catalyzed by peroxidases can be used not only for the synthesis of sulfur-substituted catechols but also for the preparation of synthetic compounds related to pheomelanins, which contain benzothiazine units. In fact, the quinone undergoes an extremely easy nucleophilic addition by thiols. For example, treating the neurotransmitter dopamine with cysteine, in the presence of HRP/H₂O₂, gives rise to 2-*S*- and 5-*S*-cysteinyl-catecholamine and a smaller amount of the 2-*S*,5-*S*-di-cysteinyl-catecholamine conjugate [48, 49] (Fig. 6.3e).

6.1.2.4 Nitration of Phenols

Nitration of phenols by peroxidases can occur through two different mechanisms. The reaction requires phenol, nitrite, and hydrogen peroxide. In the principal mechanisms, compound I and compound II are formed. Upon one-electron oxidation of the substrates, phenoxy radical and nitrogen dioxide are produced. Coupling of these species gives the nitrophenol derivatives, where the nitro group is in the *ortho* or *para* position with respect to the phenol hydroxyl group. This reaction will be described in more detail in Sect. 6.1.5.

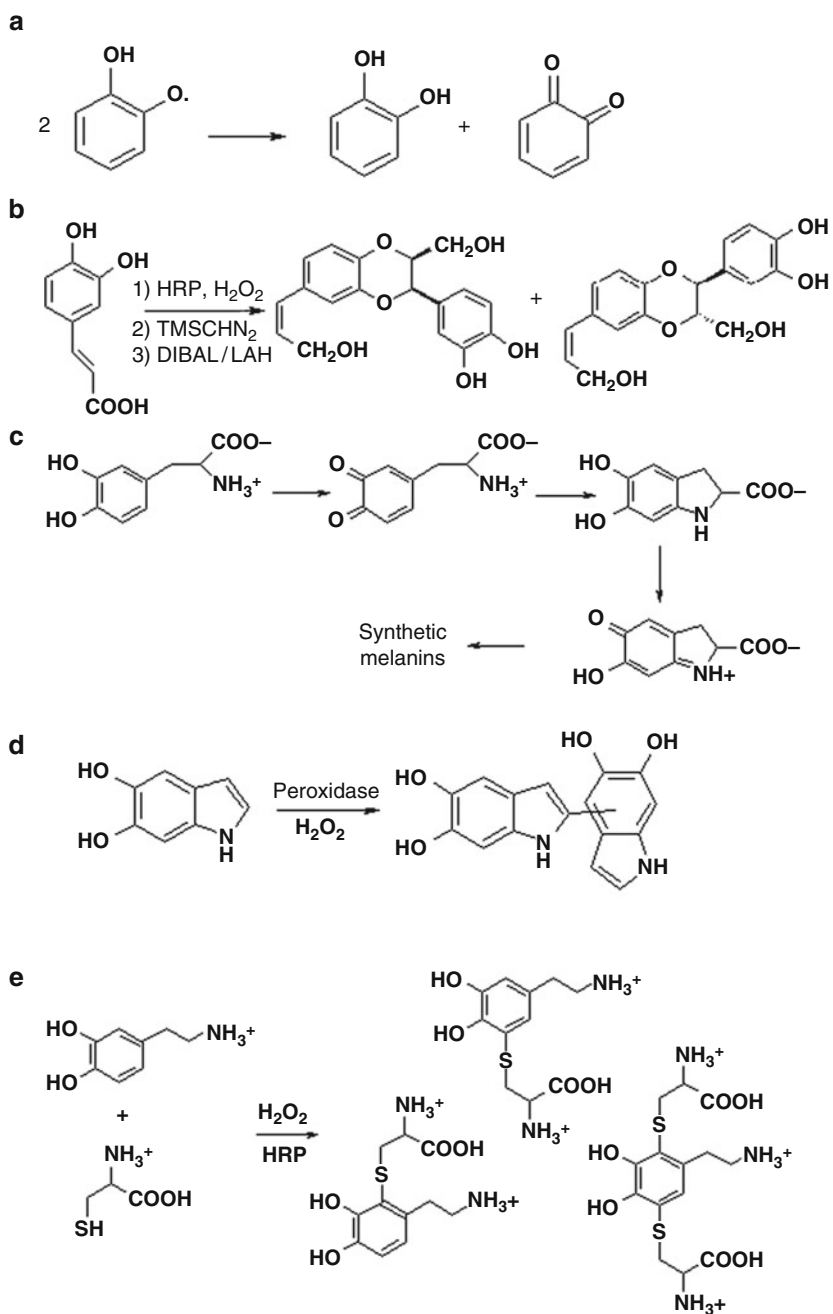


Fig. 6.3 Some examples of peroxidase-catalyzed oxidations of catechols

6.1.3 Insertion of Oxygen Atoms into Substrate Molecules

Oxygen insertion into C–H bonds is an energy demanding process requiring strong oxidants and often occurring with little regio- and stereoselectivity. Therefore, the use of peroxidases in these reactions would be advantageous to perform the process under mild conditions. In several instances, these enzymes are indeed able to carry out such transformation, and in that case, the source of the oxygen atom is generally hydrogen peroxide or, less frequently, molecular oxygen. In the first case, a direct oxygen transfer from the enzymatic active species to the bound substrate is needed. If the substrate is tightly bound to the protein in a rigid conformation, the reaction is expected to occur with high stereo or enantioselectivity, whereas when the substrate is weakly bound and/or far from the iron-oxo moiety, the stereochemical output will be poor. As a consequence, unlike the reactions driven by radical mechanisms described in Sect. 6.1.1, here the enzyme strongly determines the selectivity of the reaction. In fact, the capability of catalyzing oxygen atom insertions by peroxidases depends on the oxidative potential of its compound I form and on the substrate accessibility close to the heme site. In this respect, CPO differs from other peroxidases, in that it has a reactive compound I and allows the substrate to access to the distal cavity [19].

6.1.3.1 Epoxidation

The enantioselective epoxidation of olefins is a very important tool for the preparation of chiral building blocks. Addition of nucleophiles to the epoxide ring may occur stereospecifically thus forming bifunctional, chiral synthons. HRP binds substrates at the heme edge (see Chap. 5), and therefore it is a low efficiency catalyst for selective epoxidation. For instance, styrene is oxidized to styrene oxide, phenylacetaldehyde and benzaldehyde [50–52]. HRP mutants (F41L, F41T, H42E, H42A, H42V, and F41H/H42A) with higher accessibility of the substrate to the heme iron have been prepared. They are able to perform epoxidation of styrene with high turnover rates and produce optically active styrene epoxide but with low selectivity since other oxidative by-products are also formed [50–54].

By far, the most important peroxidase-catalyzed method for the preparation of chiral epoxides is the direct oxidation of olefins with CPO and H_2O_2 or *t*-BuOOH as oxidants [20, 23, 36]. The oxygen atom in the epoxide comes from the peroxide [55], indicating a direct oxygen transfer from compound I to the olefinic double bond. High yield and enantioselectivity are observed in some cases and can be accounted for by considering that the substrate, in particular the C=C group, must approach the Fe(IV)=O group generated within CPO. In other cases, particularly when the substrates carry bulky substituents, the stereochemical output of the reaction is modest, since the substrate cavity in the enzyme is narrow and substrate access to the heme cavity is impossible. The best performances have been obtained with *cis* alkenes where, in many cases, the observed epoxide e.e. are in excess of

95%. In contrast, *trans* olefins are often poor substrates for CPO. When the double bond is far from the chain terminus (i.e., from *cis*-3-alkenes upward), allylic hydroxylation accompanies the epoxidation. In addition, with terminal monosubstituted olefins, heme alkylation occurs, thus producing inactivation of CPO. 1-Alkenes can be profitably oxidized to epoxides by CPO only when they are not monosubstituted. A detailed description of the yields and e.e. for CPO-catalyzed epoxidation of olefins has been reported by Adams and coworkers [23].

A different approach to the epoxidation reaction promoted by CPO has been reported, which takes advantage of the capability of the enzyme to generate hypochlorite in the presence of hydrogen peroxide and chloride. ClO^- transforms olefins into halohydrins, which are then converted into epoxides. The developed process [36] makes extensive use of enzymes for the different steps involved. Thus, hydrogen peroxide was produced by the glucose-2-oxidase-catalyzed oxidation of D-glucose by molecular oxygen, and ring closure of the halohydrin was obtained by halohydrin epoxidase. The whole process has the drawback that, being dependent on the inorganic oxidant hypochlorite, the epoxides are produced with low enantioselectivity.

6.1.3.2 N-Oxidation

When HRP is used for the oxidation of aryl amines in the presence of hydrogen peroxide, the reaction proceeds through a radical mechanism and gives rise to the formation of a complex mixture of products, including oligomeric compounds (see Sect. 6.1.2). On the other hand, with CPO the N-oxidation of aryl amines to the corresponding nitroso derivatives occurs. $\text{H}_2^{18}\text{O}_2$ labeling studies show that the oxygen atom is transferred directly from compound I to the substrate nitrogen atom [20, 56, 57] (Fig. 6.4a). It has been proposed that the reaction occurs through an initial oxidation of the amine to hydroxylamine, which, after further reaction with the CPO compound I, forms the nitroso derivative [57–59].

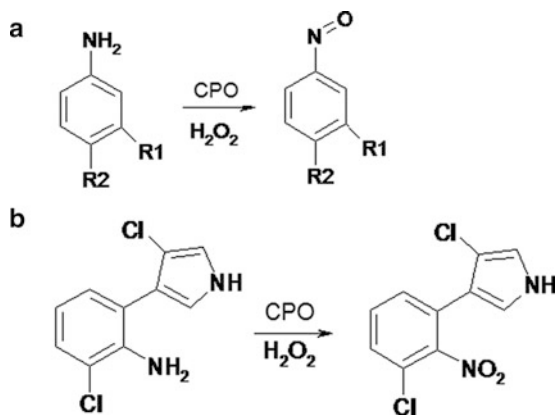


Fig. 6.4 CPO catalyzed N-oxidations of amines to nitroso derivatives, (a), where R_1 is H or Cl and R_2 is CH_3 , Cl or NO_2 ; and to a nitro derivative, (b)

Other peroxidases, albeit non-heme, are able to catalyze similar oxidations. CPO from *Pseudomonas pyrocinia* has been successfully employed for the preparation of the antibiotic pyrrolnitrin [60]. The amino group of the precursor molecule is directly transformed into a nitro group by the CPO active species (Fig. 6.4b).

6.1.3.3 Aromatic Hydroxylation

An example of insertion of an oxygen atom into unactivated aromatic rings is the hydroxylation of phenylalanine by MPO/H₂O₂ to give the *o*-, *m*-, and *p*-hydroxylated derivatives (the tyrosine isomers) [61]. When electron-rich aromatic rings such as those of phenols (*p*-cresol, tyrosine etc.) are reacted with peroxidase/H₂O₂, a complex mixture of products containing dimers and oligomers is formed, according to the radical mechanism described in Sect. 6.1.2, but no aromatic hydroxylation is observed. The latter reaction has thus potential applications, considering that it would be difficult to obtain the same products with conventional synthetic methods. Mason et al. [62, 63] and Klibanov et al. [64] showed that HRP can be successfully employed to afford selective aromatic hydroxylation but with a different approach with respect to the classical peroxidase reactions. In fact, HRP can catalyze the reaction by using molecular oxygen as the oxidant in the presence of the reducing cosubstrate dihydroxyfumaric acid. This reaction bears high potential interest since it can be applied to the preparation of compounds of pharmaceutical relevance, such as L-dopa, D-(–)-3,4-dihydroxyphenylglycine, and adrenaline from L-tyrosine, D-(–)-*p*-hydroxyphenylglycine, and L-(–)-phenylephrine, respectively [64] (Fig. 6.5).

6.1.3.4 Aliphatic Hydrocarbon Hydroxylation

The hydroxylation of aliphatic C–H bonds can be performed exclusively by CPO [65–67]. A direct oxygen transfer mechanism has been suggested, as the oxygen atom arises from the peroxide. The reaction requires an activated C–H bond since hydroxylation occurs at the allylic or benzylic positions. Both cyclic (cyclohexene)

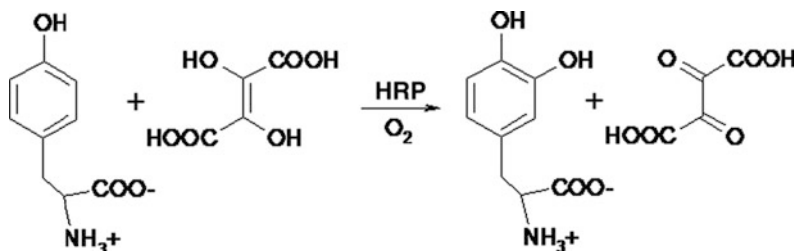


Fig. 6.5 HRP catalyzed hydroxylation of L-tyrosine to L-Dopa in the presence of dihydroxyfumaric acid

and aliphatic (3-heptene) olefins are substrates for CPO. The capacity of the enzyme to block the substrate in the active site allows performing the hydroxylation reaction with high stereoselectivity, giving the alcohol with good enantiomeric excess. An inversion in the stereochemistry passing from ethylbenzene to propylbenzene has been reported, the former substrate giving rise to the (*R*)-alcohol and the latter the (*S*)-alcohol [66]. In the oxidation of toluene by CPO, benzaldehyde and benzoic acid are produced [66]; probably, after the initial hydroxylation reaction to benzyl alcohol, CPO compound I further oxidizes the product.

6.1.3.5 Indole Oxidation

Selective indole oxidation is not an easy task and usually requires several steps with conventional synthetic organic methods. Here again, CPO allows the synthesis of oxindoles with high yields and selectivity [68, 69]. The key of the selectivity is the direct oxygen transfer from compound I to the substrates, yielding the oxindole derivative; with substituted indoles, the yield is nearly quantitative (Fig. 6.6).

6.1.3.6 Alcohol Oxidation

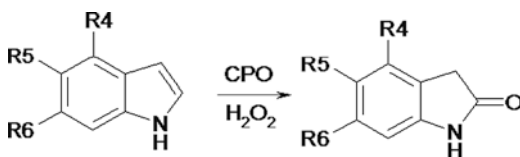
Selective oxidation of alcohols by direct oxygen transfer from the iron-oxo species is performed only by CPO, and it has been proven by $\text{H}_2^{18}\text{O}_2$ labeling studies. Since CPO has a restricted active site, the enzyme is active on primary alcohols. Examples of this reaction are the oxidation of allylic, propargylic, and benzylic alcohols to the corresponding aldehydes [70]. Also, the oxidation of the $-\text{CH}_2\text{OH}$ group in 5-hydroxymethyl-furfural to the corresponding acid has been reported [71]. Both the steps of alcohol oxidation to aldehyde and the subsequent oxidation to acid occurred with incorporation of ^{18}O -oxygen from $\text{H}_2^{18}\text{O}_2$.

6.1.3.7 Sulfoxidation

In the presence of hydrogen peroxide, or alkyl hydroperoxides, peroxidases are generally able to perform the sulfoxidation of dialkyl or alkyl aryl sulfides. When the substituents of the sulfide are different, the sulfoxide is chiral (Fig. 6.7a).

Interestingly, the enantioselectivity shown by the enzyme depends largely on its source and on the type of substrate. This is due to the possible occurrence of

Fig. 6.6 CPO catalyzed oxidation of substituted indoles into the corresponding oxindole derivatives



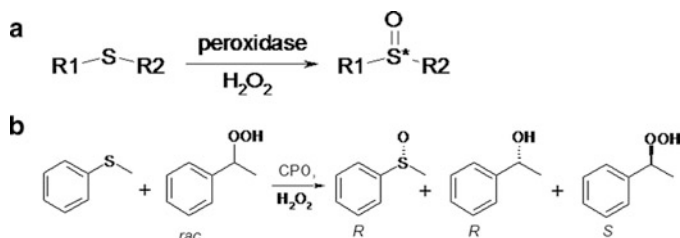
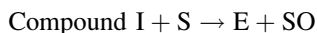


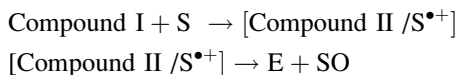
Fig. 6.7 Enantioselective catalytic sulfoxidation of sulfides

different mechanisms, the importance of which depends on how close the substrate can approach the iron(IV)-oxo group in compound I and on the capability of the enzyme to bind the substrate tightly at the active site. Experiments of ^{18}O incorporation (from $\text{H}_2^{18}\text{O}_2$) into the substrates showed that with some enzymes (like CPO), the oxygen atom in the sulfoxide is completely derived from hydrogen peroxide, and with others (like HRP), it is derived not only from $\text{H}_2^{18}\text{O}_2$ but also from water or molecular oxygen. Complete insertion of an oxygen atom from H_2O_2 into the substrate is observed when a direct oxygen transfer from the iron(IV)-oxo species to the sulfur atom occurs:

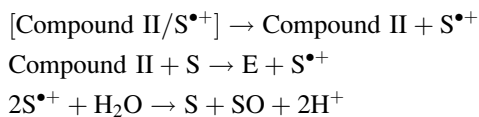


This necessarily requires a close approach of the sulfide sulfur atom to the iron center of the enzyme [19].

An oxygen transfer occurs also when a different mechanism, involving one-electron oxidation steps, occurs. Here compound I reacts with the substrate oxidizing it to a sulfur radical. If the compound II thus formed binds tightly the substrate radical, an oxygen transfer from the iron(IV)-oxo to the sulfur atom in active site cage may occur:



Also in this case, a substrate binding site close to the heme iron is necessary. But if the substrate is loosely bound near the porphyrin edge, after the first electron transfer to compound I has occurred, the substrate radical species rapidly diffuses to the bulk of the solution. The resulting compound II species oxidizes a further substrate molecule restoring the native enzyme. The $\text{S}^{\bullet+}$ species, free in the solution, dismutates independently of the enzyme forming the sulfoxide.



This mechanism requires a fast substrate dissociation from the active site. The different mechanisms can be simultaneously operative, thus justifying the partial ^{18}O incorporation into sulfoxide and modest e.e. observed in some cases.

The best efficiency, both in terms of reaction rate and product e.e., approaching 100% in several cases, was obtained with CPO. Its catalytic sulfoxidation takes advantage of the enzyme's peculiar active site, with an entrance channel that leads the substrate close to the iron atom. There are many data for the CPO activity in this reaction; in particular, for alkyl aryl sulfides and dialkyl sulfides. The paper by Adam et al. [23] gives an excellent overview of several available data. The literature shows also contrasting data, reporting from very high to moderate e.e. for the sulfoxidation of the same substrates by CPO. But it should be taken into consideration that some e.e. values must be corrected for the noncatalytic oxidation of the sulfides by H_2O_2 , the contribution of which depends on the experimental conditions and obviously yields racemic products [36]. In most of the cases, CPO forms the sulfoxide with the (*R*) absolute configuration [20].

CPO can also operate using alkyl hydroperoxides as oxidants. Also in this case, the oxygen atom inserted into the substrate comes from the peroxide, and the reaction occurs, giving rise to sulfoxides with high e.e. It should be noted that CPO strongly discriminates between the alkyl hydroperoxides and, when they are chiral, reacts with different rates with the two enantiomers. This property has been exploited for developing a method to prepare enantiopure hydroperoxides (together with enantiopure sulfoxide) from a racemic mixture of the oxidant [72]. As an example, if thioanisole is reacted with racemic 1-phenethyl hydroperoxide in the presence of CPO/ H_2O_2 , the final reaction mixture contains the (*R*)-sulfoxide, the (*R*)-alcohol, and the unreacted (*S*)-hydroperoxide with good enantiomeric excesses (Fig. 6.7b). This method suffers the problem of the low conversions. However, if an enantiopure hydroperoxide is desired, the kinetic resolution method by HRP, H_2O_2 , and guaiacol, developed by Adam et al. [30] and described in Sect. 6.1.2, is preferable.

The oxidation of organic sulfides can be performed also by other peroxidases (and also by model systems and by proteins with pseudoperoxidase activity, as reported in Sect. 6.3.2). In particular, the reactions catalyzed by HRP [73–75], LPO [19, 73, 74] and CcP [76] have been the subject of several studies. HRP differs from CPO because its heme–iron is much less easily accessible. Aromatic substrates, such as alkyl aryl sulfides, bind at the heme edge; this results in low rates and low enantiomeric excess in the sulfoxide formed. To overcome this problem, enzyme engineering has been applied to both HRP and CcP. Mutants have been prepared with the rationale of introducing in the active site of the protein a cavity suitable for accommodating the sulfide, by replacing bulky amino acids (Trp51 in CcP, His42 and Phe41 in HRP) with smaller ones. The F41L HRP mutant showed an increased reactivity with respect to the native enzyme and especially very good enantioselectivity, often above 90%, on a large number of alkyl aryl sulfides [52, 77], ranging from thioanisole (97% e.e.) to the bulkier methyl 2-naphthyl sulfide (99% e.e.) and cyclohexyl phenyl sulfide (94% e.e.).

6.1.4 Activation of Halogens

Classical peroxidases, such as HRP, in the presence of peroxide are able to oxidize iodide to I_3^- following a radical mechanism with two one-electron oxidation steps. But the term “activation of halogens” is usually meant to indicate a two-electron oxidation of halide ions (chloride, bromide, iodide) to form active halide species. There is still some debate on the nature of the active species, since there is evidence for enzymatic generation of either a free hypohalide or an enzyme-bound halogenating species (see Chap. 5). The formation of the halogenating species requires an enzyme active species with high redox potential. The $E^{o'}$ values to be considered are not the one-electron redox potentials reported in Table 6.1 but those for the compound I/iron(III) couples. Considering that the active species were the hypohalide ion, the $E^{o'}$ of the enzyme active species must be above a threshold dictated by the HOX/X^- redox potential and by the anion concentration [13]. This value, as well as that of the enzyme, depends on the pH of the solution. Among the halogenating peroxidases are the closely related human enzymes MPO, LPO, eosinophil peroxidase (EPO), and thyroid peroxidase (TPO). The $E^{o'}$ value for the compound I/iron(III) couples have been determined for the enzymes as 1.16 ± 0.01 V for MPO [78], followed by 1.10 ± 0.01 V for EPO [78], and 1.09 ± 0.01 V for LPO, [79] respectively. It follows that only MPO compound I is able to oxidize chloride to hypochlorite at pH 7.0 at reasonable rates [80–82], while EPO requires acidic pH [13]. EPO compound I is very active in the oxidation of bromide and iodide [83], and LPO compound I has barely detectable activity with bromide at neutral pH, but it oxidizes efficiently iodide. An example of chlorinating activity by human peroxidases is the transformation of taurine into taurine chloramine [84–88].

By far, the most studied chlorinating peroxidase is CPO (in particular that from *Caldariomyces fumago*, which is involved in the biosynthesis of the chlorometabolite caldariomycin). CPO is able to halogenate (Cl, Br) activated C–H bonds, such as those of 1,3-dicarbonyl compounds. The reaction can afford both the monohalogenated compound and the dihalogenated product (and also mixed chloro/bromo compounds) [89–92] (Fig. 6.8a).

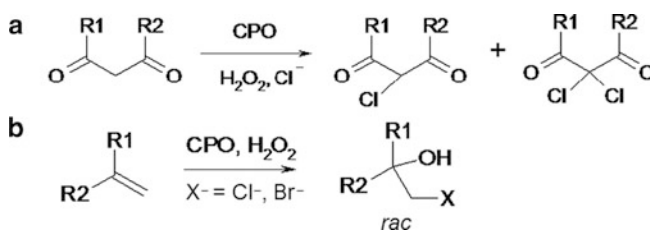


Fig. 6.8 Activation of halogens by CPO; (a) reactions with 1,3-dicarbonyl compounds; (b) halohydrins formation

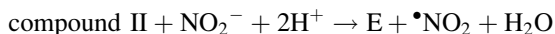
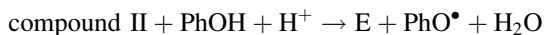
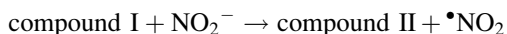
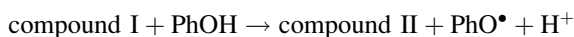
The standard CPO assay, the chlorination of monochlorodimedone to dichlorodimedone [93] is an example of the reaction on 1,3-dicarbonyl compounds. A further example of halogenation (Cl, Br) performed by CPO is that on cyclic enamines and enaminones, although with usually low yields; uracil undergoes chlorination or bromination, mainly at 5- position [94, 95], whereas pyrazole forms 4-Cl-pyrazole [96] with good yield. Interestingly, the non-heme CPO from *Pseudomonas pyrocinia* catalyzes the insertion of a chlorine atom into the indole nucleus with high regioselectivity, forming the 7-chloro-indole derivatives [97].

As discussed in the epoxide formation section, the system CPO/H₂O₂/chloride (or bromide) reacts with double bonds forming halohydrins [23, 98–100]. The selectivity in the reaction has driven the reactivity of the hypohalide ion; thus while a good regioselectivity is observed, the diastereoselectivity is almost negligible [23] (Fig. 6.8b).

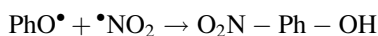
Several examples of halohydrin formation from styrene derivatives and saccharides catalyzed by CPO are reviewed by Adam and coworkers [23]. Formation of bromohydrin derivatives of some saccharides can be of interest for the preparation of bioactive compounds [72].

6.1.5 Activation of Nitrite

The insertion of a nitro group into an aromatic moiety is an important tool for the preparation or synthons since it can be easily transformed into several other functional groups. Peroxidases can be usefully employed for performing this reaction on phenols in very mild conditions in the presence of nitrite and hydrogen peroxide. In most cases, the reaction proceeds through the classical intermediates compound I and compound II, in one-electron steps. Both enzyme intermediates are capable of oxidizing nitrite to nitrogen dioxide ($E^{\circ}(\bullet\text{NO}_2/\text{NO}_2^-) = 1.04 \text{ V}$ at pH 7) [101] and the phenol to phenoxy radical:



Nitrogen dioxide is also able to generate a phenoxy radical from the phenol. Coupling of the two radicals gives rise to nitrophenol [13, 102–107]:



The regiochemistry in the nitration is dictated by the reactivity of the phenol and does not differ from that observed between the phenol and chemically, or

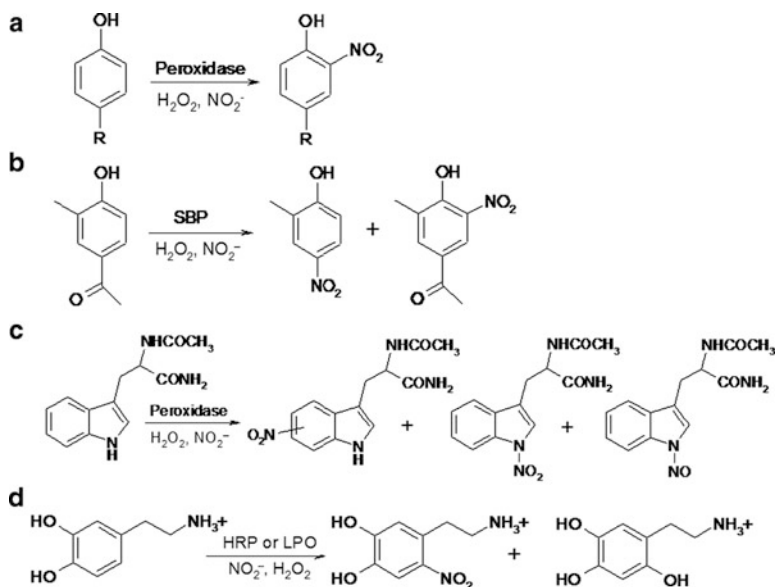


Fig. 6.9 Activation of nitrite by peroxidases; (a) and (b) nitration of phenol derivatives; (c) nitration of *N*-acetyl-tryptophan amide; (d) nitration of dopamine

electrochemically, generated nitrogen dioxide. In the case of *p*-substituted phenols, the reaction occurs at the *ortho* position with respect to the hydroxyl group (Fig. 6.9a).

It has been also reported that, with soybean peroxidase, nitration can occur with concomitant C–C cleavage if the *para* position to the hydroxyl group is occupied [107] (Fig. 6.9b).

Nitrite concentration is an important aspect to take into consideration. In fact, if the phenol is in large excess, it is the only species that reacts with the enzyme active species. In these conditions, only phenoxyl radicals are formed, giving rise to phenol dimers and oligomers, as described in Sect. 6.1.2, and little nitration products. On the other hand, large concentrations of nitrite lead to preferential phenol nitration according to a different mechanism [13, 105, 106, 108], which involves the formation of a very reactive nitrating species with chemical reactivity resembling that of peroxyxynitrite, which has been in fact proposed to be an enzyme-bound peroxyxynitrite. This species reacts with the phenols yielding nitrophenols, with comparable regiochemistry but different reaction rates [105, 106].

The ternary system of peroxidase/nitrite/hydrogen peroxide can also be advantageously used for nitration of indole derivatives. Several nitro derivatives, together with the *N*-nitro and *N*-nitroso adducts, are formed in this reaction. Interestingly, the composition of the product mixture depends on the enzyme used (LPO or HRP) and on nitrite concentration [109]. By changing the enzyme and the reaction conditions, it is possible to drive the reaction toward the *N*-nitroso derivative or the nitro-derivatives (Fig. 6.9c).

A much easier nitration reaction is that of catechol derivatives. It has been shown that HRP and LPO (and likely every peroxidase) nitrate dopamine to 6-nitrodopamine with the concomitant formation of low amounts of 6-hydroxydopamine [110] (Fig. 6.9d).

6.2 Analytical Applications of Peroxidases

The widespread application of enzyme linked immunosorbent assays (ELISAs) for analytical purposes is due to the extremely high selectivity and affinity of antibody molecules to their corresponding antigens. Since the two reaction partners are usually chromatographically and electrochemically inert, an enzyme (mainly HRP in the case of peroxidases) is used for labeling of either the antigen or the antibody, allowing both the detection of the antigen and the amplification of the primary signal. Peroxidases are increasingly applied also in the building of biosensors. These are a subgroup of chemical sensors that can be defined as self-contained integrated devices, which are able to provide specific quantitative or semiquantitative analytical information using a biological recognition element retained in direct contact with the transduction element [111]. In this section, we describe some of the most recent developments of HRP-containing ELISA kits, which have found applications in food control, in diagnostic microbiology, and as disposable amperometric immunosensors, and of peroxidase-containing bioelectrosensors, which improve the simpler colorimetric biosensors usually employed in medical diagnostic test kits [15].

6.2.1 ELISA

Among the analytical procedures developed for the determination of milk proteins in foods, ELISA is the most commonly used method both to detect and quantify hidden protein allergens. Indeed, besides having many functional properties as food ingredients, milk proteins are also a frequent cause of food allergy, especially in children. The group of Perez has recently developed two HRP-based immunoassays (indirect competitive and double antibody sandwich formats) for the detection of undeclared milk proteins (in particular, bovine β -lactoglobulin) in foods. Their results indicated that the sandwich format could detect low percentages of powdered milk added to processed food and also better discriminate between commercial foods with declared or nondeclared milk ingredients, with respect to the competitive format [112]. On the other hand, in the field of biomedical applications of ELISAs, a novel HRP immunoassay for the diagnosis of chronic *Chlamydia pneumoniae* infection has been reported. The test is based on the quantification of chlamydial lipopolysaccharide in human serum utilizing

lipopolysaccharide-binding protein as a capture molecule and HRP/*o*-phenylenediamide for chromatographic detection [113]. Although optical detection methods are most developed in terms of commercial applications, also the electrochemical detection method using immunoreactions can be applied, as it appears very promising due to the relatively simple and inexpensive equipment required [114, 115]. The group of Shim reported the development of a disposable amperometric immunosensor system for the detection of rabbit IgG (as a model analyte), based on a carbon electrode coated with a conducting polymer bearing a carboxylic acid group [116]. In this system, HRP and streptavidin were covalently bonded through their lysine residues to the polymer on the electrode, and biotinylated anti-IgG was immobilized on the electrode surface using streptavidin–biotin coupling. This sensor was based on the competitive assay between free and glucose oxidase-labeled IgG for the available binding sites of the antibody. The function of HRP bonded on the electrode is to reduce the H_2O_2 formed in the presence of glucose by the analyte–glucose oxidase conjugate, providing a catalytic current that can be monitored amperometrically depending on IgG concentration. Such a conducting polymer-based immunosensor could be applied to the detection of different compounds of interest.

6.2.2 Biosensors

Compared with other analytical techniques, electrochemical enzyme biosensors bear the advantage of high selectivity of the biological recognition elements and high sensitivity of the electrochemical transduction process. The performance of biosensors mainly depends on the amount and bioactivity of enzyme immobilized onto the electrodes; accordingly, considerable efforts have been devoted to the improvement of enzyme immobilization, in which multipurpose functional materials are commonly utilized. In this respect, a novel immobilization platform has been recently developed by synergistically using ZnO crystals and nano-sized gold particles as HRP-loading material [117]. The resulting enzyme biosensor was tested for the determination of hydrogen peroxide as a model test system, since H_2O_2 plays an important role in food industry, environmental monitoring, and clinical diagnosis. Experimental results showed that HRP could be immobilized onto the nanocomposite matrix with high loading, well-retained bioactivity, and rapid and sensitive electrochemical response to H_2O_2 without addition of any electron mediators. This enzyme immobilization strategy could represent a promising alternative to other bioactive molecules in biosensor design.

Biosensors can also represent a good method to evaluate the antioxidant status through the measurement of biomarkers, i.e., biological molecules whose chemical structure has been modified as a result of an oxidative stress condition [118]. The usefulness of biosensors to evaluate the antioxidant status lies in their ability both to improve food quality and provide early indication of some disease, or its progression, in a noninvasive way to evaluate the effectiveness of the antioxidant therapy.

Enzyme-based biosensors are very suitable for the antioxidant status evaluation, since they show excellent selectivity for biological substances and can directly determine and/or monitor antioxidant compounds in a complex media such as biological or vegetable samples without needing a prior separation step. During the course of the catalytic reaction on the electroactive substrates, the current produced at an applied potential is related to the concentration of a specific biomarker, for which the biosensor is selective. HRP-based biosensors for antioxidant status evaluation have been applied in the detection of superoxide radical [119], nitric oxide [120], glutathione [119, 121], uric acid [122, 123], and phenolic compounds [124–126].

Besides HRP, other plant peroxidases have recently been explored to find promising candidates for biosensor applications. In particular, the peroxidases from tobacco, peanut, and sweet potato have been kinetically characterized on graphite to understand the nature of the direct electron transfer (ET), finding that the fraction of enzyme molecules in direct ET varies substantially for the different plant peroxidases, depending on their anionic/cationic character and degree of glycosylation. Especially noticeable are the results obtained with sweet potato peroxidases, due to its high availability, high specific activity, and superior electrochemical characteristics that make it very attractive for further studies [127]. In another report, direct immobilization of native and recombinant (and thus nonglycosylated) forms of tobacco peroxidases (TOP) at graphite electrodes enabled the study of the bioelectrocatalytic behavior of this anionic peroxidase, both in direct and catechol-mediated reduction of H_2O_2 . In the case of the recombinant enzyme, the absence of glycosylation provided favorable adsorption/orientation on graphite for more efficient ET reactions, and the E141F mutation in the heme-binding pocket enabled achievement of a Ca^{2+} -tolerance of TOP in the reaction with H_2O_2 and a catecholic substrate [128]. The results obtained demonstrated advantageous bioelectrocatalytic properties of the recombinant form of TOP adsorbed on graphite electrodes, for further development of enzyme electrodes for detection of aromatic phenols and amines, stable toward inactivation by H_2O_2 .

Efficient bioelectrocatalysis of lignin peroxidases (LiP) has been recently reported by the group of Ferapontova, who studied the reduction of H_2O_2 promoted by LiP-graphite electrode systems, in the presence of phenols, catechols, veratryl alcohol, and some other high-redox-potential lignin model compounds acting as mediators [129]. The results showed the possibility of development of solid-phase LiP-based electrochemical biosensors for detection of recalcitrant aromatic compounds. Spring cabbage peroxidase (SCP) is a relatively poorly studied enzyme, but recent studies carried out by the group of Belcarz revealed that this enzyme possesses highly promising properties: good affinity for various substrates, great stability at ambient and low temperatures, optimum activity at neutral pH, and ability to bind to polyanionic matrices, besides low costs of extraction and purification. Moreover, SCP immobilized on modified carbon nanotubes provided a bioelectrocatalytic system, which is effective for H_2O_2 reduction and stable for long periods [130]. These properties make this enzyme a highly promising biological material for the development of biosensors.

6.3 Prospective Applications of Peroxidases in the Fine Chemical and Pharmaceutical Industries

6.3.1 Native and Modified Peroxidases

The catalytic performance of heme peroxidases can be improved by modification of the native enzymes. Such a strategy has become popular in the field of metalloproteins, where the metal-binding sites have been redesigned in different ways, to introduce structural features that are specific to other proteins or enzymes [131]. Redesign of heme proteins, in particular, gives insight into the factors governing structure and function within members of a closely related protein family and is invaluable for the developing area of de novo protein design. Moreover, in the field of industrial applications, the modification of peroxidases is noteworthy since it can enhance their operational stability and possibly improve or alter their enzymatic activity, thus producing more efficient biocatalysts. The current strategies for the modification of heme proteins follow different approaches: rational design, directed evolution, and replacement of the native heme prosthetic group (reconstitution), as summarized in Fig. 6.10 [132–160]. A detailed discussion of this topic is given in Chap. 9.

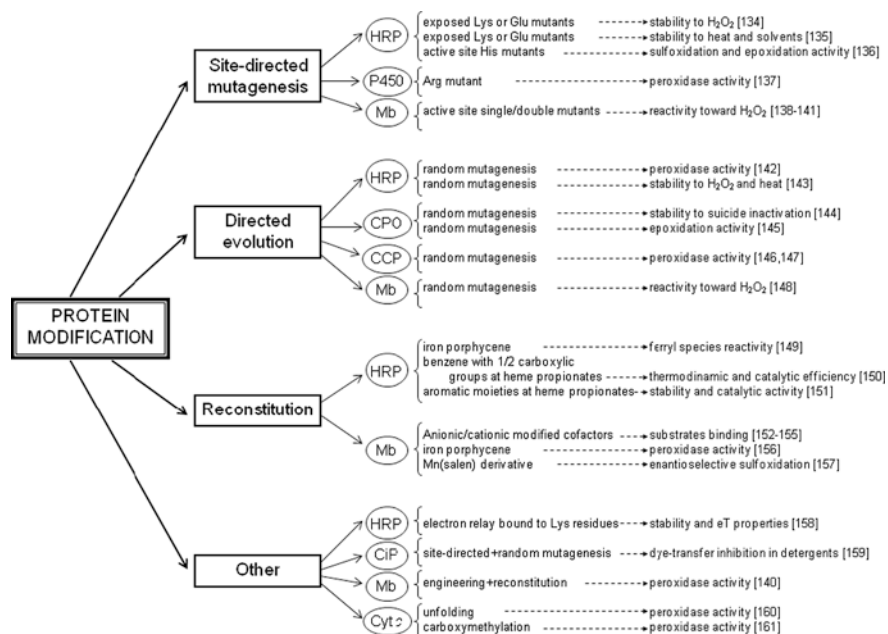


Fig. 6.10 Schematic representation of the protein modification approaches applied to four peroxidases (Horseradish, chloroperoxidase, cytochrome c, and *C. cinereous* peroxidase) and proteins with pseudoperoxidase activity (cytochrome P450, myoglobin, and cytochrome c). The dashed arrows link each specific protein modification with the properties improved

6.3.2 *Proteins with Pseudoperoxidase Activity*

Besides peroxidases, other heme-containing enzymes utilize peroxides for their specific reactions. Among these, the P450 peroxygenases represent a recently identified family of P450s that use H_2O_2 instead of O_2 as source of the oxygen atom to be introduced into the α - or β -carbon of myristic acid [161, 162]. The native enzyme not only hydroxylates myristic acid but also oxidizes 3,5,3',5'-tetramethylbenzidine, a typical peroxidase substrate, in a myristic acid-dependent reaction. Actually, since peroxidase activity was absent without the fatty acid, the latter substrate was needed for the formation of the enzyme reactive intermediate: both the peroxidase and the peroxygenase substrates compete for this reactive species during the course of their respective reactions [136]. The weak peroxidase activity of the native enzyme can be markedly enhanced by using protein engineering. Upon replacement of a single amino acid, the enzyme behaves as an almost authentic peroxidase. These results suggest that there are critical structural elements in the distal active site, which determine whether P450 peroxygenases act as peroxygenases or peroxidases; by controlling the heme distal side structure, a heme protein with a specific function can be engineered to introduce a different functionality [163]. On the other hand, Watanabe and coworkers have observed that native P450_{BSb}, the enzyme isolated from *Bacillus subtilis*, shows high peroxidase and peroxygenase activity; this enzyme efficiently and selectively hydroxylates less reactive C–H bonds in the presence of H_2O_2 , an interesting reaction for fine chemistry applications [164]. Since this enzyme never oxidizes substrates other than fatty acids that have long alkyl chains, the authors thought to change the selectivity by applying a series of short alkyl-chain carboxylic acids as decoy molecules. These species are recognized by P450 peroxygenase as substrates to make the carboxylate–Arg salt bridge but are not oxidized by the enzyme, so that a wide variety of nonnatural substrates could be oxidized by P450/ H_2O_2 . Besides one-electron oxidation of peroxidase substrates like guaiacol, the enantioselective styrene epoxidation and ethylbenzene hydroxylation were also observed, with the interesting possibility to improve both the catalytic activity and the selectivity by designing the nature and structure of the decoy molecule.

As a potential alternative to the high cost of peroxidases or P450 peroxygenases, other readily available heme proteins, such as myoglobin (Mb), hemoglobin (Hb), or cytochrome *c* (cyt *c*), and their derivatives, were explored as pseudoperoxidases, considering that protein modification can provide substantial contributions to the optimization of the new activity through both protein engineering and replacement of the natural prosthetic group with a synthetic heme (Fig. 6.10). Among the proteins that can be easily employed in peroxide-dependent reactions is Mb, which is normally involved in storage and intracellular transfer of molecular oxygen [165]. *In vivo* Mb exists prevalently as oxyMb, but high concentrations of oxidants or acidic pH may induce autoxidation of the protein with formation of metMb, the state in which Mb can exhibit a peroxidase-like behavior. Mb can be used as a biocatalyst in several peroxide-dependent reactions: oxidation [166, 167] and

nitration [168, 169] of phenolic substrates, sulfoxidation of organic sulfides [170–174], and epoxidation of alkenes [170–172, 174].

The Mb heme pocket bears structural features that are more similar to those of peroxidases than to any other protein or enzyme; this makes Mb widely employed for engineering novel metalloproteins by redesign of the existing metal-binding site [131]. Like classical peroxidases [175], Mb contains proximal (His93) and distal (His64) histidines [165], although it lacks other residues that play essential roles in promoting peroxidase activity, i.e., a distal arginine and a proximal aspartate. In addition, Mb lacks a specific cleft for substrate binding near the heme; moreover, its globular shape, the different functional oxidation state of the iron atom, and the differences in overall polarity of the active site make the catalytic activity of Mb in peroxidase type reactions markedly lower than that of the enzymes. Nevertheless, the peroxidase activity of Mb can be improved by engineering the protein, particularly in the active site features. In this respect, Mb has several advantages because of its relatively small size, compact structure, and the extensively accumulated biochemical and biophysical characterization, including a large number of X-ray crystal structures available for both the native proteins from various sources and several mutants [174]. In particular, the availability of the expression system for recombinant Mb in *E. coli* and the relatively easy methods of site-directed mutagenesis make the engineering approach of extreme importance for investigating the role of critical residues and to introduce nonnatural activities into the protein [166, 176]. Our group produced site-directed mutants of sperm whale Mb containing those amino acid residues critical for peroxide activation in peroxidases; thus the distal Thr67 was replaced with either Arg [137] or the more flexible Lys residue [138], and the double mutant T67R/S92D Mb was also obtained [139]. The reactivity toward H₂O₂, as measured by the k_1 rate constant for the formation of the intermediate compound I-like species, showed an appreciable increase for the modified Mbs (up to threefold for the T67R/S92D Mb mutant) [137–139], indicating that the positively charged residue introduced into the protein favors the cleavage of the bound hydroperoxide by a polarization effect analogous to that promoted by distal Arg in peroxidases. A greater increase in reactivity toward H₂O₂ was indeed obtained by Watanabe upon repositioning the distal His of Mb as it is in peroxidases [140], though further greater enhancement was observed for a quadruple variant of Mb generated through random mutagenesis (with a 24.7-fold increase in k_1) [147]. In the latter case, the mutations were all peripheral and far from the heme pocket, showing that protein reactivity is also controlled by still incompletely understood factors associated with the folding and local flexibility of the polypeptide backbone.

The reconstitution of Mb with a modified prosthetic group may also allow introduction of a specific binding site for exogenous substrates into the protein, thus enhancing the selectivity of Mb [151, 177]. In general, introduction of a synthetic heme–peptide complex into the protein has the effect of opening the Mb active site, thereby allowing an easier approach of the substrate to the heme, and can be exploited to fine tune substrate recognition by the reconstituted protein. The most interesting improvements in the peroxidase activity of Mb by nongenetic

methods were reported by the group of Hayashi and by our group. The work of Hayashi initially focused on the construction of a binding interface for substrates through the functionalization of the two heme propionates [151]. The chemical reactivity of Mb is in fact improved by setting a substrate binding site on the protein surface and near the entrance of the heme pocket. With the aim of creating such an artificial binding domain, Hayashi reconstituted Mb with two different types of chemically modified cofactors, either anionic [152, 153] or cationic [154], thereby obtaining Mb derivatives that form stable complexes with the substrates both by electrostatic interactions and hydrophobic contacts [154]. More recently, Hayashi also replaced the native heme of Mb with iron porphycene (an artificially created iron porphyrin isomer). Interestingly, the peroxidase activity of the reconstituted protein toward several substrates was much higher than that observed for native Mb [155]. Apo-Mb was also reconstituted with a synthetic Mn(salen) derivative that was anchored to the protein by formation of two disulfide links [156]. The Mn(salen)-reconstituted Mb exhibited an increase in the enantioselectivity of thioanisole sulfoxidation up to 51% e.e.

An interesting improvement in this field is the modification of Mb by combining the genetic and reconstitution approaches, to potentiate the different effects on the enhancement of the catalytic activity [167]. In our initial attempts, horse heart apoMb was reconstituted with protohemin modified by attachment of an Arg–Ala residue to one of the two propionate side chains, but the resulting collapse of the distal helix, leading to coordination of distal His to the sixth coordination position of the iron, hindered the binding of hydrogen peroxide to the iron and reduced the activity of the reconstituted protein [178]. However, when protohemin was modified by attachment of a His residue (heme–His), the reconstituted Mb contained a significant portion of high spin form that reacted normally with hydrogen peroxide [138]. Since the His imidazole group of the modified prosthetic group is partially protonated at physiological pH, it could facilitate peroxide cleavage in a way somewhat similar to that of distal Arg in peroxidases.

We also reconstituted the mutants T67K Mb and T67R/S92D Mb with heme–His. The catalytic oxidation of phenolic substrates by the various Mb derivatives demonstrated that the performance of Mb is enhanced in an additive fashion by engineering and cofactor reconstitution, with the heme–His reconstituted T67R/S92D Mb protein being the most efficient so far reported for any Mb derivative [139, 179]. This shows that the combined approach of protein engineering and cofactor replacement of heme proteins like Mb is indeed promising in a broader perspective, taking into account that the heme cofactor can be extensively elaborated to introduce more sophisticated substrate recognition sites and even further catalytic groups.

Similarly to Mb, Hb is also active in the catalytic oxidation of substrates by hydrogen peroxide, with rates and general behavior comparable with those of Mb. In particular, a number of research reports showed that Hb exhibits oxidizing activities and can be used as a mimetic peroxidase to catalyze the oxidation reactions of aromatic compounds [180–182], aniline [183, 184], lipids [185], styrene [186], and sulfides [187]. Again, although the activity of Hb is not comparable with

that of peroxidases, its commercial availability at low cost draws interest to the study of its pseudoperoxidase reactivity and its potential applications. Nevertheless, to date potential applications of Hb and Mb as an alternative to peroxidase have been reported only in the field of biosensors (mainly for hydrogen peroxide or organic peroxides and phenols) [188–197].

A different strategy for the production of biocatalysts involves adsorption of the protein on a solid surface; this approach is an important topic for biological, medical, and technological research, and, in particular, the immobilization process can increase the protein resistance toward inactivation by hydrogen peroxide. In the case of Mb, for example, the protein has been immobilized on zirconium phosphonates, ordered mesoporous silicates, or folded sheet materials obtaining heterogeneous biocatalysts for the oxidation of 2,2'-azino-bis(3-ethylbenzthiazoline-6-sulphonic acid) (ABTS) and aromatic substrates by hydrogen peroxide [198–200]. On the other hand, Hb has been immobilized on chitosan films enhancing both its thermal stability and catalytic activity in organic solvents [201].

Another heme protein that could be interesting from the point of view of potential biotechnological applications is cytochrome *c*, which can also be converted into an oxidative enzyme with activity mimicking that of peroxidases [202]. In this context, both the ability of cyt *c* to perform in nonaqueous media (molecular solvents and ionic liquids) [203] and the production of a cyt *c* variant resistant to heme degradation by hydrogen peroxide [204] are noteworthy. Cyt *c* has been designed by nature to promote electron transfer processes, with a heme edge exposed to the protein surface, and is provided with a basic patch of lysine residues around the heme, which could selectively interact with charged substrates in a peroxidase-like reaction. However, the heme group in cyt *c* is six-coordinated, with axial ligands His18 and Met80 and cannot catalyze chemical reactions unless one of the axial ligands, preferably Met80, is released. This could be in principle achieved by replacement of Met80 with a noncoordinating residue, but to our knowledge, only reports on nongenetic approaches aimed at inducing the loss of the native Met ligand, by unfolding in the presence of denaturing agents or carboxymethylation of the protein have appeared [159, 160]. Alternatively, cyt *c* can be proteolytically digested to the heme-peptide complexes known as microperoxidases, that will be described in the following section.

6.3.3 Heme–Peptide Complexes

The problems connected with the high cost and low stability of peroxidases, which limits their potential applications in processes of industrial interest, can be possibly overcome, at least in part, by the use of heme-peptide complexes as small-size peroxidase analogs. In this context, we will consider only the heme-peptide complexes more strictly related to the peroxidases, and will not deal with the extensive literature about catalytic oxidations by synthetic metalloporphyrins. It is difficult to reproduce in a synthetic molecule the peculiar features of complex enzymes such as

peroxidases, and particularly the high reactivity toward hydrogen peroxide and the substrates, though often an appreciable increase in the catalytic activity of the synthetic heme complexes can be obtained toward a variety of substrates even with limited rates in the reaction with hydrogen peroxide [179]. Three different approaches have been explored:

- (a) Linking a peptide residue to hemin or deuterohemin, with the aim of introducing substrate selectivity or stereoselectivity in the catalytic activity, thus partly mimicking the substrate recognition mechanism exhibited by the enzyme [205–207]
- (b) Linking a histidine residue or a peptide containing histidine to the porphyrin propionate side chain, to better model the effect of the proximal histidine in the enhancement of the heme reactivity toward hydrogen peroxide [205, 208–211]
- (c) Using microperoxidases, the heme–peptide complexes obtained from proteolytic degradation of cyt *c*, as starting point for the preparation of complexes with improved activity and controlled substrate selectivity [205, 212–214]

Synthetic and natural iron(III) porphyrins are able to generate highly reactive species upon reaction with hydrogen peroxide. In catalytic processes, the activation of the metal catalyst by peroxide is generally a slow step; in fact, synthetic systems usually lack the acid–base activation mechanism required for efficient heterolytic cleavage of the bound peroxide in the first step of the catalytic cycle [215–219]. In spite of that, the species generated by reaction between heme and peroxide is highly reactive due to the easy approach of the substrate to the porphyrin moiety and the iron–oxo group. The capability of the catalyst of discriminating between different substrates depends on the relative redox potentials of the iron active species and the substrate. Another important aspect is the mode of interaction between the two reagents; in fact, in order to have an efficient oxidation process, the substrate must easily approach the iron porphyrin complex and with a disposition favoring the electron transfer. In peroxidases, substrate discrimination is controlled by the protein backbone in the active site. In synthetic iron porphyrins, the accessible distal and proximal sites do not allow such a discrimination. In the synthetic tetraaryl iron porphyrin derivatives, it is possible to introduce charged or bulky groups on the phenyl rings in order to introduce some selectivity [220]. The two propionate substituents present in hemin and deuterohemin complexes may also give some electrostatic interaction with charged substrates. In general, it would be desirable that the design of heme–peptide complexes had a partly accessible porphyrin and a substrate binding site where, after binding, this could undergo oxidation by the iron active species.

Covalent modification of protohemin and deuterohemin complexes, by linkage of histidine residues to the propionate side chains of the porphyrins, is the standard approach followed to introduce the push effect exerted by the proximal ligand in peroxidases [205, 208–211]. To combine the activation effect given by the axial imidazole and the substrate recognition given by an appended peptide chain, two model systems were studied by our group. These complexes contain an *L*-histidine

methyl ester residue linked to one propionate group of deuterohemin and a peptide, containing an L-phenylalanine residue at position 3 or 4, linked to the other propionate arm [208]. The chelated histidine residue improves the reactivity of the model systems; it also has the effect of forcing the peptide of the other arm to fold toward the opposite (distal) side of the porphyrin. In the catalytic oxidation of the two enantiomers of tyrosine methyl ester by *tert*-butyl hydroperoxide, only the complex bearing the Phe residue in position 4 of the peptide chain exhibited enantioselectivity. This result was explained considering that chiral recognition required interaction of the substrate with the polar His residue; when this interaction is offset by the hydrophobic ring stacking between the phenol and the Phe residue prevailing when the latter is in the third (and not in the fourth) position, the substrate is not sufficiently immobilized in the catalyst/substrate adduct thus preventing the induction of appreciable stereoselectivity. In the covalent linkage of the histidine to the propionate chain, the size of the arm carrying the imidazole group is important, as strain in the coordination of the imidazole to the iron reduces the catalytic efficiency. According to molecular mechanics and dynamics, calculations showed that strain-free coordination by the imidazole to the iron centers occurs when the position of His is second or third in the peptide sequence [209]. Moreover, the chelating arms containing the His residue can exhibit a further effect on the stereoselectivity of the reaction, due to the possibility of interaction of the substrate with the chelating arm containing the chiral His residue [210]. The effect of the position of the histidine residue on the catalytic activity of heme-peptide complexes was studied also by the Nordlander's group with modified protohemins [211]. They synthesized the hemin modified by covalently linking a Gly-His-OMe or a Gly-Gly-His-OMe residue to one propionate arm of the porphyrin, the latter of which being less coordinatively strained and exhibiting the highest peroxidase reactivity.

Microperoxidases (MPs) are heme-containing peptides derived from proteolytic digestion of cyt *c*, in which the heme is covalently linked to the peptide chain through two thioether bonds [221–223]. The peptide size and sequence in MPs can be modified by changing the source of the starting cyt *c* or the type of proteolytic enzyme (i.e., trypsin, pepsin, or both of them one after the other). In all MPs, the histidine residue acting as iron proximal ligand in cyt *c* is maintained, while the second (Met) axial ligand is removed by the proteolysis. This leaves the six coordination position of the iron(III) center available to weakly bind a water molecule, allowing easy replacement by hydrogen peroxide or other exogenous ligands. The best known amongst MPs is MP8, which is obtained from the peptic and tryptic digestion of horse heart cyt *c*; it retains the amino acid residues 14–21 of the starting protein. Treatment of the protein with pepsin alone yields MP11, which contains residues 11–21; while trypsin proteolysis alone generates MP9, containing residues 14–22. In the presence of hydrogen peroxide, all these MPs form active species, which are able to oxidize several substrates, thus acting as models for peroxidases [213].

Microperoxidases are highly soluble in water and partly soluble in (polar) organic medium and can take advantage of the activating “push” effect due to the

presence of a suitably positioned axial histidine. Therefore, MPs are good starting points for the building up of heme peptide catalysts with enhanced activity and selectivity. At the same time, the presence of a rigid proximal site makes the modified MPs good probes for investigating the effect of modifications in the distal site on the reactivity of the complex. MP8 is characterized by an open distal site, which is freely accessible to both hydrogen peroxide and substrate molecules. The reduced substrate selectivity observed in the reactions of this complex is ascribable to electrostatic interaction with the protonated *N*-terminal amino group. The lack of charged residues in the distal site, which could reproduce the effect of distal histidine and arginine in peroxidases, makes the reactivity of MP8 toward H₂O₂ orders of magnitude lower than that of the enzyme.

Some modified MP8 derivatives were synthesized by our group by covalent linkage to the *N*-terminal amino group of one (Pro-MP8) or two (Pro₂-MP8) proline residues, or an *N*-protected proline carrying an aromatic fluorenyl group (Fmoc-Pro-MP8) [212]. The reactivity with hydrogen peroxide of these MP8 derivatives is controlled by the polarity around the iron and reaches the highest value with the complex containing the two proline residues [179]. The analysis of the reactivity of MPs active species toward the substrates is complicated by the complete accessibility of the porphyrin ring of the MPs by exogenous molecules. Therefore, the MP substrate oxidation is extremely rapid compared to the formation of the active species and usually occurs as a fast step in the catalytic cycle. The increase in efficiency of these complexes in a peroxidase-type reaction is significant, even if the nature of the active species is still under debate [167, 213].

The activity of several MP derivatives in the oxidation of phenolic substrates by hydrogen peroxide has been investigated by our group. The kinetic parameters show that the residues on the distal MP site alters the reactivity of the active species by controlling both the substrate approach and the ET rate, which is modulated by the phenol disposition with respect to the heme. The binding of the substrates to MP complexes, as deduced from the paramagnetic effect of the metal ion on the ¹H-NMR relaxation rates, occurs with iron–substrate proton distances in the range of 7.4–9.5 Å, which is the same range commonly observed for substrate binding to peroxidases [224–226]. The collective data show that the electrostatic interaction between substrate and MP controls substrate binding, and stacking π – π interactions seem to play an important role [179]. Moreover, polar residues near the heme facilitate the oxidation of the substrate, since they mimic the effect of the distal arginine in peroxidases in promoting compound II reduction: the efficiency of this process is so high in MP11 that its reactivity becomes comparable with that of HRP, and even larger than that in the case of the oxidation of tyramine [214]. To our knowledge, this is the highest peroxidase-like activity ever reported for a heme model system.

The emerging picture from the activity of covalently modified MPs is that to have an efficient catalyst the distal site must contain positively charged residues, which can approach the iron center; their presence increases the reactivity toward both hydrogen peroxide and the substrate. The selectivity for different substrates can take advantage of the addition of other charged or polar residues that do not necessarily have to approach the iron closely, since the ET occurs through the

porphyrin plane. Aromatic residues can be used to increase the substrate affinity through π - π stacking interactions. To maintain a good catalytic activity, reduction of the polarity around the iron by the aromatic groups should be prevented; moreover, the substrate binding site must be kept close to the porphyrin edge.

References

1. Schmid A, Dordick JS, Hauer B, Kiener A, Wubbolts M, Witholt B (2001) Industrial biocatalysis today and tomorrow. *Nature* 409:258–268
2. Sheldon RA (2008) E factor, green chemistry and catalysis: an odyssey. *Chem Commun*: 3352–3365
3. Polizzi KM, Bommaris AS, Broering JM, Chaparro-Riggers JF (2007) Stability of biocatalysts. *Curr Opin Chem Biol* 11:220–225
4. Aehle W (2007) *Enzymes in Industry – production and applications*, 3rd edn. Wiley, New York
5. Dunford HB, Stillmann JS (1976) On the function and mechanism of action of peroxidases. *Coord Chem Rev* 19:187–251
6. Anni H, Yonetani T (1992) Mechanism of action of peroxidases. In: Sigel H, Sigel A (eds) *Met Ions Biol Syst*, vol 28. Marcel Dekker, New York
7. Bosshard HR, Anni H, Yonetani T (1991) Yeast cytochrome *c* peroxidase. In: Everse J, Everse KE, Grisham MB (eds) *Peroxidases in chemistry and biology*, vol II. CRC, Boca Raton
8. Kimura S, Yamazaki I (1979) Comparisons between hog intestinal peroxidase and bovine lactoperoxidase-compound I formation and inhibition by benzhydroxamic acid. *Arch Biochem Biophys* 198:580–588
9. Hu S, Kincaid JR (1991) Resonance Raman structural characterization and the mechanism of formation of lactoperoxidase compound III. *J Am Chem Soc* 113:7189–7194
10. Taugog A, Dorris M, Doerge DR (1994) Evidence for a radical mechanism in peroxidase-catalyzed coupling. I. Steady-state experiments with various peroxidases. *Arch Biochem Biophys* 315:82–89
11. Monzani E, Gatti AL, Profumo A, Casella L, Gullotti M (1997) Oxidation of phenolic compounds by lactoperoxidase. Evidence for the presence of a low-potential compound II during catalytic turnover. *Biochemistry* 36:1918–1926
12. Marquez LA, Dunford HB (1995) Kinetics of oxidation of tyrosine and dityrosine by myeloperoxidase compounds I and II. Implications for lipoprotein peroxidation studies. *J Biol Chem* 270:30434–30440
13. Arnold J, Monzani E, Furtmüller PG et al (2006) Kinetics and thermodynamics of halide and nitrite oxidation by mammalian heme peroxidases. *Eur J Inorg Chem* :3801–3811
14. Hayashi YI (1979) The oxidation-reduction potentials of compound I/compound II and compound II/ferric couples of horseradish peroxidases A2 and C. *J Biol Chem* 254: 9101–9106
15. Green MT, Dawson JH, Gray HB (2004) Oxoiron(IV) in chloroperoxidase compound II is basic: implications for P450 chemistry. *Science* 304:1653–1656
16. Valenti P, Recanatini M, Magistretti M, Da Re P (2006) Some basic derivatives of Pummerer's ketone. *Archives der pharmazie* 314:740–743
17. Gallagher PH (1923) Mechanism of oxidation in the plant: part I. The oxygenase of bach and chodat: function of lecithins in respiration. *Biochem J* 17:515–529
18. Hewson WD, Dunford HB (1976) Stoichiometry of the reaction between horseradish peroxidase and *p*-cresol. *J Biol Chem* 251:6043–6052

19. Casella L, Gullotti M, Ghezzi R et al (1992) Mechanism of enantioselective oxygenation of sulfides catalyzed by chloroperoxidase and horseradish peroxidase. Spectral studies and characterization of enzyme-substrate complexes. *Biochemistry* 31:9451–9459
20. Colonna S, Gaggero N, Richelmi C, Pasta P (1999) Recent biotechnological developments in the use of peroxidases. *Trends Biotechnol* 17:163–171
21. Brown BR, Bocks SM (1963) Some new enzymatic reaction of phenols. In: Pridham JB (ed) *Enzyme chemistry of phenolic compounds*. Pergamon, Oxford
22. Holland HL (1992) Organic synthesis with oxidative enzymes. VCH, New York, p 341
23. Adam W, Lazarus M, Saha-Möller CR et al (1999) Biotransformations with peroxidases. In: Faber K (ed) *Advances in biochemical engineering and biotechnology*, vol 6. Springer, Berlin
24. Uyama H, Kurioka H, Kaneko I, Kobayashi S (1994) Synthesis of a new family of phenol resin by enzymatic oxidative polymerization. *Chem Lett* :423–426
25. Krawczik AR, Lipkowska E, Wróbel JT (1991) Horseradish peroxidase-mediated preparation of dimers from eugenol and isoeugenol. *Collect Czech Chem Commun* 56:1147–1150
26. Kobayashi A, Koguchi Y, Kanzaki H, Kajiyama S, Kawazu K (1994) Production of a new type of bioactive phenolic compound. *Biosci Biotechnol Biochem* 58:133–134
27. Kobayashi A, Koguchi Y, Kanzaki H, Kajiyama S, Kawazu K (1994) A new type of antimicrobial phenolics produced by plant peroxidase and its possible role in the chemical defense systems against plant pathogens. *Z Naturforsch C* 49:411–414
28. Goodbody AE, Endo T, Vukovic J et al (1988) Enzymic coupling of catharanthine and vindoline to form 3', 4'-anhydrovinblastine by horseradish peroxidase. *Planta Med* 54:136–140
29. Setälä H, Pajunen A, Rummakko P, Sipilä J, Brunow G (1999) A novel type of spiro compound formed by oxidative cross coupling of methyl sinapate with a syringyl lignin model compound. A model system for the b-1 pathway in lignin biosynthesis. *J Chem Soc Perkin Trans 1*:461–464
30. Hoch U, Adam W, Fell R, Saha-Möller CR, Schreier P (1997) Horseradish peroxidase – a biocatalyst for the one-pot synthesis of enantiomerically pure hydroperoxides and alcohols. *J Mol Catal A Chem* 117:321–328
31. Adam W, Hoch U, Saha-Möller CR, Schreier P (1995) Enzyme-catalyzed asymmetric synthesis: kinetic resolution of racemic hydroperoxides by enantioselective reduction to alcohols with horseradish peroxidase and guaiacol. *J Am Chem Soc* 117:11898–11901
32. Höft E, Hamann H-J, Kunath A, Adam W, Hoch U, Saha-Möller CR, Schreier P (1995) Enzyme-catalyzed kinetic resolution of racemic secondary hydroperoxides. *Tetrahedron Asymmetry* 6:603–608
33. Schmitt MM, Schüler E, Braun M, Häring D, Schreier P (1998) Horseradish peroxidase: an effective but unselective biocatalyst for biaryl synthesis. *Tetrahedron Lett* 39:2945–2946
34. Davin LB, Wang H, Crowell AL et al (1997) Stereoselective bimolecular phenoxy radical coupling by an auxiliary (dirigent) protein without an active center. *Science* 275:362–366
35. Boeriu CG, Oudgenoeg G, Spekking WT et al (2004) Horseradish peroxidase-catalyzed cross-linking of feruloylated arabinoxylans with α -casein. *J Agric Food Chem* 52:6633–6639
36. van Deurzen MPJ, van Rantwijk F, Sheldon RA (1997) Selective oxidations catalyzed by peroxidases. *Tetrahedron* 53:13183–13220
37. Kobayashi S, Kaneko I, Uyama H (1992) Enzymatic oxidation polymerization of o-phenylenediamine. *Chem Lett* 21:393–394
38. Pieper DH, Winkler R, Sandermann H (1992) Formation of a toxic dimerization product of 3, 4-dichloroaniline by lignin peroxidase from *Phanerochaete chrysosporium*. *Angew Chemie Int Ed* 31:68–70
39. Fukunishi K, Kitada K, Naito I (1991) A facile preparation of iminoxyl dimers by hydrogen peroxide/peroxidase oxidation of aldoximes. *Synthesis* :237–238
40. Kedderis GL, Hollemberg PF (1984) Peroxidase-catalyzed N-demethylation reactions. Substrate deuterium isotope effects. *J Biol Chem* 259:3663–3668

41. Meunier G, Meunier B (1985) Evidences for an efficient demethylation of methoxyellipticine derivatives catalyzed by a peroxidase. *J Am Chem Soc* 107:2558–2560
42. Meunier B (1991) N- and O-Demethylations catalyzed by peroxidases. In: Everse J, Everse KE, Grisham MB (eds) *Peroxidases in chemistry and biology*, vol 2. CRC, Boca Raton
43. Ferrari RP, Laurenti E, Casella L, Poli S (1993) Oxidation of catechols and catecholemines by horseradish peroxidase and lactoperoxidase: ESR spin stabilization approach combined with optical methods. *Spectrochim Acta* 49A:1261–1267
44. Donnelly DMX, Murphy FG, Polonski J, Prangé T (1987) Enzyme-mediated H₂O₂ oxidation of (E)-stilbene-3, 4-diol. *J Chem Soc Perkin Trans* 1:2719–2722
45. Matsumoto K, Takahashi H, Miyake Y, Fukuyama Y (1999) Convenient syntheses of neurotrophic americanol A and isoamericanol A by HRP catalyzed oxidative coupling of caffeic acid. *Tetrahedron Lett* 40:3185–3186
46. Prota G (1992) Melanin-producing cells. In: Jovanovich HB (ed) *Melanins and melanogenesis*. Academic Press, San Diego
47. d'Ischia M, Napolitano A, Tsiakas K, Prota G (1990) New intermediates in the oxidative polymerization of 5, 6-dihydroxyindole to melanin promoted by the peroxidase/H₂O₂ system. *Tetrahedron* 46:5789–5796
48. Ito S, Fujita K (1981) Iron- and peroxide-dependent conjugation of dopamine with cysteine: oxidative routes to the novel brain metabolite 5-S-cysteinyl-dopamine. *Biochim Biophys Acta* 672:151–157
49. Nicolis S, Zucchelli M, Monzani E, Casella L (2008) Myoglobin modification by enzyme-generated dopamine reactive species. *Chem Eur J* 14:8661–8673
50. Savenkova MI, Newmyer SL, Ortiz de Montellano PR (1996) Rescue of His-42 → Ala horseradish peroxidase by a Phe-41 → His mutation. Engineering of a surrogate catalytic histidine. *J Biol Chem* 271:24598–24603
51. Azevedo AM, Martins VC, Prazeres DM et al (2003) Horseradish peroxidase: a valuable tool in biotechnology. *Biotechnol Annu Rev* 9:199–247
52. Ozaki S-I, Ortiz de Montellano PR (1995) Molecular engineering of horseradish peroxidase: thioether sulfoxidation and styrene epoxidation by Phe-41 leucine and threonine mutants. *J Am Chem Soc* 117:7056–7064
53. Newmyer SL, Ortiz de Montellano PR (1996) Rescue of the catalytic activity of an H42A mutant of horseradish peroxidase by exogenous imidazoles. *J Biol Chem* 271:14891–14896
54. Tanaka M, Ishimori K, Mukai M, Kitagawa T, Morishima I (1997) Catalytic activities and structural properties of horseradish peroxidase distal His42 → Glu or Gln mutant. *Biochemistry* 36:9889–9898
55. Ortiz de Montellano PR, Choe YS, DePillis G, Catalano CE (1987) Structure-mechanism relationships in hemoproteins. Oxygenations catalyzed by chloroperoxidase and horseradish peroxidase. *J Biol Chem* 262:11641–11646
56. Corbett MD, Corbett BR (1985) Enzymatic N-oxidation of 4-nitroaniline. *Biochem Arch* 1:115–120
57. Doerge DR, Corbett MD (1991) Peroxygenation mechanism for chloroperoxidase-catalyzed N-oxidation of arylamines. *Chem Res Toxicol* 4:556–560
58. Corbett D, Baden DG, Chipko BR (1979) The non-microsomal production of N-(4-chlorophenyl)glycolhydroxamic acid from 4-chloronitrosobenzene by rat liver homogenates. *Bioorg Chem* 8:227–235
59. Corbett MD, Chipko BR, Batchelor AO (1980) The action of chloride peroxidase on 4-chloroaniline. N-oxidation and ring halogenation. *Biochem J* 187:893–903
60. Kirner S, van Pée KH (1994) The biosynthesis of nitro compounds: the enzymatic oxidation to pyrrolnitrin of its amino-substituted precursor. *Angew Chem Int Ed Engl* 33:352
61. Fujimoto S, Ishimitsu S, Hirayama S, Kawakami N, Ohara A (1991) Hydroxylation of phenylalanine by myeloperoxidase-hydrogen peroxide system. *Chem Pharm Bull* 39:1598–1600
62. Mason HS, Onopryenko I, Buhler D (1957) Hydroxylation; the activation of oxygen by peroxidase. *Biochim Biophys Acta* 24:225–226

63. Buhler DR, Mason HS (1961) Hydroxylation catalyzed by peroxidase. *Arch Biochem Biophys* 92:424–437
64. Klibanov AM, Berman Z, Alberti BN (1981) Preparative hydroxylation of aromatic compounds catalyzed by peroxidase. *J Am Chem Soc* 103:6263–6264
65. McCarthy MB, White RE (1983) Functional differences between peroxidase compound I and the cytochrome P-450 reactive oxygen intermediate. *J Biol Chem* 258:9153–9158
66. Zaks A, Dodds DR (1995) Chloroperoxidase-catalyzed asymmetric oxidations: substrate specificity and mechanistic study. *J Am Chem Soc* 117:10419–10424
67. Miller VP, Tschirret-Guth RA, Ortiz de Montellano PR (1995) Chloroperoxidase-catalyzed benzylic hydroxylation. *Arch Biochem Biophys* 319:333–340
68. Corbett MD, Chipko BR (1979) Peroxide oxidation of indole to oxindole by chloroperoxidase catalysis. *Biochem J* 183:269–276
69. Dawson JH (1988) Probing structure-function relations in heme-containing oxygenases and peroxidases. *Science* 240:433–439
70. Geigert J, Dalietos DJ, Neidleman SL, Lee TD, Wadsworth J (1983) Peroxide oxidation of primary alcohols to aldehydes by chloroperoxidase catalysis. *Biochem Biophys Res Commun* 114:1104–1108
71. van Deurzen MPJ, van Rantwijk F, Sheldon RA (1997) Chloroperoxidase-catalyzed oxidation of 5-hydroxymethylfurfural. *J Carbohydr Chem* 16:299–309
72. Fu H, Kondo H, Ichikawa Y, Look GC, Wong C-H (1992) Chloroperoxidase-catalyzed asymmetric synthesis: enantioselective reactions of chiral hydroperoxides with sulfides and bromohydrate of glycals. *J Org Chem* 57:7265–7270
73. Doerge DR (1986) Oxygenation of organosulfur compounds by peroxidases: evidence of an electron transfer mechanism for lactoperoxidase. *Arch Biochem Biophys* 244:678–685
74. Doerge DR, Cooray NM, Brewster ME (1991) Peroxidase-catalyzed S-oxygenation: mechanism of oxygen transfer for lactoperoxidase. *Biochemistry* 30:8960–8964
75. Kobayashi S, Nakano M, Goto T, Kimura T, Schaap AP (1986) An evidence of the peroxidase-dependent oxygen transfer from hydrogen peroxide to sulfides. *Biochem Biophys Res Commun* 135:166–171
76. Miller VP, DePillis GD, Ferrer JC, Mauk AG, Ortiz de Montellano PR (1992) Mono-oxygenase activity of cytochrome *c* peroxidase. *J Biol Chem* 267:8936–8942
77. Ozaki S-I, Ortiz de Montellano PR (1994) Molecular engineering of horseradish peroxidase. Highly enantioselective sulfoxidation of aryl alkyl sulfides by the Phe-41-Leu mutant. *J Am Chem Soc* 116:4487–4488
78. Arnhold J, Furtmüller PG, Regelsberger G, Obinger C (2001) Redox properties of the couple compound I/native enzyme of myeloperoxidase and eosinophil peroxidase. *Eur J Biochem* 268:5142–5148
79. Furtmüller PG, Arnhold J, Jantschko W, Zederbauer M, Jakopitsch C, Obinger C (2005) Standard reduction potentials of all couples of the peroxidase cycle of lactoperoxidase. *J Inorg Biochem* 99:1220–1229
80. Furtmüller PG, Burner U, Obinger C (1998) Reaction of myeloperoxidase compound I with chloride, bromide, iodide, and thiocyanate. *Biochemistry* 37:17923–17930
81. Marquez LA, Dunford HB (1994) Chlorination of taurine by myeloperoxidase. Kinetic evidence for an enzyme-bound intermediate. *J Biol Chem* 269:7950–7956
82. Furtmüller PG, Obinger C, Hsuanyu Y, Dunford HB (2000) Mechanism of reaction of myeloperoxidase with hydrogen peroxide and chloride ion. *Eur J Biochem* 267:5858–5864
83. Furtmüller PG, Burner U, Regelsberger G, Obinger C (2000) Spectral and kinetic studies on the formation of eosinophil peroxidase compound I and its reaction with halides and thiocyanate. *Biochemistry* 39:15578–15584
84. Bakkenist AR, de Boer JE, Plat H, Wever R (1980) The halide complexes of myeloperoxidase and the mechanism of the halogenation reactions. *Biochim Biophys Acta* 613:337–348
85. Winterbourn CC (1985) Comparative reactivities of various biological compounds with myeloperoxidase-hydrogen peroxide-chloride, and similarity of the oxidant to hypochlorite. *Biochim Biophys Acta* 840:204–210

86. Zuurbier KWM, Bakkenist AR, Wever R, Muijsers AO (1990) The chlorinating activity of human myeloperoxidase: high initial activity at neutral pH value and activation by electron donors. *Biochim Biophys Acta* 1037:140–146
87. Kettle AJ, Winterbourn CC (1994) Assays for the chlorination activity of myeloperoxidase. *Methods Enzymol* 233:502–512
88. Ramos DR, Garcia MV, Canle LM, Santaballa JA, Furtmüller PG, Obinger C (2007) Myeloperoxidase-catalyzed taurine chlorination: Initial versus equilibrium rate. *Arch Biochem Biophys* 466:221–233
89. Franssen MCR, van der Plas HC (1987) The chlorination of barbituric acid and some of its derivatives by chloroperoxidase. *Bioorg Chem* 15:59–70
90. Franssen MCR, Weijnen JGJ, Vincken JP, Laane C, van der Plas HC (1988) Chloroperoxidase-catalyzed halogenation of apolar compounds using reversed micelles. *Biocatalysis* 1:205–216
91. Renganathan V, Miki K, Gold MH (1987) Haloperoxidase reactions catalyzed by lignin peroxidase, an extracellular enzyme from the basidiomycete *Phanerochaete chrysosporium*. *Biochemistry* 26:5127–5132
92. Franssen MCR, Weijnen JGJ, Vincken JP, Laane C, van der Plas HC (1987) Haloperoxidase in reversed micelles: use in organic synthesis and optimisation of the system. In: Laane C, Trumper J, Lilly MD (eds) *Biocatalysis in organic media*. Elsevier, Amsterdam
93. Morris DR, Hager LP (1966) Mechanism of the inhibition of enzymatic halogenation by antithyroid agents. *J Biol Chem* 241:3582–3589
94. Itoh N, Izumi Y, Yamada H (1987) Haloperoxidase-catalyzed halogenation of nitrogen-containing aromatic heterocycles represented by nucleic bases. *Biochemistry* 26:282–289
95. Itahara T, Ide N (1987) Chloroperoxidase catalyzed halogenation of pyrimidine bases. *Chem Lett* 12:2311–2312
96. Franssen MCR, van Boven HG, van der Plas HC (1987) Enzymatic halogenation of pyrazoles and pyridine derivatives. *J Heteroatom Chem* 24:1313–1316
97. Wiesner W, van Pee KH, Lingens F (1986) Detection of a new chloroperoxidase in *Pseudomonas pyrrocinia*. *FEBS Lett* 209:321–324
98. Liu KKC, Wong CH (1992) Enzymic halohydrate of glycals. *J Org Chem* 57:3748–3750
99. Fang JM, Lin CH, Bradshaw CW, Wong CH (1995) Enzymes in organic synthesis: oxidoreductions. *J Chem Soc Perkin Trans I*:967–978
100. Coughlin P, Roberts S, Rush C, Willetts A (1993) Biotransformation of alkenes by haloperoxidases: Regiospecific bromohydrin formation from cinnamyl substrates. *Biotechnol Lett* 15:907–912
101. Stanbury DM (1989) Reduction potentials involving inorganic free radicals in aqueous solution. *Adv Inorg Chem* 33:69–138
102. van der Vliet A, Eiserich JP, Halliwell B, Cross CE (1997) Formation of reactive nitrogen species during peroxidase-catalyzed oxidation of nitrite. *J Biol Chem* 272:7617–7625
103. Burner U, Furtmüller PG, Kettle AJ, Koppenol WH, Obinger C (2000) Mechanism of reaction of myeloperoxidase with nitrite. *J Biol Chem* 275:20597–20601
104. Lehnig M (2001) N-15 Chemically induced dynamic nuclear polarization during reaction of N-acetyl-L-tyrosine with the nitrating systems nitrite/hydrogen peroxide/horseradish peroxidase and nitrite/hypochlorous acid. *Arch Biochem Biophys* 393:245–254
105. Monzani E, Roncone R, Galliano M, Koppenol WH, Casella L (2004) Mechanistic insight into the peroxidase catalyzed nitration of tyrosine derivatives by nitrite and hydrogen peroxide. *Eur J Biochem* 271:895–906
106. Roncone R, Barbieri M, Monzani E, Casella L (2006) Reactive nitrogen species generated by heme proteins: mechanism of formation and targets. *Coord Chem Rev* 250:1286–1293
107. Budde CL, Beyer A, Minir IZ, Dordick JS, Khmelnitsky YL (2001) Enzymatic nitration of phenols. *J Mol Catal B* 15:55–64
108. Brennan ML, Wu W, Fu X et al (2002) A tale of two controversies: defining both the role of peroxidases in nitrotyrosine formation in vivo using eosinophil peroxidase and

- myeloperoxidase-deficient mice, and the nature of peroxidase-generated reactive nitrogen species. *J Biol Chem* 277:17415–17427
109. Sala A, Nicolis S, Roncone R, Monzani E, Casella L (2004) Peroxidase catalyzed nitration of tryptophan derivatives. Mechanism, products and comparison with chemical nitrating agents. *Eur J Biochem* 271:2841–2852
 110. Palumbo A, Napolitano A, Barone P, d'Ischia M (1999) Nitrite- and peroxide-dependent oxidation pathways of dopamine: 6-nitrodopamine and 6-hydroxydopamine formation as potential contributory mechanisms of oxidative stress- and nitric oxide-induced neurotoxicity in neuronal degeneration. *Chem Res Toxicol* 12:1213–1222
 111. Thévenot DR, Toth K, Durst RA, Wilson GS (2001) Electrochemical biosensors: recommended definitions and classification. *Biosens Bioelectron* 16:121–131
 112. De Luis R, Lavilla M, Sánchez L, Calvo M, Pérez MD (2009) Development and evaluation of two ELISA formats for the detection of b-lactoglobulin in model processed and commercial foods. *Food Control* 20:643–647
 113. Tirola T, Jaakkola A, Bloigu A et al (2006) Novel enzyme immunoassay utilizing lipopolysaccharide-binding protein as a capture molecule for the measurement of chlamydial lipopolysaccharide in serum. *Diagn Microbiol Infect Dis* 54:7–12
 114. Skladal P (1997) Advances in electrochemical immunosensors. *Electroanalysis* 9:737–745
 115. Madou M, Tierney MJ (1993) Required technology breakthroughs to assume widely accepted biosensors. *Appl Biochem Biotech* 41:109–128
 116. Darain F, Park S-U, Shim Y-B (2003) Disposable amperometric immunosensor system for rabbit IgG using a conducting polymer modified screen-printed electrode. *Biosens Bioelectron* 18:773–780
 117. Zhang Y, Zhang Y, Wang H et al (2009) An enzyme immobilization platform for biosensor designs of direct electrochemistry using flower-like ZnO crystals and nano-sized gold particles. *J Electroanal Chem* 627:9–14
 118. Mello LD, Kubota LT (2007) Biosensors as a tool for the antioxidant status evaluation. *Talanta* 72:335–348
 119. Pastor I, Esquembre R, Micol V, Mallavia R, Mateo CR (2004) A ready-to-use fluorimetric biosensor for superoxide radical using superoxide dismutase and peroxidase immobilized in sol-gel glasses. *Anal Biochem* 334:335–343
 120. Casero E, Darder M, Pariente F, Lorenzo E (2000) Peroxidase enzyme electrodes as nitric oxide biosensors. *Anal Chim Acta* 403:1–9
 121. Mao L, Yamamoto K (2000) Amperometric biosensor for glutathione based on osmium-polyvinylpyridine gel polymer and glutathione sulfhydryl oxidase. *Electroanalysis* 12:577–582
 122. Akyilmaz E, Sezgintürk MK, Dinçkaya E (2003) A biosensor based on urate oxidase-peroxidase coupled enzyme system for uric acid determination in urine. *Talanta* 61:73–79
 123. Pérez DM, Ferrer ML, Mateo CR (2003) A reagent less fluorescent sol-gel biosensor for uric acid detection in biological fluids. *Anal Biochem* 322:238–242
 124. Imabayashi S, Kong Y, Watanabe M (2001) Amperometric biosensor for polyphenol based on horseradish peroxidase immobilized on gold electrodes. *Electroanalysis* 13:408–412
 125. Kong YT, Imabayashi S, Kano K, Ikeda T, Kakiuchi T (2001) Peroxidase-based amperometric sensor for the determination of total phenols using two-stage peroxidase reactions. *Am J Enol Vitic* 52:381–385
 126. Mello LD, Alves AA, Macedo DV, Kubota LT (2005) Peroxidase-based biosensor as a tool for a fast evaluation of antioxidant capacity of tea. *Food Chem* 92:515–519
 127. Lindgren A, Ruzgas T, Gorton L et al (2000) Biosensors based on novel peroxidases with improved properties in direct and mediated electron transfer. *Biosens Bioelectron* 15:491–497
 128. Castillo J, Ferapontova E, Hushpulia D et al (2006) Direct electrochemistry and biocatalysis of H₂O₂ reduction of recombinant tobacco peroxidase on graphite. Effect of peroxidase single-point mutation on Ca²⁺-modulated catalytic activity. *J Electroanal Chem* 588:112–121

129. Ferapontova EE, Castello J, Gorton L (2006) Bioelectrocatalytic properties of lignin peroxidase from *Phanerochaete chrysosporium* in reactions with phenols, catechols and lignin-model compounds. *Biochim Biophys Acta* 1760:1343–1354
130. Belcarz A, Ginalska G, Kowalewska B, Kulesza P (2008) Spring cabbage peroxidases – Potential tool in biocatalysis and bioelectrocatalysis. *Phytochemistry* 69:627–636
131. Lu Y, Berry SM, Pfister TD (2001) Engineering novel metalloproteins: design of metal-binding sites into native protein scaffolds. *Chem Rev* 101:3047–3080
132. Watanabe Y (2002) Construction of heme enzymes: four approaches. *Curr Opin Chem Biol* 6:208–216
133. Ryan BJ, Ó'Fágáin C (2007) Effects of single mutations on the stability of horseradish peroxidase to hydrogen peroxide. *Biochimie* 89:1029–1032
134. Ryan BJ, Ó'Fágáin C (2008) Effects of mutations in the helix G region of horseradish peroxidases. *Biochimie* 90:1414–1421
135. Savenkova MI, Kuo JM, Ortiz de Montellano PR (1998) Improvement of peroxygenase activity by relocation of a catalytic histidine within the active site of horseradish peroxidase. *Biochemistry* 37:1828–10836
136. Matsunaga I, Sumimoto T, Ayata M, Ogura H (2002) Functional modulation of a peroxygenase cytochrome P450: novel insight into the mechanisms of peroxygenase and peroxidase enzymes. *FEBS Lett* 528:90–94
137. Redaelli C, Monzani E, Santagostini L et al (2002) Characterization and peroxidase activity of a myoglobin mutant containing a distal arginine. *ChemBioChem* 3:226–233
138. Roncone R, Monzani E, Labò S, Sanangelantoni AM, Casella L (2005) Catalytic activity, stability and unfolding of engineered and reconstituted myoglobins. *J Biol Inorg Chem* 10:11–24
139. Roncone R, Monzani E, Murtas M et al (2004) Engineering peroxidase activity in myoglobin: the haem cavity structure and peroxide activation in the T67R/S92D mutant and its derivative reconstituted with protohaemin-1-histidine. *Biochem J* 377:717–724
140. Matsui T, Ozaki S, Liang E, Phillips GN, Watanabe Y (1999) Effects of the location of distal histidine in the reaction of myoglobin with hydrogen peroxide. *J Biol Chem* 274:2838–2844
141. Morawski B, Lin Z, Cirino P et al (2000) Functional expression of horseradish peroxidase in *Saccharomyces cerevisiae* and *Pichia pastoris*. *Protein Eng* 13:377–384
142. Morawski B, Quan S, Arnold FH (2001) Functional expression and stabilization of horseradish peroxidase by directed evolution in *Saccharomyces cerevisiae*. *Biotechnol Bioeng* 76:99–107
143. Rai GP, Zong Q, Hager LP (2000) Isolation of directed evolution mutants of chloroperoxidase resistant to suicide inactivation by primary olefins. *Israel J Chem* 40:63–70
144. Rai GP, Sakai S, Flórez AM, Mogollon L, Hager LP (2001) Directed evolution of chloroperoxidase for improved epoxidation and chlorination catalysis. *Adv Synth Catal* 343:1–8
145. Iffland A, Gendreizig S, Tafemeyer P, Johnsson K (2001) Changing the substrate specificity of cytochrome *c* peroxidase using directed evolution. *Biochem Biophys Res Commun* 286:126–132
146. Iffland A, Tafemeyer P, Saudan C, Johnsson K (2000) Directed molecular evolution of cytochrome *c* peroxidase. *Biochemistry* 39:10790–10798
147. Wan L, Twitchett MB, Eltis LD, Mauk AG, Smith M (1998) In vitro evolution of horse heart myoglobin to increase peroxidase activity. *Proc Natl Acad Sci USA* 95:12825–12831
148. Matsuo T, Murata D, Hisaeda Y, Hori H, Hayashi T (2007) Porphyrinoid chemistry in hemoprotein matrix: detection and reactivities of iron(IV)-oxo species of porphycene incorporated into horseradish peroxidase. *J Am Chem Soc* 129:12906–12907
149. Feng J-Y, Liu J-Z, Ji L-N (2008) Thermostability, solvent tolerance, catalytic activity and conformation of cofactor modified horseradish peroxidases. *Biochimie* 90:1337–1346
150. Song H-Y, Liu J-Z, Weng L-P, Ji L-N (2009) Activity, stability, and unfolding of reconstituted horseradish peroxidase with modified heme. *J Mol Catal B Enzym* 57:48–54
151. Hayashi T, Hisaeda Y (2002) New functionalization of myoglobin by chemical modification of heme-propionates. *Acc Chem Res* 35:35–43

152. Hayashi T, Takimura T, Ogoshi H (1995) Photoinduced singlet electron transfer in a complex formed from zinc myoglobin and methyl viologen: artificial recognition by a chemically modified porphyrin. *J Am Chem Soc* 117:11606–11607
153. Hayashi T, Tomokuni A, Mizutani T, Hisaeda Y, Ogoshi H (1998) Interfacial recognition between reconstituted myoglobin having charged binding domain and electron acceptor via electrostatic interaction. *Chem Lett* 1:1229–1230
154. Hayashi T, Ando T, Matsuda T et al (2000) Introduction of a specific binding domain on myoglobin surface by new chemical modification. *J Inorg Biochem* 82:133–139
155. Hayashi T, Murata D, Makino M (2006) Crystal structure and peroxidase activity of myoglobin reconstituted with iron porphycene. *Inorg Chem* 45:10530–10536
156. Carey JR, Ma SK, Pfister TD et al (2004) A site-selective dual anchoring strategy for artificial metalloprotein design. *J Am Chem Soc* 126:10812–10813
157. Mogharrab N, Ghourchian H, Amininasab M (2007) Structural stabilization and functional improvement of horseradish peroxidase upon modification of accessible lysines: experiments and simulation. *Biophys J* 92:1192–1203
158. Cherry JR, Lamsa MH, Schneider P et al (1999) Directed evolution of a fungal peroxidase. *Nat Biotechnol* 17:379–384
159. Diederix REM, Ubbink M, Canters GW (2002) Peroxidase activity as a tool for studying the folding of *c*-type cytochromes. *Biochemistry* 41:13067–13077
160. Prasad S, Maiti NC, Mazumdar S, Mitra S (2002) Reaction of hydrogen peroxide and peroxidase activity in carboxymethylated cytochrome *c*: spectroscopic and kinetic studies. *Biochim Biophys Acta* 1596:63–75
161. Matsunaga I, Yokotani N, Gotoh O et al (1997) Molecular cloning and expression of fatty acid α -hydroxylase from *Sphingomonas paucimobilis*. *J Biol Chem* 272:23592–23596
162. Matsunaga I, Ueda A, Fujiwara N, Sumimoto T, Ichihara K (1999) Characterization of the ybdT gene product of *Bacillus subtilis*: novel fatty acid β -hydroxylating cytochrome P450. *Lipids* 34:841–846
163. Matsunaga I, Shiro Y (2004) Peroxide-utilizing biocatalysts: structural and functional diversity of heme-containing enzymes. *Curr Opin Chem Biol* 8:127–132
164. Shoji O, Fujishiro T, Nakajima H et al (2007) Hydrogen peroxide dependent monooxygenations by tricking the substrate recognition of cytochrome P450_{BSP}. *Angew Chem Int Ed* 46:3656–3659
165. Antonini E, Brunori M (1971) Hemoglobin and myoglobin in their reactions with ligands. North-Holland, Amsterdam
166. Watanabe Y, Ueno T (2003) Introduction of P450, peroxidase, and catalase activities into myoglobin by site-directed mutagenesis: diverse reactivities of compound I. *Bull Chem Soc Jpn* 76:1309–1322
167. Roncone R, Monzani E, Nicolis S, Casella L (2004) Engineering and prosthetic-group modification of myoglobin: peroxidase activity, chemical stability and unfolding properties. *Eur J Inorg Chem* :2203–2213
168. Nicolis S, Monzani E, Roncone R, Gianelli L, Casella L (2004) Metmyoglobin catalyzed exogenous and endogenous tyrosine nitration by nitrite and hydrogen peroxide. *Chem Eur J* 10:2281–2290
169. Nicolis S, Pennati A, Perani E et al (2006) Easy oxidation and nitration of human myoglobin by nitrite and hydrogen peroxide. *Chem Eur J* 12:749–757
170. Ozaki S, Matsui T, Watanabe Y (1996) Conversion of myoglobin into a highly stereospecific peroxygenase by the L29H/H64L mutation. *J Am Chem Soc* 118:9784–9785
171. Ozaki S, Matsui T, Watanabe Y (1997) Conversion of myoglobin into a peroxygenase: a catalytic intermediate of sulfoxidation and epoxidation by the F43H/H64L mutant. *J Am Chem Soc* 119:6666–6667
172. Ozaki S-I, Yang H-J, Matsui T, Goto Y, Watanabe Y (1999) Asymmetric oxidation catalyzed by myoglobin mutants. *Tetrahedron Asymmetry* 10:183–192

173. Pironti V, Nicolis S, Monzani E, Colonna S, Casella L (2004) Nitrite increases the enantioselectivity of sulfoxidation catalyzed by myoglobin derivatives in the presence of hydrogen peroxide. *Tetrahedron* 60:8153–8160
174. Kato S, Yang H, Ueno T et al (2002) Asymmetric sulfoxidation and amine binding by H64D/V68A and H64D/V68S Mb: mechanistic insight into the chiral discrimination step. *J Am Chem Soc* 124:8506–8507
175. Gajede M, Schuller DJ, Henriksen A, Smith AT, Poulos TL (1997) Crystal structure of horseradish peroxidase C at 2.15 Å resolution. *Nat Struct Biol* 4:1032–1038
176. Ozaki S, Roach MP, Matsui T, Watanabe Y (2001) Asymmetric oxidation catalyzed by myoglobin mutants. *Acc Chem Res* 34:818–825
177. Hayashi T, Hitomi Y, Ando T et al (1999) Peroxidase activity of myoglobin is enhanced by chemical mutation of heme-propionates. *J Am Chem Soc* 121:7747–7750
178. Monzani E, Alzuet G, Casella L et al (2000) Properties and reactivity of myoglobin reconstituted with chemically modified protohemin complexes. *Biochemistry* 39:9571–9582
179. Nicolis S, Casella L, Roncone R, Dallacosta C, Monzani E (2007) Heme-peptide complexes as peroxidase models. *C R Chimie* 10:380–391
180. Chapsal JM, Bourbigot MM, Thomas D (1986) Oxidation of aromatic compounds by haemoglobin. *Water Res* 20:709–713
181. Liu ZH, Wang QL, Mao LY et al (2000) Highly sensitive spectrofluorimetric determination of ascorbic acid based on its enhancement effect on a enzyme-catalyzed reaction. *Anal Chim Acta* 413:167–173
182. Zhang K, Cai RX, Chen DH, Mao LY (2000) Determination of hemoglobin based on its enzymatic activity for the oxidation of *o*-phenylenediamine with hydrogen peroxide. *Anal Chim Acta* 13:109–113
183. Mieyal JJ, Acherman RS, Blumer JL, Freeman LS (1976) Characterization of enzyme-like activity of human hemoglobin. Properties of the hemoglobin-P-450 reductase-coupled aniline hydroxylase system. *J Biol Chem* 251:3436–3441
184. Hu X, Tang K, Liu SG, Zhang YY, Zou GL (2005) Hemoglobin-biocatalysts synthesis of a conducting polyaniline. *React Funct Polym* 65:239–248
185. Yoshida Y, Kashiba K, Niki E (1994) Free radical-mediated oxidation of lipid induced by hemoglobin in aqueous dispersion. *Biochim Biophys Acta* 1201:165–172
186. Ortiz de Montellano PR, Catalano CE (1985) Epoxidation of styrene by haemoglobin and myoglobin. Transfer of oxygen equivalents to the protein surface. *J Biol Chem* 260:9265–9271
187. Kelder PP, De Mol NJ, Janssen LHM (1989) Is hemoglobin a catalyst for sulfoxidation of chlorpromazine? An investigation with isolated purified hemoglobin and hemoglobin in monooxygenase and peroxidase mimicking systems. *Biochem Pharmacol* 38:3593–3599
188. Zhang J, Oyama M (2004) A hydrogen peroxide sensor based on the peroxidases activity of hemoglobin immobilized on gold nanoparticles-modified ITO electrode. *Electrochim Acta* 50:85–90
189. Kafi AKM, Lee D-Y, Park S-H, Kwon Y-S (2008) Potential application of hemoglobin as an alternative to peroxidases in a phenol biosensor. *Thin Solid Films* 516:2816–2821
190. Xua Y, Hua C, Hua S (2008) A hydrogen peroxide biosensor based on direct electrochemistry of hemoglobin in Hb–Ag sol films. *Sens Actuators B* 130:816–822
191. Liu X, Xu Y, Ma X, Li G (2005) A third-generation hydrogen peroxide biosensor fabricated with hemoglobin and Triton X-100. *Sens Actuators B* 106:284–288
192. Liu H-H, Wan Y-Q, Zou G-L (2006) Redox reactions and enzyme-like activities of immobilized myoglobin in aqueous/organic mixtures. *J Electroanal Chem* 594:111–117
193. Jia N, Lian Q, Wang Z, Shen H (2009) A hydrogen peroxide biosensor based on direct electrochemistry of haemoglobin incorporated in PEO–PPO–PEO triblock copolymer film. *Sens Actuators B* 137:230–234
194. Zhao C, Wan L, Jiang L, Wang Q, Jiao K (2008) Highly sensitive and selective cholesterol biosensor based on direct electron transfer of haemoglobin. *Anal Biochem* 383:25–30

195. Yang W, Li Y, Bai Y, Sun C (2006) Hydrogen peroxide biosensor based on myoglobin/colloidal gold nanoparticles immobilized on glassy carbon electrode by a Nafion film. *Sens Actuators B* 115:42–48
196. Zhang L, Tian DB, Zhu JJ (2008) Third generation biosensor based on myoglobin-TiO₂/MWCNTs modified glassy carbon electrode. *Chin Chem Lett* 19:965–968
197. Shen L, Huang R, Hu N (2002) Myoglobin in polyacrylamide hydrogel films: direct electrochemistry and electrochemical catalysis. *Talanta* 56:1131–1139
198. Bellezza F, Cipiciani A, Costantino U, Nicolis S (2004) Catalytic activity of myoglobin immobilized on zirconium phosphonates. *Langmuir* 20:5019–5025
199. Itoh T, Ishii R, Ebina T et al (2006) Encapsulation of myoglobin with a mesoporous silicate results in new capabilities. *Bioconjug Chem* 17:236–240
200. Essa H, Magner E, Cooney J, Hodnett BK (2007) Influence of pH and ionic strength on the adsorption, leaching and activity of myoglobin immobilized onto ordered mesoporous silicates. *J Mol Catal B Enzym* 49:61–68
201. Zhang Y-Y, Hu X, Tang K, Zou G-L (2006) Immobilization of hemoglobin on chitosan films as mimetic peroxidases. *Process Biochem* 41:2410–2416
202. Vazquez-Duhalt R (1999) Cytochrome *c* as a biocatalyst. *J Mol Catal B Enzym* 7:241–249
203. Laszlo JA, Compton DL (2002) Comparison of peroxidase activities of hemein, cytochrome *c* and microperoxidase-11 in molecular solvents and imidazolium-based ionic liquids. *J Mol Catal B Enzym* 18:109–120
204. Villegas JA, Mauk AG, Vazquez-Duhalt R (2000) A cytochrome *c* variant resistant to heme degradation by hydrogen peroxide. *Chem Biol* 7:237–244
205. Lombardi A, Nistri F, Pavone V (2001) Peptide-based heme-protein models. *Chem Rev* 101:3165–3189
206. Casella L, Gullotti M, De Gioia L, Monzani E, Chillemi F (1991) Synthesis, ligand binding and biomimetic oxidations of deuterohaemin modified with an undecapeptide residue. *J Chem Soc Dalton Trans* :2945–2953
207. Casella L, Gullotti M, Monzani E, De Gioia L, Chillemi F (1991) Biomimetic oxidation catalysis by iron (III) deuteroporphyrin carrying a deca-L-alanine peptide chain. *Rend Fis Acc Lincei* 2:201–212
208. Casella L, Gullotti M, De Gioia L, Bartesaghi R, Chillemi F (1993) Haem-peptide complexes. Synthesis and stereoselective oxidations by deuterohaemin-L-phenylalanyl-poly-L-alanine complexes. *J Chem Soc Dalton Trans* :2233–2239
209. Casella L, Monzani E, Fantucci P et al (1996) Axial imidazole distortion effects on the catalytic and binding properties of chelated deuterohemin complexes. *Inorg Chem* 35:439–444
210. Monzani E, Linati L, Casella L et al (1998) Synthesis, characterization and stereoselective catalytic oxidations of chelated deuterohaemin-glycyl-L-histidine complexes. *Inorg Chim Acta* 273:339–345
211. Ryabova ES, Dikiy A, Hesslein AE et al (2004) Preparation and reactivity studies of synthetic microperoxidases containing b-type heme. *J Biol Inorg Chem* 9:385–395
212. Casella L, De Gioia L, Frontoso Silvestri G (2000) Covalently modified microperoxidases as heme-peptide models for peroxidases. *J Inorg Biochem* 79:31–40
213. Dallacosta C, Monzani E, Casella L (2003) Reactivity study on microperoxidase-8. *J Biol Inorg Chem* 8:770–776
214. Dallacosta C, Casella L, Monzani E (2004) Modified microperoxidases exhibit different reactivity towards phenolic substrates. *ChemBioChem* 5:1692–1699
215. Lee WA, Yuan LC, Bruice TC (1988) Oxygen transfer from percarboxylic acids and alkyl hydroperoxides to (meso-tetraphenylporphinato)iron(III) and -chromium(III). *J Am Chem Soc* 110:4277–4283
216. Beck MJ, Gopinath E, Bruice TC (1993) Influence of nitrogen base ligation on the rate of reaction of [5, 10, 15, 20-tetrakis(2, 6-dimethyl-3-sulfonatophenyl)porphinato]iron(III) hydrate with tert-BuOOH in aqueous solution. *J Am Chem Soc* 115:21–29

217. Traylor TG, Popovitz-Biro R (1988) Hydrogen bonding to the proximal imidazole in heme protein model compounds: effects upon oxygen binding and peroxidase activity. *J Am Chem Soc* 110:239–243
218. Traylor TG, Ciccone JP (1989) Mechanism of reactions of hydrogen peroxide and hydroperoxides with iron(III) porphyrins. Effects of hydroperoxide structure on kinetics. *J Am Chem Soc* 111:8413–8420
219. Traylor TG, Xu F (1990) Mechanisms of reactions of iron(III) porphyrins with hydrogen peroxide and hydroperoxides: solvent and solvent isotope effects. *J Am Chem Soc* 112:178–186
220. Kadish KM, Smith KM, Guillard R (eds) (2003) *The porphyrin handbook. Biochemistry and binding activation of small molecules.* Academic Press, New York
221. Tsou CL (1951) Cytochrome *c* modified by digestion with proteolytic enzymes. *Biochem J* 49:362–367
222. Aron J, Baldwin DA, Marques HM, Pratt JM, Adams PA (1986) Hemes and hemoproteins. 1: Preparation and analysis of the heme-containing octapeptide (microperoxidase-8) and identification of the monomeric form in aqueous solution. *J Inorg Biochem* 27:227–243
223. Baldwin DA, Marques HM, Pratt JM (1986) Hemes and hemoproteins, 2: The pH-dependent equilibria of microperoxidase-8 and characterization of the coordination sphere of Fe(III). *J Inorg Biochem* 27:245–254
224. Modi S, Behere DV, Mitra S (1989) Binding of aromatic donor molecules to lactoperoxidase: proton NMR and optical difference spectroscopic studies. *Biochim Biophys Acta* 996: 214–225
225. Casella L, Gullotti M, Poli S et al (1991) Spectroscopic and binding studies on the stereoselective interaction of tyrosine with horseradish peroxidase and lactoperoxidase. *Biochem J* 279:245–250
226. Ortiz de Montellano PR (1992) Catalytic sites of hemoprotein peroxidases. *Annu Rev Pharmacol Toxicol* 32:89–107

Chapter 7

Grafting of Functional Molecules: Insights into Peroxidase-Derived Materials

Gibson S. Nyanhongo, Endry Nugroho Prasetyo, Tukayi Kudanga, and Georg Guebitz

Contents

7.1	Introduction	156
7.2	Production of Functional Polymers	157
7.2.1	Phenolic Resins	157
7.2.2	Cardanol	160
7.2.3	Poly(methyl methacrylate)	161
7.2.4	Acrylamide	161
7.2.5	Polystyrene	162
7.2.6	Conducting Polymers	162
7.2.7	Fluorescent Naphthol-Based Polymers	164
7.3	Surface Modification of Complex Polymers	165
7.3.1	Bonding Wood Fibers	165
7.3.2	Manufacturing of Medium Density Fiber boards	166
7.3.3	Modification of Thermomechanical Pulp	166
7.3.4	Textile Fibers	168
7.3.5	Hair Dyeing	169
7.3.6	Surface Modification of Polyphenylene-2,6-Benzobisthiazole Fibers	170
7.3.7	Biopolymer Cross-linking	171
7.4	Conclusions	172
	References	172

Abstract An insight into the progress made in applying heme peroxidases in grafting processes, starting from the production of simple resins to more complex polymers, is presented. The refinement of the different reaction conditions (solvents, concentrations of the reactants) and careful study of the reaction mechanisms have been instrumental in advancing enzymatic grafting processes. A number of processes described here show how peroxidase mediated catalysis could provide a new strategy as an alternative to conventional energy intensive procedures mediated by chemical catalysts.

7.1 Introduction

The importance of heme peroxidases in polymer chemistry is based on their ability to oxidize a variety of phenolic molecules thereby generating reactive species (phenoxy radicals). These reactive species provide ideal sites for cross-linking (coupling) desired functional molecules leading to polymerization reactions and consequently the formation of new materials. In this chapter, grafting is described as a process by which functional molecules (for example, antimicrobials and hydrophobic molecules) are enzymatically coupled to a natural or synthetic polymer; or a process by which surface activation of polymers by peroxidases and laccases is used for further binding. Horseradish peroxidase (HRP) was the first peroxidase to be employed for oxidative polymerization studies during the 1980s [1, 2]. However, the pioneering works of Dordick and coworkers during the early 1990s heralded the beginning of special interests in the application of peroxidases for grafting. Among the increasingly explored peroxidases to date are the plant [HRP and soybean peroxidases (SBP)] and fungal peroxidases (lignin peroxidases, manganese peroxidases (MnP), and versatile peroxidases). Although fungi are increasingly being regarded as new alternative sources of peroxidase for industrial purposes, plant peroxidases have played a pivotal role in our understanding of grafting functional molecules. The general scheme in enzymatic grafting of functional molecules consists of two major steps, the first is radical generation by peroxidases and the second, the coupling of oxidized functional molecules onto the target polymer (Fig. 7.1). Peroxidase alone or in the presence of electron mediators (molecules which when oxidized form highly reactive oxidizing species) oxidizes the functional molecules and/or target template polymer. The generated reactive species (functional molecules and target template molecules) cross-link resulting in the establishment of covalent bonds. The cross-linking can result in the formation of homopolymers (Fig. 7.1a), heteropolymers (Fig. 7.1b), cross-linking of two different or similar polymers (Fig. 7.1c), or coupling of small molecules to polymer surfaces (Fig. 7.1d).

Although this chapter reviews the main applications of heme peroxidases in grafting functional molecules onto natural and synthetic polymers based on the above scheme, a few examples using laccases, which also catalyze similar reactions, have also been incorporated where such similar application is lacking with peroxidases and could potentially be applied in the future. Laccases (benzenediol: oxygen oxidoreductases, EC.1.10.3.2) are multicopper containing enzymes that catalyze the oxidation of various aromatic compounds, especially phenolic compounds, concomitantly reducing molecular oxygen to water [3]. There has been great interest in the application of laccases in industry ranging from effluent treatment, food processing, diagnostic, pulp and paper industry, and the textile industry to medical and personal care applications [4]. Both enzymes are being extensively explored for functionalization of a wide variety of structurally and chemically diverse substrates, as summarized in Fig. 7.2 and later described in the chapter, with varying degrees of success.

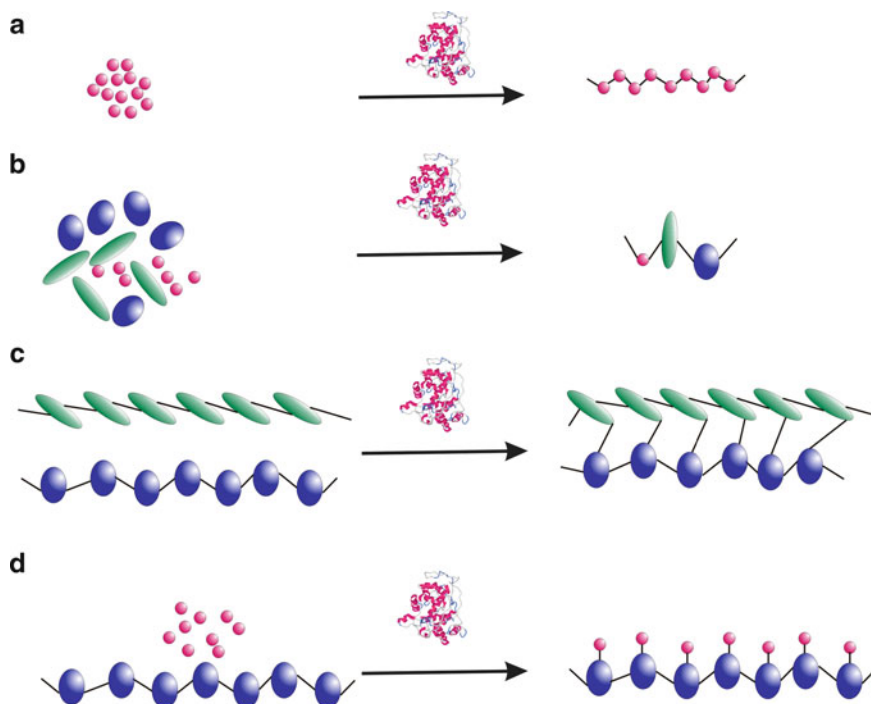


Fig. 7.1 General scheme representing peroxidase-mediated reactions: (a) homopolymerization, (b) heteromolecular coupling, (c) cross-linking, and (d) surface functionalization

7.2 Production of Functional Polymers

Enzymatic development of functional polymers for application as coating or adhesive materials, for example, has attracted much scientific interest over the years. A number of natural products ranging from plant to animal polymers are being actively investigated. In this section, the ability of heme peroxidases to mediate the production of such polymers is revised.

7.2.1 Phenolic Resins

The first demonstration of the industrial importance of heme peroxidases in grafting applications has been the development of hybrid resins from renewable sources to replace phenol–formaldehyde based resins. Phenolic resins are widely used in surface coatings, adhesives, laminates, molding, friction materials, abrasives, flame retardants, carbon membranes, glass fiber laminates, fiberboards, and protein-based wood adhesives, [5]. Table 7.1 and Fig. 7.2 summarize some of the

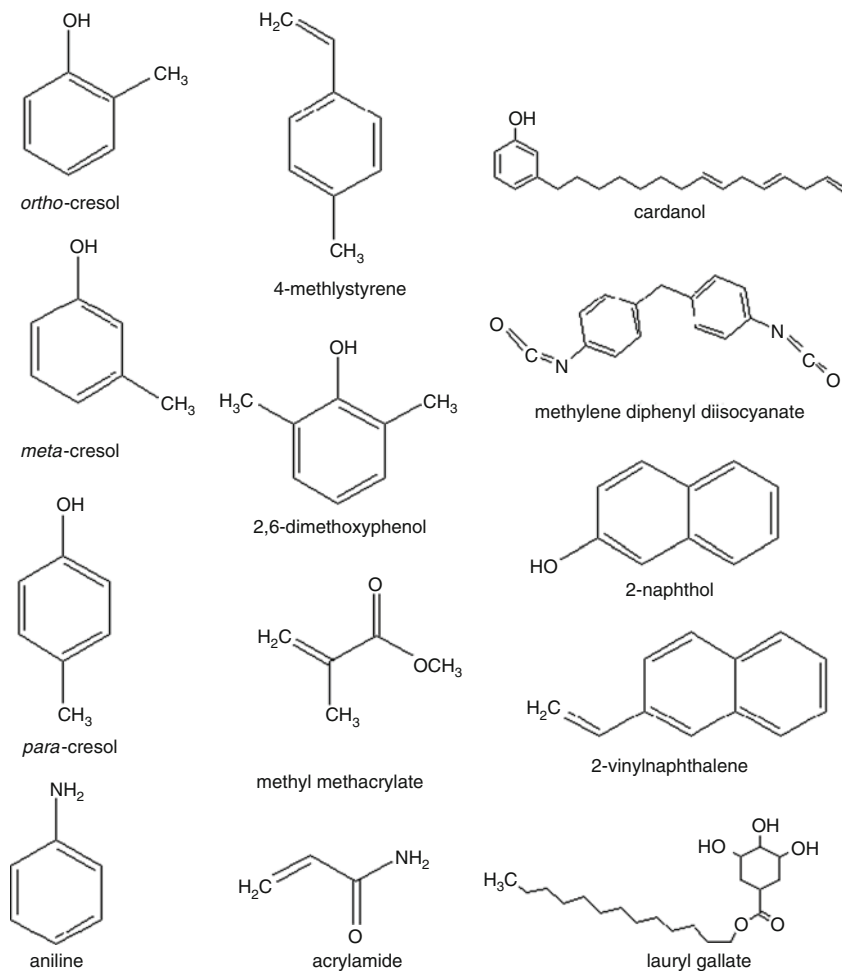


Fig. 7.2 A summary of some of the molecules used during polymer functionalization

Table 7.1 Some of the substrates used for peroxidase-mediated formation of phenolic resins

Substrates	References
Lignin + cresol	[6–8]
Kraft lignin + phenols	[9]
Milled wood lignin	[10]
2,6-Dimethylphenol	[11]
Lignocatechol	[12, 13]
Lignocresol	[5]
Brown rotted wood	[14]
Cardanol	[15–20]
Anarcardic acid	[21]

substrates investigated. Dordick and coworkers in the 1990s not only demonstrated the ability of HRP to mediate polymerization of phenolics but also the ability to incorporate phenols into lignin leading to the formation of polymers with great potential as phenolic resins.

For example, enzymatically prepared poly(*p*-phenylphenol) and poly(*p*-cresol) (Fig. 7.2) were shown to have high melting points. In addition, the poly(*p*-phenylphenol) showed much higher electrical conductivity than phenol–formaldehyde resins. These materials have potential as coating materials. Since that time the ability of HRP to oxidatively incorporate cresol (Fig. 7.2) into lignin has renewed interest in using lignin as a raw material for grafting functional molecules to obtain new functional polymers. Lignin is the second most abundant polymer on earth, constituting 30% of nonfossil organic carbon, and is currently under-utilized [22]. Approximately 2% of the lignin from the pulp and paper industry is used commercially (1 million tons/year liginosulphonates and less than 100,000 tons/year of kraft lignins) [23–25]. Lignin is currently used in polymer blends for mortar, construction systems, adhesives, biodegradable plastics, polyurethane copolymers, paints, dispersants in dyes, in pesticides, and printed circuit boards [25–30]. Although lignin has been suggested as a possible replacement for various petroleum-derived chemicals, its maximum exploitation has been hampered by its huge physico-chemical heterogeneity. However, the discovery of peroxidase and laccases which have the ability to modify lignin and create new functional polymers with good chemoselective conversion, justifies the recent progress in new lignin applications. Studies have shown that *p*- and *m*-substituted aromatic lignins can be enzymatically polymerized by peroxidases, yielding novel functional polymers [31]. It has also been shown that the copolymerization reaction did not occur with acetylated lignin or methylated lignin (i.e., with phenolic groups blocked), indicating the necessity for the peroxidase to form phenoxy radicals with both the *p*-cresol and the lignin. For example, Blinkovsky and Dordick [9] demonstrated the ability of HRP to catalyze the copolymerization of phenols with kraft lignin in aqueous–organic solvent mixtures while Grönqvist et al. [10] also showed the ability of HRP to oxidatively polymerize milled wood lignin. Thermal analysis showed that the copolymerization products resulted in a material with markedly lower glass transition temperatures and higher (and more uniform) curing exotherms. Liu et al. [6] successfully copolymerized lignin and cresol, in a reaction catalyzed by a peroxidase using a reversed micellar system. The copolymer showed quite different properties compared to native lignin, including lower glass transition temperature. Liu et al. [8] also managed to control molecular weight of the lignin/cresol polymer by adjusting the concentration of surfactant, enzyme, cresol, lignin, and the ratio of alcohol to hydrocarbon in the organic phase. The resulting polymer had good thermoset properties and could be easily recovered after precipitation. In yet another demonstration of the remarkable flexibility of enzymes, HRP-catalyzed polymerization of 2,6-dimethylphenol (Fig. 7.2) led to a polymer consisting of exclusively oxy-1,4-phenylene units [11]. Poly(oxy-2,6-dimethyl-1,4-phenylene) (polyphenylene oxide) is widely used as a high-performance engineering plastic, since the polymer has excellent chemical and physical properties.

Using SBP, Ikeda et al. [11] successfully produced polyphenol resins that could very well replace conventionally polymerized novolac and resins, without the involvement of formaldehyde. Further, the same group demonstrated the ability of laccase to mediate the synthesis of polyphenols with very similar structure to those produced by both HRP and SBP. Peroxidase-mediated polymerization of lignocatechol and lignocresol was shown to produce phenolic resins that have potential application in adhesives, as bonding agents and engineering materials [12, 13]. Recently, a highly thermostable polymer with good thermosetting properties was produced using SBP in ionic liquids [5]. Treatment of brown rot fungus-decayed wood with sodium borohydride followed by mixing with polyethylenimine resulted in a formaldehyde-free, strong, and water-resistant wood adhesive [14]. Brown rot fungi preferentially degrade cellulose and hemicelluloses in wood and in the process lignin is oxidized and demethylated, resulting in oxidized *ortho*-quinone structures [14].

7.2.2 *Cardanol*

Cardanol, a phenol derivative having a C15 unsaturated alkyl chain with 1–3 double bonds at its *meta* position (Fig. 7.2), is obtained by thermal distillation of cashew nut shell liquid [15]. Cardanol is an excellent raw material for the preparation of high grade insulating varnishes, paints, enamels, alcohol soluble resins, laminating resins, and rubber compounding. Cardanol-based resins possess outstanding resistance to softening action of mineral oils and high resistance to acids and alkaline conditions, antimicrobial properties, termite, and insect resistance. Cardanol-phenol resins were developed in the 1920s by Harvey and found use in vehicle brakes after it was observed that they had a coefficient of friction less sensitive to temperature changes than phenol-formaldehyde resins. In an effort to develop eco-friendly methods for processing cardanol, Kim et al. [16] successfully used SBP to catalyze the oxidative polymerization of cardanol yielding 62% polycardanol over 6 h. Although HRP alone was not able to oxidatively polymerize cardanol, polymerization was possible after addition of either *N*-ethyl phenothiazine or phenothiazine-10-propionic acid as a redox mediator [20]. The final hardness of the cross-linked polycardanol film exceeded 9 H scale as pencil scratch hardness, which displayed high potential as a commercial coating material and also showed excellent antibiofouling activity. Recently, by incorporating epoxide, Kim et al. [18] synthesized an epoxide-containing polycardanol in the presence of peroxidase, resulting in transparent polymeric films with high gloss surface within 3 h, reducing the time by 50% when compared to previous studies. The short curing time and increase in the hardness as compared to polycardanol were attributed to the presence of epoxide in the polymerized cardanol. Recently fungal peroxidase from *Coprinus cinereus* were successfully used to produce polycardanol with remarkable properties [17, 19]. The demonstration of the ability of fungal peroxidase to oxidize cardanol is quite interesting since the biotechnological production

techniques are improving fast in this area. Anacardic acid, a mixture of several closely related organic compounds consisting of salicylic acid substituted with an alkyl chain that has 15 or 17 carbon atoms, was enzymatically polymerized using SBP resulting in cross-linked polyanacardic acid on a solid surface to form a permanent natural coating polymer [21].

7.2.3 *Poly(methyl methacrylate)*

A novel free radical polymerization of methyl methacrylate (MMA) (Fig. 7.2) catalyzed by HRP was developed by Kalra and Gross [32]. Poly(methyl methacrylate) (PMMA) is a clear, colorless polymer used extensively for the production of scratch resistance optical products, plastics, and PVCs. Traditionally, PMMA is produced under extreme conditions ($\geq 70^\circ\text{C}$) using toxic metals. However, HRP catalyzed production of PMMA was conducted at ambient temperatures in the presence of low concentrations of hydrogen peroxide and 2,4-pentanedione, in a mixture of water and dioxane. The products were found to have syndiotactic diad fractions ranging from 0.82 to 0.87 and T_g values of about 130°C [32]. In another interesting development, a vitamin C functionalized PMMA was developed [33]. The vitamin C functionalized PMMA fully scavenged 2,2-diphenyl-1-picryl hydrazyl free radicals. This antioxidant functionalized PMMA has implications for consumer-related applications like foods, pharmaceuticals, and personal care products. Peroxidase mediated studies have also been extended to developing highly reactive polymers based on the polymerization of 2-(4-hydroxyphenyl)ethyl methacrylate with two functional groups, methacryl and phenolic groups [34]. Chemoselective polymerization of *m*-ethynylphenol, possessing two reactive groups (phenol and acetylene moieties), was successfully carried out in methanol [35]. The product is a good reactive starting polymer consisting exclusively of diacetylene derivative products. In a similar approach a highly reactive polymer product was obtained through the treatment of technical lignins (lignosulphonates, kraft, and acetosolv) that can be further reacted with other polymers [36]. This method allows for the creation of coating materials with functional purposes or designing protective paintings and can be applied in the development of composite materials, for example, in water proof papers and cardboards or even thermoplastics [36].

7.2.4 *Acrylamide*

Enzymatic polymerization of acrylamide has gained a lot of interest among researchers. This is because acrylamide (Fig. 7.2) is a precursor used in the synthesis of polyacrylamides used as water-soluble thickeners with applications in gel electrophoresis (SDS-PAGE), papermaking, synthesis of dyes, and the manufacture of permanent press fabrics. HRP-mediated free radical polymerization

of acrylamide in water was reported by Emery et al. [37], Lalot et al. [38], and Teixeira et al. [39]. These polymerizations took place when β -diketones such as 5,5-dimethyl-1,3-cyclohexanedione and 2,4-pentanedione were used as initiators. MnP produced by the basidiomycete *Bjerkandera adusta* and HRP were also shown to effectively polymerize acrylamide in the presence of 2,4-pentanedione [40]. The molecular weight of the polymer was 155,000 for MnP and 67,500 for HRP – significantly higher than 13,000 obtained by chemical synthesis using Fe-ammonium persulfate. Lalot and coworkers [37, 38] obtained a polyacrylamide with good thermal properties that could be used as a thermoplastic resin in water and at room temperature, although longer incubation times were necessary.

7.2.5 *Polystyrene*

In another show of versatile approaches in applying peroxidases, styrene was successfully polymerized. Polystyrene is a liquid hydrocarbon that is commercially manufactured through chemical means. Polystyrene is widely used commercially, for example, as packaging material, injection molded parts, UV screening agents, in disposable cutlery, and CD and DVD cases. The use of peroxidases reduces the need for heavy metals, and the reaction is carried out at ambient temperatures that require less specialty equipment [41]. Molecular weight and yield of polystyrene were shown to be influenced by solvent, concentration of hydrogen peroxide, and initiator. This enzymatic strategy was also successfully used for the synthesis of polymers from styrene derivatives, 4-methylstyrene, and 2-vinylnaphthalene (Fig. 7.2), the latter resulting in a >90% yield of polymer [41]. Recently Shan et al. [42] also reported the production of stable polymer colloids and nanospheres in emulsion.

7.2.6 *Conducting Polymers*

The production of conducting polymers is of immense industrial interest because of their wide range of applications including electronic equipment, photovoltaic cells, plastic batteries, polymer light-emitting diodes, and optical displays, [43, 44]. Polyaniline is one such extensively investigated conducting polymer, derived from a readily available monomer [45–47]. Currently, polyaniline is synthesized by oxidizing aniline (Fig. 7.2) under strongly acidic conditions and low temperature, using ammonium persulfate as the initiator of radical polymerization [48]. However, since the 1990s, peroxidase-mediated polymerization of aniline has attracted great attention because it is carried out under mild conditions. Tremendous progress has been made since then in refining the reaction conditions. HRP has been used in the synthesis of polyaniline in aqueous organic solvents [49, 50] although it showed low activity toward aniline and low stability at pH below 4.5.

The HRP-catalyzed polymerizations were preferentially *ortho* and *para* directing, resulting in branched polymeric materials, which were intractable and had poor electrical properties. However, SBP-mediated synthesis of polyaniline at 1°C in either aqueous or partially organic solvents resulted in low branching and *ortho*-coupled polyaniline at pH higher than 3.0. SBP actually outperforms HRP in terms of stability and is now used in numerous biotechnological applications [51].

In order to minimize polymer branching and facilitate processing, a large number of experimental conditions have been investigated including solvent mixtures, use of templates, and organized reaction environments such as reversed micelles. Consequently, water-soluble polyanilines using a water soluble monomer analog of aniline have been successfully made [52, 53]. These materials must be converted to the conducting form by doping (protonation) under extreme acidic conditions. However, they still remain limited in their electrical and optical properties. Although the synthesis still requires strong oxidants and/or modified aniline monomers, subsequent doping and processing limitations have been minimized.

In an attempt to overcome the low infusible character and low solubility of aniline, dispersion polymerization of aniline was conducted in water-dispersible colloidal particles that can be cast as films or blended with other materials to prepare composites. HRP mediated polymerization of aniline in a mixture of phosphate buffer and organic solvent resulted in polyaniline composed of *ortho*-directed units and *para*-directed units. Increasing the pH or adopting an organic solvent with a high dielectric constant, enhanced the production of *ortho*-directed units [54]. These *ortho*-directed polyanilines were more thermally flexible and electrically conductive.

One of the great advancements in the enzymatic polymerization of aniline was the development of the template-assisted enzymatic polymerization approach [47]. This method uses an anionic polymeric template to promote the head-to-tail coupling of aniline radicals to obtain a water-soluble electrically conductive polyaniline. The template promotes *para*-directed, head-to-tail coupling of aniline radicals and a “local” environment where the pH and charge density near the template molecule is different from that of the bulk solution [50]. This polyanion-assisted polymerization allowed the enzymatic synthesis of water-soluble complexes of conducting polyaniline with well-defined structure at pH as high as 4.3 [50]. The template-assisted enzymatic polymerization of aniline was also performed in a two-phase system [55], yielding water-soluble polyelectrolyte complexes. The polymerization of aniline was carried out in aqueous buffer at pH 4.0 using the enzyme HRP as the biocatalyst in the presence of a poly(vinylphosphonic acid) (PVP) as the polyelectrolyte polyanion template. Under these conditions appropriate control of polymerization could be achieved to tune the water solubility and conductivity of the final PVP–polyaniline macromolecular complex [56]. The template-guided synthesis of polyaniline therefore provides a unique approach for the control of polymerization of aniline to an electroactive polymer under mild conditions. To overcome the problems of rapid inactivation of HRP at high temperatures and pH below 4, during synthesis of polyaniline, a peroxidase purified from the African palm oil tree, was successfully used [57] in aqueous

buffer at pH 3.5. Strong acid polyelectrolytes, such as sulfonated polystyrene, are the most favored because they provide a lower local pH environment that serves to both charge and preferentially align the aniline monomers through electrostatic and hydrophobic interactions promoting the desired head-to-tail coupling. A water-soluble, conducting poly(*o*-toluidine)/sulfonated polystyrene exhibiting moderate electrical conductivity was produced using HRP to polymerize *o*-toluidine at room temperature and pH 4.3 [58]. Interestingly, it was found that micelles formed from aggregating, strong acid surfactant molecules such as sodium dodecylbenzenesulfonic acid, also provide suitable local template environments that lead to the formation of conducting polyaniline. HRP-mediated polymerization of substituted and unsubstituted phenols and anilines using a template of a borate-containing electrolyte or lignin sulphonate resulted in a polymer–template complex that can be used in biological sensors, antistatic, and anticorrosive coatings, among other uses [59]. Although a lot of success has been achieved regarding peroxidase catalyzed polymerization of aniline using polyelectrolyte templates such as sulfonated polystyrene [47, 50, 58], poly(vinylphosphonic acid) [56], and deoxyribonucleic acid (DNA) [56, 60], the separation of the polyaniline from the polyanion is impeded by the high degree of complexation. To overcome this problem, template-free enzymatic preparation of polymer colloids [61] and in reverse, micelles has been recently explored [43, 62]. This has been employed to obtain polyaniline particles by using poly(vinyl methyl ether) and chitosan or poly(*N*-isopropylacrylamide) as stabilizer in partial organic media. The resulting polyaniline formed dispersed colloidal particles with physicochemical properties similar to those synthesized by chemical oxidation [51, 55]. Unlike the anionic polyelectrolyte used in the template-assisted approach, steric stabilizers used in dispersion polymerization are commonly nonionic; therefore they are adsorbed on the polyaniline particles in low amounts, and most of the stabilizer can be eliminated by cycles of centrifugation and redispersion.

7.2.7 *Fluorescent Naphthol-Based Polymers*

Fluorescent polymers have attracted considerable attention because of their applications in plastic scintillators, luminescent solar concentrators, high laser resistance materials, laser dyes, and fiber optic sensors. Many fluorescent dyes are known to contain segments obtained from 2-naphthol units. A fluorescent polymer of 2-naphthol (Fig. 7.2) was prepared using HRP in reversed micelles [63]. The poly(2-naphthol) exhibited fluorescence characteristic of naphthol moieties and a second reproducible and structured emission originating from a highly conjugated chromophore. Since the polymer was synthesized in microspherical morphology, it is assumed to be easy for dispersion during coating applications. Bodtke et al. [64] also reported the synthesis of azine pigments mediated by HRP oxidative coupling of 3-alkyl-2-hydrazono-4-thiazolines and α -naphthol.

7.3 Surface Modification of Complex Polymers

Imparting new functional properties or an esthetic look to complex polymers is a fast growing area where peroxidases are actively being pursued. Basically the polymer is either oxidized by the enzyme alone or in the presence of mediators followed by grafting as shown in the general scheme in Fig. 7.3. This results in increased binding either between polymers or with introduced functional molecules.

The industrial production of “Myco-wood” in the former German Democratic Republic (1958–1965) is one of the greatest demonstrations of the industrial potential of lignolytic enzymes (peroxidases and laccases) in the wood industry. The white-rot fungi *Pleurotus ostreatus* and *T. versicolor* [65] were used to treat beech wood leading to the reduction of the density and loosening of the structure of the wood. The fungi selectively degraded lignin thereby improving machinability and water sorption properties of the wood. The obtained “myco wood” was mostly used for production of pencils, rulers, drawing tables, and wooden forms used in the glass industry [65, 66]. Based on this observation, ligninolytic enzymes (peroxidases and laccases) have become increasingly popular for wood modification.

7.3.1 Bonding Wood Fibers

Bonding of timber and wood has a history which runs into several thousand years. Traditionally the bonding of timber and wood is achieved by adding petrochemical-based adhesives which form a resinous matrix in which the particles or fibers are bonded together by mechanical entanglement or covalent cross-linking. Attempts to use enzymes to mediate bonding in wood started in the mid 1960s. Later, the use of lignosulphonates oxidized by peroxidase or laccase as binders for the production of particle boards was reported by Nimz et al. [67, 68]. They successfully produced particle boards that surpassed the requirements of transverse tensile strength (DIN 52365 test) of 0.35 MPa specified by the European standard EN 312-4. Unfortunately, the particle boards swelled in water due to the sulphonate groups present in lignosulphonate, making them suitable for indoor use only. Recently a more efficient process to reduce swelling was developed by combining laccase-oxidized lignin-based adhesive with 1% methylene diphenyl diisocyanate (Fig. 7.2) resulting in particle boards with doubled tensile strength and reduced swelling [27, 69].

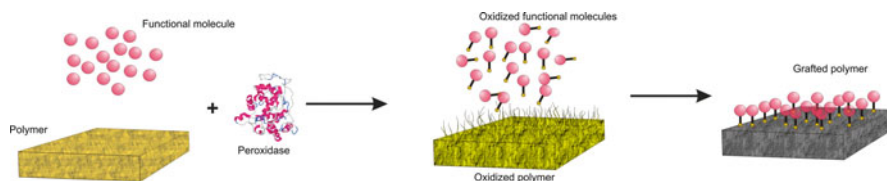


Fig. 7.3 Grafting of functional molecules – a general scheme

7.3.2 *Manufacturing of Medium Density Fiber boards*

Building on the knowledge gained with oxidative polymerization of lignin and the ability of peroxidases and/or laccases to oxidize lignin, a new strategy was developed to promote auto adhesion of lignin in wood without any additional gluing material during production of wood laminates, particle boards, and medium density fiber boards (MDF). HRP and laccase treatment of brown rotted wood produced laminates with relatively good shear strength although lower than those obtained with adhesives. Unfortunately the wood laminates swelled in water leading to delamination [70]. Forced-air-drying of MDF increased internal bond strength and reduced swelling in water. [71–74]. The enzymatic process involved oxidizing the lignin rich middle lamella exposed on the fiber surface of wood which promoted cross-linking of fibers during hot pressing of the boards. This treatment resulted in MDFs with comparable properties to traditional MDF. Both laccase and peroxidase-bonded MDF boards achieved the European standard CIN DIN 622-5. Although peroxidases gave the same results as boards treated by laccase, the requirement of hydrogen peroxide and its rapid degradation constituted its main drawback [75]. Nevertheless, these studies demonstrated the possibility of producing MDF without addition of resins. MDF from rape-straw fibers incubated with brown- and white-rot fungi in whole culture fermentation broth or wastewater have been shown to have twice the strength of MDF obtained using purified *T. versicolor* laccase [74, 76]. This observation demonstrates that refining the production process to reduce costs can give this technology competitive advantage over traditional processes.

7.3.3 *Modification of Thermomechanical Pulp*

The industrial application potential of peroxidases and laccases has been extensively studied in the pulp and paper industry. The effects of modifying the fiber chemistry of lignocellulosic pulps have been well established over the past decades. During the 1980s several research groups and patents demonstrated distinct changes in fiber properties after grafting phenolic acid groups onto pulp fibers, resulting in increased internal bond strength and hydrophobicity. Yamaguchi et al. [77, 78] utilized laccase to polymerize various phenolic compounds to form dehydrogenative polymers which were subsequently coupled to thermomechanical pulp (TMP) using peroxidase for the formation of paperboard. Incorporation of phenolics (vanillic acid, catechol, mimosa tannin, and tannic acid) from renewable sources as cross-linking agent in the presence of peroxidase from shoots of bamboo or laccase from *T. versicolor*, enabled production of TMP [77–79]. The produced TMPs had good tensile and ply-bond strength comparable to hot-pressed TMP–phenol paper boards and significantly higher than those produced in the absence of phenols. Pretreatment of TMP fibers with laccase further increased the ply-bond strength.

Pretreatment of wood chips with white-rot fungus *Trametes hirsuta* and the brown-rot *Gloeophyllum trabeum* [74, 80], *Coniophora puteana*, and *Fomitopsis pinicola* [81] reduced the required refining energy by 40% in TMP as compared with untreated wood chips. In addition, the pretreated TMPs had 3.5-times higher bending strength, 3-times higher modulus of elasticity, and at least 60% reduction in thickness swelling in water (24 h), when compared to boards pressed from untreated fibers [74, 81].

In similar studies, recent trends suggest there is much innovative research in developing functional packaging materials with antimicrobial properties aimed at reducing the need to include antimicrobial agents in food [82, 83]. Food packaging materials are mainly intended to prevent the deterioration of food, prolong shelf life of packed goods, and guarantee consumer safety. However, enzymatic grafting of molecules with antimicrobial activities is quite recent and there are no reports available for peroxidases. Nevertheless, laccase mediated grafting of phenols possessing antimicrobial activities onto unbleached kraft liner fibers was reported by Elegir et al. [84]. The paper sheets grafted with different phenolics showed greater efficacy against Gram positive and Gram negative bacteria than paper sheets treated only with monomeric phenol derivatives. Coupling or grafting reactions were negatively affected by quenching of radicals as the oxidized molecule stabilizes by resonance; a previous study reported a loss of up to 90% of radicals within a few hours in laccase-treated TMP [85]. However, coupling phenolic amines to prevent the loss of radicals through resonance increased subsequent coupling of fungicides onto amine functionalized wood using *T. hirsuta* laccase [86]. In this study, it was proposed that phenolic amines act as anchor groups creating a stable reactive surface which counteracts negative effects of radical quenching during the coupling/grafting reactions as illustrated in Fig. 7.4 [87]. This is another possible area where biocatalysis based on peroxidases could be explored.

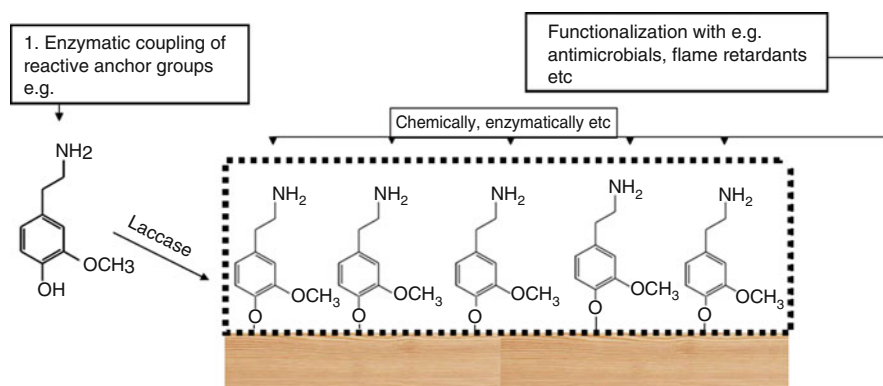


Fig. 7.4 Attachment of anchor groups (i.e., phenolic amines) to lignin moieties of wood for further functionalization

7.3.4 Textile Fibers

Two seemingly contradictory but different approaches have recently been established in applying peroxidases in the textile industry. These approaches are namely; peroxidase-mediated coupling of functional molecules on textile fibers and peroxidase-mediated removal of back stains during laundry. Peroxidase-mediated oxidation of some phenolic compounds results in colored products. Perhaps the first and most notable attractive activity of heme peroxidases which even led to their discovery was the observation by Planche in 1810 of their ability to catalyze the formation of a beautiful blue color when a tincture of gaiac resin came into contact with fresh horseradish root, long before the enzyme was known. And with respect to laccases, the more than 6,000-years-old Chinese lacquer artwork demonstrates the use of this enzyme in producing colorful artworks [27]. However, it was not until recently that this principle has been applied to color textile fibers. Wool padded with phenolic compounds (hydroquinones, dopamine, guaiacol, catechol, and ferulic acid) and incubated with HRP or laccases resulted in fibers with different color shades [88]. Mordant with chromium compounds or heating under acid conditions enabled fixation of dyes on wool fibers resulting in colored wool. The recent coating of wool with lauryl gallate (Fig. 7.2) mediated by a similar enzyme (laccase) resulted in a multifunctional textile material with antioxidant, antibacterial, and water repellent properties [89]. Similarly, enzymatic dyeing of flax was demonstrated as shown in Fig. 7.5 [90].

A German scientist, Otto Röhm, was the first to patent the use of enzymes in laundry in 1913 [91] but it was not until 1930 that the use of pancreatic enzymes in presoak solutions became popular in the detergent industry. However the application of peroxidases in laundry to prevent back staining is very recent. A peroxidase-based system for the inhibition of dye transfer during washing with laundry



Fig. 7.5 Enzymatically dyed flax samples (adopted with modifications from Kim et al 2008) [90]

detergents was developed by Conrad et al. [92]. The system uses either *Arthromyces ramosus* peroxidase (ARP) or *Coprinus cinereus* peroxidase (CiP). Both enzymes have been selected as the best catalyst for this system on the basis of their excellent catalytic properties, stability, and commercially viable productivity [93] and are now considered alternative sources of peroxidase for industrial purposes. The mechanisms of dye-transfer inhibition involve oxidation and decolorization of released dyes. To enhance the dye decolorization ability of the enzymes, phenothiazine-10-propionic acid is used as a mediator. The peroxidases oxidize phenothiazine-10-propionic acid to a highly reactive species responsible for oxidizing and decolorizing dyes in solution. This dye-transfer inhibition system is toxicologically and ecologically safe at the applied levels. Until now, a nonenzymatic method has been employed to prevent dye transfer during washing using synthetic polymers, such as poly(1-vinyl-2-pyrrolidone), which are thought to complex the dye molecules in solution. A comparison of the enzymatic and nonenzymatic dye-transfer inhibition systems showed that the enzymatic method is, in many cases, more effective than the nonenzymatic one [91]. However, comparing peroxidases with laccases, there are increasing reports applying the latter for textile fiber modification as evidenced by recent works of Tzanov et al. [94], Hadzhiyska et al. [95], Calafell et al. [96], Schroeder et al. [97], and Kim et al. [90], among others. Novozyme (Novo Nordisk, Denmark) launched a new industrial application of laccase for bleaching in denim jeans (DeniLite®) in 1996. Also, in 2001 the company Zytex (Zytex Pvt. Ltd., Mumbai, India) developed a formulation based on laccase capable of degrading indigo in a very specific way [98].

7.3.5 Hair Dyeing

Another interesting application of peroxidases is in hair dyeing. Traditional hair dyeing processes are based on the oxidative polymerization of dye precursors (phenols or aminophenols, and couplers) [99]. Hydrogen peroxide not only initiates the polymerization reaction of dye precursors but also bleaches the natural hair pigment melanin. The hair changes from darker to lighter colors and the color of the polymerized dye precursors is not shifted by the natural hair color. The general stages involved in either hair dyeing or chemical dyeing processes are summarized in Fig. 7.6. The concentrations of hydrogen peroxide needed for oxidation of dye precursors are in the range of 3% in the final application formulation. Special bleaching products contain up to 6% hydrogen peroxide to achieve bright blond shades [100]. These concentrations, when applied repeatedly, can cause hair damage. To achieve a gentler dyeing and milder oxidation process, enzymes have been proposed as better options. Since the 1960s a number of patents have been filed, claiming the application of several oxidative enzymes such as oxidases, peroxidases, and tyrosinases as substitutes for hydrogen peroxide to give a milder hair coloring process [100]. However, to our knowledge, no enzymatic hair dyeing product has appeared on the market to date. Nevertheless, recent studies are

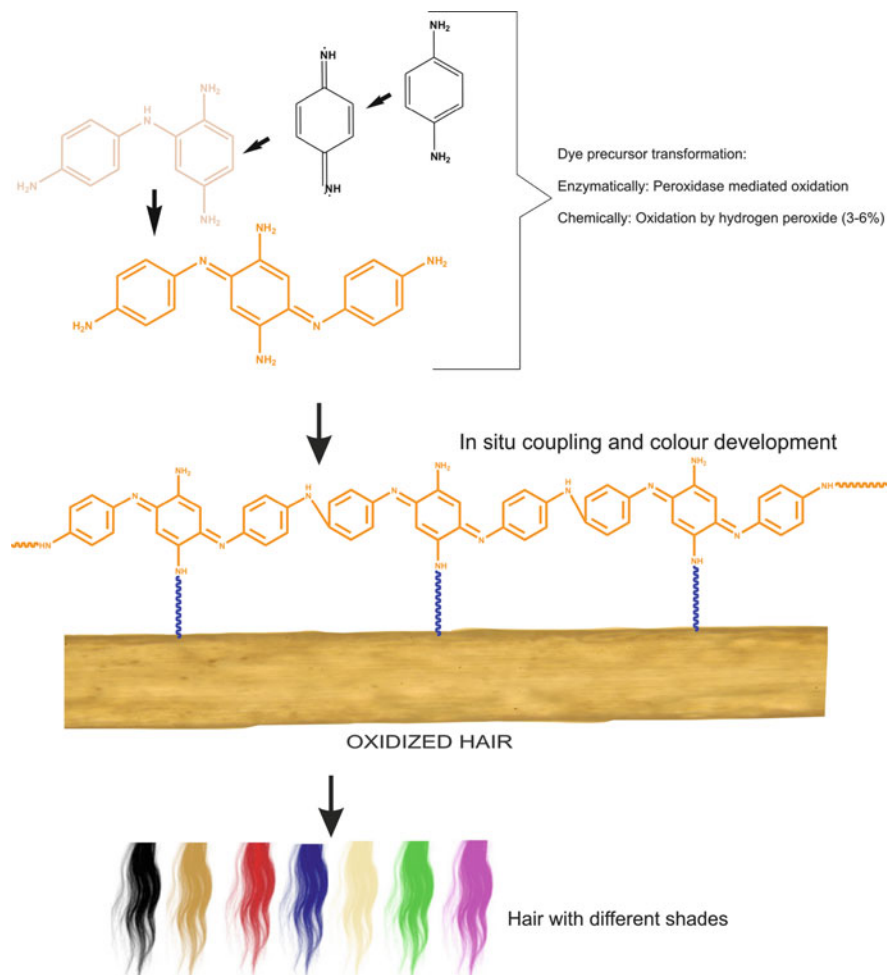


Fig. 7.6 Enzymatic and chemical hair dyeing processes

encouraging as they have shown that SBP generates more potent reactive species which are able to oxidize dye precursors at a significantly lower concentration than hydrogen peroxide itself [100].

7.3.6 Surface Modification of Polyphenylene-2,6-Benzobisthiazole Fibers

Increasing applications of oxidoreductases for modifying surface properties of synthetic polymers have been reported. A good example is surface modification

of polyphenylene-2,6-benzobisthiazole (PBO) fibers [101]. PBO fibers have been widely used since the mid twentieth century in aerospace industries and civil industries because of their excellent properties such as strength, chemical and fire resistance, light weight, and toughness [102]. Most of the conventional methods used to modify the fiber surface require strong chemical agents.

However, the surfaces of PBO fibers were modified by HRP resulting in increased hydrophilicity and facilitating the incorporation of glycol. In another interesting development, HRP was able to activate surface molecules of Kevlar fibers [103]. Kevlar fibers are organic, *para*-aramid man-made fibers which combine high strength and light weight with comfort and protection. This material is five times stronger than steel on an equal weight basis. In addition, it has high tensile strength at low weight, structural rigidity, toughness, and high resistance to chemicals and fire. HRP-mediated oxidation of the Kevlar fiber allowed the incorporation of acrylamide [103]. Surface activation mediated by HRP also enabled coupling of acrylamide onto high-density polyethylene (HDPE) leading to increased hydrophilicity and increased adsorption of water-soluble dyes [104].

7.3.7 *Biopolymer Cross-linking*

Peroxidase-mediated cross-linking of proteins results in covalent bond formation between tyrosine, cysteine, and lysine residues as demonstrated by many researchers and has been reviewed by Matheis and Whitaker [105, 106], Matheis and Whitaker [107], and Feeney and Whitaker [108]. Peroxidase-catalyzed efficient cross-linking of protein has a great potential in food baking industry because it improves the physicochemical and functional properties of food materials. A patent has been filed in relation to *in situ* cross linking of proteins, including collagen, using HRP to form biocompatible semisolid gels. These materials can be used as wound sealants, delivery vehicles, or as binding agents in food product applications [109]. Using HRP, Vacoud et al. [110] demonstrated the possibility of functionalizing polysaccharide materials by grafting a phenolic substrate (dodecyl gallate) onto chitosan. Recently, the formation of several polysaccharide-based hydrogels by an HRP-catalyzed enzymatic reaction has been reported. Kurisawa et al. [111] and Jin et al. [112] made hyaluronic acid and dextran, respectively, with Ph-OH groups and formed gels using the HRP-catalyzed oxidative reaction. The polysaccharide derivatives were synthesized by conjugation of the polysaccharides with tyramine. Recently, Ogushi et al. [113, 114] synthesized carboxymethylcellulose derivatives that are cross-linkable by the same enzymatic reaction. These polysaccharide-based hydrogels have great potential for biomedical applications, such as tissue engineering and wound healing, because of the biocompatibility of the polysaccharides.

7.4 Conclusions

We provided an overview covering the progress made in peroxidase-mediated grafting, starting from simple resins to more complex polymers, both natural and synthetic, leading to the production of materials with new properties. The refinement of the different reaction conditions (solvents, concentrations of the reactants namely monomer, enzyme, hydrogen peroxide) have been shown to influence the resulting product in terms of yield, molecular weight, and structure of the resulting polymers. A number of processes described here show how peroxidase-mediated catalysis provides a new strategy which, otherwise, would be very difficult to produce by conventional chemical catalysts. Peroxidase-mediated grafting is conducted under mild conditions without toxic reagents. Although these studies clearly demonstrate the potential applications of peroxidases at laboratory scale, commercial processes based on these enzymes have been largely confined to the diagnostic area. The first hurdle which has to be resolved to scale-up peroxidase-catalyzed processes to industrial level is the high price of the enzyme. The approach of using a bienzymatic system where glucose oxidase generate hydrogen peroxide *in situ* in the presence of peroxidase [115], could offer a possible alternative. Secondly, the fact that the hydrogen peroxide degrades rapidly at elevated temperatures also limits the application of peroxidases to processes which operate at relatively low temperature. If these challenges are not overcome, laccases will continue to be considered where peroxidases could be applied. Indeed in most of the work in textile industry, laccases have become enzymes of choice [116]. During the 1980s and early 1990s, research mainly focused on peroxidases which were thought to be key enzymes for lignin degradation. However, the difficulties associated with the fast decay of hydrogen peroxide and the inactivation of peroxidases at high hydrogen peroxide concentrations, have turned research emphasis to the use of laccases. Laccases only need O₂ as electron acceptor and are produced easily in higher amounts, but the higher redox potential of heme peroxidases as compared to laccases still favors their industrial application. Laccases from white-rot fungi can be readily purchased in large quantities for commercial applications from Novozyme (Denmark). Nevertheless, current research indicates that novel sources of fungal peroxidases are being discovered, and molecular biology approaches to improve production, activity, and stability of peroxidases are encouraging.

Acknowledgments Acknowledgment for support of this work is made to Austrian Academic Exchange Service (ÖAD) and European Union Biorenew Project [Sixth Framework Programme (FP6-2004-NMP-NI-4)].

References

1. Dordick JS (1987) Production of phenolic polymers catalyzed by horseradish peroxidase in organic solvents. Proc Mater Biotechnol Symp 225–239
2. Schnitzer M, Barr M, Hartenstein R (1984) Kinetics and characteristics of humic acids produced from simple phenols. Soil Biol Biochem 16:371–376

3. Nyanhongo GS, Schroeder M, Steiner W et al (2005) Biodegradation of 2, 4, 6-trinitrotoluene (TNT): an enzymatic perspective. *Biocatal Biotransform* 23:53–69
4. Nyanhongo GS, Gübitz GM, Sukyai P et al (2007) Oxidoreductases from *Trametes* spp. in biotechnology: A wealth of catalytic activity. *Food Technol Biotechnol* 43:248–266
5. Eker B, Zagorevski D, Zhu G et al (2009) Enzymatic polymerization of phenols in room-temperature ionic liquids. *J Mol Catal B Enzym* 59:177–184
6. Liu J, Yuan W, Lo T (1999) Copolymerization of lignin with cresol catalyzed by peroxidase in reversed micellar systems. *EJB Elect J Biotechnol* 2:82–87
7. Popp JL, Kirk TK, Dordick JS (1991) Incorporation of p-cresol into lignins via peroxidase-catalysed copolymerization in nonaqueous media. *Enzyme Microb Technol* 13:964–968
8. Liu J, Yang F, Xian M et al (2001) Molecular weight and distribution of the copolymer of lignin/phenol in the copolymerization catalyzed by peroxidase. *Macromol Chem Phys* 202:840–848
9. Blinkovsky AM, Dordick JS (1993) Peroxidase-catalyzed synthesis of lignin-phenol copolymers. *J Polym Sci A Polym Chem* 31:1839–1846
10. Grönqvist S, Viikari L, Orlandi M et al (2005) Oxidation of milled wood lignin with laccase, tyrosinase and horseradish peroxidase. *Appl Microbiol Biotechnol* 67:489–494
11. Ikeda R, Sugihara J, Uyama H et al (1996) Enzymatic oxidative polymerization of 2, 6-dimethylphenol. *Macromolecules* 29:8702–8705
12. Xia Z, Yoshida T, Funaoka M (2003) Enzymatic synthesis of polyphenols from highly phenolic lignin-based polymers (lignophenols). *Biotechnol Lett* 25:9–12
13. Yoshida T, Xia Z, Takeda K et al (2005) Peroxidase-catalyzed polymerization and copolymerization of lignin-based macromonomer (lignocresol) having high content of p-cresol and thermal properties of the resulting polymers. *Polym Adv Technol* 16:783–788
14. Li K, Geng X (2005) Formaldehyde-free wood adhesives from decayed wood. *Macromol Rapid Commun* 26:529–532
15. Ikeda R, Tanaka H, Uyama H et al (2000) A new crosslinkable polyphenol from a renewable resource. *Macromol Rapid Commun* 21:496–499
16. Kim YH, Suk An E, Keun Song B et al (2003) Polymerization of cardanol using soybean peroxidase and its potential application as anti-biofilm coating material. *Biotechnol Lett* 25:1521–1524
17. Kim YH, Won K, Kwon JM et al (2005) Synthesis of polycardanol from a renewable resource using a fungal peroxidase from *Coprinus cinereus*. *J Mol Catal B Enzym* 34:33–38
18. Kim YH, An ES, Park SY et al (2007) Enzymatic epoxidation and polymerization of cardanol obtained from a renewable resource and curing of epoxide-containing polycardanol. *J Mol Catal B Enzym* 45:39–44
19. Park SY, Kim YH, Won K et al (2009) Enzymatic synthesis and curing of polycardol from renewable resources. *J Mol Catal B Enzym* 57:312–316
20. Won K, Kim YH, An ES et al (2004) Horseradish peroxidase-catalyzed polymerization of cardanol in the presence of redox mediators. *Biomacromolecules* 5:1–4
21. Chelikani R, Kim Y, Yoon D-Y et al (2009) Enzymatic polymerization of natural anacardic acid and antibiofouling effects of polyanacardic Acid Coatings. *Appl Biochem Biotechnol* 157:263–277
22. Boerjan W, Ralph J, Baucher M (2003) Lignin biosynthesis. *Annu Rev Plant Biol* 54:519–546
23. Gargulak JD, Lebo SE (2000) In: Glasser WG, Northey RA, Schultz TP (eds) Commercial use of lignin-based materials. American Chemical Society, Washington, pp 304–320
24. Gosselink RJA, Abächerli A, Semke H et al (2004) Analytical protocols for characterisation of sulphur-free lignin. *Ind Crops Prod* 19:271–281
25. Lora JH, Glasser WG (2002) Recent industrial applications of lignin: a sustainable alternative to nonrenewable materials. *J Polym Environ* 10:39–48
26. Allen BR (1980) Pretreatment methods for the degradation of lignin. Report

27. Hüttermann A, Mai C, Kharazipour A (2001) Modification of lignin for the production of new compounded materials. *Appl Microbiol Biotechnol* 55:387–384
28. Kosbar LL, Gelorme JD, Japp RM et al (2000) Introducing biobased materials into the electronics industry. *J Ind Ecol* 4:93–105
29. Sena-Martins G, Almeida-Vara E, Duarte JC (2008) Eco-friendly new products from enzymatically modified industrial lignins. *Ind Crops Prod* 27:189–195
30. Stewart CE, Plante AF, Paustian K et al (2008) Soil carbon saturation: linking concept and measurable carbon pools. *Soil Sci Soc Am J* 72:379–392
31. Fukuoka T, Uyama H, Kobayashi S (2004) Effect of phenolic monomer structure of precursor polymers in oxidative coupling of enzymatically synthesized polyphenols. *Macromolecules* 37:5911–5915
32. Kalra B, Gross RA (2000) Horseradish peroxidase mediated free radical Polymerization of methyl methacrylate. *Biomacromolecules* 1:501–505
33. Singh A, Kaplan DL (2004) Vitamin C functionalized poly(methyl methacrylate) for free radical scavenging. *J Macromol Sci A Pure Appl Chem* 41:1377–1386
34. Uyama H, Lohavisavapanich C, Ikeda R et al (1998) Chemoselective polymerization of a phenol derivative having a methacryl group by peroxidase catalyst. *Macromolecules* 31:554–556
35. Tonami H, Uyama H, Kobayashi S et al (2000) Chemoselective oxidative polymerization of *m*-ethynylphenol by peroxidase catalyst to a new reactive polyphenol. *Biomacromolecules* 1:149–151
36. Bolle R, Aehle W (2000) Lignin-based paint. US Patent 6072015
37. Emery O, Lalot T, Brigodiot M et al (1997) Free-radical polymerization of acrylamide by horseradish peroxidase-mediated initiation. *J Polym Sci A Polym Chem* 35:3331–3333
38. Lalot T, Brigodiot M, Marechal E (1999) A kinetic approach to acrylamide radical polymerization by horseradish peroxidase-mediated initiation. *Polym Int* 48:288–292
39. Teixeira D, Lalot T, Brigodiot M et al (1999) β -Diketones as key compounds in free-radical polymerization by enzyme-mediated initiation. *Macromolecules* 32:70–72
40. Iwahara K, Hirata M, Honda Y et al (2000) Free-radical polymerization of acrylamide by manganese peroxidase produced by the white-rot basidiomycete *Bjerkandera adusta*. *Biotechnol Lett* 22:1355–1361
41. Singh A, Ma D, Kaplan DL (2000) Enzyme-mediated free radical polymerization of styrene. *Biomacromolecules* 1:592–596
42. Shan J, Kitamura Y, Yoshizawa H (2005) Emulsion polymerization of styrene by horseradish peroxidase-mediated initiation. *Colloid Polym Sci* 284:108–111
43. Cholli AL, Thiyagarajan M, Kumar J et al (2005) Biocatalytic approaches for synthesis of conducting polyaniline nanoparticles. *Pure Appl Chem* 77:339–344
44. Raitman OA, Katz E, Bückmann AF et al (2002) Integration of polyaniline/poly(acrylic acid) films and redox enzymes on electrode supports: an in situ electrochemical/surface plasmon resonance study of the bioelectrocatalyzed oxidation of glucose or lactate in the integrated bioelectrocatalytic systems. *J Am Chem Soc* 124:6487–6496
45. Cao Y, Li S, Xue Z et al (1986) Spectroscopic and electrical characterization of some aniline oligomers and polyaniline. *Synth Met* 16:305–315
46. Chiang J, MacDiarmid AG (1986) 'Polyaniline': protonic acid doping of the emeraldine form to the metallic regime. *Synth Met* 13:193–205
47. Samuelson LA, Anagnostopoulos A, Alva KS et al (1998) Biologically derived conducting and water soluble polyaniline. *Macromolecules* 31:4376–4378
48. Rannou P, Nechtschein M (1998) PANI-CSA films: Ageing and kinetics of conductivity degradation. *J Chim Phys Physico-Chimie Biol* 95:1410–1413
49. Chattopadhyay K, Mazumdar S (1999) Structural and conformational stability of horseradish peroxidase: effect of temperature and pH. *Biochemistry* 39:263–270
50. Liu W, Cholli AL, Nagarajan R et al (1999) The role of template in the enzymatic synthesis of conducting polyaniline. *J Am Chem Soc* 121:11345–11355

51. Cruz-Silva R, Arizmendi L, Del Angel M et al (2007) pH- and thermosensitive polyaniline colloidal particles prepared by enzymatic polymerization. *Langmuir* 23:8–12
52. Alva K, Marx KA, Kumar J et al (1996) Biochemical synthesis of water soluble polyanilines: poly(p-Amino Benzoic Acid). *Macromol Rapid Commun* 17:859–863
53. Alva K, Kumar J, Marx KA et al (1997) Enzymatic synthesis and characterization of a novel water soluble polyaniline: poly(2, 5 diamino benzene sulfonic acid). *Macromolecules* 30:4024–4029
54. Lim CH, Yoo YJ (2000) Synthesis of ortho-directed polyaniline using horseradish peroxidase. *Process Biochem* 36:233–241
55. Cruz-Silva R, Ruiz-Flores C, Arizmendi L et al (2006) Enzymatic synthesis of colloidal polyaniline particles. *Polymer* 47:1563–1568
56. Nagarajan R, Tripathy S, Kumar J et al (2000) An enzymatically synthesized conducting molecular complex of polyaniline and poly(vinylphosphonic acid). *Macromolecules* 33:9542–9547
57. Sakharov IY, Vorobiev AC, Leon JJC (2003) Synthesis of polyelectrolyte complexes of polyaniline and sulfonated polystyrene by palm tree peroxidase. *Enzyme Microb Technol* 33:661–667
58. Nabid MR, Entezami AA (2003) Enzymatic synthesis and characterization of a water-soluble, conducting poly(o-toluidine). *Eur Polym J* 39:1169–1175
59. Nagarajan R, Samuelson L, Tripathy S, Liu W, Kumar J, Bruno F (2003) Enzymatic polymerization of aniline or phenols around a template. US Patent 6569651
60. Nagarajan R, Liu W, Kumar J et al (2001) Manipulating DNA conformation using intertwined conducting polymer chains. *Macromolecules* 34:3921–3927
61. Cruz-Silva R, Romero-Garcia J, Angulo-Sanchez JL et al (2005) Template-free enzymatic synthesis of electrically conducting polyaniline using soybean peroxidase. *Eur Polym J* 41:1129–1135
62. Thiagarajan M, Samuelson LA, Kumar J et al (2003) Helical conformational specificity of enzymatically synthesized water-soluble conducting polyaniline nanocomposites. *J Am Chem Soc* 125:11502–11503
63. Premachandran RS, Banerjee S, Wu XK et al (1996) Enzymatic synthesis of fluorescent naphthol-based polymers. *Macromolecules* 29:6452–6460
64. Bodtke A, Pfeiffer WD, Ahrens N et al (2005) Horseradish peroxidase (HRP) catalyzed oxidative coupling reactions using aqueous hydrogen peroxide: an environmentally benign procedure for the synthesis of azine pigments. *Tetrahedron* 61:10926–10929
65. Luthardt W (1963) Myko-Holz-Herstellung, Eigenschaften und Verwendung. In: Lyr H, Gillwald W (eds) *Holzerstörung durch Pilze*. Akademie-Verlag, Berlin
66. Schmidt O (1994) *Holz- und Baumpilze*. Springer, Berlin, Heidelberg, New York
67. Nimz H, Razvy A, Maqharab I, Clad W (1972) Bindemittel bzw. Klebmittel zur Herstellung von Holzwerkstoffen sowie zur Verklebung von Werkstoffen verschiedener Art. DOS 2 221 353 German
68. Nimz H, Gurang I, Mogharab I (1976) Untersuchungen zur Vernetzung technischer Sulfitablauge. *Liebigs Annalen der Chemie*:1421–1434
69. Hüttermann A, Kharazipour A (1996) Enzymes as polymerisation catalysts. In: A. Maijanen and A. Hase (eds) *New catalysts for clean environment*. VTT Symp 163:143–148
70. Jin L, Nicholas DD, Schultz TP (1991) Wood laminates glued by enzymatic oxidation of brown-rotted lignin. *Holzforschung* 45:467–468
71. Felby C, Pedersen LS, Nielsen BR (1997) Enhanced auto adhesion of wood fibers using phenol oxidases. *Holzforschung* 51:281–286
72. Felby C, Hassingboe J, Lund M (2002) Pilot-scale production of fiberboards made by laccase oxidized wood fibers: board properties and evidence for cross-linking of lignin. *Enzyme Microb Technol* 31:736–741
73. Felby C, Olesen PO, Hansen TT (1998) Laccase catalyzed bonding of wood fibers. *Enzymes in fiber processing*. ACS Symp Ser 687:88–98

74. Unbehaun H, Dittler B, Kühne G et al (2000) Investigation into the biotechnological modification of wood and its application in the wood-based material industry. *Acta Biotechnol* 20:305–312
75. Kharazipour A, Mai C, Hüttermann A (1998) Polyphenoles for compounded materials. *Polym Degrad Stabil* 59:237–243
76. Kühne G, Dittler B (1999) Enzymatische Modifizierung nachwachsender lignocelluloser Rohstoffe für die Herstellung bindemittelfreier Faserwerkstoffe. *Zeitschrift: Holz als Rohund Werkstoff* 57:264
77. Yamaguchi H, Maeda Y, Sakata I (1992) Applications of phenol dehydrogenative polymerization by laccase to bonding among woody-fibers. *Mokuzai Gakkaishi* 38:931–937
78. Yamaguchi H, Maeda Y, Sakata I (1994) Bonding among woody fibers by use of enzymic phenol dehydrogenative polymerization. Mechanism of generation of bonding strength. *Mokuzai Gakkaishi* 40:185–190
79. Yamaguchi H, Nagamori N, Sakata I (1991) Application of the dehydrogenative polymerization of vanillic acid to bonding of woody fibers. *Mokuzai Gakkaishi* 37:220–226
80. Unbehaun H, Wolff M, Kühne G et al (1999) Mechanismen der mykologischen Transformation von Holz für die Holzwerkstoffherstellung. *Holz als Rohund Werkstoff* 57:92
81. Körner I, Kühne G, Pecina H (2001) Unsterile Fermentation von Hackschnitzelneine Holzvorbehandlungsmethode für die Faserplattenherstellung. *Zeitschrift: Holz als Rohund Werkstoff* 59:334–341
82. Appendini P, Hotchkiss JH (2002) Review of antimicrobial food packaging. *Innov Food Sci Emerg Technol* 3:113–126
83. Dainelli D, Gontard N, Spyropoulos D et al (2008) Active and intelligent food packaging: legal aspects and safety concerns. *Trends Food Sci Technol* 19:S103–S112
84. Elegir G, Kindl A, Sadocco P et al (2008) Development of antimicrobial cellulose packaging through laccase-mediated grafting of phenolic compounds. *Enzyme Microb Technol* 43:84–92
85. Grönqvist S, Rantanen K, Alen R et al (2006) Laccase-catalysed functionalisation of TMP with tyramine. *Holzforschung* 60:503–508
86. Kudanga T, Nugroho Prasetyo E, Sipilä J et al (2008) Laccase-mediated wood surface functionalization. *Eng Life Sci* 8:297–302
87. Kudanga T, Nugroho Prasetyo E, Sipilä J et al (2009) Coupling of aromatic amines onto syringylglycerol [beta]-guaiacyloether using *Bacillus* SF spore laccase: a model for functionalization of lignin-based materials. *J Mol Catal B Enzym* 61:143–149
88. Shin H, Guebitz G, Cavaco-Paulo A (2001) “In situ” enzymatically prepared polymers for wool coloration. *Macromol Mater Eng* 286:691–694
89. Hossain K, Gonzalez MD, Lozano GR et al (2009) Multifunctional modification of wool using an enzymatic process in aqueous-organic media. *J Biotechnol* 141:58–63
90. Kim S, López C, Guebitz G et al (2008) Biological coloration of flax fabrics with flavonoids using laccase from *Trametes hirsuta*. *Eng Life Sci* 8:324–330
91. Van Ee JH, Misset O, Baas EJ (1997) *Enzymes in detergency*. Marcel Dekker, New York
92. Conrad LS, Damhus T, Kirk O et al (1997) Enzymatic inhibition of dye transfer. *Inform* 8:950–957
93. Nakayama T, Amachi T (1999) Fungal peroxidase: its structure, function, and application. *J Mol Catal B Enzym* 6:185–198
94. Tzanov T, Silva C, Zille A et al (2003) Effect of some process parameters in enzymatic dyeing of wool. *Appl Biochem Biotechnol* 111:1–13
95. Hadzhiyska H, Calafell M, Gibert J et al (2006) Laccase-assisted dyeing of cotton. *Biotechnol Lett* 28:755–759
96. Calafell M, Diaz C, Hadzhiyska H et al (2007) Bio-catalyzed coloration of cellulose fibers. *Biocatal Biotransform* 25:336–340
97. Schroeder M, Aichering N, Guebitz GM et al (2006) Enzymatic coating of lignocellulosic surfaces with polyphenols. *Biotechnol J* 2:334–341

98. Rodriguez Couto S, Toca Herrera JL (2006) Industrial and biotechnological applications of laccases: a review. *Biotechnol Adv* 24:500–513
99. Umbach W (1988) *Kosmetik, Entwicklung, Herstellung und Anwendung kosmetischer Mittel*. Thieme, Stuttgart
100. Aehle W (2007) *Enzymes in industry: production and applications*. Wiley, New York
101. Wang J, Liang G, Zhao W, Zhang Z (2007) Enzymatic surface modification of PBO fibres. *Surface and Coating Technology* 201:4800–4804
102. Davies RJ, Eichhorn SJ, Riekel C et al (2004) Crystal lattice deformation in single poly (p-phenylene benzobisoxazole) fibres. *Polymer* 45:7693–7704
103. Fan G, Zhao J, Zhang Y et al (2006) Grafting modification of Kevlar fiber using horseradish peroxidase. *Polym Bull* 56:507–515
104. Zhao J, Guo Z, Liang G et al (2004) Novel surface modification of high-density polyethylene films by using enzymatic catalysis. *J Appl Polym Sci* 91:3673–3678
105. Matheis G, Whitaker JR (1984) Modification of proteins by polyphenol oxidase and peroxidase and their products. *J Food Biochem* 8:137–162
106. Matheis G, Whitaker JR (1984) Peroxidase-catalyzed cross linking of proteins. *J Prot Chem* 3:35–48
107. Matheis G, Whitaker JR (1987) A review: enzymatic cross-linking of proteins applicable to foods. *J Food Biochem* 11:309–327
108. Feeney RE, Whitaker JR (1988) Importance of cross-linking reactions in proteins. *Adv Cereal Sci Technol* 9:21–43
109. Miller DR, Tizard IR, Keeton JT, Prochaska JF (2003) System for polymerizing collagen and collagen composites in situ for a tissue compatible wound sealant, delivery vehicle, binding agent and/or chemically modifiable matrix. US Patent 6509031
110. Vachoud L, Chen T, Payne GF et al (2001) Peroxidase catalyzed grafting of gallate esters onto the polysaccharide chitosan. *Enzyme Microb Technol* 29:380–385
111. Kurisawa M, Chung JE, Yang YY et al (2005) Injectable biodegradable hydrogels composed of hyaluronic acid-tyramine conjugates for drug delivery and tissue engineering. *Chem Commun*:4312–4314
112. Jin R, Hiemstra C, Zhong Z et al (2007) Enzyme-mediated fast in situ formation of hydrogels from dextran-tyramine conjugates. *Biomaterials* 28:2791–2800
113. Ogushi Y, Sakai S, Kawakami K (2009) Phenolic hydroxy groups incorporated for the peroxidase-catalyzed gelation of a carboxymethylcellulose support: cellular adhesion and proliferation. *Macromol Biosci* 9:262–267
114. Ogushia Y, Sakaia S, Kawakami K (2007) Synthesis of enzymatically-gellable carboxymethylcellulose for biomedical applications. *J Biosci Bioeng* 104:30–33
115. Uyama H, Kurioka H, Kobayashi S (1997) Novel bienzymatic catalysis system for oxidative polymerization of phenols. *Polym J* 29:190–192
116. Ruiz-Duenas FJ, Morales M, Garcia E et al (2009) Substrate oxidation sites in versatile peroxidase and other basidiomycete peroxidases. *J Exp Bot* 60:441–452

Chapter 8

Applications and Prospective of Peroxidase Biocatalysis in the Environmental Field

Cristina Torres-Duarte and Rafael Vazquez-Duhalt

Contents

8.1	Introduction	180
8.2	Phenols	182
8.3	Halogenated Phenols	184
8.4	Chloroanilines	185
8.5	Polycyclic Aromatic Hydrocarbons	187
8.6	Endocrine Disruptive Chemicals	188
8.7	Pesticides	191
8.8	Dioxins	193
8.9	Polychlorinated Biphenyls (PCBs)	195
8.10	Dyes	196
8.11	Challenges for the Industrial Applications of Peroxidase for Environmental Purposes	198
	References	200

Abstract Environmental protection is, doubtless, one of the most important challenges for the human kind. The huge amount of pollutants derived from industrial activities represents a threat for the environment and ecologic equilibrium. Phenols and halogenated phenols, polycyclic aromatic hydrocarbons, endocrine disruptive chemicals, pesticides, dioxins, polychlorinated biphenyls, industrial dyes, and other xenobiotics are among the most important pollutants. A large variety of these xenobiotics are substrates for peroxidases and thus susceptible to enzymatic transformation. The literature reports mainly the use of horseradish peroxidase, manganese peroxidase, lignin peroxidase, and chloroperoxidase on the transformation of these pollutants. Peroxidases are enzymes able to transform a variety of compounds following a free radical mechanism, giving oxidized or polymerized products. The peroxidase transformation of these pollutants is accompanied by a reduction in their toxicity, due to a biological activity loss, a reduction in the bioavailability or due to the removal from aqueous phase, especially when the pollutant is found in water. In addition, when the pollutants are present in soil, peroxidases catalyze a covalent binding to soil organic matter. In most of cases,

oxidized products are less toxic and easily biodegradable than the parent compounds. In spite of their versatility and potential use in environmental processes, peroxidases are not applied at large scale yet. Diverse challenges, such as stability, redox potential, and the production of large amounts, should be solved in order to apply peroxidases in the pollutant transformation. In this chapter, we critically review the transformation of different xenobiotics by peroxidases, with special attention on the identified transformation products, the probable reaction mechanisms, and the toxicity reports. Finally, the design and development of an environmental biocatalyst is discussed. The design challenges are mainly focused on the enzyme stability in the presence of hydrogen peroxide and operational conditions, an enzyme with high redox potential to be able to oxidize a wide range of xenobiotics or pollutants, and the protein overexpression at large-scale in industrial microorganisms is discussed.

8.1 Introduction

Humankind faces two unprecedented challenges: Energy and Environment. Society functioning and its future progress are dependent on the availability of new and renewable sources of energy, and on the capacity to change polluting productive processes for new environment friendly processes. Together, these developments have led to a growing awareness of the central importance of the environmental sciences as humankind attempts to transition to a more sustainable relationship with the Earth and its natural resources.

Concerning pollution, there is no complete data on the world's toxic chemical releases. Nevertheless, 20 years ago, the United States started to estimate the amount of toxic chemicals that are released and published the "Toxics Release Inventory" (TRI) [1]. TRI is a database containing detailed information on nearly 650 chemicals and chemical categories that approximately 22,000 industrial and federal facilities manage through disposal or other releases, or recycling, energy recovery, or treatment. By 2007, 21,996 facilities, including federal facilities, reported 1.86 million tons of on-site and off-site disposals or other releases of the almost 650 toxic chemicals to the TRI Program, as shown in Table 8.1. Almost 87% of the total was disposed or otherwise released on-site; 13% was sent off-site for disposal. Metal mining facilities reported 28% and electric utilities reported 25% of the total chemical releases in 2007.

Many other countries operate pollution inventories, such as Austria, Canada, Denmark, Netherlands, France, Germany, Hungary, Mexico, Norway, Scotland, Spain, and Sweden. The policies do tend to differ slightly from one another. In particular, the substances requiring reporting and their associated thresholds can vary significantly. Unfortunately, not all the countries operate this kind of inventories; thus the amount of toxics released around the world remains unknown.

Nevertheless, it was estimated that about 40% of the deaths (62 million per year) is attributed to various environmental factors especially organic and chemical pollutants [2, 3]. In addition, 2.2 million infants and children die each year from diarrhea, which is caused largely by contaminated water and food [4].

Table 8.1 Data from the 2007 US Toxic Release Inventory (TRI) [1]

	Tons	Percent
<i>On-site disposal or other releases</i>		
Air	596,204	32.1
Water	105,470	5.7
Underground injection	95,034	5.1
Land	811,674	43.7
Total onsite disposal or other releases	1,608,180	86.6
<i>Off-site disposal or other releases</i>		
Underground injection	7,389	0.4
Land	178,097	9.6
POTWs and waste treatment	2,102	0.1
Other	61,610	3.3
Total off-site disposal or other releases	249,199	13.4
Total on- and off-site disposal or other releases	1,857,380	100

From these inventories and data, it is clear that society is facing an enormous problem of contamination. Many of the polluting compounds that are continuously dispersed are products of industrial activities such as phenols and halogenated phenols, polycyclic aromatic hydrocarbons (PAH's), endocrine disruptive chemicals (EDC), pesticides, dioxins, polychlorinated biphenyls (PCB's), industrial dyes, and other xenobiotics. In this chapter, we critically review the literature information on the enzymatic transformation of these polluting xenobiotics. This work is focused on peroxidases as enzymes able to transform a variety of pollutant compounds with the aim to reduce their toxicity and their environmental impact.

Perhaps the earliest report on peroxidase activity was in 1855 by Schönbein [5], who observed that certain organic compounds could be oxidized by diluted solutions of hydrogen peroxide in the presence of substances occurring in plants and animals. The name of peroxidase was first given by Linossier, who in 1898 isolated it from pus [6]. The first successful isolation and purification of a peroxidase was achieved between 1917 and 1924 by Willstatter and his coworkers [7, 8]. They used a phenolic compound, the pyrogallol (1,2,3-trihydroxybenzene), as the first experimental procedure to monitor the peroxidase activity. As described in Chap. 5 of this book, peroxidases transform substrates by a free radical mechanism. Free radicals are ubiquitous, reactive chemical entities possessing an unpaired electron. Free radical and related reactive oxygen species are largely responsible for the cell damage associated with several illnesses. Paradoxically, it is the high reactivity of free radicals that makes them a useful tool to contend against pollutants. When free radicals subtract an electron from a surrounding compound or molecule, a new free radical is formed in its place. In turn, the newly formed radical then seeks to return to its ground state by subtracting electrons with antiparallel spins from pollutant molecules. Many pollutant compounds are oxidized by heme enzymes, such as peroxidases and cytochromes P450. Thus, due to the diversity of chemical nature and properties of xenobiotics, the unspecificity of the free radical-mediated oxidation mechanism of peroxidases is an invaluable attribute for xenobiotic transformation.

8.2 Phenols

Phenol and its compounds are ubiquitous water pollutants that are present in the effluents of a variety of chemical industries such as coal refineries, phenol manufacturing, pharmaceuticals, and industries of resin, paint, dyeing, textile, leather, petrochemical, pulp mill, etc. [9]. Phenols are known to be toxic and also, some of them, hazardous carcinogenic that can accumulate in the food chain. Phenolic compounds are a public health risk and they are heavily regulated in many countries, and must be removed from wastewater before they are discharged into the environment [10]. For example, a 10 days consumption of polluted water with low concentrations (3 ppm) of 2,4-dichlorophenol can cause vomiting, paralysis, and even death in children [11, 12]. Phenol, 2-chlorophenol, and 2,4-dichlorophenol are ranked within the 250 most hazardous pollutants [13]. In addition, chlorophenols are commonly found in chlorinated water, since phenol can react with chlorine [14].

Many physical and chemical methods for phenolic compounds removal from industrial effluents, such as solvent extraction, chemical oxidation, and charcoal adsorption, are currently used [15]. However, these methods are expensive, time consuming, and less efficient because of incomplete phenolic compounds removal.

Peroxidases comprise an important class of enzymes able to catalyze the oxidative coupling reactions of a broad range of phenolic compounds [16–20]. Several research works have been focused on the development of a biotechnological process to remove phenolic compounds from polluted wastewater using peroxidases [21–23]. This enzymatic treatment offers a high degree of specificity, operation under mild conditions, high reaction rate, and reaches very low concentrations of soluble phenols [10]. Horseradish peroxidase has been used in a number of reports on the enzymatic treatment of phenolic compounds contaminated wastewater. Phenol oxidation by horseradish peroxidase and product identification as *o*-*o'*-biphenol was first reported by Danner et al., in 1973 [24]. However, recently peroxidases from other sources, such as soybean [23, 25, 26], turnip roots [27], and bitter melon [22], have been proposed as alternative to horseradish peroxidase.

Using peroxidases in the presence of hydrogen peroxide, phenolic substrates are converted catalytically to phenoxy radicals (Fig. 8.1). The phenoxy radicals produced in the enzymatic reaction step can then, in postenzymatic reactions, couple with each other or with other reactive substances present in the system [28–32]. Self-coupling of phenol molecules with each other dominates in systems that lack appropriate substrates to participate in cross-coupling reactions with phenol, leading to formation of precipitated polymeric products [9, 33] that can be readily removed from water.

Significant cross-coupling of phenol with other reactive substances usually occurs in aquatic systems in contact with soils and sediments, generally resulting in their incorporation in soil organic matter [19, 31]. Cross-coupling reactions between phenolic contaminants and various types of organic substances have been demonstrated in several investigations [32, 34–41]. For example, phenolic contaminants have been found to bind with humic substances through C–C or aryl

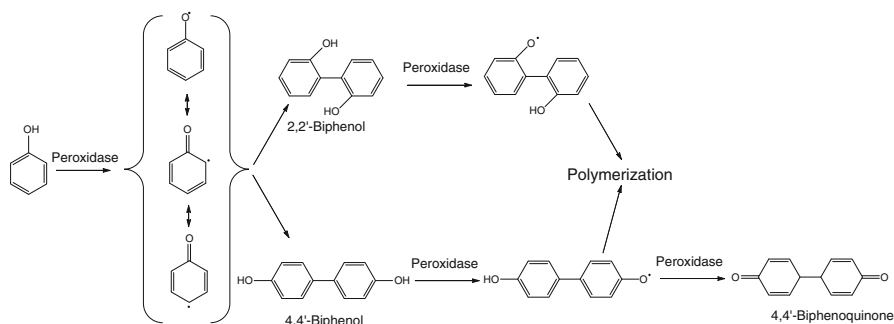


Fig. 8.1 Mechanism of phenol oxidation and polymerization by peroxidase-catalyzed reaction

ether linkages via cross-coupling [36]. Huang and Weber [42] investigated phenol conversion by horseradish peroxidase and precipitate formation. Both processes were significantly influenced by cross-coupling of phenol with dissolved organic matter, particularly in the cases of the more reactive and soluble dissolved soil organic matter. Analytical characterizations indicate that enzymatic cross-coupling leads to incorporation of phenol in the soluble organic macromolecules from soil, yielding nontoxic soluble products.

Unfortunately, during the removal process, a decrease in peroxidase activity has been observed. All peroxidases are susceptible to an oxidative inactivation in the presence of hydrogen peroxide [43]. This oxidative self-inactivation seems to occur by different catalytic-mediated pathways, including heme destruction, and oxidation of essential amino acid residues. In addition, inactivation may occur through stabilization of the phenoxy radical by a π -conjugation with the compound I and/or in less extent, by the adsorption of enzyme molecules onto the end product polymer, limiting the substrate diffusion to the active site [44]. In order to improve the operational stability of peroxidases during phenol polymerization, several additives such as polyethylene glycol (PEG) or gelatin have been studied [45, 46]. Duarte et al. [27] observed that 50 mg l^{-1} of PEG improved to 99% the removal of bisphenol, 3-chlorophenol, and *m*-cresol by free turnip peroxidase. On the other hand, the presence of PEG in the reaction mixture protected turnip peroxidase from inactivation during phenol polymerization [47]. This protection allows to extend the enzyme lifetime when it is immobilized both covalently or entrapped, increasing the number of reaction cycles with high removal efficiency. Phenol removal from a real wastewater effluent was efficiently performed by immobilized turnip peroxidase in presence of PEG. Moreover, the covalent chemical modification with PEG and immobilization of the modified turnip peroxidase showed an enhanced protein conformational and thermal stability, higher solvent tolerance, and a slight increase in catalytic efficiency. This allowed an extended reuse of the peroxidase preparation in the transformation of a highly concentrated phenol solution [48].

8.3 Halogenated Phenols

Highly halogenated phenols, including tetra- and pentahalogenated phenols, are currently used for a wide range of domestic, agricultural, and industrial purposes. Chlorophenols are among the most widely distributed pollutants. Their toxicity increases as the degree of chlorine substitution increases [49]. Pentachlorophenol and the lower chlorinated phenol, tetrachlorophenol, are intensively used as fungicides, herbicides, insecticides, and precursors in the synthesis of other pesticides. The prohibition of pentachlorophenol production in USA since 1992 and in Europe since 2000, and the production in countries such as China and India, makes it difficult to find data about total world production of chlorophenols. However, the world production of these compounds was estimated to be over 200,000 tons per year in 1980 [50] and little data is available thereafter. Pentachlorophenol is the major synthetic wood preservative currently used and it is used in a variety of applications for its biocidal properties, as an additive for shoe leather, drilling mud, paper products, and certain food packaging. Despite its uses, pentachlorophenol has been banned in many countries, and its use has been severely restricted in others; however, it is still widely used and remains an important pollutant from a toxicological perspective. The toxicology and environmental impact of pentachlorophenol has been reviewed [50–52]. Pentachlorophenol is a stable and persistent compound that can be absorbed by ingestion, inhalation and, to a lesser extent, through skin. It is metabolized and eliminated slowly. Severe exposure results in acute effects mediated by uncoupling oxidative phosphorylation. Occasionally, fatal illness occurs with tachycardia, tachypnoea, hyperthermia, sweating, and convulsions [52]. Pentachlorophenol has been classified as a weak mutagen; however, it is able to form a DNA adduct [53, 54], and thus should be considered as a potential carcinogen.

Ligninolytic fungi are able to degrade pentachlorophenol. *Phanerochaete chrysosporium* [55, 56], *Gloeophyllum striatum* [57], *Panus tigrinus* [58], and *Trametes versicolor* [59] are able to mineralize pentachlorophenol to CO₂. The proposed fungal pentachlorophenol metabolism is a multistep pathway starting with an oxidative dehalogenation mediated by extracellular peroxidases to form tetrachloro-1,4-benzoquinone. Tetrachloro-1,4-benzoquinone is further degraded by reductive dehalogenations, and then hydroxylated. *In vitro* ligninolytic peroxidases and other peroxidases are able to transform pentachlorophenol. Lignin peroxidase from *P. chrysosporium* [60–62], horseradish peroxidase [63, 64], myeloperoxidase [65], lactoperoxidase [66], microperoxidase-8 [67], versatile peroxidase from *Bjerkandera adusta* [68], and chloroperoxidase from *Caldariomyces fumago* [69] are able to transform pentachlorophenol to tetrachloro-1,4-benzoquinone by an oxidative dehalogenation in the presence of hydrogen peroxide. Then, a polymerization reaction occurs. In addition to the polymer, two other products have been detected from chloroperoxidase-mediated transformation of pentachlorophenol: tetrachloro-1,4-benzoquinone and a dimer (Fig. 8.2) [69]. Tetrachloro-1,4-benzoquinone has been also detected as product from pentachlorophenol transformation by horseradish peroxidase and lignin

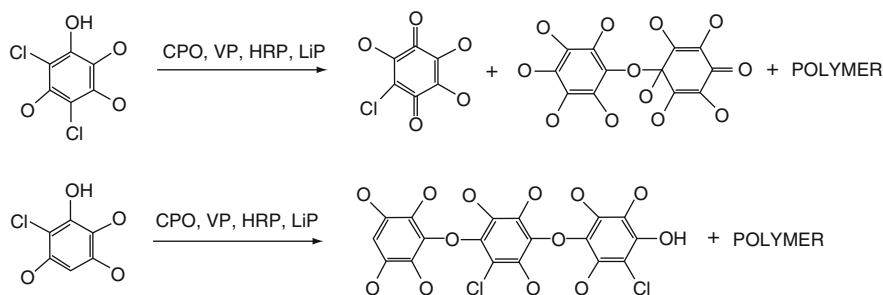


Fig. 8.2 Detected products from the peroxidase oxidation of highly halogenated phenols [69]

peroxidase, and the suggested mechanism includes the oxygen-based radical formation, followed by a radical delocalization and *p*-chlorine release [63]. The tetrachloro-1,4-benzoquinone formed has been suggested as a possible precursor for polymer formation [62]. However, a different mechanism for tetrachloro-1,4-benzoquinone formation has been proposed in which the first step is the dimer formation by phenoxyl radical condensation and then dimer decomposition forming tetrachloro-1,4-benzoquinone [69, 70]. Nevertheless, significant amounts of the highly toxic polychlorinated dibenzo-*p*-dioxins and dibenzofurans have been reported after peroxidase-catalyzed oxidation of halogenated phenols [71].

8.4 Chloroanilines

Chloroanilines are used as intermediates in the synthesis of dyestuffs, agricultural chemicals, pharmaceuticals, and others, and they can be released into the environment through industrial activity. They can also occur in the environment as biodegradation products of aniline-based pesticides. Pentachloroaniline is a major metabolite of the widely used fungicide Quintozene (pentachloronitrobenzene, PCNB) [72, 73]. This pesticide is converted to pentachloroaniline in moist soil, estuarine sediments [74], and by animal metabolism [72, 75]. Clary and Ritz [76] found increased pancreatic cancer mortality among long-term residents in areas with high application rates of PCNB. Highly chlorinated anilines can be lethal for many organisms [77]. In general, chloroaniline toxicity increases with the number of chlorine atoms, although this trend is less marked for highly substituted compounds. Tetrachloroaniline shows only slightly increased toxic effects with respect to trichloroanilines, while for pentachloroaniline, the trend of increasing toxicity is reversed since this compound was found to be less toxic than tetra-substituted anilines [78]. Its toxicity potential was also estimated with the Microtox test and with other bacterial toxicological assays [79]. Chlorinated anilines are commonly classified as polar narcotic chemicals in most QSAR studies focused on acute toxicity to aquatic organisms [80].

P. chrysosporium has been reported as able to mineralize lignin conjugates of chloroanilines and free chloroanilines [81], but no products were identified. This ability is important in order to remove these conjugates from the environment. 4-Chloroaniline and 4-chlorophenol have been transformed by oxidoreductases in the presence of humic acids, and oligomerization of the substrates or their binding to organic matter was found [41].

Peroxidase transformation of mono- and dichlorinated anilines have been extensively studied, but there is scarce information about highly halogenated anilines. From several peroxidases tested, only chloroperoxidase from *C. fumago* was able to transform highly chlorinated anilines [69]. This first report on peroxidase transformation of pentachloroaniline showed that the main product is a polymeric material, and pentachlorophenol and tetrachloro-1,4-benzoquinone are also produced (Fig. 8.3). The mechanism of pentachlorophenol production from pentachloroaniline is still unknown. However, the tetrachloro-1,4-benzoquinone seems to be a product of the pentachlorophenol intermediate and not produced directly from the pentachloroaniline as found in pentachlorophenol peroxidase transformation [69]. The identified products from the chloroperoxidase-mediated transformation of tetrachloroaniline are the polymer, which represented 87–95% of the total mass, pentachloroaniline, and three different dimers, which have been identified as minor products [69].

4-Chloronitrosobenzene has been identified as product of the chloroperoxidase transformation of 4-chloroaniline [82, 83]. This product was the only one identified

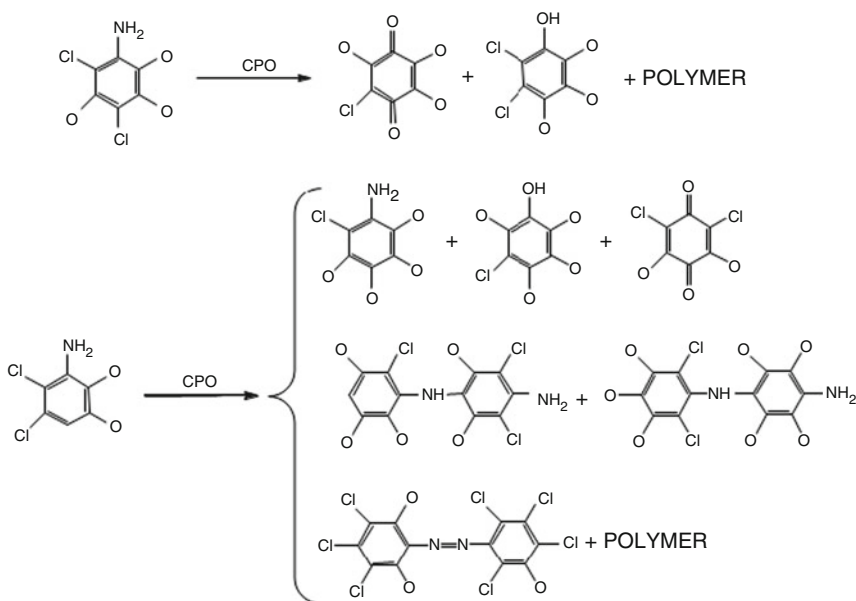


Fig. 8.3 Detected products from the peroxidase oxidation of highly halogenated anilines [69]

when no chloride was present in the reaction media at pH 6 or above. When chloride is present at pH 3 or lower, halogenated products were observed.

8.5 Polycyclic Aromatic Hydrocarbons

PAHs are composed of two or more fused aromatic rings and are components of crude oil, creosote, and coal (Fig. 8.4) [84]. Most of the contamination by PAHs is originated from the extensive use of fossil fuels as energy sources. They are priority pollutants to remove because they have been identified as procarcinogens, mutagens, and teratogenic. They are persistent in the environment, mainly due to their high hydrophobicity and low aqueous solubility, which makes their microbial biodegradation a very slow process [85].

Several oxidative enzymes have been reported to be able to catalyze the modification of polyaromatic hydrocarbons. Peroxidases and phenoloxidasases can act on specific PAH's by transforming them to less toxic or products easier to degrade. PAHs are oxidized by peroxidases such as lignin peroxidase [86, 87], manganese peroxidase [88], and by nonperoxidase hemoproteins like cytochrome P450 [89], cytochrome C [90], and hemoglobin [91] in the presence of hydrogen peroxide. The oxidation products from hemoprotein reactions on PAHs are mainly quinones and hydroxylated derivatives. Several quinones from PAHs are not mutagenic or significantly less mutagenic than the parental hydrocarbons [92]. In addition, these oxidized products are more biodegradable [93]. Thus, the enzymatic oxidation of PAHs can be considered as a detoxification process.

Unfortunately, not all PAHs are substrates for peroxidases. A correlation has been found between the ionization potential (IP) of PAHs and the specific activity of manganese peroxidase, lignin peroxidase, hemoglobin, and chloroperoxidase. A threshold value of IP was found for each enzyme. Lignin peroxidase oxidizes PAHs with IP = 7.55 eV [87], while manganese peroxidase oxidizes PAHs with IP

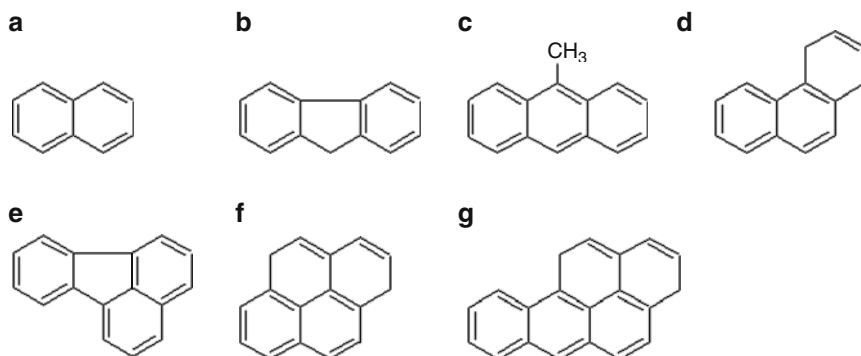


Fig. 8.4 Chemical structures of PAHs: (a) naphthalene; (b) fluoranthene; (c) 9-methylanthracene; (d) phenanthrene; (e) fluoranthene; (f) pyrene; (g) benzo(a)pyrene 4

up to 8.2 eV [88, 94]; the highest IP for hemoglobin-mediated oxidation of PAHs was 8.0 eV [95] and chloroperoxidase was able to modify PAHs with IP lower than 8.2 eV [96].

The versatile peroxidase from *B. adusta* oxidized PAHs in the presence and absence of manganese. The reaction products were the corresponding quinones, and for 9-methylanthracene, a demethylation reaction was detected [97]. In the presence of manganese, a noncompetitive inhibition was found, indicating different binding sites for Mn and PAHs [98]. Using a mutated cytochrome P450 in a peroxidative reaction in the presence of hydrogen peroxide, phenanthrene, fluoranthene, pyrene, and benzo(a)pyrene were oxidized giving mainly hydroxylated products and quinones [99].

The transformation of PAHs with the manganese peroxidase of *P. chrysosporium* required an unsaturated fatty acid, showing that this reaction is connected in some way to the manganese peroxidase-dependent lipid peroxidation known to occur in this system. This reaction seems to follow an H atom abstraction route, because the rate of transformation *in vitro* is greater than that predicted by IP [88].

The chloroperoxidase of *C. fumago* was able to transform 17 of 20 PAHs assayed [100]. In this case, only halogenated products were observed, and no oxygenated products could be detected. This biocatalytic transformation should be carefully considered because the toxicity and environmental impact of aromatic compounds may be increased.

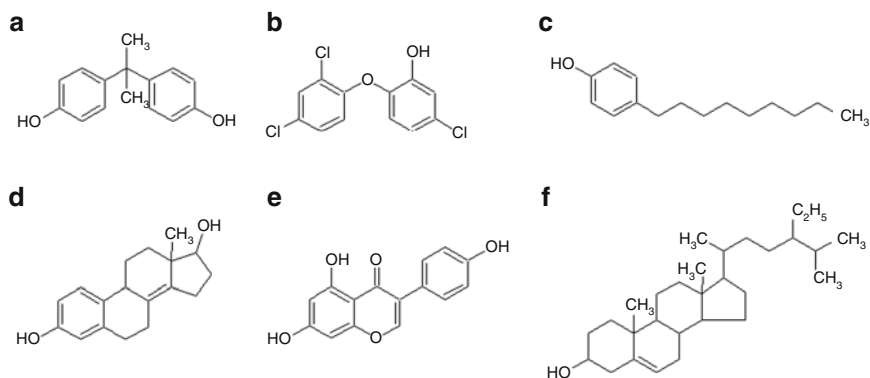
As mentioned above, not only peroxidases are able to transform PAHs. Cytochrome *c* is a hemoprotein with peroxidase-like activity in the presence of hydrogen peroxide [101]. Cytochrome *c* has a covalently bound heme prosthetic group that is important for catalysis in the presence of organic solvents, because it does not lose its heme catalytic group in these reaction systems, while peroxidases do. In addition, cytochrome *c* is active over a wide range of pH (from pH 2 to pH 11). Tinoco et al. [102] modified the cytochrome *c*; they pegylated the surface of the protein and methylated the carboxylic acids, including the propionates of the heme group. This double chemical modification significantly increased the peroxidasic activity in the transformation of different PAHs. Both activity and substrate range are increased (Table 8.2).

8.6 Endocrine Disruptive Chemicals

EDCs are a group of compounds that due to their chemical structure are able to act as agonists or antagonists of hormones. They can disturb the synthesis, secretion, transport, binding, action, and elimination of the endogenous hormones, which are responsible for maintaining homeostasis, reproduction, development, and integrity in living organisms and their progeny [103]. They are very potent estrogens; for example, the no-observed-effect concentrations for nonylphenol are as low as $6 \mu\text{g l}^{-1}$ in fish and $3.9 \mu\text{g l}^{-1}$ in invertebrates [104].

Table 8.2 Oxidation of polycyclic aromatic hydrocarbon by unmodified- and pegylated and methylated cytochrome *c* [102]

Aromatic compound	Specific activity (min^{-1})	
	Unmodified	PEG-Cyt-Met
7,12-dimethylbenzanthracene	24.59(\pm 1.52)	80.33(\pm 3.83)
1,2,3,4-dibenzanthracene	NR	16.60(\pm 2.24)
Azulene	2.26(\pm 0.29)	14.32(\pm 0.57)
3-methylcholanthrene	1.88(\pm 0.07)	10.96(\pm 0.54)
7-methylbenzo(a)pyrene	NR	7.56(\pm 0.42)
1,2,5,6-dibenzanthracene	NR	5.70(\pm 0.31)
Triphenylene	NR	5.27(\pm 1.05)
Dibenzothiophene	0.67(\pm 0.06)	4.73(\pm 0.05)
Anthracene	0.33(\pm 0.06)	3.09(\pm 0.32)
Thianthrene	0.49(\pm 0.06)	1.41(\pm 0.08)
Pyrene	0.51(\pm 0.05)	0.97(\pm 0.03)
Fluoranthene	NR	0.65(\pm 0.09)
Acenaphthene	NR	0.40(\pm 0.01)
Benzo(a)pyrene	0.22(\pm 0.02)	0.39(\pm 0.06)
Fluorene	NR	0.22(\pm 0.01)
Phenanthrene	NR	0.17(\pm 0.02)
Chrysene	NR	NR
9,10-dimethylanthracene	NR	NR
Naphthalene	NR	NR
Biphenyl	NR	NR

**Fig. 8.5** Chemical structures of EDCs: (a) bisphenol-A; (b) triclosan; (c) nonylphenol; (d) 17b-estradiol; (e) genistein; (f) b-sitosterol

A wide variety of xenobiotics can act as EDC (Fig. 8.5), bisphenol-A (BPA) and nonylphenol (NP) being the most extensively studied. They are widely dispersed in the environment, but they can mainly be found in wastewater effluents. BPA is used as a raw material for the production of polycarbonates and epoxy resins, and is present in the discharges of BPA producing factories, from installations that incorporate BPA into plastic, from leaching of plastic wastes and landfill sites.

The presence of NP in the environment is related to the biodegradation in sewage treatment plants of nonylphenol ethoxylates, which are mainly used as nonionic surfactants in domestic and industrial applications. For the EDC with estrogenic activity, it has been found that the main structural features are a phenolic ring that helps the binding to the estrogen receptor, and a hydrophobic substituent that helps the fitting in the cavity of the receptor [105]. Since they have a phenolic ring in their structure, they are especially susceptible to peroxidase degradation.

Several works report the EDC oxidation by manganese peroxidase. Using 10 U ml^{-1} of manganese peroxidase from *P. ostreatus*, 0.4 mM BPA was eliminated in 1 h. The reaction products identified indicate that the reaction is initiated by the withdrawal of one electron from the substrate to form phenoxy radicals. After electronic rearrangements, this radical would undergo random cleavage at the aromatic rings and C–C linkages to form a mixture of low molecular weight metabolites [106]. Huang and Weber [107] studied in detail the mechanism for the oxidation of BPA. They found the formation of monomers, dimers, trimers, and other compounds of high molecular weight, and the final concentration of BPA was lowered to submicromolar levels.

Estrone is a potent natural estrogen found in effluents of sewage treatment plants. Partially purified manganese peroxidase from *Phanerochaete sordida* was able to completely transform $10 \text{ }\mu\text{M}$ estrone in 2 h. This transformation was accompanied by the complete removal of estrogenic activity [108]. Tsutsumi et al. [109] used manganese peroxidase from the same fungus, and also demonstrated the

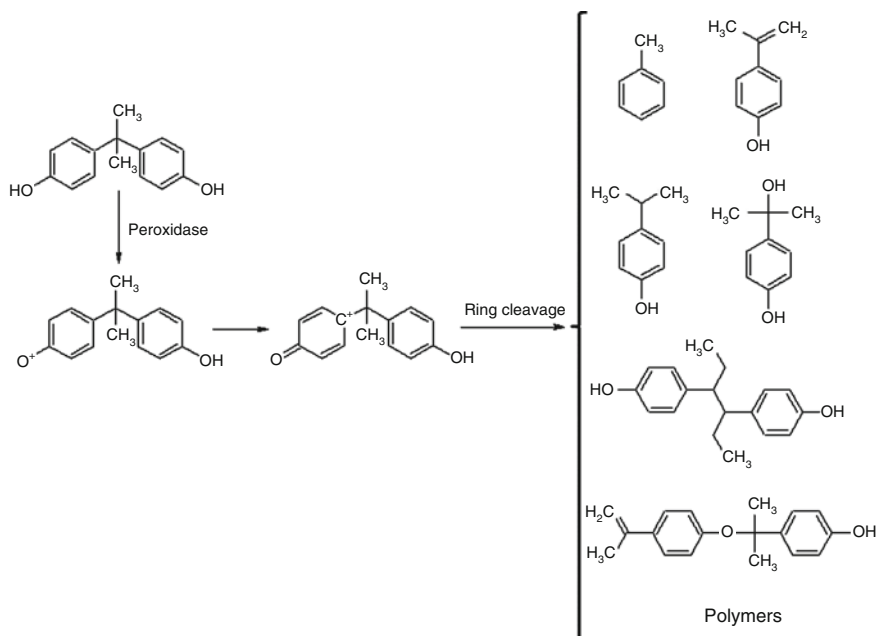


Fig. 8.6 Products identified for the transformation of BPA by peroxidases

disappearance of both BPA and NP in 1 h, but estrogenic activities only decreased to 40% and 60% after treatment, respectively. This indicates that some of the transformation products still have estrogenic activity. After 12 h, the activities were almost entirely removed, and this was correlated with the appearance of higher molecular weight compounds, probably polymerization products that due to the bulkiness would not be able to interact with the estrogen receptors (Fig. 8.6).

8.7 Pesticides

Pesticides include a broad range of substances most commonly used to control insects, weeds, and fungi. Insecticides are often subclassified by chemical type as organophosphates, organochlorines, carbamates, and pyrethroids [110]. Some studies have indicated that pesticide exposure is associated with chronic health problems or health symptoms such as respiratory problems, memory disorders, dermatologic conditions, cancer, depression, neurologic deficits, miscarriages, and birth defects [111].

The pesticide family most widely used in agricultural and residential applications is the organophosphates, which affect the nervous system by reducing the ability of the enzyme acetylcholinesterase to properly regulate the concentration of the neurotransmitter acetylcholine. If acetylcholine accumulates, the nerve impulses or neurons remain active longer than usual, overstimulating the nerves and muscles and causing symptoms such as weakness or muscle paralysis and death [112].

Jauregui et al. [113] studied the transformation of organophosphorus pesticides by white-rot fungi (Fig. 8.7). From several strains tested, the highest activities were found with *B. adusta* 8258, *P. ostreatus* 7989, and *P. chrysosporium* 3641. They depleted parathion, terbufos, azinphos-methyl, phosmet, and tribufos. The extracellular ligninolytic enzymes lignin peroxidase, manganese peroxidase, and laccase were produced by the fungi, but when the extracellular media or purified enzymes were tested, no activity on pesticides could be found. Further studies demonstrated that the microsomal fraction was able to transform the pesticides, indicating that cytochrome P450 activity may be involved. This transformation was correlated with a reduced toxicity as estimated by their capacity to inhibit acetylcholinesterase activity. The reaction products identified showed that cleavage of N–C and S–C bonds may occur.

On the other hand, Hernández et al. [114] reported the transformation of several organophosphorus pesticides by the chloroperoxidase from *C. fumago*. This enzyme was able to replace the sulfur atom by an oxygen atom, transforming the phosphorothioate group to an oxon derivative. No hydrolysis products were found nor chlorinated compounds. This enzymatic oxidation is similar to that performed by cytochromes P450, but no further cleavage was observed with chloroperoxidase, which is typical of P450-catalyzed reaction. As mentioned earlier, chloroperoxidase is also able to transform the halogenated pesticides 2,3,5,6-tetrachlorophenol and pentachlorophenol, and the main reaction products are

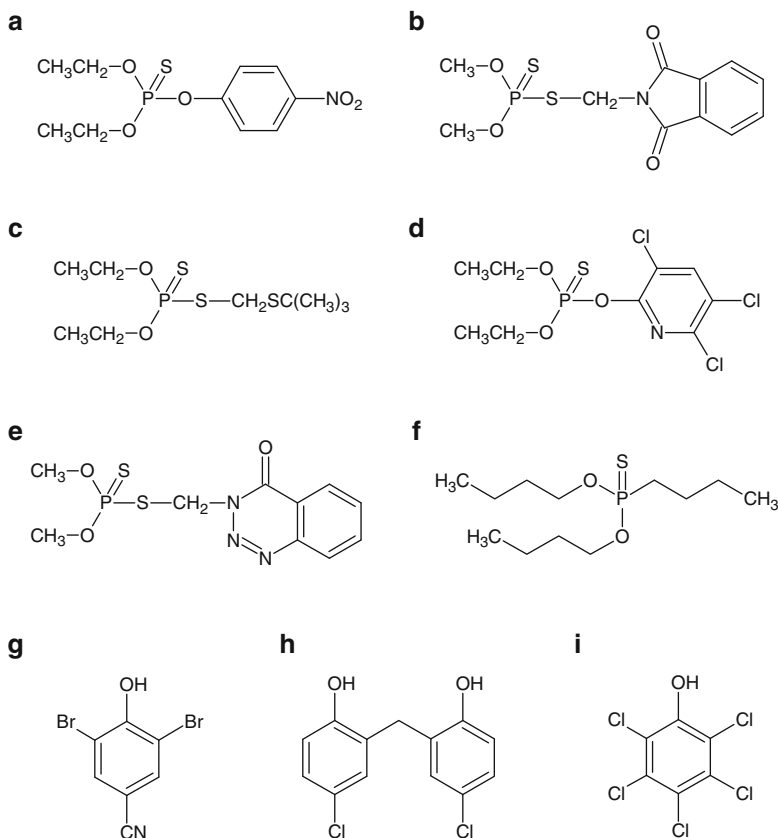


Fig. 8.7 Chemical structure of pesticides: (a) parathion; (b) phosmet; (c) terbufos; (d) chlopyrifos; (e) azinphos-methyl; (f) tribufos; (g) bomoxylin; (h) dichlorophene; (i) pentachlorophenol

polymers. For pentachlorophenol, the corresponding quinone is formed [69]. The transformation of these three pesticides by chloroperoxidase occurs with similar velocities (Table 8.3). It can be seen that the values of k_{cat} are one order of magnitude larger than for the transformation of other halogenated pesticides by versatile peroxidase. Since the peroxidase specificity on phenols is controlled by an electron transfer process, the difference in the activity constants is explained by the difference in the IP of the pesticides. The transformation of pesticides with higher IPs could be limited, as explained for PAHs [68].

Davila et al. [68] reported the transformation of the pesticides bromoxynil, dichlorophen, and pentachlorophenol by the versatile peroxidase from *B. adusta*. For the three transformed pesticides by versatile peroxidase, an oxidative dehalogenation was observed, a very important process since the halogenated pesticides are considered more persistent and toxic than the organophosphorus pesticides, because of the carbon–halogen bond. Enzymatic transformation of dichlorophen compound

Table 8.3 Kinetic parameters on the transformation of pesticides by peroxidases

Pesticide	Enzyme	k_{cat} (min^{-1})	K_M (μM)	References
Parathion	CPO (<i>C. fumago</i>)	1,092	1.2	[114]
Bromoxynil	VP (<i>B. adusta</i>)	409	31	[64]
Dichlorophene	VP (<i>B. adusta</i>)	194	32	[64]
Pentachlorophenol	CPO (<i>C. fumago</i>)	2,818	120	[65]
2,3,5,6-Tetrachlorophenol	CPO (<i>C. fumago</i>)	3,650	6	[65]

has been identified as 4-chlorophenol-2,2'-methylene-1,4-benzoquinone. This compound is not the end product from the versatile peroxidase transformation, as successive additions of enzyme and hydrogen peroxide depleted this first product to a nonidentified product. A dimer and a trimer are the main products from the peroxidase reaction on bromoxynil. Finally, the pentachlorophenol product from the versatile peroxidase transformation was unequivocally identified as 2,3,5,6-tetrachloro-1, 4-benzoquinone (chloranil).

8.8 Dioxins

Dioxins are some of the most toxic chemicals known to science. Dioxins are unwanted by products of a wide range of manufacturing processes including smelting, chlorine bleaching of paper pulp, and the manufacturing of some herbicides and pesticides. In terms of dioxin release into the environment, waste incinerators (solid waste and hospital waste) are often the worst culprits, due to incomplete burning [115]. One of the most toxic chemical in the class is 2,3,7,8-tetrachlorodibenzo-*para*-dioxin (TCDD) and probably the most toxic compound ever synthesized by man.

Although formation of dioxins is local, environmental distribution is global. Dioxins are found throughout the world in practically all ecosystems. The highest levels of these compounds are found in some soils, sediments, and food, especially dairy products, meat, fish, and shellfish. Very low levels are found in plants, water, and air [116].

There is a very broad range of toxic effects of dioxins. Many of the congeners can induce toxic responses at very low dose. The most sensitive effects are immunosuppression, developmental and reproductive toxicity, as well as neurological behavioral effects. Carcinogenic effects are induced at higher exposure. TCDD was considered a complete carcinogen by the International Agency for Research on Cancer, IARC [115].

The first report on the peroxidase transformation of dioxins was published by Hammel et al. in 1986 [116]. They transformed dibenzo[*p*]dioxin and 2-chlorodibenzo[*p*] dioxin with lignin peroxidase from *P. chrysosporium*. Later on, with the aim to elucidate the pathway for the fungal degradation of 2,7-dichlorodibenzo-*p*-dioxin, the oxidation products generated by lignin peroxidase and manganese peroxidase

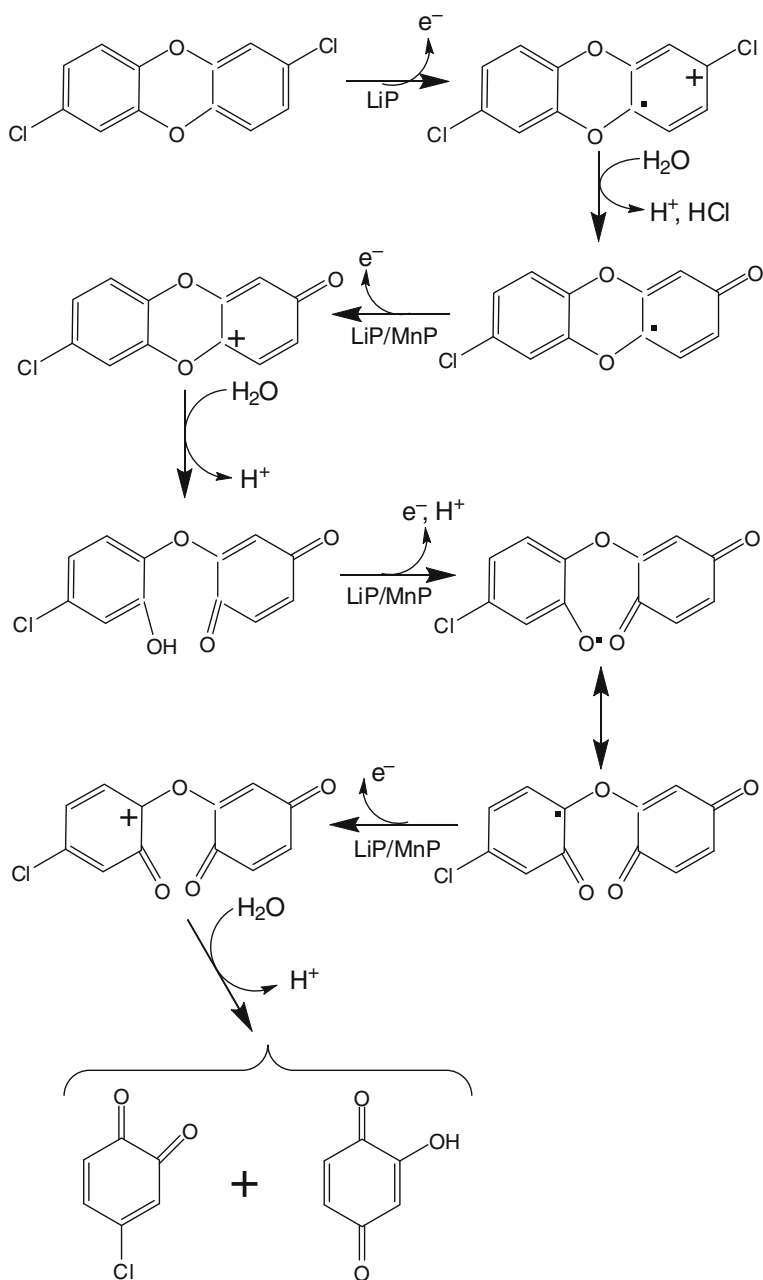


Fig. 8.8 Proposed mechanism for the dioxin oxidation catalyzed by lignin peroxidase [117]

were analyzed [117]. 2,7-Dichlorodibenzo-*p*-dioxin was slowly oxidized by lignin peroxidase to yield 4-chloro-1,2-benzoquinone and 2-hydroxy-1,4-benzoquinone. When veratryl alcohol was added to the reaction mixture, the product yields increased, but no additional products were observed. Manganese peroxidase was unable to oxidize 2,7-dichlorodibenzo-*p*-dioxin. A mechanism for the lignin peroxidase-catalyzed dioxin ring cleavage was proposed (Fig. 8.8). Both, lignin peroxidase and manganese peroxidase oxidized 1-chloro-3,4-dihydroxybenzene to 4-chloro-1,2-benzoquinone and 2-hydroxy-1,4-benzoquinone. Release of Cl⁻ was also observed. Finally, lignin peroxidase and manganese peroxidase oxidized 1-chloro-3,4-dimethoxybenzene to the *o*-quinone and 2-methoxy-1,4-benzoquinone.

Similarly to the 2,7-dichlorodibenzo-*p*-dioxin oxidation and on the basis of the products detected during lignin peroxidase oxidation of dibenzo-*p*-dioxin, it was concluded that the reaction is initiated by the one-electron oxidation of dibenzo-*p*-dioxin to its corresponding cation radical. The cation radical undergoes reactions with water to yield various quinone intermediates. The phenoxyquinone intermediates may undergo nonenzymatic as well as enzymatic reactions [118]. However, the nature of the final products is determined by the chlorine substitution pattern on the substrate. In the case of asymmetrically substituted chlorinated dibenzo-*p*-dioxin isomers, the initial attack of water on the corresponding cation radical could occur on either of the aromatic rings, leading to the formation of a large variety of products.

As mentioned above, manganese peroxidase was unable to oxidize 2,7-dichlorodibenzo-*p*-dioxin. Nevertheless, in the presence of polyunsaturated fatty acids, manganese peroxidase is able to form adducts with 2,7-dichlorodibenzo-*p*-dioxin [119].

An enzymatic method to remove dioxins from fishmeal has been investigated using *Coprinus cinereus* peroxidase, cloned and expressed in *Aspergillus* sp. and did not result in a major degradation of dioxins with only 10–15% reduction achieved [120].

In contrast, chlorophenols are transformed *in vitro* to polychlorinated dibenzo-*p*-dioxins and dibenzofurans by peroxidase-catalyzed oxidations. This has been demonstrated with bovine lactoperoxidase, horseradish peroxidase [71, 121] and myeloperoxidase [65] with 3,4,5- and 2,4,5-trichlorophenol.

8.9 Polychlorinated Biphenyls (PCBs)

Thirty years after their production ban in most industrialized countries, PCBs are still present in the environment and in the food chain. PCBs are manmade chemicals that never existed in nature until the 1900s when they started to be released into the environment by manufacturing companies and consumers. These chlorinated oils have a low degree of reactivity. They are not flammable, have high electrical resistance, good insulating properties, and are very stable even when exposed to heat and pressure. All in all, they seemed to be the perfect oil for use in dielectric fluids, and as insulators for transformers and capacitors. Uses for

PCBs quickly expanded to include hydraulic fluids, casting wax, carbonless carbon paper, compressors, heat transfer systems, plasticizers, pigments, adhesives, liquid cooled electric motors, fluorescent light ballasts, and the list goes on. PCBs make up a group of 209 individual chlorinated biphenyl rings known as congeners. They were typically manufactured as mixtures of 60 to 90 different congeners. Biodegradability is related to the amount of chlorination of a specific PCB. The biodegradability of a PCB is inversely proportional to the chlorine content. The lack of degradability of PCB compounds results in bioaccumulation of PCBs in the environment.

The most acutely toxic PCB congeners can assume relatively coplanar conformations, generally similar to that of TCDD, and are approximate stereo analogs of this compound. Toxic responses documented in mammals include thymic atrophy, a wasting syndrome, immunotoxic effects, reproductive impairment, porphyria and related liver damage, induction of specific isozymes of the cytochrome P450 system [122, 123], and cause neurological [124], developmental [125], respiratory [126], and reproductive problems as well as cancer due to estrogenic activity [127]. Due to their persistence and lipophilicity, PCBs bio-magnify once entering the aquatic food chain.

White-rot fungi have been shown to mineralize very recalcitrant environmental pollutants such as PCBs [128–130]. Even if detectable levels of lignin peroxidase and manganese peroxidase activity were present in culture supernatants, no correlation was observed among any combination of PCB congener biodegradation, mineralization, and lignin peroxidase or manganese peroxidase activity.

In plant cells, a peroxidase activity showed to be correlated with the ability of plant cultures to metabolize PCBs. Nevertheless, as mentioned above in fungal cultures, no correlation of manganese- and lignin-peroxidase activities with PCB degradation was found [131].

On the other hand, the metabolites produced by the *in vivo* PCB fungal metabolism are not quite the same as those observed upon incubation with horseradish peroxidase [132]. The peroxidase-catalyzed transformation of PCB started with a dechlorination, and although the metabolites identified were mainly chlorinated hydroxybiphenyls, benzoic acids, and nonsubstituted 1,1'-biphenyl, some higher chlorinated biphenyl isomers also appeared. In addition, it has been demonstrated that significant coupling and removal of PCBs occurs during horseradish peroxidase-catalyzed oxidative coupling reactions in the presence of natural organic matter [133].

8.10 Dyes

Synthetic dyes are mainly aromatic organic compounds, and they can be classified as cationic (basic dyes), anionic (direct, acid, and reactive dyes), or nonionic (disperse dyes) type [134]. Synthetic dyes are mainly used in the textile industries, but they have many other applications such as in printing, leather, papermaking, drug, and food industries [85]. Total world colorant production is estimated to be

about 800,000 tons per year [135]. By 2005, it was estimated that about 50,000 tons are discharged annually to wastewaters. They are very important pollutants since many commercial dyes have a high stability to light, temperature, detergents, and microbial attack, which make them resistant to biodegradation. It has been found that some dyes are mutagenic as well as carcinogenic [136]. For example, the biotransformation of azo dyes, which represent half of the dye production, produces aryl amines that can be oxidized to the corresponding *N*-hydroxy derivatives. These compounds are subsequently transformed to reactive electrophiles capable of forming covalent linkages with DNA [137]. The most toxic dyes are those containing *p*-diphenylenediamine and benzidine moieties [85].

The transformation of dyes by white-rot fungi has been extensively studied [134, 138, 139]. Eichlerová et al. [140] studied the degradation of azo and anthraquinone dyes by 30 different strains. *Dichomitus squalens*, *Ischnoderma resinosum*, and *Pleurotus calypttratus* gave the best results. The decolorization activities were correlated with the production of manganese peroxidase and laccase. Nevertheless, Rodriguez et al. [141] studied the decolorization of 23 industrial dyes with solid-state cultures of 16 different fungal strains grown on whole oats. Laccase, manganese peroxidase, lignin peroxidase, and aryl alcohol oxidase activities were determined in crude extracts. Only laccase activity correlated with the decolorization activity of the crude extracts. Two laccase isoenzymes from *Trametes hispidata* were purified, and their decolorization activity was characterized.

In the azo dyes transformation mediated by lignin peroxidase from *P. chrysosporium*, a cleavage of the azo bond was observed resulting in the production of a quinone and sulfophenyl hydroperoxides [142]. With this data, a mechanism for the peroxidase-catalyzed oxidation of phenolic-azo dyes has been proposed (Fig. 8.9). A carbonium ion is formed after two successive one-electron oxidations of the phenolic by the enzyme. When a water molecule reacts with the phenolic carbon bearing the azo linkage, an unstable hydroxyl intermediate is formed, which breaks down into a quinone and an amidophenyldiazine. The latter compound is then oxidized by oxygen into the corresponding phenyldiazene radical, which after elimination of nitrogen gives a phenyl radical finally oxidized by oxygen. This mechanism leads to the detoxification of azo dyes since no aromatic amines are formed.

Sulfonphthalein dyes have been transformed by extracellular extracts from *P. ostreatus*. The decolorizing activities were associated with manganese peroxidase and manganese-independent peroxidase enzymes. Different dyes were transformed; it was found that an increase in the degree of halogenation of dyes made them better substrates for manganese-independent peroxidase [143].

Peroxidases purified from plants have also been used for the degradation of dyes. Purified peroxidase of *Saccharum spontaneum* leaf could degrade a variety of dyes ranging from the 70% to 100% in 1 h [144]. A peroxidase of *Ipomea palmata* was also able to transform different dyes, but less effectively. A peroxidase purified from *Senna angustifolia* oxidized alizarin and purpurin anthraquinones efficiently to produce the respective bianthraquinones; the same reaction was catalyzed by horseradish peroxidase [145].

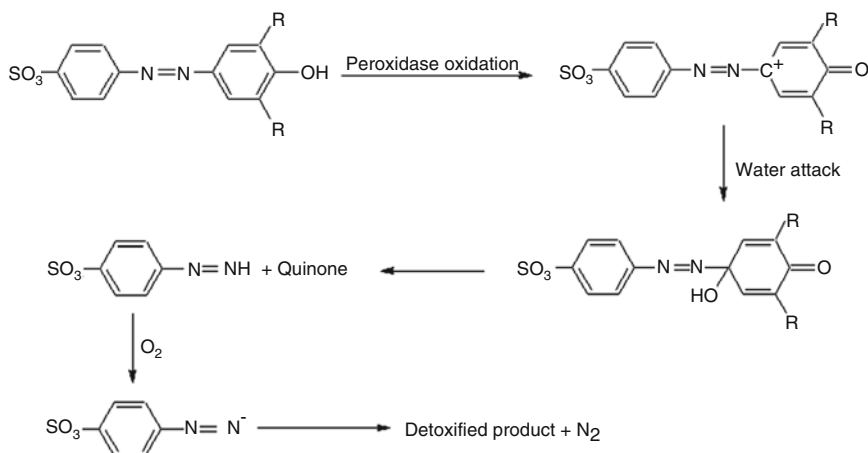


Fig. 8.9 Proposed mechanism for azo dye decolorization by peroxidases

The presence of different heavy metals in the effluents of contaminated waters can be useful for the degradation of dyes because the activity of some enzymes such as manganese peroxidase and laccase could be enhanced in the presence of metals [135].

8.11 Challenges for the Industrial Applications of Peroxidase for Environmental Purposes

In spite of their catalytic versatility and their capacity to transform a variety of pollutant compounds, peroxidases are not applied at large scale yet. The challenges that should be solved to use peroxidases for environmental purposes have been recently reviewed [146]. Three main protein engineering challenges have been identified: (a) the enhancement of operational stability, specifically hydrogen peroxide stability (see Chap. 11); (b) the increase of the enzyme redox potential in order to widen the substrate range (see Chap. 4); (c) the development of heterologous expression and industrial production (see Chap. 12).

The large-scale application of peroxidases is mainly constrained by low operational stability, arising from low stability in the presence of hydrogen peroxide [43]. This problem is largely discussed in the Chap. 11 of this book. All heme-proteins, including peroxidases, are inactivated in the presence of catalytic concentrations of their natural substrate, hydrogen peroxide. This suicide inactivation process is particularly important in the absence of reducing substrates or in the presence of an excess of hydrogen peroxide, and its mechanism has not been fully elucidated.

On the other hand, the protein engineering tools, specially applied on the peroxidase active site, could enhance the redox limitation of peroxidases widening the substrate range (see Chap. 4). The oxidative capacity of heme-peroxidases is determined by a combination of factors, such as active site topology, substrate accessibility, and redox potential [145–148]. Theoretically, peroxidase-catalyzed reactions have a thermodynamic threshold of 1.7 V, equivalent to the standard redox potential of hydrogen peroxide reduction to water. Thus, by increasing their redox potential to approach those values, the catalytic performance could be increased. A semilogarithmic correlation has been observed between the specific activity of peroxidase-catalyzed reactions and the IP of substrates [86–88, 96, 97, 149]. Data on the redox potential of peroxidase is particularly scarce. Recently, a method to estimate the redox potential of peroxidases based on the catalytic performance of the activated enzyme has been published [147]. *p*-Substituted phenols were used as substrates to estimate the redox potential for different peroxidases, and the results obtained with this catalytic method correlate well with the oxidative capacity predicted by the redox potential values of the Fe(III)/Fe(II) couple. According to these results, versatile peroxidase seems to be the more efficient enzyme in terms of oxidative capacity, as the redox potential of the activated species approaches the theoretical threshold of 1.7 V, fixed by the potential associated with the reduction of hydrogen peroxide to water.

Besides the information shown in Chap. 12 of this book, cloning and heterologous expression of peroxidases has been recently reviewed [146]. A significant research effort has been performed for the development of a recombinant expression system for fungal peroxidases. Fungal peroxidases are postranscriptionally modified, thus the recombinant system must be able to promote proper folding, which depends on the correct coordination of the prosthetic heme group, formation of disulfide bridges, and inclusion of structural calcium ions [150]. Glycosylation appears to enhance stability and solubility, but it has no effect on activity [151]. Although homologous production may be an alternative, no overproduction has been achieved so far. Traditional molecular strategies to increase heterologous protein production in fungi include the introduction of multiple copies of the gene, expression under a strong endogenous promoter, use of protease-deficient strains, and use of an appropriate signal peptide and/or fusion protein [152, 153]. As the fundamental comprehension of the expression and secretion fungal pathways advances, better techniques and experimental designs may be developed to fully exploit filamentous fungi as recombinant systems.

Finally, the design and development of an environmental biocatalyst should then focus on the production of an enzyme stable to the presence of hydrogen peroxide and operational conditions, with a high redox potential to be able to oxidize a wide range of xenobiotics or pollutants, and overexpressed at large scale in industrial microorganisms. Protein engineering, bioinformatics, bioengineering, and molecular tools, doubtless, will be able to develop biocatalysts for biotechnological processes that could be used to reduce or eliminate the environmental impact of pollutant xenobiotics.

References

1. US Environmental Protection Agency (2008) Toxics Release Inventory (TRI) Program. <http://www.epa.gov/TRI/>. Accessed 27 July 2009
2. Pimentel D, Tort M, D'Anna L et al (1998) Ecology of increasing disease: Population growth and environmental degradation. *BioScience* 48:817–826
3. Pimentel D, Cooperstei S, Randell H et al (2007) Ecology of increasing diseases: population growth and environmental degradation. *Hum Ecol* 35:653–668
4. Population Resource (2004) The Globalization of Infectious Disease. <http://www.prcdc.org/summaries/disease/disease.html>. Accessed 2 October 2004
5. Schönbein CF (1863) Ueber die Katalytische Wirksamkeit organischer Materien und deren Verbreitung in der Pflanzen- und Thierwelt. *J Prakt Chem* 98:323–344
6. Linossier G (1898) Contribution à l'étude des ferments oxidants. Sur la peroxidase du pupa. *CR Soc Biol Paris* 50:373–375
7. Willstätter R, Pollinger A (1923) Über Peroxydase (Dritte Addandlung). *Liebigs Ann Chem* 430:269–319
8. Willstätter R, Stoll A (1918) Über Peroxydase. *Liebigs Ann Chem* 416:21–64
9. Nicell JA, Al-Kassim L, Bewtra JK et al (1993) Wastewater treatment by enzyme catalyzed polymerization and precipitation. *Water Res* 27:1629–1639
10. Karam J, Nicell JA (1997) Potential applications of enzymes in waste treatment. *J Chem Technol Biotechnol* 69:141–153
11. Aoyama H, Hojo H, Takahashi KL et al (2005) A two-generation reproductive toxicity study of 2, 4-dichlorophenol in rats. *Toxicol Sci* 30:59–78
12. Kobayashi S, Fukuda T, Kawaguchi K et al (1972) Chronic toxicity of 2, 4-dichlorophenol in mice: a simple design for checking the toxicity of residual metabolites of pesticides. *J Med Soc* 19:356–362
13. US Environmental Protection Agency (1991) Superfund national priorities list for remediation. 40 CFR 423.A, Code of Federal Regulations
14. Deborde M, von Gunten U (2008) Reactions of chlorine with inorganic and organic compounds during water treatment-Kinetics and mechanisms: a critical review. *Water Res* 42:13–51
15. Aitken MD (1993) Waste treatment applications of enzymes: opportunities and obstacles. *Chem Eng J* 52:B49–B58
16. Job D, Dunford HB (1976) Substituent effect on the oxidation of phenols and aromatic amines by horseradish peroxidase compound I. *Eur J Biochem* 66:607–614
17. Dawson JH (1988) Probing structure-function relations in heme-containing oxygenases and peroxidases. *Science* 240:433–439
18. Nannipieri P, Bollag JM (1991) Use of enzymes to detoxify pesticide – contaminated soils and waters. *J Environ Qual* 20:510–517
19. Bollag JM (1992) Decontaminating soil with enzymes. *Environ Sci Technol* 26:1876–1881
20. Bollag JM (1992) Enzymes catalyzing oxidative coupling reactions of pollutants. In: Sigel H, Sigel A (eds) *Metal ions in biological systems*, vol 28. Taylor and Francis, UK
21. Husain Q, Jan U (2000) Detoxification of phenols and aromatic amines from polluted wastewater by using phenol oxidases. *J Sci Ind Res* 59:286–293
22. Akhtar S, Husain Q (2006) Potential applications of immobilized bitter melon (*Momordica charantia*) peroxidase in the removal of phenols from polluted water. *Chemosphere* 65:1228–1235
23. Bodalo A, Gomez JL, Gomez E et al (2006) Comparison of commercial peroxidases for removing phenol from water solutions. *Chemosphere* 63:626–632
24. Danner DJ, Brignac PJ Jr, Arceneaux D et al (1973) The oxidation of phenol and its reaction product by horseradish peroxidase and hydrogen peroxide. *Arch Biochem Biophys* 156:759–763

25. Caza N, Bewtra JK, Biswas N et al (1999) Removal of phenolic compounds from synthetic wastewater using soybean peroxidase. *Water Res* 33:3012–3018
26. Gomez JL, Bodalo A, Gomez E et al (2006) Immobilization of peroxidases on glass beads: an improved alternative for phenol removal. *Enzyme Microb Technol* 39: 1016–1022
27. Duarte-Vázquez MA, Ortega-Tovar M, García-Almendárez B et al (2003) Removal of aqueous phenolic compounds from a model system by oxidative polymerization with turnip (*Brassica napus* L. var purple top white globe) peroxidase. *J Chem Technol Biotechnol* 78:42–47
28. Dunford HB (1990) In: Everse J, Everse KE, Grisham HB (eds) *Peroxidase in chemistry and biology*. CRC, Ann Arbor, MI
29. Nicell JA (1994) Kinetics of horseradish peroxidase-catalysed polymerization and precipitation of aqueous 4-chlorophenol. *J Chem Technol Biotechnol* 60:203–215
30. Yu J, Taylor KE, Zou H et al (1994) Phenol conversion and dimeric intermediates in horseradish peroxidase-catalyzed phenol removal from water. *Environ Sci Technol* 28:2154–2160
31. Dec J, Bollag JM (2000) Phenoloxidase-mediated interactions of phenols and anilines with humic materials. *J Environ Qual* 29:665–676
32. Park JW, Dec J, Kim JE et al (1999) Effect of humic constituents on the transformation of chlorinated phenols and anilines in the presence of oxidoreductive enzymes or birnessite. *Environ Sci Technol* 33:2028–2034
33. Ward G, Hadar Y, Bilkis I et al (2001) Initial steps of ferulic acid polymerization by lignin peroxidase. *J Biol Chem* 276:18734–18741
34. Bollag JM, Liu SY (1985) Copolymerization of halogenated phenols and syringic acid. *Pestic Biochem Physiol* 23:261–271
35. Sarkar JM, Bollag JM, Malcolm RL (1988) Enzymatic coupling of 2, 4-dichlorophenol to stream fulvic acid in the presence of oxidoreductases. *Soil Sci Soc Am J* 52:688–694
36. Hatcher PG, Bortiatynski JM, Minard RD et al (1993) Use of high-resolution carbon-13 NMR to examine the enzymatic covalent binding of carbon-13-labeled 2, 4-dichlorophenol to humic substances. *Environ Sci Technol* 27:2096–2103
37. Dec J, Bollag JM (1994) Dehalogenation of chlorinated phenols during oxidative coupling. *Environ Sci Technol* 28:484–490
38. Roper JC, Sarkar JM, Dec J et al (1995) Enhanced enzymatic removal of chlorophenols in the presence of co-substrates. *Water Res* 29:2720–2724
39. Kim JE, Wang CJ, Bollag JM (1997) Interaction of reactive and inert chemicals in the presence of oxidoreductases: Reaction of the herbicide bentazon and its metabolites with humic monomers. *Biodegradation* 8:387–392
40. Park JW, Dec J, Kim JE et al (2000) Dehalogenation of xenobiotics as a consequence of binding to humic materials. *Arch Environ Contam Toxicol* 38:405–410
41. Park JW, Dec J, Kim JE et al (2000) Transformation of chlorinated phenols and anilines in the presence of humic acid. *J Environ Qual* 29:214–220
42. Huang Q, Weber WJ Jr (2004) Interactions of soil-derived dissolved organic matter with phenol in peroxidase-catalyzed oxidative coupling reactions. *Environ Sci Technol* 38:338–344
43. Valderrama B, Ayala M, Vazquez-Duhalt R (2002) Suicide inactivation of peroxidases and the challenge of engineering more robust enzymes. *Chem Biol* 9:555–565
44. Klibanov AM, Tu TM, Scott KP (1983) Peroxidase catalyzed removal of phenols from coal conversion wastewater. *Science* 221:259–261
45. Nakamoto S, Machida N (1992) Phenol removal from aqueous solutions by peroxidase-catalyzed reaction using additives. *Water Res* 26:49–54
46. Tatsumi K, Wada S, Ichikawa H (1996) Removal of chlorophenols from wastewater by immobilized horseradish peroxidase. *Biotechnol Bioeng* 51:126–130

47. Quintanilla-Guerrero F, Duarte-Vázquez MA, García-Almendarez BE et al (2008) Polyethylene glycol improves phenol removal by immobilized turnip peroxidase. *Bioresour Technol* 99:8605–8611
48. Quintanilla-Guerrero F, Duarte-Vázquez M, Tinoco R et al (2008) Chemical modification of turnip peroxidase with methoxypolyethylene glycol enhances activity and stability for phenols removal using the immobilized enzyme. *J Agric Food Chem* 56:8058–8065
49. Zhao F, Mayura K, Hutchinson RW et al (1995) Developmental toxicity and structure-activity relationship of chlorophenols using human embryonic palatal mesenchymal cells. *Toxicol Lett* 78:35–42
50. Ahlborg UG, Thunberg TM (1980) Chlorinated phenols: occurrence, toxicity, metabolism, and environmental impact. *Crit Rev Toxicol* 7:1–35
51. Jensen J (1996) Chlorophenols in the terrestrial environment. *Rev Environ Contam Toxicol* 146:25–51
52. Proudfoot AT (2003) Pentachlorophenol poisoning. *Toxicol Rev* 22:3–11
53. Dai J, Wright MW, Manderville RA (2003) An oxygen-bonded c8-deoxyguanosine nucleoside adduct of pentachlorophenol by peroxidase activation: evidence for ambident c8 reactivity by phenoxy radicals. *Chem Res Toxicol* 16:817–821
54. Dai J, Sloat AL, Wright MW et al (2005) Role of phenoxy radicals in DNA adduction by chlorophenol xenobiotics following peroxidase activation. *Chem Res Toxicol* 18:771–779
55. Reddy GVB, Gold MH (2000) Degradation of pentachlorophenol by *Phanerochaete chrysosporium*: intermediates and reactions involved. *Microbiology* 146:405–413
56. Shim SS, Kawamoto K (2002) Enzyme production activity of *Phanerochaete chrysosporium* and degradation of pentachlorophenol in a bioreactor. *Water Res* 36:4445–4454
57. Fahr K, Wetzstein HG, Grey R et al (1999) Degradation of 2, 4-dichlorophenol and pentachlorophenol by two brown rot fungi. *FEMS Microbiol Lett* 175:127–132
58. Leontievsky AA, Myasoedova NM, Golovleva LA et al (2002) Adaptation of the white-rot basidiomycete *Panus tigrinus* for transformation of high concentrations of chlorophenols. *Appl Microbiol Biotechnol* 59:599–604
59. Walter M, Boul L, Chong R et al (2004) Growth substrate selection and biodegradation of PCP by New Zealand white-rot fungi. *J Environ Manage* 71:361–369
60. Hammel KE, Tardone PJ (1988) The oxidative 4-dechlorination of polychlorinated phenols is catalyzed by extracellular fungal lignin peroxidases. *Biochemistry* 27:6563–6568
61. Chung N, Aust SD (1995) Veratryl alcohol-mediated indirect oxidation of pentachlorophenol by lignin peroxidase. *Arch Biochem Biophys* 322:143–148
62. Rüttimann-Johnson C, Lamar RT (1996) Polymerization of pentachlorophenol and ferulic acid by fungal extracellular lignin-degrading enzymes. *Appl Environ Microbiol* 62:3890–3893
63. Samokyszyn VM, Freeman JP, Rao Maddipati K et al (1995) Peroxidase-catalyzed oxidation of pentachlorophenol. *Chem Res Toxicol* 8:349–355
64. Choi YJ, Chae HJ, Kim EY (1999) Steady-state oxidation model by horseradish peroxidase for the estimation of the non-inactivation zone in the enzymatic removal of pentachlorophenol. *J Biosci Bioeng* 88:368–373
65. Wittsiepe J, Kullmann Y, Schrey P et al (2000) Myeloperoxidase-catalyzed formation of PCDD/F from chlorophenols. *Chemosphere* 40:963–968
66. Oberg LG, Paul KG (1985) The transformation of chlorophenols by lactoperoxidase. *Biochim Biophys Acta* 842:30–38
67. Osman AM, Posthumus MA, Veeger C et al (1998) Conversion of pentahalogenated phenols by microperoxidase-8/H₂O₂ to benzoquinone-type products. *Chem Res Toxicol* 11:1319–1325
68. Davila-Vazquez G, Tinoco R, Pickard MA et al (2005) Transformation of halogenated pesticides by versatile peroxidase from *Bjerkandera adusta*. *Enzyme Microbiol Technol* 36:223–231

69. Longoria A, Tinoco R, Vazquez-Duhalt R (2008) Chloroperoxidase-mediated transformation of highly halogenated monoaromatic compounds. *Chemosphere* 72:485–490
70. Kazunga C, Aitken MD, Gold A (1999) Primary product of the horseradish peroxidase-catalyzed oxidation of pentachlorophenol. *Environ Sci Technol* 33:1408–1412
71. Wittsiepe J, Kullmann Y, Schrey P et al (1999) Peroxidase-catalyzed *in vitro* formation of polychlorinated dibenzo-p-dioxins and dibenzofurans from chlorophenols. *Toxicol Lett* 106:191–200
72. Renner G (1980) Metabolic studies on pentachloronitrobenzene (PCNB) in rats. *Xenobiotica* 10:537–550
73. Fushiwaki Y, Tase N, Saeki A et al (1990) Pollution by the fungicide pentachloronitrobenzene in an intensive farming area in Japan. *Sci Total Environ* 92:55–67
74. Tas DO, Pavlostathis SG (2005) Microbial reductive transformation of pentachloronitrobenzene under methanogenic conditions. *Environ Sci Technol* 39:8264–8272
75. Larsen GL, Huwe JK, Bakke JE (1998) Intermediary metabolism of pentachloronitrobenzene in the control and germ-free rat and rat with cannulated bile ducts. *Xenobiotica* 28:973–984
76. Clary T, Ritz B (2003) Pancreatic cancer mortality and organochlorine pesticide exposure in California, 1989–1996. *Am J Ind Med* 43:306–313
77. de Wolf W, Opperhuizen A, Seinen W et al (1991) Influence of survival time on the lethal body burden of 2, 3, 4, 5-tetrachloroaniline in the guppy, *Poecilia reticulata*. *Sci Total Environ* 109–110:457–459
78. Argese E, Bettiol C, Agnoli F et al (2001) Assessment of chloroaniline toxicity by the submitochondrial particle assay. *Environ Toxicol Chem* 20:826–832
79. Ribo JM, Kaiser KLE (1984) Toxicities of chloroanilines to *Photobacterium phosphoreum* and their correlations with effects on other organisms and structural parameters. In: Kaiser KLE (ed) QSAR in environmental toxicology. D. Reidel, Dordrecht, The Netherlands
80. Sixt S, Altschuh J, Brüggemann R (1995) Quantitative structure-toxicity relationships for 80 chlorinated compounds using quantum chemical descriptors. *Chemosphere* 30:2397–2414
81. Arjmand A, Sandermann H (1985) Mineralization of chloroaniline/lignin conjugates and of free chloroanilines by the white rot fungus *Phanerochaete chrysosporium*. *J Agric Food Chem* 33:1055–1060
82. Corbett MD, Chipko BR, Baden DG (1978) Chloroperoxidase-catalyzed oxidation of 4-chloroaniline to 4-chloronitrosobenzene. *Biochem J* 175:353–360
83. Corbett MD, Chipko BR, Batchelor AO (1980) The action of chloride peroxidase on 4-chloroaniline. *Biochem J* 187:893–903
84. Harayama S (1997) Polycyclic aromatic hydrocarbon bioremediation design. *Curr Opin Biotechnol* 8:268–273
85. Torres E, Bustos-Jaimes I, Le Borgne S (2003) Potential use of oxidative enzymes for the detoxification of organic pollutants. *Appl Catal B* 46:1–15
86. Weber R, Gaus C, Tysklind M et al (2008) Dioxin- and POP-contaminated sites-contemporary and future relevance and challenges: overview on background, aims and scope of the series. *Environ Sci Pollut Res Int* 15:363–393
87. Ayala M, Robledo NR, Lopez-Munguia A et al (2000) Substrate specificity and ionization potential in chloroperoxidase-catalyzed oxidation of diesel fuel. *Environ Sci Technol* 34:2804–2809
88. Harford-Cross CF, Carmichael AB, Allan FK et al (2000) Protein engineering of cytochrome P450cam (CYP101) for the oxidation of polycyclic aromatic hydrocarbons. *Protein Eng* 13:121–128
89. Masaphy S, Levanon D, Henis Y et al (1995) Bioconversion of recalcitrant 4-methylthiophene to water-extractable products using lignin-degrading basidiomycete *Coriolus versicolor*. *Biotechnol Lett* 17:969–974

90. Torres E, Sandoval JV, Rosell FI et al (1995) Site-directed mutagenesis improves biocatalytic activity of iso-1-cytochrome c in polycyclic hydrocarbon oxidation. *Enzyme Microb Technol* 17:1014–1020
91. Ortiz-Leon M, Velasco L, Vazquez-Duhalt R (1995) Biocatalytic oxidation of polycyclic aromatic hydrocarbons by hemoglobin and hydrogen peroxide. *Biochem Biophys Res Comm* 215:968–973
92. Durant JL, Busby WF, Lafleur AL et al (1996) Human cell mutagenicity of oxygenated, nitrated and unsubstituted polycyclic aromatic hydrocarbons associated with urban aerosols. *Mutat Res* 371:123–157
93. Meulenberg R, Rijnaarts HHM, Doddema HJ et al (1997) Partially oxidized polycyclic aromatic hydrocarbons show an increased bioavailability and biodegradability. *FEMS Microbiol Lett* 152:145–149
94. Bogan BW, Lamar RT (1995) One-electron oxidation in the degradation of creosote polycyclic aromatic hydrocarbons by *Phanerochaete chrysosporium*. *Appl Environ Microbiol* 61:2631–2633
95. Torres E, Vazquez-Duhalt R (2000) Chemical modification of hemoglobin improves biocatalytic oxidation of PAH's. *Biochem Biophys Res Comm* 273:820–823
96. Hayashi Y, Yamazaki I (1979) The oxidation-reduction potentials of compound I/compound II and compound II/ferric couples of horseradish peroxidases A2 and C. *J Biol Chem* 254:9101–9106
97. Wang Y, Vazquez-Duhalt R, Pickard MA (2002) Purification, characterization, and chemical modification of manganese peroxidase from *Bjerkandera adusta* UAMH 8258. *Curr Microbiol* 45:77–87
98. Wang Y, Vazquez-Duhalt R, Pickard MA (2003) Manganese-lignin peroxidase hybrid from *Bjerkandera adusta* oxidizes polycyclic aromatic hydrocarbons more actively in the absence of manganese. *Can J Microbiol* 49:675–682
99. Bogan BW, Lamar RT, Hammel KE (1996) Fluorene oxidation *in vivo* by *Phanerochaete chrysosporium* and *in vitro* during manganese peroxidase-dependent lipid peroxidation. *Appl Environ Microbiol* 62:1788–1792
100. Vázquez-Duhalt R, Ayala M, Márquez-Rocha FJ (2001) Biocatalytic chlorination of aromatic hydrocarbons by chloroperoxidase of *Caldariomyces fumago*. *Phytochemistry* 58:929–933
101. Vazquez-Duhalt R (1999) Cytochrome c as biocatalyst. *J Mol Catal B Enzym* 7:241–249
102. Tinoco R, Vazquez-Duhalt R (1998) Chemical modification of cytochrome C improves their catalytic properties in oxidation of polycyclic aromatic hydrocarbons. *Enzyme Microb Technol* 22:8–12
103. Cabana H, Agathos SN (2007) Elimination of endocrine disrupting chemicals using white rot fungi and their lignin modifying enzymes: a review. *Eng Life Sci* 7:429–456
104. Soares A, Jonasson K, Terrazas E et al (2005) The ability of white-rot fungi to degrade the endocrine-disrupting compound nonylphenol. *Appl Microbiol Biotechnol* 66:719–725
105. Vazquez-Duhalt R, Marquez-Rocha F, Ponce E et al (2006) Nonylphenol, an integrated vision of a pollutant. *Appl Ecol Environ Res* 4:1–25
106. Hirano T, Honda Y, Watanabe T et al (2000) Degradation of bisphenol A by the lignin-degrading enzyme, manganese peroxidase, produced by the white-rot basidiomycete, *Pleurotus ostreatus*. *Biosci Biotechnol Biochem* 64:1958–1962
107. Huang Q, Weber WJ (2005) Transformation and removal of bisphenol A from aqueous phase via peroxidase-mediated oxidative coupling reactions: efficacy, products, and pathways. *Environ Sci Technol* 39:6029–6036
108. Tamagawa Y, Yamaki R, Hirai H et al (2006) Removal of estrogenic activity of natural steroidal hormone estrone by ligninolytic enzymes from white rot fungi. *Chemosphere* 65:97–101
109. Tsutsumi Y, Haneda T, Nishida T (2001) Removal of estrogenic activities of bisphenol A and nonylphenol by oxidative enzymes from lignin-degrading basidiomycetes. *Chemosphere* 42:271–276

110. Kamel F, Hoppin JA (2004) Association of pesticide exposure with neurologic dysfunction and disease. *Environ Health Perspect* 112:950–958
111. McCauley LA, Anger WK, Keifer M et al (2006) Studying health outcomes in farmworker populations exposed to pesticides. *Environ Health Perspect* 114:953–960
112. Engel LS, Checkoway H, Keifer MC et al (1998) Neurophysiological function in farm workers exposed to organophosphate pesticides. *Arch Environ Health* 53:7–14
113. Jauregui J, Valderrama B, Albores A et al (2003) Microsomal transformation of organophosphorus pesticides by white rot fungi. *Biodegradation* 14:397–406
114. Hernandez J, Robledo NR, Velasco L et al (1998) Chloroperoxidase-mediated oxidation of organophosphorus pesticides. *Pestic Biochem Physiol* 61:87–94
115. Schecter A, Birnbaum L, Ryan JJ et al (2006) Dioxins: an overview. *Environ Res* 101:419–428
116. Hammel KE, Kalyanaraman B, Kirk TK (1986) Oxidation of polycyclic aromatic hydrocarbons and dibenzo[p]-dioxins by *Phanerochaete chrysosporium* ligninase. *J Biol Chem* 261:16948–16952
117. Valli K, Wariishi H, Gold MH (1992) Degradation of 2, 7-dichlorodibenzo-p-dioxin by the lignin-degrading basidiomycete *Phanerochaete chrysosporium*. *J Bacteriol* 174:2131–2137
118. Joshi DK, Gold MH (1994) Oxidation of dibenzo-p-dioxin by lignin peroxidase from the basidiomycete *Phanerochaete chrysosporium*. *Biochemistry* 33:10969–10976
119. Harazono K, Watanabe Y, Fukatsu T et al (2003) Trapping of 2, 7-dichlorodibenzo-p-dioxin in aqueous solution by enzymatic reaction of fungal manganese peroxidase in the presence of polyunsaturated fatty acids. *Curr Microbiol* 47:250–254
120. Baron CP, Børresen T, Jacobsen C (2007) Comparison of methods to reduce dioxin and polychlorinated biphenyls contents in fishmeal: extraction and enzymatic treatments. *J Agric Food Chem* 55:1620–1626
121. Oberg LG, Glas B, Swanson SE et al (1990) Peroxidase-catalyzed oxidation of chlorophenols to polychlorinated dibenzo-p-dioxins and dibenzofurans. *Arch Environ Contam Toxicol* 19:930–938
122. Safe S (1984) Polychlorinated biphenyls (PCBs) and polybrominated biphenyls (PBBs): biochemistry, toxicology, and mechanism of action. *Crit Rev Toxicol* 13:319–393
123. Safe S (1990) Polychlorinated biphenyls (PCBs), dibenzo-p-dioxins (PCDDs), dibenzofurans (PCDFs), and related compounds: environmental and mechanistic considerations which support the development of toxic equivalency factors (TEFs). *Crit Rev Toxicol* 21:51–58
124. Seegal RF, Schantz SL (1994) Neurochemical and behavioral sequelae of exposure to dioxins and PCBs. In: Schecter A (ed) *Dioxins and health*. Plenum, New York, N.Y., pp 409–447
125. Patandin S, Dagnelie PC, Mulder PGH et al (1999) Dietary exposure to polychlorinated biphenyls and dioxins from infancy until adulthood: a comparison between breast-feeding, toddler, and long-term exposure. *Environ Health Perspect* 107:45–51
126. Ray S, Swanson HI (2009) Activation of the aryl hydrocarbon receptor by TCDD inhibits senescence: a tumor promoting event? *Biochem Pharmacol* 77:681–688
127. Demers A, Ayotte P, Brisson J et al (2002) Plasma concentrations of polychlorinated biphenyls and the risk of breast cancer: a congener-specific analysis. *Am J Epidemiol* 155:629–635
128. Shah MM, Barr DP, Chung N et al (1992) Use of white rot fungi in the degradation of environmental chemicals. *Toxicol Lett* 64–65:493–501
129. Thomas DR, Carswell KS, Georgiou G (1992) Mineralization of biphenyl and PCBs by the white rot fungus *Phanerochaete chrysosporium*. *Biotechnol Bioeng* 40:1395–1402
130. Novotný C, Vyas BR, Erbanová P et al (1997) Removal of PCBs by various white rot fungi in liquid cultures. *Folia Microbiol* 42:136–140
131. Chroma L, Macek T, Demnerova K et al (2000) Decolorization of RBBR by plant cells and correlation with the transformation of PCBs. *Chemosphere* 49:739–748

132. Köller G, Möder M, Cziala K (2000) Peroxidative degradation of selected PCB: a mechanistic study. *Chemosphere* 41:1827–1834
133. Colosi LM, Burlingame DJ, Huang Q et al (2007) Peroxidase-mediated removal of a polychlorinated biphenyl using natural organic matter as the sole cosubstrate. *Environ Sci Technol* 41:891–896
134. Kaushik P, Malik A (2009) Fungal dye decolorization: recent advances and future potential. *Environ Int* 35:127–141
135. Husain Q (2006) Potential applications of the oxidoreductive enzymes in the decolorization and detoxification of textile and other synthetic dyes from polluted water: a review. *Crit Rev Biotechnol* 26:201–221
136. Champagne PP, Ramsay J (2005) Contribution of manganese peroxidase and laccase to dye decoloration by *Trametes versicolor*. *Appl Microbiol Biotechnol* 69:276–285
137. Spadaro JT, Gold MH, Renganathan V (1992) Degradation of azo dyes by the lignin-degrading fungus *Phanerochaete chrysosporium*. *Appl Environ Microbiol* 58:2397–2401
138. Chagas EP, Durrant LR (2001) Decolorization of azo dyes by *Phanerochaete chrysosporium* and *Pleurotus sajorcaju*. *Enzyme Microb Technol* 29:473–477
139. Fu Y, Viraraghavan T (2001) Fungal decolorization of dye wastewaters: a review. *Bioresour Technol* 79:251–262
140. Eichlerová I, Homolka L, Lisá L et al (2005) Orange G and Remazol Brilliant Blue R decolorization by white rot fungi *Dichomitus squalens*, *Ischnoderma resinotum* and *Pleurotus calyptratus*. *Chemosphere* 60:398–404
141. Rodriguez E, Pickard MA, Vazquez-Duhalt R (1999) Industrial dye decolorization by laccases from ligninolytic fungi. *Curr Microbiol* 38:27–32
142. Chivukula M, Spadaro JT, Renganathan V (1995) Lignin peroxidase-catalyzed oxidation of sulfonated azo dyes generates novel sulfophenyl hydroperoxides. *Biochemistry* 34:7765–7772
143. Shrivastava R, Christian V, Vyas BRM (2005) Enzymatic decolorization of sulfonphthalein dyes. *Enzyme Microb Technol* 36:333–337
144. Shaffiq T, Roy J, Nair R et al (2002) Degradation of textile dyes mediated by plant peroxidases. *Appl Biochem Biotechnol* 102–103:315–326
145. Arrieta-Baez D, Roman R, Vazquez-Duhalt R et al (2002) Peroxidase-mediated transformation of hydroxy-9, 10-anthraquinones. *Phytochemistry* 60:567–572
146. Ayala M, Pickard MA, Vazquez-Duhalt R (2008) Fungal enzymes for environmental purposes, a molecular biology challenge. *J Mol Microbiol Biotechnol* 15:172–180
147. Ayala M, Roman R, Vazquez-Duhalt R (2007) A catalytic approach to estimate the redox potential of heme-peroxidases. *Biochem Biophys Res Commun* 357:804–808
148. Vazquez-Duhalt R, Westlake DWS, Fedorak PM (1994) Lignin peroxidase oxidation of aromatic compounds in systems containing organic solvents. *Appl Environ Microbiol* 60:459–466
149. Cavalieri E, Munhall A, Rogan E et al (1983) Syncarcinogenic effect of the environmental pollutants cyclopenteno[cd]pyrene and benzo[a]pyrene in mouse skin. *Carcinogenesis* 4:393–397
150. Conesa A, Punt PJ, van den Hondel CAMJJ (2002) Fungal peroxidases: molecular aspects and applications. *J Biotechnol* 93:143–158
151. Nie G, Reading NS, Aust SD (1999) Relative stability of recombinant versus native peroxidases from *Phanerochaete chrysosporium*. *Arch Biochem Biophys* 365:328–334
152. Conesa A, Punt PJ, van Luijk N et al (2001) The secretion pathway in filamentous fungi: a biotechnological view. *Fungal Genet Biol* 33:155–171
153. Punt PJ, van Vieson N, Conesa A et al (2002) Filamentous fungi as cell factories for heterologous protein production. *Trends Biotechnol* 20:200–206

Part III
Challenges in the Application
of Peroxidases

Chapter 9

Enzyme Technology of Peroxidases: Immobilization, Chemical and Genetic Modification

Adriana Longoria, Raunel Tinoco, and Eduardo Torres

Contents

9.1	Introduction	210
9.2	Immobilization	219
9.2.1	Immobilization on Inorganic Supports	220
9.2.2	Immobilization on Organic Supports	224
9.3	Chemical Modification	227
9.3.1	Chemical Modification of Superficial Amino Acids	228
9.3.2	Heme Modification	231
9.4	Genetic Engineering of Peroxidases	233
9.5	Conclusions	237
	References	237

Abstract An overview of enzyme technology applied to peroxidases is made. Immobilization on organic, inorganic, and hybrid supports; chemical modification of amino acids and heme group; and genetic modification by site-directed and random mutagenesis are included. Different strategies that were carried out to improve peroxidase performance in terms of stability, selectivity, and catalytic activity are analyzed. Immobilization of peroxidases on inorganic and organic materials enhances the tolerance of peroxidases toward the conditions normally found in many industrial processes, such as the presence of an organic solvent and high temperature. In addition, it is shown that immobilization helps to increase the Total Turnover Number at levels high enough to justify the use of a peroxidase-based biocatalyst in a synthesis process. Chemical modification of peroxidases produces modified enzymes with higher thermostability and wider substrate variability. Finally, through mutagenesis approaches, it is possible to produce modified peroxidases capable of oxidizing nonnatural substrates with high catalytic activity and affinity.

9.1 Introduction

In previous chapters, the capacity and potentiality of peroxidases to catalyze reactions of industrial, medical, environmental, and diagnosis interest has been described. However, in order to complete their application, these enzymes must reach sufficiently high levels of stability, activity, selectivity, and operational functionality.

Although the interest of scientists in peroxidase enzymes has increased tremendously during the past decades, the application of these enzymes as biocatalysts in industrial processes is still negligible. Often the low activity and the fragile nature of these enzymes make their use challenging and sometimes results in poor productivities. Different aspects including heme deactivation (Chap. 12), redox potential modulation (Chap. 4), protein denaturation, and substrate availability have to be dealt with.

In evaluating a biocatalyst for a given processing task, there are performance criteria to be met not only for the biocatalyst but also for the process. The economic feasibility of bio-processes depends on its productivity and yield. In general terms, it has been stated that the stability of the catalyst in terms of TTN (Total Turnover Number, mol of product produced by mol of biocatalyst) of around 10,000 is the minimum sufficient to justify the use of a biocatalyst in a synthesis process, and a TTN of 1×10^6 for a process on a large scale [1]. In the same way, the productivity of the reactor, measured in terms of STY (Space • Time Yield, mass of the generated product by reactor volume per time) of 100 g/(L day) is the minimum value to make a bio-process economically feasible [1]. These values depend on the particular product and market to be reached, and can vary from application to application. In the case of peroxidases, chloroperoxidase from *Caldariomyces fumago* is the most prominent enzyme due to its high TTN values. This enzyme has a TTN value greater than 860,000 for the selective oxidation of indol to oxindole [2] and 250,000 for the oxidation of thioanisole [3].

Nevertheless, for the rest of the peroxidases reported in the literature, values of specific activity and stability to temperature or storage are rather small, still far from those established for a commercial process. Therefore, the improvement of the stability, activity and catalytic productivity are highly relevant for the application of these enzymes in productive processes. Through enzymatic technology, i.e., the use of techniques to design and modify biocatalysts, it is possible to improve the functionality of enzymes in general, and peroxidases in particular (Table 9.1).

Since enzymes are proteins, the susceptibility to be chemically modified and to be immobilized depends on the reactivity of their exposed side chains of amino acids. These include the imidazole group of histidine, the indole of tryptophan, the *p*-hydroxyphenyl of tyrosine, the thioether of methionine, the thiol group of cysteine, the carboxyl groups of glutamic and aspartic acids, the carboxyl-terminal amino acids, and the amino groups of both lysine and amino-terminal amino acids. The hydroxyl groups of glycoproteins [85] or heme-propionates in hemeperoxidases [86] are targets as well.

Table 9.1 References related to the immobilization, chemical and genetical modification of peroxidases

Process	Results	References
Adsorbed horseradish peroxidase (HRP) on silica mesoporous materials	The immobilized HRP on FSM-16 and MCM-41 with pore diameter of 50 Å showed the highest enzymatic activity in toluene and thermostability in aqueous solution at a temperature of 70°C	[4]
Immobilized chloroperoxidase (CPO) on mesoporous silica materials	CPO immobilized on SBA-16 90 Å and Al-MCM-41 26 Å showed the highest activity and stability	[5]
Immobilized CPO in silica-based materials	The immobilized CPO in SBA-15 143 Å showed higher residual activity at 50°C and reusability after five reaction cycles for 4,6-dimethylidibenzothiophene oxidation	[6]
Immobilized CPO on SBA-16 mesoporous materials	The Cs ⁺ -doped material incremented the CPO load and its catalytic activity. The Cs ⁺ -doped and CPO covalent bonded materials showed a higher enzyme activity compared to physical random immobilization	[7]
Immobilized CPO on the mesoporous molecular sieve SBA-15	CPO-SBA-15 was able to oxidize indole to 2-oxoindole using H ₂ O ₂ or <i>tert</i> -butyl hydroperoxide as oxidants and it showed better conversion and pH range performance compared to native CPO	[8]
Immobilized CPO and glucose oxidase (GOx) on SBA-15 were mixed for tandem catalysis	By the use of the tandem system, a conversion of 92% of indole was reached at pH = 5.5. Also, the mixture of immobilized CPO and GOx was recycled several times without significant loss of activity	[9]
Cross-linked CPO aggregates in the pores of mesocellular foams	The CPO-CLEAs (cross-linked enzyme aggregates) supported in mesocellular foams were more stable against leaching than conventional catalysts prepared by physical adsorption of CPO on the same support	[10]
Immobilized cholesterol oxidase (COD) and HRP on tetraethyl orthosilicate-derived sol-gel films	A fast response time (5 s) and a lower limit of cholesterol of 0.5 mM was detected when a physically entrapped enzyme sandwich sol-gel film configuration was used (cholesterol detection between 2 and 10 mM)	[11]
Immobilized CPO in the mesoporous silicate material, mesocellular foam	The optimal pH at which the maximum amount of enzyme is immobilized was determined to be pH 3.4, slightly below the isoelectric point of the enzyme	[12]
Immobilized CPO on mesoporous sol-gel glass	The coupling of CPO and GOx reactions reduced the CPO inactivation in presence of H ₂ O ₂ . The stability on acetonitrile mixtures was enhanced	[13]

(continued)

Table 9.1 (continued)

Process	Results	References
Immobilized HRP on the planar surfaces and inside the cylindrical nanopores of nanocapillary array membranes (NCAMs)	when a pore size larger than size of CPO was used (200 Å) The HRP was immobilized on NCAMs planar surfaces and also inside its nanopores. Reaction velocities were estimated to be ~10-fold higher in the nanopores than for the enzyme bound to the planar surfaces	[14]
Coimmobilized lignin peroxidase (LiP) and GOx on nanoporous gold	The immobilized LiP retained 55% of its initial activity after 2 h incubation at 45°C while the free LiP was completely deactivated. By coimmobilization with GOx, a high LiP activity was achieved	[15]
Immobilized HRP on aluminum-pillared interlayered clay	The immobilized HRP exerted a perfect phenol removal over a broader range of pH from 4.5 to 9.3 and had a better storage stability than the free enzyme	[16]
Immobilized hemoglobin (Hb) on layered titanate	The immobilized Hb shows enhanced catalytic activity with maximum activities of 2.46 and 8.13 times enhancements in the 20 min average reaction rates in toluene and acetonitrile solvents, respectively	[17]
Entrapped Hb within a layered spongy Co ₃ O ₄ -based nanocomposite	The layered spongy Co ₃ O ₄ was integrated with the conductive polymer Nafion and Hb to form an Hb-Nafion-Co ₃ O ₄ composite. The film electrode showed high sensitivity (396 mA/cm ² •M) for H ₂ O ₂	[18]
Immobilized cytochrome <i>c</i> on nanodiamonds	The cytochrome <i>c</i> covalently attached to nanodiamonds surface showed good stability after ten washes and even after storage of the sample suspensions in a refrigerator (4°C) for 5 months	[19]
Immobilized soybean peroxidase (SBP) and HRP onto K ₂ SO ₄ crystals	The protein-coated microcrystals preparations showed enhanced activity in different organic solvents when tested with substrates such as guaiacol, thioanisole, and indole	[20]
Immobilized CPO on aminopropyl-glass	No differences in pH-activity and pH-stability profiles, and thermostability of the soluble and immobilized enzymes could be detected. After five uses, the immobilized CPO retained full activity between pH 6.0 and 6.7	[21]
HRP and SBP were covalently immobilized onto aldehyde glass	It was found that at an immobilized enzyme concentration in the reactor of 15 mg/L, SBP removed 5% more of 4-chlorophenol than HRP, a shorter treatment was necessary	[22]

(continued)

Table 9.1 (continued)

Process	Results	References
Immobilized HRP on magnetite	The immobilized HRP retained 100% of its activity, removed almost 100% of various chlorophenols in solution, and also the removal of total organic carbon and adsorbable organic halogen reached a 90%	[23]
CPO-coated magnetic nanoparticles with iron oxide core and polymer shell	The thick polymer shell increased the stability of the nanobiocatalyst, giving no loss of activity after recycling 11 times	[24]
Noncovalent immobilization of CPO onto talc	In contrast to the hydrophobic talc (15M00), the hydrophilic talc (CLST) was less favorable to adsorption (≤ 2.5 mg CPO/g talc); however, the CLST-CPO combination had excellent enzymatic activity (80–126%)	[25]
Immobilized HRP on gelatin in presence of NaY zeolite	The presence of NaY zeolite enhanced the activity of the HRP, and the effect was more dramatic when both the enzyme and the NaY zeolite were coimmobilized in gelatin	[26]
Coimmobilization of COD and HRP on perlite surface	The stabilities of immobilized COD and HRP to pH were higher than those of soluble enzymes. The coimmobilized enzymes retained 65% of its initial activity after 20 consecutive reactor batch cycles	[27]
Adsorbed white radish peroxidase on celite	Efficiency of immobilized peroxidase was checked in a continuous reactor where the immobilized enzyme exhibited 73% decolorization of Reactive Red 120 even after 1 month of operation	[28]
Immobilized HRP in porous silica nanoparticles	The preparation of silica particles under biocompatible conditions was possible when diglyceroxysilane was used as the precursor and PEG was added as a steric stabilizer. The immobilized HRP was stable for 100 days	[29]
Immobilized HRP and GOx on layered silicates using an avidin–biotin immobilization approach	The immobilized enzymes retained high levels of activity compared to the native enzymes and showed improved thermal behavior. In addition, the immobilized GOx retained 65% of its initial activity at 58°C	[30]
Adsorbed HRP onto silicon wafers	It was possible to reuse the same HRP-covered silicon wafer as catalyst in the polymerization of ethylene glycol dimethacrylate three times	[31]
Immobilized CPO onto epoxide derivatized silica gel	The immobilized CPO was easily obtained and no leaching of CPO from the support	[32]

(continued)

Table 9.1 (continued)

Process	Results	References
Immobilized HRP in 1-butyl-3-methylimidazolium tetrafluoroborate ionic liquid based sol-gel host materials	was detected. A better enzyme stability as function of pH and H ₂ O ₂ concentration was obtained Immobilized HRP showed a dramatically enhanced activity (about 30-fold greater than that in silica gel without ionic liquid prepared by conventional sol-gel methods) and an excellent thermostability	[33]
Immobilized Hb on stable mesoporous multilamellar silica vesicles (MSV)	The immobilization capacity of MSV for Hb was high as 522 mg/g, which was about two times larger than that of conventional SBA-15. The immobilized Hb retained 80% of its activity	[34]
Immobilized HRP in a sol-gel prepared from a detergentless microemulsion system	A microsized gel powder was prepared without additional drying and grinding steps or the addition of detergent. The immobilized HRP maintained its activity for 48 h and was stable against excess H ₂ O ₂	[35]
Coimmobilized CPO-GOx and SBP-GOx on polyurethane foam	The TTN of the CPO-GOx system in the oxidation of thioanisole and <i>cis</i> -2-heptene was 250 × 10 ³ and 10 × 10 ³ , respectively. The SBP-GOx system oxidized thioanisole ([50% ee (S)] and TTN = 210)	[3]
Immobilized CPO into polyurethane foam	The immobilized CPO mediated the selective oxidation of indole to 2-oxindole (regioselectivity: 99%) in water-saturated isooctane or 1-octanol	[36]
Immobilized HRP with chitosan in alternate layers	The enzymatic activity of the immobilized HRP was measured for long periods of time with linear response (10 min). After 1 month, 80% of the enzyme activity was preserved	[37]
Immobilized HRP on chitosan and activity in organic solvents	The catalytic efficiency of the immobilized HRP was higher when <i>o</i> -phenylene diamine was used as the substrate and minor when guaiacol was used in organic solvents	[38]
Immobilized HRP on chitosan powder	The immobilized HRP was an effective catalyst for the oxidative polymerization of aniline and it remained active after being stored in pH 6.0 buffer for more than 72 h at room temperature	[39]
Immobilized CPO on chitosan membranes	The residual activity for immobilized CPO was 99% and 58% compared with 68% and 43% for free CPO in the presence of 1.5 M urea and 300 mM H ₂ O ₂ , respectively, after 20 h	[40]

(continued)

Table 9.1 (continued)

Process	Results	References
Immobilized HRP on nonwoven polyester fabric coated with chitosan	The immobilized HRP retained 85% of its activity after 4 weeks of storage at 4°C, retained 54% of its activity after ten cycles of reuse and showed a high yield of immobilization	[41]
Immobilized HRP onto a polyacrylonitrile membrane	A membrane with a specific HRP activity of 1.15 U/g of support dry wt was obtained. After an operation period of 35 h, the enzymatic membrane had a specific productivity of 59.5 μmol of H ₂ O ₂ reduced/(h·U _{immob} HRP)	[42]
Incorporated HRP into polyelectrolyte complexes with chitosan of different molecular weights (MW 5–150 kDa)	The complex formed by 0.001% chitosan with a molecular weight of 150 kDa was most stable: when immobilized on foamed polyurethane, it retained at least 50% of the initial activity for 550 days	[43]
Entrapped CPO and HRP onto amphiphilic network	The specific activities in <i>n</i> -heptane were 1 and 2 orders of magnitude higher when CPO and HRP were encapsulated into the amphiphilic network, respectively	[44]
Immobilized HRP on gemini surfactant-polyvinyl alcohol composite film	The immobilized HRP presented good bioelectrocatalytic activity to the reduction of H ₂ O ₂ , NO ₂ ⁻ , O ₂ , and trichloroacetic acid. For H ₂ O ₂ the catalytic current was linear to its concentration (0.195–97.5 M)	[45]
Encapsulated CPO in block copolymer polymersomes assembled from polystyrene- <i>b</i> -poly(L-isocyanoalanine-(2-thiophene-3-yl-ethyl)amide)	The oxidation of two substrates by the encapsulated CPO was studied: while the oxidation of pyrogallol was limited by diffusion into the polymersome, the rate-limiting step for the oxidation of thioanisole was the turnover by the enzyme	[46]
Immobilized HRP on polyaniline activated with glutaraldehyde (PANIG)	The immobilized HRP in PANIG showed better tolerance to organic solvents, thermostability, and higher activity in the alkaline range (from pH 9.0 to 11.0) than the free enzyme	[47, 48]
Immobilized HRP on an hybrid formed by colloidal carbon microspheres dispersed in a chitosan solution	The immobilized HRP was used in the elaboration of a H ₂ O ₂ sensor. The biosensor showed a fine linear correlation with H ₂ O ₂ concentration and fast response to H ₂ O ₂ at -0.15 V	[49]
Immobilized HRP in Langmuir–Blodgett (LB) films of phospholipids (dipalmitoylphosphatidylglycerol (DPPG))	The activity detected for mixed HRP-DPPG LB films was 23% higher than the one of free enzyme. The LB technique provided a good control of molecular architecture	[50]
Immobilized HRP on different cinnamic carbohydrate esters	The thermostability of the immobilized HRP was greater than that of the free enzyme and also showed great	[51, 52]

(continued)

Table 9.1 (continued)

Process	Results	References
Encapsulated HRP on sol–gel glasses	stability during storage (33% of its residual activity after 60 days) The encapsulated HRP showed enhanced operational stability and an increased TTN (up to 6-fold) compared to the native enzyme	[53]
Immobilized manganese peroxidases (MnP) in glutaraldehyde–agarose gels	The immobilization process maintained a high percentage of MnP activity for long periods of time (50–60% after more than 1 year at room temperature storage)	[54]
Immobilized LiP and HRP on CNBr–Sephacrose 4B	In comparison to free enzymes, immobilized LiP and HRP improved their decolorization ability by factor of 2.9 and 2.6, respectively, in 48 h	[55]
Immobilized HRP on cellulosic fiber surfaces	More hydrophobic fiber surfaces result in larger enzyme–fiber binding affinity constants and higher binding heterogeneity. Also, the oxidation of the cellulosic fiber substrate increased the loading capacity per unit weight of the surface	[56]
Modified HRP by acetylation or succinylation	The modification of HRP allowed the preparation of tracer enzymes with different isoelectric points. No significant changes were observed in the molecular parameters of the modified HRP	[57]
Chemically modified HRP by using anhydrides of mono- and dicarboxylic acids and pyrrol sulfonic acid	The thermostability of the HRP was enhanced after the covalent attachment of small molecules and that phenomenon was attributed to the degree of modification, rather than the nature of the modifier	[58]
Modified CPO by using diethylpyrocarbonate	The existence of a histidine distal residue in the active site of the enzyme was elucidated by the specific chemical modification of histidine residues of CPO with diethylpyrocarbonate	[59]
Modified histidine residues of HRP with pyrocarbonates	The catalytic activity of HRP was not affected by modification of histidine residues with small-sized substituents not containing reactive groups. In contrast, electron-rich substituents disrupted the heme structure	[60]
Chemically modified myoglobin and cutinase suspended in <i>n</i> -hexane by acyl chlorides and iodine	The modification rates were slower for larger acyl chlorides, particularly with lyophilized powders. Hydration of lyophilized proteins accelerated chemical modification rates, as it did their catalytic activity	[61]

(continued)

Table 9.1 (continued)

Process	Results	References
Transferred azido groups to HRP superficial amino groups	Azido-HRP retained its catalytic activity after conjugation of a small molecule. This modified protein could also be successfully immobilized on the surface of an acetylene-covered polymersome	[62]
Modified HRP with phthalic anhydride (PA) and glucosamine hydrochloride	The modified HRP with PA and glucosamine hydrochloride showed an increased thermostability (about 10- and 9-fold, respectively) and also the removal efficiency of phenolics was increased	[63]
Chemically modified HRP by PA	The PA-modified HRP was more efficient in chlorophenols removal than native HRP and showed a greater affinity and catalytic efficiency in organic solvents	[64, 65]
Modified HRP with maleic and citraconic anhydrides	An enhanced thermostability of modified HRP with respect to native HRP was observed, and the changes were attributed to side chain reorientations of the aromatic residues of the enzyme	[66]
Chemically modified CPO by phthalic, maleic, and citraconic anhydrides	The chemical modification of CPO increased its catalytic efficiency for sulfoxidation by 12–26% and catalytic efficiency for phenol oxidation by 7–53% in aqueous buffer	[67]
Chemically modified HRP with poly (ethylene)glycol (PEG)	The modified HRP retained 70% of its original activity and was found to be soluble in benzene. Also, the modified HRP had 21% of its activity in benzene relative to that of native enzyme in aqueous solution	[68]
Chemically modified HRP with PEG aldehyde (MW 350, 1,900 and 5,000)	The isoelectric point of the native HRP (8.8) was shifted to 5.5 after the chemical modification process. The modified enzyme with the aldehyde MW 5,000 was soluble and active in organic solvents	[69]
Chemically modified HRP with PEG (from MW 350 to 5,000)	The modified HRP showed a better thermostability than the native enzyme, but there was no correlation between the length of the polymer adduct and the improvement	[70, 71]
Chemically modified LiP with PEG	The catalytic efficiency of the modified LiP in solutions containing 15% acetonitrile was over 11-fold higher than that of the native enzyme in buffer solutions (pH 4.2)	[72]
Chemically modified MnP with PEG	The modified MnP from <i>Bjerkandera adusta</i> showed greater resistance to denaturation by H ₂ O ₂ , stability to organic solvents, and greater stability to	[73]

(continued)

Table 9.1 (continued)

Process	Results	References
Chemically modified HRP with PEG was encapsulated in polyester microspheres	higher temperatures and lower pH than the native enzyme The covalent modification of HRP with PEG increased the encapsulation efficiency from 83% to about 100%, and the aggregation was less than 1% and improved its residual activity to more than 95%	[74]
Chemically modified turnip peroxidase with PEG	After the chemical modification and immobilization in a calcium alginate matrix, the enzyme showed enhanced conformational and thermal stabilities, and higher solvent tolerance	[75]
Immobilized HRP on poly(ethylene terephthalate) grafted acrylamide fiber	The temperature profile of the free HRP and the immobilized HRP revealed a similar behavior, although the immobilized HRP exhibited higher relative activity in the range from 50 to 60°C	[76]
Double chemically modified cytochrome <i>c</i> with PEG and methyl groups (PEG-Cyt-Met)	The PEG-Cyt-Met was able to oxidize more aromatic compounds than the native protein, it showed higher thermostability, and it was able to oxidize synthetic porphyrins and asphaltenes	[77-79]
Double chemically modified Hb with PEG and methyl groups	The double chemically modified Hb showed up to ten times higher activity than the unmodified protein when polycyclic aromatic hydrocarbons were used as substrates	[80]
Reconstituted HRP by modified prosthetic groups with benzene and/or carboxylic groups	The reconstitution of HRP with the modified hemes increased the thermostability both in aqueous buffer and some organic solvents, the substrate affinity, and the catalytic efficiency	[81]
Reconstituted HRP with modified hemes (esterified by phenol, <i>p</i> -nitrophenol, and <i>p</i> -methylphenol)	The reconstituted HRP with <i>p</i> -nitrophenol-modified heme derivative had a larger initial rate, affinity, catalytic efficiency, and substrate-binding efficiency than native HRP	[82]
Reconstituted HRP and myoglobin with a meso-unsubstituted iron corrole	The reconstitution of myoglobin enhanced its activity, whereas the reconstitution of HRP decreased its activity compared to native proteins	[83]
Reconstituted HRP and myoglobin with DNA oligonucleotide-modified prosthetic groups	Greater than 100-fold changes in catalytic constants were observed, depending on which oligonucleotide was incorporated in the hybrid catalyst	[84]

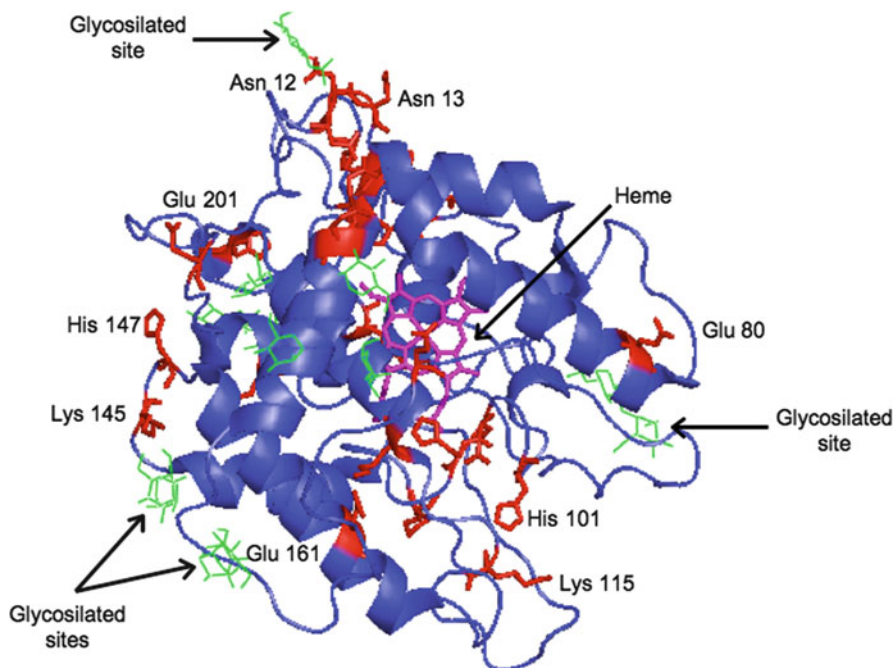


Fig. 9.1 Some potential sites for chemical modification and immobilization of chloroperoxidase, including amino acids, carbohydrate moieties, and heme group

Figure 9.1 shows the tridimensional structure of chloroperoxidase where some potential modification sites are marked. These include side chains of amino acids such as lysine, histidine, and aspartic acid, as well as the propionates from the heme group and carbohydrate moieties. To illustrate how enzyme technology has impacted the development of biocatalysts based on peroxidases, we highlight important aspects described in literature: immobilization, chemical and genetic modification of peroxidases.

9.2 Immobilization

For the purpose of this chapter, we define an immobilized enzyme as a composite consisting of two essential components: the noncatalytic structural component (carrier) and the catalytic functional component, the enzyme. Therefore, an immobilized enzyme has to be characterized by two sets of variables, the noncatalytic and the catalytic parameters [87].

The two essential functions that an immobilized enzyme performs are: the noncatalytic functions that are designed to aid separation and the catalytic ones that are designed to convert the targeted compound within a desired time and space.

Numerous efforts have been devoted to the development of insoluble immobilized enzymes for various applications. Among the benefits of using immobilized enzymes rather than their soluble counterparts are the reusability and improved stability of heterogeneous biocatalysts with the aim of reducing the production cost by efficient recycling and control of the process [88].

No matter which method is selected for immobilization, two essential needs should be balanced, the catalytic needs (expressed as productivity, STY, stability and selectivity) and the noncatalytic needs (e.g., separation, control, down-streaming process) that are required by a given application. When both needs are satisfied, the immobilized enzyme can be labeled as robust [88].

The immobilization of peroxidases can be classified in agreement with the support used for immobilization. In this way, three main types can be mentioned: on organic, inorganic, and hybrid supports. Each of them displays their own characteristics that make them catalytically attractive and potentially applicable. Next, some examples and strategies are described. Additionally, peroxidases have been immobilized for their use in biosensors development with applications in diagnosis or electronics. These interesting and novel applications are covered in Chap. 6.

9.2.1 Immobilization on Inorganic Supports

Both synthetic and natural inorganic materials such as clay, glass beads, silica-based materials, and celite have been used to immobilize peroxidases. Among them, mesoporous silicates are the most interesting due to their attractive properties, availability, and simple preparation [89].

Peroxidase immobilization on inorganic mesoporous silicates has proven to be an interesting alternative to improve enzyme functionality [4–8]. The main advantages of the periodic mesoporous silicate materials are the uniform and adjustable pore diameters (from 1.5 to 30 nm), the high specific surface area (up to 1,500 m²/g), and the high pore volume (up to 1.5 cc/g), which in principle, allows high enzyme load. The large regular repeating structures of mesoporous silicates offer the possibility of adsorbing or entrapping large biomolecules within their pores, providing a suitable microenvironment to protect the enzyme. Therefore, mesoporous materials fulfill many of the requirements for enzyme carriers: the noncatalytic component, such as large surface area, sufficient functional groups for enzyme attachment, hydrophilic character, water insolubility, chemical and thermal stability, mechanical strength, suitable particle form, regenerability, and toxicological safety [90].

Depending on the conditions and chemical precursors used for mesoporous materials synthesis, different morphologies, such as hexagonal, cubic, or lamellar, and different pore sizes can be obtained (Fig. 9.2). Additionally, these materials can easily be functionalized with organic groups to produce a variety of hybrid inorganic–organic materials with new properties, which directly affect the functionality of the enzyme [91, 92].

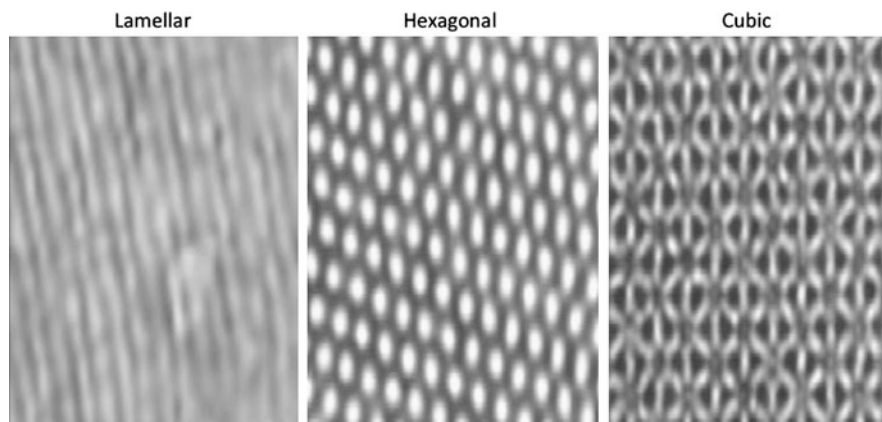


Fig. 9.2 Lamellar, hexagonal, and cubic morphologies obtained by different synthesis conditions of mesoporous materials

The immobilization of enzymes in mesoporous materials can be carried out in a covalent or noncovalent way. The first needs the formation of a covalent bond between the hydroxyl groups of the material and the reactive groups of the enzyme. It is normally necessary to modify the hydroxyl groups of the material to offer the desired reactivity towards the target groups of the enzyme. This also provides a space between the material and the enzyme to avoid steric obstructions during the immobilization process or during the biocatalytic reaction. The main advantage of covalent immobilization is the retention of the enzyme during the whole biocatalytic process. Nevertheless, some conditions of anchorage to the support can inactivate the enzyme, reducing the amount of active enzyme, hence affecting the TTN and STY, i.e., process efficiency.

For physical immobilization (noncovalent attachment) of peroxidases, the enzymes are immobilized by electrostatic interaction into the pore of the material. In order to reach high enzyme load, the material pore should be at least three times the enzyme size to enable full access to the internal pores (Fig. 9.3a). Besides, it is possible to increase the enzyme load as well as the strength of interaction by modifying the positive or negative charges of the material (Fig. 9.3b). The soft immobilization conditions of anchorage can maintain the enzyme structure and hence the catalytic activity; nevertheless, enzyme loosening is common during the catalysis process.

In the first report about immobilization of peroxidases on mesoporous materials, Takahashi and coworkers shed light on different parameters that affect the process. Using horseradish peroxidase (HRP) as a model, the authors reported that higher stability to temperature and organic solvent, important variables on industrial processes, were obtained when the size of the pore match the size of the enzyme, in such a way that the encapsulated enzyme was located in a restricted space that slowed down its free movement, preventing its denaturation [4].

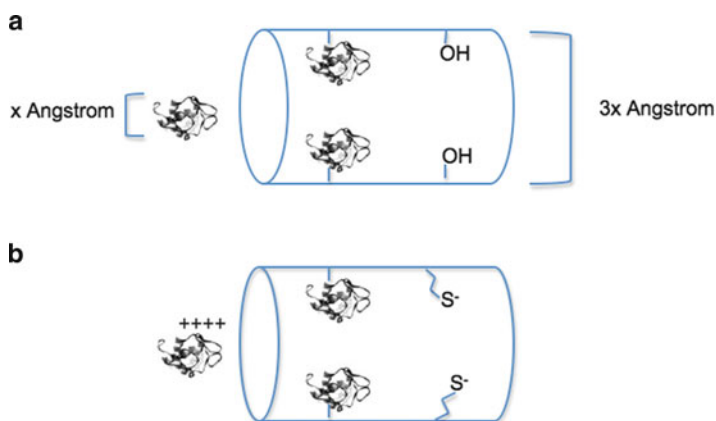


Fig. 9.3 Schematization for chemical (a) and physical (b) protein adsorption in mesoporous material. The pore size for high enzyme load should be at least three times the enzyme size

Based on the principles reported by Takahashi et al., we carried out the immobilization of chloroperoxidase from *C. fumago* on SBA (Santa Barbara Amorphous type material)-16. Chloroperoxidase (CPO) is an enzyme of molecular size of $60 \times 53 \times 46 \text{ \AA}$ that catalyzes reactions of environmental and chemical interest. The enzyme was immobilized covalently and noncovalently on SBA-16 of 90 \AA , reaching up to $6.1 \text{ mg of CPO/g of material}$. The biocatalytic preparation was assayed in the oxidation of the 4,6-dimethyldibenzothiophene (DMDBT), a recalcitrant organosulfur compound of petroleum. In order to apply a biocatalyst in the petroleum refining industry, it is necessary to have a biocatalyst stable in the conditions normally found in a refinery, such as low water activity and high temperature [93]. For this reason, the stability of immobilized CPO toward organic solvents and temperature was determined. The preparation showed improved stability towards an organic solvent and urea, although the specific activity was seriously affected by the immobilization process, falling near to 10% of the activity of the free enzyme [7].

For DMDBT oxidation, CPO physically immobilized on SBA-16 of 90 \AA had a higher thermostability than the free enzyme, retaining 50% of its activity at 45°C after 187 h while the free enzyme was half-inactivated after 68 h. This could be due to the restricted movement of the immobilized enzyme confined in the pores of this material. In contrast, the immobilization in material with a larger pore of 117 \AA did not improve the thermostability of the enzyme, probably due to the fact that larger pores did not prevent the increased conformational flexibility of the enzyme at this temperature.

Another limitation in the industrial application of peroxidases is the low stability to H_2O_2 (see Chap. 12). Here, an improvement for H_2O_2 inactivation through the physical immobilization of CPO on the mesoporous sieve SBA-15 of 130 \AA for the oxidation of indole to 2-oxoindole has been reported [8]. The performance of the immobilized enzyme was enhanced to that of the native CPO with respect to maximum conversion. According to the authors, the superior performance of

immobilized CPO was most likely a result of suppressing the oxidative deactivation due to the periodic addition of H_2O_2 resulting in a nonideal mixing. Since immobilized CPO is encapsulated within the pores of SBA-15, H_2O_2 has to diffuse into the pores, and consequently, the excess of H_2O_2 is diluted. Hence, immobilized CPO is protected from high H_2O_2 concentrations and is therefore less susceptible to oxidative deactivation, and the immobilized CPO exhibits considerably higher conversions than the free enzyme.

The deactivation of peroxidases by peroxides can be circumvented by controlling the H_2O_2 production by *in situ* generation [3, 13]. H_2O_2 can be produced by glucose oxidation with glucose oxidase (GOx) to produce H_2O_2 and D-gluconolactone; the latter then hydrolyzes rapidly to D-gluconic acid. Then the enzymatically produced H_2O_2 is used by peroxidase to catalyze the oxidation of a reduced substrate (Fig. 9.4). In the interesting work of Jung et al., the physical adsorption of CPO and GOx on the mesoporous silica molecular sieve SBA-15 of up 118 Å was studied in order to improve the stability of the enzyme vs. H_2O_2 . The bi-enzymatic catalysts obtained by physically mixing CPO-SBA-15 and GOx-SBA-15 were tested in the selective oxidation of indole to 2-oxoindole using the CPO-GOx tandem reaction. The maximum indole conversion followed the same trend as the H_2O_2 formation rate of the tandem system, reaching 92% while the conversion found for the conventional system does not exceed 88% [9].

To test the reusability of the biocatalyst, five sequential reaction cycles with CPO immobilized on SBA-16 of different pore sizes were completed [6]. The authors found that immobilization on material with larger pore, 143 Å, improved the reusability of the catalyst. Enzyme immobilized by covalent attachment to silica-based materials retained a higher residual activity after five reaction cycles than the physical approach.

In another related work [94], a periodic mesoporous organosilane derivatized with amine groups, was found to be a good support for recyclability. This material, with pore entrances large enough to allow the enzyme entry inside the pores

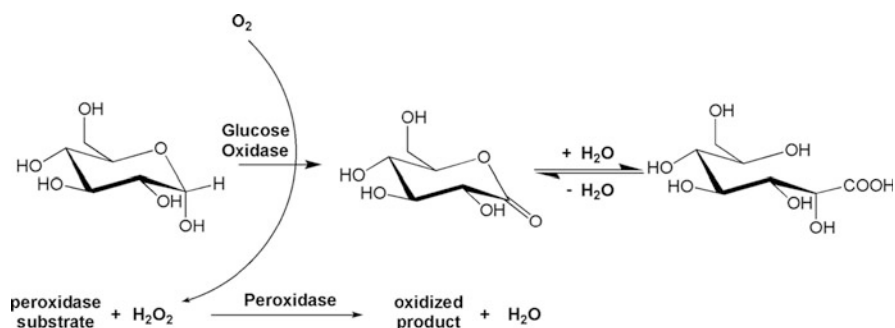


Fig. 9.4 *In situ* production of hydrogen peroxide by glucose oxidation catalyzed by glucose oxidase. The enzymatically generated hydrogen peroxide is then the oxidizing agent for the oxidation of reducing substrates by peroxidases

reached loads of 39.9 mg CPO/g support, the highest reported so far. CPO maintained 75% activity after 20 cycles when it was immobilized onto these materials.

In conclusion, it is clear that the immobilization of peroxidases into ordered porous materials with high surface areas aids the biocatalytic operation in terms of stability and activity in conditions that simulate an industrial process such as high temperature, the presence of organic solvent, and high H_2O_2 concentrations.

Other immobilization processes of peroxidases on inorganic materials have been carried out although in a less systematic way. For example, the use of CPO immobilized on microporous talc in bromohydroxylation reactions was reported [25]. Higher regioselectivities and improved oxidative stability were found for the immobilized enzyme. The covalent immobilization of CPO on epoxy-modified silica gel was also reported [32]. The immobilized CPO was more stable with respect to pH and oxidant concentration. Another approach consisted of covalently encapsulating the CPO in a highly ordered porous structure of sol-gel glass [13]. Solvent stability in acetonitrile mixtures was enhanced when a pore size larger than the size of CPO was used, i.e., 200 Å.

9.2.2 Immobilization on Organic Supports

Peroxidases have been immobilized on organic supports by different methodologies, taking advantage of the reactivity of their amino acids and the heme group. Additionally, the presence of posttranslational modifications, such as glycosylation, allows enzyme anchorage to several supports. Given to the presence of 18% of carbohydrates in CPO, an interesting methodology was reported by Sheldon's group consisting of the covalent encapsulation of the enzyme in polyurethane foam. Through this methodology, the authors reported an important improvement in the biocatalytic capacities of CPO during the regioselective oxidation of indol. The enzyme load in the polyurethane foam was up to 25 mg of CPO/g dry support. The immobilization efficiency, i.e., retained catalytic activity after immobilization, was 55%. The enzyme preparation was able to mediate the oxidation of indole into oxindole in a range of water-saturated, water-immiscible solvents, using *tert*-butyl hydroperoxide as the oxidant. The highest TTN (mol of product formed per mol of enzyme used until the catalyst was deactivated) was achieved in 1-octanol medium, followed by *n*-hexane and isooctane. TTN values ranged from 3,300 to 19,000 [36], values high enough for a process of synthesis but far from a large-scale process.

The TTN value was improved through coimmobilization with GOx, using the aforementioned strategy to produce *in situ* H_2O_2 . Coimmobilization of peroxidases with GOx into polyurethane foams afforded heterogeneous biocatalysts in which the H_2O_2 is formed inside the polymeric matrix from glucose and oxygen. The TTN of CPO in the oxidation of thioanisole and *cis*-2-heptene was increased to new maxima of 250,000 and 10,000, respectively, upon coimmobilization with GOx. The mixed biocatalyst transformed the enantioselective oxidation of thioanisole with 100% conversion and 99% enantiomeric excess (ee) [3]. Therefore, it seems

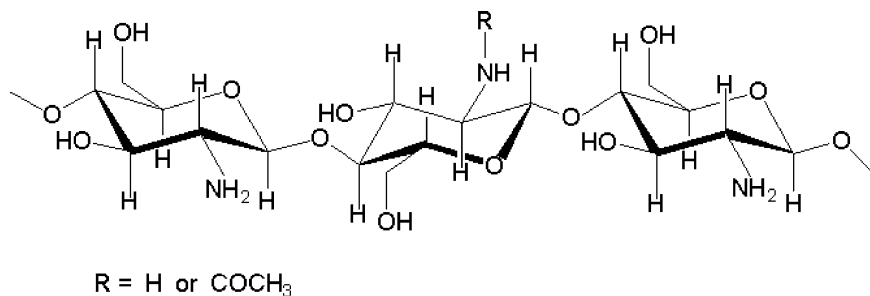


Fig. 9.5 Schematic representation of chitosan structure, a biopolymer composed of 2-amino-2-deoxy- β -D-glucose

that polyurethane foam is a good support for peroxidases containing carbohydrate moieties in the enzyme periphery, increasing the operational stability, maintaining the enzyme regioselectivity, and facilitating biocatalyst recyclability.

Another interesting organic material usually used to immobilize enzymes is chitosan [95, 96]. Chitosan is a poly((1 \rightarrow 4)-2-amino-2-deoxy- β -D-glucose) (Fig. 9.5), which is a product of deacetylation of chitin, the second polysaccharide ranked by its prevalence in nature, just after cellulose.

Chitosan is one of the most promising natural polymers, having important characteristics such as biodegradability, chemical inertness, nontoxicity, biocompatibility, high mechanical strength, good film-forming properties, and low cost [97]. The amino groups of chitosan are nucleophilic and reactive at higher pHs, allowing chitosan to be cross-linked under mild conditions to create gel matrixes of various shapes and sizes including beads, membranes, and fibers. Several enzymes such as tyrosinase, HRP, catalase, laccase, and urease have been immobilized on a matrix containing chitosan by the sol-gel method [37, 38, 96, 98–100].

The immobilization of HRP on a composite membrane of chitosan has been investigated. The membrane was prepared by coating nonwoven polyester fabric with chitosan glutamate in the presence of glutaraldehyde as a crosslinking agent. The soluble and immobilized HRP were stored at 4°C and measured at weekly intervals. The soluble HRP lost 90% of its activity after 4 weeks of storage at 4°C, whereas the immobilized HRP retained 85% of its original activity at the same time. A reusability study was carried out by measuring the activity of the immobilized HRP (stored dry at 4°C) at successive times. After 10 cycles of reuse, a decrease of 46% in relative activity was recorded. The excellent long-term stability should be attributed to the covalent interactions between the $-\text{COOH}$ and $-\text{NH}_2$ groups from the composite membrane and the HRP, which prevented the loss of the enzyme, and the biochemical environment provided by the chitosan and nonwoven-fabric, which prevented the denaturation of the enzyme. The stability of HRP against metal ion inactivation was improved after immobilization. Immobilized HRP exhibited high resistance to proteolysis by trypsin. The immobilized HRP was more resistant to inactivation by urea, Triton X-100, and organic solvents compared to its soluble counterpart [41].

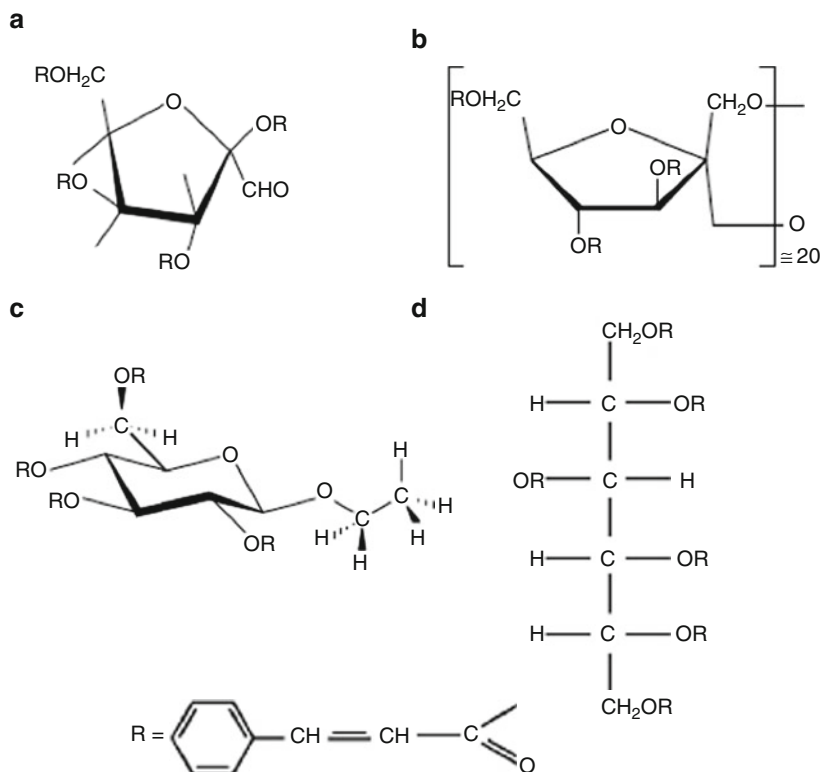


Fig. 9.6 Polymeric based on (a) D-glucosone (GSOCN), (b) inuline (INCN), (c) ethyl-D-glucopyranoside (EGSCN), or (d) D-sorbitol (SOTCN) for immobilization of peroxidases on glass beads

New polymeric organic supports based on cinnamoylated derivatives of D-glucosone (GSOCN), D-sorbitol (SOTCN), ethyl-D-glucopyranoside (EGSCN), or inuline (INCN) on glass beads [51, 52] (Fig. 9.6) were assayed for noncovalently immobilized HRP. The encapsulation by noncovalent attachment is a suitable methodology for enzyme immobilization because it is a smooth method of treatment that can maintain the structure of the enzyme, and hence its catalytic activity.

Two related works exemplify this method for peroxidases. These supports were capable of linking with the HRP enzyme in a rapid and straightforward way by means of physical adsorption interactions between the cinnamoyl groups of the immobilization support and the related groups in the tertiary structure of the protein. Immobilized enzymatic activity varied with the incubation time used (2–21 h), depending on the chemical nature of the immobilization support. The affinity of HRP for H₂O₂ and 2,2'-azino-bis(3-ethylbenzothiazolinesulfonic acid) (ABTS) was slightly lower in the case of the enzyme immobilized on the GSOCN, SOTCN, and EGSCN derivatives than in the case of the soluble enzyme. All the supports were more resistant than the soluble form to inactivation by H₂O₂ and by heat at neutral pH. When the stability and durability of the immobilized HRP

were analyzed, the cinnamoylated derivatives functioned as suitable supports for immobilizing peroxidase and to be suitable for industrial application of the enzyme [51, 52].

Sol-gel encapsulation of biological catalysts in silicate glasses has experienced a swift expansion due to the synthetic ease of enzyme entrapment procedures and to the significantly enhanced stability of the entrapped enzyme [101–103]. The activity of immobilized HRP has been employed for the asymmetric oxidation of thioanisole in acetonitrile with H_2O_2 . Encapsulation of HRP by the sol-gel method considerably enhanced its operational stability by protecting the peroxidase activity under harsh conditions. The TTN of the encapsulated HRP increased up to 6-fold ($\text{TTN} = 4.22 \times 10^3$) the rates observed with its homogeneous counterpart. The sulfoxide selectivity and the ee also increased greatly upon encapsulation. Coupling GOx reaction to the encapsulated peroxidase allowed high ee (up to 56%) and sulfoxide as sole product by elimination of side nonenantioselective and over-oxidation reactions. The heterogeneous catalyst can be recycled by simple filtration in successive runs. For every cycle, data regarding conversion, selectivity and enantioselectivity were obtained after 48 h of reaction. Similar recovery values of selectivity and enantioselectivity together with higher degrees of conversion than those obtained after 17 h confirm the robustness of the encapsulated biocatalyst [53].

Commercial supports are an attractive alternative to immobilize peroxidases. The main advantage of these materials is their wide availability, and several further functionalizations can be carried out. Among the different possibilities, the use of glutaraldehyde-activated supports is especially appropriate for immobilization in very mild conditions, even at moderately acidic pH values. Manganese peroxidases (MnP) from *Phanerochaete chrysosporium* and *Bjerkandera sp.* BOS55 were immobilized in glutaraldehyde-agarose gels. Immobilization maintained a high percentage of MnP activity for long periods of time (activity levels of 50–60% after more than 1 year at room temperature storage). Other desirable effects such as increased thermostability at 50–60°C for MnP from *Bjerkandera sp.* and higher resistance to high H_2O_2 concentrations for MnP for *P. chrysosporium* were also obtained, although the reason for the latter is still unclear. This is an interesting feature because it avoids the inactivation of the enzyme in the presence of an unbalanced concentration of H_2O_2 [54].

9.3 Chemical Modification

Chemical modifications of proteins have been carried out for a long time prior to any interest in the understanding of the chemical basis of the process. Early studies were motivated by the interest in quantitative determination of proteins and amino acids that conform its structure [104]. Intramolecular reactions occur naturally in posttranslational modifications such as disulfide bonding, glycosylation, or terminal residue cyclization. These modifications are relevant in structure–function relationships. They can produce conformational changes in order to switch between

active/inactive protein states or they can be related to a loss or gain in protein function. However, the *in vitro* chemical modification of proteins has emerged as a useful technique for protein amino acid sequence determination and in the study of the role of specific residues in the catalytic activity of an enzyme. Before the discovery of site-directed mutagenesis, the serine residue of the catalytic triad of subtilisin was converted to a cysteine by chemical modification [105, 106].

More recently, covalent chemical modification has been used as a powerful tool to enhance the functionality and stability of enzymes, for example, the covalent link of flavin to papain turned a protease into an oxido-reductase [107]. The use of this methodology was rekindled as a result of the explosion in the interest in commercial and synthetic applications of enzymes [108]. As a consequence, enzymes with new properties such as stability at extreme pH conditions, temperature, or solubility in organic solvents are being generated.

As mentioned before, the chemical modification of peroxidases is based on the reactivity of their exposed amino acids, besides their prosthetic group, ferroprotoporphyrin IX. As peroxidases are glycosylated enzymes, the hydroxyl groups of the carbohydrates can be modified as well (Fig. 9.1).

Over the years, a great variety of chemical groups have been synthesized as activated forms to be incorporated into the amino acid side chains; thus, there are great many possibilities of changing the chemical character or functionality of amino acids. On the other hand, chemical modification is a nonspecific process and produces mixtures of modified proteins. However, novel strategies of selective and efficient chemistry of proteins have been used to create site-specific or region-selective modification of single amino acids. A methodology that combines site-directed gene mutagenesis and selective synthesis allowed modification at multiple and predetermined sites in a peptide sequence [109]. For heme-enzymes, chemical modifications can be divided into modifications of the amino acids on the protein surface and modifications of the propionate groups of the heme molecule, although a combination of both has occurred as will be described below.

9.3.1 Chemical Modification of Superficial Amino Acids

In order to modify the characteristics of surface-exposed amino acids of an enzyme, both small and large molecules have been used. In an early work, small molecules such as anhydrides of mono- and dicarboxylic acids and picryl sulfonic acid (Fig. 9.7a) were used for the chemical modification of ϵ -amino groups of lysine residues of HRP. The authors found that the thermostability of the enzyme was enhanced and that phenomenon was attributed at the degree of modification, rather than the nature of the modifier. The increased thermostability of the modified enzyme was attributed to the decrease of the conformational mobility around the heme [58].

When compounds such as phthalic, maleic, and citraconic anhydrides (Fig. 9.7b) were used in the chemical modification of ϵ -amino groups of HRP and CPO, an

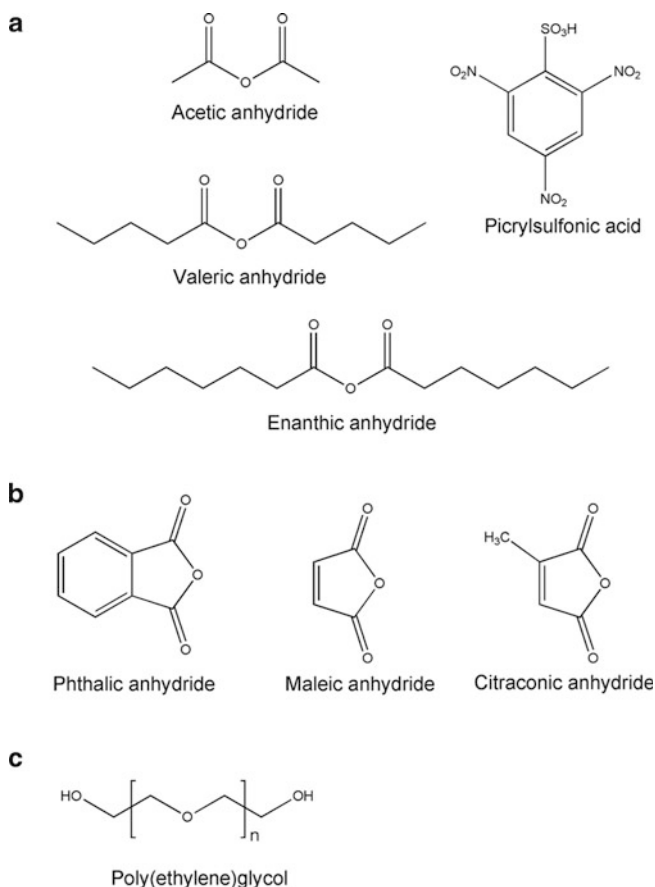


Fig. 9.7 (a) and (b) Anhydride derivatives, (c) poly(ethylene)glycol used for the chemical modification of ϵ -amino groups of horseradish peroxidase and chloroperoxidase

increased thermostability and tolerance to organic solvents was observed [63–67]. For example, the thermostability of HRP increased about 10-fold when modified with phthalic anhydride compared to native HRP [63]. The modified HRP showed a greater affinity and specificity to phenol and a higher efficiency in the removal of chlorophenols from an aqueous solution compared to native HRP either at low or at high temperature [64]. Not only was an enhanced thermostability obtained, also an increased tolerance to some organic solvents was observed for the HRP modified by phthalic anhydride. Additionally, a greater affinity and catalytic efficiency in organic solvents were observed for different substrates and the modified HRP. The improvements were attributed to conformational changes of both heme and aromatic residues surroundings [65]. In a related work where HRP was modified using maleic and citraconic anhydrides, a thermodynamic study showed that the thermal denaturation of modified HRP occurred at higher temperature than native

HRP. The existence of conformational changes was confirmed by circular dichroism studies, and the enhanced thermostability of modified HRP was attributed to side chain reorientations of aromatic residues [66].

On the other hand, when CPO was modified with citraconic, maleic, and phthalic anhydrides, catalytic efficiencies for phenol oxidation were higher compared to native CPO. Those modifications also improved their thermostability by 1–2-fold and tolerance to dimethylformamide (DMF). Circular dichroism studies showed no changes in the secondary structure of CPO, but changes in the environment of the aromatic residues were demonstrated by fluorescence studies [67]. Those findings are in agreement with those obtained for HRP modification using the same compounds. Modification with citraconic, maleic, and phthalic anhydrides represents a simple and powerful method to enhance catalytic properties, thermostability, and organic solvents tolerance of hemeperoxidases.

Poly(ethylene)glycol (PEG, Fig. 9.7c) and its derivatives are the principal representatives of large-sized molecules used in the chemical modification of heme-enzymes. The covalent attachment of PEG moieties is a procedure of great interest for enhancing the therapeutic and biotechnological potential of peptides and proteins. When PEG is properly linked to a polypeptide, it conveys its physicochemical properties, while the main biological functions, such as enzymatic activity, may be maintained [110]. PEG has been used in the chemical modification of enzymes principally because of its amphiphilic character. That characteristic conveys organic solvent solubility to the enzymes without loss in water solubility. For example, when HRP was modified with 2,4-bis(O-methoxypolyethyleneglycol)-6-chloro-s-triazine, 60% of the amino groups were modified, 70% of the enzymatic activity in aqueous solution was maintained, and it was found to be soluble in benzene. The enzymatic activity of the modified HRP in benzene was of 21% relative to that of unmodified enzyme in aqueous solution, and no changes in heme environment were observed [68]. After chemical modification of HRP with PEG aldehyde (MW 5,000), the isoelectric point (pI) was shifted from 8.8 in the native HRP to 5.5 for the modified enzyme. Even with this dramatic pI change, no significant differences in enzymatic activity in aqueous buffer were detected. The enzyme modified with the aldehyde was soluble and active in organic solvents such as toluene, dioxane, and methylene chloride, but it was more sensitive to H₂O₂ inhibition in toluene than in aqueous buffer [69].

Enzymes modified using PEG not only gained solubility in organic solvents but also showed an enhanced thermostability. When HRP was modified using methoxy-PEG (mPEG, MW 350–5,000) activated by nitrophenylchloroformate (mPEGpn), it became a modified enzyme with better thermostability than the native enzyme, but no correlation between the length of the mPEGpn used and the improvement in thermostability was found. After that, HRP was modified with mPEG (MW 5,000) activated by cyanuric chloride (mPEGcc). The number of modified lysine residues increased, but the thermal behavior of mPEGcc-modified HRP was similar to that of mPEGpn-modified HRPs. In all cases, the modification did not markedly change the stability in organic solvents [70]. In a related work, the modification of lysine residues of HRP by mPEG (MW 5,000) improved its stability towards pH. Similar

to other cases of PEG modification, an increased thermostability was found. The stabilization of modified HRP appeared to occur by suppressing initial unfolding and by lessening the extent of inactivation of the final enzyme form [71].

Besides HRP, other peroxidases have been modified with PEG. For example, the chemical modification of lignin peroxidase (LiP) from *P. chrysosporium* with PEG produced an enzyme that retained 100% of its activity over pentachlorophenol (PCP) in aqueous solutions. The activity of modified LiP was found to be over 2-fold that of the native enzyme in the presence of 10% (v/v) acetonitrile. Also, the solubility of PCP was enhanced by the addition of acetonitrile to aqueous solutions: in the presence of 15% (v/v) acetonitrile, the solubility was 10-fold higher (from 0.06 to 0.65 mM). The increase of PCP solubility in buffer solutions (pH 4.2) containing 15% acetonitrile permitted an increase in the catalytic efficiency of the modified enzyme in unoptimized reactor systems from 44 to 480 mol PCP/mol LiP·h [72]. On the other hand, the modified MnP from *Bjerkandera adusta* UAMH 8258 and the native enzyme showed similar catalytic properties in the oxidation of Mn(II) and other substrates such as 2,6-dimethoxyphenol, veratryl alcohol, guaiacol, and ABTS. However, the modified MnP showed greater resistance to denaturation by H₂O₂ and stability to organic solvents such as acetonitrile, DMF, tetrahydrofuran, methanol, and ethanol. The PEG-modified MnP also showed greater stability to higher temperatures and lower pH than the native enzyme [73].

Heme-proteins with *in vitro* peroxidase activity such as horse heart cytochrome *c* [77] and human hemoglobin [80] were also modified with PEG. The surface hydrophobicity from human hemoglobin was enhanced by chemical modification of superficial amino groups using PEG [80]. However, the heme environment (active site) of horse heart cytochrome *c* was altered as a consequence of the chemical modification of its superficial free amino groups. The catalytic efficiency of PEG-modified cytochrome for aromatic substrates was higher than that of native cytochrome [77]. This modified cytochrome showed activity at temperatures higher than 100°C and an optimal PEG/protein mass ratio of 2.8 was found, producing a fully thermostable biocatalyst at 80°C. Tertiary, secondary, and active site structures were analyzed by fluorescence, circular dichroism, and UV/visible spectroscopies. Besides its disordered structure, the pegylated protein showed a lower unfolding rate at the active site than the unmodified one. A shell-like structure seems to protect the heme environment, in which PEG is coiled on the protein surface with a primary shield of rigid water molecules, solvating the hydrophilic region of bound-PEG, and the PEG hydrophobic regions interacting with the hydrophobic clusters on protein surface [78].

9.3.2 Heme Modification

Regarding the chemical modification of the heme molecule located in the active site of peroxidases and other heme-proteins with peroxidase activity, a few examples are now discussed. Free carboxylic groups of heme from horse heart cytochrome *c*

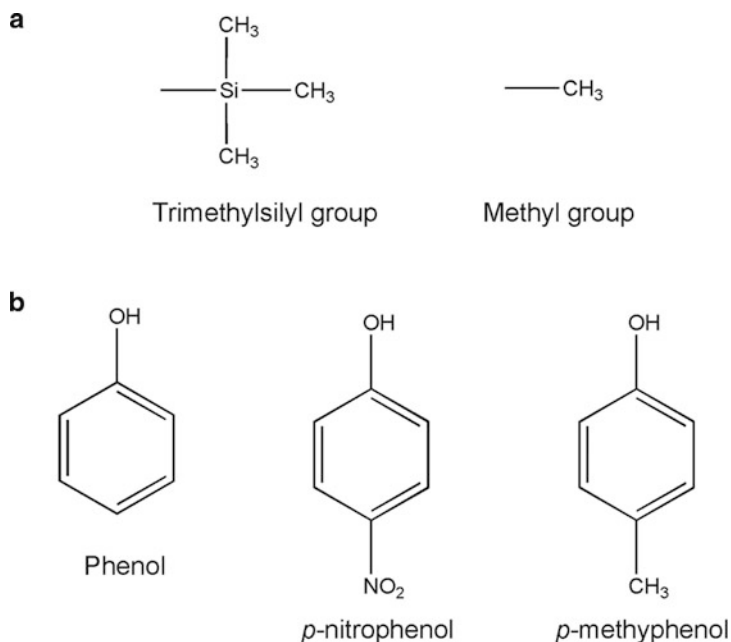


Fig. 9.8 Structures of chemical compounds for the esterification of the propionates groups of heme from (a) cytochrome *c* and (b) horseradish peroxidase

were modified by chemical reaction with methyl and trimethylsilyl compounds (Fig. 9.8a). The catalytic efficiency of methyl-modified cytochrome increased compared to native cytochrome. A subsequent process combining the alkylation of free carboxylic groups to form methyl esters with the modification of free amino groups with PEG enhanced the ability to oxidize 17 aromatic compounds from 20 tested, while the unmodified protein was only able to oxidize eight compounds [77]. After the double chemical modification of cytochrome *c* (called PEG-Cyt-Met), a particle that consisted of 85% PEG and only 14% protein was obtained. The higher activity of PEG-Cyt-Met could be a consequence of the conformational change of the active site by a disruption of the methionine-iron bond. Low temperature EPR on the PEG-Cyt-Met showed a pentacoordinated high spin iron, as in the case of peroxidases, while in the unmodified cytochrome *c*, the iron is hexacoordinated and low spin [111]. This could explain the enhanced catalytic efficiency of the double modification, where the PEG-Cyt-Met appeared to acquire a peroxidase nature. Also, the PEG-Cyt-Met was able to transform a variety of synthetic porphyrins and the petroporphyrin-rich asphaltene fraction in a ternary solvent mixture composed of methylene chloride, methanol, and phosphate buffer. The highest activity was found in the ternary systems with low water content (5%). Using hydrophobic peroxides, such as *tert*-butyl and cumene hydroperoxides, the operational life of the biocatalyst was extended. No reaction could be detected with the unmodified cytochrome *c* [79]. Asphaltene-rich deposits represent vast energetic resources

that motivate the investigation and the innovation of upgrading technologies, including biotechnological strategies.

Human hemoglobin was also modified by methyl esterification of its free carboxylic groups and by covalent coupling of PEG MW 5,000 to its free amino groups. The double modified hemoglobin (PEG–Met–hemoglobin) was assayed for the oxidation of 11 polycyclic aromatic hydrocarbons (PAHs) and two organosulfur aromatic compounds. Acenaphthene, anthracene, azulene, benzo(a)pyrene, fluoranthene, fluorene, phenanthrene, and pyrene were transformed to their respective quinones, while no biocatalytic reaction could be detected for chrysene and biphenyl. PEG–Met–hemoglobin showed up to 10 times higher activity than the unmodified protein. The equilibrium substrate-binding constants for unmodified and PEG–Met–hemoglobins showed that the catalytic enhancement could be attributed to the affinity increase for hydrophobic substrates in the modified protein [80]. As can be seen, the approach of double chemical modification of peroxidases and heme-proteins has proven to be useful in the improvement of their functionality and most importantly their ability to transform highly recalcitrant compounds.

Other approach used in the chemical modification of the heme group was the esterification of the HRP heme-propionates using phenol, *p*-nitrophenol, and *p*-methylphenol (Fig. 9.8b). These synthetic hemes were inserted to the apo-HRP to give a novel HRP, respectively. Reconstituted HRP with *p*-nitrophenol-modified heme had a larger initial rate, affinity, catalytic efficiency, and substrate-binding efficiency than native HRP in aqueous buffer and some organic solvents. The reconstituted HRPs showed higher thermostability and tolerance to DMF because of the active site hydrophobicity increase. The initial rate, affinity, catalytic efficiency, and substrate-binding efficiency increased with the increase of electron-withdrawing efficiency of substituents at 4-position of the phenols used to synthesize the heme derivatives, and contrariwise, the stability decreased. The changes on the catalytic properties and stability were related to the changes on the conformation of HRP due to the modification of the environment around the active site and an increase of α -helix content. This work showed an interesting strategy to improve peroxidase activity and stability through the increase of the hydrophobicity and the electron-withdrawing efficiency of the heme group [82].

In summary, it has been shown that chemical modification provides a rapid and inexpensive method to enhance the catalytic efficiency, thermostability, and organic solvent tolerance of peroxidases. The improvement of these characteristics leads to the generation of robust biocatalysts with higher potential usefulness in the industrial field.

9.4 Genetic Engineering of Peroxidases

Genetic engineering has been used to improve the selectivity and activity of enzymes and also to reach some other desirable properties for working in conditions found in industrial processes such as fluctuations in pH and high temperature [112].

Site-directed mutagenesis allows making one or more changes in any specific zone in the enzyme, normally carried out in or near the active site. In random mutagenesis, mutations are made in different parts of the enzyme, close or far from the active site [113, 114].

Genetic modifications by site-directed and random mutagenesis have been proven with peroxidases, obtaining in both cases interesting results, although in most of the reported cases, these studies are made to understand the relationship between structure and mechanism and not to enhance the catalytic functions for biotechnological applications [115–117].

By using these methods, Smith and coworkers were able to transform HRP into an enzyme capable of catalyzing oxygenations similar to cytochrome P450, i.e., insertion of oxygen in C–H bonds. The authors patented novel heme-based peroxidases from HRP modified at positions 38, 41, and 42 with stereoselectivity and activity similar to that of the cytochromes P450, but without the need for ancillary enzymes or reagents [118]. Substitution of all three residues simultaneously has been found to leave the catalytic cleft in a high spin state, contrary to the native enzyme with its low spin state, enabling faster catalytic activity after contact with the oxidizing agent and the reducing substrate. For aromatic substrates, high specificities were observed for the novel enzymes, with dissociation constants at the micromolar level. Thus, the enzymes generated from this invention may be used as generic biocatalysts to oxidize substrates in a stereoselective manner for processing or for the resolution of chiral mixtures. Notably, enzymatic turnover was stable in 50 mM H₂O₂. The interaction with the reducing substrate prior to the binding of H₂O₂ could protect the enzyme from the inactivation. In another interesting patent report from the same authors, a new peroxidase from *Coprinus cinereus*, was generated with the capacity of oxidizing a nonnatural substrate. The peroxidase mutant capable of oxidizing veratryl alcohol, wherein a residue was substituted by tryptophan in position 179, along with one or more acidic amino acid residues in sufficient proximity to the indole ring of the tryptophan proved to be able to enhance the stability of any charge on the indole ring and/or substrate or intermediate formed therewith. The original peroxidase is not normally capable of oxidizing veratryl alcohol to any significant degree, by which it is meant that such activity is not measurable, or is less than 1% of that of LiP [119]. Savenkova and coworkers used site directed mutagenesis to improve the peroxygenase activity of HRP. The strategy of the authors was based on decreasing the steric interference between the substrate and the ferryl oxygen in the native enzyme. In order to reach this goal, they removed His42 due to its location in the center of the access channel over the heme iron atom and it was mutated by valine. Because His42 is a critical catalytic residue, the authors relocated the histidine at position 38, replacing the native arginine (R38H/H42V). The access channel was enlarged also by replacing Arg38 by alanine (R38A). These two mutants showed peroxygenative catalysis efficiency of 190 and 1,400 higher as sulfoxidation catalyst, and 25- and 26-fold as epoxidation catalyst, respectively [120].

The increase of the access to the ferryl iron atom was also applied to cytochrome *c* peroxidase. In the work of Iffland et al., several mutants of cytochrome *c*

peroxidase (CCP) from *Saccharomyces cerevisiae* were produced through directed molecular evolution. In all of the selected mutants, the distal arginine (Arg48), which is fully conserved in the superfamily of peroxidases, was mutated to histidine. This allows generating mutants with increased activity against guaiacol, a classical peroxidase substrate. In this way, the substrate specificity of CCP changed from the protein cytochrome *c* to a small organic molecule. After three rounds of DNA shuffling and screening, mutants which possessed a 300-fold increased activity against guaiacol and up to 1,000-fold increased specificity for this substrate relative to that for the natural substrate were isolated [121]. It seems that the mutation Arg48His in CCP increases the steric access of the phenolic substrate to both the distal His52 and the ferryl oxygen. This would facilitate the required proton transfer from the phenol to either the distal His52 or the ferryl oxygen of compound II. The same strategy was applied to cytochrome *c*, a protein capable to oxidize several compounds by a mechanism similar to peroxidases [121]. Indeed, in the work of Torres et al., yeast cytochrome *c*, an electron transfer protein with peroxidase activity, was subjected to site-directed mutagenesis to open the access channel to the active site. The increase in the channel size was reached by changing the Phe 82, which is in the access entrance to the heme group, by a smaller amino acid, Gly, achieving ten times increase in the catalytic efficiency of the biocatalyst [122].

Genetic variants of peroxidases with improved catalytic abilities with respect to native enzymes have been developed through changes in amino acids moved away from the active site or the channel of access to heme by random mutagenesis. For example, in the work of Morawski et al., mutants of HRP were generated by different cycles of random mutagenesis. The produced mutants in each cycle displayed improvements in the specific activity against ABTS and guaiacol. Through two and three cycles of random mutagenesis, two different variants with higher activity were obtained. These variants presented seven (R93L, T102A, L131P, N135N -codon change-, L223Q, T257T -codon change-, V303E) and nine (N47S, T102A, G121G -codon change-, L131P, N135N -codon change-, L223Q, P226Q, T257T -codon change-, P289P -codon change-) mutations, respectively, most of them located in the periphery of the enzyme (Fig. 9.9). In terms of specific activity against ABTS, the variant of the second cycle was 5.4 times more active than the native enzyme, whereas the variant of the third cycle was 2.8 times more active [123].

Regarding CPO, probably the most versatile enzyme among peroxidases, directed evolution was successfully applied to produce an enzyme more resistant to suicide inactivation during primary olefin epoxidation [124]. Plasmid vectors containing error-prone copies of the CPO gene and a hygromycin B resistance marker gene were used to transform *C. fumago* spheroplasts and to produce mutant libraries. Three mutants were isolated after the third and fourth rounds of mutation and screening. The variants coming from the third round contained each one five mutations (V19A, D45G, H148R, V250A, S252P and V19A, D45G, L95P, V250A, S252P, respectively); meanwhile the mutant from the fourth round bore seven mutations (A19V, D45G, I64S, L95P, F125S, V250A and S252P). All the mutated residues were located at the periphery of the enzyme, far away from the heme

prosthetic group and the active site of CPO (Fig. 9.10). The enantioselectivity of the mutants on *cis*- β -methyl styrene and styrene is similar to that of the wild-type CPO. This suggests that the active site stereochemistry is not affected in the mutant enzymes. But somehow, CPO mutations must alter the geometry of the CPO active

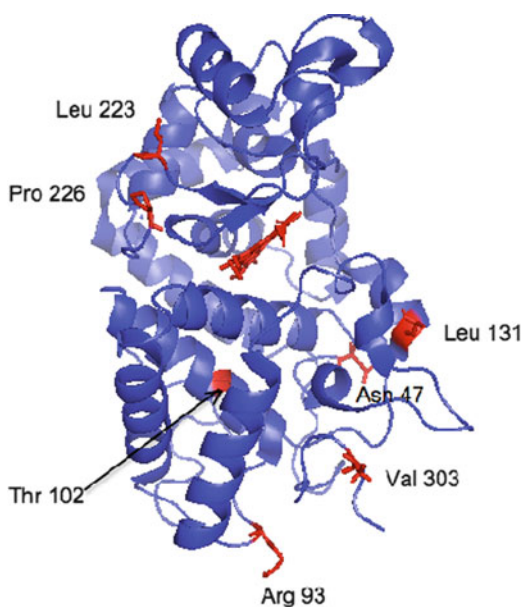


Fig. 9.9 Amino acid substitutions in the periphery of horseradish peroxidase found to be responsible for improvements in the specific activity against ABTS and guaiacol [123]

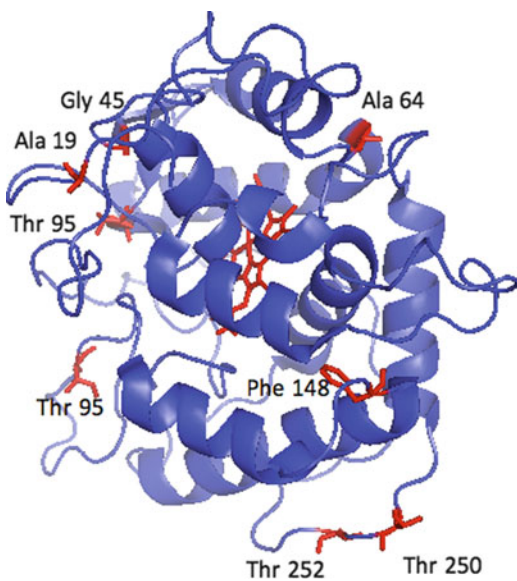


Fig. 9.10 Amino acid substitutions in the periphery of chloroperoxidase that promoted its resistance to suicidal inactivation by primary olefins [124]

site in such a way that it either protects the heme prosthetic group from the *N*-alkylation reaction, which inactivates the enzyme, or promotes the release of product from the *N*-alkylated enzyme [124].

In a closely related work, mutants of CPO were produced with higher epoxidation activity than the wild type enzyme. Up to 8-fold increase in the epoxidation activity was reached by one of the mutants, which had seven amino acid mutations (D131H, H147R, P203P -codon change-, V249A, S251P, A267A -codon change-, N284S) [125].

The results illustrate the ability of directed molecular evolution and site-directed mutagenesis technologies to deliver solutions about biotechnological problems of limited performance of peroxidase enzymes, approaching peroxidases as viable industrial biocatalysts.

9.5 Conclusions

Enzyme technology is a powerful tool to produce peroxidase-based biocatalyst with higher potential to be applied in industrial biotechnological processes. Immobilization of peroxidases on inorganic and organic materials enhances the tolerance of peroxidases towards the conditions normally found in many industrial processes, such as the presence or an organic solvent and high temperature. In addition, it is shown that immobilization helps to increase the total turnover number at levels high enough to justify the use of a peroxidase-based biocatalyst in a synthesis process. Chemical modification of peroxidases produces modified enzymes with higher thermostability and wider substrate variability. Finally, through mutagenesis approaches, it is possible to produce modified peroxidases capable to oxidize non-natural substrates with high catalytic activity and affinity.

Acknowledgment Acknowledgment for support of this work is made to National Council of Science and technology (CONACyT I003-CB2007-01-80986), PROMEP/103.5/09/4194, and ICyTDF PIFUTP08 148.

References

1. Bommarius AS, Riebel BR (2004) Biocatalysis, fundamentals and applications. Wiley, Weinheim
2. Seelbach K, van Deurzen MPJ, van Rantwijk F et al (1997) Improvement of the total turnover number and space-time yield for chloroperoxidase catalyzed oxidation. *Biotechnol Bioeng* 55:283–288
3. van de Velde F, Lourenço ND, Bakker M et al (2000) Improved operational stability of peroxidases by coimmobilization with glucose oxidase. *Biotechnol Bioeng* 69:286–291
4. Takahashi H, Li B, Sasaki T et al (2000) Catalytic activity in organic solvents and stability of immobilized enzymes depend on the pore size and surface characteristics of mesoporous silica. *Chem Mater* 12:3301–3305

5. Terrés E, Montiel M, Le Borgne S et al (2008) Immobilization of chloroperoxidase on mesoporous materials for the oxidation of 4,6-dimethyldibenzothiophene, a recalcitrant organic sulfur compound present in petroleum fractions. *Biotechnol Lett* 30:173–179
6. Montiel C, Terrés E, Domínguez JM et al (2007) Immobilization of chloroperoxidase on silica-based materials for 4,6-dimethyl dibenzothiophene oxidation. *J Mol Catal B Enzym* 48:90–98
7. Aburto J, Ayala M, Bustos-Jaimes I et al (2005) Stability and catalytic properties of chloroperoxidase immobilized on SBA-16 mesoporous materials. *Microporous Mesoporous Mater* 83:193–200
8. Hartmann M, Streb C (2006) Selective oxidation of indole by chloroperoxidase immobilized on the mesoporous molecular sieve SBA-15. *J Porous Mater* 13:347–352
9. Jung D, Streb C, Hartmann M (2008) Oxidation of indole using chloroperoxidase and glucose oxidase immobilized on SBA-15 as tandem biocatalyst. *Microporous Mesoporous Mater* 113:523–529
10. Jung D, Paradiso M, Wallacher D et al (2009) Formation of cross-linked chloroperoxidase aggregates in the pores of mesocellular foams: characterization by SANS and catalytic properties. *ChemSusChem* 2:161–164
11. Kumar A, Malhotra R, Malhotra BD et al (2000) Co-immobilization of cholesterol oxidase and horseradish peroxidase in a sol-gel film. *Anal Chim Acta* 414:43–50
12. Han YJ, Watson JT, Stucky GD et al (2002) Catalytic activity of mesoporous silicate-immobilized chloroperoxidase. *J Mol Catal B Enzym* 17:1–8
13. Borole A, Dai S, Cheng CL et al (2004) Performance of chloroperoxidase stabilization in mesoporous sol-gel glass using in situ glucose oxidase peroxide generation. *Appl Biochem Biotechnol* 113:273–285
14. Wang Z, King TL, Branagan SP et al (2009) Enzymatic activity of surface-immobilized horseradish peroxidase confined to micrometer-to nanometer-scale structures in nanocapillary array membranes. *Analyst* 134:851–859
15. Qiu H, Li Y, Ji G et al (2009) Immobilization of lignin peroxidase on nanoporous gold: Enzymatic properties and in situ release of H₂O₂ by co-immobilized glucose oxidase. *Bioresour Technol* 100:3837–3842
16. Cheng J, Yu SM, Zuo P (2006) Horseradish peroxidase immobilized on aluminum-pillared interlayered clay for the catalytic oxidation of phenolic wastewater. *Water Res* 40:283–290
17. Wang Q, Gao Q, Shi J (2004) Enhanced catalytic activity of hemoglobin in organic solvents by layered titanate immobilization. *J Am Chem Soc* 126:14346–14347
18. Lu X, Zou G, Li J (2007) Hemoglobin entrapped within a layered spongy Co₃O₄ based nanocomposite featuring direct electron transfer and peroxidase activity. *J Mater Chem* 17:1427–1432
19. Huang LCL, Chang HG (2004) Adsorption and immobilization of cytochrome c on nanodiamonds. *Langmuir* 20:5879–5884
20. Kreiner M, Parker MC (2005) Protein-coated microcrystals for use in organic solvents: application to oxidoreductases. *Biotechnol Lett* 27:1571–1577
21. Kadima TA, Pickard MA (1990) Immobilization of chloroperoxidase on aminopropyl-glass. *Appl Environ Microbiol* 56:3473–3477
22. Bódalo A, Bastida J, Máximo MF et al (2008) A comparative study of free and immobilized soybean and horseradish peroxidases for 4-chlorophenol removal: protective effects of immobilization. *Bioprocess Biosyst Eng* 31:587–593
23. Tatsumi K, Wada S, Ichikawa H (1996) Removal of chlorophenols from wastewater by immobilized horseradish peroxidase. *Biotechnol Bioeng* 51:126–130
24. Wang W, Xu Y, Wang DIC et al (2009) Recyclable nanobiocatalyst for enantioselective sulfoxidation: facile fabrication and high performance of chloroperoxidase-coated magnetic nanoparticles with iron oxide core and polymer shell. *J Am Chem Soc* 131:12892–12893
25. Aoun S, Chebli C, Baboulène M (1998) Noncovalent immobilization of chloroperoxidase onto talc: catalytic properties of a new biocatalyst. *Enzyme Microb Technol* 23:380–385

26. Carvalho RH, Lemos F, Cabral JMS et al (2007) Influence of the presence of NaY zeolite on the activity of horseradish peroxidase in the oxidation of phenol. *J Mol Catal B Enzym* 44:39–47
27. Torabi SF, Khajeh K, Ghasempur S et al (2007) Covalent attachment of cholesterol oxidase and horseradish peroxidase on perlite through silanization: activity, stability and co-immobilization. *J Biotechnol* 131:111–120
28. Satar R, Husain Q (2009) Applications of celite-adsorbed white radish (*Raphanus sativus*) peroxidase in batch process and continuous reactor for the degradation of reactive dyes. *Biochem Eng J* 46:96–104
29. Voss R, Brook MA, Thompson J et al (2007) Non-destructive horseradish peroxidase immobilization in porous silica nanoparticles. *J Mater Chem* 17:4854–4863
30. Chalkias NG, Giannelis EP (2007) An avidin-biotin immobilization approach for horseradish peroxidase and glucose oxidase on layered silicates with high catalytic activity retention and improved thermal behavior. *Ind Biotechnol* 3:82–88
31. Naves AF, Carmona-Ribeiro AM, Petri DFS (2007) Immobilized horseradish peroxidase as a reusable catalyst for emulsion polymerization. *Langmuir* 23:1981–1987
32. Petri A, Gambicorti T, Salvadori P (2004) Covalent immobilization of chloroperoxidase on silica gel and properties of the immobilized biocatalyst. *J Mol Catal B Enzym* 27:103–106
33. Liu Y, Wang M, Li J et al (2005) Highly active horseradish peroxidase immobilized in 1-butyl-3-methylimidazolium tetrafluoroborate room-temperature ionic liquid based sol–gel host materials. *Chem Commun* :1778–1780
34. Zhu Y, Shen W, Dong X et al (2005) Immobilization of hemoglobin on stable mesoporous multilamellar silica vesicles and their activity and stability. *J Mater Res* 20:2682–2690
35. Shin MJ, Park JY, Park K et al (2007) Novel sol-gel immobilization of horseradish peroxidase employing a detergentless micro-emulsion system. *Biotechnol Bioprocess Eng* 12:640–645
36. van de Velde F, Bakker M, van Rantwijk F et al (2001) Chloroperoxidase-catalyzed enantioselective oxidations in hydrophobic organic media. *Biotechnol Bioeng* 72:523–529
37. Schmidt TF, Caseli L, dos Santos Jr DS et al (2009) Enzyme activity of horseradish peroxidase immobilized in chitosan matrices in alternated layers. *Mat Sci Eng C* 29: 1889–1892
38. Bindhu LV, Abraham ET (2003) Immobilization of horseradish peroxidase on chitosan for use in nonaqueous media. *J Appl Polym Sci* 88:1456–1464
39. Jin Z, Su Y, Duan Y (2001) A novel method for polyaniline synthesis with the immobilized horseradish peroxidase enzyme. *Synth Met* 122:237–242
40. Zhang LH, Bai CH, Wang YS et al (2009) Improvement of chloroperoxidase stability by covalent immobilization on chitosan membranes. *Biotechnol Lett* 31:1269–1272
41. Mohamed SA, Aly AS, Mohamed TM et al (2008) Immobilization of horseradish peroxidase on nonwoven polyester fabric coated with chitosan. *Appl Biochem Biotechnol* 144:169–179
42. Leirião PRS, Fonseca LJP, Taipa MA et al (2003) Horseradish peroxidase immobilized through its carboxylic groups onto a polyacrylonitrile membrane: Comparison of enzyme performances with inorganic beaded supports. *Appl Biochem Biotechnol* 110:1–10
43. Veselova IA, Kireiko AV, Shekhovtsova TN (2009) Catalytic activity and the stability of horseradish peroxidase increase as a result of its incorporation into a polyelectrolyte complex with chitosan. *Appl Biochem Microbiol* 45:125–129
44. Bruns N, Tiller JC (2005) Amphiphilic network as nanoreactor for enzymes in organic solvents. *Nano Lett* 5:45–48
45. Liu L, Zhao F, Liu L et al (2009) Improved direct electron transfer and electrocatalytic activity of horseradish peroxidase immobilized on gemini surfactant-polyvinyl alcohol composite film. *Colloid Surf B Biointerf* 68:93–97
46. de Hoog HM, Nallani M, Cornelissen JLLM et al (2009) Biocatalytic oxidation by chloroperoxidase from *Caldariomyces fumago* in polymersome nanoreactors. *Org Biomol Chem* 7:4604–4610

47. Fernandes KF, Lima CS, Pinho H et al (2003) Immobilization of horseradish peroxidase onto polyaniline polymers. *Process Biochem* 38:1379–1384
48. Fernandes KF, Lima CS, Lopes FM et al (2004) Properties of horseradish peroxidase immobilised onto polyaniline. *Process Biochem* 39:957–962
49. Chen X, Li C, Liu Y et al (2008) Electrocatalytic activity of horseradish peroxidase/chitosan/carbon microsphere microbio-composites to hydrogen peroxide. *Talanta* 77:37–41
50. Schmidt TF, Caseli L, Viitala T et al (2008) Enhanced activity of horseradish peroxidase in Langmuir–Blodgett films of phospholipids. *Biochim Biophys Acta* 1778:2291–2297
51. Rojas-Melgarejo F, Rodríguez-López JN, García-Cánovas F et al (2004) Immobilization of horseradish peroxidase on cinnamic carbohydrate esters. *Process Biochem* 39:1455–1464
52. Rojas-Melgarejo F, Rodríguez-López JN, García-Cánovas F et al (2004) Stability of horseradish peroxidase immobilized on different cinnamic carbohydrate esters. *J Chem Technol Biotechnol* 79:1148–1154
53. Ferrer ML, Levy D, Gomez-Lor B et al (2004) High operational stability in peroxidase-catalyzed non-aqueous sulfoxidations by encapsulation within sol-gel glasses. *J Mol Catal B Enzym* 27:107–111
54. Mielgo I, Palma C, Guisan JM et al (2003) Covalent immobilisation of manganese peroxidases (MnP) from *Phanerochaete chrysosporium* and *Bjerkandera sp.* BOS55. *Enzyme Microb Technol* 32:769–775
55. Ferrer I, Dezotti M, Durán N (1991) Decolorization of Kraft effluent by free and immobilized lignin peroxidases and horseradish peroxidase. *Biotechnol Lett* 13:577–582
56. Di Risio S, Yan N (2009) Adsorption and inactivation behavior of horseradish peroxidase on cellulosic fiber surfaces. *J Colloid Interf Sci* 338:410–419
57. Rennke HG, Venkatachalam MA (1979) Chemical modification of horseradish peroxidase. Preparation and characterization of tracer enzymes with different isoelectric points. *J Histochem Cytochem* 27:1352–1353
58. Ugarova NN, Rozhkova GD, Berezin IV (1979) Chemical modification of the ϵ -amino groups of lysine residues in horseradish peroxidase and its effect on the catalytic properties and thermostability of the enzyme. *Biochim Biophys Acta* 570:31–42
59. Blanke SR, Hager LP (1990) Chemical modification of chloroperoxidase with diethyl-pyrocyanate. Evidence for the presence of an essential histidine residue. *J Biol Chem* 265:12454–12461
60. Urrutigoity M, Baboulène M, Lattes A (1991) Use of pyrocyanates for chemical modification of histidine residues of horseradish peroxidase. *Bioorg Chem* 19:66–76
61. Rees DG, Halling PJ (2001) Chemical modification probes accessibility to organic phase: proteins on surfaces are more exposed than in lyophilized powders. *Enzyme Microb Technol* 28:282–292
62. van Dongen SFM, Teeuwen RLM, Nallani M et al (2009) Single-step azide introduction in proteins via an aqueous diazo transfer. *Bioconjug Chem* 20:20–23
63. Liu JZ, Song HY, Weng LP et al (2002) Increased thermostability and phenol removal efficiency by chemical modified horseradish peroxidase. *J Mol Catal B Enzym* 18:225–232
64. Song HY, Liu JZ, Xiong YH et al (2003) Treatment of aqueous chlorophenol by phthalic anhydride-modified horseradish peroxidase. *J Mol Catal B Enzym* 22:37–44
65. Song HY, Yao JH, Liu JZ et al (2005) Effects of phthalic anhydride modification on horseradish peroxidase stability and structure. *Enzyme Microb Technol* 36:605–611
66. Liu JZ, Wang TL, Huang MT et al (2006) Increased thermal and organic solvent tolerance of modified horseradish peroxidase. *Protein Eng Des Sel* 19:169–173
67. Liu JZ, Wang M (2007) Improvement of activity and stability of chloroperoxidase by chemical modification. *BMC Biotechnol* 7:23–30
68. Takahashi K, Nishimura H, Yoshimoto T et al (1984) A chemical modification to make horseradish peroxidase soluble and active in benzene. *Biochim Biophys Res Commun* 121:261–265

69. Wirth P, Soupe J, Tritsch D et al (1991) Chemical modification of horseradish peroxidase with ethanal-methoxypolyethylene glycol: solubility in organic solvents, activity, and properties. *Bioorg Chem* 19:133–142
70. Garcia D, Marty JL (1998) Chemical modification of horseradish peroxidase with several methoxypolyethylene glycols. *Appl Biochem Biotechnol* 73:173–184
71. Garcia D, Ortega F, Marty JL (1998) Kinetics of thermal inactivation of horseradish peroxidase: stabilizing effect of methoxypoly(ethylenglycol). *Biotechnol Appl Biochem* 27:49–54
72. Wang P, Woodward CA, Kaufman EN (1999) Poly(ethylene glycol)-modified ligninase enhances pentachlorophenol biodegradation in water-solvent mixtures. *Biotechnol Bioeng* 64:290–297
73. Wang Y, Vazquez-Duhalt R, Pickard MA (2002) Purification, characterization, and chemical modification of manganese peroxidase from *Bjerkandera adusta* UAMH 8258. *Curr Microbiol* 45:77–87
74. Al-Azzam W, Pastrana EA, King B et al (2005) Effect of the covalent modification of horseradish peroxidase with poly(ethylene glycol) on the activity and stability upon encapsulation in polyester microspheres. *J Pharm Sci* 94:1808–1819
75. Quintanilla-Guerrero F, Duarte-Vázquez MA, Tinoco R et al (2008) Chemical modification of turnip peroxidase with methoxypolyethylene glycol enhances activity and stability for phenol removal using the immobilized enzyme. *J Agric Food Chem* 56:8058–8065
76. Temoçin Z, Yiğitoğlu M (2009) Studies on the activity and stability of immobilized horseradish peroxidase on poly(ethylene terephthalate) grafted acrylamide fiber. *Bioprocess Biosyst Eng* 32:467–474
77. Tinoco R, Vazquez-Duhalt R (1998) Chemical modification of cytochrome C improves their catalytic properties in oxidation of polycyclic aromatic hydrocarbons. *Enzyme Microb Technol* 22:8–12
78. Garcia-Arellano H, Valderrama B, Saab-Rincón G et al (2002) High temperature biocatalysis by chemically modified cytochrome c. *Bioconj Chem* 13:1336–1344
79. Garcia-Arellano H, Buenostro-Gonzalez E, Vazquez-Duhalt R (2004) Biocatalytic transformation of petroporphyrins by chemical modified cytochrome c. *Biotechnol Bioeng* 85:790–798
80. Torres E, Vazquez-Duhalt R (2000) Chemical modification of hemoglobin improves biocatalytic oxidation of PAHs. *Biochem Biophys Res Commun* 273:820–823
81. Feng JY, Liu JZ, Ji LN (2008) Thermostability, solvent tolerance, catalytic activity and conformation of cofactor modified horseradish peroxidase. *Biochimie* 90:1337–1346
82. Song HY, Liu JZ, Weng LP et al (2009) Activity, stability, and unfolding of reconstituted horseradish peroxidase with modified heme. *J Mol Catal B Enzym* 57:48–54
83. Matsuo T, Hayashi A, Abe M et al (2009) Meso-unsubstituted iron corrole in hemoproteins: remarkable differences in effects on peroxidase activities between myoglobin and horseradish peroxidase. *J Am Chem Soc* 131:15124–15125
84. Glettenberg M, Niemeyer CM (2009) Tuning of peroxidase activity by covalently tethered DNA oligonucleotides. *Bioconj Chem* 20:969–975
85. Harris JM (1992) Poly(ethylene glycol) chemistry: biotechnical and biomedical applications. Plenum, New York
86. Araiso T, Dunford HB (1981) Effect of modification of heme propionate groups on the reactivity of horseradish peroxidase. *Arch Biochem Biophys* 211:346–351
87. Cao L, van Langen L, Sheldon RA (2003) Immobilised enzymes: carrier-bound or carrier-free? *Curr Opin Biotechnol* 14:387–394
88. Cao L (2005) Immobilised enzymes: science or art? *Curr Opin Chem Biol* 9:217–226
89. Hoffmann F, Cornelius M, Morell J et al (2006) Periodic mesoporous organosilicas (PMOs): past, present, and future. *J Nanosci Nanotechnol* 6:265–288
90. Hartmann M (2005) Ordered mesoporous materials for bioadsorption and biocatalysis. *Chem Mater* 17:4577–4593

91. Yiu HHP, Wright PA (2005) Enzymes supported on ordered mesoporous solids: a special case of an inorganic-organic hybrid. *J Mater Chem* 15:3690–3700
92. Hudson S, Cooney J, Magner E (2008) Proteins in mesoporous silicates. *Angew Chem Int Ed Engl* 47:8582–8594
93. Vazquez-Duhalt R, Torres E, Valderrama B et al (2002) Will biochemical catalysis impact the petroleum refining industry? *Energy Fuels* 16:1239–1250
94. Hudson S, Cooney J, Hodnett BK et al (2007) Chloroperoxidase on periodic mesoporous organosilanes: immobilization and reuse. *Chem Mater* 19:2049–2055
95. Duran N, Rosa MA, D'Annibale A et al (2002) Applications of laccases and tyrosinases (phenoloxidases) immobilized on different supports: a review. *Enzyme Microb Technol* 31:907–931
96. Sun WQ, Payne GF (1996) Tyrosinase-containing chitosan gels: a combined catalyst and sorbent for selective phenol removal. *Biotechnol Bioeng* 51:79–86
97. Urugami T, Tokura S (2006) Material science of chitin and chitosan. Springer, Berlin
98. Çetinus AS, Öztop HN (2003) Immobilization of catalase into chemically crosslinked chitosan beads. *Enzyme Microb Technol* 32:889–894
99. D'Annibale A, Stazi SR, Vinciguerra V et al (1999) Characterization of immobilized laccase from *Lentinula edodes* and its use in olive-mill wastewater treatment. *Process Biochem* 34:697–706
100. Liang ZP, Feng YQ, Meng SX et al (2005) Preparation and properties of urease immobilized onto glutaraldehyde cross-linked chitosan beads. *Chin Chem Lett* 16:135–138
101. Pierre AC (2004) The sol-gel encapsulation of enzymes. *Biocatal Biotransform* 22:145–170
102. van Unen DJ, Engbersen JFJ, Reinhoudt DN (2001) Sol-gel immobilization of serine proteases for application in organic solvents. *Biotechnol Bioeng* 75:154–158
103. Park CB, Clark DS (2002) Sol-gel encapsulated enzyme arrays for high-throughput screening of biocatalytic activity. *Biotechnol Bioeng* 78:229–235
104. Means GE, Feeney RE (1998) Chemical modifications of proteins: a review. *J Food Biochem* 22:399–425
105. Polgar L, Bender ML (1966) A new enzyme containing a synthetically formed active site. Thiolsubtilisin. *J Am Chem Soc* 88:3153–3154
106. Neet KE, Koshland DE Jr (1966) The conversion of serine at the active site of subtilisin to cysteine: a 'chemical mutation'. *Proc Natl Acad Sci USA* 56:1606–1611
107. Kaiser ET (1988) Catalytic activity of enzymes altered at their active sites. *Angew Chem Int Ed Engl* 27:913–922
108. DeSantis G, Jones JB (1999) Chemical modification of enzymes for enhanced functionality. *Curr Opin Biotechnol* 10:324–330
109. van Kasteren SI, Kramer HB, Jensen HH et al (2007) Expanding the diversity of chemical protein modification allows post-translational mimicry. *Nature* 446:1105–1109
110. Veronese FM (2001) Peptide and protein PEGylation: a review of problems and solutions. *Biomaterials* 22:405–417
111. Busi E, Howes BD, Pogni R et al (2000) Modified cytochrome c/H₂O₂ system: spectroscopic EPR investigation of the biocatalytic behaviour. *J Mol Catal B Enzym* 9:39–48
112. Hibbert EG, Dalby PA (2005) Directed evolution strategies for improved enzymatic performance. *Microb Cell Fact* 4:29
113. Joyce GF (2004) Directed evolution of nucleic acid enzymes. *Annu Rev Biochem* 73:791–836
114. Williams GJ, Nelson AS, Berry A (2004) Directed evolution of enzymes for biocatalysis and the life sciences. *Cell Mol Life Sci* 61:3034–3046
115. Saab-Rincón G, Valderrama B (2009) Protein engineering of redox-active enzymes. *Antioxid Redox Signal* 11:167–192
116. Mester T, Tien M (2001) Engineering of a manganese-binding site in lignin peroxidase isozyme H8 from *Phanerochaete chrysosporium*. *Biochem Biophys Res Commun* 284:723–728

117. Raven EL, Çelik A, Cullis PM et al (2001) Engineering the active site of ascorbate peroxidase. *Biochem Soc Trans* 29:105–111
118. Smith AT, Ngo E (2007) Novel peroxidases and uses. Patent number WO/2007/020428, PCT/GB2006/003045
119. Smith AT, Doyle WA (2006) Engineered peroxidases with veratryl alcohol oxidase activity. Patent number WO/2006/114616, PCT/GB2006/001515
120. Savenkova MI, Kuo JM, Ortiz de Montellano PR (1998) Improvement of peroxygenase activity by relocation of a catalytic histidine within the active site of horseradish peroxidase. *Biochemistry* 37:10828–10836
121. Iffland A, Tafelmeyer P, Saudan C et al (2000) Directed molecular evolution of cytochrome c peroxidase. *Biochemistry* 39:10790–10798
122. Torres E, Sandoval JV, Rosell FI et al (1995) Site-directed mutagenesis improves the biocatalytic activity of iso-1-cytochrome c in polycyclic hydrocarbon oxidation. *Enzyme Microb Technol* 17:1014–1020
123. Morawski B, Lin Z, Cirino P et al (2000) Functional expression of horseradish peroxidase in *Saccharomyces cerevisiae* and *Pichia pastoris*. *Protein Eng* 13:377–384
124. Rai GP, Zong Q, Hager LP (2000) Isolation of directed evolution mutants of chloroperoxidase resistant to suicide inactivation by primary olefins. *Isr J Chem* 40:63–70
125. Rai GP, Sakai S, Flórez AM et al (2001) Directed evolution of chloroperoxidase for improved epoxidation and chlorination catalysis. *Adv Synth Catal* 343:638–645

Chapter 10

Reactor Engineering

Juan M. Lema, Carmen López, Gemma Eibes, Roberto Taboada-Puig,
M. Teresa Moreira, and Gumersindo Feijoo

Contents

10.1	Characteristics of Peroxidative Reactions Influencing Reactor Design	246
10.1.1	Enzyme	246
10.1.2	Oxidizing Agent	247
10.1.3	Mediators	248
10.1.4	Additives	248
10.1.5	Oxygen	249
10.1.6	Temperature and pH	249
10.1.7	Agitation	250
10.1.8	Immobilization	251
10.1.9	Presence of Organic Solvents	251
10.2	Reactor Configuration	252
10.2.1	Discontinuous Stirred Tank Reactor	253
10.2.2	Continuous Stirred Tank Reactor	257
10.2.3	Membrane Reactor	259
10.2.4	Plug Flow Reactor	262
10.2.5	Electrochemical Reactor	265
10.3	Enzymatic Membrane Reactor	266
10.3.1	Dye Decolorization in a One-Stage Enzymatic Membrane Reactor	266
10.3.2	Other Applications of One-Stage Enzymatic Membrane Reactors	273
10.3.3	Two-Stage Enzymatic Membrane Reactor	275
10.4	Biphasic Reactors	279
10.4.1	Solvent Selection	279
10.4.2	Effect of Substrates and Cosubstrates of VP	280
10.4.3	Selection of a Surfactant	281
10.4.4	Enhancement of Mass Transfer and Enzyme Stability	281
10.4.5	Degradation of Anthracene in TPPB	283
	References	284

Abstract In this chapter, the engineering aspects of processes catalyzed by peroxidases will be presented. In particular, a discussion of the existing technologies that utilize peroxidases for different purposes, such as the removal of recalcitrant compounds or the synthesis of polymers, is analyzed. In the first section, the essential variables controlling the process will be investigated, not only those that

are common in any enzymatic system but also those specific to peroxidative reactions. Next, different reactor configurations and operational modes will be proposed, emphasizing their suitability and unsuitability for different systems. Finally, two specific reactors will be described in detail: enzymatic membrane reactors and biphasic reactors. These configurations are especially valuable for the treatment of xenobiotics with high and poor water solubility, respectively.

10.1 Characteristics of Peroxidative Reactions Influencing Reactor Design

The design of an enzyme-based process should investigate the influence of different variables affecting the performance of the system. Enzyme concentration, temperature, agitation, and pH are key factors in any enzymatic reaction. However, there are specific considerations for peroxidase-catalyzed reactions, for instance, the compounds involved in the catalytic cycle (oxidizing agent, mediators). All of these factors will influence the choice of the reactor and/or the feasibility of the process since it is directly related to the cost of the enzyme, the limiting variable. We will emphasize the effect of any of those variables in the stability of peroxidases and the strategies used in the operation of enzymatic reactors.

10.1.1 Enzyme

The selection of the most suitable enzyme for a certain purpose mainly depends on its biocatalytic characteristics. Once a correct choice has been made, it is important to minimize the expenses associated with the enzyme use, as the economic feasibility of enzymatic processes is likely to depend on the cost of the enzyme production. In this context, several authors showed that the performance of various peroxidase processes was independent of enzyme purity [1, 2], even suggesting that the crude enzyme was protected from inactivation [3, 4]. Microfiltration and subsequent ultrafiltration stages are sufficient to separate biomass and concentrate the enzyme for an economically viable operation [2, 5].

The enzyme concentration is a parameter that is commonly optimized during the operation of an enzymatic reactor [6, 7]. Enzyme concentration must be balanced with peroxide, substrate, and mediator concentration from a stoichiometric point of view. If the concentrations of substrate, peroxide, or mediator (when required) are limiting, any further increase in enzyme concentration causes a significant change in the reaction rate. Higher reaction yields can only be reached by varying those operational conditions rather than by adding more enzyme [7]. Once the optimal enzyme/peroxide/substrate ratio is established, kinetics can be responsible for the limitation of the process. In that case, increasing enzyme concentration will boost the enzyme reaction rate [8].

In order to preserve enzyme activity during the reaction process, special attention must be paid on the substrates that cause direct or indirect enzyme inactivation. Since peroxide is a strong peroxidase inhibitor, a low peroxide/enzyme ratio must be selected. When treating phenolic compounds, the polymeric products obtained from the action of peroxidases also cause enzyme inactivation [9]. If the enzyme is inactivated, not only is the reaction hindered but, sometimes, there is a direct oxidation of the substrate by the peroxide, which causes an enantioselective reduction in some synthetic reactions [10, 11]. In these cases, an appropriate enzyme concentration and usually an adequate enzyme addition strategy are considered [8].

10.1.2 Oxidizing Agent

Hydrogen peroxide is the most widespread oxidizing agent for the two-electron oxidation of the native peroxidase, but other organic peroxides may also be used [12]. In several synthetic applications of chloroperoxidase (CPO), tert-butyl hydroperoxide (TBHP) has replaced H_2O_2 as an electron donor. The use of TBHP is reasonable because tert-butyl alcohol, the product from TBHP, was previously shown to exert a stabilizing effect on CPO. Furthermore, the organic peroxide is also beneficial in the presence of organic solvents because it partitions between the two phases and the enzyme is then protected from peroxide-induced inactivation [13, 14]. In particular, CPO not only catalyzed peroxidative reactions but it was also reported to catalyze the aerobic oxidation of various substrates with the combination of molecular oxygen as a primary oxidant and dihydroxyfumaric acid (DFA) or ascorbic acid (AA) as a sacrificial reductant [11].

High concentrations of H_2O_2 lead to inactivation of hemoproteins, including peroxidases, in a process known as “suicide inactivation” (see Chap. 11). However, CPO is significantly resistant to suicide inactivation because of its intrinsic catalase activity [15]. Low concentrations of metal ions, amino-acids such as histidine, tyrosine, and cysteine, were demonstrated to protect horseradish peroxidase (HRP) against this process [16]. The presence of high molecular weight polyethylene glycol (PEG) has also been demonstrated to greatly reduce enzyme inactivation [17].

Due to the double effect that H_2O_2 produces in the catalytic activity of peroxidases, both as substrate and inhibitor, the concentration of this compound must be selected very carefully. A low peroxide/enzyme ratio preserves the enzyme against inactivation, although a minimum peroxide/substrate ratio must be reached to avoid stoichiometric limitations. The most appropriate peroxide/substrate ratio can be predicted from both the catalytic cycle of the enzyme and the reaction mechanism. Considering MnP for the degradation of Orange II as an example, 1 mol of H_2O_2 enzymatically generates 2 mol of Mn^{3+} , which are the acceptors of 2 mol of electrons produced during the oxidation of 1 mol of Orange II [18]. An equimolar H_2O_2 /Orange II ratio should be enough for the degradation of Orange II,

a hypothesis which was experimentally verified [19]. Other authors also studied the best H_2O_2 /phenol ratio for the degradation of phenol by HRP and soybean peroxidase (SBP), with ratios of 1 or 1.5 [7, 20]. A lower H_2O_2 concentration leads to lower reaction yields, although higher concentrations cause enzyme inactivation.

On the other hand, strategies based on protein engineering can be used for the conformational stabilization of the enzyme to be resistant to H_2O_2 [21]. Other approaches have been used to avoid inactivation of peroxidases by maintaining low concentrations of H_2O_2 in the medium, such as the step-addition or the continuous and progressive addition of H_2O_2 by a peristaltic pump [5, 22], the use of a H_2O_2 -stat for a controlled concentration in the medium [23], H_2O_2 generation by electrochemical methods [24], or by coupling a H_2O_2 producing enzymatic reaction, as for instance with glucose oxidase [25]. Kinetic models for the suicide inactivation of peroxidases have been widely described, even considering the addition of excess substrate (which would preclude the inactivation) or other protective substances [26–29].

10.1.3 Mediators

Redox mediators are compounds that broaden the degrading capacity of enzymes, enhancing their specificity to a wider range of substrates/recalcitrant compounds as well as the degradation efficiency [30]. Low molecular weight, diffusible redox mediators not only may provide high redox potentials required for the degradation of recalcitrant substances but are also able to migrate into the aromatic structure of the compound. Some compounds that have been used as mediators are 1-hydroxybenzotriazole, veratryl alcohol, violuric acid, 2-methoxy-phenothiazone, 3-hydroxyanthranilic acid, anthraquinone 2,6-disulfonic acid, 2,2-azino-bis(3-ethylbenzothiazoline-6-sulfonic acid), *N*-hydroxyacetanilide, phenol red, 3,3', 5,5'-tetramethyl benzidine, dichlorophenol red, 2,2',6,6'-tetramethylpiperidine-*N*-oxyl radical, syringaldehyde and acetosyringone, and others [30, 31].

On the other hand, unsaturated lipids may act as secondary mediators of the MnP/Mn system, in a mechanism known as lipid peroxidation, which is a free radical chain-reaction proceeding via the oxidation of unsaturated lipids [32, 33]. Thiols may also undergo oxidation by MnP/Mn and produce thiyl radicals, which in turn mediate in the oxidation of a variety of compounds [34].

10.1.4 Additives

The addition of some compounds to enzymatic reactions catalyzed by peroxidases is a common technique that fulfils several purposes: (1) to increase the solubility of organic substrates and (2) to enhance the enzyme lifetime by preserving it from inactivation.

The phenoxy radicals generated in the catalytic treatment of phenolic compounds attack the active site of the enzyme [35]. Other authors stated that the inactivation is caused by the lack of contact between the substrate and the enzyme resulting from entrapment of the enzyme by the polymers formed in the reaction [36]. When this kind of inactivation occurs, the application of hydrophilic additives (PEG, gelatine, borate) with a greater affinity for the polymers than the enzyme helps protect the enzyme and greatly enhances its catalytic lifetime [3]. Absorbents such as chitosan, activated carbon, or activated diethyl aminoethyl (DEAE) cellulose were also applied to remove colored reaction products from phenolic degradation by peroxidases [37]. Furthermore, the attachment of PEG to peroxidases can effectively increase the compatibility between the enzyme and some organic solvents, thus increasing solubility and activity (see Chap. 9) [38]. Also polymers such as PEG and polyethyleneimine (PEI) were observed to have a protective effect against peroxide inactivation of CPO [39].

10.1.5 Oxygen

Oxygen is not an essential parameter in the operation of peroxidase reactors, unless an electroenzymatic reactor is being operated, where oxygen has to be bubbled in the cathode for the electrochemical generation of H_2O_2 [40]. In particular cases, the presence of dissolved oxygen (DO) is required for the aerobic oxidation of DFA or AA by CPOs. Although the effect of DO on the stability of peroxidases has not been analyzed profoundly, a beneficial effect on the production of fungal peroxidases in *in vivo* cultures has been reported [41, 42]. Furthermore, lignin peroxidase (LiP) was demonstrated to be stable for long periods (more than 4 days) at high DO concentrations [43].

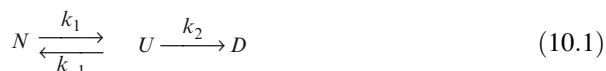
Interestingly, DO has been utilized as a control parameter to establish steady state conditions during the operation of a continuous enzymatic reactor for dye decolorization [8]. An unexpected decrease in the level of DO was the warning signal of the loss of peroxidase activity or dye overload, whereas the sudden increase reflected an extra dosing of H_2O_2 , which would probably imply higher enzyme deactivation rate.

10.1.6 Temperature and pH

Temperature and pH are variables that are frequently evaluated during the optimization of a specific process [44–47]. The choice of operation temperature always represents a compromise between enzyme activity and stability, since temperature exerts opposite effects on both. Even though each enzyme usually has its specific pH and temperature for a maximal activity, it may change when immobilized into a support or when using different substrates (see Chap. 9) [48]. The pH dependence

can even be temperature-dependent [48]. Both parameters not only affect the reaction rate and enzyme stability but also may play an important role in the process, as for instance in resolution of racemic mixtures [48] or the solubility of products [49]. Hence, optimal conditions for pH and temperature should be reevaluated in each specific case of study.

Commonly, the thermal denaturation of proteins is often discussed in terms of the Lumry–Eyring model, which involves two steps: reversible unfolding and irreversible alteration of the unfolded state to produce the final denatured state, which is unable to fold back to the native protein.



where N is the native state, U is the reversible unfolded state, and D is a final irreversible denatured state [50]. k_1 , k_{-1} , and k_2 are the rate constants for reversible denaturation, renaturation, and irreversible denaturation stage, respectively. However, simpler mathematical models that are particular cases of the whole Lumry–Eyring model are often utilized. In particular, the model that includes only one irreversible step, assuming that $k_2 \gg k_1$ and $k_2 \gg k_{-1}$, has been frequently described. In this model, enzyme inactivation is described according to a first-order one-step mechanism, and customary k_d is considered to present an Arrhenius-type dependence on temperature [51].

10.1.7 Agitation

Although there are a significant number of publications reporting enzyme deactivation due to parameters such as pH and temperature, much less is known about the cause of enzyme deactivation due to hydrodynamic shear stress. Elias and Joshi [52] studied the damage produced by shear forces in enzymes and concluded that (1) some proteins deactivate only due to hydrodynamic shear; (2) for those proteins, the rate of deactivation increases in the presence of gas–liquid interface; (3) some proteins do not get deactivated no matter how high the applied hydrodynamic shear is, in the absence of gas–liquid interface; and (4) for the proteins that need gas–liquid interface for deactivation, the rate of deactivation increases with an increase in the hydrodynamic shear.

Concerning peroxidases, there is not much information about their inactivation by mechanical stress. Venkatadri and Irvine concluded that the loss of LiP activity under agitated conditions (100–200 rpm) was due to mechanical forces [43]. The effect of two of the most applied agitation modes (magnetic and mechanical stirring) in the stability of soluble MnP was studied by our group, and we could not appreciate differences between both modes. When using immobilized enzymes, magnetic stirring sometimes decreased the support integrity, and this may have an impact on immobilized enzyme stability. However, our results showed that even MnP immobilized on agarose beads resulted in the same stability with magnetic and mechanical

agitation both at low or high agitation speed. Significantly, agitation has a double effect in biphasic reactors where a second immiscible phase is present [53]. Increasing agitation rate would augment the interfacial area, and interfacial interaction is the main cause of enzyme inactivation in the presence of organic solvents [54].

10.1.8 Immobilization

Enzyme stabilization is a major concern, since poor stability is usually the limiting factor in any enzyme reactor operation. Enzyme immobilization is the most relevant strategy for enzyme stabilization [55]. Enzyme immobilization inside a porous solid can enhance the operational stability of the enzyme because the matrix may hinder the rotational freedom of the protein, and hence the unfolding induced by any distorting agent (pH, heat, organic solvents) may occur to a lesser extent (see Chap. 9) [56, 57]. These possible conformational changes of the protein are more limited when the immobilization takes place by means of multipoint covalent attachment, which contributes to the rigidity of the enzyme [56]. Furthermore, immobilization allows an easy enzyme recovery from the reaction medium and the reuse of the catalyst. Continuous operation is to a large extent linked to immobilized enzymes, since only high stability justifies the use of a continuous reactor in most cases [58].

Several studies have demonstrated the improved stability of peroxidases when they were subjected to immobilization. Akhtar and Husain observed that bitter gourd peroxidase (BGP) was able to remove higher percentage of phenols over a wider range of pH when immobilized on a bioaffinity support [37]. Sasaki et al. highlighted an improvement of thermal stability of MnP immobilized on FSM-16 mesoporous material [59]. Furthermore, some other studies demonstrated a protective effect of peroxidase immobilization against inactivation by H_2O_2 [7, 20]. The different behavior of immobilized peroxidases with respect to soluble ones points out the necessity of an optimization of the process conditions when immobilized enzyme is used. Nevertheless, the possible improvement in stability should balance the usual decrease in kinetic rates, due to substrate transfer limitations to reach the enzyme inside the support.

10.1.9 Presence of Organic Solvents

The use of organic solvents is an alternative to enhance availability of hydrophobic substances, either substrates or products of the reaction, as well as to reduce side reactions. The first studies of peroxidase catalysis in water-miscible and water-immiscible organic solvents were initiated by Dordick and Klibanov using commercial HRP, one of the most often investigated enzymes [60, 61]. Several studies have been focused on the effect of solvents in peroxidase structure and function

[62, 63], as well as the evaluation of their potential applications in the presence of organic solvents [62, 64–67], gaining attention on the utilization of ionic liquids [68, 69]. All those studies are crucial for the later application of enzymes in bioreactor systems; however, peroxidase reactors containing organic solvents are still on the early stages [38].

Two possibilities arise when using organic solvents, which determine the technology and the characteristics of the bioreactor: single-phase systems and biphasic systems. Single-phase systems are based on the use of water-miscible cosolvents to increase solubility of poorly soluble substances. This type of system can considerably reduce mass-transfer limitations with faster reaction rates. The most important criterion in selecting a miscible solvent is its compatibility with the maintenance of enzymatic activity. Hydrophilic solvents have greater tendency to strip bound water from enzyme molecules [70], therefore higher enzymatic inactivation than that with immiscible organic solvents is expected. In this context, solvent presence in the medium is narrowed by enzyme stability, which also limits the amount of solubilized substrate. Another disadvantage of using single-phase systems is the required recovery and reutilization of the solvent after enzymatic catalysis, envisaging an economical and environmentally friendly operation.

Single-phase systems may also be based on the use of nearly anhydrous organic solvents. In this specific case, the incompatibility of enzymes and organic reaction media can be overcome in a number of ways, e.g., by enzyme immobilization or by modifying the enzyme to render it soluble in organic solvents [71, 72]. However, the applicability of this system is limited, since many important biotransformations involve both hydrophobic and hydrophilic substrates, products and/or cofactors that are insoluble in the same reaction medium.

In biphasic reactors or two-phase partitioning bioreactors (TPPB), the substrate is located mostly in the immiscible phase and diffuses to the aqueous phase. The enzyme catalyzes conversion of the substrate at the interface and/or in the aqueous phase. The product/s of the reaction then may partition to the organic phase. The system is self-regulated, as the substrate delivery to the aqueous phase is only directed by the partitioning ratio between the two phases and the enzymatic reaction rate [53]. The use of ionic liquid/supercritical carbon dioxide for enzyme-catalyzed transformation is gaining attention [69].

10.2 Reactor Configuration

The development of an enzyme reactor for large-scale applications involves a series of decisions and compromises beginning with the choice of the reactor configuration, including the operational mode. Each following step is dependent on the other decisions taken and will influence the overall efficiency and economics of the final process. Compromises need to be made about the reactor type and the operating strategy, directly related to the kinetic behavior and characteristics of the enzyme and/or support in immobilized systems [73]. In the next paragraphs, a discussion

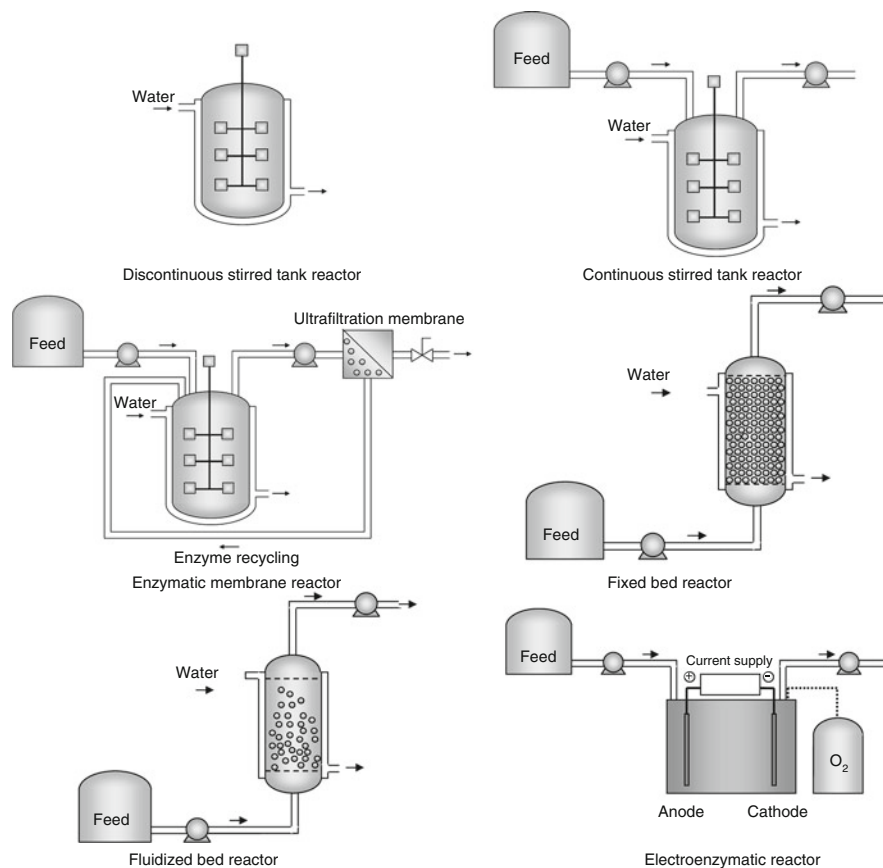


Fig. 10.1 Schemes of several reactor configurations for peroxidative reactions

about the different enzyme reactor configurations is presented (Fig. 10.1), emphasizing the scenarios where each of them are more appropriate (Table 10.1). Examples in literature are summarized in Table 10.2.

10.2.1 Discontinuous Stirred Tank Reactor

The discontinuous stirred tank reactor represents one of the most traditional reactor configurations for enzymatic reactions. It consists of a stirred tank where the enzyme, substrates, and cofactors are added at the beginning of the operation with no inlet and/or outlet stream during the reaction time. This type of reactor is usually considered to present an ideal hydrodynamic behavior; therefore, the reactor is supposed to be completely mixed and the concentration of all

Table 10.1 Suitability of some reactor configurations for peroxidative reactions

Reactor configuration	High suitability	Low suitability
Discontinuous stirred tank reactor	Lab-scale purposes Batteries of experiments about the effect of operational variables (T, pH, buffer, . . .) in conversion and/or turnover number Kinetic studies Product inhibition	Industrial-scale purposes
Continuous stirred tank reactor	High volumes of influent Substrate inhibition	Costly enzymes
Enzymatic membrane reactor	Expensive enzymes with low stabilization by immobilization Substrates or products with low solubility in aqueous solution Undesirable by-products formed during the reaction Hydrolysis of high molecular weight substrates	Polymerization reactions
Plug flow reactor	Continuous operation Space restrictions Product inhibition Catalyst sensitive to shear stress Viscous substrates	Small particles (use fluidized beds) Polymerization reactions (use fluidized beds)
Electroenzymatic reactor	In place controlled generation of hydrogen peroxide	Particles in suspension (use membraneless systems)

the components identical in every reactor point, although variable during the time course of the reaction. The process will be finally stopped when an adequate conversion is reached [94].

Batch reactors based on peroxidases are mainly applied for degradation purposes (see Chap. 8). LiP, manganese peroxidase (MnP), HRP, SBP, and CPO were used for the oxidation of phenolic compounds [3, 6, 7, 9, 20, 38, 74, 75, 95], decolorization of dye-containing effluents [5, 22], and pulp biobleaching [59]. In the field of synthesis, CPO is the most versatile and promising of the peroxidases (see Chap. 6). It was applied in discontinuous operation for epoxidations [78, 79], enantioselective oxidations of alcohols to aldehydes [14, 48], halogenations [77, 80], hydroxylations, and oxidation of indole to oxindole, which is an important drug precursor [96].

High conversion with an optimal reaction rate [7, 11, 75, 95], increase of the turnover numbers, i.e., the moles of substrate converted per mole of enzyme deactivated [3, 75, 95], and high stereospecificity of the compound of interest are targets of particular interest in the operation of these batch reactors [10, 11, 48, 77]. The achievement of these goals requires the study of different variables: type and concentration of peroxide, substrates and cofactors, enzyme activity and purity, composition of the reaction medium, pH, temperature, or agitation. Such optimization requires a deep knowledge of the system and a mathematical model that represents it satisfactorily. The kinetic model obtained in batch experiments is the

Table 10.2 Applications of different reactor configurations for peroxidative reactions

Reactor configuration	Enzyme	Reaction	References
Discontinuous stirred tank reactor	Soybean peroxidase	Degradation of phenols	[6, 7, 20, 74]
	Horseradish peroxidase	Phenol removal	[3, 7, 9, 20, 75, 76]
	Chloroperoxidase	Enantioselective oxidation of sulfides	[11, 15, 77]
		Enantioselective oxidation of racemic epoxyalcohols	[15, 48]
		Oxidation of benzyl alcohol	[14]
		Epoxidation of styrene	[78]
		Asymmetric oxidations	[79]
		Halogenation reactions	[80]
	Manganese peroxidase	Decolorization of dyes	[5, 19, 22]
	Lignin peroxidase	Pulp biobleaching	[59]
Bitter gourd peroxidase	Pentachlorophenol biodegradation	[38]	
Continuous stirred tank reactor	Horseradish peroxidase	Removal of phenols	[37]
		Phenol removal	[49, 75, 76, 81]
		Decomposition of hydrogen peroxide	[82]
Enzymatic membrane reactor	Soybean peroxidase	Removal of aromatic compounds	[83]
	Manganese peroxidase	Phenol removal	[84]
Plug flow	Chloroperoxidase	Dye decolorization	[8, 85]
	Horseradish peroxidase	Oxidation of indole to oxindole	[86]
Fixed bed	Horseradish peroxidase	Phenol and aromatic amines	[76, 83]
	<i>Coprinus cinereus</i> peroxidase	Phenolic waste stream	[2]
Fluidized bed	Horseradish peroxidase	Phenol	[87]
	Soybean peroxidase	Phenol and <i>p</i> -chlorophenol	[88, 89]
Electrochemical (No membrane)	Horseradish peroxidase	Phenol	[47]
	Lignin peroxidase	Veratryl alcohol	[40]
	Horseradish peroxidase	2,4,6-trinitrotoluene	[24]
	<i>Aspergillus oryzae</i> peroxidase	Azo dye	[90]
	Horseradish peroxidase	Petrochemical wastewater	[91]
	Horseradish peroxidase	Textile wastewater	[92]
	Horseradish peroxidase	Phenol	[93]

basis for any bioreactor calculation, design, or optimization. The reaction kinetics of peroxidases can be defined using a first- or second-order Michaelis–Menten model with respect to the substrate and first-order linear dependence relative to inactivators such as hydrogen peroxide [19, 76].

Different drawbacks arise from the application of peroxidases: (1) the enzymatic inactivation, usually caused by the presence of high concentrations of hydrogen peroxide, which oxidizes the porphyrin ring [15]; moreover, when phenolic compounds are being treated, the phenoxy radicals produced as intermediates

spontaneously form insoluble polymers, which entrap the enzyme in a shell, also causing its inactivation [3]; and (2) the expense of the enzyme at the end of the enzymatic process [11, 74]. In order to overcome these problems, some strategies concerning the design of the system can be proposed:

(a) *Fed-batch reactor*

When the enzyme is inhibited by the substrates, a strategy of substrate addition in consecutive loads can be developed. As peroxidases are very sensitive to the presence of high hydrogen peroxide concentrations, the continuous feeding of peroxide allows the enzyme to preserve the activity longer and reach high conversion levels. The addition of peroxide can be performed in pulses [48] or continuously by means of a peristaltic pump [14]. The flow of peroxide can be determined from an analysis of the consumption rate of the system [5] or by a feed-on-demand addition method by which the peroxide concentration is monitored and adjusted *in situ* by a peroxide-stat device [5, 9, 37]. The feed-on-demand system has as main advantage the fitting to the requirements of the process, as peroxide consumption may change during the reaction.

In the particular case of phenolic compounds degradation, the polymeric products resulting from the enzymatic reaction cause the inactivation of the peroxidase. In that case, a strategy of dropwise addition of enzyme has been proposed, where the reactor receives fresh enzyme solution continuously. The rate of formation of free radicals is reduced and hence, their concentration falls and the amount of enzyme available grows, as a result of lower inactivation [9].

(b) *Immobilized enzyme reactor*

It is well known that immobilization techniques may improve enzyme stability and have a protective effect against inactivation [7]. Moreover, immobilized enzymes are easy to recover and reuse at the end of a discontinuous process. Immobilized peroxidases protected against peroxide inactivation were extensively applied in batch systems (see Chap. 9) [7, 20, 37, 59, 78, 95].

(c) *Membrane reactor*

Although the use of membrane reactors for the retention of the enzyme is mostly applied in continuous processes, some authors used a membrane batch reactor in order to reuse the enzyme in consecutive cycles [11, 74]. Flock et al. used a membrane unit coupled to the reactor with recycling of both permeate and retentate streams to the reactor vessel. A valve at the outlet of the membrane maintained pressure within the range fixed by the manufacturer [74]. Pasta et al. operated a reactor with the membrane inside, emptied the reactor content at scheduled times, and thereafter, replenished it with fresh solution of the substrate and the oxidizing system [11].

(d) *Two-stage reactor*

Some peroxidases can oxidize the substrate by means of an intermediate compound. This is the case of MnP, which requires the presence of Mn^{2+} ion, which is

oxidized by the enzyme to Mn^{3+} and in turn, oxidizes the substrate. A two-stage system was applied to the pulp-biobleaching by MnP [59]. In the first stage, the enzyme, hydrogen peroxide, and the chelating buffer were added to a vessel to obtain the Mn^{3+} -chelate complex. A membrane at the outlet retained the enzyme, and the Mn^{3+} -chelate complex was able to pass to a second vessel containing unbleached kraft pulp. By this system, the enzyme can be applied in consecutive cycles.

10.2.2 Continuous Stirred Tank Reactor

High labor and handling costs as well as the start-up and shutdown times required to fill and empty the reactor are important drawbacks in a batch operation. Continuous flow systems are nearly always more cost-effective than batch reactors, especially when large volumes are to be treated, i.e., the main application of this reactor configuration is wastewater treatment. The removal of phenolic compounds from waters has been performed using SBP and HRP in continuous stirred tank reactor (CSTR) [49, 75, 76, 81, 83, 84].

A CSTR is a reactor configuration with continuous inlet and outlet flows, constant operative volume, perfect mixing, and homogeneous content [97]. Immediately after being fed into the reactor, the concentration of the influent is reduced to the level corresponding to steady-state. In the particular case of peroxidase enzyme reactors, this effect implies that the concentration of substrate, hydrogen peroxide, and enzyme are lowered immediately causing a reduction in the inactivation of the enzyme through free radical bonding or compound III formation [49]. Furthermore, the catalytic lifetime is also extended by maintaining low levels of enzyme activity in the reaction mixture [82]. Apart from diminishing enzyme requirements, the performance of peroxidase-catalyzed reactions in CSTR aims to increase the efficiency and catalytic turnover of the process [49].

The main variable of design for a CSTR is the hydraulic retention time (HRT), which represents the ratio between volume and flow rate, and it is a measure of the average length of time that a soluble compound remains in the reactor. Capital costs are related to HRT, as this variable directly influences reactor volume [83]. HRT can be calculated by means of a mass balance of the system; in that case, kinetic parameters are required. Some authors obtained kinetic models from batch assays operating at the same reaction conditions, and applied them to obtain the HRT in continuous operation [10, 83, 84]. When no kinetic parameters are available, HRT can be estimated from the time required to complete the reaction in a discontinuous process. One must take into account that the reaction rate in a continuous operation is slower than in batch systems, due to the low substrate concentration in the reactor. Therefore, HRT is usually longer than the total time needed in batch operation [76].

Once the volume is defined, other elements in the equipment comprise peristaltic pumps for the inlet and outlet streams. Working with peroxidases, two inlets are

necessary to prevent inactivation, as hydrogen peroxide and the enzyme cannot be part of the same feed mixture [10, 81, 82]. When the feed is pumped to the reactor, variables such as concentration of substrates and products and enzymatic activity are measured. The steady-state is achieved when the variables reach a constant value [49, 81]; this time is considered to be more or less threefold the HRT. For the optimization of turnover numbers, the ratio between peroxide and substrate concentration in the feed has special relevance. Peroxide concentration must be enough to perform the oxidation while minimizing compound III formation and thus, enzyme requirements [75, 83].

One significant problem in the CSTR operation is the washout of the enzyme with the outlet stream. In order to exploit the total lifetime of the enzyme, some authors increased the values of HRT by using very low flow rates or very large reactor volumes [76]. The large size of the reactor would not balance the saving of enzyme. In order to overcome this drawback, some strategies can be developed:

(a) *Operation of multiple CSTRs in series*

When several CSTRs are operated in series, only the first one receives fresh feed. The influent to each subsequent reactor corresponds to the effluent of the previous one. To find the correspondence between one single CSTR reactor and several ones in series and with the objective of maintaining an equivalent HRT, the volume of one single reactor is divided into the total number of reactors in series.

Due to the small reactor volumes, concentration of substrate, enzyme, and peroxide are not allowed to decrease in a high extent in the first stages. A high substrate concentration favors reaction kinetics. However, high concentrations of enzyme and peroxide may cause inactivation due to free radical bonding, which is more pronounced in the initial reactor stages [83]. In order to decrease enzyme inactivation, the biocatalyst and peroxide can be supplied to each stage of the reactor system in smaller doses [49]. In this case, when the number of stages increases, both peroxide and enzyme concentration decrease and inactivation is minimized [49].

(b) *Application of additives*

In the presence of hydrophilic synthetic polymers such as PEG, the apparent rate of enzyme inactivation can be reduced: a 200-fold increase of enzyme lifetime has been reported in some cases [36]. This aspect can reduce catalyst requirements and improve turnover and economical feasibility of the process. In continuous reactors treating phenolic compounds, the inactivation rate is reduced and the presence of additives has less beneficial effects than in discontinuous systems. This is due to the decreased reaction rate and, hence, decreased production rate of phenoxy radicals. Even so, the presence of PEG reduces the retention time required [81].

(c) *Immobilized enzyme reactors*

One of the most extensively applied techniques to retain and reuse the enzyme in continuous operation is the immobilization onto a support. The outlet port is provided with a nylon membrane to retain the solid biocatalyst inside the

reactor [84]. The main disadvantage of this system is the unfeasibility to maintain a continuous operation when the immobilized enzyme is deactivated. In that case, the process must be stopped to take out the deactivated enzyme and refill the reactor with new immobilized one.

10.2.3 Membrane Reactor

When looking for an economically feasible enzymatic system, retention and reuse of the biocatalyst should be taken into account as potential alternatives [98, 99]. Enzymatic membrane reactors (EMR) result from the coupling of a membrane separation process with an enzymatic reactor. They can be considered as reactors where separation of the enzyme from the reactants and products is performed by means of a semipermeable membrane that acts as a selective barrier [98]. A difference in chemical potential, pressure, or electric field is usually responsible from the movement of solutes across the membrane, by diffusion, convection, or electrophoretic migration. The selective membrane should ensure the complete retention of the enzyme in order to maintain the full activity inside the system. Furthermore, the technique may include the integration of a purification step in the process, as products can be easily separated from the reaction mixture by means of the selective membrane.

Enzymatic membrane reactors are classified in three main categories:

1. *Direct contact enzymatic reactors*

In this class of reactors, substrates are fed to the region of the system that contains the enzyme, ensuring a direct contact between them and immediate enzymatic action. The separation of the biocatalyst can be performed in the same reactor or by coupling an external membrane unit.

2. *Enzymatic reactors with enzyme immobilized into the membrane*

As immobilization usually leads to higher enzyme stability, the enzyme is immobilized into the matrix or onto the membrane in this type of reactors. The enzymatic reaction and product separation occur simultaneously [100, 101]. The immobilization can be based on a covalent interaction between the activated groups of the membrane and functional groups of the protein [102]; adsorption by electrostatic interactions enzyme-support [103]; entrapment in the polymeric matrix during the process of membrane preparation [104]; or encapsulation [105]. The main weak points of these reactors are the loss of enzymatic activity during membrane formation, the complexity to replace new active enzyme when deactivation occurs, and the stability of the biocatalyst during storage [106]. Moreover, although diffusion is the primary mass transfer mechanism, the reactors can be operated with ultrafiltration fluxes and transmembrane pressure differences, which enhance mass transfer rates [107, 108].

3. *Extractive-membrane enzymatic reactors*

The operation principle is based on the selective extraction of substrates from the feed stream and/or products from the reaction mixture by specific membranes. The enzyme–substrate contact occurs once the substrate has diffused through the membrane to the enzymatic region [98]. The generated products diffuse again through the membrane to reach the outlet stream. The main difficulty of these reactors is that the diffusion is the main mechanism of substrate and product transport. Therefore, the kinetics of the process tends to decrease [109].

The first step for the design of an EMR is to select the type of reactor. Extractive membrane reactors are desirable when one of the substrates or products is poorly soluble in aqueous solution or when an undesirable by-product has to be separated, as the membrane acts as a solvent extraction step [99]. Immobilized enzyme reactors are usually applied with materials that enable enhancement of enzymatic stability or preserve enzyme from deactivation by a direct contact with an organic solvent [99]. Finally, direct-contact membrane reactors are the most versatile alternative in processes with soluble compounds.

Although the main advantage of this class of reactors is the retention and reuse of the enzyme, some effects usually cause a decrease of enzymatic activity [110]: (1) enzyme leakage through the membrane; (2) adsorption of the enzyme onto the membrane, which causes alterations in enzyme conformation; (3) interactions with the membrane material, which may influence the stability of the enzyme; (4) shear forces and friction near the membrane [98]; and (5) peroxide deactivation.

The major purpose when operating EMRs is to prevent these enzymatic activity losses, which can be performed following some steps:

(a) *Selection of the membrane*

Two main criteria for the membrane selection are pore size and material. As peroxidases usually have sizes in the range of 10–80 kDa, ultrafiltration membranes with a molecular cutoff between 1 and 50 kDa are the most adequate to prevent enzyme leakage [99]. The materials commonly applied to ultrafiltration membranes are synthetic polymers (nylon, polypropylene, polyamide, polysulfone, cellulose and ceramic materials [101]). The adequate material depends on a great number of variables. When enzyme is immobilized into the matrix, this must be prepared at mild conditions to preserve the enzymatic activity. In the case of enzyme immobilization onto the membrane, this should be activated with the reactive groups necessary to interact with the functional groups of the enzyme. If an extractive system is considered, the selection of the hydrophilicity or hydrophobicity of the membrane should be performed according to the features of reactants, products, and solvents. In any case, the membrane should not interfere with the catalytic integrity of the enzyme.

(b) *Selection of flow rate through the membrane*

The flow through the membrane is normally controlled using a peristaltic pump and a needle valve on the outlet to control the pressure, which must be maintained

below a limit value provided by the membrane manufacturer [74]. When the configuration includes a recycling flow from the membrane to the reactor, the recycling flow rate should be high enough to ensure homogeneity in the enzyme confinement place (reactor vessel and piping) but avoiding shear forces and friction, which cause activity decrease [111].

Before starting up the system, some initial tests should be performed in order to check if the enzyme activity is completely retained into the system. It would be also important to evaluate if the enzyme is trapped in the membrane and the potential activity loss [8]. An activity decrease could point out a wrong membrane or flow rate selection.

(c) *Hydrogen peroxide addition*

Having in mind the inhibitory effect of hydrogen peroxide on peroxidases, the procedure of peroxide addition influences the preservation of the enzymatic activity into the system. The peroxide can be added in a portionwise, continuous, or feed-on-demand mode, by using a peroxide-stat [8, 86], as was mentioned before in Sect. 10.1.2. When adding peroxide in a continuous mode, a low concentration of this reactant and thus less enzyme deactivation are ensured.

(d) *Enzyme addition*

Enzyme must be injected during the reaction to ensure constant activity in the case of enzyme activity losses [8]. A dropwise addition of peroxidase [86] usually results in higher enzyme consumption and, thus, lower turnover numbers than in continuous addition [8].

This measure should be only considered after optimizing the design (membrane selection) and performance of the system. The addition of enzyme not only represents one of the major operational costs of the reactor but also causes pressure drops over the membrane and can be responsible for other problems such as concentration polarization and fouling [101]. Concentration polarization results from the accumulation of molecules at the boundary layer close to the membrane, and can be solved by backflushing the membrane. In that case, the configuration of two parallel membranes in a continuous process may solve the problem, as one of them can be operating while the other one is being cleaned. Fouling is the consequence of deposition or adsorption of particles onto the membrane surface that cause a modification of the structure and, thus, changes in the filtration properties of the membrane. This process is irreversible and defines the life time of the membrane [98].

Although some efforts are being made to develop EMRs based on the immobilization of peroxidases onto the membrane [106, 112], the most applied configurations correspond to the use of direct contact reactors for wastewater treatment, with SBP and MnP applied to effluents containing both phenols [74] and dyes [8, 85]. Some attempts were made to apply an EMR for the synthesis of oxindole from indole by CPO [86]. However, the reactor was only stable for a short period (10 residence times). Afterward, the polymerization of oxindole yielded a solid substance, which blocked the membrane, causing enzyme deactivation and the reduction of the total turnover numbers compared to those obtained in batch assays.

10.2.4 Plug Flow Reactor

A plug flow reactor is a tubular reactor in which the feed enters at one end of a cylindrical tube and the product stream leaves at the other end, moving as a “plug” with no mixing or diffusion along the flow path. Hence, the properties of the flowing stream will vary from one point to another, ideally only in the axial direction. The validity of the assumptions will depend on the geometry of the reactor and the flow conditions. Deviations from the ideality relate to the following circumstances (1) mixing in longitudinal direction due to vortices and turbulence and (2) incomplete mixing in radial direction in laminar flow conditions. The plug flow reactor is advantageous for processes with product inhibition, since the enzyme interacts with low product concentrations across a significant fraction of the axial direction [97]. When compared to CSTR, a significantly higher catalyst productivity is obtained due to the profiles of substrate and products inside the tubular reactor [113].

As described in CSTR, HRT may be estimated from the time required to complete the catalysis in batch studies. The simplest configuration of a plug flow reactor consists of a storage tank containing the substrate and the peroxidase. At the reactor inlet, this flow is merged with a smaller flow of hydrogen peroxide. Semibatch additions of the enzyme either in the influent or at different positions of the reactor are also possible [83]. In a similar way, step-addition of hydrogen peroxide in the plug-flow system may improve the enzymatic conversion, by reducing the rate of enzyme inactivation by peroxide. This operational control of peroxide and enzyme concentration, as for instance by their step addition, may reduce operating costs considerably. Furthermore, the addition of protective additives may reduce the minimum enzyme dose and hence, the total expenses [114].

A more stable operation can be obtained by a partial recirculation of the effluent. It should be noticed that recirculation flows higher than that of the influent may lead to a certain degree of mixture and the reactor may behave as a CSTR. Furthermore, it is not advisable for processes in which enzymes are inhibited by products. Sometimes, it can be useful to control operational variables such as pH or temperature, since recirculation can reduce gradients through the reactor. In systems forming insoluble products, such as phenol polymerization, the settling of the precipitate may cause mechanical mixing in the plug flow reactor. In this scenario, a tank in which the reaction and settling occur simultaneously is recommended, which simplifies the operating requirements [114].

The plug flow reactor has been mainly utilized for the removal of phenol in waste streams by HRP [76, 83] and *Coprinus cinereus* peroxidase [2]. According to Buchanan et al. [83], who modeled the kinetics of the HRP-aromatic substrate system and applied to PFR and CSTR, plug-flow configuration is recommended when working with low HRT, since considerably less enzyme would be required for equal phenol removal. However, for long HRTs, a multiple-stage CSTR would be more efficient than a PFR, due to the lower rate of enzyme inactivation.

From a practical point of view, a prolonged operation of a reactor with enzyme in suspension is not feasible. Procedures to retain the enzyme in the tubular reactor have been developed in order to maintain high enzymatic activity and to avoid enzyme washout. A plug-flow reactor operated with immobilized enzyme is known either as a fixed bed reactor or a fluidized bed reactor, depending on the characteristics of the flow pattern and the immobilized enzyme. Since mechanical stirring is not required in plug flow reactors, the support material is not damaged by the impeller, which may be a drawback in CSTR with immobilized enzyme.

10.2.4.1 Fixed Bed Reactor

The fixed-bed or packed-bed reactor is the type of reactor used almost exclusively in commercial scale operations, due to its high efficiency, ease of operation, and general simplicity [115]. The fixed bed reactor is characterized by a steady flow of the substrate through a bed that contains the immobilized enzyme. The essential advantage of fixed bed reactors is simple operation in continuous mode. On the other hand, there are certain issues unique to fixed bed reactors, such as pressure loss through the bed, which depend on the height, porosity, flow, and the effluent characteristics, as well as the geometry of the support. A trade-off between small particles with low diffusional resistance, which will cause high pressure drops and larger particles resulting in diffusion limited reaction rates, but lower pressure drop is required in packed beds [115]. Furthermore, in polymerization reactions or when insoluble products are formed, these would lead to clogging phenomena and to an increase of the pressure drop. Another particularity of fixed beds is that effective temperature or pH control may be difficult. However, this drawback is largely misleading in the case of temperature control since most enzyme-catalyzed reactions have low heats of reaction.

The efficiency of the operation is conditioned by three main factors (1) active enzyme concentration, (2) mass transfer rate, and (3) operational parameters, such as plugging. Mass transfer rate depends in large part upon the linear velocity of the fluid through the bed. Hence, in order to maximize the efficiency, high L/D ratios are required, which may also reduce back mixing. However, the length of the bed is limited by the pressure that immobilized particles may withstand [116]. Flow rate, L/D ratio, pH, and temperature are some of the operational parameters that should be optimized for an efficient operation. In Shukla et al., a fixed bed reactor is used for phenol oxidation by HRP [87]. At least three cycles were needed for 80% phenol removal under the optimal L/D ratio, HRT, temperature, and substrate concentration.

10.2.4.2 Fluidized Bed Reactor

In a fluidized bed reactor, the immobilized enzyme is maintained in suspension by the inlet flow. Depending on the geometric characteristics of the reactor and the

operational conditions (liquid flow rate, size and density of solid particles, etc.), the behavior of the liquid phase may be similar either to a plug flow or a homogeneous system. It can be operated with smaller particles compared to a fixed bed reactor, because plugging is not so frequent and pressure drop is lower than in fixed beds. In addition, flow distribution through the reactor radial section is more uniform, which minimizes the formation of preferential paths [113]. The main problem is related to its hydrodynamic complexity, which frequently leads to an unstable operation. Furthermore, fluidized bed reactors present a narrow range of operational conditions. The regime of flow rates is limited, on the one hand, by the minimum rate at which the particles are suspended (minimum fluidizing velocity), and on the other hand, by the maximum rate where the particles tend to leave the reactor (terminal velocity) [97]. When small particles are used with densities similar to that of the fluid, low linear rates are required in order to avoid the washout of the particles. Under these conditions, mass transfer can govern the overall rate. On the other hand, unstable operation may occur if the fluidizing velocity is similar to that of sedimentation [116].

Frequently, a porous plate acting as liquid distributor is placed at the bottom of the column and a mesh in the upper part of the column so that the immobilized biocatalyst can be fluidized. Different configurations of fluidized bed reactors have been proposed, as for instance, a conical-shaped unit in which transversal surface is increased in flow direction, which allows the progressive expansion of the bed and then reducing the pressure drop at the top of the reactor [116]. Among the different operational variables that should be considered for an optimized enzymatic conversion, bed height, surface area of the support, feed flow rate, substrate concentration, and hydrogen peroxide concentration are highlighted.

The fluidized bed reactor has been used for phenol removal instead of fixed bed as most of the products formed are insoluble. The operation in packed bed reactors would lead to clogging phenomena and undesirable pressure drop [47, 88]. When deactivation of biocatalysts occurs and regeneration is needed, the liquid–solid circulating fluidized bed is a worthy alternative, as demonstrated for phenol polymerization [89]. The continuous enzymatic polymerization was carried out in a riser section and a downcomer was used for the regeneration of the coated immobilized particles.

10.2.4.3 Two-Stage Reactor

The combination of a second unit in peroxidase reactors may be helpful in different situations, depending on the nature of the substrate to be treated. For instance, a two-stage reactor system for the continuous decolorization of direct dyes was used [44]. The first unit consisted on a fixed bed reactor connected to a second column of activated silica, which helped in the adsorption of toxic reactive species, therefore reducing the biotoxicity of the effluent. The same system was applied for the decolorization of textile effluents and was capable of decolorizing 40% effluent even after 2 months of continuous operation [45].

10.2.5 Electrochemical Reactor

An electroenzymatic reactor is an advanced electrochemical process, which combines enzymatic catalysis and the electrogeneration of hydrogen peroxide. The process is an interesting strategy since enzymes are activated through an electrode reaction without addition of H_2O_2 . In this way, common difficulties associated with storing and transporting such an unstable chemical are avoided. Protons are generated at the anode surface by water dissociation, move to the cathode by electromigration and convection in an electric field, and then hydrogen peroxide is generated at the cathode via a two-electron reaction (Fig. 10.2).

The rate of H_2O_2 formation has been known to vary due to the effects of the applied potential, but also depending on the concentration and pH, for example [91]. The applied voltage has to be evaluated in order to obtain the maximum current efficiency for the electrogeneration of H_2O_2 [90]. At high voltages, oxygen can be converted to water molecules via a four-electron reaction, so the hydrogen peroxide concentration does not linearly increase with the current and available O_2 , reaching a limiting value. The electrode configuration is also an important parameter, and considering the sequence of H_2O_2 generation, an anode–cathode configuration has been demonstrated to be more effective [91]. Furthermore, inactivating concentrations of H_2O_2 should be avoided, as well as high concentration of other strong oxidants generated by the electric field, such as ozone or hydroxyl radical, which may attack the active site of the enzymes [91]. Other factors that should be taken into account are enzyme dosage, temperature, and the solution pH [24, 40].

Membranes enhancing the proton passage in order to prevent the reverse reaction at the anode and allowing the efficient electrogeneration of H_2O_2 are frequently used in electroenzymatic reactors. However, the membrane reactor may lead to sharp rises in the incidental expenses and make the reactor system more complex. Hence, its application at large-scale is not feasible. In this context, membraneless devices have been proposed, which are simpler and cheaper than the membrane devices for the electrogeneration of H_2O_2 . This was first proposed for electrolyzing

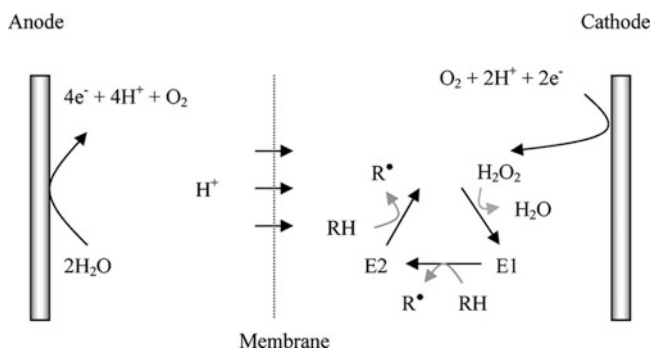


Fig. 10.2 Proposed mechanism of the electroenzymatic method (adapted from [40])

water to produce alkaline and/or acidic water [117] and only recently applied for the electroenzymatic oxidation with peroxidases [93].

The electrical potential and/or current required for electroenzymatic treatment have been shown to be lower than those needed in electrochemical treatment, which are not economically viable for large-scale. Electroenzymatic oxidation by peroxidases was proposed for the oxidation of veratryl alcohol by LiP [40]. Then, electroenzymatic reactors have been used for the treatment of petrochemical wastewater [91], dyes, and textile wastewater [90, 92, 118] and phenol streams [93] utilizing peroxidase immobilized onto inorganic porous Celite beads or directly onto the electrode. The integration of a second electrochemical reactor, which generated hypochlorite in the presence of sodium chloride, has been used for indirect oxidation of the reaction products of the electroenzymatic treatment [91].

10.3 Enzymatic Membrane Reactor

Application of EMRs to peroxidase-catalyzed reactions is still limited. The progress on immobilized enzyme reactors is mainly focused on the preparation of immobilized enzyme membranes and the study of enzyme distribution and membrane stability [106, 112]. On the other hand, most of the development is in direct contact enzyme reactors for degradation of pollutants (see Chap. 8) [8, 74] and synthesis purposes (see Chap. 6) [86]. A stirred tank reactor coupled to an ultrafiltration membrane for the retention of the enzyme represents a promising configuration. This enables us (1) to work with free enzyme, avoiding mass transfer limitations; (2) to retain unreacted substrates with high molecular weights; (3) to separate products through the membrane, achieving a purification step. When operating with peroxidases associated with a low molecular weight intermediate, i.e., MnP with Mn^{2+} , a promising new application of this configuration is being developed. In the first stage, the enzymatic oxidation of Mn^{2+} to Mn^{3+} takes place in presence of the enzyme, peroxide and Mn^{2+} ; the oxidized Mn^{3+} passes through the membrane to a second vessel, where the oxidation of the substrate occurs. This configuration is usually called two-stage EMR. In this section, some useful applications of one and two-stage EMRs using peroxidases are detailed.

10.3.1 *Dye Decolorization in a One-Stage Enzymatic Membrane Reactor*

The removal of dyes in industrial wastewaters is a major concern due to the high environmental impact caused by the presence of these pollutants [119]. Azo dyes represent a class of dyes extensively used in industry, and their complex structure presents several characteristics that can be extrapolated to many xenobiotics and contaminants, such as those with aromatic structure, azo linkage, and sulfonic group.

Satisfactory results concerning the degradation of the azo dye Orange II by the enzyme MnP from *Bjerkandera* sp were achieved in discontinuous assays [22]. The effect of factors such as addition of H_2O_2 , concentration of Mn^{2+} and organic acids, initial enzymatic activity, or pH was investigated, and the optimization of these parameters allowed us to reach a degradation of 90% for 100 mg/L of Orange II after 10 min [22]. Considering the industrial application of peroxidases for the degradation of real wastewaters, enzymatic activity savings must be intensely considered, as the enzyme is usually one of the most costly factors of these kinds of processes. Two strategies must be followed: (1) to search for a system that allows the retention and reuse of the enzyme and (2) to optimize the operational conditions in order to prevent enzyme deactivation.

10.3.1.1 Reactor Selection

Taking into account the inhibitory effect of H_2O_2 on the enzyme, a continuous operation in a stirred tank reactor was selected, as it enables us to maintain a low concentration of substrates in the reaction vessel. Enzymatic immobilization was considered as a possible alternative to retain the enzyme in the reactor with an enhanced enzymatic activity. However, the loss of enzymatic activity during the immobilization process and the diffusional problems associated with the use of immobilized enzymes induced us to reject the possibility of using immobilized MnP [120]. A membrane coupled to the CSTR was selected as the best alternative, considering that no polymerization occurs during oxidation of Orange II [18] and, thus, products discharge across the membrane.

10.3.1.2 Selection of the Ultrafiltration Membrane

The choice of the most adequate membrane considered variables such as pore size, material, shape, and contact area. Since MnP has a molecular weight of around 45 kDa, a membrane with a molecular weight cutoff of 10 kDa should ensure the retention of the most of the enzymatic activity. Polyethersulfone synthetic material was observed not to interfere with substrates, products, aqueous medium, or enzyme. A spiral-wound module supporting a flat-sheet shape [121] provides a high contact area in a small volume, and allows high permeate flow rates, thus preventing fouling problems. Therefore, a 10 kDa Prep/ScaleTM-TFF membrane into the corresponding spiral cartridge (Millipore, Billerica, MA) was coupled to a CSTR for the continuous decolorization of an effluent containing the azo dye Orange II. Measuring the rejection coefficients for enzyme and substrate proved the suitability of the membrane for the process. Solutions containing Orange II and MnP were forced to flow through the membrane for 1 h, and their concentrations in the retentate and permeate flows were analyzed. Coefficients of 0.02 and 1 were obtained for dye and enzyme, respectively. Moreover, an enzymatic solution was continuously pumped to the membrane and recycled to the reactor, and no activity

loss was observed after 3 h. These experiments support the appropriate selection of the membrane, as neither enzymatic adsorption nor activity loss due to shear stress were observed [8].

10.3.1.3 Reactor Configuration

The enzymatic reactor consisted of a 500 mL-continuous tank reactor BIOSTAT Q (Braun-Biotech International) coupled to the ultrafiltration membrane. The additional volume of the ultrafiltration unit and piping was around 150 mL. Three solutions were added to the reactor by means of three variable speed peristaltic pumps, containing (a) Orange II, Mn^{2+} and oxalic acid; (b) H_2O_2 ; and (c) MnP . Another peristaltic pump was used in order to feed the effluent into the ultrafiltration unit (Fig. 10.3). The recycling:feed flow ratio was maintained at 12:1, as this flow rate allowed an adequate homogeneity of the enzymatic mixture but prevented the polarization or fouling of the membrane.

10.3.1.4 Reactor Operation

The two main purposes when operating the EMR for the degradation of effluents containing dyes are (1) to achieve high degree of decolorization, in order to obtain effluents with low dye concentration and (2) to attain high turnover number or

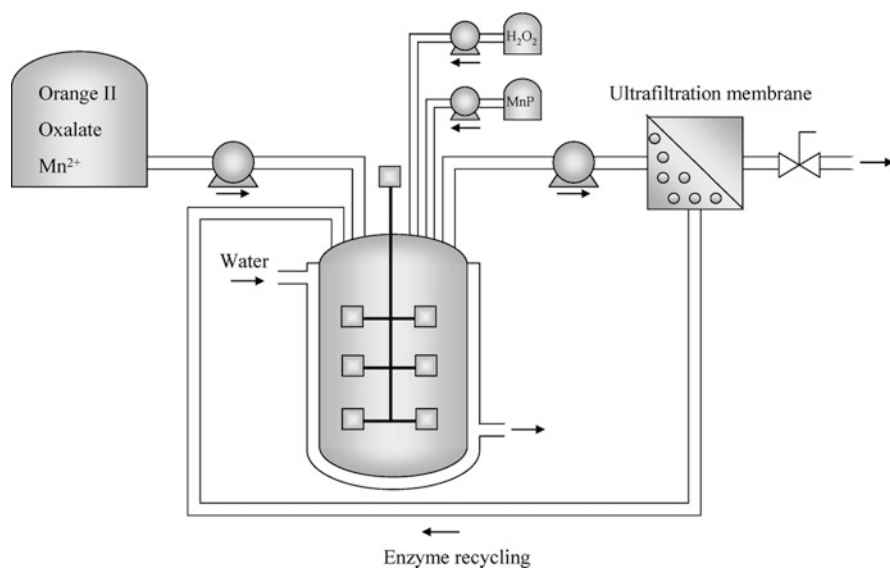


Fig. 10.3 Scheme of an enzymatic membrane reactor for the decolorization of the azo dye Orange II by manganese peroxidase

efficiency of the process, defined as the ratio between degradation rate and enzyme consumption. Some parameters were followed: Orange II concentration in the reactor vessel and in the effluent, MnP activity and DO concentration.

A first experiment with a single addition of MnP at the beginning of the operation was carried out in order to determine the enzyme consumption and thus the requirement of enzymatic activity. This feeding rate: 37 ± 2 U/(L h) was applied in the following experiments by means of two different strategies: stepwise addition (one pulse per hour) or continuous addition [8]. The continuous addition of enzyme allowed a high decolorization level (95.7%) with less enzymatic requirements than those of the stepwise addition experiment. An improvement of 69% in terms of efficiency was reached (Table 10.3).

The effect of H_2O_2 addition rate and HRT was analyzed simultaneously. Experiments with H_2O_2 addition rates of 15–50 $\mu\text{mol}/(\text{L min})$ and HRT of 15–60 min were carried out. A high addition of peroxide favors the kinetics of the process although it has inhibitory effect on the enzyme stability. On the other hand, a low addition rate prevents enzyme deactivation, but it can be inadequate to achieve a high extent of decolorization. In that case, an increase of HRT is required to maintain decolorization yields. Figure 10.4 shows that the highest efficiencies were achieved with low HRT, which correspond to decolorization yields lower than 90%. Only for HRT of 60 min did the concentration in the effluent represent less than 10% of the initial dye concentration. Under these conditions, the highest efficiency was obtained when adding 15 $\mu\text{mol}/(\text{L min})$ of H_2O_2 .

The HRT is directly related to the Orange II loading rate (OLR) for an influent with constant dye concentration. The appropriate ratio $H_2O_2/\text{Orange II}$ should be that given by the degradation mechanism of Orange II [18]: 1 mol of H_2O_2 enzymatically generates 2 mol of Mn^{3+} , which are the acceptors of 2 mol of electrons produced during the oxidation of 1 mol of Orange II. Based on this theoretical conclusion, an equimolar ratio should be the most suitable for the Orange II degradation. In fact, working at HRT of 60 min and 15 $\mu\text{mol}/(\text{L min})$ of H_2O_2 addition rate, a value close to unity was obtained for the ratio $H_2O_2/\text{Orange II}$. When the addition of peroxide increased, kinetics increased, but enzyme deactivation caused a loss of efficiency. Similarly, if addition of peroxide decreased and the ratio $H_2O_2/\text{Orange II}$ was lower than 1, the reaction rate would be very slow and a low decolorization yield would be obtained.

Table 10.3 Effect of MnP addition mode in dye decolorization (A) and efficiency (B) in the enzymatic membrane reactor with an Orange II concentration in the influent of 100 mg/L and HRT of 1 h

MnP addition mode	MnP (U/L)	MnP addition rate (U/(L h))	Decolorization (%)	Efficiency (mg/U)
Single addition	200–108	0	91.0	–
Fed-batch addition	100–250	62.8	96.3	1.53
Continuous addition	225	37.2	95.7	2.58

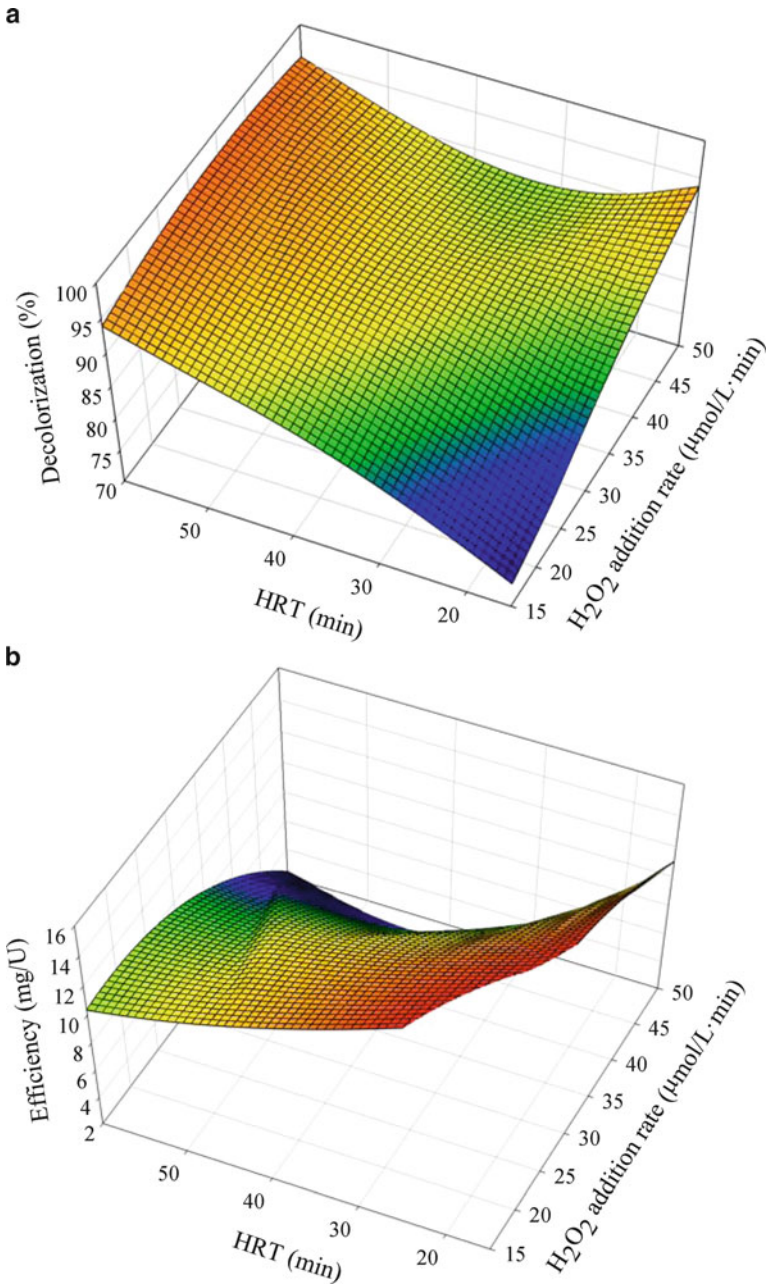


Fig. 10.4 Effect of HRT and H_2O_2 addition rate in dye decolorization (a) and efficiency (b) in the enzymatic membrane reactor with an Orange II concentration of 100 mg/L

10.3.1.5 Control Systems

The design, optimization, and control of the EMR for the decolorization of Orange II require the implementation of a control system. Two control systems were developed (a) a feedforward system based on the knowledge of kinetics and reactor hydraulics and (b) a feedback system based on the concentration of DO into the reactor, which was observed to be a main variable that provides extensive information about the development of the process.

(a) *Feedforward control system*

A kinetic model of Orange II degradation was deduced from experiments performed in discontinuous operation, with continuous H_2O_2 addition in order to maintain very low levels of peroxide in the reactor and preserve enzymatic activity. Two variables were considered to determine the kinetic behavior: Orange II concentration and H_2O_2 addition rate. Although Orange II is not a direct substrate for MnP, it is the final electron donor and the limiting substrate for the enzymatic degradation. H_2O_2 addition rate was considered instead of H_2O_2 concentration, as the latter is nearly zero in experiments with continuous addition of peroxide, whereas the kinetics were observed to be directly dependent on the peroxide addition rate [19]. The kinetic equation followed a Michaelis–Menten model for the dye concentration and a first-order linear dependence with respect to H_2O_2 addition rate (Fig. 10.5).

Considering both the mass balance corresponding to a CSTR and the kinetic equation, a dynamic model was established and validated for steady-state continuous operation of the EMR (Fig. 10.6). Moreover, the model was analyzed to foresee the deviations of the steady-state that occur when short-term changes in operational conditions take place (Fig. 10.7). Higher Orange II loading rates resulting from a more concentrated influent or a variation of HRT caused an increase in dye concentration in the effluent, which was predicted accurately by the dynamic model. The validation was also observed when modifications in the peroxide addition rate occurred.

(b) *Feedback control system*

DO concentration was observed to be a very significant variable in the operation of the enzymatic reactor for Orange II decolorization. Oxygen is generated from the reaction between Mn^{3+} and H_2O_2 [122, 123], and it is consumed in the Orange II degradation pathway [18]. The concentration of oxygen in the reactor achieves equilibrium between production and consumption during steady-state operation; when a deviation from the steady-state takes place, a change in oxygen concentration occurs.

An increase of OLR implies an increase of oxygen consumption with respect to oxygen production and, thus, a decrease of oxygen concentration (Fig. 10.7). On the other hand, an increase in H_2O_2 :Orange II ratio causes an increase of oxygen concentration in the reactor. This indicates that DO could be a good parameter to

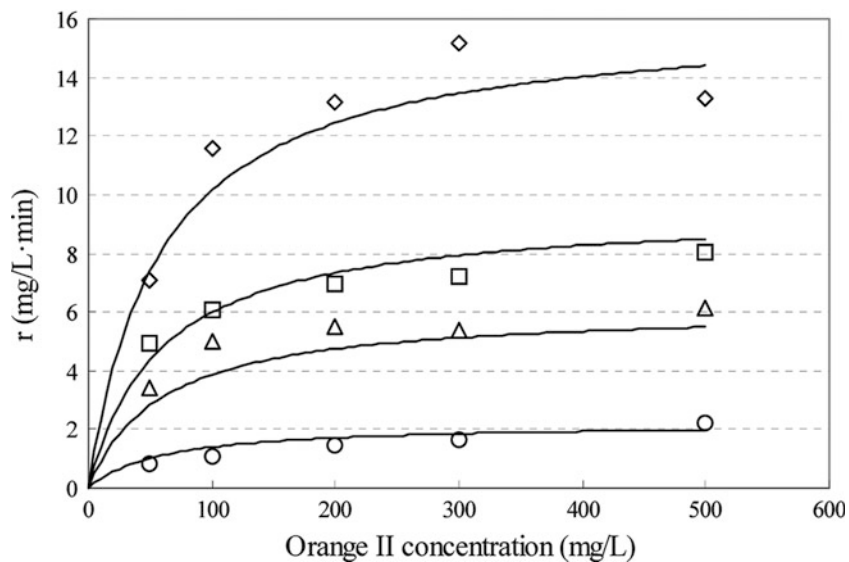


Fig. 10.5 Validation of the kinetic model in discontinuous experiments as a function of the Orange II concentration and the H_2O_2 addition rate: (*open diamond*) $50 \mu\text{mol}/(\text{L min})$; (*open square*) $25 \mu\text{mol}/(\text{L min})$; (*open triangle*) $15 \mu\text{mol}/(\text{L min})$; (*open circle*) $5 \mu\text{mol}/(\text{L min})$; (*Lines*) kinetic model. $V = 25 \text{ mL}$; Initial MnP 200 U/L ; oxalic acid 1 mM ; Mn^{2+} $33 \mu\text{M}$; H_2O_2 addition rate $50 \mu\text{mol}/(\text{L min})$; pH 4.5

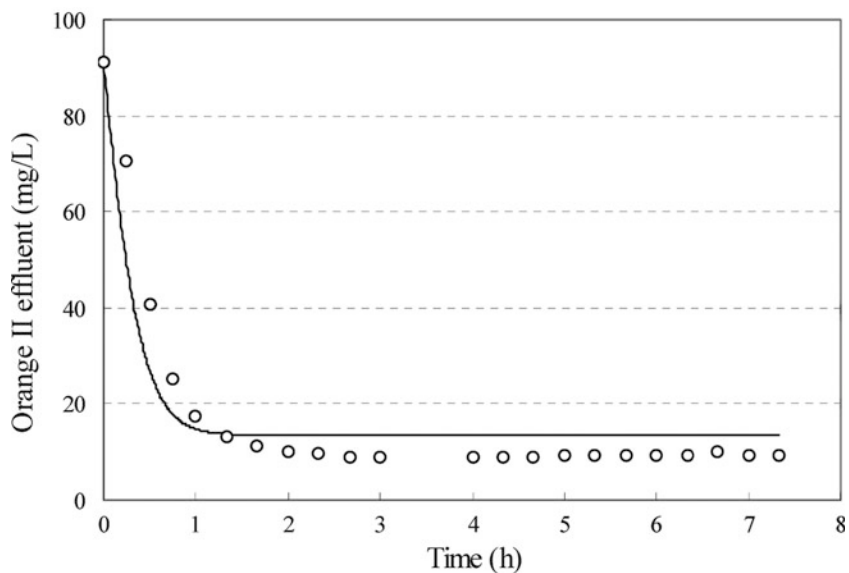


Fig. 10.6 Experimental (*open circle*) and simulated data (*Line*) in the enzymatic membrane reactor with HRT of 72 min. Initial Orange II concentration 91.1 mg/L ; H_2O_2 addition rate $15 \mu\text{mol}/(\text{L min})$

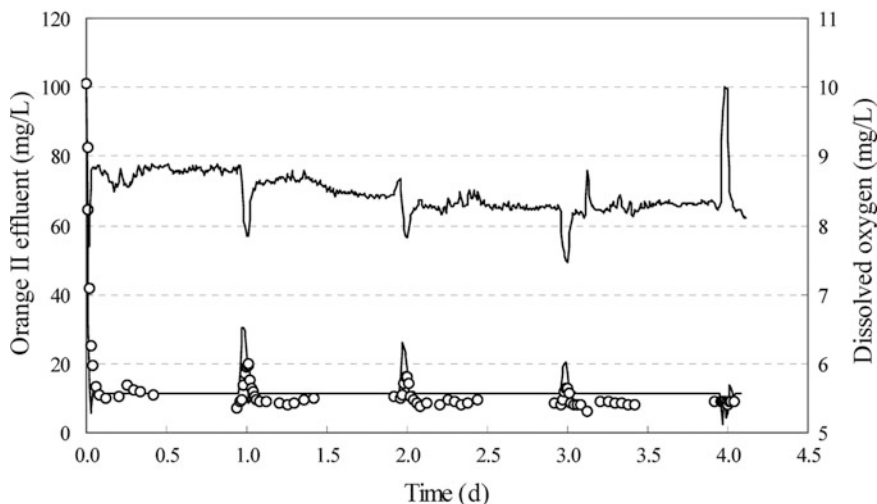


Fig. 10.7 Experimental (*open circle*) and simulated (*thin broken line*) Orange II concentration in the effluent and (*complete line*) dissolved oxygen in nonsteady-state conditions. Orange II in the influent: 100 mg/L, HRT: 1 h, H_2O_2 addition rate: $15 \mu\text{mol}/(\text{L min})$ and room temperature. The conditions of the operational stages and 1-h perturbations were: at 1 day, 200 mg/L of Orange II in the influent; at 2 day, HRT of 0.5 h; at 3 day, H_2O_2 addition rate of $7.5 \mu\text{mol}/(\text{L min})$; at 4 day, H_2O_2 addition rate of $30 \mu\text{mol}/(\text{L min})$

control the system, as the appropriate variables could be modified after the detection of the alteration in the outlet variable.

Finally, the enzyme deactivation in the EMR could be modeled by a first-order linear dependence with respect to H_2O_2 addition rate [19]. The integration of this equation in the kinetic model allows simulation of the process efficiency as a function of H_2O_2 addition rate, HRT, and Orange II concentration in the influent, and helps determine the best operational conditions.

10.3.2 Other Applications of One-Stage Enzymatic Membrane Reactors

10.3.2.1 Treatment of Phenolic Effluents

Phenols are aromatic compounds present in wastewaters from agricultural and industrial activities, especially coal and petroleum refineries and plastics, resins, dyes, ceramic, and forestry industries [6, 124]. Phenols reduce the concentration of DO in water [125]. This fact makes them toxic to some aquatic species at low concentrations; furthermore, some of them are suspected to be carcinogenic [6] and add odor and taste to drinking water [126].

An initial experiment for the degradation of synthetic water containing 100 mg/L of phenol was performed in batch operation, with a controlled addition of H_2O_2 to preserve the enzymatic activity. The initial concentration of phenol totally disappeared after 2 h. Considering pseudo-first order kinetics, a value of 0.906 h^{-1} was calculated for the pseudo-first order constant, with a related half-life time ($t_{1/2}$) of 0.765 h. An EMR, using the same configuration than that proposed for the decolorization of effluents containing Orange II, carried out the continuous treatment of the phenolic effluent. A HRT of 2 h was selected from the time required to complete the degradation of 100 mg/L of phenol in batch assays. In steady state operation (Fig. 10.8), 88% of phenol was degraded with a consumption of $11.3 \text{ U MnP}/(\text{L h})$, which resulted in an efficiency of $3.9 \text{ mg phenol}/\text{U}$. From the values achieved in the steady state and considering pseudo-first order kinetics for the degradation of phenol, a pseudo-first order constant was calculated: $k = 3.67 \text{ h}^{-1}$, which corresponded to a half-life time of 0.189 h. The continuous operation in an EMR allows a fourfold reduction of the half-life time for an effluent containing 100 mg/L of phenol, and an increase of the process efficiency. The retention of the enzyme and the preservation of the catalytic activity contribute highly to making the EMR a feasible and economically competitive system for the application of peroxidases.

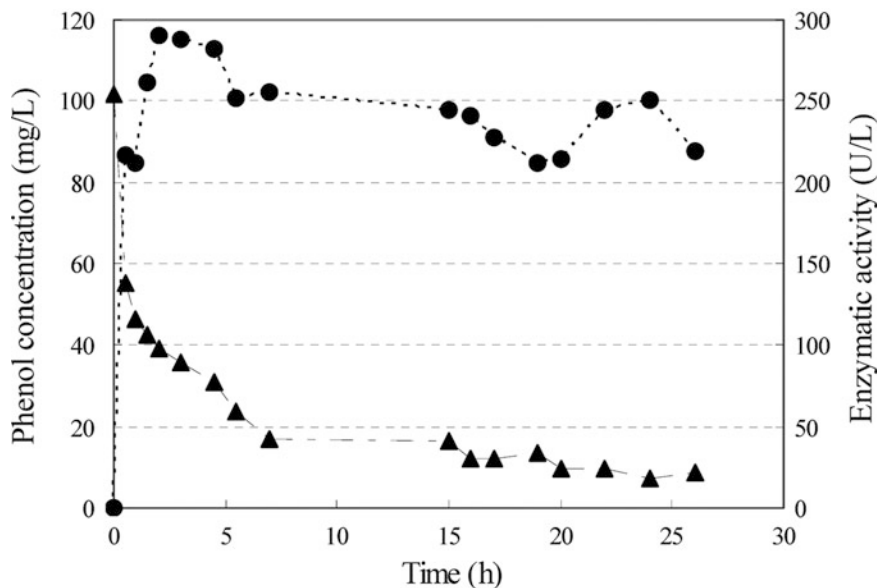


Fig. 10.8 Phenol concentration (*closed triangle*) and enzymatic activity (*closed circle*) in an enzymatic membrane reactor with HRT of 120 min. Initial phenol concentration 100 mg/L; oxalic acid 1 mM; Mn^{2+} 33 μM ; H_2O_2 addition rate 15 $\mu\text{mol}/(\text{L min})$; pH 4.5

10.3.2.2 Oxidation of Indole to Oxindole

A continuously operated reactor including an ultrafiltration membrane was applied to the oxidation of indole to oxindole catalyzed by CPO from *Caldariomyces fumago* [86]. The membrane was placed inside the reactor, held by sealing rings. Peroxide was supplemented continuously with a low flow rate, in order to prevent deactivation of the enzyme. CPO was added to the reactor in two identical pulses, at the beginning of the operation and after six HRT. A high conversion (around 80%) was achieved after two to three HRT and maintained during ten HRT. Nevertheless, the pressure drop over the membrane increased from 2 to 8 bar at the end of the operation. This problem was due to the slow polymerization of oxindole, which yielded a solid black substance able to obstruct the membrane. Furthermore, a high enzyme deactivation was observed, causing a decrease of the total turnover number.

10.3.3 Two-Stage Enzymatic Membrane Reactor

The *in vitro* oxidation of organic recalcitrant compounds by peroxidases requires that the enzyme, cofactors, and the compound to be degraded are all present in the reaction mixture [8, 22, 127, 128]. However, one main drawback found is that there is an important consumption and destabilization of the enzyme in the process, which may limit the applicability of the enzymatic process.

The definition of a more efficient enzymatic system could be based on the separation of the catalytic cycle of the enzyme and the degradation step by the Mn^{3+} reactive species in MnP systems. The Mn^{3+} -chelates present several advantages in their use as oxidants. They are more tolerant to protein denaturing conditions such as extremes of temperature, pH, oxidants, organic solvents, detergents, and proteases, and they are smaller than proteins; therefore, they can penetrate microporous barriers inaccessible to proteins. The optimization of the production of the Mn^{3+} -chelate will have to be compatible with the minimal consumption and deactivation of the enzyme.

The development of a two-stage degradation system, where the biocatalytic Mn^{3+} -chelate is produced in an enzymatic reactor and withdrawn for the degradation reactor is then proposed. In the first reactor, the enzyme would react with H_2O_2 , organic acid, and Mn^{2+} to render the Mn^{3+} -chelate complex. The biocatalytically generated Mn^{3+} -chelate would be recovered from the enzymatic mixture by an ultrafiltration membrane, which permits the recycling of the enzyme to the enzymatic reactor to assure minimal consumption as well as the separation of the generated complex. This species would be forwarded to a second degradation reactor, to carry out the degradation of a xenobiotic; in this case, an industrial azo dye (Orange II) was considered as a model compound.

The optimization of the two-stage process has to be conducted taking into account the following specific factors: (a) those parameters that may directly affect the catalytic cycle: the type and concentration of organic acids, Mn^{2+} , H_2O_2 , as well

as the influence of temperature and pH on the stability of the complex and (b) those which may affect the degradation of the dye. Finally, both the enzymatic and the degradation reactors were coupled in a continuous operation to perform the degradation of the dye and to evaluate the efficiency of the process in terms of the amount of pollutant degraded per unit of enzyme consumed.

The enzymatic system used for the continuous production of Mn^{3+} -malonate is presented in Fig. 10.3. It is composed by a stirred tank reactor (200-mL working volume) operated in continuous mode coupled to a 10 kDa cutoff ultrafiltration membrane (Prep/Scale-TFF Millipore), which permits the recycling of the enzyme to the reaction vessel. The enzyme was recycled in a recycling:feed flow ratio of 12:1.

The generation of the Mn^{3+} -chelate in batch mode was monitored spectrophotometrically for 11 h. The reaction conditions were similar to those of the determination of the manganese-dependent activity, except for the lack of the phenolic substrate (2,6-dimethoxyphenol) so that the Mn^{3+} -chelate could be monitored directly. Figure 10.9 shows a typical time course of Mn^{3+} -chelate generation by the enzyme Versatile Peroxidase (VP). From the analysis of the data, we observed that there is a steady slope in the generation of the Mn^{3+} -chelate from the beginning of the experiment, reaching a maximum around 240 μM . After the maximum, a slight decay at very slow rate was observed from 1.5 to 11 h, indicating that the complex is rather stable during the evaluated period.

The optimization of different variables carried out in batch experiments indicated that the highest amount of Mn^{3+} -malonate was achieved when the conditions were: 30 mM malonate; 2 mM MnSO_4 ; 0.3 mM H_2O_2 ; pH 4–4.5. Among the

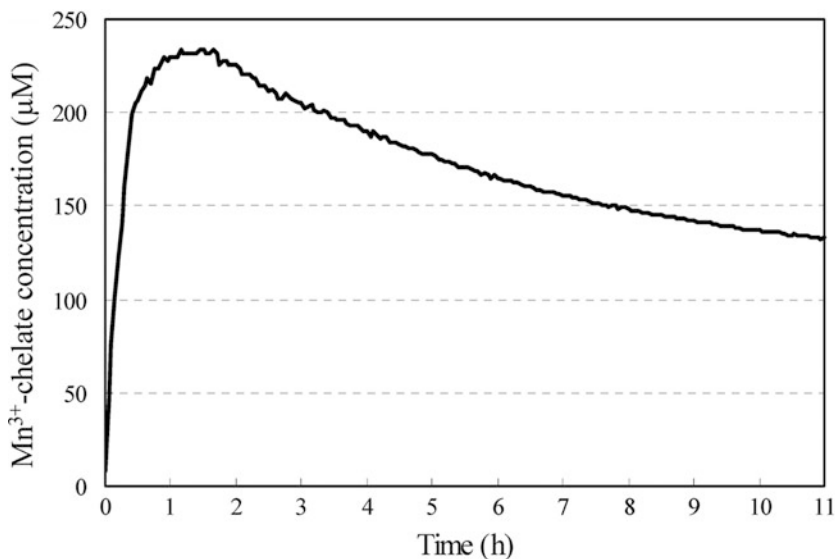


Fig. 10.9 Time course of formation of Mn^{3+} -chelate catalyzed by VP

different parameters evaluated, the concentration of H_2O_2 was found to be crucial on the action of the enzyme. The concentration of H_2O_2 must be strictly controlled, since an excessively concentrated reagent would cause the inactivation of the enzyme, yet an excessively low concentration may limit the reaction rate and extent. The continuous addition of H_2O_2 at a controlled flow may permit the progressive participation of H_2O_2 in the catalytic cycle through a suitable regeneration of the oxidized form of the enzyme, minimizing the peroxide-dependent inactivation of the peroxidase [128].

The decolorization of the azo dye Orange II by Mn^{3+} -chelate was performed in batch with the complex that had been previously produced in the enzymatic reactor. The capability of the complex to degrade Orange II was evaluated under different initial concentrations of the dye, from 10 to 22 mg/L, whereas the initial concentration of the complex was 165 μM (Fig. 10.10). In all these cases, the complex was able to degrade the dye reaching the same percentage of degradation, 80–85%.

Different concentrations of the Mn^{3+} -chelate, from 70 to 200 μM , were evaluated to maximize the degradation extent and rate (Fig. 10.11). It was observed that the higher the initial concentration of the complex, the higher the degradation. Thus, when the concentration of the oxidizing agent was 200 μM , the percent of degradation was 90%, and when the initial concentration was 70 μM , degradation was 42.5%.

Thereafter, the continuous production of the complex Mn^{3+} -malonate was carried out in a stirred reactor coupled with an external ultrafiltration membrane. The continuous reactor production of Mn^{3+} -chelate was coupled with a degradation

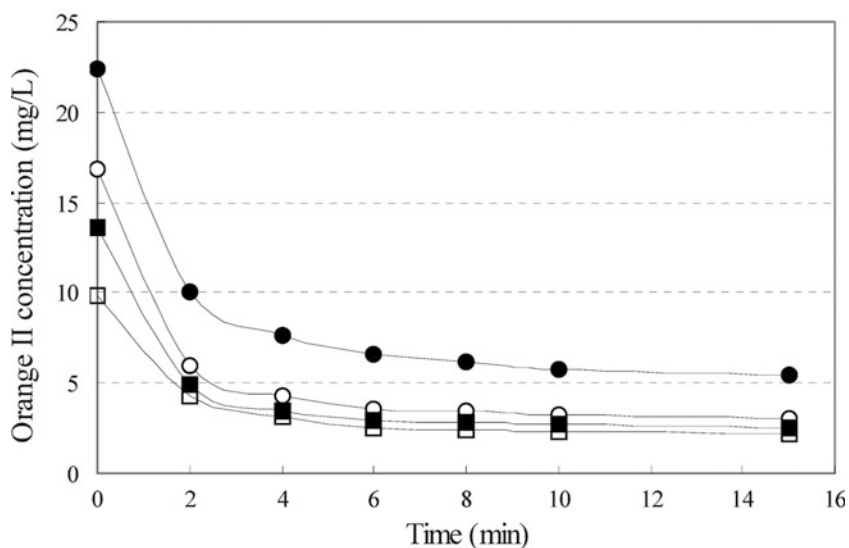


Fig. 10.10 Influence of the initial dye concentration on the degradation extent (closed circle) 22 mg/L; (open circle) 17 mg/L; (closed square) 14 mg/L; (open square) 11 mg/L

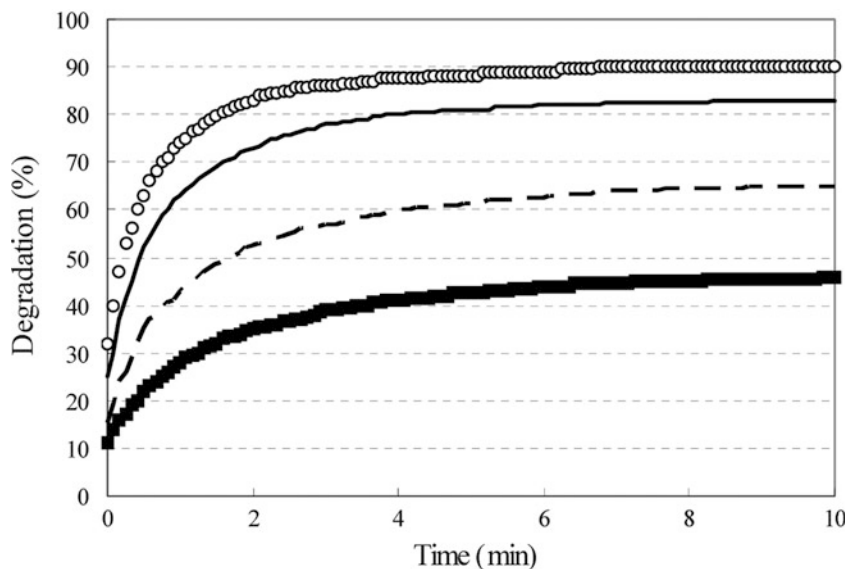


Fig. 10.11 Kinetics of degradation of Orange II with different initial concentrations of Mn^{3+} -malonate: (filled square) 70 μM , (broken thick line) 110 μM , (complete thick line) 165 μM , (open circle) 200 μM

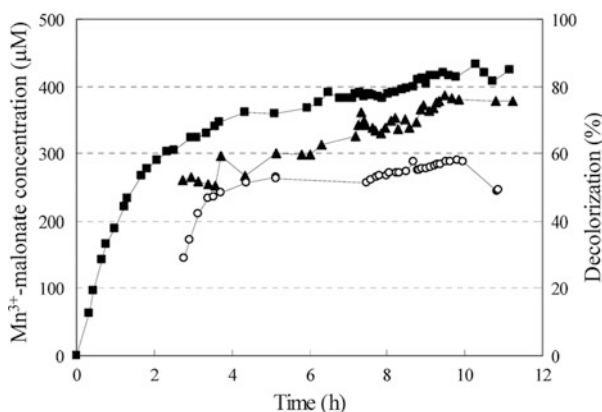


Fig. 10.12 Profile of production of Mn^{3+} -malonate and degradation of Orange II: (closed square) Mn^{3+} -malonate produced in the enzymatic reactor; (closed triangle) Mn^{3+} -malonate introduced in the oxidation reactor; (open circle) decolorization of Orange II

system, operating with the azo dye Orange II. From the previous results, this compound presented a satisfactory degradation rate and its spectrophotometric monitorization is simple and straightforward. The possibility of carrying out the optimization of the enzymatic and degradation reactions independently is one of the points of this system. According to the results, the two-stage system was operative and attained high levels of dye decolorization (Fig. 10.12). The fact that only the

Mn^{3+} reactive species participate in the degradation reactor assured minimal consumption of the enzyme, a factor that may be essential in the application of the peroxidases for degradation.

10.4 Biphasic Reactors

Poorly soluble substrates are likely to be inaccessible for the reaction with the enzyme. A similar scenario occurs in polymerization reactions, where the conversion results in low yields due to the lower solubility of the polymeric products. In this way, nonaqueous enzymology has emerged in the last years to further widen the versatility of the enzymatic catalysis. Solubility of hydrophobic compounds in organic solvents is usually orders of magnitude higher than in water. An example is anthracene, which is nearly insoluble in water (0.07 mg/L), whereas its solubility in solvents such as methanol and trichloromethane increases to a large extent (1×10^4 and 33×10^4 times higher, respectively).

The use of biphasic reactors (with immiscible solvents) tries to overcome the restrictions described for monophasic reactors (miscible solvents) (1) the concentration of substrate or products in biphasic reactors could be increased even to g/L (instead of mg/L), depending on the solubility of the substrate in the immiscible solvent considered; (2) the enzyme remains in the aqueous phase and can be easily recycled; and (3) the solvent, after the enzymatic treatment and depleted in substrate, could be separated from the aqueous phase, used to extract the substrate and returned to the aqueous phase for a further batch treatment.

This section presents the oxidation of a poorly soluble compound, the tricyclic PAH anthracene, by the enzyme VP in a biphasic reactor. The optimization of the operation of the TPPB will be focused in four critical aspects:

1. Selection of the appropriate solvent, with special emphasis on the partition coefficient of anthracene, enzyme activity, and stability, and solvent viscosity
2. Study of the parameters involved in the catalytic cycle of the enzyme: hydrogen peroxide, malonate, and pH control
3. Selection of an appropriate surfactant, in terms of enzyme interaction
4. Enhancement of mass transfer of the substrate from the organic phase varying agitation and by the addition of a surfactant

10.4.1 Solvent Selection

First, the most appropriate solvent was selected for the operation of the TPPB. The selected solvent should present suitable physical and chemical characteristics such as low solubility in water, low volatility, and inert for the enzyme, i.e., not oxidized by the action of the catalyst. Furthermore, two main factors should be considered

for the selection of the solvent: (1) the partition coefficient of anthracene in the solvent and (2) the enzyme/solvent interaction.

The partition coefficient (K_{SW}) is the ratio of concentrations of a specific compound in an immiscible solvent and water at equilibrium. Solvents with high partition coefficients can sequester the target compound, thus limiting its availability for the enzyme action in the aqueous phase [129]. The partition coefficient for anthracene was determined in 15 solvents from different nature: mineral oils, vegetable oils, alcohols, hydrocarbons, and others. The values of $\log K_{SW}$ obtained ranged from 3.7 (silicone oil) to 5.2 (undecanone). Among the solvents evaluated, two were selected for a further study: the solvent with the lowest partition coefficient (silicone oil, $\log K_{SW}$ 3.7) and a solvent with an intermediate value (dodecane, $\log K_{SW}$ 4.5) [53].

The inactivation of VP caused by the interfacial interaction at different agitation rates was also evaluated. When the agitation rate is increased, the interfacial surface is also enhanced, leading to a higher enzyme inactivation [54]. The enzyme was exposed to different interfacial areas by modifying the agitation rate: 400, 600, and 800 rpm. Enzyme inactivation in silicone oil (7, 61 and 138 U/(L h), respectively) was lower than in dodecane (12, 81 and 143 U/(L h), respectively) even at higher interfacial areas, since silicone oil has a lower interfacial tension [53].

In summary, silicone oil led to lower partition coefficient and lower enzyme inactivation, compared to dodecane. Consequently, silicone oil was selected for subsequent experiments.

10.4.2 Effect of Substrates and Cosubstrates of VP

The parameters affecting the catalytic cycle of VP were investigated to optimize anthracene oxidation in TPPBs operated with silicone oil. Hydrogen peroxide addition rates ranging from 1 to 25 $\mu\text{mol}/(\text{L min})$ were evaluated. The flow rate selected was 5 $\mu\text{mol}/(\text{L min})$ since the highest degradation rate was achieved at a high efficiency (Table 10.4). In these experiments, a marked pH increase was observed throughout the reaction time. In order to avoid this pH increase and to favor enzyme stability, malonate concentration was first increased to 33 and

Table 10.4 Results of the set of experiments at different addition rates of H_2O_2 and malonate concentration

H_2O_2 ($\mu\text{mol}/(\text{L min})$)	1	5	15	25	
Degradation rate (mg/(L h))	0.16	0.38	0.28	0.27	
Efficiency (mg/U)	0.047	0.046	0.016	0.016	
Malonate (mM)	10	33	66	10 ^a	5 ^a
Degradation rate (mg/(L h))	0.29	0.36	0.39	0.42	0.42
Efficiency (mg/U)	0.042	0.046	0.033	0.079	0.074

^apH was controlled by addition of malonic acid 250 mM

66 mM, but stability was only possible when pH was controlled by the addition of malonic acid.

10.4.3 Selection of a Surfactant

Surfactants are frequently used in detergents and food products to alter the properties of solution interfaces, mediating between immiscible phases because of their hydrophobic and hydrophilic moieties. The addition of surfactants increases the concentration of hydrophobic compounds in the water phase by solubilization or emulsification above a specific threshold, the critical micellar concentration (CMC), where surfactant molecules aggregate to micelles [130]. Two widely utilized nonionic surfactants, Tween 80 and Triton X-100, were evaluated in terms of enzyme interaction, by calculating the inactivation coefficient (k_d) under static conditions. Concentrations lower than CMC were studied in order to avoid diffusional limitations in the interaction of the enzyme and the PAH in the micellar phase. The concentration 0.25 CMC was considered the most favorable for the enzyme, with Triton X-100 being the surfactant that led to the lowest inactivation coefficients for all the concentrations tested and was 2.5 times lower than k_d in control experiment.

10.4.4 Enhancement of Mass Transfer and Enzyme Stability

An effective transfer of substrates from the organic to the aqueous phase is required in the operation of a TPPB. In biphasic reactors at a specific agitation rate and in absence of the enzyme, the mass transfer of substrate is defined by (10.2):

$$\frac{dS_w}{dt} = k_L a (S^* - S_w). \quad (10.2)$$

After integration and linearization, (10.3) is obtained:

$$\ln(S^* - S_w) = \ln S^* - k_L a t \quad (10.3)$$

from which the mass transfer coefficient ($k_L a$) is calculated when data of anthracene in the aqueous phase (S_w) during time is provided and being S^* the anthracene concentration under equilibrium conditions. Mass transfer coefficients of anthracene at different agitation rates (from 200 to 300 rpm), with different viscosities of silicone oil (10, 20, and 50 cSt) and 0.25 CMC of Triton X-100 were determined. Below the CMC, the surfactant is present as dispersed molecules (monomers), and as expected, no increase of anthracene water solubility was observed in the present work.

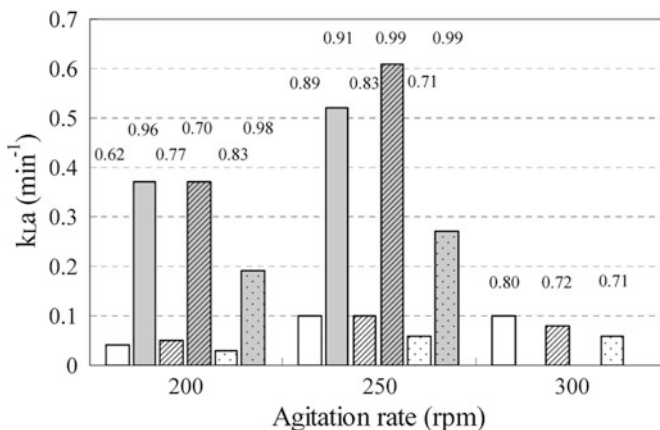


Fig. 10.13 Calculated mass transfer coefficients k_{La} and regression coefficient, r^2 , for each condition of agitation rate, viscosity of silicon oil and presence of Triton (0.25 CMC). *White columns*: water based medium; *gray columns*: Triton X-100 medium; *void columns*: 10 cSt silicone oil; *striped columns*: 20 cSt silicone oil; *dotted columns*: 50 cSt silicone oil

As presented in Fig. 10.13, the effect of Triton X-100 at 0.25 CMC was remarkable. Mass transfer coefficients were 5-fold higher than those obtained in absence of surfactant. The dispersion of nonaqueous-phase, leading to an increase in contact area, and the facilitated transport of the pollutant, probably due to reduction of surface tension or interaction of the pollutant with single surfactant molecules, may explain this increase of the mass transfer coefficients at concentrations lower than CMC [131]. On the other hand, mass transfer coefficients increased slightly when the agitation rate was increased from 200 to 250 rpm, which was coincident with the formation of the emulsion. The effect of increasing to 300 rpm had little impact on the mass transfer coefficients. The value of k_{La} with Triton at 300 rpm was not determined due to an inefficient separation of both phases. Finally, silicone oil of 10 and 20 cSt led to similar results, while solvent with 50 cSt always led to lower mass transfer coefficients.

The conditions that most favored mass transfer of anthracene (250 and 300 rpm and presence of Triton X-100) were evaluated in terms of enzyme inactivation as well as all viscosities of silicone oil. Inactivation coefficients, k_d , were calculated according to first-order kinetics (Fig. 10.14). The increase of the agitation rate to 300 rpm did not have a remarkable effect on the inactivation in presence of Triton, whereas in aqueous medium inactivation coefficients slightly increased. The viscosity of solvent does not seem to affect inactivation, except for 10 cSt, which led to the highest values.

The results presented in this work suggest that the susceptibility of VP to inactivation can be reduced by protection mechanisms associated with the surfactant. Similar protection of peroxidases from inactivation by various additives has been demonstrated in previous studies using phenols as the substrate [132].

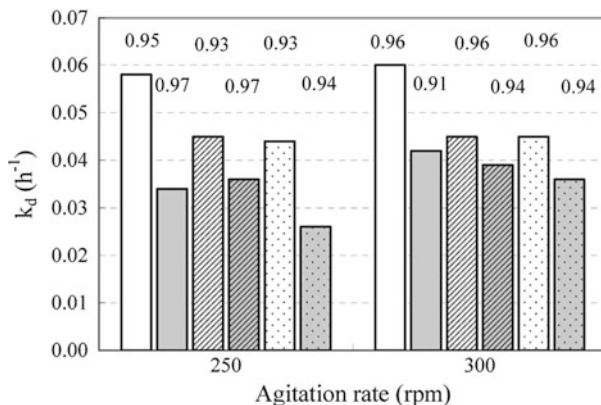


Fig. 10.14 Calculated enzymatic decay coefficients k_d and regression coefficient, r^2 , for each condition of agitation rate, viscosity of silicon oil and presence of Triton (0.25 CMC). *White columns*: water based medium; *gray columns*: Triton X-100 medium; *void columns*: 10 cSt silicone oil; *striped columns*: 20 cSt silicone oil; *dotted columns*: 50 cSt silicone oil

10.4.5 Degradation of Anthracene in TPPB

Once mass transfer and enzyme inactivation was studied, the degradation of anthracene was evaluated in a TPPB. *In vitro* degradation experiments were carried out at 250 rpm, since 300 rpm did not give any improvement in mass transfer and enzyme stability. Furthermore, the overall effect of the different viscosities was evaluated for the maximization of anthracene removal by VP.

A summary of the outcomes in terms of the average anthracene degradation rate (in 38 h) and efficiency is presented in Fig. 10.15. The increase of viscosity led to higher degradation rates and in parallel, higher efficiencies. A similar effect was observed for experiments with Triton X-100.

On the other hand, the presence of Triton increased the removal rate. The highest degradation rate was obtained with silicone oil 50 cSt in presence of 0.25 CMC Triton X-100 and at 250 rpm. Mass transfer experiments demonstrated that lower viscosities favored increased mass transfer coefficients. However, it seems that there were no mass transfer limitations in the degradation experiments, and other effects such as enzyme protection were more important to increase anthracene removal. As the interfacial area decreases for high solvent viscosity, the interfacial interaction with the enzyme also decreases, which is the main mechanism for the inactivation of biocatalysts by organic solvents [54].

In conclusion, we would like to point out that the availability of poorly soluble compounds can be enhanced by increasing the total surface area between the solvent and the aqueous phase by modifying the agitation and by the addition of Triton X-100. The system greatly benefits from surfactant addition through the increase of mass transfer of pollutant from organic to aqueous phase, owing to the decrease in interfacial tension and the protecting effect on the enzyme.

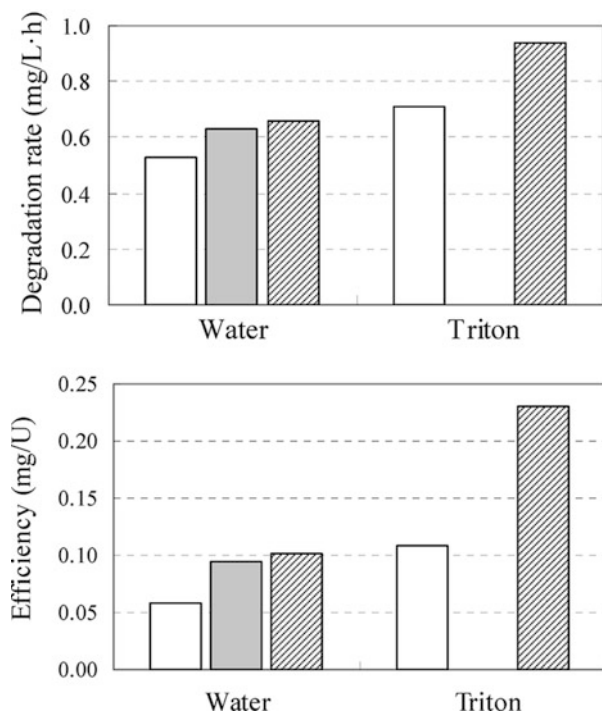


Fig. 10.15 Evaluation of different operational conditions for the degradation of anthracene in TPPB. *White columns*: 10 cSt silicone oil; *gray columns*: 20 cSt silicone oil and *striped columns*: 50 cSt silicone oil

Acknowledgments This work was funded by the Spanish Ministry of Education and Science (CTQ2007-66788/PPQ) and by Xunta de Galicia (PGIDIT06PXIB265088PR).

References

1. Alberti BN, Klibanov AM (1982) Peroxidase for removal of hazardous aromatics from industrial wastewaters. In: Exemer JH (ed) Detoxification of hazard waste. Ann Arbor Science, Ann Arbor
2. Mao X, Buchanan ID, Stanley SJ (2006) Development of an integrated enzymatic treatment system for phenolic waste streams. *Environ Technol* 27:1401–1410
3. Cooper VA, Nicell JA (1996) Removal of phenols from a foundry wastewater using horseradish peroxidase. *Water Res* 30:954–964
4. Masuda M, Sakurai A, Sakakibara M (2001) Effect of enzyme impurities on phenol removal by the method of polymerization and precipitation catalyzed by *Coprinus cinereus* peroxidase. *Appl Microb Biotechnol* 57:494–499
5. Moreira MT, Palma C, Mielgo I et al (2001) In vitro degradation of a polymeric dye (Poly R-478) by manganese peroxidase. *Biotechnol Bioeng* 75:362–368

6. Bódalo A, Gómez JL, Gómez E et al (2006) Removal of 4-chlorophenol by soybean peroxidase and hydrogen peroxide in a discontinuous tank reactor. *Desalination* 195:51–59
7. Gómez JL, Bódalo A, Gómez E et al (2006) Immobilization of peroxidases on glass beads: an improved alternative for phenol removal. *Enzyme Microb Technol* 39:1016–1022
8. López C, Moreira MT, Feijoo G et al (2004) Dye decolorization by manganese peroxidase in an enzymatic membrane bioreactor. *Biotechnol Prog* 20:74–81
9. Entezari MH, Mostafai M, Sarafraz-yazdi A (2006) A combination of ultrasound and a biocatalyst: removal of 2-chlorophenol from aqueous solution. *Ultrason Sonochem* 13:37–41
10. Colonna S, Gaggero N, Richelmi C et al (1999) Recent biotechnological developments in the use of peroxidases. *Trends Biotechnol* 17:163–168
11. Pasta P, Carrea G, Monzani E et al (1999) Chloroperoxidase-catalyzed enantioselective oxidation of methyl phenyl sulfide with dihydroxyfumaric acid/oxygen or ascorbic acid/oxygen as oxidants. *Biotechnol Bioeng* 62:489–493
12. Everse J, Everse KE, Grisham MB (1991) *Peroxidases in chemistry and biology*. CRC, Boca Raton
13. Kiljunen E, Kanerva LT (2000) Chloroperoxidase-catalysed oxidation of alcohols to aldehydes. *J Mol Catal B Enzym* 9:163–172
14. Samra BK, Andersson M, Adlercreutz P (1999) Chloroperoxidase catalysed oxidation of benzyl alcohol using tert-butyl hydroperoxide oxidant in organic media. *Biocatal Biotransfor* 17:381–391
15. Manoj KM, Hager LP (2001) Utilization of peroxide and its relevance in oxygen insertion reactions catalyzed by chloroperoxidase. *Biochim Biophys Acta* 1547:408–417
16. Mahmoudi A, Nazari K, Khosraneh M et al (2008) Can amino acids protect horseradish peroxidase against its suicide-peroxide substrate? *Enzyme Microb Technol* 43:329–335
17. Buchanan ID, Nicell JA (1998) Kinetics of peroxidase interactions in the presence of a protective additive. *J Chem Technol Biotechnol* 72:23–32
18. López C, Valade AG, Combourieu B et al (2004) Mechanism of enzymatic degradation of the azo dye Orange II determined by *ex situ* ^1H nuclear magnetic resonance and electrospray ionization-ion trap mass spectrometry. *Anal Biochem* 335:135–149
19. López C, Moreira MT, Feijoo G et al (2007) Dynamic modeling of an enzymatic membrane reactor for the treatment of xenobiotic compounds. *Biotechnol Bioeng* 97:1128–1137
20. Bódalo A, Bastida J, Máximo M et al (2008) A comparative study of free and immobilized soybean and horseradish peroxidases for 4-chlorophenol removal: protective effects of immobilization. *Bioprocess Biosyst Eng* 31:587–593
21. Miyazaki C, Takahashi H (2001) Engineering of the H_2O_2 -binding pocket region of a recombinant manganese peroxidase to be resistant to H_2O_2 . *FEBS Lett* 509:111–114
22. Mielgo I, López C, Moreira MT et al (2003) Oxidative degradation of azo dyes by manganese peroxidase under optimized conditions. *Biotechnol Prog* 19:325–331
23. van Deurzen MPJ, Seelbach K, Van Rantwijk F et al (1997) Chloroperoxidase: use of a hydrogen peroxide-stat for controlling reactions and improving enzyme performance. *Biocatal Biotransfor* 15:1–16
24. Lee K, Gu MB, Moon S-H (2003) Degradation of 2, 4, 6-trinitrotoluene by immobilized horseradish peroxidase and electrogenerated peroxide. *Water Res* 37:983–992
25. Lan J, Huang X, Hu M et al (2006) High efficient degradation of dyes with lignin peroxidase coupled with glucose oxidase. *J Biotechnol* 123:483–490
26. Moosavi-Movahedi AA, Nazari K, Ghadermarzi M (1999) Suicide inactivation of peroxidase by H_2O_2 : kinetic equations for peroxidatic oxidation reaction of guaiacol and determination of the kinetic parameters. *Ital J Biochem* 48:9–17
27. Khosraneh M, Mahmoudi A, Rahimi H et al (2007) Suicide-Peroxide inactivation of microperoxidase-11: a kinetic study. *J Enzyme Inhib Med Chem* 22:677–684
28. Nazari K, Mahmoudi A, Khosraneh M et al (2009) Kinetic analysis for suicide-substrate inactivation of microperoxidase-11: a modified model for bisubstrate enzymes in the presence of reversible inhibitors. *J Mol Catal B Enzym* 56:61–69

29. Hiner AN, Rodríguez-López JN, Arnao MB et al (2000) Kinetic study of the inactivation of ascorbate peroxidase by hydrogen peroxide. *Biochem J* 348:321–328
30. Husain M, Husain Q (2008) Applications of redox mediators in the treatment of organic pollutants by using oxidoreductive enzymes: a review. *Crit Rev Environ Sci Technol* 38:1–42
31. Goodwin DC, Grover TA, Aust SD (1996) Redox mediation in the peroxidase-catalyzed oxidation of aminopyrine: possible implications for drug-drug interactions. *Chem Res Toxicol* 9:476–483
32. Bao W, Fukushima Y, Jensen JKA et al (1994) Oxidative degradation of non-phenolic lignin during lipid peroxidation by fungal manganese peroxidase. *FEBS Lett* 354:297–300
33. Kapich A, Hofrichter M, Vares T et al (1999) Coupling of manganese peroxidase-mediated lipid peroxidation with destruction of nonphenolic lignin model compounds and C-14-labeled lignins. *Biochem Biophys Res Commun* 259:212–219
34. Wariishi H, Valli K, Renganathan V et al (1989) Thiol-mediated oxidation of nonphenolic lignin model compounds by manganese peroxidase of *Phanerochaete chrysosporium*. *J Biol Chem* 264:14185–14191
35. Klibanov AM, Tu T, Scott KP (1983) Peroxidase-catalysed removal of phenols from coal-conversion waste waters. *Science* 221:259–261
36. Nakamoto S, Machida N (1992) Phenol removal from aqueous solutions by peroxidase-catalyzed reaction using additives. *Water Res* 26:49–54
37. Akhtar S, Husain Q (2006) Potential applications of immobilized bitter melon (*Momordica charantia*) peroxidase in the removal of phenols from polluted water. *Chemosphere* 65:1228–1235
38. Wang P, Woodward CA, Kaufman EN (1999) Poly(ethylene glycol)-modified ligninase enhances pentachlorophenol biodegradation in water-solvent mixtures. *Biotechnol Bioeng* 64:290–297
39. Andersson M, Andersson MM, Adlercreutz P (2000) Stabilisation of chloroperoxidase towards peroxide dependent inactivation. *Biocatal Biotransform* 18:457–469
40. Lee K, Moon SH (2003) Electroenzymatic oxidation of veratryl alcohol by lignin peroxidase. *J Biotechnol* 102:261–268
41. Moreira MT, Palma C, Feijoo G et al (1998) Strategies for the continuous production of ligninolytic enzymes in fixed and fluidised bed bioreactors. *J Biotechnol* 66:27–39
42. Faison BD, Kirk TK (1985) Factors involved in the regulation of a ligninase activity in *Phanerochaete chrysosporium*. *Appl Environ Microbiol* 49:299–304
43. Venkatadri R, Irvine RL (1990) Effect of agitation on ligninase activity and ligninase production by *Phanerochaete chrysosporium*. *Appl Environ Microbiol* 56:2684–2691
44. Matto M, Husain Q (2009) Decolorization of direct dyes by immobilized turnip peroxidase in batch and continuous processes. *Ecotoxicol Environ Saf* 72:965–971
45. Matto M, Husain Q (2009) Decolorization of textile effluent by bitter melon peroxidase immobilized on concanavalin A layered calcium alginate-starch beads. *J Hazard Mater* 164:1540–1546
46. Alam MZ, Mansor MF, Jalal KCA (2009) Optimization of decolorization of methylene blue by lignin peroxidase enzyme produced from sewage sludge with *Phanerochaete chrysosporium*. *J Hazard Mater* 162:708–715
47. Bayramoglu G, ArIca MY (2008) Enzymatic removal of phenol and *p*-chlorophenol in enzyme reactor: horseradish peroxidase immobilized on magnetic beads. *J Hazard Mater* 156:148–155
48. Kiljunen E, Kanerva LT (1999) Novel applications of chloroperoxidase: enantioselective oxidation of racemic epoxyalcohols. *Tetrahedron Asymm* 10:3529–3535
49. Nicell JA, Bewtra JK, Biswas N et al (1993) Reactor development for peroxidase catalyzed polymerization and precipitation of phenols from wastewater. *Water Res* 27:1629–1639
50. Haifeng L, Yuwen L, Xiaomin C et al (2008) Effects of sodium phosphate buffer on horseradish peroxidase thermal stability. *J Thermal Anal Calorim* 93:569–574

51. Zamorano LS, Vilarmau SB, Arellano JB et al (2009) Thermal stability of peroxidase from *Chamaerops excelsa* palm tree at pH 3. *Int J Biol Macromol* 44:326–332
52. Elias C, Joshi J (1998) Role of hydrodynamic shear on activity and structure of proteins. *Adv Biochem Eng Biotechnol* 59:47–71
53. Eibes G, Moreira MT, Feijoo G et al (2007) Operation of a two-phase partitioning bioreactor for the oxidation of anthracene by the enzyme manganese peroxidase. *Chemosphere* 66:1744–1751
54. Ross AC, Bell G, Halling PJ (2000) Organic solvent functional group effect on enzyme inactivation by the interfacial mechanism. *J Mol Catal B Enzym* 8:183–192
55. Guisán JM (2006) Immobilization of enzymes and cells. Humana, New Jersey
56. Mateo C, Palomo JM, Fernandez-Lorente G et al (2007) Improvement of enzyme activity, stability and selectivity via immobilization techniques. *Enzyme Microb Technol* 40:1451–1463
57. Eggers DK, Valentine JS (2001) Molecular confinement influences protein structure and enhances thermal protein stability. *Protein Sci* 10:250–261
58. Illanes A (2009) Enzyme biocatalysis: principles and applications. Springer, Berlin
59. Sasaki T, Kajino T, Li B et al (2001) New pulp biobleaching system involving manganese peroxidase immobilized in a silica support with controlled pore sizes. *Appl Environ Microbiol* 67:2208–2212
60. Kazandjian RZ, Dordick JS, Klibanov AM (1986) Enzymatic analyses in organic solvents. *Biotechnol Bioeng* 28:417–421
61. Dordick JS, Marletta MA, Klibanov AM (1986) Peroxidases depolymerize lignin in organic media but not in water. *Proc Natl Acad Sci USA* 83:6255–6257
62. Torres E, Siminovich B, Barzana E et al (1998) Thermodynamic hydrophobicity of aqueous mixtures of water-miscible organic solvents predicts peroxidase activity. *J Mol Catal B Enzym* 4:155–159
63. Ryu K, Dordick JS (2002) How do organic solvents affect peroxidase structure and function? *Biochemistry* 31:2588–2598
64. Dai L, Klibanov AM (2000) Peroxidase-catalyzed asymmetric sulfoxidation in organic solvents *versus* in water. *Biotechnol Bioeng* 70:353–357
65. Eibes G, Cajthaml T, Moreira MT et al (2006) Enzymatic degradation of anthracene, dibenzothiophene and pyrene by manganese peroxidase in media containing acetone. *Chemosphere* 64:408–414
66. Vázquez-Duhalt R, Westlake DWS, Fedorak PM (1994) Lignin peroxidase oxidation of aromatic compounds in systems containing organic solvents. *Appl Environ Microbiol* 60:459–466
67. Takahisa O, Shin-ichiro T, Hiroshi U et al (1999) Soluble polyphenol. *Macromol Rapid Commun* 20:401–403
68. Eker B, Zagorevski D, Zhu GY et al (2009) Enzymatic polymerization of phenols in room-temperature ionic liquids. *J Mol Catal B Enzym* 59:177–184
69. Okrasa K, Guibé-Jampel E, Therisod M (2003) Ionic liquids as a new reaction medium for oxidase-peroxidase-catalyzed sulfoxidation. *Tetrahedron Asymm* 14:2487–2490
70. Klibanov AM (2001) Improving enzymes by using them in organic solvents. *Nature* 409:241–246
71. Van de Velde F, Bakker M, van Rantwijk F et al (2001) Chloroperoxidase-catalyzed enantioselective oxidations in hydrophobic organic media. *Biotechnol Bioeng* 72:523–529
72. Kamiya N, Okazaki S-y, Goto M (1997) Surfactant-horseradish peroxidase complex catalytically active in anhydrous benzene. *Biotechnol Techniques* 11:375–378
73. Weetall HH, Pitcher WHJ (1986) Scaling up an immobilized enzyme system. *Science* 232:1396–1403
74. Flock C, Bassi A, Gijzen M (1999) Removal of aqueous phenol and 2-chlorophenol with purified soybean peroxidase and raw soybean hulls. *J Chem Technol Biotechnol* 74:303–309
75. Siddique MH, St Pierre CC, Biswas N et al (1993) Immobilized enzyme catalyzed removal of 4-chlorophenol from aqueous solution. *Water Res* 27:883–890

76. Wu Y, Taylor KE, Biswas N et al (1999) Kinetic model-aided reactor design for peroxidase-catalyzed removal of phenol in the presence of polyethylene glycol. *J Chem Technol Biotechnol* 74:519–526
77. Fu H, Kondo H, Ichikawa Y et al (2002) Chloroperoxidase-catalyzed asymmetric synthesis: enantioselective reactions of chiral hydroperoxides with sulfides and bromohydroxylation of glycals. *J Org Chem* 57:7265–7270
78. Zhu G, Wang P (2005) Novel interface-binding chloroperoxidase for interfacial epoxidation of styrene. *J Biotechnol* 117:195–202
79. Zaks A, Dodds DR (1995) Chloroperoxidase-catalyzed asymmetric oxidations: substrate specificity and mechanistic study. *J Am Chem Soc* 117:10419–10424
80. Libby RD, Thomas JA, Kaiser LW et al (1982) Chloroperoxidase halogenation reactions. Chemical versus enzymic halogenating intermediates. *J Biol Chem* 257:5030–5037
81. Nicell JA, Saadi KW, Buchanan ID (1995) Phenol polymerization and precipitation by horseradish peroxidase enzyme and an additive. *Bioresour Technol* 54:5–16
82. Horta A, Álvarez JR, Luque S (2007) Analysis of the transient response of a CSTR containing immobilized enzyme particles. Part II. Minimum existence criterion and determination of substrate effective diffusivity and main reaction rate constant. *Biochem Eng J* 33:116–125
83. Buchanan ID, Nicell JA, Wagner M (1998) Reactor models for horseradish peroxidase-catalyzed aromatic removal. *J Environ Eng* 124:794–802
84. Gómez JL, Bódalo A, Gómez E et al (2008) A transient design model of a continuous tank reactor for removing phenol with immobilized soybean peroxidase and hydrogen peroxide. *Chem Eng J* 145:142–148
85. López C, Mielgo I, Moreira MT et al (2002) Enzymatic membrane reactors for biodegradation of recalcitrant compounds. Application to dye decolourisation. *J Biotechnol* 99:249–257
86. Seelbach K, Van Deurzen MPJ, Van Rantwijk F et al (1997) Improvement of the total turnover number and space-time yield for chloroperoxidase catalyzed oxidation. *Biotechnol Bioeng* 55:283–288
87. Shukla SP, Devi S (2005) Covalent coupling of peroxidase to a copolymer of acrylamide (AAm)-2-hydroxyethyl methacrylate (HEMA) and its use in phenol oxidation. *Process Biochem* 40:147–154
88. Gómez JL, Bódalo A, Gómez E et al (2007) Experimental behaviour and design model of a fluidized bed reactor with immobilized peroxidase for phenol removal. *Chem Eng J* 127:47–57
89. Trivedi U, Bassi A, Zhu J-X (2006) Continuous enzymatic polymerization of phenol in a liquid-solid circulating fluidized bed. *Powder Technol* 169:61–70
90. Kim GY, Lee KB, Cho SH et al (2005) Electroenzymatic degradation of azo dye using an immobilized peroxidase enzyme. *J Hazard Mater* 126:183–188
91. Cho SH, Lee HJ, Moon SH (2008) Integrated electroenzymatic and electrochemical treatment of petrochemical wastewater using a pilot scale membraneless system. *Process Biochem* 43:1371–1376
92. Cho SH, Shim J, Moon SH (2009) Detoxification of simulated textile wastewater using a membraneless electrochemical reactor with immobilized peroxidase. *J Hazard Mater* 162:1014–1018
93. Cho SH, Shim J, Yun SH et al (2008) Enzyme-catalyzed conversion of phenol by using immobilized horseradish peroxidase (HRP) in a membraneless electrochemical reactor. *Appl Catal A* 337:66–72
94. Casas C, González G, Lafuente FJ et al (1998) *Ingeniería Bioquímica*. Editorial Síntesis S.A., Madrid
95. Gómez JL, Bódalo A, Gómez E et al (2008) A covered particle deactivation model and an expanded Dunford mechanism for the kinetic analysis of the immobilized SBP/phenol/hydrogen peroxide system. *Chem Eng J* 138:460–473
96. van Deurzen MPJ, Van Rantwijk F, Sheldon RA (1997) Selective oxidations catalyzed by peroxidases. *Tetrahedron* 53:13183–13220

97. Levenspiel O (1999) Chemical Reaction Engineering, 3rd edn. Wiley, New York
98. Prazeres DMF, Cabral JMS (1994) Enzymatic membrane bioreactors and their applications. *Enzyme Microb Technol* 16:738–750
99. Rios GM, Belleville MP, Paolucci D et al (2004) Progress in enzymatic membrane reactors – a review. *J Membr Sci* 242:189–196
100. Gekas VC (1986) Artificial membranes as carriers for the immobilisation of biocatalysts. *Enzyme Microb Technol* 8:450–461
101. Prazeres DMF, Cabral JMS (2001) Enzymatic membrane reactors. In: Cabral JMS, Mota M, Tramper J (eds) *Multiphase bioreactor design*. Taylor & Francis, London
102. Guisan JM, Bastida A, Blanco RM et al (1997) Immobilization of enzymes acting on macromolecular substrates. Reduction of steric problems. In: Bickerstaff GF (ed) *Methods in biotechnology immobilization of enzymes and cells*. Humana, Totowa, NJ
103. Lante A, Crapisi A, Krastanov A et al (2000) Biodegradation of phenols by laccase immobilised in a membrane reactor. *Process Biochem* 36:51–58
104. Isono Y, Nakajima M (2000) Membrane phase separation of aqueous/alcohol biphasic mixture and its application for enzyme bioreactor. *Prog Biotechnol* 2000:63–68
105. Bohdziewicz J (1998) Biodegradation of phenol by enzymes from *Pseudomonas sp.* immobilized onto ultrafiltration membranes. *Process Biochem* 33:811–818
106. Amounas M, Innocent C, Cosnier S et al (2000) A membrane based reactor with an enzyme immobilized by an avidin-biotin molecular recognition in a polymer matrix. *J Membr Sci* 176:169–176
107. Curcio S, Calabrò V, Iorio G (2006) A theoretical and experimental analysis of a membrane bioreactor performance in recycle configuration. *J Membr Sci* 273:129–142
108. Gumí T, Fernández-Delgado Albacete J, Paolucci-Jeanjean D et al (2008) Study of the influence of the hydrodynamic parameters on the performance of an enzymatic membrane reactor. *J Membr Sci* 311:147–152
109. Kelsey LJ, Pillarella MR, Zydney AL (1990) Theoretical analysis of convective flow profiles in a hollow-fiber membrane bioreactor. *Chem Eng Sci* 45:3211–3220
110. Katuri KP, Mohan SV, Sridhar S et al (2009) Laccase-membrane reactors for decolorization of an acid azo dye in aqueous phase: process optimization. *Water Res* 43:3647–3658
111. Narendranathan TJ, Dunnill P (1982) The effect of shear on globular proteins during ultrafiltration: studies on alcohol dehydrogenase. *Biotechnol Bioeng* 24:2103–2107
112. Liu ZM, Dubremetz JF, Richard V et al (2005) Useful method for the spacial localization determination of enzyme (peroxidase) distribution on microfiltration membrane. *J Membr Sci* 2005:2–7
113. Buchholz K, Kasche V, Bornscheuer UT (2005) *Biocatalysis and enzyme technology*. Wiley, Weinheim
114. Wu Y, Taylor KE, Biswas N et al (1998) A model for the protective effect of additives on the activity of horseradish peroxidase in the removal of phenol – a kinetic investigation. *Enzyme Microb Technol* 22:315–322
115. Pitcher W (1978) Design and operation of immobilized enzyme reactors. In: Ghose T, Fiechter A, Blakebrough A (eds) *Advances in biochemical engineering*. Springer, Berlin
116. Lema JM, Roca E (1998) Biorreactores no convencionales. In: Gódia F, López J (eds) *Ingeniería Bioquímica*. Editorial Síntesis, Madrid
117. Ando S, Haraga H, Miyahara H et al (1996) Membraneless water electrolyzer. Toto, US
118. Shim J, Kim GY, Yeon SH et al (2007) Degradation of azo dye by an electroenzymatic method using horseradish peroxidase immobilized on porous support. *Korean J Chem Eng* 24:72–78
119. López C, Moreira MT, Feijoo G et al (2007) Technologies for the treatment of effluents from textile industries. *Afinidad* 64:561–573
120. Mielgo I, Palma C, Guisán JM et al (2003) Covalent immobilisation of manganese peroxidases (MnP) from *Phanerochaete chrysosporium* and *Bjerkandera sp.* BOS55. *Enzyme Microb Technol* 32:769–775

121. Giorno L, Drioli E (2000) Biocatalytic membrane reactors: applications and perspectives. *Trends Biotechnol* 18:339–349
122. Aitken MD, Irvine RL (1990) Characterization of reactions catalyzed by manganese peroxidase from *Phanerochaete chrysosporium*. *Arch Biochem Biophys* 276:405–414
123. Pérez J, Jeffries TW (1992) Roles of manganese and organic acid chelators in regulating lignin degradation and biosynthesis of peroxidases by *Phanerochaete chrysosporium*. *Appl Environ Microbiol* 58:2402–2409
124. Feijoo G, Lema JM (1995) Treatment of forest industry effluents with toxic and recalcitrant compounds by white-rot fungi. *Afinidad* 52:171–180
125. Kibret M, Somitsch W, Robra KH (2000) Characterization of a phenol degrading mixed population by enzyme assay. *Water Res* 34:1127–1134
126. Hill GA, Robinson CW (1975) Substrate inhibition kinetics: Phenol degradation by *Pseudomonas putida*. *Biotechnol Bioeng* 17:1599–1615
127. Suzuki K, Hirai H, Murata H et al (2003) Removal of estrogenic activities of 17[β]-estradiol and ethinylestradiol by ligninolytic enzymes from white rot fungi. *Water Res* 37:1972–1975
128. Eibes G, Lu Chau T, Feijoo G et al (2005) Complete degradation of anthracene by Manganese Peroxidase in organic solvent mixtures. *Enzyme Microb Technol* 37:365–372
129. Efrogmson RA, Alexander M (1995) Reduced mineralization of low concentrations of phenanthrene because of sequestering in nonaqueous-phase liquids. *Environ Sci Technol* 29:515–521
130. Edwards DA, Luthy RG, Liu Z (1991) Solubilization of polycyclic aromatic hydrocarbons in micellar nonionic surfactant solutions. *Environ Sci Technol* 25:127–133
131. Volkering F, Breure AM, Van Andel JG et al (1995) Influence of nonionic surfactants on bioavailability and biodegradation of polycyclic aromatic hydrocarbons. *Appl Environ Microbiol* 61:1699–1705
132. Kim EY, Chae HJ, Chu KH (2007) Enzymatic oxidation of aqueous pentachlorophenol. *J Environ Sci* 19:1032–1036

Chapter 11

Deactivation of Hemeperoxidases by Hydrogen Peroxide: Focus on Compound III

Brenda Valderrama

Contents

11.1	Molecular Bases of the H ₂ O ₂ -Dependent Deactivation of Peroxidases	291
11.1.1	Compound III Formation Pathways	292
11.1.2	Compound III Decay Pathways	296
11.2	Structure and Electronic Configuration of Compound III	298
11.2.1	Optical Spectrum of Compound III in the Visible Region	298
11.2.2	Circular Dichroism Spectrum of Compound III	299
11.2.3	Magnetic Circular Dichroism Spectrum of Compound III	300
11.2.4	Electron Paramagnetic Resonance Spectrum of Compound III	301
11.2.5	Resonance Raman Spectrum of Compound III	302
11.2.6	Theoretical Study of Compound III Model Systems	304
11.2.7	Mössbauer Spectroscopy of Compound III	305
11.2.8	X-ray Diffraction Crystallography of Compound III	305
11.3	Conclusions	307
	References	308

Abstract Peroxidases use H₂O₂ as electron acceptor in order to catalyze a variety of oxidative reactions through a catalytic cycle with two intermediates. Additionally to these intermediates, a third species (Compound III) is produced when ferric peroxidases are exposed to an excess of H₂O₂. Compound III is a peroxy-Fe^{III}– porphyrin free radical, the best described of the intermediates leading to the irreversible deactivation of the enzymes. This chapter aims to describe the structure, stability, formation, and decay of Compound III as fundamental knowledge required to understand, and potentially to control, the peroxidases H₂O₂-dependent deactivation process.

11.1 Molecular Bases of the H₂O₂-Dependent Deactivation of Peroxidases

Industrial innovation aimed to the replacement of conventional chemical processes into biotechnological ones marks the road for sustainable industrial practices [1].

The driving forces for these changes are energetic and environmental considerations directed to reduce or eliminate the use and generation of hazardous substances [2]. Enzymes are key elements of clean industrial practices since they are naturally endowed with exquisite selectivity and catalytic efficiency at ambient temperature. In particular, peroxidases have interesting potential applications in many different fields, being mostly used in biosensors [3, 4] and immunoassays [5]. Additionally, peroxidases have been recently introduced in several industrial processes: i.e., Kraft pulp bleaching [6–8], in dye decolorization and detoxification [9], as detergents additives [10], in synthesis of specialty chemicals [11–13], in degradation of aromatic compounds and other xenobiotics [14–16], in waste water treatment [17], as antioxidants [18], as indicators for food processing [5], in bioelectrodes [19], and in the synthesis of conducting plastics [20].

However promising, present and future commercial uses have been limited by the low stability of peroxidases in the presence of their natural substrate, hydrogen peroxide (H_2O_2) [21]. In spite of being a widely known phenomenon, it was not until recently that a mechanistic model was proposed [22, 23]. Encouraging reports indicate that this liability is susceptible of manipulation [24–27] and even the isolation of a novel isoenzyme, which is naturally resistant to deactivation [28], leads us to think that eventually we will be able to design H_2O_2 -resistant variants by means of dedicated strategies [29]. Deeper knowledge of the H_2O_2 -dependent deactivation of peroxidases will undoubtedly facilitate the development of more robust biocatalysts. Discussion of this process is focused on information gathered from heme peroxidases belonging to the peroxidase–catalase superfamily (see Chap. 2), for which most of the experimental evidence is available.

11.1.1 *Compound III Formation Pathways*

Extensive investigations on the catalytic mechanism of classical peroxidases resulted in a consensus model involving five different iron species [30, 31]. These species are ferrous, ferric, Compound I, Compound II, and Compound III (Fig. 11.1). As discussed in Chap. 5, after the reaction of ground state (GS) Fe^{III} porphyrin with H_2O_2 , Compound I (CI) is formed, a cationic oxo Fe^{IV} porphyrin-based π -free radical. Electron paramagnetic resonance (EPR) studies established that, in peroxidases of classes I and III, the second oxidation equivalent in CI is present as a porphyrin-based free radical [32, 33]. In peroxidases from fungal sources, electron abstraction from the protein results in the formation of a different species with the free radical based in a residue close to the porphyrin.

A fraction of the Compound I population engages in the catalase shortcut by reacting with a second molecule of H_2O_2 , restoring GS and releasing molecular oxygen [28, 34, 35]. In the presence of external electron sources, such as aromatic molecules, Compound I reacts with 1 equivalent of a one-electron reducing agent, generating Compound II (CII), which is an oxo Fe^{IV} porphyrin without the associated free radical. CII oxidizes a second molecule of substrate to form Fe^{III}

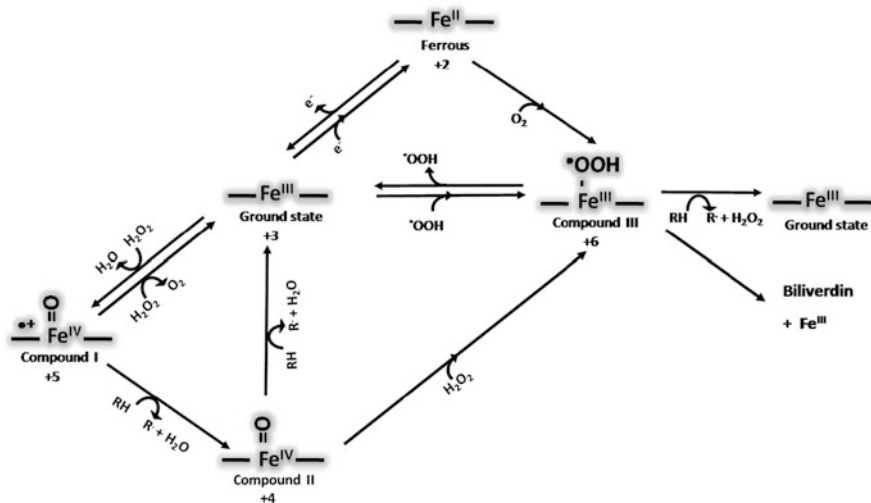


Fig. 11.1 Relationship among catalytic intermediates of peroxidases. The formal oxidation state of each species is indicated by the numbers +2 to +6. The formal oxidation state of the species directly correlates with the relative energy content of the intermediates. The entry and exit of external electron donors/acceptors is indicated. In spite of its high oxidation state, Compound III is relative inert given the stability provided by the $\text{Fe(II)}\cdot\text{O}_2$, $\text{Fe(III)}\cdot\text{O}_2^-$ and $\text{Fe(IV)}\cdot\text{O}_2^{2-}$ resonance forms. Nevertheless, amino acid residues may rescue the free radical of Compound III, restore the iron atom ferric state, and allocate the free radical into a low redox potential site in the protein backbone. When the porphyrin performs as an electron donor, a different reaction occurs, resulting in tetrapyrrole bleaching and iron release

porphyrin. Return of CII to GS seems to be preceded by dissociation of a hydroxyl anion as suggested from resonance Raman studies using ^{18}O -labeled H_2O_2 [36, 37]. In these studies, Hashimoto et al. demonstrated that the iron-bound oxygen atom in Compound II is exchangeable with oxygen atoms from bulk water but only at pH values above 6.9 or 8.8 for horseradish A2 and C isoenzymes, respectively. However, the most probable source for the proton is not water itself but a protonated His residue placed within two Å of the iron-bound oxygen in CII.

From CII, a competition between an electron-donor substrate and H_2O_2 is established to either restore GS or form Compound III (CIII), a peroxy Fe^{III} porphyrin free-radical [23, 38–40]. CIII of peroxidases was first reported by Keilin and Mann in the reaction of horseradish peroxidase with a large excess of H_2O_2 [41]. CIII is analogous to oxyhemoglobin (oxy-Hb) and to oxymyoglobin (oxy-Mb) since all of them contain low-spin heme iron with His and dioxygen in the fifth and sixth ligand position, respectively [42, 43]. Equivalent species have been detected in other heme proteins, such as cytochrome *c* [44], cytochrome *c* peroxidase [45], horseradish peroxidase A2, lignin peroxidase [46], bovine liver catalase [47], *Aspergillus nidulans* catalase [48], and manganese peroxidase [49].

The kinetic model for the H_2O_2 -dependent deactivation of peroxidases from classes I and III is similar, in that it is time-dependent and show saturation kinetics.

However, the average number of turnovers an enzyme molecule is able to perform before deactivation varies substantially among preparations: two turnovers for ascorbate peroxidase [50], 238 for horseradish peroxidase A2 [28], 265 for horseradish peroxidase C [51], and 81,000 for Zo peroxidase [28].

CII converts into CIII when exposed to H_2O_2 but not to other strong oxidizers such as alkyl hydroperoxides or peroxybenzoate derivatives [41, 52]. The selectivity pattern, taken along with evidence of formation of intermediate ferric species, may suggest that in this reaction, H_2O_2 acts as a reductant instead of an oxidant [53]. Reaction of CII with H_2O_2 to form CIII is dependent on pH, being faster at acidic pH values, indicating that an ionizable group with a pK_a between 7.1 and 9.1 is involved [52–54].

The latter values closely resemble the experimental data obtained for the deprotonation of the iron-bound oxygen of horseradish peroxidases A2 and C in the absence of H_2O_2 [36, 37] and are far from the observed pK_a for H_2O_2 in solution [55]. It is well known that the heterolytic cleavage of H_2O_2 during the formation of CI is facilitated by the abstraction of a peroxide proton by the side chain of a conserved residue in the distal cavity, His in plant peroxidases, and Glu in chloroperoxidase [21, 56]. A similar role has been proposed for a distal His residue during the autoxidation of oxy-Mb [57] and for H_2O_2 activation by cytochrome *c* peroxidase [58].

The addition of an external reductant has been shown to reduce deactivation of hemeproteins by precluding the formation of CIII through the competition with H_2O_2 for CII, as indicated above [51]. This assumption suggests that the redox properties of the added substrate would influence the electron-abstraction partition between sources controlling the stability of the enzyme under normal operation conditions. A good correlation between the substrate ionization potential value and the total turnover number of the peroxidase has been demonstrated whether using natural amino acids, amino acid derivatives, or substituted aromatic compounds [24, 27, 50, 59]. The ability of exogenous substrates with low redox potential to preclude formation of CIII strongly supports our previously published model, which suggests the existence of simultaneous and competing electron transfer pathways [23].

CIII may also be formed through reactions different from those of the peroxidasic cycle described above (a) oxygenation of Fe^{II} porphyrin or (b) reaction of Fe^{III} porphyrin (GS) with superoxide anion (Fig. 11.1). Rate constants for these reactions are compiled in Table 11.1.

Binding of molecular oxygen to Fe^{II} porphyrin, in a process equivalent to that of hemoglobin, is formally spin-forbidden. However, the reaction proceeds, thanks to the property of the porphyrin to tune the spin states of the reactants to be close in energy, resulting in spin inversion and reversible binding [65]. In peroxidases, where the heme iron is in the ferric state, it has been observed that the iron atom is close to the porphyrin plane and that the strong iron–His proximal bond weakens the iron–oxygen bond, rendering the system more reactive [66]. Structurally, spin inversion seems to be based on the movement of iron into the heme plane so as to trigger a transition from a tense to a relaxed state resulting in oxygen binding [67].

Table 11.1 Catalytic constants reported for peroxidase catalyzed reactions. CI – Compound I, CII – Compound II, CIII – Compound III, GS – Ground state, R – Reduced iron

Enzyme	Reaction	Rate	Comments	Reference
Myeloperoxidase	Ferrous + O ₂ → CIII	$1.1 \times 10^4 \text{ M}^{-1} \text{ s}^{-1}$	At 25°C, pH 7.0. Rate doubles at pH 5.0	[60]
	CIII → GS + •OOH	$6 \times 10^{-2} \text{ s}^{-1}$	At 25°C, pH 8.0. Rate increases fourfold at pH 6.0	[60]
Lactoperoxidase	Ferrous + O ₂ → CIII	$1.8 \times 10^5 \text{ M}^{-1} \text{ s}^{-1}$	At 25°C, pH 7.0. Oxygen binding is reversible with a $K_D = 6 \mu\text{M}$	[61]
Horse radish peroxidase C	Ferrous + O ₂ → CIII	$5.3 \times 10^4 \text{ M}^{-1} \text{ s}^{-1}$	At 25°C, pH 7.0	[62]
	CI + H ₂ O ₂ → GS + O ₂	$5 \times 10^2 \text{ M}^{-1} \text{ s}^{-1}$		[52]
	CIII → GS + •OOH	$8.2 \times 10^{-3} \text{ s}^{-1}$	At 25°C, pH 7.0. Formed from ferrous heme iron and oxygen	[62]
	CIII → GS + •OOH	$2.7 \times 10^4 \text{ s}^{-1}$	At 5°C, pH 7.0	[52]
Horse radish peroxidase A2	CII + H ₂ O ₂ → CIII	$13 \text{ M}^{-1} \text{ s}^{-1}$	At 5°C, pH 7.0	[52]
	CII + H ₂ O ₂ → GS + •OOH	$2.1 \text{ M}^{-1} \text{ s}^{-1}$	At 5°C, pH 7.0	[52]
	GS + •OOH → CIII	$10^7 \text{ M}^{-1} \text{ s}^{-1}$	RT, pH 5–5.5	[63]
	GS + H ₂ O ₂ → CI	$4.6 \times 10^4 \text{ M}^{-1} \text{ s}^{-1}$	RT, pH 6.1	[28]
	CII + RH → GS + •R + H ₂ O	$5.3 \times 10^5 \text{ M}^{-1} \text{ s}^{-1}$	RT, pH 6.1	[28]
	GS + •OOH → CIII	$>10^3 \text{ M}^{-1} \text{ s}^{-1}$	RT, pH 6.1	[28]
	GS + H ₂ O ₂ → CI	$6.0 \times 10^5 \text{ M}^{-1} \text{ s}^{-1}$	RT, pH 6.1	[28]
Zo peroxidase	CII + RH → GS + •R + H ₂ O	$3.6 \times 10^4 \text{ M}^{-1} \text{ s}^{-1}$	RT, pH 6.1	[28]
Lignin peroxidase	CIII → GS + •OOH	$\sim 1.0 \times 10^{-3} \text{ s}^{-1}$	RT, pH 3.0	[46]
Horse radish peroxidase	GS + •OOH → CIII	$20 \text{ M}^{-1} \text{ s}^{-1}$	RT, pH 7.0	[53]
Bovine liver catalase	GS + •OOH → CIII	$4.5 \times 10^4 \text{ M}^{-1} \text{ s}^{-1}$	RT, pH 9.0	[64]
	GS + •OOH → CIII	$4.6 \times 10^6 \text{ M}^{-1} \text{ s}^{-1}$	RT, pH 5.0	[64]
	CII + H ₂ O ₂ → CIII	$6.1 \times 10^4 \text{ M}^{-1} \text{ s}^{-1}$	25°C, pH 7.0–7.5	[47]

Aside from the classical examples of hemoglobin and myoglobin, reaction of ferrous heme iron with O_2 in hemeperoxidases has been reported for myeloperoxidase [60], horseradish peroxidase C [62], bovine liver catalase [68], lignin peroxidase [46], and lactoperoxidase [61]. With the exception of lactoperoxidase, the binding of O_2 is irreversible and CIII engages in one or more of the decay pathways described below.

Generation of CIII from GS occurs when the enzyme acts as an oxidase in the presence of superoxide ion. This reaction has been observed in horseradish peroxidase isoenzymes C and A2 [28, 53, 63], lignin peroxidase [46], myeloperoxidase [69], and bovine liver catalase [64]. The rate constant for the reaction of GS with superoxide increases with a decrease of pH suggesting that the reacting species is $\bullet HO_2$ instead of $\bullet O_2^-$ [64]. The physiological relevance of the hydroxyperoxyl radical has been recently reassessed [70].

11.1.2 Compound III Decay Pathways

At least three formal resonance forms can be written for CIII: $Fe^{II}-O_2$, $Fe^{III}-\bullet O_2^-$, and $Fe^{IV}-O_2^{2-}$. The potential reactivity of CIII in each one of these resonance forms depends on (1) dissociation of O_2 from the ferrous resonance form, as occurs with lactoperoxidase [61]; (2) dissociation of $\bullet O_2^-$, yielding ferric heme as has been described for myeloperoxidase [60], lignin peroxidase [46], and horseradish peroxidase C; (3) one-electron reduction of the $Fe^{III}-\bullet O_2^-$ resonance form to produce the peroxide species O_2^{2-} , which, upon protonation, could either dissociate as H_2O_2 or convert the ferric heme protein into CI; (4) a net two-electron reduction of the complex that results in transfer of two-electron deficient oxygen atom to the porphyrin ring or to a substrate bound at the active site, such as a halide anion (in the case of chloroperoxidase) or an organic molecule (in the case of cytochrome P450) [22].

Only three of the theoretical decay pathways for CIII have been experimentally described. First, CIII returns to GS after catalyzing the one-electron oxidation of a substrate molecule (pathway 3) [46, 71]. This substrate molecule may be external or internal. In the latter case, CIII might undergo electron transfer with the surrounding protein, resulting in the formation of an oxidized side-chain group in a reaction similar to that previously described for lignin peroxidases [38, 72–74]. Amino acid-based free radicals have been detected in cytochrome *c* [75], metmyoglobin [76], prostaglandin H synthase [77, 78], ascorbate peroxidase [79], versatile peroxidase [80], and lignin peroxidase [81, 82] after treatment with excess H_2O_2 . In some cases, the amino acid-based free radical is located in the vicinity of the porphyrin, while in other cases, it is stabilized in the outskirts of the protein. It is well known that protein-based radical damage may be propagated within protein structures and that in most cases, transient short-lived species react rapidly with a range of targets to yield other radicals [83].

Protein-based free radicals might travel back and forth between the protein backbone and proximal side-chains until reaching the lowest-reduction potential

site available. The ultimate sink for oxidizing equivalents in proteins is Cys residues [72], although Trp- and Tyr-based free radicals have been observed after the examination of a number of peptide radicals [84]. Transfer reactions within heme proteins have been observed in myoglobin [85], hemoglobin [86], and leghemoglobin [87]. These hemeprotein-derived radicals generate intermolecular cross-links through the formation of di-Tyr links. Tyr-mediated self-oligomerization has been observed during the oxidative inactivation of myoglobin [88], cytochrome P450 [89], and lactoperoxidase [90, 91]. Occasionally, hemeproteins oligomerize with other proteins through the formation of di-Tyr links, as has been described between cytochrome *c* and α -synuclein [92].

Second, and given the vicinity of the bound peroxy radical to the porphyrin ring in CIII, this species might reach the tetrapyrrole structure and perform a two-electron oxidation of the porphyrin moiety yielding biliverdin and soluble Fe^{III} (pathway 4). This speculation is supported by the existence of an inactive species, different from, but related to, CIII characterized by heme bleaching, which has been observed in ascorbate peroxidase [50], hemoglobin [93], myoglobin [94], horseradish peroxidase [95], microperoxidase-11 [96], cytochrome P450 [97], chloroperoxidase [98], *Coprinus cinereus* peroxidase [99], as well as in the non-peroxidasic hemeprotein prostaglandin H synthase [100]. Heme compounds are particularly susceptible to oxidative attacks at the *meso* position to form biliverdin ring systems, and the dependence of this process on exogenous peroxide has been demonstrated [72, 101]. Such oxidation readily leads to rupture or elimination of the carbon bridges linking the pyrrole rings, resulting in cleavage of the porphyrin macrocycle and formation of an open chain tetrapyrrolic structure [95, 102, 103]. The release of heme iron during the formation of these species confirms that they are associated with heme degradation.

Finally, the spontaneous liberation of free radicals via the unimolecular decay of CIII is feasible, since the peroxy radical is not covalently bound to the porphyrin (pathway 2). This assumption is supported by experimental evidence, which demonstrates that in the presence of excess H_2O_2 and no reductant, CIII decays irreversibly into GS and superoxide species in lignin peroxidase [46], horseradish peroxidase [104], myeloperoxidase [51, 105, 106].

The integrity of the heme group after decay of CIII may be corroborated by different methods, including residual catalytic activity or spectroscopic methods. It has been reported that the decay product of horseradish peroxidase CIII presents a diminished intensity of the Soret band (proportional to the loss of peroxidasic activity) and the appearance of a new signal at 670 nm. This compound was named p670 and has been explained as the accumulation of verdoheme [53, 107].

CIII is less active than CI or CII; however, it can still oxidize a number of electron donors. Whether the electron abstraction reaction is direct or indirect has not been addressed regularly. Nevertheless, the latter mechanism is sustained by recent results using horseradish peroxidase and myeloperoxidase [106, 108, 109].

11.2 Structure and Electronic Configuration of Compound III

Several lines of evidence are required to completely define the structure of heme groups and their associated ligands (a) optical spectra in the visible region, (b) EPR spectra, (c) the oxidation state of the compound, and (d) proof of the identity of the sixth ligand of the heme iron atom [45]. Structural information of other protein elements can be complemented with the use of proteomic tools and X-ray diffraction crystallography.

The optical and magnetic spectra of a heme protein reflect the reciprocal perturbations of the iron atom and the porphyrin upon their electronic configuration. The heme iron atom perturbs the porphyrin spectrum depending on its valence and by the number and strength of the interactions with the immediately adjacent Z-ligand atoms, either proximal or distal to the heme. The ligand on the proximal side of the heme, which is contributed by the protein, seems to be the same for all the derivatives of any given protein [110]: the identity of the proximal ligand is His in hemoglobin, myoglobin, and in peroxidases from classes I, II, and III [43, 111–113], Cys in chloroperoxidase [114] and peroxygenase [115], or Cys in dioxygen activating enzymes cytochrome P450 and nitric oxide synthase [116]. In peroxidases, the His ligand, hydrogen bonded to an Asp residue, which imparts a more imidazolate character to the proximal ligand, is good enough for binding, activating, and splitting distal ligands such as H₂O₂ but not O₂ [117].

All the catalytic intermediates of the peroxidase catalytic cycle as well as CIII present characteristic spectroscopic properties, which provide invaluable information on the structure of the porphyrin and its ligands. Here we discuss the evidence regarding the structure of Compound III.

11.2.1 Optical Spectrum of Compound III in the Visible Region

Electronic spectra of metalloproteins find their origins in (1) internal ligand absorption bands, such as $\pi \rightarrow \pi^*$ electronic transitions in porphyrins; (2) transitions associated entirely with metal orbitals ($d-d$ transitions); and (3) charge-transfer bands between the ligand and the metal. Optical spectra of porphyrins in the visible region predominantly reflect the electronic structure of the porphyrin itself. In CIII, the most conspicuous signal is the Soret band with a maximum at 416 nm and secondary maxima at 540 and 580 nm (Fig. 11.2). The spectrum indicates that the heme iron in this species is $d_{1/2}^5$ with two oxygen atoms occupying the sixth ligand position [45]. The oxidation state of the ligand, considered separately, is the oxidation state of the complex minus that ascribed to the iron, which is III. In order to accommodate this number of oxidizing equivalents within the two oxygen atoms, we write: [Protein (heme $d_{1/2}^5$) •OO⁻¹]^{VI}, which may be also described to be a peroxy-Fe^{III}porphyrin. It should be noted that the electronic configuration of CIII is identical to that of oxymyoglobin and oxyhemoglobin, yet these compounds exhibit striking differences in their ability to dissociate oxygen or to be reduced by dithionite [43, 57].

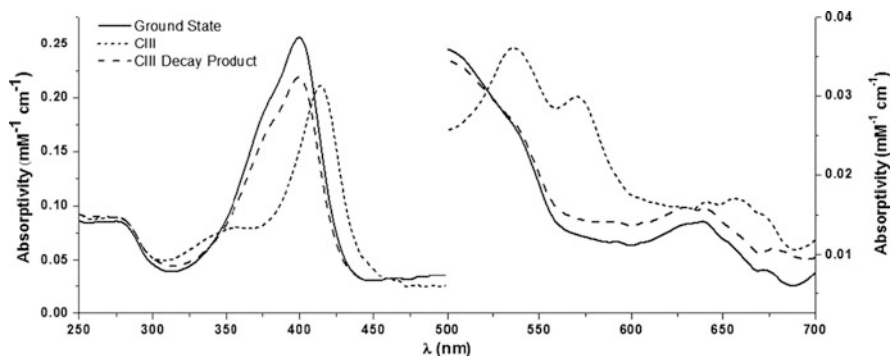


Fig. 11.2 Optical absorption spectra of horseradish peroxidase A2 in 10 mM phosphate buffer, pH 6.1. Spectra were recorded before the addition of a 500 M excess of H_2O_2 at room temperature, Ground state (*filled line*); after 5 min of incubation, Compound III (*dotted line*); and after 24 h incubation, Compound III decay product (*dashed line*)

11.2.2 Circular Dichroism Spectrum of Compound III

Absorption spectra using a source of polarized light provide more information than regular absorption spectra. The presence of the heme chromophore in peroxidases gives rise to several new circular dichroism (CD) bands due to the heme electronic transitions. Although the heme group is highly symmetric, theoretical calculations have shown that significant optical activity of the heme transitions arises from the interactions of heme with amino acid residues in the protein [118]. The first heme band CD spectra were simultaneously reported for hemoglobin [119], leghemoglobin [120], and horseradish peroxidase isoenzymes A1 and C1 [121].

In the ultraviolet region, plant peroxidases present a positive band at 191 nm and negative bands at 208 and 221 nm, reflecting the substantial helical content of the enzymes [121]. In the 250–290 nm range, horseradish A2 peroxidase presents a negative band at 285 nm and fine structure bands at 262 and 268 nm (Fig. 11.3). In addition, horseradish C peroxidase has a band at 280 nm, whereas A1 peroxidase has a shoulder at 291 nm [121].

The CD spectra of peroxidases in the heme absorption region are highly sensitive to the conformation of the heme group inside the protein cavity and to the dipole–dipole coupling interactions between the porphyrin and the surrounding aromatic amino acid side chains [122, 123]. In this region, GS horseradish A2 peroxidase presents a band at 311 nm and the intense CD Soret band at 412 nm with a shoulder at 354 nm (Fig. 11.3). The main differences between the CD spectrum of CIII compared to that of GS are a reduction of the CD band at 311 nm and a red-shift of the Soret CD band to 430 nm with the disappearance of the 354 nm shoulder. Additionally a broad band, possibly composed by a series of shoulders, appears from 350 to 400 nm. During spontaneous decay, the CD spectrum of CIII slowly returns to that of GS, with the characteristic reduction of the Soret band due to porphyrin destruction (see above).

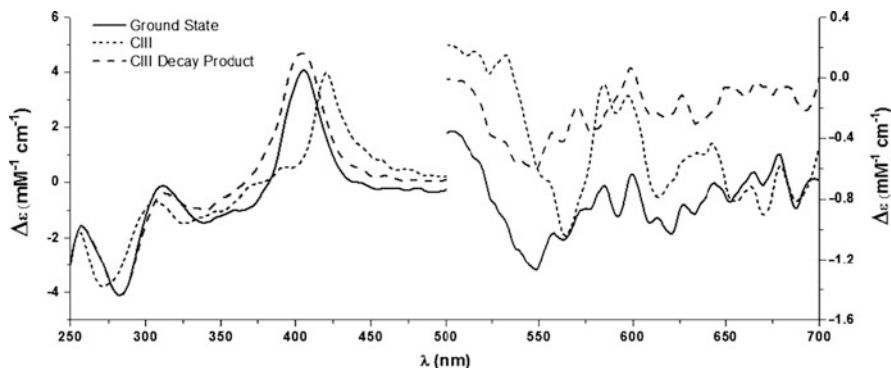


Fig. 11.3 Circular dichroism spectra of horseradish peroxidase A2 in 10 mM phosphate buffer, pH 6.1. Spectra were recorded before the addition of a 500 M excess of H_2O_2 at room temperature, Ground state (*filled line*); after 5 min of incubation, Compound III (*dotted line*); and after 24 h of incubation, Compound III decay product (*dashed line*)

11.2.3 Magnetic Circular Dichroism Spectrum of Compound III

In the presence of a magnetic field, even nonchiral molecules exhibit CD spectra, which can be measured by the technique called magnetic circular dichroism (MCD). The intensity developed by the spin-orbit coupling between excited states and between GS and excited states can be exploited, particularly at low temperature, which generates more intense metal-centered $d-d$ transitions relative to absorption spectra. Although the theoretical analysis of MCD spectra is usually complex, they are particularly sensitive to the spin state of the heme iron and a powerful fingerprint for the identification of bound ligands. The complexity arises from the existence of extra transitions (e.g., charge-transfer transitions including iron-porphyrin and axial ligands) overlapped in the Soret region, and from the Faraday C term contribution from the iron electronic states, which appears to be critical in the Soret region more than in the visible region even at room temperature. From these facts, it has been presumed that the Q band MCD can be used as a quantitative measure more easily than the Soret band MCD [124].

The MCD spectra of CIII of horseradish peroxidase recorded at -40 and -146°C are similar to those obtained for the oxygenated complexes of myoglobin and hemoglobin, in that the apparent Faraday A terms are observed both in the Soret and Q regions (Fig. 11.4) [125]. However, the magnitude of the Q band of Compound III is smaller than that from the oxygen complexes of hemoglobin and myoglobin but larger than the value for the oxygen complex of cytochrome P450 [124]. These results are in accordance with the fact that the oxygen in CIII is more reactive than in hemoglobin or myoglobin, but less than in cytochrome P450. Thus it seems that the differences in the electron distribution in the Fe-O complex directly correlate oxygen reactivity and its electron density.

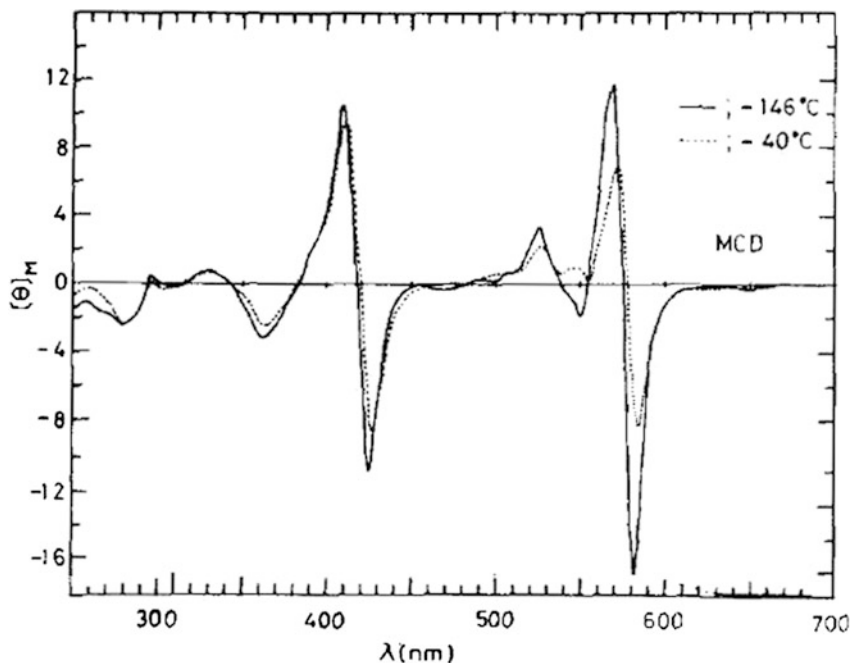


Fig. 11.4 Magnetic circular dichroism of horseradish peroxidase recorded at -40 and -146°C . Adapted from Nozawa et al. [124]

11.2.4 *Electron Paramagnetic Resonance Spectrum of Compound III*

EPR detects unpaired electrons in a sample by their absorption of energy from continuous microwave irradiation (X-band, ca. 9–10 GHz), when the sample is placed in a strong magnetic field (around 0.3 T). EPR spectra completely define the electronic configuration of a heme iron atom [42, 126–128]. In other cases, EPR spectra give indirect evidence concerning the electronic configuration of the heme iron atom as it interacts with its environment [24, 80, 129, 130]. Particularly in the case of Compound III, which is diamagnetic and therefore displays no EPR signal, other lines of evidence are required to determine the electronic configuration of the heme iron atom with confidence. Interactions between the intrinsic spin of one electron and the intrinsic spin of another electron are called spin–spin coupling. For these elements, this coupling can shift the electron orbital energy levels. When two electron wave-functions overlap in this manner, the spins couple in an antiferromagnetic manner, combining so as to exactly cancel their paramagnetism.

Compound III exhibits no EPR at very low temperature and therefore seems to be diamagnetic [45]. This phenomenon seems to arise from the close proximity of two atoms (the heme iron atom and the peroxy radical) harboring unpaired

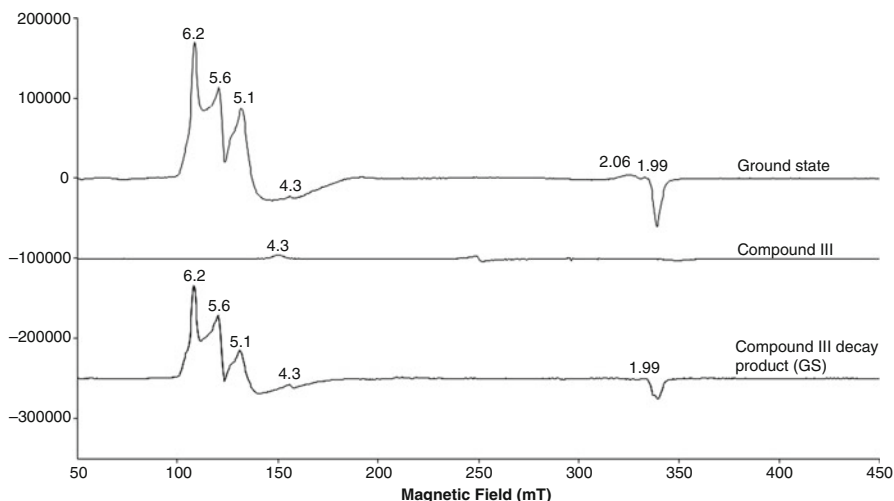


Fig. 11.5 20 K X-band ($\nu = 9.38$ GHz) resonance paramagnetic (EPR) spectra of horseradish peroxidase A2 (0.2 mM) in 10 mM phosphate buffer, pH 6.1. Spectra were recorded before the addition of a 500 M excess of H_2O_2 at room temperature, Ground state (*upper line*); after 2 min of incubation, Compound III (*intermediate line*); and after 20 h incubation, Compound III decay product (*lower line*). Identified G values are marked

electrons in the same structure with a finite amount of electronic overlap between them indicating equilibrium between resonant forms. During spontaneous decay of CIII, the signals in the EPR spectrum slowly appear to match that of GS, with the characteristic reduction of the Soret band due to porphyrin destruction (Fig. 11.5).

11.2.5 Resonance Raman Spectrum of Compound III

As in Raman spectroscopy, Resonance Raman spectroscopy gives information about molecular vibrational frequencies. These frequencies are in the range of 10^{12} – 10^{14} Hz, and correspond to radiation in the infrared region of the electromagnetic spectrum. This spectroscopy involves laser excitation finely tuned to be near to an absorption band of the sample, corresponding to an electronic transition. Certain vibrational modes, those coupled to the electronic transition, exhibit greatly increased Raman scattering signals in the resulting spectrum overwhelming that of all other electronic transitions in the sample, reducing the complexity of the spectrum, and allowing us to look at only a few vibrational modes at a time. The sensitivity of the method approaches that of absorption spectrophotometry, while the high resolution characteristic of vibrational spectroscopy is preserved, even in dilute sample solutions (as low as 10^{-8} M) at room temperature [131].

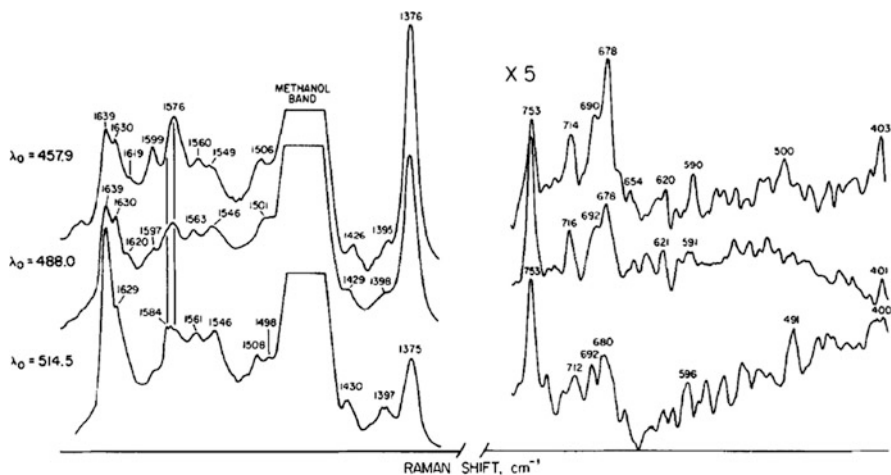


Fig. 11.6 Resonance Raman spectra of compound III of horseradish peroxidase (0.2 mM) in 10 mM phosphate buffer, pH 7.8, containing 30% v/v methanol at -10°C excited at three different wavelengths. Instrumental conditions: spectral slit width 5 cm^{-1} ; laser power, 30 mW; acquisition time, 40 min. Reproduced with permission from [139]

If the resonant electronic transition is associated with a site of biological activity, then the technique offers a sensitive probe for structural features of the site. Heme proteins afford particularly informative resonance Raman spectra, with a rich assortment of porphyrin ring vibrations, which can be classified and analyzed via their symmetry properties [132–134]. Some of these frequencies are sensitive to the structural features of spin- and oxidation-state changes of the heme group. These can be used to monitor the structural consequences of ligation or electron transfer in heme proteins [66, 135–138].

The Raman spectra of the HRP CIII excited at 457.9, 488.0, and 514.5 nm contains four bands that are known to be sensitive to the structure and electron distribution of the heme group (Fig. 11.6) [139]. The increase in the frequencies of bands 1,506, 1,584, and $1,639\text{ cm}^{-1}$ observed when oxygen becomes coordinated at the sixth site was attributed to core expansion of the porphyrin ring brought about when the iron atom is pulled into the plane of the macrocycle [139]. On the other hand, the frequencies of bands 1,376 and $1,639\text{ cm}^{-1}$ are thought to be sensitive to changes in the π^* orbital occupancy of the porphyrin [139]. Back donation from the iron d_{π} orbitals, which is more efficient for Fe^{II} , weakens the porphyrin bonds and lowers these frequencies. The band $1,376\text{ cm}^{-1}$ observed in HRP CIII can thus be attributed to either the presence of Fe^{III} in the form of $\text{Fe}^{\text{III}}\text{-O}_2^{\bullet-}$ complex or to $\text{Fe}^{\text{II}}\text{-O}_2$ complex in which oxygen acts as a good π -acid to compete with the porphyrin for the iron d_{π} electrons [66, 139].

The degree of back donation is very sensitive to the match between iron d_{π} and oxygen π^* orbital energies. The proximal His in CIII apparently acts as a stronger field ligand than in oxy-Mb, driving up the energy of the iron d_{π} orbitals closer to

that of the oxygen π^* orbitals and promoting greater π -bonding. This greater back donation is probably also facilitated by the fact that the iron atom is closer to the porphyrin plane in CIII, leading to better orbital overlap. At the same time, the energy of the d_z^2 orbital would also be raised. This would decrease the strength of the σ -bond formed by the overlap of a filled oxygen σ orbital with the iron d_z^2 orbital, widening the energy gap between the oxygen π^* -orbital with which it overlaps [140].

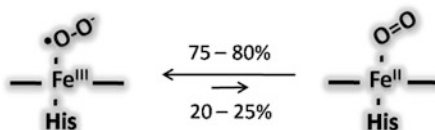
Thus, a plausible explanation for the data is that CIII has a stronger σ -bond to the proximal His than oxy-Mb. This results in a *trans* effect that apparently causes a net weakening of the iron–oxygen bond, but leads to more extensive back donation into oxygen π^* orbitals. The increased electron density in these antibonding orbitals can at least partly explain the greater degree of oxygen activation in CIII compared to oxy-Mb. This should weaken the O–O bond and activate it for use as an electron acceptor. This line of reasoning concerning the influence of the proximal His state of hydrogen bonding and ionization on heme reactivity is similar in kind to that advanced by others [66].

11.2.6 Theoretical Study of Compound III Model Systems

The theoretical study of heme groups has become more common in recent years because of the appearance of new methodologies and the increase in computer power. In particular, the application of the IMOMM (Integrated Molecular Orbital Molecular Mechanics), a hybrid Quantum Mechanics/Molecular Mechanics (QM/MM) scheme, has allowed the accurate study of transition metal systems [140–142].

The literature is rich in discussions about the nature of the Fe–O bond. In principle, the electronic structure of oxyheme could be described as singlet oxygen bound to low-spin iron ($\text{Fe}^{\text{II}}\text{-O}_2$) or as a superoxide radical antiferromagnetically coupled to low-spin iron ($\text{Fe}^{\text{III}}\text{-O}_2\cdot^-$). Jensen et al. have used density functional methods to calculate fully relaxed potential energy curves of the seven lowest electronic states during the binding of O_2 to a realistic model of ferrous deoxyheme [65], concluding that their results are closest to an $\text{Fe}^{\text{III}}\text{-O}_2\cdot^-$ description, in accordance with earlier DFT calculations [143]. However, the spin densities are far from ± 1 , which clearly shows that the electronic structure cannot be fully described by a single configuration but as a mixture of 75–80% $\text{Fe}^{\text{III}}\text{-O}_2\cdot^-$ and 20–25% $\text{Fe}^{\text{II}}\text{-O}_2$ [140] (Fig. 11.7). This is in accordance with the experimental observation that a quantum mixture of approximately two thirds ferric and one-third ferrous states gives the best agreement with Mössbauer [144] and EPR spectra.

Fig. 11.7 Simultaneous electronic configurations of Compound III as estimated by density functional methods [65]



Interestingly, whereas the spin densities on iron and O_2 vary appreciably for the various states, the charges are much more similar. However, this variation is fully consistent with the spin densities, giving a lower charge for low-spin states, which are better shielded from the nuclei. Thus, the total electron density (charge) is quite rigid in the states. The spin density, however, differs significantly within the various states. Therefore, the notion of $Fe^{III}-O_2\bullet^-$ and $Fe^{II}-O_2$ is only justified in terms of spin density and not in terms of the charge [65, 140, 142].

11.2.7 Mössbauer Spectroscopy of Compound III

Mössbauer spectroscopy probes high-energy transitions in the atomic nucleus and is based on the phenomenon of Recoil-free γ -ray Resonance Absorption. At a sufficiently low temperature, a significant fraction of the nuclei embedded in a crystal lattice may emit or absorb γ -rays without any recoil. In contrast, under normal conditions, atomic nuclei recoil when they emit or absorb γ -rays, and the wavelength varies with the amount of recoil. The strictly monochromatic γ -radiation emitted from the excited nucleus of a suitable isotope during a radioactive decay pathway can therefore be absorbed by the same isotope in the sample. The interest of the method lies in the fact that, if energy transitions occur within the nucleus itself, the magnitude will depend on the density and arrangement of extranuclear electrons, i.e., on the chemical state of the atoms.

Mössbauer spectroscopy provides valuable information on the electronic configuration, the nature of the surrounding ligands and the symmetry of the ligand field of ^{57}Fe -substituted heme groups. The effects of the electronic structure on the iron nucleus are transmitted primarily via two hyperfine interactions: the isomer shift (δ in mm/s) and the electric quadrupole splitting (ΔE_Q). The observed isomer shift gives information about the metal oxidation and spin states and the nature of the ligands coordinated to the iron. From a structural point of view, the quadrupole splitting is dependent on electric field gradients at the nucleus and reflects the asymmetry of the electric field surrounding the metal center.

The spectrum of CIII japanese radish peroxidase exhibits two widely splitted lines with a quadrupole splitting $\Delta E_Q = 2.37 \text{ mm s}^{-1}$ and an isomer shift $\delta_{Fe} = 0.29 \text{ mm s}^{-1}$ at 77°K [145], very similar to those observed in oxyhemoglobin [144], a horseradish peroxidase [146]. The electronic structure of the iron is apparently determined by the $Fe-O_2$ bond with a marginal contribution of the fifth, axial ligand provided by the protein (Fig. 11.8).

11.2.8 X-ray Diffraction Crystallography of Compound III

The three-dimensional structures of plant peroxidases from *Arabidopsis* [112], barley [147], horseradish [112], peanut [111], and soybean [148] have been

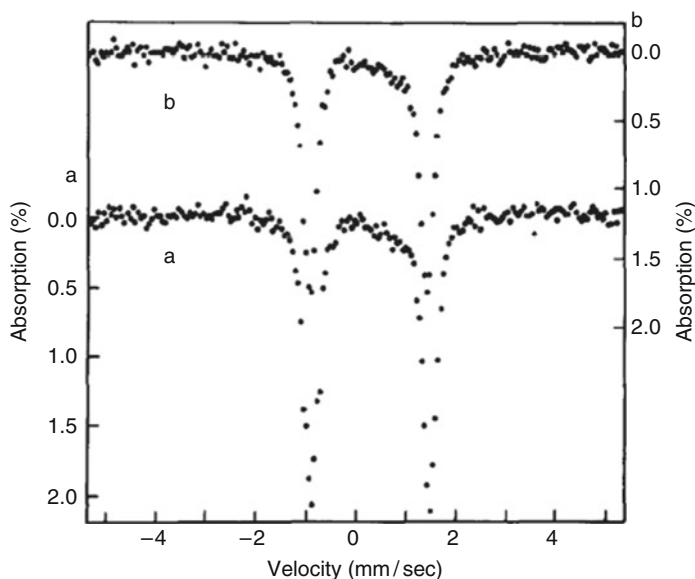


Fig. 11.8 Mössbauer absorption spectrum of Japanese radish peroxidase a-hydrogen peroxide Compound III at (a) 77°K and (b) 195°K. Reproduced with permission from [145]

determined by X-ray crystallography. Based on this evidence, specific roles for particular amino acid residues and structural motifs or regions have been proposed and, in some cases, confirmed using site-directed mutagenesis or other spectroscopic techniques.

An understanding of the H_2O_2 -dependent deactivation mechanism or heme peroxidases in structural terms requires detailed structures for the redox intermediates. The three dimensional structure of CIII at atomic levels by X-ray diffraction crystallography has been achieved by the use two different experimental strategies.

Miller et al. reported the 2.2 Å structure of CIII of recombinant yeast cytochrome *c* peroxidase as a model for Compound 0, the transient enzyme:peroxide complex (Fig. 11.9a) [149]. A mutant cytochrome *c* peroxidase known to stabilize the formation of CIII was crystallized as GS and the crystals were converted into the $\text{Fe}^{\text{II}}\text{-O}_2$ complex and diffracted. In the resultant model, oxygen atom O_A is bound to the heme iron at a distance of 1.8 Å and to oxygen atom O_B at a distance of 1.29 Å. The dioxygen molecule bond to iron is tilted, facilitating the formation of a hydrogen bond between oxygen atom O_A and $\text{N}_\epsilon\text{H}$ of Trp 51. Oxygen atom O_B interacts with two water molecules (596 and 648), which are part of a larger hydrogen bond network with residues His 52 and Arg 48 in the distal cavity.

Berglund et al. reported the 1.6 Å structure of CIII of recombinant horseradish peroxidase C isoenzyme as part of a multicrystal data collection strategy aimed to the visualization of the peroxidasic catalytic pathway at atomic levels

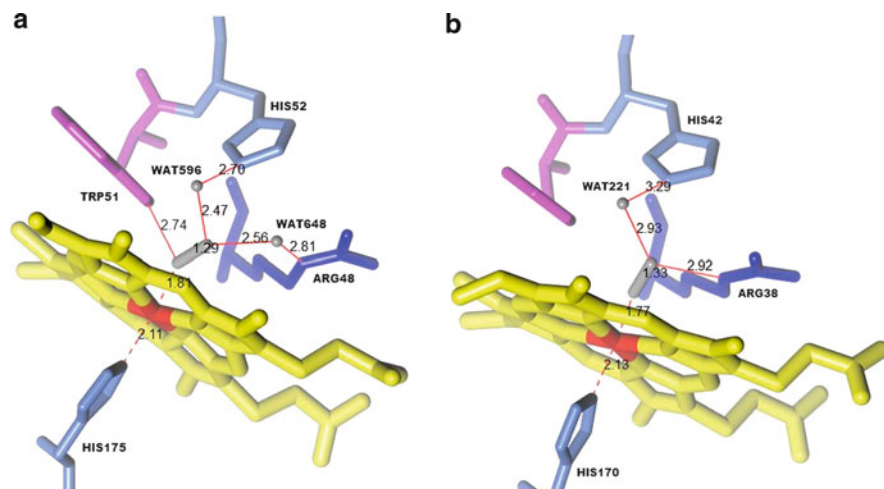


Fig. 11.9 Heme environment of (a) recombinant cytochrome *c* peroxidase Compound III (PDB 1DCC) [149] and (b) recombinant horseradish peroxidase C Compound III (PDB 1H57) [110]. Hydrogen bonds are depicted as *filled lines* and coordination bonds as *dashed lines*

(Fig. 11.9b) [110]. In this model, the dioxygen bound to the heme iron has a significant superoxide character in a bent conformation with oxygen atom O_A bound to the heme iron at a distance of 1.8 Å. In the original model, oxygen atom O_B formed hydrogen bonds with the Nε2 atom of His 42 (2.9 Å), the N1 atom of Arg 38 (2.9 Å), and with a water molecule (2.9 Å). However, comparison with the model proposed by Miller et al. suggests an alternative organization scheme involving the indirect interaction of oxygen atom O_B with His 42 through water molecule 221 as depicted in Fig. 11.9b.

11.3 Conclusions

Heme peroxidases are able to catalyze reactions of dehydrogenation and polymerization of aromatic compounds, epoxidation, and heteroatoms oxidation reactions, all of which can be used for valuable applications including the synthesis of fine chemicals and optically and biologically active compounds. However, present and future commercial uses have been limited by the low stability of peroxidases in the presence of their natural substrate, H₂O₂. We have gained deeper insight into the deactivation mechanism and its intermediates in the last years. From the known intermediates, Compound III has been the best described, since it has been observed in all reported cases. The aim of this chapter was to revise the current knowledge on the deactivation mechanism and to present a catalog of methodologies, which have

been applied to the characterization of Compound III in terms of its structure, stability, formation, and decay. We consider that the ability to control Compound III may be the most promising strategy for the eventual to control of the H₂O₂-dependent deactivation process of heme peroxidases.

Acknowledgments I am indebted to Paloma Gil for advice and helpful discussions, to Rebecca Pogni for the use of EPR facilities in the University of Siena, and to Ricardo Paredes for assistance in figure preparation. Original research presented here was funded by Papiit-UNAM 202407 and by the Executive Program of Scientific and Technological Cooperation Mexico-Italy 2006–2009.

References

1. DeSimone LD, Popoff F (1997) The business link to sustainable development. MIT, Cambridge, MA
2. Anastas PT, Warner JC (1998) Green chemistry: theory and practice. Oxford University Press, New York, NY
3. Ramos MC, Torrijas MC, Diaz AN (2001) Enhanced chemiluminescence biosensor for the determination of phenolic compounds and hydrogen peroxide. *Sens Actuators* 73:71–75
4. Iwuoha EI, Joseph S, Zhang Z et al (1998) Drug metabolism biosensors: electrochemical reactivities of cytochrome P450cam immobilized in synthetic vesicular systems. *J Pharm Biomed Anal* 17:1101–1110
5. Ingram DT, Lamichhane CM, Rollins DM et al (1998) Development of a colony lift immunoassay to facilitate rapid detection and quantification of *Escherichia coli* O157:H7 from agar plates and filter monitor membranes. *Clin Diagn Lab Immunol* 5:567–573
6. Paice MG, Jurasek KL (1984) Peroxidase catalyzed color removal from bleach plant effluent. *Biotechnol Bioeng* 26:477–480
7. Michel FC, Dass SB, Grulke EA et al (1991) Role of manganese peroxidase and lignin peroxidase of *Phanerochaete chrysosporium* in the decolorization of Kraft bleach plant effluent. *Appl Environ Microbiol* 57:2368–2375
8. Ferrer I, Dezotti M, Duran N (1991) Decolorization of Kraft effluent by free and immobilized lignin peroxidases and horseradish peroxidase. *Biotechnol Lett* 13:577–582
9. Husain Q (2006) Potential applications of the oxidoreductive enzymes in the decolorization and detoxification of textile and other synthetic dyes from polluted water: a review. *Crit Rev Biotechnol* 26:201–221
10. Xu F (2005) Applications of oxidoreductases: recent progress. *Ind Biotechnol* 1:38–50
11. Lipovšek D, Antipov E, Armstrong KA et al (2007) Selection of horseradish peroxidase variants with enhanced enantioselectivity by yeast surface display. *Chem Biol* 14:1176–1185
12. van Rantwijk F, Sheldon RA (2000) Selective oxygen transfer catalyzed by heme peroxidases: synthetic and mechanistic aspects. *Curr Opin Biotechnol* 11:554–564
13. van Deurzen MPJ, van Rantwijk F, Sheldon RA (1997) Selective oxidations catalyzed by peroxidases. *Tetrahedron* 53:13183–13220
14. Hammel KE, Kayanaraman B, Kirk TK (1986) Oxidation of polycyclic aromatic hydrocarbons and dibenzo(p)dioxins by *Phanerochaete chrysosporium* ligninase. *J Biol Chem* 36:16948–16952
15. Hammel KE, Tradone PJ (1988) The oxidative 4-dechlorination of polychlorinated phenols is catalyzed by extracellular fungal lignin peroxidase. *Biochemistry* 27:6563–6568
16. Field JA, de Jong E, Feijoo-Costa G et al (1993) Screening for ligninolytic fungi applicable to the biodegradation of xenobiotics. *Trends Biotechnol* 11:44–49

17. Klibanov AM, Tu T-M, Scott KL (1983) Peroxidase catalyzed removal from coal-conversion waste waters. *Science* 221:259–261
18. Patel M, Day BJ (1999) Metalloporphyrin class of therapeutic catalytic antioxidants. *Trends Pharm Sci* 20:359–364
19. Gaspar S, Popescu IC, Gazaryan IG et al (2000) Biosensors based on novel plant peroxidases: a comparative study. *Electrochim Acta* 46:255–264
20. Liu W, Kumar J, Tripathy S et al (1999) Enzymatically synthesized conducting polyaniline. *J Am Chem Soc* 121:71–78
21. Park JB, Clark DS (2006) Deactivation mechanisms of chloroperoxidase during biotransformations. *Biotechnol Bioeng* 93:1190–1195
22. Valderrama B, Ayala M, Vazquez-Duhalt R (2002) Suicide inactivation of peroxidases and the challenge of engineering more robust enzymes. *Chem Biol* 9:555–565
23. Valderrama B, Vazquez-Duhalt R (2005) Electron-balance during the oxidative self-inactivation of cytochrome c. *J Mol Cat B Enz* 35:41–44
24. Valderrama B, Garcia-Arellano H, Giansanti S et al (2006) Oxidative stabilization of iso-1-cytochrome c by redox-inspired protein engineering. *FASEB J* 20:1233–1235
25. Kitajima S, Shimaoka T, Kurioka M et al (2007) Irreversible crosslinking of heme to the distal tryptophan of stromal ascorbate peroxidase in response to rapid inactivation by H₂O₂. *FEBS J* 274:3013–3020
26. Ryan BJ, Ó'Fágáin C (2007) Effects of single mutations on the stability of horseradish peroxidase to hydrogen peroxide. *Biochimie* 89:1029–1032
27. Mahmoudi A, Nazari K, Khosraneh M et al (2008) Can amino acids protect horseradish peroxidase against its suicide-peroxide substrate? *Enzyme Microb Technol* 43:329–335
28. Gil-Rodríguez P, Ferreira-Batista CV, Vazquez-Duhalt R et al (2008) A novel heme peroxidase from *Raphanus sativus* intrinsically resistant to hydrogen peroxide. *Eng Life Sci* 8:286–296
29. Saab-Rincon G, Valderrama B (2009) Protein engineering of redox-active enzymes. *Antioxid Redox Signal* 11:167–192
30. Dunford HB (1999) Heme peroxidases. Wiley, New York, NY
31. Keilin D, Hartree EF (1951) Purification of horseradish peroxidase and comparison of its properties with those of catalase and methaemoglobin. *Biochem J* 49:88–106
32. Patterson WR, Poulos TL, Goodin DB (1995) Identification of a porphyrin π -cation radical in ascorbate peroxidase Compound I. *Biochemistry* 34:4342–4345
33. Roberts JE, Hoffman BM, Rutter R et al (1981) Electron-nuclear double resonance of horseradish peroxidase compound I. Detection of the porphyrin π -cation radical. *J Biol Chem* 256:2118–2121
34. Hiner ANP, Hernández-Ruíz J, Williams GA et al (2001) Catalase-like oxygen production by horseradish peroxidase must predominantly be an enzyme-catalyzed reaction. *Arch Biochem Biophys* 392:295–302
35. Iwamoto H, Kobayashi T, Hasegawa E et al (1987) Reaction of human myeloperoxidase with hydrogen peroxide and its true catalase activity. *J Biochem* 101:1407–1412
36. Hashimoto S, Nakajima R, Yamazaki I et al (1986) Oxygen-exchange between the Fe(IV)=O-Heme and bulk water for the A2 isozyme of horseradish-peroxidase. *FEBS Lett* 208:305–307
37. Hashimoto S, Tatsuno Y, Kitagawa T (1986) Resonance Raman evidence for oxygen exchange between the Fe^{IV}=O Heme and bulk water during enzymic catalysis of horseradish peroxidase and its relation with the heme-linked ionization. *Proc Natl Acad Sci USA* 83:2417–2421
38. Cai DY, Tien M (1989) On the reactions of lignin peroxidase compound III (isozyme H8). *Biochem Biophys Res Commun* 162:464–469
39. Cai D, Tien M (1992) Kinetic studies on the formation and decomposition of compounds II and III. Reactions of lignin peroxidase with H₂O₂. *J Biol Chem* 267:11149–11155

40. Arnao MB, Acosta M, del Rio JA et al (1990) A kinetic study on the suicide inactivation of peroxidase by hydrogen peroxide. *Biochim Biophys Acta* 1041:43–47
41. Keilin D, Mann T (1937) On the haematin compound of peroxidase. *Proc R Soc Lond Ser B Biol Sci* 122:119–133
42. Blumberg WE, Peisach J, Wittenberg BA et al (1968) The electronic structure of protoheme proteins. I. An electron paramagnetic resonance and optical study of horseradish peroxidase and its derivatives. *J Biol Chem* 243:1854–1862
43. Wittenberg JB, Wittenberg BA, Peisach J et al (1970) On the state of the iron and the nature of the ligand in oxyhemoglobin. *Proc Natl Acad Sci USA* 67:1846–1853
44. Barr DP, Mason RP (1995) Mechanism of radical production from the reaction of cytochrome *c* with organic hydroperoxides – an ESR spin-trapping investigation. *J Biol Chem* 270:12709–12716
45. Peisach J, Blumberg WE, Wittenberg BA et al (1968) The electronic structure of protoheme proteins. III. Configuration of the heme and its ligands. *J Biol Chem* 243:1871–1880
46. Wariishi H, Gold MH (1990) Lignin peroxidase compound III. Mechanism of formation and decomposition. *J Biol Chem* 265:2070–2077
47. Lardinois OM (1995) Reactions of bovine liver catalase with superoxide radicals and hydrogen peroxide. *Free Radic Res* 22:251–274
48. Lardinois OM, Rouxhet PG (1994) Characterization of hydrogen peroxide and superoxide degrading pathways of *Aspergillus niger* catalase: a steady-state analysis. *Free Radic Res* 20:29–50
49. Wariishi H, Akileswaran L, Gold MH (1988) Manganese peroxidase from the basidiomycete *Phanerochaete chrysosporium*: spectral characterization of the oxidized states and the catalytic cycle. *Biochemistry* 27:5365–5370
50. Hiner AN, Rodríguez-López JN, Arnao MB et al (2000) Kinetic study of the inactivation of ascorbate peroxidase by hydrogen peroxide. *Biochem J* 348:321–328
51. Hiner AN, Hernández-Ruiz J, García-Cánovas F et al (1995) A comparative study of the inactivation of wild-type, recombinant and two mutant horseradish peroxidase isoenzymes C by hydrogen peroxide and m-chloroperoxybenzoic acid. *Eur J Biochem* 234:506–512
52. Nakajima R, Yamazaki I (1987) The mechanism of oxypoxidase formation from ferryl peroxidase and hydrogen peroxide. *J Biol Chem* 262:2576–2581
53. Adediran SA, Lambeir AM (1989) Kinetics of the reaction of compound II of horseradish peroxidase with hydrogen peroxide to form compound III. *Eur J Biochem* 186:571–576
54. Shimizu N, Kobayashi K, Hayashi K (1989) Kinetics of the reaction of superoxide anion with ferric horseradish peroxidase. *Biochim Biophys Acta* 995:133–137
55. Edwards J, Ormsby D (2009) Dissociation constants of inorganic acids in aqueous solutions. Institute of Fundamental Sciences Chemistry Resources. <http://ifs.massey.ac.nz/resources/chemistry/dissociation/inorgacids.htm>
56. Newmyer SL, Ortíz de Montellano PR (1995) Horseradish peroxidase His-42 ->Ala, His-42->Val, and Phe-41->Ala mutants. *J Biol Chem* 270:19430–19438
57. Shikama K (1998) The molecular mechanism of autoxidation for myoglobin and hemoglobin: a venerable puzzle. *Chem Rev* 98:1357–1374
58. Poulos TL, Freer ST, Alden RA et al (1980) The crystal structure of cytochrome *c* peroxidase. *J Biol Chem* 255:575–580
59. Tesoriere L, Allegra M, D'Arpa D et al (2001) Reaction of melatonin with hemoglobin-derived oxoferryl radicals and inhibition of the hydroperoxide-induced hemoglobin denaturation in red blood cells. *J Pineal Res* 31:114–119
60. Jantschko W, Furtmuller PG, Zederbauer M et al (2004) Kinetics of oxygen binding to ferrous myeloperoxidase. *Arch Biochem Biophys* 426:91–97
61. Jantschko W, Furtmuller PG, Zederbauer M et al (2005) Reaction of ferrous lactoperoxidase with hydrogen peroxide and dioxygen: an anaerobic stopped-flow study. *Arch Biochem Biophys* 434:51–59

62. Rodríguez-López JN, Smith AT, Thorneley RNF (1997) Effect of distal cavity mutations on the binding and activation of oxygen by ferrous horseradish peroxidase. *J Biol Chem* 272:389–395
63. Sawada Y, Yamazaki I (1973) One-electron transfer reactions in biochemical systems. 8. Kinetic study of superoxide dismutase. *Biochim Biophys Acta* 327:257–265
64. Shimizu N, Kobayashi K, Hayashi K (1984) The reaction of superoxide radical with catalase. Mechanism of the inhibition of catalase by superoxide radical. *J Biol Chem* 259:4414–4418
65. Jensen KP, Ryde U (2004) How O₂ binds to heme – reasons for rapid binding and spin inversion. *J Biol Chem* 279:14561–14569
66. Van Wart HE, Zimmer J (1985) Resonance Raman evidence for the activation of dioxygen in horseradish oxyperoxidase. *J Biol Chem* 260:8372–8377
67. Scheidt WR, Reed CA (1981) Spin-state stereochemical relationships in iron porphyrins – implications for the hemoproteins. *Chem Rev* 81:543–555
68. Metodiewa D, Dunford HB (1992) Spectral studies of intermediate species formed in one-electron reactions of bovine liver catalase at room and low temperatures. A comparison with peroxidase reactions. *Int J Rad Biol* 62:543–553
69. Cuperus RA, Muijers AO, Wever R (1986) The superoxide dismutase activity of myeloperoxidase; formation of compound III. *Biochim Biophys Acta* 871:78–84
70. De Grey AD (2002) HO₂*: the forgotten radical. *DNA Cell Biol* 21:251–257
71. Dordick JS, Klivanov AM, Marletta MA (1986) Horseradish peroxidase catalyzed hydroxylations: mechanistic studies. *Biochemistry* 25:2946–2951
72. Grey CE, Hedstrom M, Adlercreutz P (2007) A mass spectrometric investigation of native and oxidatively inactivated chloroperoxidase. *ChemBioChem* 8:1056–1062
73. Barr DP, Aust SD (1994) Conversion of lignin peroxidase compound III to active enzyme by cation radicals. *Arch Biochem Biophys* 312:511–515
74. Chung N, Aust SD (1995) Inactivation of lignin peroxidase by hydrogen peroxide during the oxidation of phenols. *Arch Biochem Biophys* 316:851–855
75. Barr DP, Gunther MR, Deterding LJ et al (1996) ESR spin-trapping of a protein-derived tyrosyl radical from the reaction of cytochrome *c* with hydrogen peroxide. *J Biol Chem* 271:15498–15503
76. Gunther MR, Tschirret-Guth RA, Witkowska HE et al (1998) Site-specific spin trapping of tyrosine radicals in the oxidation of metmyoglobin by hydrogen peroxide. *Biochem J* 330:1293–1299
77. DeGray JA, Lassmann G, Curtis JF et al (1992) Spectral analysis of the protein-derived tyrosyl radicals from prostaglandin H synthase. *J Biol Chem* 267:23583–23588
78. Shi W, Hoganson CW, Espe M et al (2000) Electron paramagnetic resonance and electron nuclear double resonance spectroscopic identification and characterization of the tyrosyl radicals in prostaglandin H synthase I. *Biochemistry* 39:4112–4121
79. Hiner ANP, Martínez JI, Arnao MB et al (2001) Detection of a tryptophan radical in the reaction of ascorbate peroxidase with hydrogen peroxide. *Eur J Biochem* 268:3091–3098
80. Ruíz-Dueñas FJ, Pogni R, Morales M et al (2009) Protein radicals in fungal versatile peroxidase. *J Biol Chem* 284:7986–7994
81. Blodig W, Doyle WA, Smith AT et al (1998) Autocatalytic formation of a hydroxy group at C beta of Trp171 in lignin peroxidase. *Biochemistry* 37:8832–8838
82. Doyle WA, Blodig W, Veitch NC et al (1998) Two substrate interaction sites in lignin peroxidase revealed by site-directed mutagenesis. *Biochemistry* 37:15097–15105
83. Hawkins CL, Davies MJ (2001) Generation and propagation of radical reactions on proteins. *Biochim Biophys Acta* 1504:196–219
84. Prutz WA (1990) Free radical transfer involving sulphur peptide functions. In: Chatgililoglu C, Asmus KD (eds) *Sulfur-centered reactive intermediates in chemistry and biology*. Plenum, New York

85. Wilks A, Ortiz de Montellano PR (1992) Intramolecular translocation of the protein radical formed in the reaction of recombinant sperm whale myoglobin with H₂O₂. *J Biol Chem* 267:8827–8833
86. Giulivi C, Cadenas E (1998) Heme protein radicals: formation, fate and biological consequences. *Free Radic Biol Med* 24:269–279
87. Davies MJ, Puppo A (1992) Direct detection of a globin-derived radical in leghaemoglobin treated with peroxides. *Biochem J* 281:197–201
88. Tew D, Ortiz de Montellano PR (1988) The myoglobin protein radical. Coupling of Tyr-103 to Tyr-151 in the H₂O₂-mediated cross-linking of sperm whale myoglobin. *J Biol Chem* 263:17880–17886
89. Zgoda VG, Karuzina II, Archakov AI (1999) Heme and apoprotein modification of cytochrome P450 2B4 during its oxidative inactivation in monooxygenase reconstituted system. *Free Radic Biol Med* 26:620–632
90. Lardinois OM, Medzihradsky KF, Ortiz de Montellano PR (1999) Spin trapping and protein cross-linking of the lactoperoxidase protein radical. *J Biol Chem* 274:35441–35448
91. Lardinois OM, Ortiz de Montellano PR (2000) EPR spin-trapping of a myeloperoxidase protein radical. *Biochem Biophys Res Commun* 270:199–202
92. Ruf RAS, Lutz EA, Zigoneanu IG et al (2008) α -Synuclein conformation affects its tyrosine-dependent oxidative aggregation. *Biochemistry* 47:13604–13609
93. Nagababu E, Rifkind JM (2000) Heme degradation during autoxidation of oxyhemoglobin. *Biochem Biophys Res Commun* 273:839–845
94. Catalano CE, Choe YS, Ortiz de Montellano PR (1989) Reactions of the protein radical in peroxide-treated myoglobin. Formation of a heme-protein cross-link. *J Biol Chem* 264:10534–10541
95. Nakajima R, Yamazaki I (1980) The conversion of horseradish peroxidase C to a verdohemoprotein by a hydroperoxide derived enzymatically from indole-3-acetic acid and by m-nitroperoxybenzoic acid. *J Biol Chem* 255:2067–2071
96. Sector A, Zhou W, Ma WC et al (2000) Investigation of the mechanism of action of microperoxidase-11, (MP-11), a potential anti-cataract agent, with hydrogen peroxide and ascorbate. *Exp Eye Res* 71:183–194
97. He K, Bornheim LM, Falick AM et al (1998) Identification of the heme-modified peptides from cumene hydroperoxide-inactivated cytochrome P450 3A4. *Biochemistry* 37:17448–17457
98. Lambeir AM, Dunford HB (1985) Oxygen binding to dithionite-reduced chloroperoxidase. *Eur J Biochem* 147:93–96
99. Chang HC, Holland RD, Bumpus JA et al (1999) Inactivation of *Coprinus cinereus* peroxidase by 4-chloroaniline during turnover: comparison with horseradish peroxidase and bovine lactoperoxidase. *Chem Biol Interact* 123:197–217
100. Mahy JP, Gaspard S, Delaforge M et al (1994) Reactions of prostaglandin-H synthase with monosubstituted hydrazines and diazenes – formation of iron(II)-diazene and iron(III)-sigma-alkyl or iron(III)-sigma-aryl complexes. *Eur J Biochem* 226:445–457
101. Sigman JA, Wang X, Lu Y (2001) Coupled oxidation of heme by myoglobin is mediated by exogenous peroxide. *J Am Chem Soc* 123:6945–6946
102. O'Carra P (1975) Heme-cleavage: biological systems and chemical analogs. In: Smith K (ed) *Porphyrin and metalloporphyrins*. Elsevier, The Netherlands
103. Brown SB (1976) A model for the formation of bile-pigments isomers in vivo and in vitro. *Biochem J* 159:23–27
104. Smith AM, Morrison WL, Milham PJ (1982) Oxidation of indole-3-acetic acid by peroxidase: involvement of reduced peroxidase and compound III with superoxide as a product. *Biochemistry* 21:4414–4419
105. Winterbourn CC, Garcia RC, Segal AW (1985) Production of the superoxide adduct of myeloperoxidase (compound III) by stimulated human neutrophils and its reactivity with hydrogen peroxide and chloride. *Biochem J* 228:583–592

106. Ximenes VF, Catalani LH, Campa A (2001) Oxidation of melatonin and tryptophan by and HRP cycle involving Compound III. *Biochem Biophys Res Commun* 287:130–134
107. Adediran SA (1996) Kinetics of the formation of p-670 and of the decay of Compound III of horseradish peroxidase. *Arch Biochem Biophys* 327:279–284
108. Ximenes VF, Silva SO, Rodrigues MR et al (2005) Superoxide-dependent oxidation of melatonin by myeloperoxidase. *J Biol Chem* 280:38160–38169
109. Ximenes VF, Pessoa AS, Padovan CZ et al (2009) Oxidation of melatonin by AAPH-derived peroxy radicals: Evidence of a pro-oxidant effect of melatonin. *Biochim Biophys Acta* 1790:787–792
110. Berglund GI, Carlsson GH, Smith AT et al (2002) The catalytic pathway of horseradish peroxidase at high resolution. *Nature* 417:463–468
111. Poulos TL, Schuller DJ, Ban N et al (1996) The crystal structure of peanut peroxidase. *Structure* 4:311–321
112. Nielsen KL, Indiani C, Henriksen A et al (2001) Differential activity and structure of highly similar peroxidases. Spectroscopic, crystallographic, and enzymatic analyses of lignifying *Arabidopsis thaliana* peroxidase A2 and horseradish peroxidase A2. *Biochemistry* 40:1103–11021
113. Choinowski T, Blodig W, Winterhalter KH et al (1999) The crystal structure of lignin peroxidase at 1.70 angstrom resolution reveals a hydroxy group on the C-beta of tryptophan 171: A novel radical site formed during the redox cycle. *J Mol Biol* 286:809–827
114. Sundaramoorthy M, Ternier J, Poulos TL (1995) The crystal structure of chloroperoxidase: a heme peroxidase-cytochrome P450 functional hybrid. *Structure* 3:1367–1378
115. Pecyna MJ, Ullrich R, Bittner B et al (2009) Molecular characterization of aromatic peroxygenase from *Agrocybe aegerita*. *Appl Microbiol Biotechnol* 84:885–897
116. Sono M, Roach MP, Coulter ED et al (1996) Heme-containing oxygenases. *Chem Rev* 96:2841–2888
117. Poulos TL (1996) The role of the proximal ligand in heme enzymes. *J Biol Inorg Chem* 1:356–359
118. Hsu MC, Woody RW (1971) The origin of the heme Cotton effects in myoglobin and hemoglobin. *J Am Chem Soc* 93:3515–3525
119. Sugita Y, Nagai M, Yoneyama Y (1971) Circular dichroism of hemoglobin in relation to the structure surrounding the heme. *J Biol Chem* 246:383–388
120. Nicola NA, Minasian E, Appleby CA et al (1975) Circular dichroism studies of myoglobin and leghemoglobin. *Biochemistry* 14:5141–5149
121. Strickland EH, Kay E, Shannon LM et al (1968) Peroxidase isoenzymes from horseradish roots. *J Biol Chem* 243:3560–3565
122. Myer YP, Pande A (1978) Circular dichroism studies of hemoproteins and heme models. The porphyrins 3:271–322
123. Das TK, Mazumdar S, Mitra S (1995) Heme CD as a probe for monitoring local structural changes in hemoproteins: alkaline transition in hemoproteins. *J Chem Sci* 107:497–503
124. Nozawa T, Kobayashi N, Hatano M et al (1980) Magnetic circular-dichroism on oxygen complexes of hemoproteins – correlation between magnetic circular-dichroism magnitude and electronic-structures of oxygen complexes. *Biochim Biophys Acta* 626:282–290
125. Vickery L, Nozawa T, Sauer K (1976) Magnetic circular dichroism studies of myoglobin complexes. Correlations with heme spin state and axial ligation. *J Am Chem Soc* 98:343–350
126. Andersson KK, Barra A-L (2002) The use of high field/ frequency EPR in studies of radical and metal sites in proteins and small inorganic models. *Spectrochim Acta A* 58: 1101–1112
127. Hagen WR (2006) EPR spectroscopy as a probe of metal centres in biological systems. *Dalton Trans* 2006:4415–4434
128. Ubbink M, Worrall JAR, Canters GW et al (2002) Paramagnetic resonance of biological metal centers. *Annu Rev Biophys Biomol Struct* 31:393–422

129. Ivancich A, Jakopitsch C, Auer M et al (2003) Protein-based radicals in the catalase-peroxidase of *Synechocystis* PCC6803: a multifrequency EPR investigation of wild-type and variants on the environment of the heme active site. *J Am Chem Soc* 125:14093–14102
130. Zucchi MR, Nascimento OR, Faljoni-Alario A et al (2003) Modulation of cytochrome c spin states by lipid acyl chains: a continuous-wave electron paramagnetic resonance (CW-EPR) study of haem iron. *Biochem J* 370:671–678
131. Wang Y, Van Wart HE (1993) Raman and resonance Raman spectroscopy. *Methods Enzymol* 226:319–373
132. Spiro TG (1975) Biological applications of resonance Raman-spectroscopy – Heme proteins. *Proc R Soc Lond Ser A Math Phys Eng* 345:89–105
133. Spiro TG (1988) Biological applications of Raman spectroscopy, vol 3. Resonance Raman spectra of heme proteins and other metalloproteins. Wiley, New York, NY
134. Smulevich G, Feis A, Howes BD (2005) Fifteen years of Raman spectroscopy of engineered heme containing peroxidases: what have we learned? *Acc Chem Res* 38:433–440
135. Das TK, Couture M, Ouellet Y et al (2001) Simultaneous observation of the O-O and Fe-O₂ stretching modes in oxyhemoglobins. *Proc Natl Acad Sci USA* 98:479–484
136. Sitter AJ, Reczek CM, Termer J (1986) Comparison of the heme structures of horseradish peroxidase compounds X and II by resonance Raman spectroscopy. *J Biol Chem* 261:8638–8642
137. Sitter AJ, Reczek CM, Termer J (1985) Heme-linked ionization of horseradish peroxidase compound II monitored by the resonance Raman Fe (IV) = O stretching vibration. *J Biol Chem* 260:7515–7522
138. Franzen S, Bohn B, Poyart C et al (1995) Evidence for sub-picosecond heme doming in hemoglobin and myoglobin: a time-resolved resonance Raman comparison of carbon monoxy and deoxy species. *Biochemistry* 34:1224–1237
139. Zimmer J, Van Wart HE (1982) Resonance Raman spectrum of horseradish peroxidase compound III: comparison with oxyhemoglobin. *Biochem Biophys Res Commun* 108:977–981
140. Jensen KP, Roos BO, Ryde U (2005) O₂-binding to heme: electronic structure and spectrum of oxyheme, studied by multiconfigurational methods. *J Inorg Biochem* 99:45–54
141. Maseras F (2000) The IMOMM method opens the way for the accurate calculation of “real” transition metal complexes. *Chem Commun* 2000:1821–1827
142. Torrens F (2003) Nature of Fe-III-O-2, Fe-II-CO and Fe-III-CN complexes of hemoprotein models. *Polyhedron* 22:1091–1098
143. Rovira C, Kunc K, Hutter J et al (1997) Equilibrium geometries and electronic structure of iron-porphyrin complexes: a density functional study. *J Phys Chem A* 101:8914–8925
144. Tsai TE, Groves JL, Wu CS (1981) Electronic structure of iron-dioxygen bond in oxy Hb A and its isolated oxy and oxy chains. *J Chem Phys* 74:4306–4314
145. Maeda Y, Morita Y (1967) Mossbauer effect in peroxidase-hydrogen peroxide compounds. *Biochem Biophys Res Commun* 29:680–685
146. Schulz CE, Rutter R, Sage JT et al (1984) Mossbauer and electron paramagnetic resonance studies of horseradish peroxidase and its catalytic intermediates. *Biochemistry* 23:4743–4754
147. Henriksen A, Welinder KG, Gajhede M (1998) Structure of barley grain peroxidase refined at 1.9-Å resolution. A plant peroxidase reversibly inactivated at neutral pH. *J Biol Chem* 273:2241–2248
148. Henriksen A, Mirza O, Indiana C et al (2001) Structure of soybean seed coat peroxidase: a plant peroxidase with unusual stability and haem-apoprotein interactions. *Protein Sci* 10:108–115
149. Miller MA, Shaw A, Kraut J (1994) 2.2 Å structure of oxy-peroxidase as a model for the transient enzyme: peroxide complex. *Nat Struct Mol Biol* 1:524–531

Chapter 12

Heterologous Expression of Peroxidases

Sandra de Weert and B. Christien Lokman

Contents

12.1	Production of Peroxidases in <i>E. coli</i>	316
12.2	Production of Peroxidases in <i>Saccharomyces cerevisiae</i> and <i>Pichia</i> spp.	317
12.3	Production of Peroxidases in Baculovirus	318
12.4	Production of Peroxidases in White-Rot Fungi	319
12.5	Production of Peroxidases in Filamentous Fungi	320
12.6	Production of Heme-Peroxidases in <i>Aspergillus</i>	321
	12.6.1 Expression Systems and Detection	321
	12.6.2 Large-Scale Production with Bioreactors	323
12.7	Bottlenecks for Heterologous Protein Expression in Filamentous Fungi	324
	12.7.1 The Secretory Pathway of <i>Aspergillus</i>	325
	12.7.2 Limitations to Protein Production	326
12.8	Conclusions	329
	References	329

Abstract The industrial importance of peroxidases has led to much research in the past two decades on the development of a cost effective and efficient production process for peroxidases. Unfortunately, even today, no clear answers can be given to questions such as (1) should the peroxidase be expressed in bacteria, yeast, or fungi? (2) which is the optimal production strain (e.g., protease deficient, heme overproducing)? (3) which expression vector should be chosen? and (4) what purification method should be used? Strategies that have proven successful for one peroxidase can fail for another one; for each individual peroxidase, a new strategy has to be developed. This chapter gives an overview of the heterologous production of heme containing peroxidases in various systems. It focuses on the heterologous production of fungal peroxidases as they have been subject of considerable research for their industrial and environmental applications. An earlier study has also been performed by Conesa et al. [1] and is extended with recent proceedings.

12.1 Production of Peroxidases in *E. coli*

The benefits of *E. coli* as an expression organism are manifold. The ease of manipulation and cultivation on a large-scale makes it an attractive and a cost efficient host organism for overproduction of peroxidases. Several commercial expression systems are available, and tricks and improvements for heterologous protein production using *E. coli* are well documented (for a review see: Structural Genomics Consortium [2]). However, in previous studies, *E. coli* has not always proven to be the optimal production system for peroxidases. Expression of peroxidases in *E. coli* results in many cases in the production of catalytically inactive enzymes in inclusion bodies. Protein reconstitution to yield active enzymes is possible only after tedious and commercially unattractive treatment with heme, Ca^{2+} , urea, and/or high pressure [3–8]. On the other hand, it can be a useful system for site-directed mutagenesis, gene evolution studies, and the production of low amounts of enzyme for other purposes than direct industrial applications, such as crystallization and preliminary protein characterization. Despite the disadvantages of using *E. coli* as a host organism, two different peroxidases were produced recently in a soluble form. The novel ligninolytic peroxidase gene (ACLnP) from the poroid brown-rot fungus *Antrodia cinnamomea* has been successfully expressed in *E. coli* strain M15 under the control of the T5 promoter. The native, nonglycosylated recombinant protein was capable of oxidizing the redox mediator veratryl alcohol, and also decolorized bromophenol blue and 2,6-dimethoxyphenol dyes, suggesting a functional extracellular peroxidase activity [9].

A second successful example is the production of the fungal versatile peroxidase from *Bjerkandera adusta* in *E. coli* strain BL21. In the presence of hemin, 12 mg/L of recombinant, soluble protein could be produced [10]. In Sect. 12.7, heme will be described as a limiting factor for overproduction of heme peroxidases. Also, nonfungal peroxidases have been expressed in *E. coli*, e.g., the chloroperoxidase (CPO) encoding gene from *Pseudomonas pyrrocinia* [11]. This heme-lacking enzyme was overproduced 800-fold in *E. coli* in comparison with the production level in *P. pyrrocinia*. In Table 12.1, a brief overview of the heterologous production of heme peroxidases with *E. coli* as host strain are listed.

Table 12.1 Production of peroxidases in *E. coli*

Protein	Organism	Result	Ref.
CPO	<i>Caldariomyces fumago</i>	Insoluble in inclusion bodies	[8]
CPO	<i>Pseudomonas pyrrocinia</i>	27 mg CPO/5 g cells (800 × overexpr.)	[11]
LiP	<i>Phanerochaete chrysosporium</i>	Insoluble in inclusion bodies	[5]
LiP	<i>Trametes cervina</i>	Insoluble in inclusion bodies	[4]
ACLnP	<i>Antrodia cinnamomea</i>	60% of total protein	[9]
MnP	<i>Phanerochaete chrysosporium</i>	Insoluble in inclusion bodies	[7]
Msp2	<i>Marasmius scorodonius</i>	Insoluble in inclusion bodies	[3]
VPO	<i>Bjerkandera adusta</i>	Soluble form, 12 mg/L	[10]

CPO Chloroperoxidase; LiP Lignin peroxidase; ACLnP *Antrodia cinnamomea* peroxidase; LiP Lignin peroxidase; MnP Manganese peroxidase; Msp2 Msp2 peroxidase; VPO Versatile peroxidase

12.2 Production of Peroxidases in *Saccharomyces cerevisiae* and *Pichia* spp.

S. cerevisiae is the most exploited eukaryotic microorganism in biotechnology; applications include fermentative processes, heterologous protein production, and high-throughput studies. The availability of efficient and robust expression systems is essential for all these applications. Maya et al. [12] have recently revised new expression systems and the improvements of classical ones. It is well established today that heterologous production of proteins is connected with different stress reactions. The production of a heterologous protein at a high level may either directly limit other cellular processes by competing for their substrates, or indirectly interfere with metabolism, if their synthesis is inhibited. As a result, stress reactions of the cell are induced, for example, the unfolded protein response (UPR) in *S. cerevisiae* (as well as some other yeasts). This response is reviewed by Mattanovich et al. [13]. Stress responses, like UPR, are described in more detail in Sect. 12.7 with respect to heterologous production in *Aspergillus* sp. Although *S. cerevisiae* is frequently used in heterologous protein production, limited success has been obtained with the production of peroxidases. So far only *Arthromyces ramosus* peroxidase, ARP (Gouka et al. personal communication), *Coprinus cinereus* peroxidase, CiP/ARP [14], and the vanadium-containing chloroperoxidase from the fungus *Curvularia inaequalis* have been produced with reasonable success in *S. cerevisiae* [15]. Attempts to express the genes encoding CPO [16] and *P. chrysosporium* peroxidases [17] did not result in any detectable extracellular protein. Similarly, production of Msp2 was undetectable when using *S. cerevisiae* or *Pichia pastoris* as host organisms [3].

On the other hand, *Pichia* expression systems have been successful in a few cases, such as the production of manganese peroxidase and lignin peroxidase from *Phanerochaete chrysosporium* using *P. pastoris* [18] and *Pichia methanolica* [19] as host organisms, respectively. For the production of manganese peroxidase (rMnP) in *P. pastoris*, the optimum pH and temperature for a standardized fed-batch fermentation process were determined. Experiments demonstrated that rMnP production is highest at pH 6, reaching 2,000 U/L, whereas cultivation of *P. chrysosporium* mycelia in stationary flasks for production of heme peroxidases is commonly conducted at low pH (pH 4.2). Further studies revealed that degradation at low pH was caused by intracellular proteases that are released from dead and lysed yeast cells during the fermentation. In the case of rMnP production in *P. methanolica*, the choice of signal peptide proved to be of importance. The cDNA encoding for lignin peroxidase was expressed in *P. methanolica* under the control of the inducible alcohol oxidase (AUG1) promoter, which was followed by either the lignin peroxidase leader peptide of *P. chrysosporium* or the *S. cerevisiae* alpha-factor signal peptide. The use of alpha-factor signal peptide resulted in a 2-fold increase in extracellular activity: 1,933 U/L versus 932 U/L with the lignin peroxidase signal peptide. The *lipH2* gene, encoding lignin peroxidase, was also expressed successfully under control of the AOX1 promoter and the É-factor secretion signal from the PICZalpha expression vector in *P. pastoris*. Lignin peroxidase activity reached a

Table 12.2 Production of peroxidases in the yeast *S. cerevisiae* and *Pichia*

Protein	Organism	Host	Result	Ref.
CPO	<i>Caldariomyces fumago</i>	<i>S. cerevisiae</i>	No extracellular protein	[16]
CPO*	<i>Curvularia inaequalis</i>	<i>S. cerevisiae</i>	100 mg/L	[15]
LiP	<i>Phanerochaete chrysosporium</i>	<i>S. cerevisiae</i>	No extracellular protein	[17]
LiP	<i>Phanerochaete chrysosporium</i>	<i>P. methanolica</i>	932 U/L and 1,933 U/L	[19]
LiPH2	<i>Phanerochaete chrysosporium</i>	<i>P. pastoris</i>	15 U/L	[20]
MnP	<i>Phanerochaete chrysosporium</i>	<i>P. pastoris</i>	2,000 U/L	[18]
MnP	<i>Phanerochaete chrysosporium</i>	<i>S. cerevisiae</i>	No extracellular protein	[17]
Msp2	<i>Marasmius scorodoni</i>	<i>S. cerevisiae</i>	Undetectable	[3]
Msp2	<i>Marasmius scorodoni</i>	<i>P. pastoris</i>	Undetectable	[3]
CiP/ARP	<i>Coprinus cinereus</i>	<i>S. cerevisiae</i>	0.02 U/mL	[14]
ARP	<i>Arthomyces ramosus</i>	<i>S. cerevisiae</i>	0.5 mg/L	Gouka et al. (personal communication)
ARP	<i>Arthomyces ramosus</i>	<i>P. pastoris</i>	21 mg/L	[22]

CPO Chloroperoxidase; *CPO** nonheme chloroperoxidase; *LiP* Lignin peroxidase; *LiPH2* Lignin peroxidase H2 isozyme; *MnP* Manganese peroxidase; *CiP* *Coprinus cinereus* peroxidase; *ARP* *Arthomyces ramosus* peroxidase

maximum of 15 U/L after 12 h induction, which was an order of magnitude below the level of activity obtained with *P. methanolica* [20]. Also, improvement of ARP production was obtained when *P. pastoris* was used as a host strain instead of *S. cerevisiae*. In the *arp* expression vector of *P. pastoris*, the expression was controlled by the promoter of *P. pastoris* alcohol oxidase, *Paox 1* [21]. Developments with respect to the *Pichia* expression system have had an impact on not only the expression levels that can be achieved but also the activity of various heterologous proteins [22]. In Table 12.2, a brief overview of the heterologous production of heme peroxidases in *S. cerevisiae* and *Pichia* sp. as host production strains is listed.

12.3 Production of Peroxidases in Baculovirus

The baculovirus expression vector system (BEVS) is now widely used for recombinant protein production [23]. Unfortunately, this system suffers from low yields and high production costs, and therefore is inappropriate for industrial scaling-up. Several peroxidases have been successfully produced on a small scale (Table 12.3) using the baculovirus expression system, such as MnP isozyme H4 and LiP isozymes H2 and H8 [17, 24, 25].

Table 12.3 Production of peroxidases in baculovirus

Protein	Organism	Result	Ref.
CPO	<i>C. fumago</i>	Inactive protein	[16]
LiP	<i>P. chrysosporium</i>	0.4 mg/mL after hemin addition	[24]
LiP	<i>P. chrysosporium</i>	Active protein	[25]
MnP	<i>P. chrysosporium</i>	35.7 U/L after hemin addition	[17]

CPO Chloroperoxidase; LiP Lignin peroxidase; MnP Manganese peroxidase

Table 12.4 Production of peroxidases in white-rot fungi

Protein	Organism	Host	Result	Ref.
LiP	<i>P. chrysosporium</i>	<i>P. chrysosporium</i>	2 mg/mL (<i>gpd</i> expr. syst.)	[30]
MnP	<i>P. chrysosporium</i>	<i>P. chrysosporium</i>	2 μ mol/mL/min (<i>gpd</i> expr. syst.)	[28]
MnP	<i>D. squalens</i>	<i>P. chrysosporium</i>	1–1.5 mg/L (<i>gpd</i> expr. system)	[29]
MnP2	<i>P. ostreatus</i>	<i>P. ostreatus</i>	7,300 U/L; 30-fold overproduction	[27]
MnP3	<i>P. ostreatus</i>	<i>P. ostreatus</i>	1,700 U/L	[26]

LiP Lignin peroxidase; MnP Manganese peroxidase

12.4 Production of Peroxidases in White-Rot Fungi

Various industrially relevant peroxidases come from white-rot fungi, and overproduction of these enzymes in a homologous host has been a promising option. The first genetic modification of the white-rot fungus *Pleurotus ostreatus* with an expression system harboring recombinant genes was reported by Irie et al. [26]. Recombinant manganese peroxidase isozyme MnP3 constructs, under the control of *P. ostreatus* *sdil* expression signals, were introduced into the wild-type *P. ostreatus* strain by cotransformation. This resulted in the isolation of a recombinant strain with a higher level of MnP activity than the wild-type fungus.

Overproduction of the recombinant versatile peroxidase MnP2 has also been successful by combining a homologous recombinant gene expression system and optimizing the culture conditions for *P. ostreatus* [27]. Furthermore, homologous production has been achieved for *P. chrysosporium* manganese and lignin peroxidases; and the thermostable manganese peroxidase from *Dichomitus squalens* has been expressed using recombination in *P. chrysosporium* [28–30]. These genes were expressed under control of the constitutively expressed glyceraldehyde phosphate dehydrogenase (*gpd*) promoter (Sect. 12.6.1). Although some of the approaches described above resulted in active recombinant proteins, the production levels were still not sufficient for large-scale industrial production. The main obstacle for using *P. chrysosporium* as enzyme producer is the productivity, which at the moment is difficult to solve due to the poor understanding of the regulatory mechanisms in response to different culture conditions. Singh and Chen [31] suggest in their critical review that further investigation might lead to the development of improved strains for large-scale production. Table 12.4 summarizes the results described above.

12.5 Production of Peroxidases in Filamentous Fungi

Another promising expression system, which has proven to be suitable for high level protein production, is that of filamentous fungi such as *Aspergillus* and *Trichoderma*. Filamentous fungi have been used as sources of metabolites and enzymes for centuries. They have an extraordinary capacity for protein production and they have been exploited for the production of various homologous and recombinant proteins [32, 33]. Initial studies on overproduction of peroxidases in filamentous fungi resulted in only limited success. Expression of both the *P. radiata* lignin peroxidase in *T. reesei* [34] and the *C. fumago* CPO in *A. nidulans* [16] failed to produce any extracellular protein, and only traces of extracellular peroxidase activity were detected upon expression of the *P. chrysosporium* lignin peroxidase (liP H8) in a *A. niger* F38 strain, which is able to degrade aromatic compounds present in olive oil waste waters [35].

In contrast, the *C. cinereus* peroxidase, the *P. chrysosporium* MnP, and the *Pleurotus eryngii* manganese peroxidase MnPL2 have been successfully produced as active proteins in *Aspergillus* spp. [36–38]. Since initial production yields obtained in these studies were low compared to those typical for other fungal proteins, an intensive study has been performed on the heterologous production of *P. chrysosporium* manganese peroxidase and lignin peroxidase [39], and *C. fumago* chloroperoxidase in *Aspergillus* [40]. This study revealed that initial yields of 10 mg/L recombinant MnP in shake-flasks could be improved up to 500 mg/L in controlled batch fermentations. The addition of hemin and over-expression of the chaperone calnexin [41] had a positive effect on MnP production. This effect will be discussed in more detail in Sect. 12.7.2. In the case of lignin peroxidase, the enzyme was secreted into the extracellular medium, although the protein was not active, presumably due to incorrect processing of the secreted enzyme. The *C. fumago* chloroperoxidase was also successfully expressed in *A. niger*. The recombinant enzyme was produced in the culture medium as an active protein and could be purified by a three-step purification procedure.

Besides addition of heme, the influence of culture temperature on heterologous production of peroxidases has also been reported. For example, lowering the culture temperature from 28 to 19°C enhanced the level of active versatile peroxidase of *P. eryngii* 5.8-fold and reduced the effective proteolytic activity of the *A. nidulans* host strain by 2-fold. In this way, a maximum peroxidase activity of 466 U/L was reached [42]. Efficient heterologous production of peroxidases is not always dependent on the availability of heme. The heterologous production of *Arthromyces ramosus* peroxidase (ARP) has been analyzed in *A. awamori* under the control of the inducible endoxylanase promoter. Secretion of active ARP was achieved at up to 800 mg/L in shake flask cultures without addition of hemin [43]. This represents a 1,600-fold increase in production compared to ARP production in *S. cerevisiae* and 38-fold increase compared to ARP production in *P. pastoris* (see Sect. 12.2). These observations support that several filamentous fungi are more effective secretors of proteins than yeast strains like *S. cerevisiae* and *P. pastoris*. Also for

Table 12.5 Production of peroxidases in filamentous fungi

Protein	Organism	Host	Result	Ref.
CPO	<i>Caldariomyces fumago</i>	<i>A. niger</i>	Active protein	[40]
CPO	<i>Caldariomyces fumago</i>	<i>A. nidulans</i>	No extracellular protein	[16]
LiP	<i>Phanerochaete chrysosporium</i>	<i>A. niger</i>	Traces of peroxidase activity	[35]
LiP	<i>Phlebius radiata</i>	<i>T. reesei</i>	No extracellular protein	[34]
LiP	<i>Phanerochaete chrysosporium</i>	<i>A. niger</i>	No activity, incorrect processing	[39]
LiP	<i>Phanerochaete chrysosporium</i>	<i>A. awamori</i>	No activity, incorrect processing	[46]
MnP	<i>Phanerochaete chrysosporium</i>	<i>A. oryzae</i>	5 mg/L, heme addition	[39]
MnP	<i>Phanerochaete chrysosporium</i>	<i>A. niger</i>	5–10 mg/L	[39]
MnPL2	<i>Pleurotus eryngii</i>	<i>A. nidulans</i>	Active protein, heme addition	[36]
CiP	<i>Corpinus cinereus</i>	<i>A. oryzae</i>	~1,000 U/mL, heme addition	[47]
ARP	<i>Arthromyces ramosus</i>	<i>A. awamori</i>	~800 mg/L active protein	[43]
VPO	<i>Pleurotus eryngii</i>	<i>A. nidulans</i>	466 U/L	[42]
DyP	<i>Geotrichum candidum</i>	<i>A. oryzae</i>	42-fold compared to native DyP	[44]

CPO Chloroperoxidase; LiP Lignin peroxidase; MnP Manganese peroxidase; MnPL2 *Pleurotus eryngii* manganese peroxidase; CiP *Coprinus cinereus* peroxidase; ARP *Arthromyces ramosus* peroxidase; VPO Versatile peroxidase; DyP dye-decolorizing peroxidase

the efficient production of the dye-decolorizing peroxidase DyP from *Geotrichum candidum* Dec 1 in *A. oryzae*, no exogenous heme was supplemented [44]. Production of DyP could be further improved by use of solid-state instead of submerged culture [45]. Different production facilities will be further discussed in Sect. 12.6. In Table 12.5, an overview of the heterologous production of peroxidases in filamentous fungi is listed. Despite all efforts of the past 10–15 years, there is still no clearly optimal production system or strategy in filamentous fungi. The bottlenecks encountered during overproduction of peroxidases and some optimization strategies will be discussed in more detail in Sect. 12.7.

12.6 Production of Heme-Peroxidases in *Aspergillus*

In Sect. 12.5, we presented an overview of the production of peroxidases in filamentous fungi. In this section, more detail will be given to the heterologous production of peroxidases using *Aspergillus* as a host organism. The use of different expression systems and large-scale production in bioreactors will be discussed.

12.6.1 Expression Systems and Detection

Genetic tools have enabled us to express genes encoding homologous and heterologous proteins. Many studies have revealed increased production when strong promoters, more gene copies, or reduced proteolytic activity were tested in relation to protein production. Glyceraldehyde 3-phosphate dehydrogenase plays a central

role in glycolysis and gluconeogenesis. The constitutive glyceraldehyde 3-phosphate dehydrogenase promoter (*gpd*) from *A. nidulans* has shown to be successful in protein production. The isolation and characterization of this *gpd* promoter of *A. nidulans* was performed in 1988 by Punt et al. [48]. Nowadays this promoter has been isolated from a variety of microorganisms and used in efficient expression systems [49].

A. awamori secretes large amounts of glucoamylase (GLA) upon growth in medium supplemented with hexose sugars and polymer sugars or starch [50]. Little or no glucoamylase is secreted when this strain is cultivated in the presence of glycerol and xylose. The inducible promoter of the glucoamylase gene, *PglaA*, has been successfully used for heterologous protein production in different organisms. By placing the green fluorescent protein (GFP) gene adjacent to *PglaA*, it was shown that although xylose acted as a repressor, xylose-limited cultures still showed expression of GFP [51]. The xylose concentration was too low to cause repression of the promoter; however, repression increased with increasing xylose concentrations [52]. Also fusions between a gene encoding a heterologous protein and a gene encoding a well secreted fungal protein have shown to be well expressed. The first example was described by Ward et al [53] fusing the genes encoding glucoamylase and bovine chymosin. The yield of the GLA-fused chymosin was significantly increased compared to the unfused chymosin. As a result, more studies on these GLA fusions were performed [54] to modify and optimize heterologous protein production. Nowadays tailoring existing enzymes for other or improved activities is an ongoing topic of research, and directed evolution has emerged as a new and powerful technology to develop and modify existing enzymes for industrial application [55].

Finally, to determine the concentration and activity of heterologous proteins, an efficient assay is needed. Methods can vary from detection of peroxidase activity in liquid or solid media and are based on the oxidation of a colorless substrate. Figure 12.1 shows the detection of ArP production by *A. awamori* in a plate assay. The fungus is grown on inducing media and after sufficient growth, an

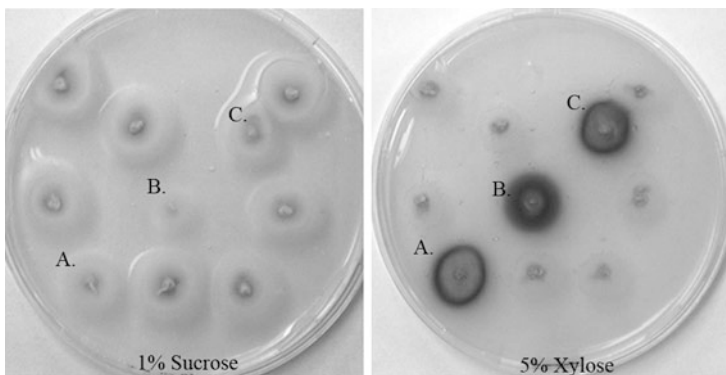


Fig. 12.1 *o*-Anisidine plate assay of peroxidase producing *A. awamori* strains

agar layer containing *o*-anisidine is placed over the colony. The colorless substrate is oxidized and subsequently forms an orange product, which can be detected by eye. Also the decolorization of dyes by oxidation is frequently used to demonstrate peroxidase activity [56, 57]; these methods can be used for screening initial transformants. Once confirmed, quantification is necessary. Measuring activity in culture supernatant or during enzyme purification usually involves use of a colorimetric method, based on measuring the change in absorbance of substrates like ABTS in time.

12.6.2 Large-Scale Production with Bioreactors

As shown in Table 12.5, the initial yields of heterologous peroxidases are often much lower than is normally achieved with homologous proteins and insufficient for industrial applications. Approaches to increase peroxidase production include adequate strain selection, heme supplementation, overexpression of chaperones, and controlled fermentations. By using controlled fermentation, the physiological conditions can be optimized in order to improve production yields.

One of the important parameters is pH. During growth in industrial settings, the pH may drop resulting in an increased activity of acidic extracellular proteases, which will degrade the heterologous produced peroxidase. Growth at a neutral pH is important and can be controlled well in bioreactors. For example, MnP production during buffered batch fermentations in shake flasks, using *A. niger* as host strain, was improved from 10 mg/L to 500 mg/L. The experiments demonstrated that MnP production was most efficient at neutral pH and suggested that higher production rates were related to protein degradation at low pH by acidic proteases [39]. These observations were also supported by studies of the effects of pH and temperature on recombinant manganese peroxidase (rMnP) production by *P. pastoris* [18]. The optimal pH and temperature for a standardized fed-batch fermentation process for rMnP production in *P. pastoris* were determined to be pH 6 and 30°C, respectively. *P. pastoris* constitutively expressed the manganese peroxidase (*mnpI*) cDNA from *P. chrysosporium*, and the rMnP had similar kinetic characteristics and pH activity and stability ranges as the wild-type MnP. Cultivation of *P. chrysosporium* mycelia in stationary flasks for production of heme peroxidases is commonly conducted at low pH (pH 4.2). However, shake flask and fed-batch fermentation experiments with *P. pastoris* demonstrated that rMnP production is highest at pH 6, with rMnP concentrations in the medium declining rapidly at pH less than 5.5. Investigations of the cause of low rMnP production at low pH were consistent with the hypothesis that intracellular proteases are released from dead and lysed yeast cells during the fermentation that are active against rMnP at pH less than 5.5 [18]. To circumvent the negative effect of acidification of the culture medium, one could consider the use of *A. awamori* as host strain. In contrast to *A. niger*, the pH does not decrease below 6.0 during cultivation, resulting in less activity of acidic proteases. A dependence of recombinant peroxidase production

on cultivation temperature was found during the production of versatile peroxidase in bioreactors using *A. nidulans* as host strain [42]. Lowering the culture temperature from 28 to 19°C enhanced the level of active *P. eryngii* peroxidase 5.8-fold and reduced the effective proteolytic activity twofold. A maximum peroxidase activity of 466 U/L was reached. However, the positive effect of a reduced cultivation temperature has been proven to be strain dependent. The same optimization scheme was applied to a recombinant *Aspergillus niger*. With this strain, the peroxidase activity was not improved, while the effective proteolytic activity was increased between 3- and 11-fold compared to that obtained with *A. nidulans* [42]. The results described above suggest that for each host strain and recombinant protein, a combination of the optimum pH and temperature in bioreactors should be established.

Besides submerged fermentations (SMF), solid-state fermentations (SSF) might be an attractive option. SSF appears to possess several biotechnological advantages such as higher fermentation productivity, higher end-concentration of products, higher product stability, lower catabolic repression, cultivation of microorganisms specialized for water-insoluble substrates or mixed cultivation of various fungi, and lower demand on sterility due to the low water activity used in SSF [58]. Hölker et al. [58] clearly demonstrate in their review that as long as the cultivation volume is kept in the liter scale, SSF represents the superior technology considering process productivity, product quality, and processing costs. However, SSF is difficult to scale up because of the build-up of gradients in temperature, pH, moisture, oxygen, substrate, and the need to generate a large amount of inoculum. Despite the disadvantages, there are examples of the heterologous production of peroxidases using SSF. The productivity of a peroxidase (DyP) originating from *G. candidum* was enhanced in *A. oryzae* when SSF was used instead of SMF. The yield of 5.3 g DyP per kg of wheat bran corresponded to the yield of a 56 kg submerged culture. The productivity per carbon gram of the medium in the solid-state culture was 4.1-fold higher than in the submerged culture. These elevated production levels were suggested not to be due to improvement of DyP expression efficiency but to the increase of total cell mass per gram of medium [45]. Information is lacking on the optimal large-scale production processes of heterologous peroxidases by filamentous fungi, possibly due to the bottlenecks on small scale; this area needs to be explored in future research projects.

12.7 Bottlenecks for Heterologous Protein Expression in Filamentous Fungi

Filamentous fungi are known for their extraordinary capacity of secreting large amounts of proteins, metabolites, and organic acids as described above. However, whereas large amounts of homologous proteins can be produced in industrial fermentation processes, production yields for heterologous proteins are often rather low. Despite the commercial use of fungi as secretion machinery, limitations have

been encountered as well. These limitations have stimulated research in the field of genetics of protein secretion. Bottlenecks in the secretion pathway of filamentous fungi will be discussed.

12.7.1 The Secretory Pathway of *Aspergillus*

In Fig. 12.2, a schematic view is presented of the secretory pathway in filamentous fungi. In short, proteins to be secreted start their journey by entering the endoplasmic reticulum (ER). At the ER, key processes like translation, signal recognition, translocation and modifications take place. It is here that proteins are folded and undergo glycosylation, disulfide bridge formation, subunit assembly, or phosphorylation. When they leave the ER, the proteins are packed into vesicles to be transported to the Golgi compartment. In this compartment, further modifications are performed (e.g., further glycosylation). Once the proteins leave the Golgi, they are packed into secretory vesicles and transported to the plasma membrane to be secreted. When proteins do not reach the extracellular space, they are targeted to intracellular compartments such as vacuoles. From there, they become either resident proteins or undergo proteolytic degradation.

Expression of mutated or heterologous proteins disrupts protein folding in the ER and generates ER stress. A signaling network called Unfolded Protein Response (UPR) is activated, and foldase and chaperone expression is upregulated, thereby increasing the capacity of the secretory pathway (Fig. 12.3). UPR is a cellular response to increased concentrations of misfolded proteins. Misfolded proteins are expelled to the cytosol by Sec61, a protein complex that forms channels in the ER membrane. An ER transmembrane kinase, Ire1p, is activated upon unfolded proteins and subsequently, together with a tRNA ligase, Rlg1p, splices *HAC1* primary transcript. The mRNA passes to the cytoplasm, and the transcription factor Hac1p activates the UPR target genes (Fig. 12.3). In addition, a response called ER

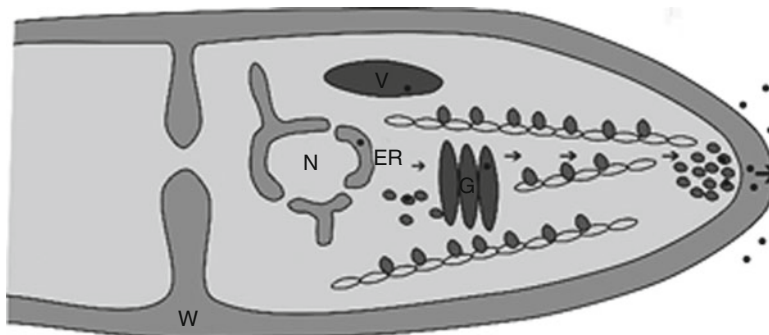


Fig. 12.2 Schematic view of the fungal secretory pathway. N: nucleus, ER: endoplasmic reticulum, V: vacuole, G: Golgi compartment, W: cell wall; *filled circles*: protein. *Arrows* indicate path of protein for secretion

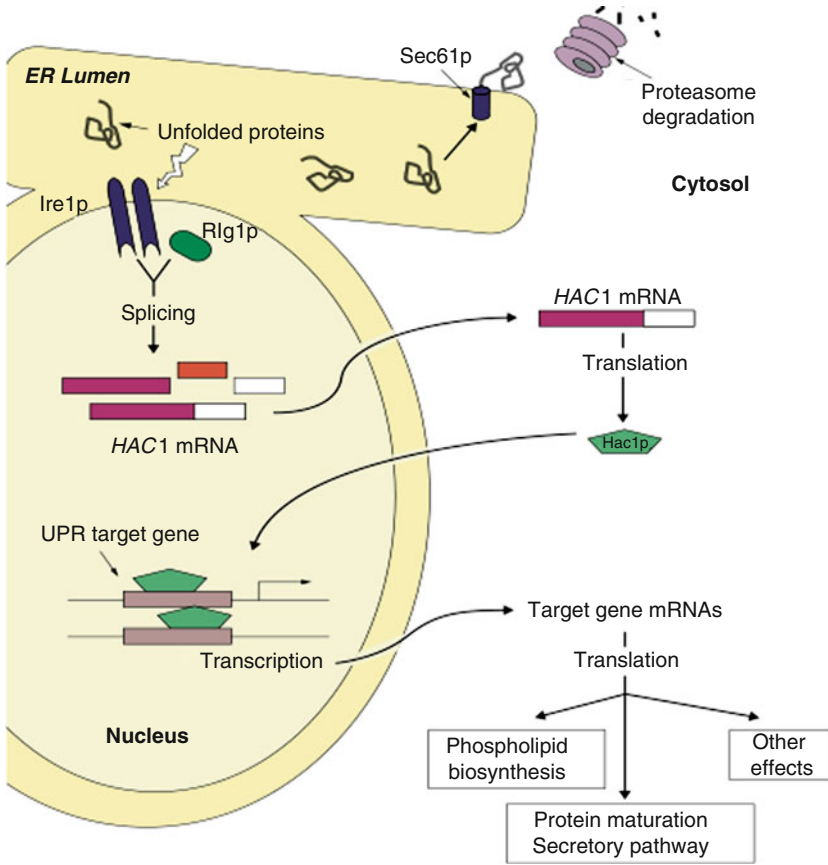


Fig. 12.3 The unfolded proteins in the endoplasmic reticulum turn on the unfolded protein response (UPR) and ER-associated degradation (ERAD). The presented model was adapted from McCracken and Brodsky [59]

associated degradation (ERAD) targets terminally misfolded proteins to the proteasome to undergo degradation [60]. This is achieved by retrotranslocation from the ER to the cytosol where the protein is ubiquitinated. Although the sensor for ERAD is not known, it has been suggested that the sensor involved in UPR is very closely related [61].

12.7.2 Limitations to Protein Production

12.7.2.1 Glycosylation and Proteolysis

Limitations in protein production may originate from transcriptional to (post) translational factors. The ubiquitous form of posttranslational modification is

glycosylation. It occurs by the attachment of a glycan to a protein through an asparagine residue, called *N*-glycosylation, or through a hydroxylysine, hydroxyproline, serine, or a threonine, called *O*-glycosylation. Glycosylation is not only important for protein stability but also for secretion and localization. Unusual fungal glycan structures on a heterologous protein can influence the activity, stability, and overall operational performance. Fungal glycosylation can result in incorrect folding and subsequent degradation of the protein. In early studies, it was found that proteases can be a possible bottleneck when producing proteins of interest [62]. Although numerous studies have been performed to minimize proteolysis [63, 64], it is still an interesting topic of research. Studies on protease regulation in *A. nidulans* show a complicated regulatory path [65, 66]. Disruption of specific protease genes will only partly solve the problem of proteolysis. Therefore, identifying genes involved in regulation of multiple protease genes is considered a feasible option. In this way, expression of several protease genes can be managed simultaneously. It was shown that the deletion of *pepA*, the major extracellular protease gene of *A. niger* encoding aspergillopepsin, resulted in a low extracellular protease activity [67]. However, a strain mutated in the *prtT* gene showed an even lower protease activity [68]. Sequence analysis revealed distinct features of a Zn(II)₂Cys₆-binuclear cluster protein. Northern analysis of this *prtT* gene showed constitutive expression of two upstream promoters (700 bp apart) and suggests regulation at the posttranscriptional level [68].

12.7.2.2 Protein Folding and Maturation

Another limitation involves protein maturation. Proteins have to fold and mature into their native form to be functional. This process takes place in the ER and is assisted by chaperones and foldases. Foldases catalyze slow processes such as disulfide bridge formation that are essential for functional confirmation. Chaperones are helper proteins that bind to non native proteins to prevent incorrect protein–protein interactions, and aid in translocating extracellular proteins. Foldases and chaperones are not restricted to the ER but are also present in the cytosol, mitochondria, chloroplasts, and periplasm [69]. These chaperones and foldases are involved in the quality control of protein structures and this process takes place in the ER. Chaperones and foldases present in filamentous fungi are listed in Table 12.6. One of them, the binding protein BiP, is a member of the heat shock 70 protein family (HSP70) and is localized in the lumen of the ER due to the K/HDEL signal [70, 71]. BiP is involved in a number of processes like protein folding, assembly in the ER and in the degradation of proteins that do not mature properly. Under normal cell conditions, there is a basal expression of BiP, which is increased once there is cellular stress.

Calnexin and its soluble homologous calreticulin belong to the family of lectin-like chaperones. Their task is to interact with the partially trimmed monoglycosylated N-linked oligosaccharides and therefore contribute to an important part of the maturation and quality control mechanisms of glycoproteins [72]. The expression

Table 12.6 ER Chaperones and foldases in filamentous fungi

Protein	Category	Function	Gene
BiP	Chaperone	Translocation folding, quality control	<i>bipA</i>
Protein disulfide isomerase and PDI related proteins	Foldase, Chaperone	Disulfide formation, disulfide isomerization, folding	<i>pdiA; tigA; prpA</i>
Peptidyl-propyl <i>cis-trans</i> isomerase	Foldase	Interconversion of peptidyl-propyl imide bonds	<i>cypB; FKBP22</i>
Calnexin	Chaperone, Lectin	Folding of glycoproteins	<i>clxA</i>

of foldases and chaperones is induced upon ER stress, which on its term is induced by the amount of unfolded proteins. It has been shown that UPR induces the expression of BiP [73]. Studies have been performed to increase the heterologous protein production by overexpressing chaperones and foldases [41]. In some cases, it has been successful [74, 75], and in other cases, it had no or even a negative effect on protein secretion [76, 77].

In the case of rMnP expressed in *A. niger*, overexpression of Bip resulted in a considerable reduction of MnP activity to almost undetectable levels, while calnexin had a positive effect [41]. Total protein levels were equal for both overexpression strains; however, Western analysis confirmed the protein levels of MnP, corresponding to the activity results. A similar observation was reported by Dorner et al. [78, 79] in CHO cells for heterologous protein production. BiP overexpression is able to increase the intracellular levels but not the level of secreted proteins [76, 80]. The reason for these different results is not clear and not easy to understand. It could be related to the multifunctional character of this chaperone since it is involved in several processes in the ER. Translocation into the ER and protein folding can be predicted as advantageous but other processes like ERAD of misfolded proteins can have a disadvantage. The level of BiP overexpression can have an influence on the production of heterologous proteins [74]. In contrast to the results of BiP overexpression, overexpression of calnexin is positively influencing the heterologous protein production with a 4–5-fold increase. Calnexin can contribute to the maturation of heterologous proteins [41]. It was also suggested that calnexin can have a function in incorporation of the cofactor [81] by providing sufficient time for this incorporation. This variety of results suggest that the effect on heterologous protein production may be related to a specific protein–chaperon/foldases system [41].

12.7.2.3 Cofactor Incorporation

Incorporation and availability of cofactors can be limiting factors in the production of heterologous proteins [33]. Heme has been often shown to be limited in its availability and incorporation into fungal peroxidases. Addition of hemin to growth

media has been reported to improve peroxidase production [38, 39]. However, this strategy is not suited for industrial applications since hemin is expensive and difficult to implement [38]. Uptake of hemin by filamentous fungi has not yet been demonstrated. Hemin supplementation can contribute to improve peroxidase production, but since heme is involved in many essential processes [82], it can also directly or indirectly affect the efficiency of these processes. In mammalian systems, it has been shown that hemin can act as an inhibitor of the proteasome [83]. Inhibition of this system might have an effect on protein production by interference with the UPR and ERAD systems. Whether this phenomenon also occurs in *Aspergillus* species remains to be revealed. However, it has been demonstrated that overexpression of the first two enzymes of the heme biosynthesis pathway increased the production of *C. cinereus* peroxidase in *Aspergillus oryzae* 4-fold [38].

12.8 Conclusions

Heterologous heme peroxidase production has been a well-studied topic during the past years. Although some bottlenecks operating at the level of expression, production, and cofactor incorporation have been identified, many are still to be elucidated. Although production of an enzyme can be exceptionally efficient in one production host, other enzymes can completely fail to be produced in the same organism and vice versa. The enzyme can be unstable and degraded, or produced but not active. To find general traits involved in heterologous protein production and construct an optimal production strain for a wide range of peroxidases is a great challenge. This makes heterologous protein production an interesting field of research for years to come.

References

1. Conesa A, Punt PJ, van den Hondel CAMJJ (2002) Fungal peroxidases: molecular aspects and applications. *J Biotechnol* 93:143–158
2. Consortium SG (2008) Protein production and purification. *Nat Methods* 5:12
3. Zelena K, Zorn H, Nimtz M et al (2009) Heterologous expression of the *msp2* gene from *Marasmius scorodoni*us. *Arch Microbiol* 191:397–402
4. Miki Y, Morales M, Ruiz-Duenas FJ et al (2009) *Escherichia coli* expression and in vitro activation of a unique ligninolytic peroxidase that has a catalytic tyrosine residue. *Protein Expr Purif* 68:208–214
5. Doyle WA, Smith AT (1996) Expression of lignin peroxidase H8 in *Escherichia coli*: folding and activation of the recombinant enzyme with Ca²⁺ and haem. *Biochem J* 315: 15–19
6. Whitwam R, Tien M (1996) Heterologous expression and reconstitution of fungal Mn peroxidase. *Arch Biochem Biophys* 333:439–446
7. Whitwam RE, Gazarian IG, Tien M (1995) Expression of fungal Mn peroxidase in *E. coli* and refolding to yield active enzyme. *Biochem Biophys Res Commun* 216:1013–1017

8. Zong Q, Osmulski PA, Hager LP (1995) High-pressure-assisted reconstitution of recombinant chloroperoxidase. *Biochemistry* 34:12420–12425
9. Huang ST, Tzean SS, Tsai BY et al (2009) Cloning and heterologous expression of a novel ligninolytic peroxidase gene from poroid brown-rot fungus *Antrodia cinnamomea*. *Microbiology* 155:424–433
10. Mohorcic M, Bencina M, Friedrich J et al (2009) Expression of soluble versatile peroxidase of *Bjerkandera adusta* in *Escherichia coli*. *Bioresour Technol* 100:851–858
11. Wolframm C, Lingens F, Mutzel R et al (1993) Chloroperoxidase-encoding gene from *Pseudomonas pyrocinia*: sequence, expression in heterologous hosts, and purification of the enzyme. *Gene* 130:131–135
12. Maya D, Quintero MJ, de la Cruz Munoz-Centeno M et al (2008) Systems for applied gene control in *Saccharomyces cerevisiae*. *Biotechnol Lett* 30:979–987
13. Mattanovich D, Gasser B, Hohenblum H et al (2004) Stress in recombinant protein producing yeasts. *J Biotechnol* 113:121–135
14. Sawai-Hatanaka H, Ashikari T, Tanaka Y et al (1995) Cloning, sequencing, and heterologous expression of a gene coding for *Arthromyces ramosus* peroxidase. *Biosci Biotechnol Biochem* 59:1221–1228
15. Hemrika W, Renirie R, Macedo-Ribeiro S et al (1999) Heterologous expression of the vanadium-containing chloroperoxidase from *Curvularia inaequalis* in *Saccharomyces cerevisiae* and site-directed mutagenesis of the active site residues His(496), Lys(353), Arg (360), and Arg(490). *J Biol Chem* 274:23820–23827
16. Sigle RO (1993) Expression of chloroperoxidase for site-specific mutagenesis, in Department of Biochemistry, University of Illinois, Illinois, p 144
17. Pease E, Tien M (1991) Lignin degrading enzymes from the filamentous fungus *Phanerochaete chrysosporium*. Plenum, New York
18. Jiang F, Kongsaree P, Schilke K et al (2008) Effects of pH and temperature on recombinant manganese peroxidase production and stability. *Appl Biochem Biotechnol* 146:15–27
19. Wang H, Lu F, Sun Y et al (2004) Heterologous expression of lignin peroxidase of *Phanerochaete chrysosporium* in *Pichia methanolica*. *Biotechnol Lett* 26:1569–1573
20. Wang W, Wen X (2009) Expression of lignin peroxidase H2 from *Phanerochaete chrysosporium* by multi-copy recombinant *Pichia* strain. *J Environ Sci* 21:218–222
21. Cereghino JL, Cregg JM (2000) Heterologous protein expression in the methylotrophic yeast *Pichia pastoris*. *FEMS Microbiol Rev* 24:45–66
22. Macauley-Patrick S, Fazenda ML, McNeil B et al (2005) Heterologous protein production using the *Pichia pastoris* expression system. *Yeast* 22:249–270
23. Hitchman RB, Possee RD, King LA (2009) Baculovirus expression systems for recombinant protein production in insect cells. *Recent Pat Biotechnol* 3:46–54
24. Johnson TM, Li JK (1991) Heterologous expression and characterization of an active lignin peroxidase from *Phanerochaete chrysosporium* using recombinant baculovirus. *Arch Biochem Biophys* 291:371–378
25. Johnson TM, Pease EA, Li JK et al (1992) Production and characterization of recombinant lignin peroxidase isozyme H2 from *Phanerochaete chrysosporium* using recombinant baculovirus. *Arch Biochem Biophys* 296:660–666
26. Irie T, Honda Y, Watanabe T et al (2001) Homologous expression of recombinant manganese peroxidase genes in ligninolytic fungus *Pleurotus ostreatus*. *Appl Microbiol Biotechnol* 55:566–570
27. Tsukihara T, Honda Y, Sakai R et al (2006) Exclusive overproduction of recombinant versatile peroxidase MnP2 by genetically modified white rot fungus, *Pleurotus ostreatus*. *J Biotechnol* 126:431–439
28. Mayfield MB, Kishi K, Alic M et al (1994) Homologous expression of recombinant manganese peroxidase in *Phanerochaete chrysosporium*. *Appl Environ Microbiol* 60:4303–4309

29. Li D, Youngs HL, Gold MH (2001) Heterologous expression of athermostable manganese peroxidase from *Dichomitus squalens* in *Phanerochaete chrysosporium*. Arch Biochem Biophys 385:348–356
30. Sollewijn Gelpke MD, Mayfield-Gambill M, Lin Cereghino GP et al (1999) Homologous expression of recombinant lignin peroxidase in *Phanerochaete chrysosporium*. Appl Environ Microbiol 65:1670–1674
31. Singh D, Chen S (2008) The white-rot fungus *Phanerochaete chrysosporium*: conditions for the production of lignin-degrading enzymes. Appl Microbiol Biotechnol 81:399–417
32. van den Hondel CAMJJ, Punt PJ, van Gorcom RF (1992) Production of extracellular proteins by the filamentous fungus *Aspergillus*. Antonie Van Leeuwenhoek 61:153–160
33. Punt PJ, van Biezen N, Conesa A et al (2002) Filamentous fungi as cell factories for heterologous protein production. Trends Biotechnol 20:200–206
34. Saloheimo M, Barajas V, Niku-Paavola ML et al (1989) A lignin peroxidase-encoding cDNA from the white-rot fungus *Phlebia radiata*: characterization and expression in *Trichoderma reesei*. Gene 85:343–351
35. Aifa MS, Sayadi S, Gargouri A (1999) Heterologous expression of lignin peroxidase of *Phanerochaete chrysosporium* in *Aspergillus niger*. Biotechnol Lett 21:849–853
36. Ruiz-Duenas FJ, Martinez MJ, Martinez AT (1999) Heterologous expression of *Pleurotus eryngii* peroxidase confirms its ability to oxidize Mn(2+) and different aromatic substrates. Appl Environ Microbiol 65:4705–4707
37. Stewart P, Whitwam RE, Kersten PJ et al (1996) Efficient expression of a *Phanerochaete chrysosporium* manganese peroxidase gene in *Aspergillus oryzae*. Appl Environ Microbiol 62:860–864
38. Elrod SLC, Jones JR (1997) A method for increasing hemoprotein production in filamentous fungi. International patent application
39. Conesa A, van den Hondel CA, Punt PJ (2000) Studies on the production of fungal peroxidases in *Aspergillus niger*. Appl Environ Microbiol 66:3016–3023
40. Conesa A, van De Velde F, van Rantwijk F et al (2001) Expression of the *Caldariomyces fumago* chloroperoxidase in *Aspergillus niger* and characterization of the recombinant enzyme. J Biol Chem 276:17635–17640
41. Conesa A, Jeenes D, Archer DB et al (2002) Calnexin overexpression increases manganese peroxidase production in *Aspergillus niger*. Appl Environ Microbiol 68:846–851
42. Eibes GM, Lu-Chau TA, Ruiz-Duenas FJ et al (2009) Effect of culture temperature on the heterologous expression of *Pleurotus eryngii* versatile peroxidase in *Aspergillus* hosts. Bioprocess Biosyst Eng 32:129–134
43. Lokman BC, Joosten V, Hovenkamp J et al (2003) Efficient production of *Arthromyces ramosus* peroxidase by *Aspergillus awamori*. J Biotechnol 103:183–190
44. Sugano Y, Nakano R, Sasaki K et al (2000) Efficient heterologous expression in *Aspergillus oryzae* of a unique dye-decolorizing peroxidase, DyP of *Geotrichum candidum* Dec1. Appl Environ Microbiol 66:1754–1758
45. Sugano Y, Matsuo K, Shoda M (2001) Efficient production of a heterologous peroxidase, DyP from *Geotrichum candidum* Dec 1, on solid-state culture of *Aspergillus oryzae* RD005. J Biosci Bioeng 92:594–597
46. Conesa A (2001) Overproduction of fungal peroxidases in filamentous fungi, in Molecular Microbiology. Leiden University, Leiden, pp 55–64
47. Andersen H, Jensen, E, Welinder K (1992) A process for producing heme proteins. European patent application PCT/DK1992/000088
48. Punt PJ, Dingemans MA, Jacobs-Meijnsing BJ et al (1988) Isolation and characterization of the glyceraldehyde-3-phosphate dehydrogenase gene of *Aspergillus nidulans*. Gene 69:49–57
49. De Maeseneire SL, Dauvrin T, Jonniaux JL et al (2008) Cloning and characterization of the glyceraldehyde-3-phosphate dehydrogenase gene and the use of its promoter for expression in *Myrothecium gramineum*, a novel expression host. FEMS Microbiol Lett 281:140–146

50. Nunberg JH, Meade JH, Cole G et al (1984) Molecular cloning and characterization of the glucoamylase gene of *Aspergillus awamori*. *Mol Cell Biol* 4:2306–2315
51. Santerre Henriksen AL, Even S, Muller C et al (1999) Study of the glucoamylase promoter in *Aspergillus niger* using green fluorescent protein. *Microbiology* 145:729–734
52. Ganzlin M, Rinas U (2008) In-depth analysis of the *Aspergillus niger* glucoamylase (*glaA*) promoter performance using high-throughput screening and controlled bioreactor cultivation techniques. *J Biotechnol* 135:266–271
53. Ward M, Wilson LJ, Kodama KH et al (1990) Improved production of chymosin in *Aspergillus* by expression as a glucoamylase-chymosin fusion. *Nat Biotechnol* 8:435–440
54. Gouka RJ, Punt PJ, van den Hondel CAMJJ (1997) Efficient production of secreted proteins by *Aspergillus*: progress, limitations and prospects. *Appl Microbiol Biotechnol* 47:1–11
55. Turner NJ (2009) Directed evolution drives the next generation of biocatalysts. *Nat Chem Biol* 5:567–573
56. Shakeri M, Sugano Y, Shoda M (2007) Production of dye-decolorizing peroxidase (rDyP) from complex substrates by repeated-batch and fed-batch cultures of recombinant *Aspergillus oryzae*. *J Biosci Bioeng* 103:129–134
57. Lopez C, Moreira MT, Feijoo G et al (2004) Dye decolorization by manganese peroxidase in an enzymatic membrane bioreactor. *Biotechnol Prog* 20:74–81
58. Holker U, Hofer M, Lenz J (2004) Biotechnological advantages of laboratory-scale solid-state fermentation with fungi. *Appl Microbiol Biotechnol* 64:175–186
59. McCracken AA, Brodsky JL (2000) A molecular portrait of the response to unfolded proteins. *Genome Biol* 1:1013.1–1013.3
60. Bonifacino JS, Weissman AM (1998) Ubiquitin and the control of protein fate in the secretory and endocytic pathways. *Annu Rev Cell Dev Biol* 14:19–57
61. Travers KJ, Patil CK, Wodicka L et al (2000) Functional and genomic analyses reveal an essential coordination between the unfolded protein response and ER-associated degradation. *Cell* 101:249–258
62. van den Hombergh JP, Fraissinet-Tachet L, van de Vondervoort PJ et al (1997) Production of the homologous pectin lyase B protein in six genetically defined protease-deficient *Aspergillus niger* mutant strains. *Curr Genet* 32:73–81
63. Berka RM, Kodama KH, Rey MW et al (1991) The development of *Aspergillus niger* var. *awamori* as a host for the expression and secretion of heterologous gene products. *Biochem Soc Trans* 19:681–685
64. Broekhuijsen MP, Mattern IE, Contreras R et al (1993) Secretion of heterologous proteins by *Aspergillus niger*: production of active human interleukin-6 in a protease-deficient mutant by KEX2-like processing of a glucoamylase-hIL6 fusion protein. *J Biotechnol* 31:135–145
65. Katz ME, Bernardo SM, Cheetham BF (2008) The interaction of induction, repression and starvation in the regulation of extracellular proteases in *Aspergillus nidulans*: evidence for a role for CreA in the response to carbon starvation. *Curr Genet* 54:47–55
66. Katz ME, Gray KA, Cheetham BF (2006) The *Aspergillus nidulans xprG* (*phoG*) gene encodes a putative transcriptional activator involved in the response to nutrient limitation. *Fungal Genet Biol* 43:190–199
67. Mattern IE, van Noort JM, van den Berg P et al (1992) Isolation and characterization of mutants of *Aspergillus niger* deficient in extracellular proteases. *Mol Gen Genet* 234:332–336
68. Punt PJ, Schuren FH, Lehmbeck J et al (2008) Characterization of the *Aspergillus niger prtI*, a unique regulator of extracellular protease encoding genes. *Fungal Genet Biol* 45:1591–1599
69. Gething MJ, Sambrook J (1992) Protein folding in the cell. *Nature* 355:33–45
70. Bole DG, Hendershot LM, Kearney JF (1986) Posttranslational association of immunoglobulin heavy chain binding protein with nascent heavy chains in non-secreting and secreting hybridomas. *J Cell Biol* 102:1558–1566
71. Munro S, Pelham HR (1986) An Hsp70-like protein in the ER: identity with the 78 kd glucose-regulated protein and immunoglobulin heavy chain binding protein. *Cell* 46:291–300

72. Helenius A, Trombetta ES, Hebert DN et al (1997) Calnexin, calreticulin and the folding of glycoproteins. *Trends Cell Biol* 7:193–200
73. van Gemeren IA, Punt PJ, Drint-Kuyvenhoven A et al (1997) The ER chaperone encoding *bipA* gene of black *Aspergilli* is induced by heat shock and unfolded proteins. *Gene* 198:43–52
74. Harmsen MM, Bruyne MI, Raue HA et al (1996) Overexpression of binding protein and disruption of the *PMR1* gene synergistically stimulate secretion of bovine prochymosin but not plant thaumatin in yeast. *Appl Microbiol Biotechnol* 46:365–370
75. Tate CG, Whiteley E, Betenbaugh MJ (1999) Molecular chaperones stimulate the functional expression of the cocaine-sensitive serotonin transporter. *J Biol Chem* 274:17551–17558
76. Hsu TA, Eiden JJ, Bourgarel P et al (1994) Effects of co-expressing chaperone BiP on functional antibody production in the baculovirus system. *Protein Expr Purif* 5:595–603
77. Robinson AS, Bockhaus JA, Voegler AC et al (1996) Reduction of BiP levels decreases heterologous protein secretion in *Saccharomyces cerevisiae*. *J Biol Chem* 271:10017–10022
78. Dorner AJ, Krane MG, Kaufman RJ (1988) Reduction of endogenous GRP78 levels improves secretion of a heterologous protein in CHO cells. *Mol Cell Biol* 8:4063–4070
79. Dorner AJ, Wasley LC, Kaufman RJ (1992) Overexpression of GRP78 mitigates stress induction of glucose regulated proteins and blocks secretion of selective proteins in Chinese hamster ovary cells. *EMBO J* 11:1563–1571
80. Punt PJ, van Gemeren IA, Drint-Kuijvenhoven J et al (1998) Analysis of the role of the gene *bipA*, encoding the major endoplasmic reticulum chaperone protein in the secretion of homologous and heterologous proteins in black *Aspergilli*. *Appl Microbiol Biotechnol* 50:447–454
81. Nauseef WM, McCormick SJ, Goedken M (1998) Coordinated participation of calreticulin and calnexin in the biosynthesis of myeloperoxidase. *J Biol Chem* 273:7107–7111
82. Hamza I (2006) Intracellular trafficking of porphyrins. *ACS Chem Biol* 1:627–629
83. Guo GG, Gu M, Etlinger JD (1994) 240-kDa proteasome inhibitor (CF-2) is identical to delta-aminolevulinic acid dehydratase. *J Biol Chem* 269:12399–12402

Chapter 13

A Compendium of Bio-Physical-Chemical Properties of Peroxidases

Humberto Garcia-Arellano

Contents

Physico-chemical properties of some hemeperoxidases	336
Physico-chemical properties of Lignin peroxidase isoenzymes from <i>Phanerochaete chrysosporium</i>	336
Physicochemical properties of horseradish peroxidase isoenzymes	337
Affinity constants (K_M) for some horseradish peroxidase isoenzymes	337
Molar extinction coefficient of some hemeperoxidases	338
Redox potential of hemeperoxidases	339
Kinetic parameters for some hemeperoxidases	340
Half-life of hemeperoxidases against hydrogen peroxide	343
Optimum pH for the oxidation of different compounds by hemeperoxidases	343
Some common inhibitors of hemeperoxidases	344
Aminoacid sequences of hemeperoxidases	345
References	349

Physico-chemical properties of some hemeperoxidases

Enzyme source	Molecular weight (kDa)	Carbohydrate content (%)	Isoelectric point	References
Catalase				
Bovine liver	240 (homotetramer) 57 (monomer)	Not detected	5.4	[1–3]
Goat liver	220–236 (homotetramer) 220 (homotetramer) 60 (monomer)	Not detected	– 5.8–6.1	[4] [5]
<i>Aspergillus niger</i>	385 (homotetramer) 97 (monomer)	8.3 Neutral sugar and 1.9 Glucosamine	–	[6]
Chloroperoxidase				
<i>Caldariomyces fumago</i>	42	25–30		[7, 8]
Cytochrome c				
Horse heart	12.4	–	10.6	[9]
Lignin-peroxidase				
<i>Phanerochaete chrysosporium</i>	42	13	3.5	[10]
<i>Phanerochaete chrysosporium</i> EM446	41 42–43 39–43	– 21 6	– – –	[11, 12] [13] [14]
<i>Phanerochaete chrysosporium</i> BKM-F-1767 isoenzymes	39.5–42.5 38–43	12–39 –	3.70–4.65 3.3–4.7	[15] [16]
Manganese-peroxidase				
<i>Phanerochaete chrysosporium</i> EM446	46 45–47	– 17	– –	[11, 17, 18] [13]
<i>Phanerochaete chrysosporium</i> ATCC 24725	46	–	4.0–4.4	[19]
<i>Trichophyton rubrum</i> LSK-27	42	–	8.2	[20]
<i>Panus tigrinus</i> CBS 577.79	50.5	5.3	4.07	[21]
Versatile peroxidase				
<i>Pleurotus eryngii</i> CBS 613.91 isoenzymes	43	5–7	3.65–3.75	[22]
<i>Pleurotus eryngii</i> ATCC 90787 isoenzymes	37–43	–	3.65–3.7	[23]

Physico-chemical properties of Lignin peroxidase isoenzymes from *Phanerochaete chrysosporium*

Isoenzyme	Mw (kDa)	Carbohydrate content (%)	pI	pH optimum	H ₂ O ₂		Veratryl alcohol			References
					K _M (μM)	k _{cat} /K _M (M ⁻¹ s ⁻¹) × 10 ⁴	k _{cat} (s ⁻¹)	K _M (μM)	k _{cat} /K _M (M ⁻¹ s ⁻¹) × 10 ⁴	
LiP1	39.5	12	4.65	2.3	85	45	38.3	171	22	[15]
LiP2	40	39	4.15	3.2	130	27	34.7	116	30	[15]
LiP3	42	19	3.85	2.3	85	26	22	83	26	[15]
LiP4	42	17	3.80	2.3	91	30	27	143	19	[15]
LiP5	42.5	17	3.70	2.5	140	33	45.7	200	23	[15]
I	39				47			95		[14]
II	41	6			32			71		[14]
III	43				39			55		[14]

Physicochemical properties of horseradish peroxidase isoenzymes

Isoenzyme	Mw (kDa)	Carbohydrate content (%)	pI	ϵ (mM ⁻¹ cm ⁻¹) ^a	References
Acid peroxidases					
A1	48	~18	3.5	102	[24, 25]
A2	41	~18	3.5	102	[24, 25]
A2	43	~18	3.5	97	[24, 25]
Neutral peroxidases					
B1	42.7	17.5	5.75	102.8	[26]
B2	42.8	18.4	7.15	102.3	[26]
B3	41.2	16.8	7.10	102.0	[26]
C1	41.7	19.0	9.40	101.3	[26]
C2	42.1	21.0	9.63	102.3	[26]
Basic peroxidases					
E1	38.8	12.8	10.60	97.2	[27]
E2	39	14.1	10.63	104.2	[27]
E3	33.9	0.9	>12	111.3	[27]
E4	33.7	0.8	>12	111.2	[27]
E5	37.3	4.2	>12	115.9	[27]
E6	33.9	1.7	>12	91.2	[27]

^aMeasured at 401 nm for acidic isoenzymes and 403 nm for neutral and basic isoenzymes

Affinity constants (K_M) for some horseradish peroxidase isoenzymes^a

Peroxidase isoenzyme	pH optimum	K_{Mapp} (H ₂ O ₂), mM	K_{Mapp} (<i>o</i> -dianisidine), mM	K_{Mapp} (oxaloacetate), mM
A1	5.8	10.0	0.9	0.7
A2	5.6	18.8	2.0	2.3
A3	5.6	3.8	1.1	2.2
B	5.0	1.7	0.1	0.4
C	5.0	1.6	0.1	0.4
D	5.0	1.4	0.7	0.4
E	5.0	1.5	0.3	0.4

^aAdapted from Kay et al. [28]

Molar extinction coefficient of some hemeperoxidases

Enzyme source	Wavelength (nm)	Millimolar extinction coefficient ϵ ($\text{mM}^{-1}\text{cm}^{-1}$)	Conditions	References
Catalase				
Bovine liver	278	77.8		[4]
	280	69.7		[29]
	405	70.3		[4]
	405	92.6		[29]
	405	13.5 ^a	Obtained on the basis of dry weight of two preparations after heating at 105°C for 20 h	[1, 5, 30]
Horse erythrocyte	405	324		[31]
	277	68.8		[32]
	405	89.4		[32]
<i>Aspergillus niger</i>	406	360		[6]
Chloroperoxidase				
<i>Caldariomyces fumago</i>	398	91.2	Oxidized	[33]
	403	75.3	Oxidized	[7]
	406	87.4	Oxidized, pH 5.2	[34]
	409	68.7	Reduced	[7]
	550	13.7	Reduced	[7]
	542	10.8	Reduced	[7]
Cytochrome C	543	10.9	Reduced pH 5.2	[34]
Horse heart	409	106	Oxidized, pH 7.0	[35]
	550	29.5	Reduced, pH 7.0	[36]
Lignin peroxidase				
<i>Phanerochaete chrysosporium</i>	407	133.3	pH 4.5	[12]
	409	169	Oxidized	[37]
	409	102	pH 4.5	[10]
	409	162–182	Estimated for six isoenzymes from the strain BKM-F-1767	[16]
	435	92.8	pH 4.5, reduced enzyme	[12]
	420	55	pH 4.5, 21 μM H_2O_2	[10]
	500	8.1	pH 4.5	[12]
	502	5	pH 4.5	[10]
	544	3.4	pH 4.5, 21 μM H_2O_2	[38]
	556	11	pH 4.5, reduced enzyme	[12]
Manganese peroxidase				
<i>Phanerochaete chrysosporium</i>	406	129.3	pH 4.5	[17]
	433	109	pH 4.5, reduced enzyme	[17]
	502	9.9	pH 4.5	[17]
	554	13	pH 4.5, reduced enzyme	[17]
Peroxidase				
Horseradish	403	102	McIlvaine citrate–phosphate buffers with constant ionic strength of 0.25 M	[39]
	403	98		[40]
Soybean	403	94.6	McIlvaine citrate–phosphate buffers with constant ionic strength of 0.25 M	[39]
Versatile peroxidase				
<i>Pleurotus eryngii</i> ATCC 90787	406	150		[23]

^a $A_{1\text{cm}}^{1\%}$ value. If a molecular weight of 240 kDa is considered, this value is converted in $324 \text{ mM}^{-1} \text{ cm}^{-1}$

Enzyme source	Redox potential of the Fe ³⁺ /Fe ²⁺ couple (mV)	Notes	References
Redox potential of hemeperoxidases			
Catalase			
Bovine liver	-50	Catalase immobilized on multiwall carbon nanotubes glassy-carbon electrode and assayed in phosphate buffer solution at pH 6.5	[41]
Chloroperoxidase	-52	Bromine-modified silver electrode in 0.1 M KNO ₃	[42]
<i>Caldariomyces fumago</i>	-138	Electrode potentials were measured with a platinum electrode against an Ag/AgCl half cell and assayed at pH 6.9	[43]
	-140		[44]
	+144	Electrode potentials were measured with a platinum electrode against an Ag/AgCl half cell and assayed at pH 3.0	[43]
Cytochrome c			
Horse heart	-66	Bromine-modified silver electrode in 0.1 M KNO ₃	[42]
Lignin peroxidase			
<i>Panerochaete chrysosporium</i>	-130		[44]
<i>Panerochaete chrysosporium</i> BKM-F-1767	-142 to -127	Oxidation-reduction potentials of several isoenzymes	[45]
Manganese peroxidase			
<i>Panerochaete chrysosporium</i>	-90		[44]
<i>Panerochaete chrysosporium</i> BKM-F-1767	-99 to -88	Oxidation-reduction potentials of different isoenzymes	[45]
Peroxidase			
Horseradish	-183		[44]
	-133	Standard calomel electrode (SCE)	[40]
Versatile peroxidase			
<i>Bjerkandera adusta</i>	50	A platinum disk was used as working electrode. The reference electrode was a silver-silver chloride electrode. Analysis at pH 7.0	[44]

Kinetic parameters for some hemeperoxidases

Substrate	k_{cat} (min^{-1})	K_M (mM)	k_{cat}/K_M ($\text{mM}^{-1}\text{min}^{-1}$)	Relevant conditions	References
Catalase (Bovine liver)					
H_2O_2	91			Estimated in the oxidation of pyrogallol to purpurogallin	[46]
	35			Hydrogen peroxide decomposition	[47]
	25.16			Hydrogen peroxide decomposition	[48, 49]
	10.9			50 mM Phosphate buffer pH 7.0, 37°C	[50]
	9.24×10^6		108.2×10^3	Hydrogen peroxide decomposition	[51]
	600×10^6		24×10^6	Hydrogen peroxide decomposition	[52]
Chloroperoxidase (<i>Caldariomyces fumago</i>)					
H_2O_2	4.3				[46]
	3.650	30×10^{-3}	121.7×10^3	Estimated in the oxidation of 2,3,5,6-tetrachlorophenol	[53]
	2.818	0.10	28.2×10^3	Estimated in the oxidation of pentachlorophenol	[53]
	2.157	0.27	8×10^3	Estimated in the oxidation of 2,3,5,6-tetrachloroaniline	[53]
2,3,5,6-tetrachlorophenol		0.12		Estimated in the presence of H_2O_2	[53]
Pentachlorophenol		38×10^{-3}		Estimated in the presence of H_2O_2	[53]
2,3,5,6-tetrachloroaniline		90×10^{-3}		Estimated in the presence of H_2O_2	[53]
Peroxyphenylacetic acid		1.64			[46]
Thioanisole	19,900		12.1×10^3	Monoxygenase activity	[54]
Phenol	1,500	0.35	4.3×10^3	Peroxiase activity	[54]
2,4-dimethyl dibenzothioephene	523	2.24×10^{-3}	234×10^3	Parameters obtained from Hill equation where $K_M = K_{M1}$ and $n = 2.03$	[55]
Parathion	1,092	1.2×10^{-3}	910×10^3	Oxidation reaction in the presence of H_2O_2	[56]
H_2O_2	1,053	0.53	1,992	Oxidation of parathion	[56]
Styrene	729	324	2.25	Oxidation of styrene in ternary solvent mixtures in the presence of 200 mM of <i>t</i> -butyl hydroperoxide	[57]
Cytochrome <i>c</i> (Horse heart)					
H_2O_2	17.04	25.2	0.68	Pyrene oxidation reaction in 60 mM phosphate buffer pH 6.1, 30°C.	[58]
	80.4	27.4	3.1	Pyrene concentration 35 μM	[59]
Pyrenol chloride	52.2	12.5	4.1	Thianthrene oxidation reaction in 60 mM phosphate buffer pH 6.1	[60]
Pyrene	17.04	29.3×10^{-3}	5.81×10^2	90% tetrahydrofuran	[58]
Thianthrene	80.4	46.6	1.73	Oxidation reaction in 60 mM phosphate buffer pH 6.1, 5 mM H_2O_2	[59]
<i>iso</i> -1-Cytochrome <i>c</i> (<i>Saccharomyces cerevisiae</i>)				60 mM phosphate buffer pH 6.1	
H_2O_2	684	69.7	9.81	Oxidation of pyrenol blue in 60 mM phosphate buffer pH 6.0.	[61]
				Values estimated for the T-5A, C102T variant	
Pyrenol chloride	178	10.5	16.9	Pyrenol chloride oxidation in 60 mM phosphate buffer pH 6.0	[61]
Pyrene	18.6	9.7	1.91	Pyrene oxidation reaction in 60 mM phosphate buffer pH 6.1	[61]

(Continued)		k_{cat} (min^{-1})	K_M (mM)	k_{cat}/K_M ($\text{mM}^{-1}\text{min}^{-1}$)	Relevant conditions	References
<i>o</i> -toluidine		16.2×10^3	2.6	6.23×10^3	30 mM sodium phosphate buffer, pH 7.0	[63]
Peroxyphenylacetic acid		44.16×10^3	40×10^{-3}	248×10^3		[46]
ABTS		48.6×10^3	178×10^{-3}	180×10^3	Mellvaine-citrate buffer pH 6.8, 25°C, 0.5 mM H_2O_2 pH 5.0, 25°C	[39]
1,2,4,5-Tetramethoxybenzene		37.5×10^3	1.2×10^{-3}	31.3×10^6	50 mM sodium tartrate, pH 3.0, 0.5 mM H_2O_2	[62]
Peroxidase (Soybean)						
ABTS		73.8×10^3	173×10^{-3}	426×10^3	Mellvaine-citrate buffer pH 6.8, 25°C, 0.5 mM H_2O_2	[39]
		160×10^3	45×10^{-3}	3.6×10^6	Mellvaine-citrate buffer pH 5, 25°C, 0.5 mM H_2O_2	[39]
Versatile peroxidase						
H_2O_2			6×10^{-3} – 10×10^{-3}		<i>Pleurotus eryngii</i> CBS 613.91, isoenzymes in the presence of 0.1 mM Mn^{2+} at pH 5.0	[22, 23]
			2×10^{-3} – 3×10^{-3}		Estimated in the oxidation of syringol in the absence Mn^{2+} at pH 3.0 by <i>Pleurotus eryngii</i> ATCC 90787 isoenzymes	[65]
Mn^{2+}			20×10^{-3}		<i>Pleurotus eryngii</i> CBS 613.91, isoenzymes in the presence of 0.1 mM H_2O_2 at pH 5.0	[22, 23]
		4.74×10^3	48×10^{-3}	98.7×10^3	Estimated for <i>Pleurotus eryngii</i> ATCC 90787 PS1 isoenzyme in the presence of H_2O_2 at pH 5.0	[65]
		4.68×10^3	0.2	23.4×10^3	Estimated for <i>Pleurotus eryngii</i> ATCC 90787 PS3 isoenzyme in the presence of H_2O_2 at pH 5.0	[65]
2,6-Dimethoxyphenol			10×10^{-3}		<i>Pleurotus eryngii</i> CBS 613.91, isoenzymes in the presence of 0.1 mM Mn^{2+} and 0.1 mM H_2O_2 at pH 5.0	[22, 23]
2,6-Dimethoxyphenol			160×10^{-3} – 250×10^{-3}		<i>Pleurotus eryngii</i> CBS 613.91, isoenzymes in the presence of 0.1 mM H_2O_2	[22, 23]
Veratryl alcohol			3–3.5		<i>Pleurotus eryngii</i> CBS 613.91, isoenzymes in the presence of 0.1 mM H_2O_2 at pH 3.0	[22, 23]
Veratryl alcohol		240	3.5	68.6	Estimated for <i>Pleurotus eryngii</i> ATCC 90787 PS1 isoenzyme, Mn^{2+} independent reaction at pH 3.0	[65]
Reactive Black 5		300	2×10^{-3}	150×10^3		[65]
Methoxyhydroquinone		240	17×10^{-3}	14.1×10^3		[65]

Half-life of hemeperoxidases against hydrogen peroxide

Enzyme	Source	Half-life, $t_{1/2}$ (min) ^a	References
Chloroperoxidase	<i>Caldariomyces fumago</i>	115	[66, 67]
	<i>Caldariomyces fumago</i> CMI 89362	186	[68]
Cytochrome c	Horse heart	1.45	[66]
		0.63 ^b	[69]
		11.5 ^{b,c}	[69]
		7.7 ^{b,d}	[69]
		19.8	[59]
<i>iso</i> -1-Cytochrome c	<i>Saccharomyces cerevisiae</i>	5.25	[60, 67]
		8.3	[70]
Lignin peroxidase	<i>Phanaerochaete chrysosporium</i>	6.2	[66, 67]
Manganese peroxidase Peroxidase	<i>Phanaerochaete chrysosporium</i>	8.5	[66, 67]
		2.95	[71]
			33
Versatile peroxidase	<i>Coprinus cinnereus</i>	15	[44]
	<i>Berjkandera adusta</i>	1.3	[66]

^aData obtained from suicide inactivation process in the presence of 1 mM H₂O₂. The half-life was obtained from the first-order inactivation constant

^bInactivation constants were determined in the oxidation of 2,3,7,8,12,13,17,18-Octaethyl-21H,23H-porphine nickel(II), (NiOEP). Reaction was assayed in the ternary system methylene chloride/methanol/water, 65:30:5 v/v

^cHalf-life against 1 mM *tert*-butyl hydroperoxide

^dHalf-life against 1 mM cumene hydroperoxide

Optimum pH for the oxidation of different compounds by hemeperoxidases

Enzyme source	Optimum pH	Observations	References
Chloroperoxidase			
<i>Caldariomyces fumago</i>	2.7	Halide dependent activity (Chlorination reaction)	[72–74]
	6.0	Halide independent activity, <i>N,N,N',N'</i> -tetramethyl- <i>p</i> -phenylenediamine oxidation (TMPD)	[73]
	4–7	Halide independent activity	[74]
Lignin peroxidase			
<i>Phanerochaete chrysosporium</i> EM446	3.0	Veratryl alcohol oxidation	[10–12]
	3.5	Bromination of monochlorodimedone	[75]
<i>Phanerochaete chrysosporium</i> BKM-F-1767	2.3–3.2	Veratryl alcohol oxidation by LiP isoenzymes	[15]
Manganese peroxidase			
<i>Phanerochaete chrysosporium</i>	4.5	Oxidation of ABTS or phenol red. Activity was negligible below pH 2.0 and above pH 6.5	[17]
<i>Trichophyton rubrum</i> LSK-27	4.5	Oxidation of 2,6-dimethoxyphenol	[20]
<i>Phanerochaete chrysosporium</i>	5.0	Oxidation of Mn ²⁺ in lactate buffer and 40 μM H ₂ O ₂	[18]
Versatile peroxidase	5.0	Oxidation of Mn ²⁺	[22]

(continued)

(Continued)

Enzyme source	Optimum pH	Observations	References
<i>Pleurotus eryngii</i> CBS 613.91 isoenzymes	4.0	Oxidation of 2,6-dimethoxyphenol in the presence of Mn ²⁺	[22]
	3.0	Oxidation of 2,6-dimethoxyphenol or veratryl alcohol in the absence of Mn ²⁺	[22]
Catalase			
Bovine liver	7.0	Hydrogen peroxide decomposition	[5, 48]
Goat liver	7.0		[5]
Human erythrocyte	4.0–8.5		[76]
Peroxidase			
Soybean	5.5	Oxidation of ABTS, guaiacol and <i>p</i> -cresol	[39]
Horseradish	6	Oxidation of 5-aminosalicylic acid	[77]
	4.5	Oxidation of esculetin	[78]
Cytochrome <i>c</i>			
Horse heart	6–7	Oxidation of dibenzothiophene in the presence of 1 mM hydrogen peroxide	[60]

Some common inhibitors of hemeperoxidases

Enzyme	Inhibitor	Observations	References
Manganese peroxidase			
<i>Phanerochaete chrysosporium</i> ME446	NaN ₃ , KCN, EDTA	Each at 1 mM	[11]
<i>Phanerochaete chrysosporium</i> BKM-F-1767 (ATCC 24725)	Fe ³⁺ , Fe ²⁺ , Co ²⁺ , Cu ²⁺ and ascorbic acid at 0.1 mM each, H ₂ O ₂ above 0.2 mM	Estimated in the oxidation of vanillylacetone in the presence of H ₂ O ₂ and Mn ²⁺	[13]
<i>Phanerochaete chrysosporium</i> Lignin peroxidase	Sodium pyrophosphate 0.5 mM	52% inhibition on the ABTS oxidation	[17]
<i>Phanerochaete chrysosporium</i> ME446	NaN ₃ , KCN, EDTA, thiourea 2-keto-4-thiomethyl butyric acid (KTBA)	Each at 1 mM Noncompetitive inhibitor	[11, 79] [14]
Versatile peroxidase			
<i>Pleurotus eryngii</i> ATCC 90787 isoenzymes	Reactive Black 5	High concentration causes substrate inhibition	[65]
Catalase			
Bovine liver	Adamantane (<i>k</i> _i 0.07 mM) ^a , Benzene (<i>k</i> _i 38 mM)	Constants estimated in the oxidation of pyrogallol	[46]
	3,3'-Diaminobenzidine, aromatic diamines		[80]
Peroxidase			
Horseradish	NaN ₃	Noncompetitive inhibitor (<i>k</i> _i 1.1 mM)	[50]

(continued)

(Continued)

Enzyme	Inhibitor	Observations	References
	1-butyl-3-methylimidazolium tetrafluoroborate	Weak noncompetitive inhibitor (k_i 2.9 M)	[81]
	Gallic acid; resorcinol; 2,4-dinitroresorcinol; 2-amino-4-nitrophenol	Competitive inhibitors	[77]

^a k_i inhibition constant

Aminoacid sequences of hemeperoxidases

Catalase – Bovine liver – (*Bos taurus*)

PDB entry code: 1TGU

UniProtKB reference: P00432

```

      10      20      30      40      50      60
...|...| ...|...| ...|...| ...|...| ...|...| ...|...|
ADNRDPASDQ MKHWKEQRAA QKPDVLTGG GNPVGDKLS LTVGPRGPLL VQDVVFTDEM

      70      80      90     100     110     120
...|...| ...|...| ...|...| ...|...| ...|...| ...|...|
AHFDRERIEP RVVHAKGAGA FGYFEVTHDI TRYSKAKVFE HIGKRTPIAV RFSTVAGESG

     130     140     150     160     170     180
...|...| ...|...| ...|...| ...|...| ...|...| ...|...|
SADTVRDPERG FAVKFYTEDG NWDLVGNNTP IFFIRDALLF PSFIHSQKRN PQTHLKDPDM

     190     200     210     220     230     240
...|...| ...|...| ...|...| ...|...| ...|...| ...|...|
VWDFWSLRPE SLHQVSFLFS DRGIPDGHRH MDGYGSHTFK LVNADGEAVY CKFHYKTDQG

     250     260     270     280     290     300
...|...| ...|...| ...|...| ...|...| ...|...| ...|...|
IKNLSVEDAA RLAHEDPDYG LRDLFNAIAT GNYPSWTLYI QVMTFSEAEI FPFNPFDLTK

     310     320     330     340     350     360
...|...| ...|...| ...|...| ...|...| ...|...| ...|...|
VWPHGDYPLI PVGKLVLRNR PVNYFAEVEQ LAFDPSNMPP GIEPSPDKML QGRLFAYPDT

     370     380     390     400     410     420
...|...| ...|...| ...|...| ...|...| ...|...| ...|...|
HRHRLGPNYL QIPVNCPYRA RVANYQRDGP MCMMDNQGGA PNYYPNSFSA PEHQPSALEH

     430     440     450     460     470     480
...|...| ...|...| ...|...| ...|...| ...|...| ...|...|
RTHFSGDVQR FNSANDDNVT QVRTFYLVKLV NEEQRKRLCE NIAGHLKDAQ LFIQKKAVERN

     490     500
...|...| ...|...| ...|...|
FSDVHPEYGS RIQALLDKYN EEKPKN

```

Chloroperoxidase (*Caldariomyces fumago*)

PDB entry code: 1LLP

UniProtKB reference: P04963

```

      10      20      30      40      50      60
...|...|...|...|...|...|...|...|...|...|...|...|
E E P G S G I G Y P Y D N N T L P Y V A P G P T D S R A P C P A L N A L A N H G Y I P H D G R A I S R E T L Q N A F L N

      70      80      90     100     110     120
...|...|...|...|...|...|...|...|...|...|...|...|
H M G I A N S V I E L A L T N A F V V C E Y V T G S D C G D S L V N L T L L A E P H A F E H D H S F S R K D Y K Q G V A

     130     140     150     160     170     180
...|...|...|...|...|...|...|...|...|...|...|...|
N S N D F I D N R N F D A E T F Q T S L D V V A G K T H F D Y A D M N E I R L Q R E S L S N E L D F P G W F T E S K P I

     190     200     210     220     230     240
...|...|...|...|...|...|...|...|...|...|...|...|
Q N V E S G F I F A L V S D F N L P D N D E N P L V R I D W W K Y W F T N E S F P Y H L G W H P P S P A R E I E F V T S

     250     260     270     280     290
...|...|...|...|...|...|...|...|...|...|...|...|
A S S A V L A A S V T S T P S S L P S G A I G P G A E A V P L S F A S T M T P F L L A T N A P Y Y A Q D P T L G P N D

```

Cytochrome *c* – Horse heart – (*Equus caballus*)

PDB entry code: 1HRC

UniProtKB reference: P00004

```

      10      20      30      40      50      60
...|...|...|...|...|...|...|...|...|...|...|...|
X G D V E K G K K I F V Q R C A Q C H T V E K G G K H K T G P N L H G L F G R K T G Q A P G F T Y T D A N K N K G I T W

      70      80      90     100
...|...|...|...|...|...|...|...|...|...|...|...|
K E E T L M E Y L E N P K K Y I P G T K M I F A G I K K K T E R E D L I A Y L K K A T N E

```

iso-1-Cytochrome *c* (*Saccharomyces cerevisiae*)

PDB entry code: 1YCC

UniProtKB reference: P00044

```

      10      20      30      40      50      60
...|...|...|...|...|...|...|...|...|...|...|...|
T E F K A G S A K K G A T L F K T R C L Q C H T V E K G G P H K V G P N L H G I F G R H S G Q A E G Y S Y T D A N I K K

      70      80      90     100
...|...|...|...|...|...|...|...|...|...|...|...|
N V L W D E N N M S E Y L T N P K K Y I P G T K M A F G G L K K E K D R N D L I T Y L K K A C E

```

Lignin peroxidase (*Phanerochaete chrysosporium*)

PDB entry code: 1LLP

UniProtKB reference: P49012

```

      10      20      30      40      50      60
...|...|...|...|...|...|...|...|...|...|...|...|
ATCANGKTVG DASCCAWFDV LDDIQANMFH GGQCGAEAHE SIRLVFHDSI AISPAMEARG

      70      80      90     100     110     120
...|...|...|...|...|...|...|...|...|...|...|...|
KFGGGGADGS IMIFDTIETA FHPNIGLDEV VAMQKPFVQK HGVTTPGDFIA FAGAVALSNC

     130     140     150     160     170     180
...|...|...|...|...|...|...|...|...|...|...|...|
PGAFPQMFFT GRKPATQPAP DGLVPEPFHT VDQIARVND AGEFDELELV WMLSAHSVAA

     190     200     210     220     230     240
...|...|...|...|...|...|...|...|...|...|...|...|
VNDVDPTVQG LPFDSTPGIF DSQFFVETQF RGTLPFGSGG NQGEVESGMA GEIRIQTDHT

     250     260     270     280     290     300
...|...|...|...|...|...|...|...|...|...|...|...|
LARDSRTACE WQSFVGNQSK LVDDFQFIFL ALTQLGQDPN AMTDCSDVIP LSKPIPGNGP

     310     320     330     340
...|...|...|...|...|...|...|...|...|...|...|...|
FSFFPPGKSH SDIEQACAET PFPSSLVTLPG PATSVARIPP HKA

```

Manganese peroxidase (*Phanerochaete chrysosporium*)

PDB entry code: 1MNP

UniProtKB reference: Q02567

```

      10      20      30      40      50      60
...|...|...|...|...|...|...|...|...|...|...|...|
AVCPDGTRVS HAACCAFIPL AQDLQETIFQ NECGEDAHEV IRLTFHDAIA ISRSQGPKAG

      70      80      90     100     110     120
...|...|...|...|...|...|...|...|...|...|...|...|
GGADGSMLLF PTVEPNFSAN NGIDDSVNNL IPFMQKHNTI SAADLVQFAG AVALSNCPGA

     130     140     150     160     170     180
...|...|...|...|...|...|...|...|...|...|...|...|
PRLEFLAGRP NKTIAAVDGL IPEPQDSVTK ILQRFEDAGG FTPFEVSVLL ASHSVARADK

     190     200     210     220     230     240
...|...|...|...|...|...|...|...|...|...|...|...|
VDQTIDAAPF DSTPFTFDTQ VFLEVLLKGV GFPGSANNTG EVASPLPLGS GSDTGEMRLQ

     250     260     270     280     290     300
...|...|...|...|...|...|...|...|...|...|...|...|
SDFALAH DPR TACIWQGFVN EQAFMAASFR AAMSKLAVLG HNRNSLIDCS DVVPVPKPAT

     310     320     330     340     350
...|...|...|...|...|...|...|...|...|...|...|...|
GQPAMFPAST GPQDLELSCP SERFPTLTTQ PGASQSLIAH CPDGSMSCPG VQFNPGA

```

Peroxidase – Horseradish – (*Armoracia rusticana*)

PDB entry code: 1ATJ

UniProtKB reference: P00433

```

      10      20      30      40      50      60
.....|.....|.....|.....|.....|.....|
QLTPTFYDNS CPNVSNIVRD TIVNELRSDP RIAASILRLH FHDCFVNGCD ASILLDNTTS

      70      80      90     100     110     120
.....|.....|.....|.....|.....|.....|
FRTEKDAFGN ANSARGFPVI DRMKAAVESA CPRTVSCADL LTIAAQQSVT LAGGPSWRVP

     130     140     150     160     170     180
.....|.....|.....|.....|.....|.....|
LGRRDSLQAF LDLANANLPA PFFTLPLQKD SFRNVGLNRS SDLVALSGGH TFGKNQCRFI

     190     200     210     220     230     240
.....|.....|.....|.....|.....|.....|
MDRLYNFSNT GLPDPTLNTT YLQTLRGLCP LNGNLSALVD FDLRTPPTIFD NKYYVNLLEEQ

     250     260     270     280     290     300
.....|.....|.....|.....|.....|.....|
KGLIQSDQEL FSSPNATDPI PLVRSFANST QTFNFAFVEA MDRMGNITPL TGTQGIQLRN

.....|
CRVVNS

```

Versatile peroxidase (*Pleurotus eryngii*)

PDB entry code: 3FKG

UniProtKB reference: O74953

```

      10      20      30      40      50      60
.....|.....|.....|.....|.....|.....|
ATCDDGRTTA NAACCILFPI LDDIQENLFD GANCGEVHE SLRLTFHDAI GFSPTLGGGG

      70      80      90     100     110     120
.....|.....|.....|.....|.....|.....|
ADGSIIAFDT IETNFPANAG IDEIVSAQKP FVAKHNISAG DFIQFAGAVG VSNCPPGGVRI

     130     140     150     160     170     180
.....|.....|.....|.....|.....|.....|
PFFLGRPDAV AASPDHLVPE PFDSVDSILA RMGDAGFSPV EVVWLLASHS IAAADKVDPS

     190     200     210     220     230     240
.....|.....|.....|.....|.....|.....|
IPGTPFDSTP EVFDSQFFIE TQLKGRFLPG TADNKGEAQS PLQGEIRLQS DHLLARDPQT

     250     260     270     280     290     300
.....|.....|.....|.....|.....|.....|
ACEWQSMVNN QPKIQNRFAA TMSKMALGQ DKTKLIDCSD VIPTPPALVG AAHLPAFDSL

     310     320     330
.....|.....|.....|
SDVEQACAAT FFPALTADPG PVTSVPPVPG S

```

References

1. Prakash K, Prajapati S, Ahmad A et al (2002) Unique oligomeric intermediates of bovine liver catalase. *Protein Sci* 11:46–57
2. Murthy MRN, Reid TJ III, Sicignano A et al (1981) Structure of beef liver catalase. *J Mol Biol* 152:465–499
3. Samejima T, Kamata M, Shibata K (1962) Dissociation of bovine liver catalase at low pH. *J Biochem* 51:181–187
4. Deutsch HF, Seabra A (1955) Immunochemical studies and assay of catalase. *J Biol Chem* 214:455–462
5. Miyahara T, Takeda A, Hachimori A et al (1978) On the heterogeneity of catalase from goat liver. Purification and characterization. *J Biochem* 84:1267–1276
6. Kikuchi-Torii K, Hayashi S, Nakamoto H et al (1982) Properties of *Aspergillus niger* catalase. *J Biochem* 92:1449–1456
7. Morris DR, Hager LP (1966) Chloroperoxidase. I. Isolation and properties of the crystalline glycoprotein. *J Biol Chem* 241:1763–1768
8. Perez DI, Van Rantwijk F, Sheldon RA (2009) Cross-linked enzyme aggregates of chloroperoxidase: synthesis, optimization and characterization. *Adv Synth Catal* 351:2133–2139
9. Margoliash E (1952) Purification of cytochrome *c*. *Nature* 170:1014–1015
10. Tien M, Kirk TK (1984) Lignin-degrading enzyme from *Phanerochaete chrysosporium*: purification, characterization, and catalytic properties of a unique H₂O₂-requiring oxygenase. *Proc Natl Acad Sci USA* 81:2280–2284
11. Kuwahara M, Glenn JK, Morgan MA et al (1984) Separation and characterization of two extracellular H₂O₂-dependent oxidases from ligninolytic cultures of *Phanerochaete chrysosporium*. *FEBS Lett* 169:247–250
12. Gold MH, Kuwahara M, Chiu AA et al (1984) Purification and characterization of an extracellular H₂O₂-requiring diarylpropane oxygenase from the white rot basidiomycete, *Phanerochaete chrysosporium*. *Arch Biochem Biophys* 234:353–362
13. Paszczynski A, Huynh VB, Crawford R (1986) Comparison of ligninase-I and peroxidase-M2 from the white-rot fungus *Phanerochaete chrysosporium*. *Arch Biochem Biophys* 244:750–765
14. Renganathan V, Miki K, Gold MH (1985) Multiple molecular forms of diarylpropane oxygenase, an H₂O₂-requiring, lignin-degrading enzyme from *Phanerochaete chrysosporium*. *Arch Biochem Biophys* 241:304–314
15. Glumoff T, Harvey PJ, Molinari S et al (1990) Lignin peroxidase from *Phanerochaete chrysosporium*. Molecular and kinetic characterization of isozymes. *Eur J Biochem* 187:515–520
16. Farrell RL, Murtagh KE, Tien M et al (1989) Physical and enzymatic properties of lignin peroxidase isoenzymes from *Phanerochaete chrysosporium*. *Enzyme Microb Technol* 11:322–328
17. Glenn JK, Gold MH (1985) Purification and characterization of an extracellular Mn(II)-dependent peroxidase from the lignin-degrading basidiomycete, *Phanerochaete chrysosporium*. *Arch Biochem Biophys* 242:329–341
18. Glenn JK, Akileswaran L, Gold MH (1986) Mn(II) oxidation is the principal function of the extracellular Mn-peroxidase from *Phanerochaete chrysosporium*. *Arch Biochem Biophys* 251:688–696
19. Leisola M, Meussdoerffer F, Waldner R et al (1985) Production and identification of extracellular oxidases of *Phanaerochaete chrysosporium*. *J Biotechnol* 2:379–382
20. Bermek H, Yazici H, Öztürk MH et al (2004) Purification and characterization of manganese peroxidase from wood-degrading fungus *Trichophyton rubrum* LSK-27. *Enzyme Microb Technol* 35:87–92

21. Petruccioli M, Frascioni M, Quarantino D et al (2009) Kinetic and redox properties of MnP II, a major manganese peroxidase isoenzyme from *Panus tigrinus* CBS 577.79. *J Biol Inorg Chem* 14:1153–1163
22. Martínez MJ, Ruiz-Dueñas FJ, Guillén F et al (1996) Purification and catalytic properties of two manganese peroxidase isoenzymes from *Pleurotus eryngii*. *Eur J Biochem* 237:424–432
23. Ruiz-Dueñas FJ, Martínez MJ, Martínez AT (1999) Molecular characterization of a novel peroxidase isolated from the ligninolytic fungus *Pleurotus eryngii*. *Mol Microbiol* 31:223–235
24. Hiner ANP, Hernández-Ruiz J, Arnao MB et al (1996) A comparative study of the purity, enzyme activity, and inactivation by hydrogen peroxide of commercially available horseradish peroxidase isoenzymes A and C. *Biotechnol Bioeng* 50:655–662
25. Shannon LM, Kay E, Lew JY (1966) Peroxidase isozymes from horseradish roots. I. Isolation and physical properties. *J Biol Chem* 241:2166–2172
26. Aibara S, Yamashita H, Mori E et al (1982) Isolation and characterization of five neutral isoenzymes of horseradish peroxidase. *J Biochem* 92:531–539
27. Aibara S, Kobayashi T, Morita Y (1981) Isolation and properties of basic isoenzymes of horseradish peroxidase. *J Biochem* 90:489–496
28. Kay E, Shannon LM, Lew JY (1967) Peroxidase isozymes from horseradish roots. II. Catalytic properties. *J Biol Chem* 242:2470–2473
29. Deutsch HF (1952) The properties of various crystalline horse erythrocyte catalase preparations. *Acta Chem Scand* 6:1516–1521
30. Prajapati S, Bhakuni V, Babu KR et al (1998) Alkaline unfolding and salt-induced folding of bovine liver catalase at high pH. *Eur J Biochem* 255:178–184
31. Furuta H, Hachimori A, Ohta Y et al (1974) Dissociation of bovine liver catalase into subunits on acetylation. *J Biochem* 76:481–491
32. Deutsch HF (1951) A highly active horse erythrocyte catalase. *Acta Chem Scand* 5:815–819
33. Bai C, Bo H, Jiang Y et al (2010) Inactivation of chloroperoxidase by arginine. *Process Biochem* 45:312–316
34. Hollenberg PF, Hager LP, Blumberg WE et al (1980) An electron paramagnetic resonance study of the high and low spin forms of chloroperoxidase. *J Biol Chem* 255:4801–4807
35. Ahmad A, Madhusudanan KP, Bhakuni V (2000) Trichloroacetic acid and trifluoroacetic acid-induced unfolding of cytochrome *c*: stabilization of a native-like folded intermediate. *Biochim Biophys Acta Protein Struct Mol Enzymol* 1480:201–210
36. Margoliash E, Schejter A (1966) Cytochrome *c*. *Adv Protein Chem* 21:113–286
37. Baciocchi E, Gerini MF, Lanzalunga O et al (2002) Lignin peroxidase catalysed oxidation of 4-methoxymandelic acid. The role of mediator structure. *Tetrahedron* 58:8087–8093
38. Tien M, Kent Kirk T (1983) Lignin-degrading enzyme from the hymenomycete *Phanerochaete chrysosporium* burds. *Science* 221:661–663
39. Kamal JKA, Behere DV (2003) Activity, stability and conformational flexibility of seed coat soybean peroxidase. *J Inorg Biochem* 94:236–242
40. Howes BD, Brissett NC, Doyle WA et al (2005) Spectroscopic and kinetic properties of the horseradish peroxidase mutant T171S. Evidence for selective effects on the reduced state of the enzyme. *FEBS J* 272:5514–5521
41. Salimi A, Noorbakhsh A, Ghadermarz M (2005) Direct electrochemistry and electrocatalytic activity of catalase incorporated onto multiwall carbon nanotubes-modified glassy carbon electrode. *Anal Biochem* 344:16–24
42. Rezaei-Zarchi S, Saboury AA, Norouzi P et al (2007) Electrochemical recognition of metalloproteins by bromide-modified silver electrode – a new method. *Int J Mol Sci* 8: 723–735
43. Makino R, Chiang R, Hager LP (1976) Oxidation-reduction potential measurements on chloroperoxidase and its complexes. *Biochemistry* 15:4748–4754
44. Ayala M, Pickard MA, Vazquez-Duhalt R (2008) Fungal enzymes for environmental purposes, a molecular biology challenge. *J Mol Microbiol Biotechnol* 15:172–180

45. Millis CD, Cai D, Stankovich MT et al (1989) Oxidation-reduction potentials and ionization states of extracellular peroxidases from the lignin-degrading fungus *Phanerochaete chrysosporium*. *Biochemistry* 28:8484–8489
46. McCarthy MB, White RE (1983) Functional differences between peroxidase compound I and the cytochrome P-450 reactive oxygen intermediate. *J Biol Chem* 258:9153–9158
47. Cetinus SA, Oztop HN (2003) Immobilization of catalase into chemically crosslinked chitosan beads. *Enzyme Microb Technol* 32:889–894
48. Cetinus SA, Oztop HN (2000) Immobilization of catalase on chitosan film. *Enzyme Microb Technol* 26:497–501
49. Abe K, Makino N, Anan FK (1979) pH dependency of kinetic-parameters and reaction-mechanism of beef-liver catalase. *J Biochem* 85:473–479
50. Aksoy Y, Balk M, Ogus I et al (2004) The mechanism of inhibition of human erythrocyte catalase by azide. *Turk J Biol* 28:65–70
51. Jürgen-Lohmann DL, Legge RL (2006) Immobilization of bovine catalase in sol-gels. *Enzyme Microb Technol* 39:626–633
52. Voet D, Voet JG (1995) Mechanism of enzyme action. *Biochemistry*, 2nd edn. Wiley, New York
53. Longoria A, Tinoco R, Vázquez-Duhalt R (2008) Chloroperoxidase-mediated transformation of highly halogenated monoaromatic compounds. *Chemosphere* 72:485–490
54. Liu JZ, Wang M (2007) Improvement of activity and stability of chloroperoxidase by chemical modification. *BMC Biotechnol*. doi:10.1186/1472-6750-7-23
55. Montiel C, Terrés E, Domínguez JM et al (2007) Immobilization of chloroperoxidase on silica-based materials for 4, 6-dimethyl dibenzothiophene oxidation. *J Mol Catal B Enzym* 48:90–98
56. Hernandez J, Robledo NR, Velasco L et al (1998) Chloroperoxidase-mediated oxidation of organophosphorus pesticides. *Pestic Biochem Physiol* 61:87–94
57. Tziaila AA, Kalogeris E, Gournis D et al (2008) Enhanced catalytic performance and stability of chloroperoxidase from *Caldariomyces fumago* in surfactant free ternary water-organic solvent systems. *J Mol Catal B Enzym* 51:24–35
58. Garcia-Arellano H (2002) Diseño de un biocatalizador termoestable por modificación química de hemoproteínas. PhD Thesis, Universidad Nacional Autónoma de México
59. Tinoco R, Vazquez-Duhalt R (1998) Chemical modification of cytochrome *c* improves their catalytic properties in oxidation of polycyclic aromatic hydrocarbons. *Enzyme Microb Technol* 22:8–12
60. Vazquez-Duhalt R (1999) Cytochrome *c* as a biocatalyst. *J Mol Catal B Enzym* 7:241–249
61. Torres E, Sandoval JV, Resell FI et al (1995) Site-directed mutagenesis improves the biocatalytic activity of *iso-1*-cytochrome *c* in polycyclic hydrocarbon oxidation. *Enzyme Microb Technol* 17:1014–1020
62. Kersten PJ, Kalyanaraman B, Hammel KE et al (1990) Comparison of lignin peroxidase, horseradish peroxidase and laccase in the oxidation of methoxybenzenes. *Biochem J* 268:475–480
63. Gilabert MA, Fenoll LG, García-Molina F et al (2004) Kinetic characterization of phenol and aniline derivatives as substrates of peroxidase. *Biol Chem* 385:795–800
64. Smith AT, Sanders SA, Thorneley RNF et al (1992) Characterisation of a haem active-site mutant of horseradish peroxidase, Phe41 →Val, with altered reactivity towards hydrogen peroxide and reducing substrates. *Eur J Biochem* 207:507–519
65. Camarero S, Sarkar S, Ruiz-Dueñas FJ et al (1999) Description of a versatile peroxidase involved in the natural degradation of lignin that has both manganese peroxidase and lignin peroxidase substrate interaction sites. *J Biol Chem* 274:10324–10330
66. Valderrama B, Vazquez-Duhalt R (2005) Electron-balance during the oxidative self-inactivation of cytochrome *c*. *J Mol Catal B Enzym* 35:41–44
67. Villegas JA, Mauk AG, Vazquez-Duhalt R (2000) A cytochrome *c* variant resistant to heme degradation by hydrogen peroxide. *Chem Biol* 7:237–244

68. LaRotta CE, D'Elia E, Bon EPS (2007) Chloroperoxidase mediated oxidation of chlorinated phenols using electrogenerated hydrogen peroxide. *Electron J Biotechnol* 10:24–36
69. Garcia-Arellano H, Buenrostro-Gonzalez E, Vazquez-Duhalt R (2004) Biocatalytic transformation of petroporphyrins by chemical modified cytochrome *c*. *Biotechnol Bioeng* 85: 790–798
70. Valderrama B, Garcia-Arellano H, Giansanti S et al (2006) Oxidative stabilization of *iso*-1-cytochrome *c* by redox-inspired protein engineering. *FASEB J* 20:1233–1235
71. Arnao MB, Acosta M, del Rio JA et al (1990) A kinetic study on the suicide inactivation of peroxidase by hydrogen peroxide. *Biochim Biophys Acta* 1041:43–47
72. Wagenknecht HA, Claude C, Woggon WD (1998) New enzyme models of chloroperoxidase: improved stability and catalytic efficiency of iron porphyrinates containing a thiolato ligand. *Helv Chim Acta* 81:1506–1520
73. Kadima TA, Pickard MA (1990) Immobilization of chloroperoxidase on aminopropyl-glass. *Appl Environ Microbiol* 56:3473–3477
74. Thomas JA, Morris DR, Hager LP (1970) Chloroperoxidase. VII. Classical peroxidatic, catalytic, and halogenating forms of the enzyme. *J Biol Chem* 245:3129–3134
75. Renganathan V, Miki K, Gold MH (1987) Haloperoxidase reactions catalyzed by lignin peroxidase, an extracellular enzyme from the basidiomycete *Phanerochaete chrysosporium*. *Biochemistry* 26:5127–5132
76. Chance B (1952) Effect of pH upon the reaction kinetics of the enzyme-substrate compounds of catalase. *J Biol Chem* 194:471–481
77. Karasyova EI, Naumchik IV, Metelitz DI (2003) Activation of peroxidase-catalyzed oxidation of aromatic amines with 2-aminothiazole and melamine. *Biochemistry* 68:54–62
78. Munoz-Munoz JL, Garcia-Molina F, Varon R et al (2007) Kinetic characterization of the oxidation of esculetin by polyphenol oxidase and peroxidase. *Biosci Biotechnol Biochem* 71:390–396
79. Glenn JK, Morgan MA, Mayfield MB et al (1983) An extracellular H₂O₂-requiring enzyme preparation involved in lignin biodegradation by the white rot basidiomycete *Phanerochaete chrysosporium*. *Biochem Biophys Res Commun* 114:1077–1083
80. Darr D, Fridovich I (1985) Inhibition of catalase by 3, 3'-diaminobenzidine. *Biochem J* 226:781–787
81. Hong ES, Kwon OY, Ryu K (2008) Strong substrate-stabilizing effect of a water-miscible ionic liquid [BMIM][BF₄] in the catalysis of horseradish peroxidase. *Biotechnol Lett* 30:529–533

Index

A

Absorption maxima, 81
Acetylcholinesterase, 191
Acrylamide
 basidiomycete, 162
 Bjerkandera adusta, 162
 dyes, 161
 Fe-ammonium persulfate, 162
 papermaking, 161
 2,4-pentanedione, 162
 polyacrylamides, 161
Activity, 226
Adhesive, 157
Affinity constants, 337
Agrocybe aegerita, 46, 51, 98
Alcohols, 126, 134
Alkyl hydrazines, 89
Amines, 120, 124
Aminofluoren, 96
Anilines, 96, 115
Animal peroxidase superfamily, 39–42
Ascorbate peroxidase, 39, 80
Aspergillus, 325–326
Aspergillus, 320
Azide, 89, 91, 94
Azo dyes, 197

B

Basidiomycete peroxidases, 43–46
Biocatalysis, 3
Biocatalysts, 2, 4, 210
Bioeconomy, 1
Bioengineering, 4
Biomimetics, 66
Bioplomyer
 biomedical, 171
 cross-linking, 171

 cysteine, 171
 dextran, 171
 hyaluronic acid, 171
 hydrogels, 171
 lysine, 171
 polysaccharide, 171
 proteins, 171
 tyrosine, 171
Bioreactors, 323–324
Biosensors, 133, 139
Biotechnology, 1, 2
Bjerkandera adjusta, 85, 184, 188, 192
Bottlenecks, 325

C

Caldariomyces fumago, 98, 100, 184, 186,
 188, 191
Cardanol
 anacardic acid, 161
 Coprinus cinereus, 160
 curing, 160
 epoxide, 160
 polycardanol, 160
Catalase, 345
Catalase–peroxidase KatG, 86–88
Catalysts, 227
Catalytic cycle, 81
Catalytic tryptophan, 39, 49–51
Catechols, 115, 121, 132, 134
Cation, 95
Cation radical, 195
CcP. *See* Cytochrome *c* peroxidase
Chlorite, 99
Chloroanilines, 185
Chloroperoxidase (CPO), 3, 40, 43, 46, 48,
 51, 52, 54, 100, 186–188, 191, 192, 211,
 219, 222, 224, 228, 230, 235, 236, 346

- Chlorophenols, 195
 Chlorpromazine, 97, 98
 CIP. *See* *Coprinopsis cinerea* peroxidase
 Circular dichroism, 299, 300
 Coating
 bonding, 160
 brown rot fungi, 160
 copolymerization, 159
 cresol, 159
 2,6-dimethylphenol, 159
 formaldehyde, 160
 hybrid resins, 157
 lignin, 159
 lignosulphonates, 159
 phenol-formaldehyde, 159
 polyethylenimine, 160
 poly(oxy-2,6-dimethyl-1,4-phenylene), 159
 poly(p-cresol), 159
 poly(p-phenylphenol), 159
 Cofactor, 62
 Cofactor incorporation, 328–329
 Coimmobilization, 214, 224
 Complex polymers
 binders, 165
 bonding, 165
 cross-linking, 165
 lignolytic enzymes, 165
 mediators, 165
 Mycowood, 165
 Pleurotus ostreatus, 165
 resins, 165
 Trametes versicolor, 165
 white-rot fungi, 165
 Compound 0, 83
 Compound ES, 85
 Compound I, 81, 83–84, 99
 Compound II, 81, 85
 Compound III, 81, 85–86, 291
 Compound III decay pathways, 296–297
 Compound III model systems, 304–305
 Compound X, 99
 Conducting polymers
 ammonium persulfate, 162
 aniline, 162
 electrical conductivity, 164
 electroactive, 163
 ortho-directed, 163
 para-directed, 163
 poly(vinylphosphonic acid), 163
 polyaniline, 162
 polyelectrolytes, 164
 sodium dodecylbenzenesulfonic acid, 164
 sulfonated polystyrene, 164
 template-assisted, 163
 template-free, 164
Coprinopsis cinerea (syn. *Coprinus cinereus*), 39
Coprinopsis cinerea peroxidase (CIP), 39, 46
 CPO. *See* Chloroperoxidase
 Crystal structure, 93
 Cyclopropanone hydrate, 89
 Cytochrome *c* (cyt *c*), 136, 139–141, 187, 188, 346
 Cytochrome *c* peroxidase (CcP), 38–40, 50, 80, 82, 94, 114, 128, 235
 Cytochrome P450, 181, 187, 188, 191
- D**
 Decolorization, 213
 Degradation, 247, 248, 254–256, 266, 267, 274–280, 283–284
 Dibenzofurans, 185
Dichomitus squalens, 197
 Di-heme cytochrome *c* peroxidase (di-heme CcP), 40, 42
 Di-heme peroxidase family, 7
 MauG, 26
 Dimerization, 95
 Dioxins, 181, 185, 193
 Distal arginine, 82
 Distal histidine, 82
 Dye decolorization, 249, 255, 264, 266–274, 277, 278
 Dye-decolorizing peroxidase (DyP), 40, 43, 46, 48, 53–54
 Dye-transfer inhibition, 169
 Dyp-type peroxidases family, 7
- E**
 Electron paramagnetic resonance (EPR), 83, 301–302
 Electron transfer theory, 72
 Enantioselectivity, 113, 123, 126, 138, 141
 Endocrine disruptive chemicals, 181, 188–191
 Enzyme, 219
 Enzyme linked immunosorbent assay (ELISA), 132
 Eosinophil peroxidase (EPO), 39, 40, 89, 98
 Epoxidation, 123, 124, 136, 137
 EPR. *See* Electron paramagnetic resonance
 Estimated redox potentials, 68
 Estrogenic activity, 191
 Expression systems, 321–323
 Extended X-ray fine structure (EXAFS), 83

F

- Fe(III)/Fe(II) couple, complexed with protoporphyrin, 62
- Fermentations, 323
- Fiber boards
 - brown and white-rot, 166
 - fiber surface, 166
 - particle boards, 166
 - rape-straw fibers, 166
 - wood laminates, 166
- Filamentous fungi, 320
- Fluorescent
 - 3-alkyl-2-hydrazono-4-thiazolines, 164
 - chromophore, 164
 - α -naphthol, 164
 - 2-naphthol, 164
 - poly (2-naphthol), 164
- Free radical, redox potential, 70

G

- Geobacter sulfurreducens*, 40, 42
- Geotrichum*, 43, 53
- Geotrichum* DyP, 40, 46, 48, 54
- Gloeophyllum striatum*, 184
- Glycosylation, 326–327
- Green chemistry, 1
- Guaiacol, 94, 95

H

- Hair dyeing
 - hydrogen peroxide, 169
 - tyrosinases, 169
- Half-life, 343
- Halogenated pesticides, 191, 192
- Halogenated phenols, 181, 184
- Halogenation, 130
- Halogens, 129
- Haloperoxidase family, 7
 - CCPO, 30
- Hammett equation, 96
- Hb. *See* Hemoglobin
- Heme desolvation, 62
 - dielectric constant, 66
 - iron oxidation states, 67
- Heme electrochemistry, 66
 - electrochemical data, 62
 - theoretical tools, 66
- Heme-haloperoxidase, 8
- Heme modification, 91
- Heme peroxidases, 316, 321
- Heme-protein crosslinking, 88–89
- Heme-thiolate peroxidases, 37, 43, 46, 51–53, 55
- Hemoglobin (Hb), 136, 138, 187

- Herbicides, 193
- Heterologous production, 316
- High spin, 82
- HOB_r, 90
- H₂O₂-dependent deactivation, 293
- Hormones, 188
- Horseradish peroxidase, 182–184, 337
 - isoenzymes, 337
- Horseradish peroxidase (HRP), 39, 40, 80, 82, 93, 94, 225, 227–229, 233, 234
- Humic substances, 182
- Hydroxylation, 125, 126, 136
- Hypohalides, 99

I

- Immobilization, 219, 221
- Indoles, 115, 126, 130, 131
- Industrial dyes, 181
- Inhibitors, 344, 345
- Insecticides, 191
- Ionization potential, 67, 187
- Ipomea palmata*, 197
- Iron–oxygen bond, 84, 85
- Iron protoporphyrin IX, 80
- Ischnoderma resinosum*, 197
- iso*-1-Cytochrome *c*, 346
- Isoelectric point, 336
- Isoniazid, 97, 98

K

- k_{cat} , 336, 340, 341
- K_M , 336, 340, 341

L

- Laccase, 191, 197, 198
- Lactoperoxidase (LPO), 39, 40, 42, 80, 88, 98, 184
- Large-scale, 323–324
- Leptoxyphium fumago* (syn. *Caldariomyces fumago*), 40, 43, 46, 48, 51
- Lignin, 97
- Ligninolytic peroxidases, 37, 39, 44, 46–51, 53
- Lignin peroxidase (LiP), 39, 40, 46, 48–51, 80, 82, 86, 134, 184, 187, 191, 193, 196, 197, 217, 234, 336, 347
 - isoenzymes, 336
- Long range electron transfer (LRET), 49–50, 55
- LPO. *See* Lactoperoxidase

M

- Magnetic circular dichroism, 300, 301
- Magnetite, 213
- Malondialdehyde, 97

- Manganese oxidation site, 47–49
Manganese peroxidase (MnP), 39, 44, 46–48, 97, 187, 188, 190, 191, 193, 196–198, 217, 231, 347
Marasmius scorodoni, 46, 54
Mb. *See* Myoglobin
Measured redox potentials, 68
 δ -Meso edge of heme, 94
Mesoporous, 211, 223
Mesoporous silicates, 220
9-Methoxyellipticine, 101
4-Methylanisole, 100
Microperoxidases (MPs), 141
MnP. *See* Manganese peroxidase
Molar extinction coefficient, 338
Molecular weight, 336
Mössbauer, 83
Mössbauer spectroscopy, 305
MP8, 141
MPO. *See* Myeloperoxidase
MPs. *See* Microperoxidases
Mutants, 123, 128, 137
Mutation, 134
Mycobacterium tuberculosis, 86
Myeloperoxidase (MPO), 39, 40, 42, 80, 88, 89, 98, 184
Myoglobin (Mb), 136, 139
- N**
Nanocapillary, 212
Nernst equation, 72
Nitration, 121, 130, 131, 136
Nitrite, 92
Nitromethane, 89
Nonylphenol, 190
- O**
Optical spectrum, 298, 299
Optimum pH, 343, 344
Organophosphorus pesticides, 191, 192
Oxidative ability, 66
 Fe(III)/Fe(II) redox potential, 67
 threshold, 67
Oxidative polymerization of dye precursors, 169
- P**
P450, 136
PAH. *See* Polycyclic aromatic hydrocarbon
Panus tigrinus, 184
Particle
 boards, 165
 lignosulphonates, 165
 methylene diphenyl diisocyanate, 165
P-chloronitroaniline, 100
PEG. *See* Polyethylene glycol
Pentachlorophenol, 184, 186, 191, 192
Peroxidase, 134, 156, 231, 235, 348
Peroxidase activity, 322
Peroxidase-based processes, 3
Peroxidase-catalase superfamily, 7, 67
 ascorbate peroxidase, 19
 catalase–peroxidase, 19
 class I peroxidase, 7
 class II peroxidase, 7
 class III secretory peroxidases, 7
 cytochrome c peroxidase, 19
 KatGs, 19
 lignin peroxidases, 7, 23
 manganese peroxidases, 7, 17
 plant secretory peroxidases, 7
 versatile peroxidases, 7, 23
Peroxidase–cyclooxygenase superfamily, 7
 chordata peroxidases, 7
 cyclooxygenases, 7
 eosinophil peroxidase, 16
 lactoperoxidase, 16
 myeloperoxidase, 16
 peroxicins, 7
 peroxidasins, 7
 peroxidockerins, 7
 peroxinectins, 7
 primordial peroxidases, 7
 thyroid peroxidase, 16
Peroxidases, 2, 4, 210, 222, 224, 226, 228
Pesticides, 181, 185, 191, 193
Phanerochaete chrysosporium, 40, 44, 46–48, 50, 85, 94, 184, 186, 188, 193, 197
Phanerochaete sordida, 190
Phenol, 182, 183
Phenolic compounds, 182
Phenolic resins, 157
Phenol polymerization, 183
Phenols, 95, 96, 115, 116, 121, 125, 130, 131, 134, 139, 141, 142, 192
Phenoxy radical, 185
Phenoxy radicals, 182
Phenylbutazone, 97
Phenylhydrazine, 91, 94
Plant, fungal and bacterial peroxidase superfamily, 38–39, 46
Pleurotus calyptratus, 197
Pleurotus eryngii, 41, 85
Pleurotus ostreatus, 44, 46, 190
Pollution, 180
Polychlorinated biphenyls, 181, 195–196

- Polycyclic aromatic hydrocarbon (PAH), 181, 187–188, 279, 281
- Polyethylene glycol, (PEG), 183, 230
- Poly(methylmethacrylate)
- antioxidant, 161
 - 2-(4-hydroxyphenyl)ethyl methacrylate, 161
 - methyl methacrylate, 161
 - m-ethynylphenol, 161
 - technical lignins, 161
 - vitamin C functionalized, 161
- Polymers, 157
- chemistry, 156
 - enzymatically, 156
 - enzymatic grafting, 156
 - grafting functional molecules, 156
 - horseradish peroxidase, 156
 - laccases, 156
 - polymerization reactions, 156
- Polyphenylene-2,6-benzobisthiazole fibers
- acrylamide, 171
 - Kevlar fiber, 171
 - polyethylene, 171
- Polystyrene
- branched polymeric, 163
 - doping, 163
 - 4-methylstyrene, 162
 - reversed micelles, 163
 - styrene, 162
 - templates, 163
 - 2-vinylnaphthalene, 162
- Porphyrin radical, 83–84
- Porphyrins, 140
- Poulos–Kraut mechanism, 83
- Primary coordination sphere of iron, 64, 69
- Productivity, 220
- Protein folding, 327–328
- Protein radical, 84–85
- Proteins, 322
- Proximal histidine, 70, 82
- redox potential, 70
- Push-pull concept, 70
- R**
- Radicals, 113–117, 120, 121
- Rate constants, 99
- Reactor configuration, 246, 252–267
- biphasic reactor, 246, 251, 252, 279–284
 - continuous stirred tank reactor (CSTR), 253–255, 257–259, 262, 267
 - discontinuous stirred tank reactor, 253–257
 - electrochemical reactor, 265–266
 - electroenzymatic reactor, 249, 253, 254, 265, 266
 - enzyme concentration, 247
 - fixed bed reactor, 253, 255, 263
 - fluidized bed reactor, 253, 255, 263–264
 - membrane reactor, 246, 253–256, 259–261, 265–279
 - plug flow reactor, 254, 255, 262–264
 - two-stage reactor, 256–257, 264, 275–279
- Reconstitution, 135, 137, 138
- Redox, 199
- Redox potential, 61, 95, 198, 199, 339
- covalent linkages, 70
 - errors in redox potential, 72
 - hard–soft acid–base principle, 64
 - local charges, 65
 - mammalian peroxidases, 72
 - noncatalytic Fe(III)/Fe(II), 67
 - porphyrin substituents, 65
 - relative impact of different factors, 66
 - relevant redox couples, 67
 - thermodynamics, 62–64
- Redox titrations, 71
- Regioselectivity, 123, 130
- Resonance Raman, 83
- Resonance Raman spectroscopy, 302
- Reusability, 223
- S**
- Saccharum spontaneum*, 197
- Secretory pathway, 325–326
- Selectivity, 220
- Self-inactivation, 183
- Senna angustifolia*, 197
- Solvent, 247, 249, 251–252, 260, 275, 279, 280, 282, 283
- Soybean peroxidase, 131
- Space, Time Yield (STY), 221
- Spectroelectrochemistry, 71
- Spring cabbage peroxidase, 134
- Stability, 220, 225, 228
- Stereoselectivity, 113, 115, 123, 126, 140, 141
- Stopped-flow spectrophotometry, 72
- Styrene, 100
- Substituted hemes, 94
- Substrate access channel, 93
- Suicide inactivation, 198
- Sulfoxidation, 126, 128, 137, 138
- Sweet potato, 134
- Synthetic dyes, 196

T

Textile fibers

- Chinese lacquer, 168
- decolorization, 169
- dye-transfer inhibition, 169
- enzymatic dyeing, 168
- gaiac resin, 168
- indigo, 169
- lauryl gallate, 168
- novozyme, 169
- phenolic, 168
- poly(1-vinyl-2-pyrrolidone), 169

Textile industry, 168

Thermomechanical pulp (TMP)

- anchor groups, 167
- antimicrobial, 167
- bacteria, 167
- Coniophora puteana*, 167
- Fomitopsis pinicola*, 167
- food, 167
- fungicides, 167
- Gloeophyllum trabeum*, 167
- Gram negative, 167
- Gram positive, 167
- packaging, 167
- paperboard, 166
- phenolic amines, 167
- phenolics, 166
- ply-bond, 166
- reactive surface, 167
- TMP-phenol, 166
- Trametes hirsuta*, 167

Thiocyanate, 91

Thyroid peroxidase (TPO), 39

TMP. *See* Thermomechanical pulp

Tobacco peroxidases, 134

Total turnover number (TTN), 210, 221, 224, 227

Toxics release inventory, 180

TPO. *See* Thyroid peroxidase*Trametes cervina*, 85*Trametes hispida*, 197*Trametes versicolor*, 184

2,4,6-Trichlorophenol, 101

TTN. *See* Total turnover number**V**

Veratryl alcohol, 86, 101

Veratryl radical, 97

Veratryl radical cation, 86

Versatile peroxidase (VP), 39–41, 46, 47, 49–51, 184, 188, 192, 276, 279–283, 348

W

White-rot fungal peroxidases, 43–44, 55

X

Xenobiotics, 181

X-ray crystallography, 306

Y

Yeast, 38, 40